A TRIBUTE TO

"Studies of the Physical Properties of Hardened Portland Cement Paste"

by T.C. Powers and T.L. Brownyard

Foreword by H.J.H. Brouwers

In their pioneering work, Powers and Brownyard were the first to systematically investigate the reaction of cement and water and the formation of hydrated cement paste. In the late 1940s, in a series of landmark papers, they presented a model for the cement paste in which unreacted cement, free water (capillary porosity), and the hydration product (which is porous in itself, that is, the gel porosity) were distinguished. They introduced the concept of nonevaporable water (water retained in P-dried state) and gel water (additional water retained upon saturation): their specific volumes are lower than that of free water, causing chemical shrinkage and creating capillary space. Careful execution of experiments resulted in the quantity and specific volume of both nonevaporable water and gel water. Powers and Brownyard were among the first who employed new theories and techniques such as adsorption, B.E.T surface area, XRD, and calorimetry. Critical paste properties were measured by extensive and carefully executed experiments, including the amount of retained water and the chemical shrinkage associated with the hydration reaction. These properties were further related to the content of the four most important clinker phases, viz. alite, belite, aluminate, and ferrite. Additionally, the composition of the cement paste was related to engineering properties such as compressive strength, shrinkage, porosity, water permeability, and freezing/thawing resistance. The impact of this standard work is paramount and their concepts and the results are used in contemporary cement and concrete science (Taylor (1997), Neville (2000)). Czernin (1959), Locher (1975), Hansen (1986), Jensen and Hansen (2001), Brouwers (2004, 2005, 2007), and Livingston et al. (2007) presented more detailed discussions on the authors' work, validated and confirmed the key findings using contemporary techniques, and also extended the approach to new research areas.

Both Powers and Brownyard performed their research at the Portland Cement Association (PCA), at that time located in Chicago, Illinois. Information about the life and work of Dr. Treval Clifford Powers can be collected, but Dr. Theodore Lucius Brownyard seems somehow to have disappeared, no further records of him after 1948 can be found by this author.

Dr. Treval Clifford Powers;
February 8, 1900, Palouse (Washington),
June 30, 1997, Green Valley (Arizona).

Dr. Powers received a Bachelor of Arts degree from Willamette University in 1925, majoring in chemistry. He worked for PCA from 1930 until his retirement in 1965. For the next 7 years, he taught, lectured, and consulted internationally in the field of cementitious materials before moving to Arizona.

On the occasion of his retirement, a symposium was sponsored by the Highway Research Board, to which workers from all over the world contributed. In 1966, it was published as the monumental Special Report No. 90 by the Highway Research Board (1966).

Probably unknown to most people working in the field of cement and concrete is that after his retirement, Dr. Powers studied "The Phenomenon of Inflation." His unorthodox economic theory resulted in the book *Leakage: The Bleeding of the American Economy* (Benchmark, 1996), which has been hailed as a pivotal work in the field of macroeconomics. Besides his research on the structure of fresh and hardened cement paste, Dr. Powers is also known for his mortar and concrete research on consistency, workability, rheology, durability, unsoundness, shrinkage and swelling, abrasion resistance, sulfate resistance, frost resistance etc. and is author of the book *The Fresh Properties of Concrete* (1968). Dr. Powers won the ACI Wason Research Medal in 1933, 1940, and together with Dr. Brownyard in 1948. He became an Honorary Member of ACI in 1961 and received the ACI Arthur R. Anderson Award in 1976. He also received the Sanford E. Thompson Award of the American Society for Testing and Materials (ASTM) in 1957.

Dr. Brownyard was born in Ensley Township, Newaygo County, Michigan, on June 6, 1905. In 1930, he entered The Johns Hopkins University in Baltimore as Francis P. Garvan Fellow at Large, and obtained his Doctor of Philosophy degree in 1934. His PhD thesis is entitled "The Retention of Water Vapor by Alumina," and in this work advanced techniques (P-drying, water-vapor adsorption) were employed that were also used later in his work with Dr. Powers and reported in their paper series. Dr. Brownyard joined the research group of Dr. Powers at the PCA in 1937, where he stayed until 1943 when he was called up by the Navy as a Lieutenant U.S. Naval Reserve. He served in the United States Naval Air Transportation Service (Navigation) throughout the war years and remained with the Navy until at least May 1948. The results reported in their paper series from 1947-1948 therefore concern their work done at the PCA many years before.

In what follows in this special volume, their entire series (9 Parts), is included. The reader is warmly encouraged to read all these nine parts of this remarkable landmark publication.

References

Brouwers, H. J. H., 2004, "The Work of Powers and Brownyard Revisted: Part 1," *Cement and Concrete Research*, V. 34, pp. 1697-1716.

Brouwers, H. J. H., 2005, "The Work of Powers and Brownyard Revisted: Part 2," *Cement and Concrete Research*, V. 35, pp. 1922-1936.

Brouwers, H. J. H., 2007, "The Work of Powers and Brownyard Revisted: Part 3," Proceedings, 12th International Congress on the Chemistry of Cement, Montréal, 8-13th July 2007, W1-05.6, J. J. Beaudoin, J. M. Makar, and L. Raki, eds., National Research Council of Canada, Montreal, Canada.

Czernin, W., 1959, "Die physikalische Beschaffenheit der Hydratationsprodukte," *Zement und Beton*, V. 16, pp. 10-15. (in German)

Hansen, T. C., 1986, "Physical Structure of Hardened Cement Paste, A Classical Approach," *Materials and Structures*, V. 19, pp. 423-436.

Highway Research Board, 1966, *Symposium on Structure of Portland Cement Paste and Concrete*, Highway Research Board Special Report No. 90, Washington D.C.

Jensen, O. M., and Hansen, P. F., 2001, "Water-Entrained Cement-Based Materials I. Principles and Theoretical Background," *Cement and Concrete Research*, V. 31, pp. 647-654.

Livingston, R. A.; Nemes, N. M.; and Neumann, D. A., 2007, "States of Water in Hydrated Cement Paste: Powers and Brownyard Revisited," *Proceedings*, 12th International Congress on the Chemistry of Cement, Montréal, July, T1-03.3, J. J. Beaudoin, J. M. Makar, and L. Raki, eds., National Research Council of Canada, Montreal, Canada.

Locher, F. W., 1975, "Volumenänderungen bei der Zementerhärtung," Sonderheft aus Zement und Beton, Heft 85/86, pp. 1-4. (in German)

Neville, A.M., 2000, *Properties of Concrete*, fourth edition, Prentice Hall/Pearson, Harlow, U.K., 844 pp.

Taylor, H. F. W., 1997, *Cement Chemistry*, second edition, Thomas Telford, London, 480 pp.

H.J.H. Brouwers, *Department of Civil Engineering, Faculty of Engineering Technology, University of Twente , Enschede (The Netherlands)*
The author studied Mechanical Engineering at Eindhoven University of Technology (the Netherlands) from 1981 until 1986. After his study, he worked at Akzo Nobel Central Research in Arnhem (NL) on plastic production processes and products. He completed a PhD thesis on the heat and mass transfer in plastic heat exchangers and condensers in 1990. Since 1992, he has been appointed at the University of Twente. His research interests include sustainable building and construction materials. He was appointed a Guest Professor at Wuhan University of Technology (China) in 2007.

Title 43-5a —a part of PROCEEDINGS, AMERICAN CONCRETE INSTITUTE Vol. 43

JOURNAL
of the
AMERICAN CONCRETE INSTITUTE
(copyrighted)

Vol. 18 No. 2 7400 SECOND BOULEVARD, DETROIT 2, MICHIGAN October 1946

Studies of the Physical Properties of Hardened Portland Cement Paste*

By T. C. POWERS†
Member American Concrete Institute

and T. L. BROWNYARD‡

IN NINE PARTS

SYNOPSIS

This paper deals mainly with data on water fixation in hardened portland cement paste, the properties of evaporable water, the density of the solid substance, and the porosity of the paste as a whole. The studies of the evaporable water include water-vapor-adsorption characteristics and the thermodynamics of adsorption. The discussions include the following topics:

1. Theoretical interpretation of adsorption data
2. The specific surface of hardened portland cement paste
3. Minimum porosity of hardened paste
4. Relative amounts of gel-water and capillary water
5. The thermodynamics of adsorption
6. The energy of binding of water in hardened paste
7. Swelling pressure

*Received by the Institute July 8, 1946—scheduled for publication in seven installments; October 1946 to April, 1947.
†Manager of Basic Research, Portland Cement Assn. Research Laboratory, Chicago 10, Ill.
‡Navy Dept., Washington, D. C., formerly Research Chemist, Portland Cement Assn. Research Laboratory, Chicago 10, Ill.

FOREWORD

This paper deals with the properties of hardened portland cement paste. The purpose of the experimental work on which it is based was to bring to light as much information as is possible by the methods of colloid chemistry and physics. Owing to the war, the original program, which included only a part of the field to be explored, was not completed. Moreover, the interpretation of the data is incomplete, partly because of the inability of the authors to comprehend their meaning, and partly because of the need of data from experiments yet to be made.

Although the work is incomplete, it represents a considerable amount of time and effort. Experimental work began in a small way in 1934 and continued until January 1943. Some additional work was done in 1945 during the preparation of this paper. The first three years was a period of intermittent work in which little of permanent value was accomplished beyond the development of apparatus and procedures. This phase of the work presented many problems, some of which have never been solved to our complete satisfaction.

The interpretation of the results of experiments also presented many difficulties. During the course of our experiments, important new developments in colloid science were coming to light through a series of papers from other laboratories. It was necessary to study these papers as they appeared and to seek their applications to our problems. The result is that the theory on which much of our present interpretation is based is one that did not exist when our work began and is one that is still in the process of development. The reader may note that many of the papers referred to in Part 3 were not published until 1940 or later.

The theory referred to is that of multimolecular adsorption by Brunauer, Emmett, and Teller as first given in 1938 and as amplified in the paper by Brunauer, Deming, Deming, and Teller in 1940. In justification for the use of such a recent and unfinished development, we may note in the first place that a remarkable number of papers by various authors have appeared since 1940 strongly supporting the kind of use that we have made of the theory, particularly the estimation of surface area. In the second place, the basic conclusions reached through the

use of the theory might have been reached from a strictly empirical analysis of the data. However, it is difficult to imagine how a picture of the hardened paste as detailed as the one presented in this paper could have been drawn without adopting theoretically justified assumptions.

The paper is composed of nine parts. Part 1 contains a review of previous work done in this field and discusses various experimental methods. Part 2 elaborates on the principal method used in the present study, namely, the measurement of water-fixation. It also presents the empirical aspects of the data so that the reader may become familiar with facts to be dealt with.

Part 3 presents the theories upon which an interpretation of the data in Part 2 can be based. It gives also a partial analysis of most of the experimental data given in Part 2 in the light of the adopted basis of interpretation. Part 4 is a discussion of the thermodynamics of moisture-content changes in hardened paste and the phenomena accompanying those changes. It is thus an extension of the earlier discussion of theory.

In Part 5 data are presented pertaining to the volumes of different phases in the paste. The interpretation of these data involves the use of factors developed in the preceding parts of the paper. The final result is a group of diagrams illustrating five different phases, the relative proportions of each, and how those relative proportions change as hydration progresses.

The relationship between the physical characteristics of the hardened cement paste and compressive strength of mortars is discussed in Part 6. A similar discussion of permeability and absorptivity is given in Part 7.

A study of the freezing of water in hardened paste is presented in Part 8. The conditions under which ice can exist in the paste are described and empirical equations are given for the amounts of water that are freezable under designated conditions.

The properties of portland cement paste as they appear in the light of these studies are described in Part 9. This part amounts to a summary of the outcome of the study, at its present incomplete stage, without details of experimental procedures, or theoretical background.

As mentioned in the first paragraph, a particular point of view as to the meaning of the data has been adopted. Specifically, we have assumed, on the basis of evidence given in the paper, that the various phenomena discussed are predominantly of physical rather than chemical nature. The result of the study therefore constitutes a hypothesis, or series of hypotheses, rather than a rigorous presentation of established facts. Considering the present state of our knowledge, we believe this policy to be more fruitful than one of trying to maintain a strictly un-

biased view as to the meaning of the data. As written, the paper represents the thinking of one group of workers (influenced, of course, by many others), and it implicitly invites independent investigations of the same field by any who may have good reason to adopt a different point of view. To this end, we have appended tabulations of the original data.

Though we thus concede the possibility of other interpretations, we nevertheless feel confident that a large part of the present interpretation will withstand logical criticism. However, it seems very likely that corrections and changes of emphasis will develop as experimental work continues, and as further advances are made in fundamental colloid science.

The paper is directed primarily toward all who are engaged in research on portland cement and concrete. However, it may be of considerable interest to many who seek only to understand concrete as they work with it in the field. Studied in connection with earlier papers on the characteristics of paste in the plastic state,* this paper affords a comprehensive, though incomplete, picture of the physical nature of portland cement paste. It, therefore, pertains to any phase of concrete technology that involves the physical properties of the cement paste. This means that the paper should find application to most phases of concrete technology.

For the most part, the reader will find few items of data that bear directly on specific questions or problems. Successful application of this study to research or practical technology requires some degree of comprehension of the work in its entirety. Consequently, it is not likely that a single, casual reading will reveal much that is of value to one not already familiar with the methods and background of this type of investigation.

ACKNOWLEDGMENTS

We are deeply indebted to Mark L. Dannis and Harold Tarkow, not only for their long and painstaking labor with the various experiments, but also for their contributions to an understanding of the results. Mark Dannis made most of the adsorption and specific-volume measurements and Harold Tarkow performed the freezing experiments reported in Part 8.

We are grateful to Gerald Pickett, whose constructive criticism was of great value throughout most of the period of study.

*Bull. 2, "The Bleeding of Portland Cement Paste, Mortar and Concrete," by T. C. Powers, P.C.A. Research Laboratory (1939); Bull. 3, "Rate of Sedimentation," by Harold H. Steinour, P.C.A. Research Laboratory (1944), reprinted from *Ind. Eng. Chem. 36*, 618; 840; 901 (1944); Bull. 4, "Further Studies of the Bleeding of Portland Cement Paste," by Harold H. Steinour, P.C.A. Research Laboratory (1945).

We are especially indebted to Harold H. Steinour, who took time from his own work to carry on the final volumenometer work described in Part 5. Also, he helped prepare the discussion of thermodynamics in Part 4 and gave much valuable criticism of various other parts of the paper.

To Virginia Atherton, who made many of the hundreds of computations, typed the manuscript, and corrected printer's proof we express our kindest thanks.

Part 1. A Review of Methods That Have Been Used for Studying the Physical Properties of Hardened Portland Cement

CONTENTS

Starting as a suspension of cement particles in water, portland cement paste becomes a solid as the result of chemical and physical reactions between the constituents of the cement and water. A solidified paste of typical characteristics is capable of giving up or absorbing a volume of water equal to as much as 50 per cent of the apparent volume of the

paste. These facts engender the idea that whatever the chemical constitution of the new material produced by chemical reaction, the new material is laid down in such a way as to enclose water-filled, interconnected spaces. That is, the hydration product appears to be not a continuous, homogeneous solid, but rather it appears to be composed of a large number of primary units bound together to form a porous structure. It seems self-evident that the manner in which the primary units are united, that is, the physical structure of the paste, is closely related to the quality of the paste and is therefore something about which we should be well informed.

Freyssinet[1]* discerned the need for knowledge of paste structure and devised a hypothesis about the setting and hardening process and about the structure of the hardened paste. Giertz-Hedström,[2] an active contributor to this subject, has given an excellent review of publications on this subject. This review, together with Bogue's[3] earlier one of a slightly different aspect of the subject, obviates the necessity of an extensive historical review at this time.

A program of studies of the properties of the hardened paste was begun in this laboratory in 1934. It has consisted mainly of studies of the fixation of water, but has also included measurements of the heat-effects accompanying the regain of water by the previously dried paste, measurements of the freezing of the water in the saturated paste, and various other related matters.

This work has yielded a considerable amount of information on the physical aspects of hardened paste. It contributes to the knowledge of the chemical constitution of the hydration products only in a negative way; that is, it shows that some of the current information on the constitution of the hydration products must be incorrect. Later parts of this paper will give an account of these studies.

METHODS FOR STUDYING THE PHYSICAL PROPERTIES OF THE HARDENED PASTE†

The question of structure can be broken down into three parts: first, the question as to the chemical constitution of the hydration products, which includes the question of structure of the ultimate parts; second, the question of the structure of the smallest primary aggregations of the ultimate parts; third, the question of how the primary aggregations are assembled and how they are held together. A review of some of the work done by earlier investigators follows.

Microscopic examinations

The light-microscope. The effectiveness of the microscope as a means of studying the structure of the hardened paste is limited because the

*See references end of Part 1.
†See also the review by Giertz-Hedström (Ref. 3).

units of the essential part of the structure are too small to be seen. The results obtained by Brown and Carlson[4] are typical. They, like others, observed that the hardened paste is predominantly "amorphous," so far as the microscope can reveal. Embedded in this amorphous mass are the remnants of unhydrated clinker grains, crystals of calcium hydroxide, and sometimes crystals of other compounds.

Kühl[5] reported that thin sections of hardened cement paste showed ". . . a residue of undecomposed cement particles, separated by a gray and only slightly differentiated mass which gives a feebly diffused luminescence in polarized light. Even under the highest magnification individual particles cannot be distinguished in this material, which is obviously almost entirely ultramicroscopic in structure." However, on examining the same specimens 20 years later he found that ". . . the passage of years had resulted in fundamental changes. No longer (was the material) uniform and only slightly differentiated under polarized light as was the case a few months after their preparation. They now showed a definitely increased (polarized-light) transmission and, most noteworthy of all, their properties were markedly different according to the percentages of water with which they had been gaged. The specimens gaged with the greatest amount of water showed the greatest changes while those mixed with the least water had undergone considerably less modification." The changes mentioned were such as to suggest that the originally colloidal material had gradually changed toward the microcrystalline state, the change being greater the higher the original water content.

Useful information has been obtained by microscopic observations of the hydration of cement in the presence of relatively large quantities of water. But it is unlikely that the structure developed under these conditions is the same as that developed in pastes; hence, conclusions about the normal structure drawn from observations of this kind are open to question.[6] For example, Le Chatelier[7] observed that when a large quantity of water was used, needlelike crystals of microscopic dimensions soon developed. He concluded from this that similar, though submicroscopic, crystals developed under all conditions.

Brownmiller[8] described the results of microscopic examinations of hardened paste by means of reflected light. The method is a modification of that described by Tavasci[9] and Insley[10] for studying the constitution of clinker. In addition to the use of etchants to bring different phases into contrast, Brownmiller treated the surface with a dye which was taken up by the so-called amorphous material and the microcrystalline phases. Although Brownmiller's primary object was to develop the experimental technique, some of his conclusions concerning the nature of hardened paste and the hydration process are of considerable

interest. He found that there was ". . . no microscopic evidence of channeling of water into the interior of cement particles to selectively hydrate any single major constituent. Hydration seems to proceed by the gradual reduction in the size of the particles as a function of the surface exposed." This conclusion seemed to be based on the appearance of the coarser particles that remained unhydrated after the first day.

Brownmiller found that a Type III* cement having a specific surface of 2600 appeared to be almost completely hydrated after one day in a sealed vial and six days in water. A Type I cement having a specific surface of 1800 showed an unhydrated residue of about 15 per cent after one day in a sealed vial and 28 days in water. The water-cement ratio of the original paste was 0.4 by weight in both cases.

The only microcrystalline hydrate mentioned by Brownmiller was calcium hydroxide. This was found as clusters of fine crystals embedded in what Brownmiller called the hydrogel.

Brownmiller found that the etched surface of the 7-day-old paste made of Type I cement showed "an extremely complicated but interesting structure. A close examination . . . shows that the cement hydrogel is not a formless mass but has an intricate structure."

The electron microscope. Eitel[11] used the electron microscope for photographing the hydration products of some of the constituents of portland cement. The article consulted gives almost no details concerning the method of preparing the samples that were photographed. It appears that the samples were taken from dilute suspensions of the hydrated material. Presumably, samples of $Ca(OH)_2$ were taken from saturated or supersaturated "milk of lime" and hydration products of C_3S and C_3A from saturated solutions of water in isobutyl alcohol. The isobutyl alcohol was used to dilute the water and thus make possible a relatively high concentration of the solid with respect to water and at the same time a dilute suspension. Since the isobutyl alcohol was saturated with water, the chemical activity of the water was unaffected by the presence of the isobutyl alcohol.

Several photographs of these preparations (magnifications ranging from 7200 to 36000) were published. The $Ca(OH)_2$ taken from milk of lime as well as that formed from the hydrolysis of C_3S appeared as hemispheres ranging in size from about 0.1 to 0.5 micron. The calcium silicate hydrate appeared as thin crystalline needles about one-half

*See A.S.T.M. Designation C150-44 where five types of portland cement are defined as follows:
Type I —For use in general concrete construction when the special properties specified for Types II, III, IV, and V are not required.
Type II —For use in general concrete construction exposed to moderate sulfate action, or where moderate heat of hydration is required.
Type III—For use when high early strength is required.
Type IV —For use when a low heat of hydration is required.
Type V —For use when high sulfate resistance is required.

micron long. The C_3A appeared mainly as rounded particles ("roses") about 0.1 micron in diameter. Referring to these and apparently to other observations, Eitel concluded that although the hydration products of portland cement are predominantly colloidal, they appear crystalline—not amorphous—to the electron microscope.

Sliepcevich, Gildart, and Katz,[12] reported the results of attempts to photograph the hydration products of portland cement and the major constituents hydrated separately. Most of the photographs published were of samples prepared as follows: 0.5 to 0.75 g of portland cement or a cement constituent was mixed with about 10 cc of purified water and allowed to stand. At the desired age the specimen for photographing was obtained by taking a drop of the supernatant liquid and allowing it to evaporate on a collodion film previously prepared. The material on this film was thus whatever dissolved or suspended material the drop contained.

In some respects the results were like those found by Eitel. Photographs of calcium hydroxide appeared like those of Eitel but whereas Eitel concluded that the particles were hemispheres, Sliepcevich, Gildart, and Katz concluded that they were spheres. From each material the latter investigators usually found material of several geometric forms. Some of the material appeared amorphous and some crystalline. As did Eitel, those investigators found the majority of crystals to be in the colloidal size range.

The significance of these results is open to question until it is known definitely just what relation the samples obtained in the manner described have to the hydration products making up the mass of a hardened cement paste.

X-ray examinations

The results of X-ray examinations were summarized by Giertz-Hedström[13] as follows: "X-ray examinations of hardened cement have so far given little beyond a confirmation of what has been shown by the microscope. The presence of clinker remains and crystallized calcium hydroxide is thus confirmed by Brandenburger.[14] The structure of the main mass, the "cement gel," is, however, such as to give, at least for the present, no clear guidance in the X-ray diagrams. This may be due to its lacking a crystalline structure or other regular fine structure or to the crystals being so small or deformed (for example bent needles) that no definite interferences are obtained."

Bogue and Lerch[15] mention the use of X-ray analysis in connection with microscopic examination. The X-ray confirms the microscopic indication that unaltered beta or gamma dicalcium silicate remained in pastes after 2 years of curing. X-ray diffraction patterns from both

hydrated tricalcium silicate and hydrated dicalcium silicate showed at the end of 2 years no evidence of the development of a new crystalline structure such as would be expected if the hydrates were to change from the theoretically unstable gel state to the stable microcrystalline state. As mentioned above, evidence of the beginning of such a change within a period of 20 years was reported by Kühl.

Water fixation

Because direct observation fails to answer many questions concerning the structure, properties, and behavior of hardened portland cement paste, indirect methods of study have been used. The principal one is that of studying the manner in which water is held in the hardened paste.

Isotherms and isobars. The fixation of water by water-containing solids is usually measured in terms of the amounts of water held at various vapor pressures with temperature constant, or in terms of the amounts held at various temperatures with pressure constant. The curves obtained by the first method are called *isotherms.* Those obtained by the second method are called *isobars.* Both of these methods have been used in the study of hardened portland cement paste. The nature of the hydration or dehydration curve depends on the manner in which the water is combined and on other factors to be discussed.

Binding of water in hydroxides. In metallic hydroxides, which represent one class of compounds that may be included among hydrates, the elements of water are present as *OH*-groups that are strongly bound by the metallic ions. This is usually recognized in writing the formulas of metallic hydroxides; thus, calcium hydroxide is usually given the formula $Ca(OH)_2$ rather than $CaO.H_2O$.

Water bound by covalent bonds. In many hydrates, the water molecule retains its identity to a large degree, i.e., H_2O is a unit in the structure. An example is $MgCl_2.6H_2O$. In this hydrate the six molecules of water are bound to the magnesium ion by covalent bonds and are arranged around the magnesium ion in an octahedral grouping. To indicate this, the formula should be written $Mg(H_2O)_6Cl_2$, for this more nearly represents the structure.

Water bound by hydrogen bonds. There is another type of compound in which the water molecule remains intact and is bound to the compound by one or both of its hydrogen atoms. The molecules so held are said to be bound by hydrogen bonds. $CuSO_4.5H_2O$ and $NiSO_4.7H_2O$ are hydrates in which one of the water molecules is bound in this way.

* * * * *

Water held in a compound by any of the types of bond described above is properly regarded as being chemically bound. The removal of

water from such hydrates necessarily gives rise to a new solid phase and hence the isotherms and isobars of these hydrates should show well marked steps in accordance with the phase rule. Fig. 1a gives, for example, the relationship between water content and vapor pressure for the hydrates of copper sulfate.

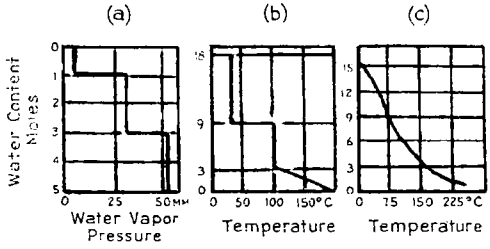

Fig. 1 – Univariant and bivariant dehydration curves
(a) Isothermal p-x curve for $CuSO_4.5H_2O$
(b) Isobaric T-x curve for $Cr_2(SO_4)_3.18H_2O$ The first $15H_2O$ come off along a univariant curve, the remaining $3H_2O$ being zeolitic
(c) Zeolitic dehydration of green $Cr_2(SO_4)_3.15H_2O$
(Curves and caption from Emeleus & Anderson)

Zeolitic water. One type of microcrystalline hydrate, which comprises the zeolites and several basic salts and hydroxides of bivalent metals, gives smooth isotherms or isobars. Fig. 1c is an example of an isobar from $Cr_2(SO_4)_3.15H_2O$. Water held in this type of compound is called zeolitic water.

According to Emeleus and Anderson[16] zeolitic water is regarded as being packed between the layers of the crystal or in the interstices of the structure. A distinguishing characteristic of zeolitic water is that it may be removed without giving rise to a new solid phase. Its removal may, however, change the spacing between successive layers of the crystal.

Water held in such a way as to exhibit the behavior described above is sometimes referred to as being in a state of zeolitic solution or solid solution.[17]

Lattice water. Emeleus and Anderson[16] distinguish a type of hydrate in which there is water of crystallization "that cannot be supposed to be associated chemically with the principal constituents of the crystal lattice." As an example, they cite potassium alum, $KAl(SO_4)_2.12H_2O$. There is little question that six of the twelve molecules of water are linked to the aluminum ion by covalent bonds. The remaining six molecules are known to be arranged octahedrally around the potassium ion but at such a large distance from it as to suggest to Emeleus and Anderson that the interaction is very weak and hence that the water is not chemically bound to the potassium ion. This perhaps represents a borderline case between chemically bound water and zeolitic water, which is supposed not to be chemically bound. The fact that exactly six molecules of water are associated with the potassium ion is accounted for by the geometry of the crystal lattice. The removal of these six molecules of water presumably gives rise to a new crystalline phase,

however, and hence the isobars and isotherms should be stepped. When more information on this type of hydrate becomes available, perhaps many of the examples cited will have to be placed in one of the classifications listed above.

Adsorbed water. In addition to any water held by the chemical forces mentioned above, a small amount per unit of surface is held by surface forces. These forces, physical rather than chemical, are known collectively as van der Waal's forces.[18] If the specific surface of the solid phase is small, the amount so held is usually undetectable. But if the specific surface is very large, as it is for colloidal material, then physically adsorbed water can be a large fraction of the total held under given conditions; indeed, anhydrous solids such as quartz powder can hold relatively large amounts of water by surface adsorption if the powder is extremely fine. Zeolitic water can be regarded as adsorbed water, the "surfaces" in this case being certain planes in the crystal, as described above. The subject of adsorption will be treated much more fully in later sections of this paper.

Interpretation of isobars

Influence of surface adsorption. From what was said above it might appear that by means of isobaric or isothermal dehydration data water held in microcrystalline hydrates could readily be distinguished from that held as zeolite water, in solid solution, or by adsorption. It will be developed below that such a distinction can be drawn under some circumstances but not under others. The complication can best be illustrated by describing the work of Hagiwara.[19] Theoretically, the vapor pressure of the water in a very small crystal of a hydrate should be greater than that of a larger crystal of the same substance at the same temperature. Consequently, a mixture containing various sized crystals should exhibit a range in vapor pressures according to the range in particle size. Practically, the effect is not noticeable unless the particle size range extends into the range of colloidal dimensions. Theoretically, very small natural crystals or very small fragments of large crystals should behave similarly, though not necessarily identically. Consequently, the results of experiments with preparations made by pulverizing macrocrystals should be indicative of the general effects of changing particle size and particle-size range.

Hagiwara pulverized crystalline hydrates and obtained the isobar for each preparation. In one series of experiments, he used $Al_2O_3.3H_2O$ prepared by the method of Bonsdorff.[20] The original crystals were of microscopic size. The preparation was dried to constant weight in a desiccator over concentrated H_2SO_4 to establish the initial water content, which was determined by igniting a portion of the material. Samples thus dried were then heated in an electric oven at 100C for 30 minutes

after which they were cooled in a desiccator and weighed. Finally, the amount of residual water was found by ignition. This was repeated on other samples at temperatures ranging from 90 to 220C as indicated in Fig. 2. Heating at 170C and at higher temperatures was continued until further heating caused no more change in the dry weight. The total heating period at these higher temperatures was not less than 5 hours and at 210C was 20 hours.

Although the corners are somewhat rounded, there is a well defined step in the isobar* at approximately 205C, where the water content decreases from 3 molecules to one molecule. This is in good agreement with the result obtained by Weiser and Milligan.[21] The rounded corner is the usual result in such experiments; very sharply defined corners are the exception.

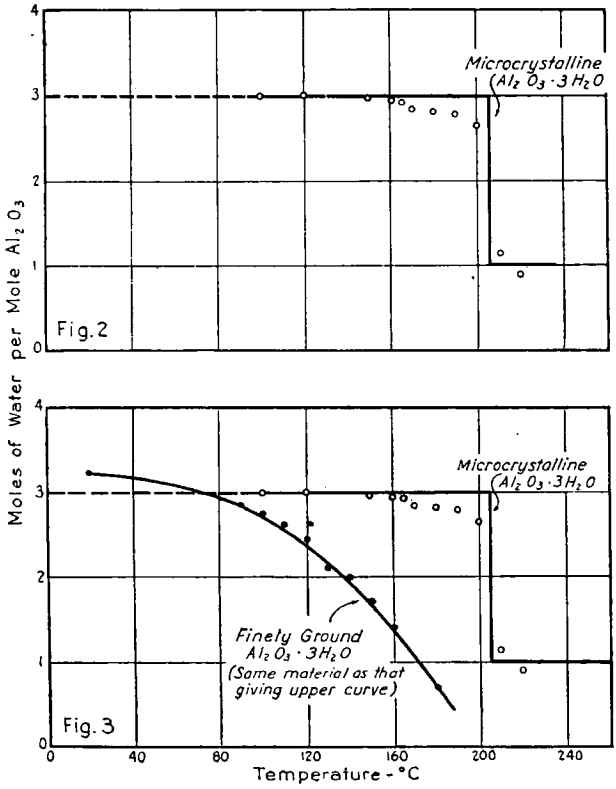

Fig. 2 & 3 – Isobars for $Al_2O_3.3H_2O$

Data from T. Hagiwara
Alexander: Colloid Chemistry
Vol. I, pp. 647-658
The Chemical Catalog Co.
Inc. (N.Y.) 1926

*Although the curves in Fig. 2 and 3 are called isobars and the text indicates that isobaric conditions were intended, it seems probable that isobaric conditions were not actually maintained. If the heating of the sample was done in an oven in the presence of room air, the actual vapor pressure in the oven would vary with the humidity of the room air and would be different at different temperatures. However, over the temperature range used in the experiment the variations in pressure were probably small. At any rate it is not likely that had strictly isobaric conditions been maintained the outcome would have been significantly different.

Hagiwara then ground a portion of the dried preparation in an agate mortar for 1½ hours, using fine quartz powder as a grinding aid, thus greatly reducing the particle size. The experiments were repeated with this finely ground material with the results shown in Fig. 3, where the results shown in Fig. 2 are reproduced for comparison. A comparison of the curves in Fig. 3 shows three significant effects of reducing the size of the crystals:

(1) All semblance of a step is absent in the curve for the finely ground sample.

(2) The initial water content of the finely ground material is higher by 0.25 mole than that of the unground material. This additional water must have come from the atmosphere during the grinding. (The initial water content is that of the sample after it is dried to constant weight in a desiccator over conc. H_2SO_4.)

(3) The water is lost from the finely ground sample at a much lower temperature than from the unground material.

Hagiwara made a similar series of experiments with $Fe_2O_3.H_2O$ with the results shown in Fig. 4. The curve for the unground macrocrystalline material shows a well defined step. The curve for "Grind A," the shorter period of grinding, still shows a step though the corners are somewhat more rounded than for the unground hydrate and the step occurs at a lower temperature. When the grinding was more prolonged, "Grind B," the step disappeared and the initial water content increased to 1.54 molecules. Grinding had little effect on the temperature at which the final water content was reached.

It appears from Hagiwara's results that a hydrate in which the water is bound by chemical bonds may still yield a smooth isobar if the sample is made up of a mixture of particles of various sizes, the smallest particles being very small. This has a significant bearing on the interpretation of isobars in general. When a solid that has water for one of its con-

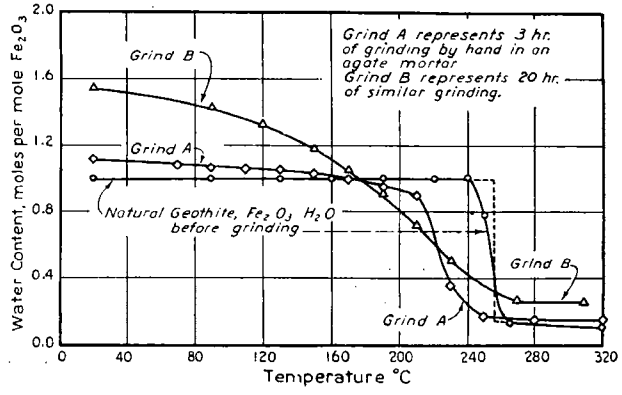

Fig. 4 – Effect of prolonged grinding on the isobars of $Fe_2O_3.H_2O$
Hagiwara, Colloid Chemistry Alexander Ed., Vol. I, pp. 647-58 (1926)

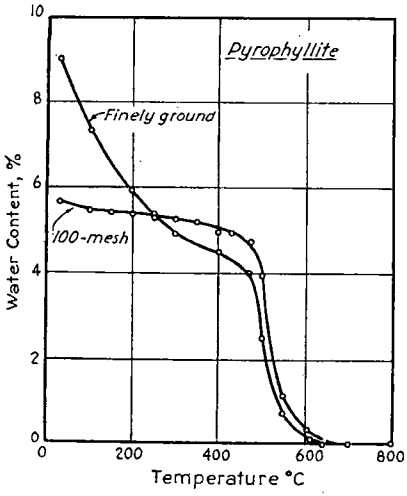

Fig. 5 – Isobar for pyrophyllite
Data from Kelley, Jenny and Brown
Soil Sci. v. 41, p. 260 (1936)

stituents yields a stepped isobar, it can usually* be concluded that the solid is a well crystallized hydrate. When, however, the isobar is a smooth curve without steps, it may represent a sample of the hydrate comprising particles of various sizes or it may represent a material in which the water is not bound by chemical bonds in the usual sense of this term. It appears also that a lack of steps in an isobar is not sufficient evidence that the hydrate has a zeolitic structure, for neither of the hydrates with which Hagiwara experimented was of that nature.

The other effect of fine grinding, namely, the increase in the initial water content brought about by grinding, is fully as significant as the one just mentioned. It must be assumed that the water in excess of that required by the formula is held by forces of a kind different from those that hold the hydrate water. The effect is clearly a surface effect, for the initial water content is much higher after the longer period of grinding than after the shorter period. (Compare "Grind B" with "Grind A" in Fig. 4.) It seems reasonable to suppose that this excess water is held by adsorption forces, i.e., forces which reside in the surface of the crystal and which came into prominence after the specific surface of the hydrate had been greatly increased by grinding.

This aspect of the effect of fine grinding is further emphasized by the results of experiments made by Kelley, Jenny, and Brown.[22] These authors studied the effect of grinding on the isobars of clay minerals. See Fig. 5. The isobar for the 100-mesh sample shows a well marked step near 500C and thus gives unmistakable evidence that the mineral is a microcrystalline hydrate. Comparing this with the isobar for the finely ground pyrophyllite, we see that the isobars are very nearly

*But not always. See remarks below on silicia gel.

identical above 400C. Each exhibits a well marked step; the steps occur at very nearly the same temperature; however, the height of the step is slightly less for the finely ground sample. Below 250C, the finely ground sample shows a larger water content than the 100-mesh sample. That is, just as with the materials Hagiwara used, after grinding there is initially a large amount of water in the finely ground sample in excess of the hydrate water represented by the nearly vertical portion of the isobar. This additional water must have been acquired from the atmosphere during grinding and must be held by some mechanism other than that which holds the hydrate water. It seems most unlikely that the excess water is zeolitic water, since fine grinding could hardly increase the total interplanar area of zeolite crystals.

Interpretation of isotherms

Isotherms of hydrates. The usual behavior of a hydrate when the water-vapor pressure around it is varied at constant temperature is illustrated in Fig. 6. This isotherm shows well defined steps with the corners slightly rounded, as indicated by the dotted lines. What the effect of pulverizing such material on the shape of the isotherm might be is not known directly from experiment, for apparently no experiments of this kind have been published. Presumably, a sufficient amount of grinding would produce a smooth isotherm, by virtue of the change in particle size and particle-size range. It might also be presumed that in a saturated condition the minute crystals would retain more water than corresponds to the highest hydrate. These presumptions follow from considerations given above in connection with the isobars.

Isotherms of gels. The appearance of a well defined step in the isotherm of a solid is not always positive proof of the existence of a hydrate of definite chemical composition. Fig. 7 illustrates this point.[23] As the arrow indicates, the isotherm was obtained by progressively lowering the water vapor pressure. Just below a pressure of 4 mm Hg, the isotherm becomes very steep, a fact which might be taken to indicate the existence of hydrates having the formulas $SiO_2.1\frac{1}{2}H_2O$ and $SiO_2.H_2O$. Fig. 8 shows the same isotherm as well as that obtained by progressively increasing the vapor pressure, the "rehydration isotherm" as it is sometimes called. Note that the latter gives no evidence of a hydrate. Weiser, Milligan, and Holmes investigated this matter fully by preparing silica gel from the same materials at various temperatures ranging from 0 to 100C and from other materials at various temperatures and under various conditions. Not all preparations exhibited the vertical section in the dehydration isotherm. Gels prepared at low temperatures exhibited a step at a higher water content than gels prepared at a high temperature. The samples prepared at 100C and aged at this temperature for a few hours, and hence under conditions favoring crystal

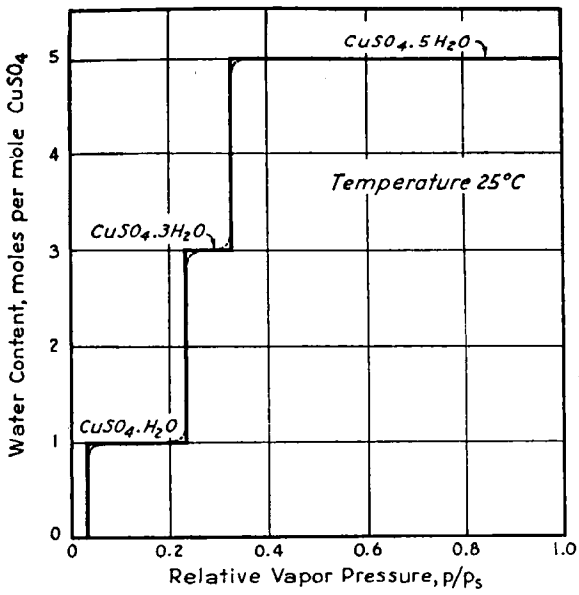

Fig. 6 – Water content vs. vapor pressure curve of $CuSO_4$

Collins and Menzies, J. Phys. Chem. v. 40, pp. 379-97 (1936)

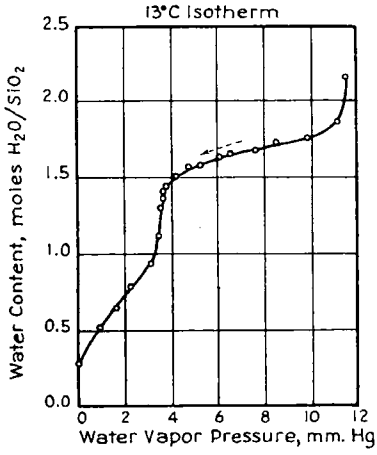

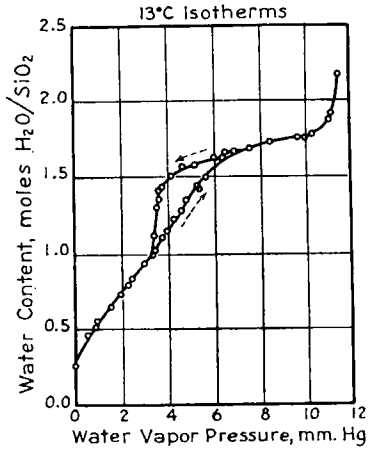

Fig. 7—(left) Dehydration isotherm for silica gel prepared from water glass at 25C

Weiser, Milligan and Holmes, J. Phys. Chem. v. 46, p. 586 (1942)

Fig. 8 (right)—Dehydration and rehydration isotherms for silica gel prepared from water glass at 25C

Weiser, Milligan and Holmes, J. Phys. Chem. v. 46, p. 586 (1942)

growth, gave no evidence of a step. No evidence of a step appeared in the rehydration isotherm of any preparation. No preparation gave evidence of crystallinity when examined by the electron diffraction method. These authors concluded that the step that occurs in the dehydration isotherm of some of the preparations is not evidence of the existence of a hydrate but is rather the result of a peculiarity of the physical structure of these gels. It follows from this conclusion that the structure of the gels prepared at low temperatures differs from that of the gels prepared at high temperatures, and there is evidence that this change in structure accompanying the increase in temperature of preparation is progressive.

Fig. 8 illustrates also the phenomenon called "sorption hysteresis." This will be discussed in another part of this paper.

* * * * *

The foregoing review shows that the interpretation of isobars and isotherms is not always a simple matter. Particularly, when the isotherm is smooth throughout, alternative interpretations must be considered carefully in the light of other pertinent information.

Water content vs. temperature curves (isobars) from hardened portland cement paste

Review of published data. In this laboratory Wilson and Martin[24] obtained a group of isobars from hardened portland cement paste. The hardened paste was ground to pass the 28-mesh sieve and then was dried to constant weight at a constant temperature in a stream of air maintained at a low, constant water vapor pressure by bubbling the air through concentrated sulfuric acid.* The dry sample was then ignited at 1000C and the loss on ignition was taken as the water retained at the temperature of drying. Various drying temperatures were used, ranging from 50 to about 600C.† The resulting isobars are given in Fig. 9. Lea and Jones[25] obtained the isobars shown in Fig. 10. These authors plotted the loss in water rather than the amount retained.

In general those curves are not like those obtained from crystalline hydrates having definite amounts of water of crystallization. The nearly vertical rise in the curves between 400 and 450C, seen clearly in the curves of Lea and Jones, is attributed to the decomposition of $Ca(OH)_2$.

Krauss and Jörns[26] obtained isobars for the hardened paste at a constant vapor pressure of 7 mm *Hg* by using the instrument shown in Fig. 11. The sample is placed in A, which can be detached from the rest of the apparatus and which serves as a weighing bottle in following the changes in weight of the sample. With A in place as shown, the

*The air was freed of CO_2 by suitable means to prevent carbonation.
†The procedure used does not maintain strictly isobaric conditions, for the pressure would vary with temperature. However, the pressure is so small under all conditions that variations can usually be neglected.

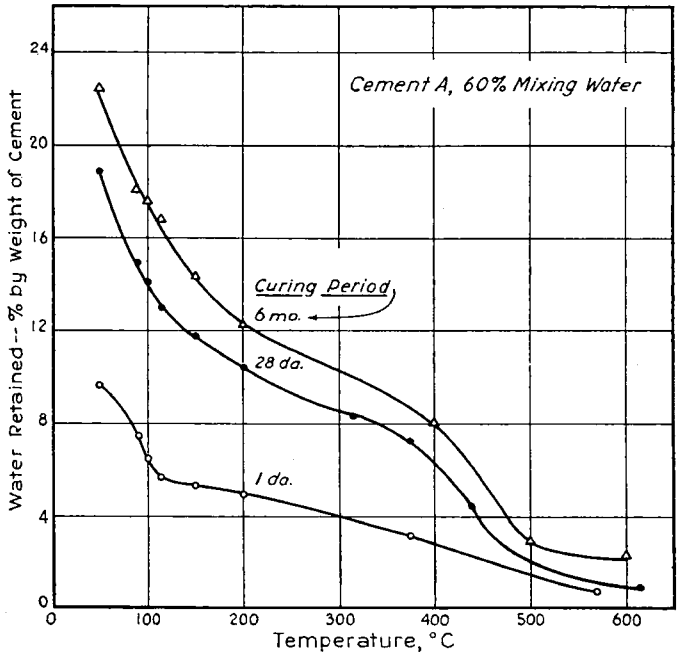

Fig. 9 – Effect of drying temperature on water retained, temperature range 50 to 600C
Wilson and Martin, J. Am. Concrete Inst. v. 31, p. 272 (1935)

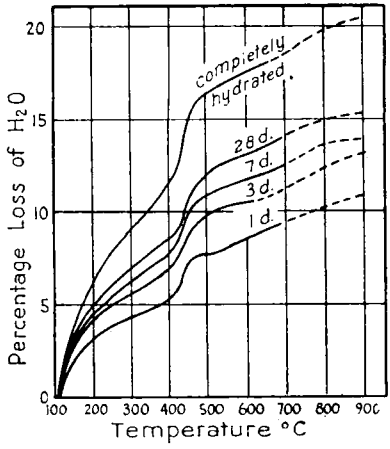

Fig. 10—Loss-on-heating curves for hardened neat cement, w/c = 0.22
Lea & Jones, J. Soc. Chem. Ind., v. 54, p. 63, 1935

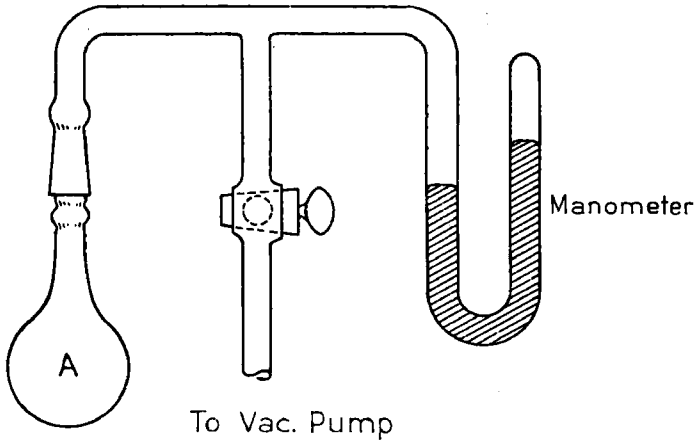

Fig. 11 – Krauss & Jorns' Apparatus

system is evacuated, thus removing water vapor as well as air. Periodically, the removal of water is interrupted by closing the stopcock and the water vapor pressure is observed. If the equilibrium pressure exceeds 7 mm *Hg*, the value chosen by Krauss and Jörns, the stopcock is opened and more water is removed by pumping. This process is repeated until at room temperature the equilibrium vapor pressure of the sample is less than 7 mm *Hg*. The temperature of the sample is then slowly raised until the pressure is exactly 7 mm. The loss of water to

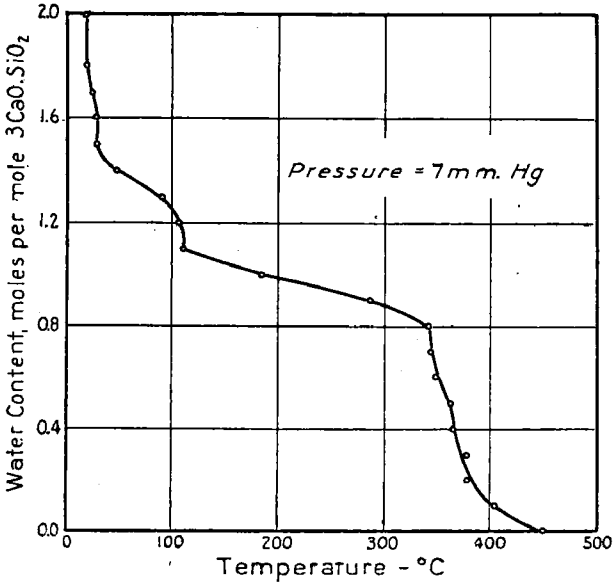

Fig. 12 – Isobar for hardened $3CaO.SiO_2$*
*Probably a mixture of C_2S and $Ca(OH)_2$ (See text)
Data from Krauss and Jorns, Zement v. 20, p. 317 (1931)

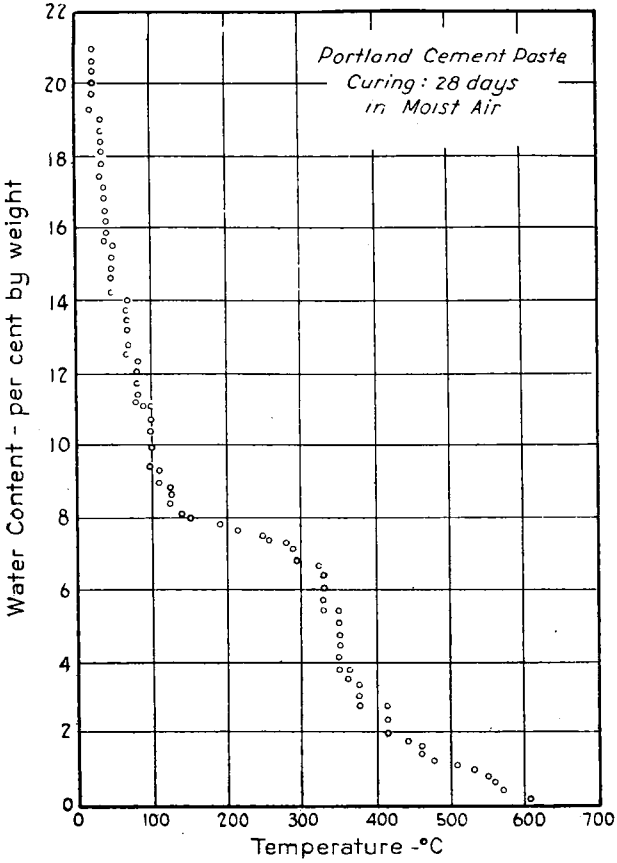

Fig. 13 – Isobar for portland cement paste obtained by Krauss and Jorns.
Zement v. 20, p. 343 (1931)

this point is determined by weighing A. Beyond this point, water is removed in small amounts by evacuation and after each decrement the temperature of the sample is raised until the pressure is exactly 7 mm *Hg*. Thus, the isobar is obtained. The results obtained by Krauss and Jörns are given in Fig. 12, 13, and 14.

Fig. 12 represents a sample described as tricalcium silicate (C_3S)* mixed with enough water to correspond with the formula $3CaO.SiO_2.2H_2O$. The mixture was cured in saturated air 24 hours before the measurements were started. There is a *suggestion* of a step in the isobar

*Throughout this discussion the compositions of portland cements will be described in terms of the compound composition computed by the methods of L. A. Dahl, *Rock Products* v. 32 (23) p. 50, (1929) and R.H. Bogue, *Ind. Eng. Chem.* (Anal. Ed.) v. 1 (4) p. 192, (1929) or PCAF Paper No. 21 (1929). The following abbreviations will be used.

$C_3S = 3CaO.SiO_2$ $\quad C_3A = 3CaO.Al_2O_3$
$C_2S = 2CaO.SiO_2$ $\quad C_4AF = 4CaO.Al_2O_3.Fe_2O_3$

On this basis the composition is computed on the assumption that the iron and alumina compunds are C_4AF and C_3A. Swayze, Am. J. Sci. v. 244, pp. 1-30, 65-94, (1946) has recently shown that the iron oxide occurs in a phase having the general formula $C_6A_xF_{(3-x)}$ (in which x may vary from 0 to 2) which includes C_4AF as a special case. After it becomes possible to make allowance for this finding, discussions in later parts of this paper may need recasting in different terms. It seems unlikely, however, that any of the arguments or deductions would be greatly altered.

near 100C and a prominent step near 350C. The latter probably represents the decomposition of calcium hydroxide. A compound that might be represented by the break at 100C is not identified. Owing to the manner of its preparation (from a melt), the material thought to be tricalcium silicate was probably a mixture of dicalcium silicate and calcium hydroxide.

Fig. 13 represents a paste cured 28 days in moist air. There appear to be numerous closely spaced steps in this isobar. Krauss and Jörns believed that these steps were sufficiently distinct to indicate the presence of several hydrates having definite chemical formulas.

Fig. 14 represents a paste that had been cured several hours in boiling water* and then stored in the air of the laboratory for several years. As can be seen, the isobar has several well defined steps.

Endell[27] determined isobars for hardened paste, but he arbitrarily limited the heating period at any one temperature to one hour. There is evidence in his results that this was not always sufficient for the attainment of equilibrium. The isobars he obtained do not exhibit any features not exhibited by those reproduced in this paper.

Meyers[28] published isobars for hardened pastes and for hydrated samples of the pure compounds C_3S, C_2S, C_3A, C_4AF, and CaO hydrated separately (Fig. 15). The samples were heated in a vacuum in which the water vapor pressure was maintained at about 0.1 micron. Under these conditions the dissociation temperature of calcium hydroxide was found to be about 380-400F (193-204C). Neat hydrated cement heated under the same conditions showed a step at about 430F; presumably the step was due to the decomposition of calcium hydroxide. The conditions described for the experiments were such as to suggest that the difference between the dissociation temperature of the sample of $Ca(OH)_2$ and that of the $Ca(OH)_2$ in the hydrated cement was probably due to a difference in vapor pressure, the pressure being higher under the conditions that prevailed when the hydrated cement was tested.

The isobars for hydrated C_3S and C_2S show steps near 400F that may also be attributed to calcium hydroxide. The isobars for hydrate C_3A and C_4AF show a large step near 240F.

Discussion of isobars. The data of Krauss and Jörns seem to indicate that hydrated cement contains a series of hydrates besides $Ca(OH)_2$. However, the other curves, including those published recently by Meyers, indicate that the curves are smooth, except for one step in the neighborhood of 400F that is apparently due to microcrystalline $Ca(OH)_2$.

Since the structure of the hardened paste is predominantly of submicroscopic texture, a smooth isobar is to be expected whether the

*The specimen was a part used in the German Standard Test for Soundness.

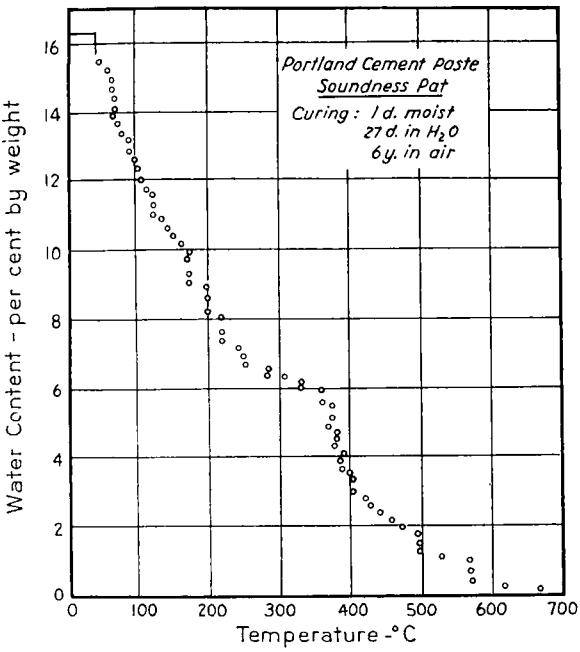

Fig. 14 – Isobar for portland cement paste obtained by Krauss and Jorns.
Zement v. 20, p. 343 (1931)

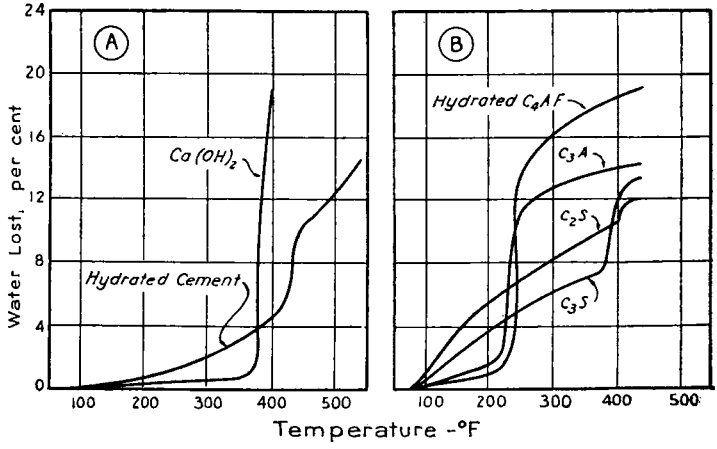

Fig. 15 – Isobars obtained by S. L. Meyers
Pit and Quarry (July, 1942)

hydration products are crystalline or not. As will be shown later, the specific surface of the hydrated material is so high that if the structure is of granular nature the granules must be of colloidal dimensions. If the particles were all of exactly the same size and constitution, a step in the isobar might be expected, despite the smallness of the particles. Without any a priori reason for assuming such uniformity in particle size, there is no basis for expecting anything but a smooth isobar except for the effect of calcium hydroxide already noted.

In general the isobars do not tell much about the hydration products. However, when the isobars are considered together with the information obtained with the microscope and X-ray, they may be considered to show that the hydration products are, for the most part, not in the microcrystalline state.*

Meyers' data on the four compounds C_3S, C_2S, C_3A, and C_4AF hydrated separately are of special interest. Note that both of the alumina-bearing compounds lost large amounts of water at about 250F. Since these two compounds usually constitute 20 per cent or more of the cement, a step on the curve for portland cement, or at least a sharp increase in slope, should occur at about 240F (116C) if those compounds are present in the hydrated cement. The fact that no such indication has been found can be taken as evidence that the hydration products of cement are not a simple mixture of the same hydration products that form when the compounds are hydrated separately; at least, they differ radically with respect to physical state, whether they do with respect to constitution or not.

Water content vs. vapor pressure curves at constant temperature (isotherms)

Jesser[30] was apparently the first to study the relationship between water content and vapor pressure for hardened paste at constant temperature. He used the method of van Bemmelen,[31] i.e., he left the specimens in a closed container over a solution of a salt or of H_2SO_4 at constant temperature, until they reached equilibrium with the vapor pressure of the solution. Starting with the saturated condition, he progressively subjected the samples to lower and lower humidities, finally drying them over concentrated H_2SO_4. He then subjected them to progressivly higher humidities, finally storing them over a solution having a relative vapor pressure of 0.98. After this he determined a second drying curve. His results are given in Fig. 16.

*Throughout this discussion a distinction will be made between the colloidal and microcrystalline states. The term "colloid" refers to any material, crystalline or not, having a specific surface of a higher order than particles visible with the light microscope. A colloidal material may exist as discrete particles or as gels, the latter being regarded as aggregations of once discrete colloidal particles. The term "microcrystalline" refers to ordered aggregations of molecules, atoms, or ions, at least large enough to be seen with a light microscope. The adjective "amorphous" is not used as the synonym of "colloidal" for such usage tends to obscure the fact that colloidal particles may themselves be crystalline, that is, of ordered structure. The possibility of crystalline colloids has long been recognized by colloid chemists. The actual existence of such colloids has been demonstrated by means of the electron microscope.[29]

Jesser used prisms about 1½x1½x4 in. made of neat paste having a water-cement ratio of 0.25 by weight. On the average, he left each prism at a given humidity about six weeks and assumed that this was sufficient time for equilibrium to be attained. Experiments in this laboratory, in which prisms of smaller cross section (1x1 in.) having a higher water-cement ratio (and consequently, a higher drying rate) were dried over dilute H_2SO_4 by much the same procedure, showed that 6 weeks was insufficient for the attainment of constant weight. Moreover, in specimens as large as those used by Jesser, hydration of the cement continues at an appreciable rate at the higher relative vapor pressures, especially in specimens cured only three days. These facts make the interpretation of his results difficult. The results are of interest none the less because they were the first to indicate the similarity between the behavior of the hardened paste and that of typically colloidal substances such as silica gel.

One striking fact in Jesser's results is that the first drying curve is not reversible. Work done in this laboratory confirms this.

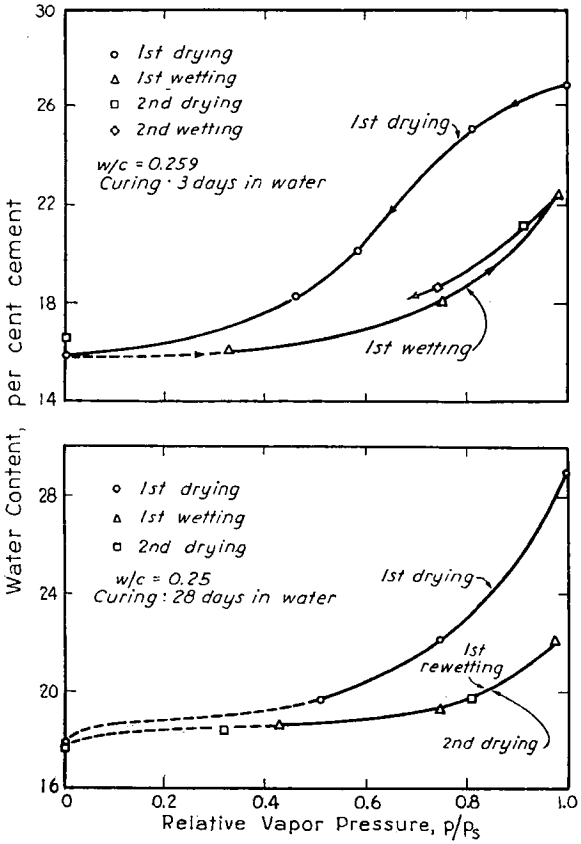

Fig. 16 – Water content versus relative vapor pressure.
Leopold Jesser, Zement v. 16, p. 741 (1927)

Fig. 17 – Diagram for apparatus used by Giertz-Hedstrom for determining isotherms for hardened cement paste

Zement v. 20, p. 672 (1931)

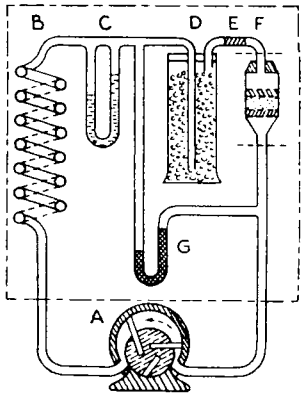

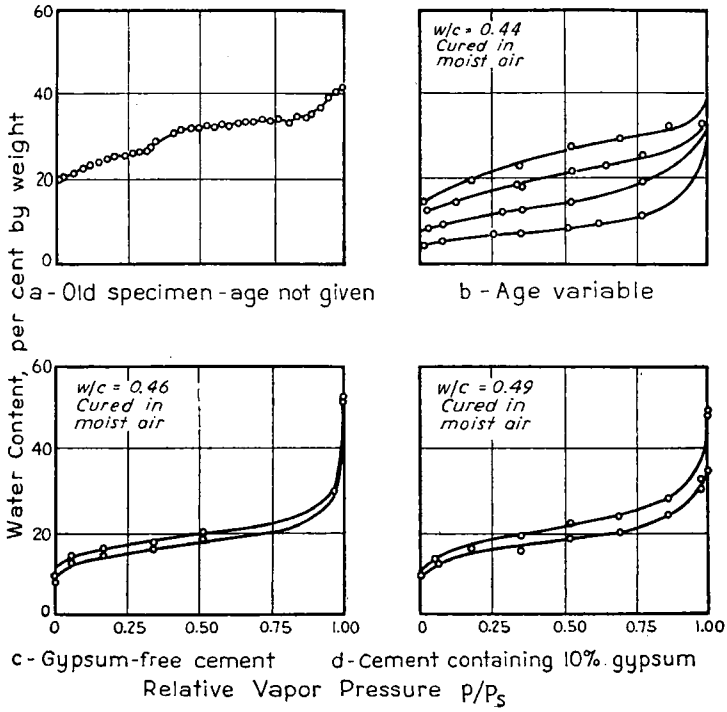

Fig. 18 – Isotherms for hydrated cement

Giertz-Hedstrom, Zement v. 20, p. 734 (1941)

Giertz-Hedström[32] published a number of isotherms for hardened paste. His procedure can be explained with the aid of Fig. 17. A pump, A, circulated air through a copper coil, B, a flow-meter, C, a wash bottle, D, and the sample-holder, F. The wash bottle, D, contained dilute H_2SO_4 and was partly filled with glass beads. The manometer, G, measured the pressure drop across D and F. The apparatus, except for the pump, was kept at a constant temperature in an air thermostat. A 1-g sample of pulverized, saturated paste was placed in F, which was detachable and served as a weighing bottle. Air was passed through the sample until periodic weighing showed that it had reached constant weight. When this point was reached, the H_2SO_4-solution first used in D, which was made very dilute to give a high relative vapor pressure, was replaced by a more concentrated solution and the sample was dried to constant weight at the lower relative vapor pressure. This procedure was repeated with progressively more concentrated H_2SO_4-solutions, and ended with concentrated H_2SO_4, so that several points were obtained along the isotherm. Giertz-Hedström's results are given in Fig. 18.

Berchem[33] has published isotherms for hardened cement and for hardened specimens of three of the principal compounds of portland cement. His method was essentially the method of Giertz-Hedström. As shown in Fig. 19 he obtained no experimental points at vapor pressures above $p = 0.63\ p_s$.

So far as the authors know, Jesser, Giertz-Hedström, and Berchem are the only investigators who have published isotherms for hardened portland cement pastes.*

Relationship between isotherms and isobars. In general, isotherms and isobars give information about the fixation of different portions of the water in the hardened paste. The isotherms give information about the fixation of that part of the water that is evaporable at a constant temperature, usually near room temperature; the isobars, on the other hand, give information about the fixation of the water that is not evaporable at room temperature. An exception is the work of Krauss and Jörns who, instead of determining isobars at a very low water vapor pressure as is commonly done, determined isobars at a vapor pressure of 7 mm *Hg*. This corresponds to a relative vapor pressure of approximately 0.3 at 25C. Thus, the range of their isobars overlaps the lower part of the isotherms given above as well as those determined in this laboratory.

Significance of isotherms. The isotherms, like the isobars, indicate that the hydration products are predominantly colloidal. They can be interpreted so as to give information about the volume and surface

*Gessner[34] has also studied the relationship between water content and relative vapor pressure of cement pastes. However, instead of determining a complete isotherm for a single sample, a different sample was used at each relative vapor pressure. Moreover, the procedure was such that the extent of chemical reaction and the water-cement ratio were different for each. Thus, many variables are involved and it is difficult to interpret the curves.

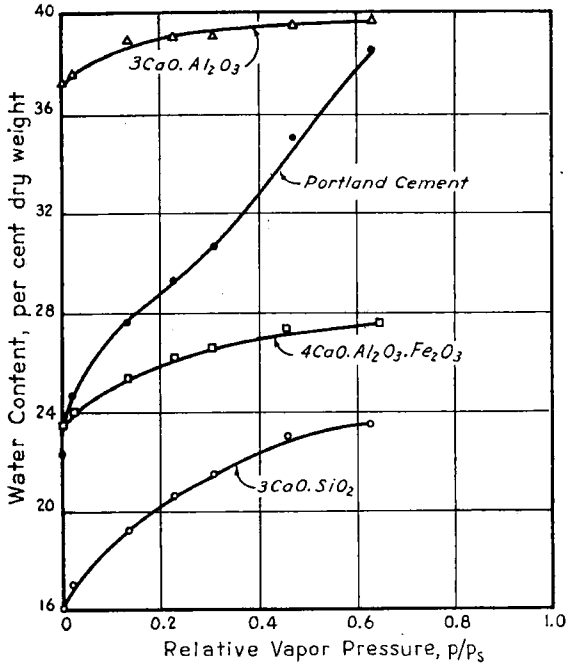

Fig. 19 – Water content vs. vapor pressure relationship
Berchem, Diss. Eidg. Techn. Hochschule, Zurich (1936)

area of the solid phase and other significant features of the properties and behavior of hardened paste. The presentation of such data and their interpretation are the main purpose of this paper.

Studies of water fixation by means of freezing tests

Studies of water fixation by means of freezing tests in various materials such as soils and plants have been reported by several investigators. Similar studies of hardened portland cement paste were reported by Giertz-Hedström[35] and by von Gronow[36]. With respect to this method Giertz-Hedström[37] says: "In all these tests the treatment is comparable with a reduction in water vapor pressure, that is to say, a form of drying out but with the addition of a different complication for each method."*

In a later paper the work done in this laboratory on the freezing of water in hardened portland cement pastes will be described.

SUMMARY OF PART 1

The material presented in Part 1 attempts to review the most significant information obtained by other investigators on the physical properties of hardened portland cement paste. It describes the experimental procedures and presents the test data of several important investigations.

*See also F. M. Lea, *Cement and Cement Manufacture*, v. 5, p. 395 (1932).

From reported microscopic studies it can be concluded that hardened cement paste is predominantly of submicroscopic texture. The only microcrystalline hydrate consistently reported is calcium hydroxide. Brownmiller found this to occur in clusters of very small crystals in the "cement gel." Although the gel state is theoretically unstable, Bogue and Lerch found no evidence of change toward the microcrystalline state over a period of 2 years. However, Kühl found evidence of such a change in pastes about 20 years old.

X-ray analyses do no more than confirm results of the microscopic method.

The relatively few reported observations made with the electron microscope indicate that the hydration products of portland cement may be colloidal but not amorphous. That is, they may be made up of submicroscopic crystals.

Several studies of physical properties of paste have been made by studying the fixation of water in hardened portland cement paste. Such studies are based on the fact that the characteristics of hydration or dehydration curves depend on both the physical and chemical characteristics of the materials involved. In hydroxides the water loses its chemical identity and appears in the structure as *OH*-groups. In many compounds it is bound molecularly by covalent bonds. In a third type of compound some of the water is bound by hydrogen bonds. In all the types of binding just mentioned the amount of water combined can usually be represented in a definite chemical formula and when the particles are of microscopic size or larger, such hydrates are stable through definite ranges of temperature and pressure.

In bodies of the zeolite type the water molecules are believed to be packed in the interstices of the solid structure and they are relatively loosely bound to the solid.

Any solid is capable of holding a small amount of water or other substance on its exposed surface by adsorption. The quantity held in this manner can be large when the specific surface of the solid is very high.

The amount of zeolitic water or adsorbed water held by a solid depends on the temperature and pressure of the water vapor surrounding the solid and the amount varies continuously with changes in either pressure or temperature.

A graph of the relationship between water content and temperature at constant vapor pressure is called an "isobar." The shape of the isobar of a hydrous solid depends on the specific surface of the solid and upon the nature of the combination between the solid and the water. Microcrystalline hydrates give stepped isobars having one or more steps.

The same hydrates reduced to submicroscopic particles of various sizes produce smooth isobars, showing more water in combination at the lower temperatures and less water at the higher temperatures than does the same material in the microcrystalline state. The isobar for zeolitic or for adsorbed water is a smooth curve under all conditions.

A graph of the relationship between water content and water vapor pressure at constant temperature is called an "isotherm." For microcrystalline hydrates the isotherm, like the isobar, is stepped. The material retains more water at low vapor pressures and less at high vapor pressures than does the same material in the microcrystalline state. This conclusion is based partly on experimental data and partly on inference from the isobaric relationships.

Under certain conditions isotherms from silica gel show a step similar to that of a microcrystalline hydrate. The resemblance is superficial, however, as other information shows that no definite hydrate exists over any given pressure range.

Isobars from portland cement paste have been obtained by several investigators. The findings of different investigators vary in some details. In general they show that the isobar is a smooth curve except for one step that is attributed to the decomposition of calcium hydroxide.

Isobars from the four principal compounds of portland cement, hydrated separately, show that the hydrates of C_3S and C_2S resemble that from portland cement, whereas the hydrates of C_3A and C_4AF show mainly the characteristics of microcrystalline hydrates, a step occurring at about 240F when vapor pressure is about 0.1 micron. The fact that Meyers found no step on the isobars for portland cement at 240F is evidence that the hydrates of C_3A and C_4AF that occur in portland cement are not the same, at least with respect to physical state, as those which form when these compounds are hydrated separately.

Isotherms from portland cement pastes have been obtained by a few investigators. The isotherms give information about the fixation of that part of the water that is evaporable at a constant temperature, usually near room temperature, whereas the isobars give the information about the fixation of that part of the water that is not evaporable at room temperature. The isotherms that have been obtained agree with the isobars in indicating that the water in hardened paste is *not* held as it is in microcrystalline compounds. Instead, the manner of binding is similar to that between water and silica gel.

Some studies of water fixation by a freezing-out procedure have been reported. The method is fundamentally similar to the drying-out procedure and the results obtained have about the same significance.

The data on the isothermal relationship between water content and vapor pressure obtained before the present investigation are too few to throw much light on the question of paste structure. Several of the earlier investigations were conducted under what are now known to be faulty test conditions.

REFERENCES

(1) E. Freyssinet, *Science et Industrie*, Jan., 1933.

(2) S. Giertz-Hedström, "Proc. Symposium on the Chemistry of Cements," p. 505 (Stockholm 1938).

(3) R. H. Bogue, "A Digest of the Literature on the Nature of the Setting and Hardening Processes in Portland Cement," Portland Cement Association Fellowship Paper No. 17 (Oct. 1928).

(4) L. S. Brown and R. W. Carlson, *Proc. A.S.T.M.* v. 36, Pt. II, 332 (1936).

(5) Hans Kühl, "Cement Chemistry and Theory and Practice," p. 34, Concrete Publications Ltd., London.

(6) Ref. 5, p. 36.

(7) Henri Le Chatelier, *Compt. rend.* v. 94, p. 13 (1882) "The Constitution of Hydraulic Mortars," (1887). Translated by J. L. Mack, McGraw-Hill, New York (1905).

(8) L. T. Brownmiller, ACI JOURNAL, Jan. 1943; *Proceedings* v. 39, p. 193 (1943).

(9) B. Tavasci, Richerche sulla Constituzione del Clinker di Cemento Portland, *Giorn. chem. ind. applicata*, p. 583 (Nov. 1934).

(10) H. Insley, *J. Res.* Natl. Bur. Stds. v. 17, p. 353 (1936).

(11) W. Eitel, *Angewandte Chemie*, v. 54, p. 185-193 (1941).

(12) C. M. Sliepcevich, L. Gildart and D. L. Katz, *Ind. Eng. Chem.* v. 35, p. 1178 (1943).

(13) Stockholm Symposium, p. 513. (See Ref. 2)

(14) E. Brandenburger, *Schweizer Archiv*, p. 45, 1937.

(15) R. H. Bogue and Wm. Lerch, *Ind. Eng. Chem.* v. 26, p. 837 (1934), or Paper No. 27, Portland Cement Association Fellowship, National Bureau of Standards, Washington, D. C.

(16) H. J. Emeleus and J. S. Anderson, "Modern Aspects of Inorganic Chemistry," D. van Nostrand, Inc., p. 163, New York, 1942.

(17) R. M. Barrer, *Trans. Faraday Soc.* v. 40, p. 374 (1944).

(18) Stephen Brunauer, "The Adsorption of Gases and Vapors," Vol. I, Chapter 7, Princeton University Press, 1943.

(19) T. Hagiwara. In "Colloid Chemistry" by J. Alexander, Chapter 38, The Chemical Catalog Co., 1926.

(20) P. A. Bonsdorff, *Pogg. Ann.* v. 27, p. 275 (1833).

(21) H. B. Weiser and W. O. Milligan, *J. Phys. Chem.* v. 38, p. 1175 (1934).

(22) W. P. Kelley, Hans Jenny, and S. M. Brown, *Soil Sci.* v. 41, p. 260 (1936).

(23) H. B. Weiser, W. O. Milligan and J. Holmes, *J. Phys. Chem.* v. 46, p. 586 (1942).

(24) R. Wilson and F. Martin, ACI JOURNAL, Jan.-Feb., 1935; *Proceedings* v. 31, p. 272.

(25) F. M. Lea and F. E. Jones, *J. Soc. Chem. Ind.* v. 54, p. 63 (1935).

(26) F. Krauss and G. Jörns, *Zement* v. 20, pp. 314, 341 (1931); also *ibid* v. 19, p. 1054 (1930).

(27) K. Endell, *Zement*, v. 15, p. 823 (1926).

(28) S. L. Meyers, *Pit and Quarry*, v. 35 p. 97, July, 1942.

(29) Thomas F. Anderson, "The Study of Colloids with the Electron Microscope," from "Recent Advances in Colloid Science," Interscience Pub. Co., New York, (1942).

(30) L. Jesser, *Zement* v. 16, p. 741 (1927); v. 18, p. 161 (1929). Earlier reports in "Protokoll der Generalversammlungen des Vereines der Osterr." *Zementfabrikanten*, 1912, 1913, and 1914.
(31) J. M. van Bemmelen, "Die Absorption," Dresden, 1910.
(32) S. Giertz-Hedström, *Zement* v. 20, pp. 672, 734 (1941).
(33) Hans Berchem, Dissertation, Eidg. Tech. Hochschule, Zürich, 1936.
(34) H. Gessner, *Kolloid Zeitschrift* v. 46 (3) (1928); v. 47 (1-2) (1929).
(35) S. Giertz-Hedström, *Zement* v. 20, p. 672 (1931).
(36) H. E. von Gronow, *Zement* v. 25 (1936).
(37) Stockholm Symposium, p. 517. (See Ref. 2)

Part 2—Studies of Water Fixation, is scheduled for the November 1946 Journal

Title 43-5b —a part of PROCEEDINGS, AMERICAN CONCRETE INSTITUTE Vol. 43

JOURNAL
of the
AMERICAN CONCRETE INSTITUTE
(copyrighted)

Vol. 18 No. 3 7400 SECOND BOULEVARD, DETROIT 2, MICHIGAN November 1946

Studies of the Physical Properties of Hardened Portland Cement Paste*

By T. C. POWERS†
Member American Concrete Institute
and T. L. BROWNYARD‡

PART 2. STUDIES OF WATER FIXATION

CONTENTS

*Received by the Institute July 8, 1946—scheduled for publication in seven installments; October 1946 to April, 1947. In nine parts: Part 1. "A Review of Methods That Have Been Used for Studying the Physical Properties of Hardened Portland Cement Paste"—ACI Journal, October, 1946. Part 2. "Studies of Water Fixation"—Appendix to Part 2. Part 3. "Theoretical Interpretation of Adsorption Data." Part 4. "The Thermodynamics of Adsorption"—Appendix to Parts 3 and 4. Part 5. "Studies of the Hardened Paste by Means of Specific-Volume Measurements." Part 6. "Relation of Physical Characteristics of the Paste to Compressive Strength." Part 7. "Permeability and Absorptivity." Part 8. "The Freezing of Water in Hardened Portland Cement Paste." Part 9. "General Summary of Findings on the Properties of Hardened Portland Cement Paste."

†Manager of Basic Research, Portland Cement Assn. Research Laboratory, Chicago 10, Ill.
‡Navy Dept., Washington, D. C., formerly Research Chemist, Portland Cement Assn. Research Laboratory. Chicago 10, Ill.

INTRODUCTION

In the preceding part of this paper some of the methods of studying hydrated portland cement paste were reviewed and the principal results obtained by previous investigators were presented. In this part of the paper the studies of water fixation carried out in this laboratory will be described.*

As shown in the first section, water fixation has claimed the interest of several investigators. The reason for such interest is not hard to find. Some of the water associated with hardened cement paste is obviously a constituent of the new solids produced by chemical reactions. If all such water is driven from the paste, the cohesion of the paste is destroyed. Another part of the water, amounting in saturated paste to as much as 50 percent of the volume of the paste, or even more, is free to leave the hardened paste without destroying the cementing value of the material. It does, however, have important effects on the hardened paste: the paste shrinks as water is lost and swells as it is gained; the strength and hardness of the hardened paste vary with its degree of saturation; some of this water is freezable and is thus a source of disruptive pressures that tend to disintegrate concrete exposed to weather. Furthermore, the amount of water that is free to come and go in response to changes in ambient conditions is an index to the degree of porosity of

*The characteristics of the cements mentioned in this part may be found in the Appendix to Part 2.

the hardened paste. The porosity is obviously an important property of the material related directly to its quality.

One incentive for studying the fixation of water in hardened paste was the possibility that suitable measurements of the manner in which the water is associated with the solids would provide the means of estimating the nature and size of the pores in the paste. It was hoped that such knowledge would simplify the problem of relating the chemical and physical characteristics of the cement to its quality. This hope arose rather directly from the hypothesis of Freyssinet[1]* which had a major influence on our choice of experimental procedure. The chosen procedure was intended to yield information on the porosity and pore-size distribution of the hardened paste and other information that might bear on the questions of volume change, durability, plastic flow, etc.

Porosity. To speak, as above, of the porosity of hardened paste is likely to be misleading unless the term is properly qualified. The word "porosity" can be interpreted differently according to past experience or to the chosen criterion as to what constitutes porosity. Certainly, the term is misleading here if it calls to mind such materials as felt or sponge.

Whether or not a material is considered to be porous depends in part on the means employed for detecting its porosity. If a material were judged by its perviousness alone, the decision would rest primarily on the choice of medium used for testing its perviousness. For example, vulcanized rubber would be found impervious, and hence, non-porous, if tested with mercury, but if tested with hydrogen it would be found highly porous. The perviousness of hardened cement paste to water and other fluids is direct evidence of the porosity of the paste.

Regardless of the size of the pore, a substance near enough to the boundary of the pore is attracted toward the boundary by one or more types of force known collectively as forces of adsorption. These forces are sufficiently intense to compress a fluid that comes within their range. If the fluid is a vapor, the degree of compression may be very great; the vapor may be liquefied or solidified; if the fluid is already a liquid, it may undergo further densification on making contact with the solid surface. Since the range of the forces causing such effects is very small—a few hundredths or thousandths of a micron—only a negligible part of the enclosed space in pores of microscopic or macroscopic dimensions is within the range of surface forces. However, when the pores are of the same order of magnitude as the range of surface-forces, it follows that a large portion, or all, of the enclosed space is within the range of surface forces. For this reason, substances containing a large volume of sub-

*See references, end of Part 2.

microscopic pores exhibit properties and behavior not noticeable in ordinary porous bodies. For example, porous bodies of submicroscopic (colloidal) texture shrink and swell markedly on changing the liquid content of the pores, the magnitude of the effect being controlled by the intensity of attraction between the solid and the liquid. Moreover, changes in liquid content alter such properties as strength, elasticity, heat content, and other properties that in non-colloidal solids are virtually constant at a given temperature. Some of these effects will be the subject of discussion farther on.

CLASSIFICATION OF WATER IN HARDENED PASTE

The present discussion aims to elucidate those features of a hardened paste that are revealed by the relative proportions of the total water content that fall in three different categories, as follows:

(*1*) *Water of constitution.*

As used here, this term refers to water of crystallization or water otherwise chemically combined; it refers to water that is a part of the solid matter in a hardened paste.

(*2*) *Water bound by surface-forces—adsorbed water.*

(*3*) *Capillary water.*

This is that water which occupies space beyond the range of the surface-forces of the solid phase.

The above classification is of little practical use, for as yet no way has been devised for actually separating the total water content into such divisions. On drying, water of category (2) and of category (3) are lost simultaneously. Furthermore, not all the water in these two categories can be removed without removing also some of the water of constitution (category (1)). Nevertheless, since evaporation or condensation is the most feasible means of manipulating it, the total water must be studied first with respect to the relative volatilities exhibited by different portions of it. From such data, means of estimating the amounts of water in the three categories given above have been developed, as will be shown.

The water in a saturated, hardened paste is classified in this paper according to its volatility as follows: The water that is retained by a sample of cement paste after it has been dried at 23 C to constant weight in an evacuated desiccator over the system $Mg(ClO_4)_2.2H_2O + Mg(ClO_4)_2.4H_2O$ as a desiccant* is regarded, in this discussion, as "fixed" or "combined" water. To avoid any unintentional commitments as to the state of combination of this part of the water, it is called *non-evaporable water.* The rest of the water in a saturated specimen is called the *evapor-*

*The material is purchased as "Dehydrite"—$Mg(ClO_4)_2$. The two molecules of water are added at the time of use. See Drying of Samples.

able water. The non-evaporable water probably includes most of the water of constitution, but not all of it, for at least one of the hydrates, calcium sulfoaluminate, is partially decomposed when the evaporable water is removed. On the other hand, it is not certain that all the non-evaporable water is water of constitution, for it is possible that some of it can be removed (by slightly raising the temperature) without decomposing any compound present. (See Part 1, Isobars from Portland Cement Paste.) In this connection, a reading of Lea's paper "Water in Set Cement" is recommended.[2]

MATERIALS AND EXPERIMENTAL PROCEDURES

The materials used for these studies were hardened neat cement pastes, pastes of cement and pulverized silica, or cement-sand mortars made with a wide variety of commercial and laboratory-prepared cements. The experimental procedures differed somewhat from time to time and with the type of specimen employed. The general features of the procedures will be described here, and certain other details will be given at appropriate points in other sections of this paper. A detailed description of the materials and methods of the various projects will be found in the Appendix to Part 2.

PREPARATION OF SPECIMENS

Neat cement cylinders

(Series 254-K4B and 254-MRB). Neat cement specimens were prepared, usually at a water-cement ratio of 0.5 by weight, by molding the mixed paste in cylindrical wax-impregnated paper molds ⅞-in. by 6-in. long. In some investigations cylindrical molds of other types were used. The molds were stoppered and laid in water horizontally as soon as they were filled, and the stoppers were removed after about 24 hours so that the curing water might have ready access to the cement paste.

In mixing the pastes, 200 g of cement was mixed with the desired amount of water in a kitchen-type mixer. The mixer was operated at top speed for two minutes and then the paste was allowed to rest for three minutes, and finally mixed again for two minutes. This procedure was followed to avoid the effects of certain types of premature stiffening, whether or not the cements showed any such tendency.

Mortar specimens

The majority of the mortar specimens were made from the mixes shown in Table 1.

As indicated in the Table 1, the aggregate consisted of standard Ottawa sand (20-30 mesh) and pulverized silica, the latter being of about the same specific surface as the cement. The quantity of silica was

TABLE 1—MIXES FOR MORTAR SPECIMENS
(Series 254-8-9-10-11)

Mix	Proportion by weight			Batch quantities in grams		
	Cement	Pulverized silica	Standard sand	Cement	Pulverized silica	Standard sand
A	1.00	—	1.64	1400	—	2300
B	1.00	0.33	2.30	1000	330	2300
C	1.00	0.71	3.65	750	530	2300

such as to give all the mixes about the same total (absolute) volume of cement + silica + water.

The water-cement ratios were adjusted to give a 1½-2-in. slump (6-inch cone) and varied through a small range with the different cements used. The values (after bleeding) were about 0.33, 0.45, and 0.58 for mixes A, B, and C, respectively.

The batches were mixed in a small power-driven, open-tub mixer. Each batch was first mixed 30 seconds dry and then for 2 minutes after the water was added. Two operators working simultaneously then made duplicate slump tests and returned the slump samples to the mixing tub. After remixing the material for 30 seconds, 2x2-in. cubes and 2x2x9½-in. prisms were cast in watertight, three-gang molds which had been previously weighed.

Measurements were made from which the air contents and the loss of water due to bleeding could be computed. This procedure was as follows: Before each cube mold was filled, its outside surface was carefully cleaned and, after filling, the mold and contents were weighed. Then the mold was placed in saturated air. After two hours, water that had accumulated at the top through settlement was carefully removed with absorbent paper and the mold again was weighed. The molds were then immersed in water at 70 F where they remained for at least 12 hours. They were then removed from the water, dried with paper and again weighed. Following this the specimens were removed from the molds, weighed in air surface-dry, and then in water so as to obtain the weight and volume of the material. The cubes were then stored in a fresh supply of water at 70 F where they remained until test or until they were 28 days old. Those that were scheduled for tests beyond 28 days were then stored in the fog room at 70 F.

During the water storage the water was changed periodically to prevent the building up of high alkali concentration.

At the scheduled time of test the cubes were again weighed in the surface-dry condition and under water. Those that had had a period of

storage in moist air were placed in water one day before the scheduled test date to allow them to absorb water if they could.

The data obtained in this manner made it possible to ascertain the average amount of original unhydrated cement, silica, sand, water, and air in each group of companion hardened specimens.

The prisms were treated in the same way as the cubes except that the measurements of settlement (bleeding) were not made.

Truncated cones

In one of the earlier investigations (Series 254-7) mortar specimens were cast in watertight, truncated cones of 4-in. base, 2-in. top diameter, and 6-in. height. Measurements similar to those made on the cubes were made on these cones before and after removing the molds. This gave accurate data on the settlement and the final proportions of the ingredients of the mixtures.

TESTING OF MORTAR SPECIMENS

At the scheduled test ages, which usually ranged from 7 days to 6 months, two cubes of a kind were tested for compressive strength. Throughout these procedures the cubes were carefully kept wet and, after being tested, cubes of a kind were placed immediately in airtight containers.

PREPARATION OF SAMPLES FOR STUDIES OF HARDENED PASTE

Mortar specimens

The tested mortar cubes in airtight containers, mentioned above, were taken from the containers as soon after the strength test as possible and passed quickly through a small jaw crusher. The crushed material was immediately transferred to a nest of sieves (No. 4-8-14-28-35-100-150) already cleaned, assembled, and sealed at the joints with wide rubber bands. The sieves were shaken on a sieving machine for 5 or 10 minutes and then, to prevent losses of water by evaporation, the nest of sieves was opened in the moist room and the material caught between the 35- and 100-mesh or, in some series, between the 48- and 100-mesh sieves, was transferred to a screw-top sample bottle. This material, which consisted of granules of hardened cement paste or hardened paste and pulverized silica, was used for the studies to be described.

Neat cement cylinders and mortar cones

The neat cement cylinders and mortar cones were weighed in air and in water by procedures somewhat like that described for the mortar cubes. Then, since no physical tests were made on these specimens, they were immediately passed through the jaw crusher and a granular sample was obtained by the procedure described above. In some of the earliest tests

the crushing was done with mortar and pestle, but this procedure permitted too much drying and carbonation of the material.

Neat cement slabs

For the most recent project of this study (Series 254-18) the test samples were very thin, neat-cement slabs. These were prepared from cylinders by sawing off slices and then grinding the slices on a glass plate with carborundum dust and water. By this method the slabs were reduced to an average thickness of about 0.3 mm. When saturated, they were translucent.

DRYING OF SAMPLES

The granular samples described above, in quantities not exceeding 15 g, were placed in wide-mouthed weighing bottles and stored in vacuum desiccators with anhydrous magnesium perchlorate (Dehydrite). (The desiccators were exhausted with a Cenco Hyvac pump.) When an excess of the anhydrous desiccant was used, the effective drying agent was a mixture of $Mg(ClO_4)_2$ and $Mg(ClO_4)_2.2H_2O$. With the thought of avoiding the dehydration of the calcium hydroxide, we used a quantity of anhydrous magnesium perchlorate in each desiccator such that when the original compound had combined with all the water given up by the samples the desiccant had become a mixture of $Mg(ClO_4)_2.2H_2O$ and $Mg(ClO_4)_2.4H_2O$; that is, this was the mixture that determined the final water vapor pressure in the desiccator. (Although this was the intention, there is some evidence in the data that the desired result was not always realized. In some cases the final desiccant was probably the mixture $Mg(ClO_4)_2 + Mg(ClO_4)_2.2H_2O$. Some of these cases are mentioned in later discussions, but it was impossible to identify all cases with certainty.)

In some of the earlier projects other desiccants were used, namely, P_2O_5, H_2SO_4, and CaO. In some the drying was done in desiccators containing air instead of in vacuum desiccators. However, most of the data reported here were obtained by the procedure described above.

Reproducibility of results

To test the reproducibility of results obtained by the drying procedure used for the greater part of this investigation, four sets of samples, each comprising 11 companion portions, were prepared from a single neat paste specimen 3½ months old. The results are given in Table 2.

The differences among the figures in any one column indicate the degree of variation among the samples in a given desiccator. The figures for the average loss for the different sets indicate the variations, if any, between conditions in different desiccators. The average losses for sets A and B are slightly higher than for sets C and D. Sets A and B were

TABLE 2—REPRODUCIBILITY OF DRYING LOSSES

Cement: Laboratory blend of 4 commercial brands, Lot 13495
Nominal w/c = 0.50 by wt.
Curing: 3½ months in water

Sample No.	Loss of water—% by wt.			
	A	B	C	D
1	19.81	20.14	19.75	19.87
2	20.06	20.01	19.84	19.80
3	19.93	20.10	19.85	19.96
4	19.99	20.13	19.66	19.89
5	20.06	20.10	19.67	19.82
6	20.09	20.07	19.86	19.84
7	19.98	20.04	19.93	19.87
8	20.00	20.09	19.63	19.87
9	20.13	20.03	19.84	19.84
10	20.00	20.04	19.74	19.79
11	19.72	20.20	19.58	19.90
Average	19.98	20.09	19.76	19.86

dried immediately after they were prepared. Sets C and D were stored in screw-top sample bottles for about one week before they were dried. It seems, therefore, that the smaller loss from sets C and D was probably due to the additional hydration of these two sets during the one-week waiting period.

DETERMINATION OF NON-EVAPORABLE WATER

One-gram portions of the samples dried as described above were heated at about 1000 C for about 15 minutes. The samples were cooled and weighed and then given a 5-minute reheat to check the completeness of ignition. The amount of loss minus the ignition loss of the original cement is called the non-evaporable water content of the sample.

The computation involves the assumption that the weight of the non-evaporable water is exactly equal to the increase in ignition loss. Such an assumption introduces some error. In the first place the original cement was not pre-dried as were the hydrated samples before determining loss on ignition. Hence, the ignition loss as reported for the original cement might be slightly above the value correct for this computation. A second, more serious, source of error arises from ignoring the increase in the amount of combined carbon dioxide. Although precautions against exposure of the granular samples of hardened paste to carbon dioxide were taken, some carbonation did occur. Tests made on 15 different samples showed that in 60 percent of the cases carbonation amounted to less than 0.5 percent of the weight of the original cement. However, carbonation as high as 1.9 percent was found. When carbonation has occurred, the loss on ignition of the carbonated sample will be greater

than the non-evaporable water content before carbonation occurred. The increase is about 0.59 times the weight of CO_2 combined. For example, if the loss on ignition is 0.2 g per g of cement greater than the original loss on ignition, and if the CO_2 content has increased by 0.005 g per g of cement, the non-evaporable water would be 0.2 minus the quantity (0.005 x 0.59) = 0.197. Thus, in this example, the assumption that the increase in loss on ignition is equal to the non-evaporable water results in an error of about 1.5 percent. At earlier stages of hydration, when the loss on ignition is smaller, the relative error would be considerably greater for the same amount of carbonation.

Since the necessary data are available on only a few of the samples and since also there is some question as to the accuracy of the figures for amount of carbonation, no attempt to correct loss on ignition for CO_2 was made in preparing the data for this report. Variations in the amount of carbonation among the various samples undoubtedly contributes to the random variations that will be noted.

Degree of desiccation of dried samples

The degree of desiccation obtained by the drying procedure described above is indicated by the data given in Table 3, which gives also the results obtained with other desiccants. For brevity, only one of the two components of the desiccating mixture is given. The samples tested were neat cement pastes (original w/c (by wt.) = 0.5), that had been cured 1 year in water. Each paste was made with a different cement, the group representing a wide range in chemical composition.

It will be noted that with any given desiccant, the percentages of non-evaporable water for the different pastes differ over a considerable range. However, it is significant that all the results obtained with one desiccant bear a virtually constant ratio to the results obtained with another. This is shown in Table 4, where the results are expressed as

TABLE 3
(Data from Series 254-K4B)

Paste No.	Water retained at equilibrium with the desiccant indicated, % by wt. of cement in specimen			
	P_2O_5	$Mg(ClO_4)_2$	$Mg(ClO_4)_2.2H_2O$	H_2SO_4 conc.
4S	18.3	21.4	22.8	22.3
5S	17.4	20.6	22.0	22.7
7Q	21.4	25.4	26.6	27.1
7P	21.1	25.2	26.5	27.1
7S	20.6	24.6	25.9	26.5
11S	17.6	20.9	22.2	22.5

TABLE 4

Paste No.	Amount of water retained relative to that retained by $Mg(ClO_4)_2.2H_2O$			
	P_2O_5	$Mg(ClO_4)_2$	$Mg(ClO_4)_2.2H_2O$	H_2SO_4, conc.
4S	0.80	0.94	1.00	0.98*
5S	0.79	0.94	1.00	1.03
7Q	0.80	0.95	1.00	1.02
7P	0.80	0.95	1.00	1.02
7S	0.79	0.95	1.00	1.02
11S	0.79	0.94	1.00	1.02

*This value is probably in error—too low. In another group of tests, the ratio for conc. H_2SO_4 was found to be 1.08. Possibly the sulfuric acid used in this second group had a slightly higher water vapor pressure than the acid represented in the table.

ratios to the quantity retained over a mixture of magnesium perchlorate dihydrate and magnesium perchlorate tetrahydrate.

The published information on the actual water vapor pressures maintained by these desiccants is not entirely satisfactory. The values given in Table 5, below, are the most reliable that can be found. Note that these values are upper limits; the actual water vapor pressures may be much lower.

TABLE 5

Drying agent	Residual water at 25 C		
	Mg. per liter	Relative vapor pressure, p/p_s*	Reference
P_2O_5	$<2.5 \times 10^{-5}$	$<1 \times 10^{-6}$	(1)
$Mg(ClO_4)_2$(anhyd.)	$<3 \times 10^{-3}$	$<130 \times 10^{-6}$	(3)
H_2SO_4	$<3 \times 10^{-3}$	$<130 \times 10^{-6}$	(2)
CaO	$<3 \times 10^{-3}$	$<130 \times 10^{-6}$	(3)

*p = existing water vapor pressure. p_s = water vapor pressure over a plane surface of pure water—the "saturation pressure" at a given temperature.

(1) Morley, *J. Am. Chem. Soc.* v. 26, p. 1171 (1904).
(2) Morley, *Am. J. Sci.* v. 30, p. 141 (1885).
(3) Bower, Bureau Stds. J. Research v. 12, p. 246 (1934).

The data for CaO are open to question. Evidence to be presented in Part 4 indicates that the equilibrium relative vapor pressure of water over CaO may be much less than the value given.

The data for P_2O_5 and H_2SO_4 are the result of very painstaking measurements and are probably close to the correct ones. The results in Table 4 bear this out. The amount of water retained by pastes dried over P_2O_5 is less than that retained over any other desiccant; that re-

tained over H_2SO_4, conc., is more. With respect to $Mg(ClO_4)_2$(anhyd.), the water vapor pressure maintained by this desiccant is certainly far less than the upper limit given in Table 5. The data in Table 4, together with the data given on page 286, indicate that the relative vapor pressure is well below 24 x 10^{-6}, the vapor pressure of water at dry ice temperature (-78 C) relative to "saturation pressure" at 25 C.

Data on the vapor pressure over $Mg(ClO_4)_2.2H_2O$ are not available in the literature. However, the data on page 286, indicate that it is about 24 millionths of the "saturation pressure."

A method of drying more commonly used than the isothermal procedures just discussed is that of oven-drying at a temperature at or slightly above the normal boiling point of water. To compare the degree of desiccation obtained from such oven-drying with that obtained isothermally over $Mg(ClO_4)_2.2H_2O + Mg(ClO_4)_2.4H_2O$, four samples that had previously been dried by the latter procedure were placed in an oven at 105 C and allowed to come to constant weight. The results are shown in Table 6.*

TABLE 6

No. of Sample	Loss in weight in oven—% of non-evaporable water content as found by isothermal drying over $Mg(ClO_4)_2.2H_2O$ + $Mg(ClO_4)_2.4H_2O$
16213	10
16214	11
16198	10
15669	13

Stability of hydrates

The figures given in the foregoing paragraphs indicate the "degree of dryness" produced by the method adopted for this investigation in terms of the amount of water retained by the paste and the relative vapor pressure of this residual water, called non-evaporable water. An attempt will now be made to indicate the amount of water retained by the hydrated compounds of portland cement when dried by this procedure.

The microscope reveals that both microcrystalline and colloidal materials occur in hardened paste, the colloidal material appearing as an amorphous mass enclosing microcrystalline $Ca(OH)_2$ and unhydrated residues of the original cement grains. Any such microcrystalline hy-

*In this test no attempt was made to control the water vapor pressure in the oven. This is the incorrect procedure that has frequently been used in studies of this kind.

drate will remain unaltered during the process of drying if its dissociation pressure is lower than the vapor pressure maintained by the drying agent. If the dissociation pressure of the hydrate is higher than the vapor pressure maintained by the drying agent, dehydration is possible but not certain; only direct trial will tell whether it will occur under the conditions of the experiment. Under suitable experimental conditions, the hydrate will lose one or more gram-molecular weights of water per mole of hydrate without appreciable change in vapor pressure, the amount lost being determined by the nature of the hydrate.

As was shown in Part 1, the water content of *colloidal* hydrates bears no small-whole-number, molar ratio to the anhydrous material (except perhaps by chance) and none of it can be removed without a corresponding change in the equilibrium water vapor pressure. That is, the water content of a colloidal hydrate varies continuously with changes in ambient conditions. The colloidal material in hardened cement pastes predominates over non-colloidal constituents to such a degree that the dehydration process shows only the characteristics associated with colloidal material and therefore the dehydration curves do not indicate directly the extent to which the microcrystalline material becomes decomposed.

The extent to which the hydrates of the major compounds of portland cement are dehydrated under the drying conditions described can be estimated from the data given in Table 7. The data pertain to products obtained by hydrating the compounds separately. The first eight lines of data show the amounts of water retained by C_3S (under the drying conditions described) after various periods of hydration. They show that the amount is greater the longer the period of hydration. However, a maximum would be expected, though it is not clearly indicated by these data.

As brought out in Part 1, the figures given in Table 7 should be regarded as single points on smooth isobars and therefore have no unique significance. Had the temperature of drying been higher, the amount of water retained at any given age would have been less, and vice versa. On the other hand, if the hydration products were microcrystalline hydrates, each hydrate would probably be stable over a considerable temperature range, with pressure constant, or over a pressure range with temperature constant.

The alumina-bearing compounds that occur in portland cement clinker, *when hydrated separately*, produce microcrystalline hydrates having definite amounts of water of crystallization. A list of several compounds is given in Table 8, together with information as to their stability in the presence of $Mg(ClO_4)_2.2H_2O$, CaO, or P_2O_5.

TABLE 7—FIXED WATER IN HYDRATED C_2S AND C_3S AS REPORTED BY SEVERAL INVESTIGATORS

Compound	Nominal w/c by wt.	"Fixed water" at age indicated, grams per gram of original anhydrous material					
		3 days	7 days	28 days	6 mo.	1 year	3 years
C_3S^a	0.35	0.103	—	0.146	0.150	0.190	—
C_3S^b	0.40	0.198	—	—	—	0.213	—
C_3S^c	0.78	—	—	—	—	—	0.31
C_3S^d	0.33	—	0.103	0.143	0.207	—	—
"	0.45	—	0.102	0.147	0.224	—	—
"	0.60	—	0.104	0.150	0.238	—	—
"	1.00	—	0.110	0.161	0.254	—	—
C_2S^a	0.30	0.013	—	0.034	0.108	0.122	—
C_2S^b	0.40	0.019	—	0.043	—	0.138	—
C_2S^c	0.33	—	—	—	—	—	0.09
C_2S^d	0.33	—	0.020	0.036	0.134	—	—
"	0.45	—	0.020	0.032	0.142	—	—
"	0.60	—	0.016	0.025	0.120	—	—
"	1.00	—	0.017	0.026	0.130	—	—

a — R. H. Bogue and Wm. Lerch, PCAF Paper, No. 27.
The specimens were cured in vials with excess water present. Material ground to pass 100 mesh, 90 percent to pass 200. "Fixed water" is the loss on heating at 1000 C from samples pulverized and dried in an oven at 105 C with no control of the water vapor pressure in the oven.

b — R. H. Bogue, Effects of Phase Composition on the Volume Stability of Portland Cement, PCAF (1940) (mimeographed)
The specimens were cured in vials with no extra water. The material was "ground to approximately 2200 cm^2/gm." "Fixed water" as in *a*.

c — This laboratory
The specimens were molded and cured in extraction-thimbles surrounded with water. The silicates were each ground to give 85 percent passing the No. 200 sieve, but the trisilicate was nevertheless the finer. p/p_s at equilibrium was about 0.5×10^{-6}. The amount of water was determined by heating at 1000 C.

d — F. P. Lasseter, Chemical Reactions in the Setting of Portland Cement—Dissertation, Columbia University, 1939.
The specimens were cured in vials with extra water present. Samples of -100 mesh material were dried 3 hr. at 105 C in "dry CO_2-free air."

The first compound listed, the high-sulfate form of calcium sulfoaluminate, may occur in hardened paste to the extent that gypsum is present for its formation (assuming an excess of C_3A). The data indicate that all but 9 of the 32 molecules of water of crystallization may be lost. In an average cement containing 1.7 percent SO_3, all of which reacted to form the calcium sulfoaluminate, the amount of hydrated sulfoaluminate per gram of cement would be about 0.09 g. About 0.03 g of this would be lost on drying.

The second item in Table 8 refers to the low sulfate form of calcium sulfoaluminate, a compound which probably does not form under the conditions prevailing in the hardening of the pastes used here. If it did occur, the data indicate that 2 of the 12 molecules of water of crystallization might be lost on drying over $Mg(ClO_4)_2.2H_2O$.

The hexahydrate of C_3A evidently would not be dehydrated by $Mg(ClO_4)_2.2H_2O$. The 12-hydrate of C_3A is reduced to about the 8-hydrate on drying over $Mg(ClO_4)_2.2H_2O$. $C_4A.12H_2O$ is not dehydrated by the conditions used for this study.

TABLE 8

Compound	Number of molecules of water retained in the presence of the desiccant indicated		
	$Mg(ClO_4)_2.2H_2O$	CaO	P_2O_5
$C_3A.3CaSO_4.32H_2O$	9[a]	8[b]	7.5[c,d]
$C_3A.CaSO_4.12H_2O$	10[a]	—	8 [c,d]
$C_3A.6H_2O$ (cubic)	—	6[e]	—
$C_3A.12H_2O$ (hex)	—	8[e]	—
$C_4A.12H_2O$	—	—	12[f]

a — This laboratory.
b — Jones: Symposium on the Chemistry of Cements (Stockholm, 1938), p. 237.
c — Forsen: *Zement* v. 19, pp. 1130, 1255 (1930); v. 22, pp. 73, 87, 100 (1933).
d — Mylius: *Acta Acad. Aboensis* v. 7, p. 3 (1933); see *b*.
e — Thorvaldson, Grace & Vigfusson: *Can. J. Res.* v. 1, p. 201 (1929).
f — Assarsson: Symposium on the Chemistry of Cements (Stockholm, 1938), p. 213.

It thus appears that of the various microcrystalline hydrates that can be formed from the constituents of portland cement only the calcium sulfoaluminate would be decomposed to an appreciable extent; it would lose 72 percent of its water of crystallization. After a long period of hydration, the water held by the hydration products of C_3S and C_2S amounts to 20 to 30 percent and 10 to 14 percent of the weight of the original material, respectively.

Before this subject is closed it should be said that the occurrence of the microcrystalline hydrates of C_3A in hardened paste, particulary $C_3A.6H_2O$, is very doubtful. Several observations indicate this. One is the fact that drying-shrinkage is greater for cements of high C_3A content. This cannot be explained on the basis that C_3A combines with water to form the hexahydrate $C_3A.6H_2O$, since that crystal does not lose water under the conditions of ordinary shrinkage tests.

DETERMINATION OF TOTAL EVAPORABLE WATER

The water that a sample is capable of holding in addition to the non-evaporable water is called the *evaporable water*, as defined before. The procedure for determining the evaporable water content of granulated samples is as follows: About 5 grams of the sample to be saturated is placed in a 50-ml Erlenmeyer flask fitted with a special stopper that permits either the introduction of water from a burette or a stream of dried air free from CO_2. At the start, water is slowly dropped onto the sample from the burette until the sample, upon being shaken, gathers into a lump and clings to the flask. Dry air is then passed over the sample while it is vigorously shaken by hand. After 2 minutes of this treatment, the flow of air is stopped and the shaking of the flask is continued. If the sample persists in gathering into a lump, the drying is continued for 2 more minutes. This procedure is continued until the particles just fail to cling to each other and to the flask. The total water

TABLE 9—DATA ON TOTAL WATER CONTENT OF SATURATED SAMPLES

Series 254-MRB

Cement No.	Age at test, days	w_o/c	Total water at test, w_t/c				w_n/c
			Original specimen	Granules			
				SSD 1	*SSD 2*	*SSDO*	
1	2	3	4	5	6	7	8
14900	126	0.45	0.526	0.508	0.515	0.527	0.227
14901	126	0.39	0.498	0.491	0.493	0.503	0.223
14902	133	0.39	0.515	0.501	0.495	0.511	0.227
14903	133	0.42	0.527	0.511	0.516	0.526	0.227
14904	162	0.42	0.489	0.490	0.481	0.499	0.228
14905	162	0.41	0.493	0.490	0.482	0.502	0.230
14906	173	0.48	0.551	0.550	0.541	0.567	0.236
14907	173	0.41	0.464	0.461	0.458	0.474	0.219
14908	200	0.39	0.487	0.479	0.475	0.492	0.225
14909	200	0.48	0.562	0.548	0.546	0.572	0.226
14910	204	0.46	0.521	0.513	0.510	0.535	0.228
14911	204	0.46	0.536	0.526	0.521	0.546	0.229
14912	212	0.49	0.551	0.547	0.541	0.568	0.225
14913	212	0.41	0.478	0.477	0.476	0.493	0.221
14914	222	0.42	0.495	0.487	0.499	—	0.225
14915	222	0.44	0.518	0.520	0.517	0.530	0.224
Average			0.513	0.506	0.504	0.523	0.226

SSD = Saturated, surface-dry.
SSD1 = Granulated sample (100-48 mesh) dried in vacuo over $(MgClO_4)_2.2H_2O$ and then resaturated in the presence of air
SSD2 = Granulated sample dried in the same way as *SSD1*, and resaturated in a vacuum.
SSDO = Granulated sample of original, undried material brought to the *SSD* condition by adding water in the presence of air
w_n/c = Non-evaporable water, g per g of cement.
w_o/c = Original water-cement ratio by wt., corrected for bleeding
w_t/c = Total water-cement ratio at time of test

held by the sample in this condition, minus the non-evaporable water, is the total evaporable water as defined above.

Data from 40 such determinations showed that the average difference in the values obtained in duplicate determinations by a given operator was 0.36 percent of the dry weight. In three cases out of 40, the difference in values was more than 1 percent. Other experiments showed that the results obtained by two operators working independently did not differ more than did duplicate determinations made by a given operator.

The procedure just described permits water to enter previously dried granules from all sides simultaneously. Since the dried grains are known to contain a considerable amount of adsorbed air, the question arises as to how completely the air is displaced by the water. To answer this question, some dried samples were evacuated, so as to remove most of the adsorbed air, and then the water for saturation was introduced in the absence of air. Companion samples were treated in the presence of air in the usual manner.

TABLE 10—DATA ON TOTAL WATER CONTENT OF SATURATED SAMPLES
Series 254-K4B

Ref. No.	Age at test, days	w_o/c	Total water at test, w_t/c			w_n/c
			Original specimen	Granules		
				SSD	*SSDO*	
1	2	3	4	5	6	7
1-S	180	0.470	0.556	0.543	0.557	0.223
1-P	180	0.473	0.577	0.559	0.576	0.233
1-Q	*180	0.425	0.521	0.502	0.515	0.229
4-S	144	0.463	0.522	0.510	0.525	0.179
4-P	138	0.460	0.548	0.512	0.535	0.177
4-Q	138	0.450	0.518	0.495	0.515	0.177
5-S	150	0.427	0.502	0.498	0.510	0.165
5-P	146	0.453	0.542	0.509	0.519	0.159
5-Q	150	0.456	0.533	0.514	0.527	0.165
6-S	196	0.471	0.529	0.508	0.530	0.215
6-Q	191	0.447	0.532	0.512	0.536	0.222
7-P	164	0.473	0.570	0.556	0.575	0.240
7-Q	171	0.480	0.548	0.549	0.564	0.239
11-P	164	0.445	0.521	0.516	0.532	0.186
11-Q	172	0.440	0.515	0.509	0.516	0.190
15-S	202	0.485	0.558	0.536	0.561	0.217
15-Q	202	0.445	0.555	0.529	0.544	0.220
16-P	223	0.464	0.540	0.525	0.541	0.226
16-Q	223	0.456	0.516	0.502	0.520	0.225
20-S	170	0.472	0.549	0.543	0.554	0.231
20-P	167	0.462	0.551	0.542	0.555	0.233
20-Q	176	0.436	0.520	0.508	0.519	0.226
Average		0.455	0.537	0.520	0.540	0.208

SSD = Saturated, surface-dry.
SSDO = Granulated sample of original, undried material brought to the *SSD* condition by adding water in the presence of air
w_n/c = Non-evaporable water, g per g of cement
w_o/c = Original water-cement ratio by wt., corrected for bleeding
w_t/c = Total water-cement ratio at time of test

Results are given in columns 5 and 6 of Table 9. (Table 9 gives also other data confirming those in Table 10. The averages 0.506 and 0.504 for the ordinary and vacuum procedures, respectively, show that the air has no appreciable influence on the results.

DISCUSSION OF GRANULAR SAMPLES

Since most of the experiments to be described were made with granular samples of the original specimens, it is necessary to consider the extent to which the granules differ from the original material.

Neat cement—effect of granulation on porosity

Table 10 gives water content data for a group of neat cement specimens and the granular samples prepared from them. The original specimens were 1x7-in. neat cement cylinders that had been stored under water for the periods shown in column 2. During the curing period, they gained in weight, the average gain being 0.082 gram per gram of cement (0.537-0.455).

From each specimen one granular sample (100-48 mesh) was prepared and then saturated by adding excess water to the granules. The excess was evaporated until the saturated surface-dry condition was reached. The results are given in column 6. A comparison of columns 4 and 6 will show that if the difference shown is significant, we may conclude that the saturated granules held slightly more water than the original specimen did at time of test. This indication is somewhat more definite in Table 9. Compare columns 4 and 7. This proves that in specimens of this kind the small granules have very nearly the same porosity as the original specimen, and it indicates that even though the original specimens were stored continuously under water, they did not remain fully saturated. This indication was supported by the dry appearance of the freshly crushed cylinders.

Neat cement—effect of drying on porosity of granules

Other samples of each specimen were dried over $Mg(ClO_4)_2.2H_2O$ and then brought to the saturated surface-dry condition. The results, given in column 5 of Table 9, should be compared with those in column 6. Also in Table 9 compare columns 5 and 6 with column 7. The average water content of the dried and resaturated granules is about 96 percent of that of the saturated granule that had not been dried.

This shows that the drying of the granules produced a permanent shrinkage that reduced the porosity of the granules below that of the paste in the original specimen. In samples of this kind (moderately low w/c, well cured) the effect is small. In specimens of higher w/c and lesser degree of hydration, the effect should be larger.

Mortar specimens—effect of granulation on porosity of paste

The mortar specimens used in these studies were made with non-absorptive, quartz sand. Consequently, all water originally in the specimen (after bleeding) as well as that absorbed during curing is held in the paste, and data showing differences between the total water contents of the original specimens and that of the granular samples represent differences in the degree of saturation, or in the porosity, of the hardened paste, just as they do with neat specimens.

Data of this kind were obtained from mortar cubes for specimens of different ages and different water-cement ratios. Typical results are given in Fig. 2-1, A and B.

The cement represented in A is a slow hardening type; that in B is normal.

In each diagram the circled dots represent the total water content of the original specimen; the crosses, the total water content of the dried-and-resaturated granules; and the triangles, the granules that were saturated without preliminary drying.

It is apparent that for specimens cured 28 days or more, the relationships are about as were found for the neat pastes described above. However, at earlier ages, especially for the slow hardening cement, the granules show less porosity than the pastes of the original specimens, the difference being greater, the higher the original water-cement ratio.

These results seem to indicate that during the early stages of hydration the paste contains voids nearly as large as the granules of the samples and that as hydration proceeds, these larger voids disappear.

On the whole, these results show that the porosity of a granular sample is about the same as that of the pastes in the original specimen except for specimens having pastes of very high porosity. A granular sample that has been dried has a smaller total pore volume than the original paste. From other data it is known that this effect, in well cured specimens, diminishes with decrease in the original water-cement ratio and probably becomes negligible at about $w_o/c = 0.3$ by weight.

METHODS OF STUDYING THE EVAPORABLE WATER

As shown by the earlier work reviewed in Part 1, when a specimen of hardened paste at room temperature is exposed to water vapor or to air containing water vapor, its water content spontaneously changes until equilibrium between the water held in the specimen and the outside water vapor is established. The establishment of equilibrium involves a change in moisture content of the sample, for the nature of the hardened paste is such that at a given temperature the relationship between vapor pressure of the water in the hardened specimen and the water content is represented by a smooth curve. Moreover, the nature of the paste is such that a specimen can remain saturated only when it is in contact with saturated water vapor or with liquid water.

Much of the work to be reported here consisted in determining the relationships between the evaporable water content and the vapor pressure for various samples of hardened cement paste. The taking up of moisture from the atmosphere will be referred to as *adsorption*, and the reverse will be called *desorption*, even though other processes might be involved. The plotted results will be called *adsorption* and *desorption isotherms*, respectively. When speaking of both processes collectively or of the processes in general without specifying the direction of moisture change, the term *sorption* will be used.

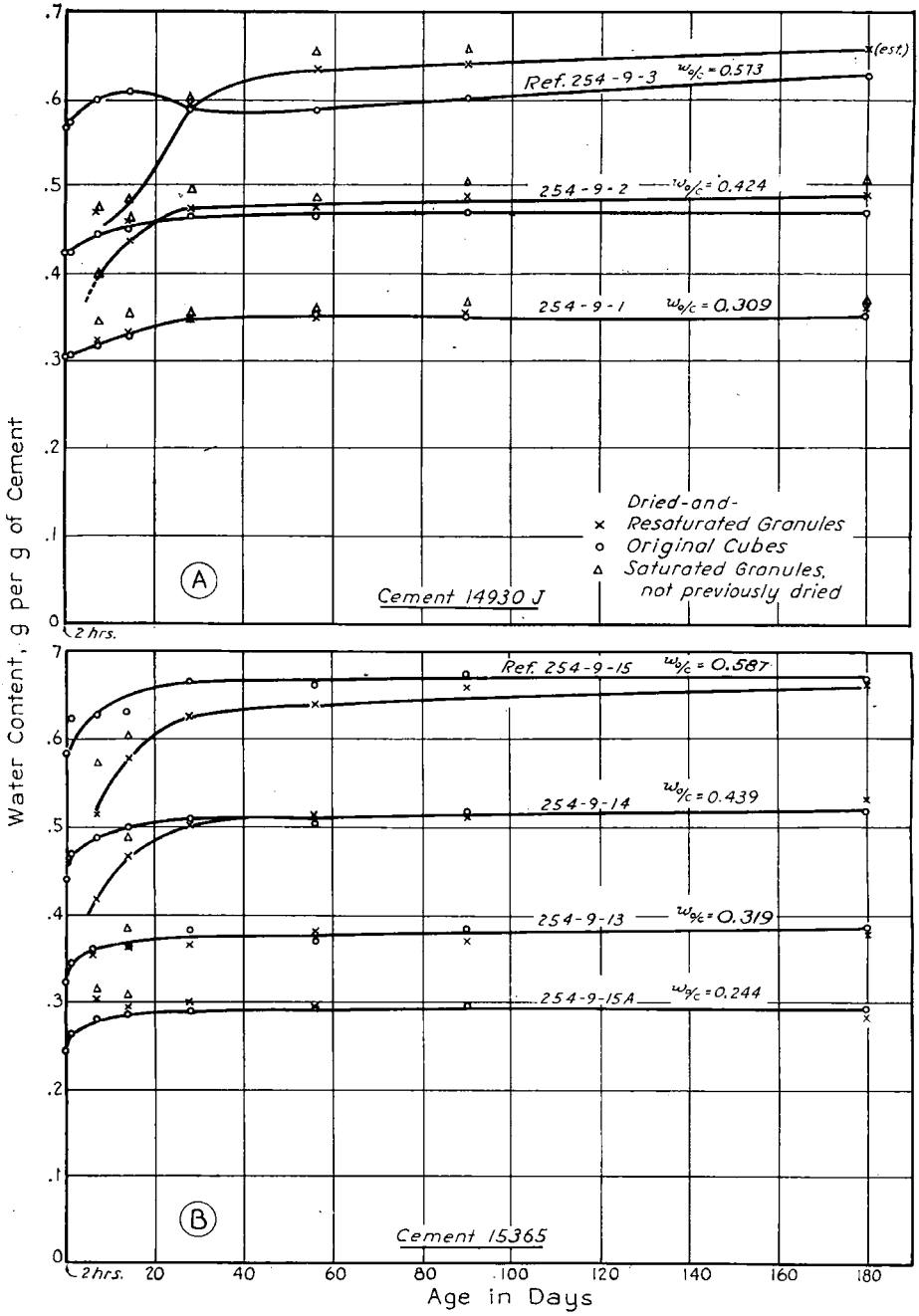

Fig. 2-1—Comparison of water content of intact cubes with that of granular samples from from the same cubes

THE APPARATUS FOR SORPTION MEASUREMENTS

Two types of apparatus were used for sorption measurements. In one the samples were exposed to water vapor only and in the other the samples were exposed to CO_2-free air containing controlled amounts of water vapor. The first is referred to as the *high-vacuum apparatus* and the second as the *air-stream apparatus*.

High-vacuum apparatus

The high-vacuum apparatus used for these studies is illustrated schematically in Fig. 2-2. As shown, two samples may be kept under test simultaneously. The samples may be either small granules or thin wafers. If granules, they are contained in small buckets made of platinum foil which are suspended on helical springs made of quartz in the two chambers marked C. If the samples are wafers, they are suspended from the springs by platinum hooks.

After the air has been pumped out, water vapor of known pressure is admitted to chamber C. The pressure of the vapor is indicated directly by the oil in manometer D. The arrangement is such that during the adsorption process the sample is never subjected to a higher vapor pressure than that with which it will finally be in equilibrium. This is an important feature of the method, for experience has shown that if the ambient vapor pressure is allowed to change as the samples approach equilibrium, the equilibrium-weight is different from what it would have been had the vapor pressure been maintained constant. This is due to the phenomenon of hysteresis, discussed later on.

The changes in weight of the sample are observed by measuring the changes in length of the quartz springs by means of a cathetometer. The spring-cathetometer combination has a sensitivity of about 0.2 mg. With a live load of about 400 mg this gives adequate accuracy.

The water vapor pressure is generated by the water (or ice) in bulb A or bulb B. Bulb B is used for the lowest pressure of the range employed which is that of water at the temperature of dry ice wetted with alcohol, -78 C. For all higher vapor pressures cock 2 is closed and 1 is open, thus utilizing bulb A. The temperature of the water (or ice) in A is controlled by a cryostat, which is maintained at any desired temperature down to -25 C within about $\pm$ 0.05 C.

For the highest pressure used, a small amount of water is distilled from A into the bottom of C and stopcock 1 is then closed. By maintaining the temperature of the tube outside the 25 C air-bath above 25 C, the water vapor pressure in C is, theoretically, maintained at 23.756 mm of *Hg*, the saturation pressure of water at 25 C. Accurate measurements at this vapor pressure, or at any vapor pressure above about 95 percent of the saturation pressure, cannot be obtained by this method because of condensation on the springs.

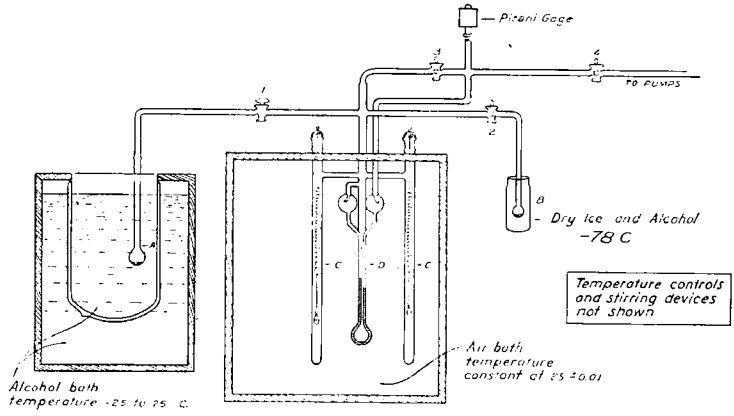

Fig. 2-2—High vacuum sorption apparatus

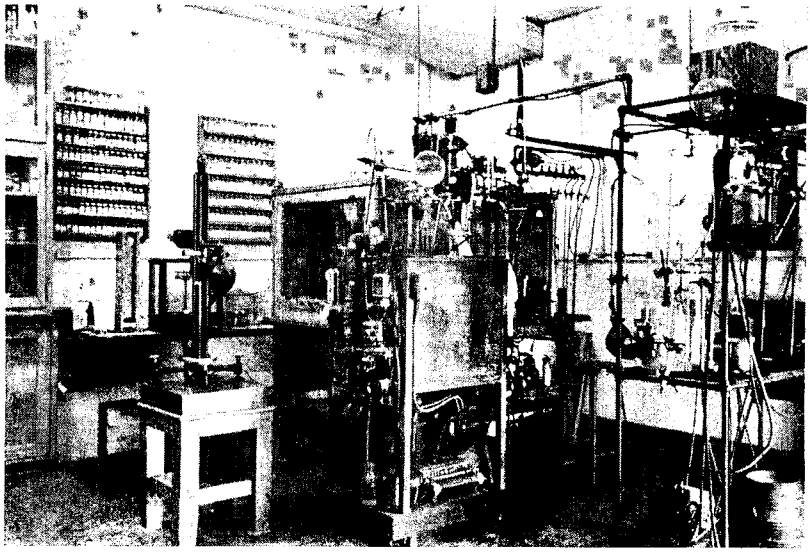

Fig. 2-3—General view of apparatus

Between cocks 3 and 4 a Pirani-type vacuum gage is attached so as to indicate the pressure on the "zero" side of the manometer. This is to make certain that the readings on the manometer are not vitiated by slow leaks on the zero side.

To check against leaks on the other "pressure" side of stopcock 3, the temperature of the bath surrounding A is measured by means of an eight-junction thermocouple and a type-K potentiometer. The vapor pressure of the ice or water in bulb A can then be ascertained from handbook data. Any discrepancies between the pressure shown at D and the pressure indicated by the temperature at A that are greater

than the inaccuracy of measurement would be indicative of pressure from gas other than water vapor.

A general view of the apparatus is given in Fig. 2-3. The cabinet in the foreground contains the controlled bath for bulb A. The large cabinet in the middle background is the 25 C air-bath. This cabinet is the same as that used for the air-stream apparatus to be described below. It can be used for both methods simultaneously, although that has not been done as yet.

The cabinet in the foreground is the cryostat. It contains a cylindrical vessel of about 10-gallon capacity filled with alcohol. This is cooled by the refrigeration unit mounted under the cabinet. A one-gallon container is mounted, submerged to its upper rim, in this alcohol bath. The container is a double-walled glass vessel with air between the walls. It contains the alcohol in which bulb A, Fig. 2-2, is immersed. By means of an electrical heater and thermoregulator, the temperature of this one-gallon bath is maintained at whatever level is desired. The thermoregulator is a laboratory-made, toluene-mercury type. It operates through an electronic switch and Mercoid relay.

The air in the large cabinet is kept in rapid circulation by means of two electric fans and two air-driven windshield fans. The cabinet is cooled by continuously circulating cold alcohol through a copper coil inside the cabinet. The circulated alcohol is cooled by means of another coil dipping into the outer alcohol bath of the cryostat described in the foregoing paragraph.* The cabinet is heated by an electric heater (about 200 watts). The input to the electric heater is controlled by a laboratory-made, toluene-mercury thermoregulator that operates through an electronic switch and Mercoid relay. The sensitivity of the regulator is about 0.005 C. The variation in temperature at any given point does not exceed 0.01 C, and the average temperatures at different points do not differ more than 0.02 C.

Air-stream apparatus

The air-stream apparatus is built in and around the large cabinet just described. It was designed to deliver 11 streams of air simultaneously, each stream having a different water content and hence different water vapor pressure. The following description pertaining to one of the air streams is applicable also to the rest.

The air to be conditioned is taken from the compressed air supply of the laboratory. The air pressure is reduced to 3 lb. per sq. in. by means of two diaphragm-type pressure-reduction valves connected in series. The low-pressure air is then delivered to a train of one-gallon bottles such as is illustrated in the lower part of Fig. 2-4. The first bottle

*This arrangement is used at present. For most of the period covered by this paper cold tap water from the building supply was used, but this often failed its purpose during the summer.

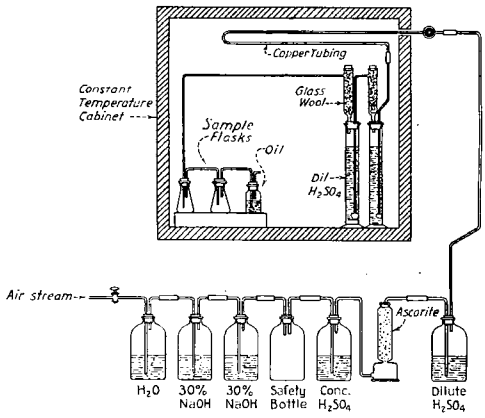

Fig. 2-4—Schematic diagram of one of the air conditioning trains for adsorption tests

contains water, and the next two sodium hydroxide solutions. The water bottle at the head of the train prevents the formation of sodium carbonate in the inlet tube of the caustic-soda bottles. Next in line is an empty bottle for safety and this is followed by a bottle of concentrated sulfuric acid (specific gravity 1.84) to dry the air. The dry air is then delivered to a tower of Ascarite to remove any traces of carbon dioxide that might have escaped the caustic-soda solutions. The air stream then passes through a 3-gallon bottle containing dilute sulfuric acid. The output of this bottle is divided into two streams, one of which is shown in Fig. 2-4. The strength of the acid in the large bottle just mentioned is so regulated that it gives the air passing through it a water content somewhat below that desired for either of the two streams taken from the bottle. This slightly-too-dry air then is piped into the constant temperature cabinet where it circulates, first through a length of copper tubing to permit the temperature to reach 25 C and then through two towers of sulfuric acid connected in series as shown in the upper part of Fig. 2-4. The second stream taken from the bottle is led similarly to another pair of acid-towers, regulated to give a different vapor pressure. The strength of the acid in the towers is carefully regulated to have exactly the vapor pressure desired in the outgoing stream of air. To insure equilibrium between the stream of air and the acid the air is dispersed as fine bubbles by means of porous plugs fastened to the ends of the inlet tubes. (These porous plugs were made in the laboratory by sintering granulated glass in a crucible.) To remove entrained droplets of acid, each tower is equipped with a glass-wool filter as shown.

The outgoing stream of air is led through rubber connections to an Erlenmeyer flask containing the sample under test. As the air passes the dry granules, they absorb some of the water vapor. This continues until the vapor pressure of the water in the sample becomes equal to that of the water vapor in the air stream.

Two samples are run simultaneously by connecting sample-flasks in tandem as shown. The outgoing stream of air from the second flask bubbles through a mineral oil contained in a 6-oz. bottle and then escapes to the interior of the cabinet. The mineral-oil trap prevents back-diffusion of moisture and carbon dioxide from the air in the cabinet to the sample.

Eleven such pairs of sample-bottles in the cabinet make it possible to obtain simultaneously 11 points on the adsorption curves for each of two materials.

Because the air delivered to the acid towers inside the cabinet is in each case slightly drier than the output from the towers, the level of the acid in the towers gradually subsides during the continuous flow of the air streams. About once a month it is necessary to replenish the towers by adding distilled water. This is done by means of glass tubes (not shown in sketch) leading from the stoppers in the tops of the acid towers through the top of the cabinet. Similarly, the acid in the large bottles outside (under) the cabinet and the caustic-soda solutions are renewed about once a month.

During the development period, the water content of each air stream was measured by passing a measured volume of the air through weighing tubes filled with P_2O_5. The relative vapor pressure of each stream was then computed from the law for perfect gases. A number of such measurements showed that the water vapor pressure in the air streams differed from that which could be computed from the strength of the acid by less than 0.025 mm of mercury or a difference in p/p_s* of less than 0.001. When this was learned, the air streams were considered always to be at equilibrium with the acids in the towers.

The sample flasks were removed from the cabinet once daily and weighed on a chemical balance, care being taken to minimize the exposure of the granules. A typical record of the results of such weighings is shown in Fig. 2-5. This diagram shows that for those samples exposed to water vapor of relatively low pressure the weights reached a maximum and thereafter declined. At vapor pressures of 0.8 p_s or higher the weight either remained constant after one or two days or else continued to increase steadily, though very slightly, with time, this tendency being more pronounced the higher the vapor pressure. The increase in weight just mentioned is believed to be due to hydration of fresh surfaces of clinker residues exposed on crushing the original sample.

The behavior of the specimens exposed to the drier atmospheres is not understood. The phenomenon was not observed when using the high-vacuum apparatus. From this it may be inferred that the presence of air

*p = vapor pressure of air steam
p_s = saturation vapor pressure of water

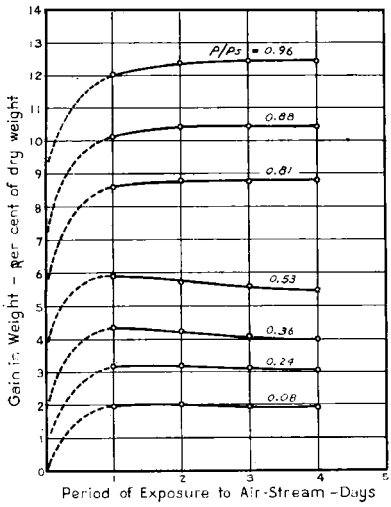

Fig. 2-5—Typical relationship between gain in weight and period of exposure

may have something to do with the result. However, as will be shown later, the major aspects of the results obtained in the presence of air are essentially the same as those obtained in the absence of air.

Inasmuch as the decrease in weight shown by the lower curves in Fig. 2-5 continued for as long as two weeks, it was decided to use maximum rather than final weights. There was some question as to whether the final weight was any more significant than the maximum weight; also, since the decline from the maximum represented but a small percentage of the total gain, it did not seem justifiable to retard the experimental work to the extent necessary to get final weights.

Reproducibility of results

The reproducibility of the data obtained in the manner just described is illustrated in Table 11. These are results from two sets of samples made from the same specimen, each set being tested independently. The corresponding figures are in very good agreement except at the two highest pressures. Such differences were commonly observed and were probably due to different degrees of proximity to equilibrium.

Comparisons such as those that are given in Table 11 were made at other times during the course of these experiments, with similar results. Nevertheless, there is reason to believe that in some groups of tests the variability was considerably greater than would be expected from such data as those presented above. Possibly such variations are due not so much to variations in the adsorption measurements themselves as to variations in auxiliary tests as when the samples contained pulverized silica and therefore required a chemical analysis for the estimation of cement content. The discrepancies that will be noted among the various

TABLE 11—REPRODUCIBILITY OF THE ISOTHERMS

Cement: 16189
Initial w/c: 0.50
Curing: 6 weeks in water

Relative vapor pressure p/p_s	Total water-content of sample indicated, % by weight of cement	
	A	B
0.0 (non-evap. H_2O)	15.47	15.42
0.08	17.98	18.03
0.16	18.87	18.94
0.32	20.10	20.28
0.39	20.82	20.98
0.46	21.44	21.65
0.53	22.02	22.09
0.60	22.82	22.90
0.70	24.82	24.76
0.81	27.52	27.53
0.88	30.43	29.69
0.96	35.31	34.60

data yet to be presented are often such as would result from errors in the determination of the cement content of the sample. The data obtained from samples of neat cement were less erratic.

Use of ordinary desiccators

In some auxiliary work, neither the air-stream nor high-vacuum apparatus was used. Instead, samples were placed in ordinary air-filled desiccators in the presence of a suitable desiccating agent. The samples were weighed from time to time until the results indicated equilibrium to have been reached.

Theoretically, the results obtained in this way should, in most respects, be the same as those obtained by the methods already described. Actually, the results from the samples dried in desiccators did not agree very well with the results obtained by the other two methods. The cause of the discrepancy is not known. It was observed, however, that the rate of absorption in an air-filled desiccator is very much less than that in vacuum or air stream. This suggests the possibility that the exposure of samples was terminated too soon, that is, that they did not approach equilibrium as closely in the air-filled desiccators as they did when tested by either of the other two methods. Another possibility is that, owing to the longer exposure and to the continued presence of air, samples tested in desiccators might have become carbonated sufficiently to influence the final results. At any rate this method is not recommended.

RESULTS OF THE SORPTION MEASUREMENTS—EMPIRICAL ASPECTS OF THE DATA

General features

Fig. 2-6 and Tables 12 to 17 record a run made with the high-vacuum

apparatus illustrated in Fig. 2-2. In this case the sample was a very thin wafer of hardened neat cement paste described in Table 12, w_o/c = 0.5 by weight. In its initial, saturated state it weighed 380.5 mg, as indicated by the uppermost point in Fig. 2-6. After the sample was installed, the air was pumped out of the apparatus. The initial pumping period was made brief to avoid overdrying the sample. The object was to remove the air from the chamber without removing water from the sample, if possible. To maintain the water vapor pressure as high as possible during the pumping a small amount of water was introduced into the sample chamber before the pumping began. The desired result was not obtained; the pump removed the water vapor so rapidly that nearly half the evaporable water in the sample was removed during only 6 minutes of pumping.

As soon as the initial pumping was finished, the sample was subjected to a vapor pressure of 0.94 p_s. Owing to the losses suffered during the initial pumping, the sample gained in weight at this pressure until it reached equilibrium at a weight of 374.4 mg. Then the pressure was lowered step by step and the rest of the points appearing on the desorption curve were obtained. At the final weight, 309.8 mg, the sample was at equilibrium with the vapor pressure of the ice at -78 C, the temperature of dry ice.

As soon as the evaporable water had been removed, the vacuum pumps were operated for many hours so as to remove as much air from the system as possible. Then the vapor pressure was increased stepwise, thus establishing the adsorption curve shown.

As shown in Fig. 2-6, the adsorption and desorption curves coincided only at pressures below 0.1 p_s. (As a matter of fact, it is not certain that the curves coincided over this range, but it seems probable that they did so.) Studies of other materials[3] show that in the range of pressures where the curves form a loop, innumerable curves within the loop can be produced under suitable experimental conditions. If the process of adsorption or desorption is reversed at any point short of the horizontal extremes of the loop, the part of the curve that had previously been generated will not be retraced but instead the points will cut across the loop. If at any stage of adsorption in this range the process is reversed, the resulting downward curve will cross over from the adsorption to the desorption curve. If the desorption curve is reversed, then a new rising curve will cross over toward the adsorption curve, but instead of joining the adsorption curve the new curve will rise more or less parallel to the adsorption curve, the loop being closed only at the saturation point. Thus, it is possible to obtain points representing thermodynamic equilib-

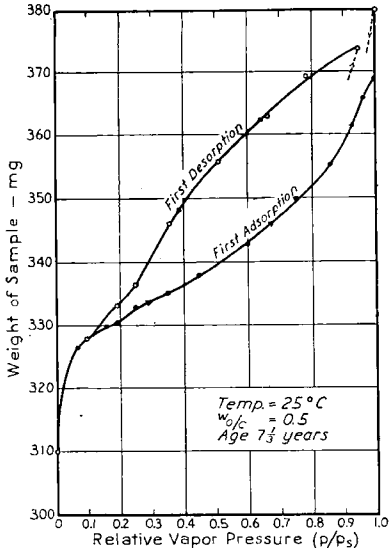

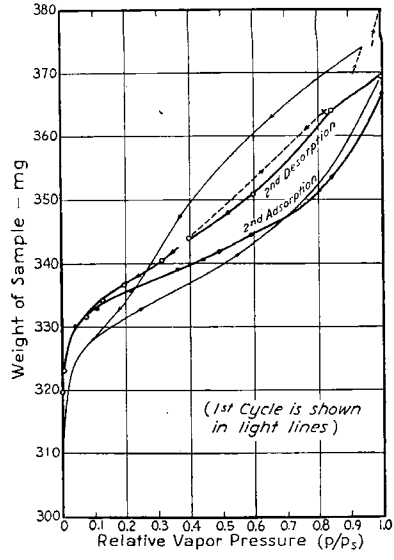

Fig. 2-6A (upper left)—Data from Tables 12 and 13

Fig. 2-6B (upper right)—Data from Tables 14 and 15

Fig. 2-6C (lower right)—Sorption isotherms for cement slab made from cement 13495

High vacuum apparatus. Data from Tables 16 and 17

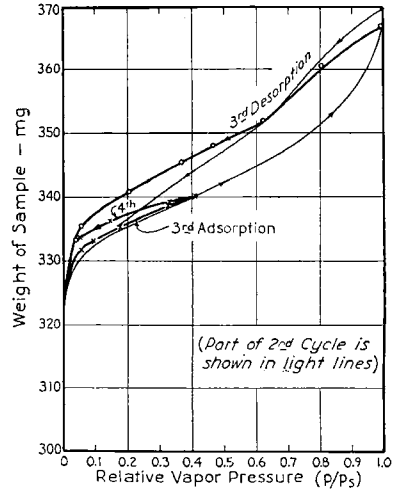

rium* between the evaporable water in the sample and the ambient water vapor anywhere between the desorption and adsorption curves.

*Chemists tend to question whether or not these should be called equilibrium points. They feel that, like points representing chemical equilibrium, a given point should be attainable from either side.

However, the requirement that a state of equilibrium must be approachable from either side with the same result does not properly apply to all physical equilibria. See for example the "ink bottle theory" of sorption hysteresis (Brunauer, p. 398). This theory shows that different amounts of water could be in equilibrium with the same vapor pressure. This is not to say that the conditions pictured in developing the ink bottle theory actually exist in hardened paste. It merely refutes the idea that equilibrium between water content and vapor pressure requires that only one water content can be associated with a given vapor pressure.

A paper by W. O. Smith (Sorption in an Ideal Soil, Soil Sci. v. 41, p. 209, (1936)) is especially pertinent. He showed by geometrical analysis that in an assemblage of spheres holding water by capillary condensation, different amounts of water can be in thermodynamic equilibrium with the same vapor pressure. Such equilibrium is reversible in the sense that the same *surface curvature* should be established at a given vapor pressure, regardless of the direction of approach. See Part 3, Capillary Condensation.

TABLE 12—FIRST DESORPTION CURVE FOR SLAB PREPARED FROM CEMENT 13495

High-vacuum apparatus
Age 7 years, 116 days
Original w/c = 0.50 by wt.

p/p_s (p_s = 23.756 mm of Hg)	Wt. of sample, mg	Evaporable water in the sample	
		mg	Fraction of dry wt. of sample ($=w$)
1.000	380.5	70.7	.2485
?	346.8 (a)	37.0	.1194
0.942	374.4	64.6	.2085
0.780	369.3	59.5	.1921
0.663	363.1	53.3	.1720
0.509	355.8	46.0	.1485
0.351	346.1	36.3	.1139
0.250	336.5	26.7	.0862
0.193	333.4	23.6	.0762
0.099	328.0	18.2	.0587
0.000	309.8	00.0	.0000

(a) Weight after 6 minutes of pumping—vapor pressure unknown.

TABLE 13—FIRST ADSORPTION DATA FOR SLAB PREPARED FROM CEMENT 13495

High-vacuum apparatus

p/p_s (p_s = 23.756 mm of Hg)	Wt. of sample, mg	Evaporable water in the sample	
		mg	Fraction of dry wt. of sample ($=w$)
0.000	309.8	00.0	.0000
0.064	326.7	16.9	.0545
0.155	329.8	20.0	.0646
0.193	330.7	20.9	.0675
0.249	332.1	22.3	.0720
0.350	335.1	25.3	.0817
0.446	338.0	28.2	.0910
0.598	343.0	33.2	.1072
0.745	351.0	41.2	.1330
0.855	356.6	46.8	.1511
0.959	366.4	56.6	.1827
0.995	369.6	59.8	.1930
1.000		67.0 (est.)	.2162 (est.)

TABLE 14—SECOND DESORPTION CURVE FOR SLAB PREPARED FROM CEMENT 13495

High-vacuum apparatus

p/p_s ($p_s = 23.756$ mm of Hg)	Wt. of sample, mg	Evaporable water in the sample	
		mg	Fraction of dry wt. of sample ($=w$)
0.995	369.6	50.0	.1565
0.848	364.1	44.5	.1392
0.594	350.7	31.1	.0973
0.397	344.0	24.4	.0763
0.82*	364.3	44.7	.1399
0.314	340.5	20.9	.0654
0.194	336.7	17.1	.0535
0.128	334.2	14.6	.0457
0.078	331.7	12.1	.0379
0.004	323.4	3.8	.0119
0.000	319.6	0.0	.0000

*Temperature controls failed and caused unintentional rise in pressure.

TABLE 15—SECOND ADSORPTION CURVE FOR SLAB PREPARED FROM CEMENT 13495

High-vacuum apparatus

p/p_s ($p_s = 23.756$ mm of Hg)	Wt. of sample, mg	Evaporable water in the sample	
		mg	Fraction of dry wt. of sample ($=w$)
0.000	319.6	0.0	.0000
0.042	330.4	10.8	.0338
0.112	333.2	13.6	.0426
0.220	335.7	16.1	.0504
0.364	339.0	19.4	.0607
0.450	340.7	21.1	.0660
0.596	344.7	25.1	.0785
0.806	351.4	31.8	.0995
1.00 (?)	366.8	47.2	.1477

TABLE 16—THIRD DESORPTION OF SLAB PREPARED FROM CEMENT 13495

High-vacuum apparatus.

p/p_s (p_s=23.756 mm of Hg)	Wt. of sample, mg	Evaporable water in the sample	
		mg	Fraction of dry wt. of sample ($=w$)
1.00 (?)	366.8	45.8	.1427
0.807	360.8	39.8	.1240
0.624	352.0	31.0	.0966
0.467	348.0	27.0	.0841
0.370	345.3	24.3	.0757
0.202	340.9	19.9	.0620
0.052	335.3	14.3	.0445
0.043	334.2	13.2	.0411
0.000	321.0	00.0	.0000

TABLE 17—THIRD PARTIAL ADSORPTION AND PARTIAL DESORPTION DATA FROM SLAB PREPARED FROM CEMENT 13495

High-vacuum apparatus

p/p_s (p_s=23.756 mm of Hg)	Wt. of sample, mg	Evaporable water in the sample	
		mg	Fraction of dry wt. of sample ($=w$)
0.000	321.0	0.0	.0000
0.052	332.3	11.3	.0352
0.094	333.2	12.2	.0380
0.178	335.4	14.4	.0448
0.321	338.7	17.7	.0552
0.405	340.1	19.1	.0595
0.326	339.2	18.2	.0567
0.146	336.5	15.5	.0483
0.049	333.6	12.6	.0392

The lack of reversibility as described above is shown by materials of various kinds.

Although the phenomenon has not been investigated extensively here, there is little reason to doubt that portland cement pastes all show essentially the behavior described above. This matter of hysteresis is significant and should be kept in mind in connection with the theoretical discussion that follows later in this paper. It is a principal reason for believing that ordinary laws of chemical reaction cannot be applied to the reactions involving the gain or loss of evaporable water.

Besides the effects common to many materials, portland cement paste exhibits certain irreversible phenomena not found among some other types of materials. This is shown in Fig. 2-6B, where the second desorption-and-adsorption curves of the sample are given.

A break in the second desorption curve at $p = 0.395\ p_s$ will be noted. After equilibrium at this pressure had been established, the cryostat was set to produce a lower pressure, but during the night the temperature controls failed, the pressure rose to $p = 0.82\ p_s$ and the sample-weight increased, giving the point indicated by the cross. (This point probably does not represent an equilibrium value, but is close to it.) When proper operation of the cryostat was restored, the point at $p = 0.315\ p_s$ was obtained.

The light-line curves in Fig. 2-6B are those of Fig. 2-6A, shown for comparison. The marked difference between the first and second cycles is believed to be due to two factors: One is the irreversible shrinkage (described in Part 1) that reduces the capacity of the sample for evaporable water. The other is the additional hydration of the cement in the sample that occurs while the sample is subjected to vapor pressures above about $0.8\ p_s$. Although these samples had been stored in water for several years they seem to have contained unhydrated clinker that was exposed when the thin wafers were prepared.

No explanation for one feature of the irreversibility has been found. Note that on the first desorption the minimum weight reached was 309.8 mg. On the second desorption the minimum weight was 319.6 mg. Continued hydration has the effect of increasing the minimum weight, but the increase shown here is much too great to be accounted for in this way. It is possible that the observed minimum weight for the first desorption was in error by several milligrams. However, the original data offer no clue as to the nature or cause of the error, if there was one.

Fig. 2-6C shows the third desorption and a partial third adsorption curve. The third *de*sorption curve differs from both the first and second desorption curves, but the third *ad*sorption is practically the same as the second adsorption. In fact, when the results are expressed as percentage of the minimum weight, the second and third adsorption curves are identical. Tests on other samples show that after the first cycle of drying and wetting the adsorption curves are reproducible. But the indications of a limited amount of data are that the desorption curves are greatly influenced by small variations in experimental conditions and are difficult to reproduce exactly.

On the third desorption, Fig. 2-6C, after the weight corresponding to $0.4\ p_s$ had been established, the pressure was intentionally lowered stepwise with the result indicated by the graph. This illustrates what

was said above about the irreversibility of this process in the range of pressures where the curves form a loop. Note that the points cut across the loop and join the desorption curve. This behavior is similar in character to that obtained with other materials[3]. It should be noted, however, that the vapor pressure at which the loop closes is much lower than that observed with other materials. Moreover, the loop closes at a much lower pressure than would be predicted from Cohan's hypothesis[4].

The size and shape of the hysteresis loop, and the course of the curve when the process is reversed within the limits of the loop, are probably characteristic of the physical structure of the hardened paste[4,5]. At any rate the whole phenomenon cannot be understood until these loops can be adequately interpreted. However, practically all the measurements reported in this paper were of adsorption only. Therefore, the interpretation of the adsorption curve is the only part of the problem that can be considered here.

Along with the measurements described above, measurements were made on the sample described in Table 18. This sample was prepared from a neat-cement cylinder that had been molded under high pressure with w/c only 0.12 by weight.

The results are given in Tables 18 to 23 and in Fig. 2-7, all three cycles being shown on the same graph. The features pointed out in Fig. 2-6 can be seen here also, and others besides. Note that the effect of the reversal in pressure that occurred during the second desorption was somewhat different from that on the other specimen. Note also that the lower parts of the second and third desorption cycles are identical. The indication is that with a specimen as dense as this, the paste becomes "stabilized" after the first drying so that desorption as well as adsorption curves are reproducible, provided that the specimen is always saturated at the start. The differences among the desorption curves in the upper range are believed to be due to slight differences in the degree of saturation at the beginning of the desorption part of the cycle.

Comparison of the results obtained with high-vacuum and air-stream apparatus

Fig. 2-8 and Tables 24 and 25 give adsorption data for two granulated pastes, the data being obtained first with the air-stream apparatus and then, about three years later, with the high-vacuum apparatus. The granules had been sealed in glass ampoules during the three-year interval. The later tests were made on samples from the same lot of granules as the earlier ones, but not on the same samples as used in the first test. Thus, the curves obtained by each method were first-adsorption curves.

The granules had originally been dried by the regular procedure used in connection with the air-stream method, that is, over Dehydrite in a

TABLE 18—FIRST DESORPTION CURVE ON SLAB PREPARED FROM CEMENT 14675

High-vacuum apparatus
Age 4 years 29 days
Original w/c = 0.12 by weight
Molded under 24,000 lb/in² pressure

p/p_s (= x) (p_s = 23.756 mm of Hg)	Wt. of sample, mg	Evaporable water in sample		
		mg	Fraction of dry wt. of paste (= w)	
1.000	664.4	47.8	0.0775	Initial wt. sat'd
?	647.9	31.3	0.0508	Wt. after 6 min. pumping
1.000	742.8	126.2	0.2046	Droplets condensed on sample
0.942	656.4	39.8	0.0645	
0.780	653.3	36.7	0.0595	
0.663	652.0	35.4	0.0574	
0.509	649.7	33.1	0.0537	
0.351	647.4	30.8	0.0500	
0.250	643.4	26.8	0.0435	
0.193	641.5	24.9	0.0404	
0.099	638.1	21.5	0.0349	
0.000	616.6	00.0	0.0000	

TABLE 19—FIRST ADSORPTION CURVE ON SLAB PREPARED FROM CEMENT 14675

High-vacuum apparatus

p/p_s (= x) (p_s = 23.756 mm of Hg)	Wt. of sample, mg	Evaporable water in sample	
		mg	Fraction of dry wt. of paste (= w)
0.000	616.6	00.0	0.0000
0.064	627.6	11.0	0.0178
0.155	629.9	13.3	0.0216
0.193	630.2	13.6	0.0221
0.249	631.5	14.9	0.0242
0.350	632.7	16.1	0.0261
0.446	634.0	17.4	0.0282
0.598	638.7	22.1	0.0358
0.745	642.5	25.9	0.0420
0.855	645.8	29.2	0.0474
0.959	653.8	37.2	0.0603
1.000	664.4*	47.8	0.0775

*Original weight.

TABLE 20—SECOND DESORPTION CURVE ON SLAB PREPARED FROM CEMENT 14675

High-vacuum apparatus

p/p_s (= x) (p_s = 23.756 mm of Hg)	Wt. of sample, mg	Evaporable water in sample	
		mg	Fraction of dry wt. of paste (= w)
1.000 (a)	685.1	68.5	0.1111
0.957	656.4	39.8	0.0645
0.848	653.8	37.2	0.0603
0.594	648.7	32.1	0.0521
0.397	646.4	29.8	0.0483
0.82 (b)	650.7	34.1	0.0553
0.314	642.2	25.6	0.0415
0.194	639.4	22.8	0.0370
0.128	637.6	21.0	0.0341
0.078	635.8	19.2	0.0311
0.004	622.0	5.4	0.0088
0.000	616.6	0.0	0.0000

(a) Water visible on sample.
(b) Temperature controls failed and caused pressure to rise.

TABLE 21—SECOND ADSORPTION CURVE FOR SLAB PREPARED FROM CEMENT 14675

High-vacuum apparatus

p/p_s (= x) (p_s = 23.756 mm of Hg)	Wt. of sample, mg	Evaporable water in sample	
		mg	Fraction of dry wt. of paste (= w)
0.000	616.6	0	0
0.042	626.1	9.5	0.0154
0.112	629.4	12.8	0.0208
0.220	631.0	14.4	0.0234
0.364	633.0	16.4	0.0266
0.450	634.5	17.9	0.0290
0.596	638.7	22.1	0.0358
0.806	644.3	27.7	0.0449
1.000	662 (est)	45.4 (est)	0.0736 (est)

TABLE 22—THIRD DESORPTION CURVE FOR SLAB PREPARED FROM CEMENT 14675

High-vacuum apparatus

p/p_s (= x) (p_s = 23.756 mm of Hg)	Wt. of sample, mg	Evaporable water in sample	
		mg	Fraction of dry wt. of paste (= w)
0.807	655.3	38.7	0.0628
0.624	647.9	31.3	0.0508
0.467	645.1	28.5	0.0462
0.370	643.3	26.7	0.0433
0.202	639.2	22.6	0.0367
0.052	634.8	18.2	0.0295
0.043	632.5	15.9	0.0258
0.000	616.6	00.0	0.0000

TABLE 23—THIRD PARTIAL ADSORPTION AND PARTIAL DESORPTION CURVES FOR SLAB PREPARED FROM CEMENT 14675

High-vacuum method

p/p_s (= x) (p_s = 23.756 mm of Hg)	Wt. of sample, mg	Evaporable water in sample	
		mg	Fraction of dry wt. of paste (= w)
0.00	616.6	0	0
0.052	627.6	11.0	0.0178
0.094	628.9	12.3	0.0199
0.178	631.1	14.5	0.0235
0.321	633.3	16.7	0.0271
0.405	634.2	17.6	0.0285
0.326	633.8	17.2	0.0279
0.146	631.6	15.0	0.0243
0.049	628.7	12.1	0.0196

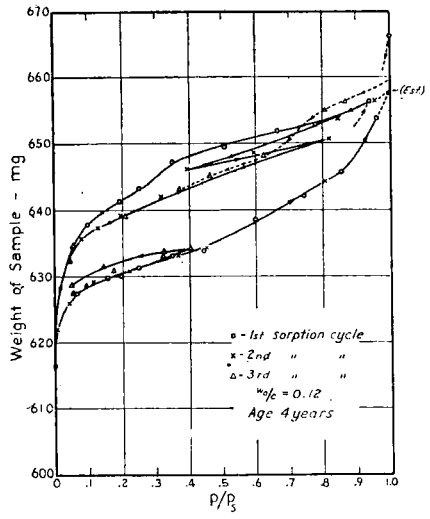

Fig. 2-7—Sorption isotherms for neat cement slab made from cement 1 4675
Data from Tables 18 to 23

vacuum desiccator. In the high-vacuum procedure these granules were exposed to the vapor pressure generated by ice at the temperature of dry ice, the lowest pressure used. After the final exposure to this low pressure in the high-vacuum apparatus, the samples were ignited. The final weights compared with those obtained after the earlier tests are given below:

	Sample No.	
	9-15A-6M	K4B-1Q
Loss on ignition as dried originally (g/g)	0.1428	0.1927
Loss on ignition as dried in high-vacuum apparatus (g/g)	0.1506	0.1922

Note that the water content of K4B-1Q was the same (within the limits of probable error) under both drying conditions and that therefore the sample as received from the sealed ampoule was not changed by the exposure to the lowest vapor pressure used in the high-vacuum apparatus. As mentioned in connection with Table 5, above, this provides data for estimating the vapor pressure of the desiccant used in earlier tests. The vapor pressure over ice at dry ice temperature (-78 C) is given as 0.56 microns of mercury.[5] The pressure relative to the saturation pressure at 25 C is therefore about 24×10^{-6}.

The data for the other sample, 9-15A-6M, indicate that the two drying conditions were not exactly alike, the amount of water removed in the original drying being somewhat greater than that removed in the

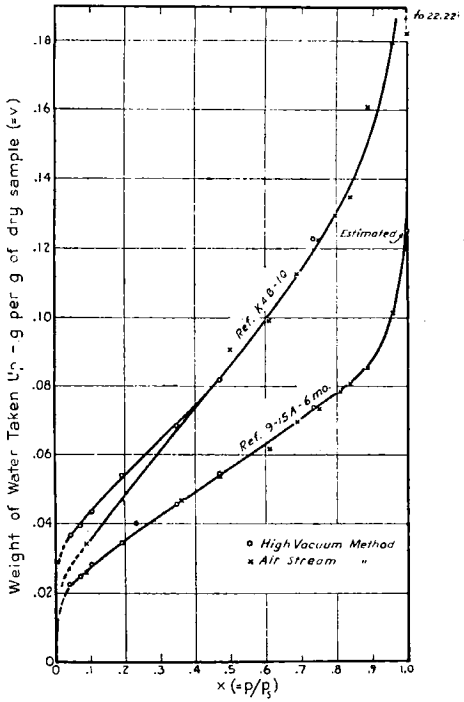

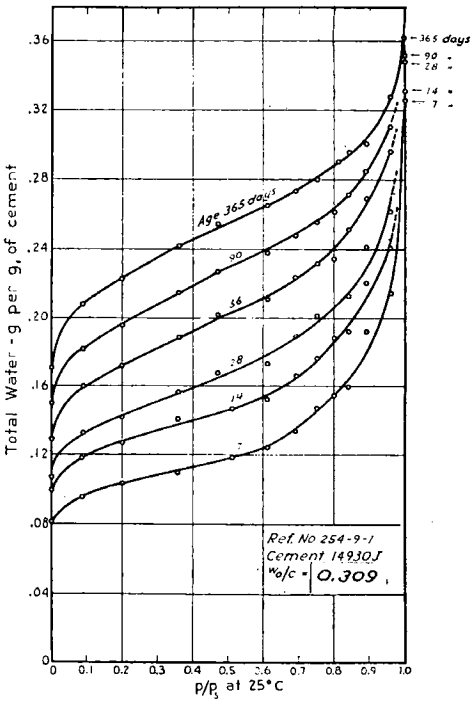

Fig. 2-8 (left)—Adsorption isotherms (25 C) for granular samples
Data from tables 24 and 25, Part 2, and from Tables A-8 and A-27 of Appendix to Part 2

Fig. 2-9 (right)—Adsorption isotherms showing effect of curing (air-stream apparatus)

TABLE 24—FIRST ADSORPTION CURVE FOR GRANULAR SAMPLE 9-15A-6M

High-vacuum method

p/p_s (= x)	Wt. of sample, mg	Evaporable water in the sample	
		mg	Fraction of dry wt. of sample (=w)
0.00	431.3	0.0	.0000
0.055	441.1	9.8	.0227
0.073	442.0	10.7	.0249
0.104	443.6	12.3	.0284
0.193	446.3	15.0	.0347
0.244	448.5	17.2	.0400
0.349	450.9	19.6	.0455
0.472	454.7	23.4	.0542
0.738	463.1	31.8	.0738
1.000			.1250*

*Observed value 0.1569, but known to be too high because of condensation in sample and spring. 0.1250 is based on the estimated water content of the sample in the saturated state.

TABLE 25—ADSORPTION CURVE FOR GRANULAR SAMPLE K4B-1Q

High-vacuum method

p/p_s (= x)	Wt. of sample, mg	Evaporable water in the sample	
		mg	Fraction of dry wt. of sample (= w)
0.00	542.2	0.0	.0000
0.055	562.2	20.0	.0369
0.073	563.7	21.5	.0395
0.104	566.3	24.1	.0442
0.193	571.4	29.2	.0541
0.244	574.0	31.8	.0587
0.349	579.4	37.2	.0686
0.472	586.6	44.4	.0819
0.738	608.9	66.7	.1230
1.000			.2295*

*Original water content after drying and resaturating.

high-vacuum apparatus. This would indicate that the vapor pressure over the magnesium perchlorate hydrate is somewhat less than that over ice at -78 C. However, there is some reason to believe, as pointed out before, that the drying agent in the original tests was sometimes inadvertently $Mg(ClO_4)_2 + Mg(ClO_4)_2.2H_2O$ instead of $Mg(ClO_4)_2.2H_2O + Mg(ClO_4)_2.4H_2O$. This could be one of those instances.

In regard to the course of the curves over the lower range of vapor pressures, we will show later that theoretically the presence of air should reduce the amount of adsorption in the manner shown by the plotted data for K4B-1Q. That is, the two series of points for this sample differ only as they theoretically should. It will be seen later that in other important respects the two series of points have the same significance and that the two methods give essentially the same result.

The two series of points for sample 9-15A-6M fall practically on the same line. Theoretically, the crosses should drop below the circles in the low-pressure range. The fact that they do not can be accounted for by the data given above showing that the sample used in the original tests (air-stream method) was dried to a lower water content than the sample used in the later tests (high-vacuum method). It will be seen later that the drier the sample the higher the "knee" of the adsorption curve. It therefore seems that by chance alone the effect of the difference in initial water content exactly offset the effect of the presence of air.

These data indicate that adsorption in the presence of air is essentially the same as that in the absence of air when the small effect of the air itself is taken into account. This is important, for it shows that the

interpretations worked out by other investigators for adsorption from a pure gas phase can be applied with modifications to the adsorption of water vapor from a mixture of air and water vapor.

It should be noted that practically all the data given in this paper were obtained by the air-stream method. *Unless otherwise stated, it is correct to assume that all adsorption data were obtained by the air-stream method.*

Effect of extent of hydration on the position of the adsorption curve

Fig. 2-9 gives a group of adsorption curves for a given kind of paste at different stages of hydration. The paste was obtained from mortar prisms that had been cured continuously in water for periods ranging from 7 days to one year. The results shown are typical except that they represent a Type IV, rather than a Type I, cement. Since the plots of water contents are expressed in terms of the weight of the original cement in the sample, the ordinates at $p/p_s = 0$ give the amounts of non-evaporable water and those at $p/p_s = 1$* give the total water contents at saturation. The curves illustrate the following general conclusions that are applicable to all samples tested, regardless of original water-cement ratio, age, or type of cement.

(1) The total water held at saturation ($p/p_s = 1$) increases as the length of the curing period increases.

(2) The non-evaporable water content also increases.

(3) The amount of water held at any intermediate vapor pressure increases with the length of the curing period.

(4) The evaporable water content, which is the difference between the total and the non-evaporable water, *de*creases as the length of the curing period increases.

The changes that take place during the period of curing are illustrated in another way in Fig. 2-10. This, like Fig. 2-9, represents a group of samples that were similar except for the extent of hydration at the time of test; they were prepared from mortar cubes all made from the same mix. Here the bottom curve represents the non-evaporable water and the top the total water content. The intermediate curves represent the water content after the originally dry samples had reached equilibrium with the relative vapor pressures indicated on the curves.

Note that all curves originate at (0,0) except the upper one. This one begins at a point representing the original water-cement ratio (corrected for bleeding). That is, zero age represents the time before any hydration takes place. At that time all the water in the sample will

*The topmost point has been plotted at $p/p_s = 1$ despite the fact that consideration of the effect of dissolved alkalies shows that it should be plotted at a lower p/p_s. This point is discussed further in connection with the effect of dissolved alkalies in Part 3.

have a relative vapor pressure of 1.0* and not any of it would be held if exposed to an atmosphere having any lesser water vapor pressure. At any time after hydration begins, only a part of the water can be lost in an atmosphere having an appreciable vapor pressure.

The rise of the top curve is due to absorption of water by the specimen from the curing tank. The points represent dried-and-resaturated granules and therefore are probably slightly below the level representing the capacity of the paste before drying, as explained before.

The rise of the bottom curve indicates the progress of hydration and, as will be shown later, is proportional to the increase in volume of the solid phase of the paste. The heights of the next three curves above the bottom curve (p/p_s = 0.09; 0.19; and 0.36) are believed to depend on the total surface area of the solid phase and hence to depend primarily on the quantity of gel present. It will be shown later that the positions of these lower curves are independent of the total porosity of the sample. Although this particular plotting does not make it apparent, it is a fact that the position of the points representing pressures greater than about 0.475 p_s depend on the total porosity of the sample as well as on the extent of hydration. The basis for these interpretations and the uses made of the information are subjects treated in later parts of this paper.

Fig. 2-11 gives some of the same data that appear in Fig. 2-9 in terms of a unit weight of dry paste rather than weight of original cement as before. It therefore shows the evaporable water only. Note that as the length of the period of wet curing increases, the total evaporable water decreases and the amount held at low vapor pressures increases. Since the total evaporable water may be taken as a measure of the total porosity of the hardened paste, this graph shows that the amount of water held at vapor pressures near the saturation pressure depends on the porosity of the sample. On the other hand, the amounts of water held at low pressures appear here to vary inversely with the porosity. However, it will be proved that the amount held at low pressure does not depend on porosity.

Influence of original water-cement ratio (w_o/c) on the shape of the adsorption curve

Fig. 2-12 to 2-15 present adsorption curves for samples having different water-cement ratios but the same degree of hydration as measured by the non-evaporable water content. The points for these curves were obtained by interpolations on plots such as that shown in Fig. 2-10. The four figures represent three different cements, two different degrees of hydration, and three (in one case, four) different water-cement ratios. Considered together, they show that differences in age and original water-cement ratio have no influence on the shape of the lower part of the ad-

*Again neglecting the effect of dissolved alkalies.

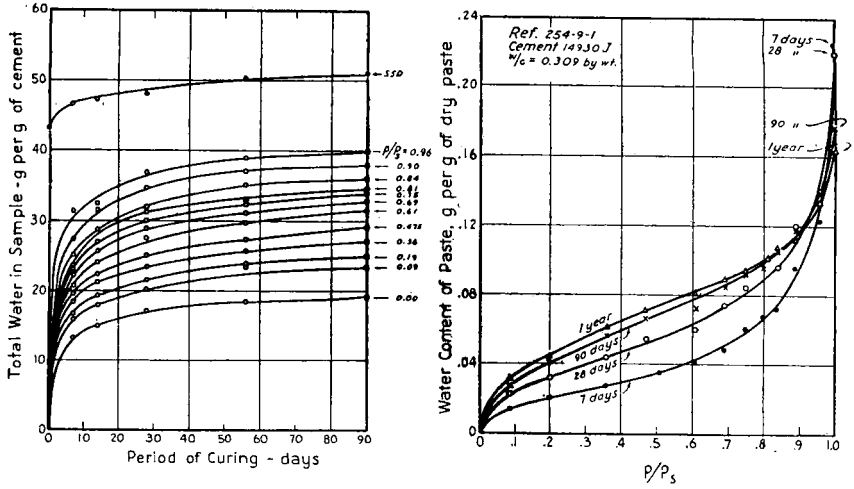

Fig. 2-10 (left)—Changes in amounts of water held at any given vapor pressure as influenced by the length of the curing period
Cement 15007J-Ref. 9-5 $w_o/c = 0.433$

Fig. 2-11 (right)—Adsorption isotherms showing evaporable water only

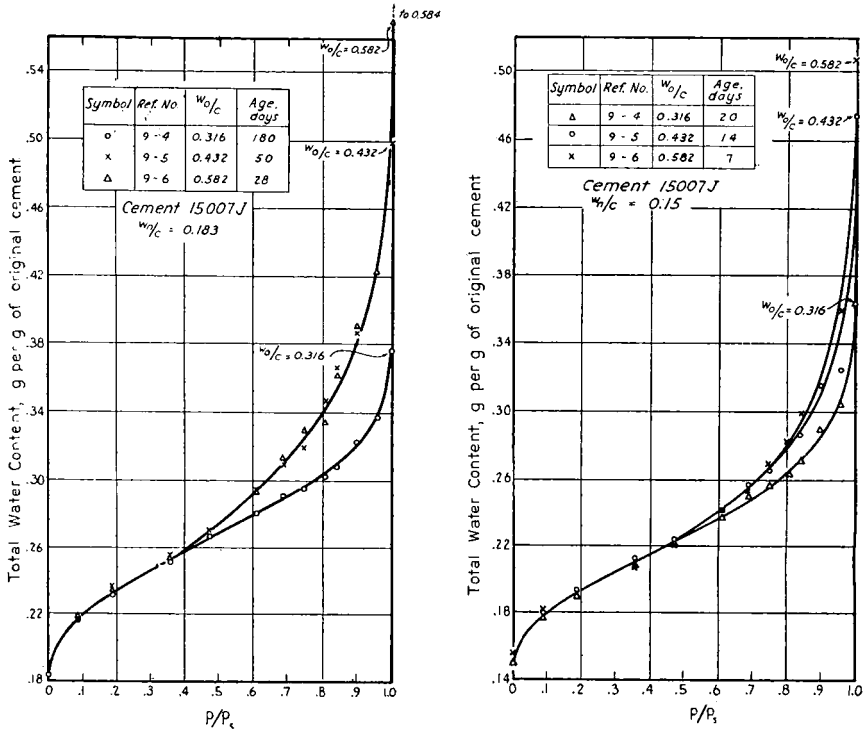

Fig. 2-12 (left)—Adsorption isotherms for samples of different w_o/c but equal non-evaporable water
Fig. 2-13 (right)—Adsorption isotherms for samples of different w_o/c but equal non-evaporable water

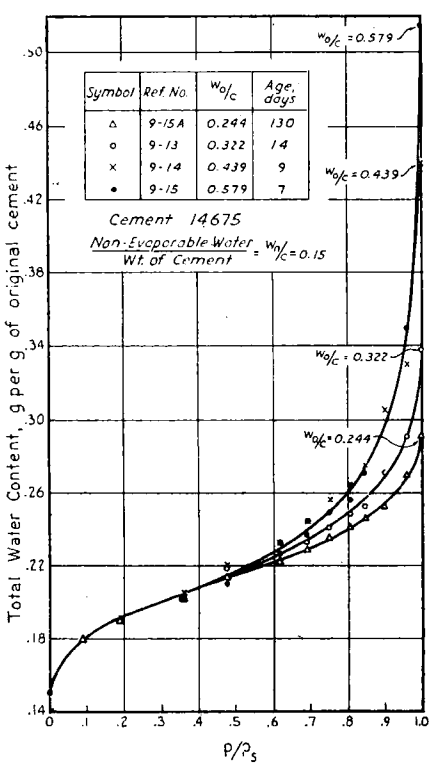

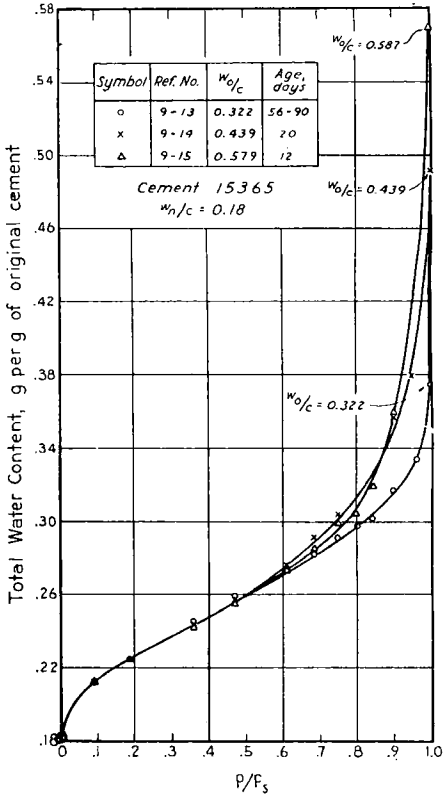

Fig. 2-14 (left)—Adsorption isotherms for samples of different w_o/c but equal non-evaporable water

Fig. 2-15 (right)—Adsorption isotherms for samples of different w_o/c but equal non-evaporable water

sorption curves apart from the effect on the level of the starting point: at a given degree of hydration the same curve holds for all ages and water ratios. In other words, the amount of water taken up in the lower third of the range of vapor pressures depends only on the extent of hydration and hence only on the increase in quantity of hydration-product in the sample. On the other hand, the total amount of evaporable water depends upon the porosity of the solid phase which *at a given degree of hydration* depends upon the original water-cement ratio.

The data just considered show that the lower third of the adsorption curve has the same shape for different ages and different porosities of samples made from the same cement. Fig. 2-16 and 2-17 are presented to show that the lower third of the curves have the same shape not only for these conditions but also for different cement compositions. These plots are like those of Fig. 2-12 to 2-15 except that the scale of ordinates is the ratio of the amount of water taken up at a given pressure to the

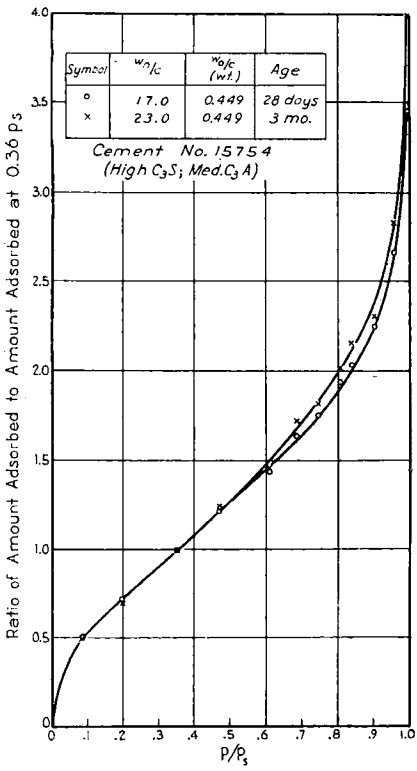

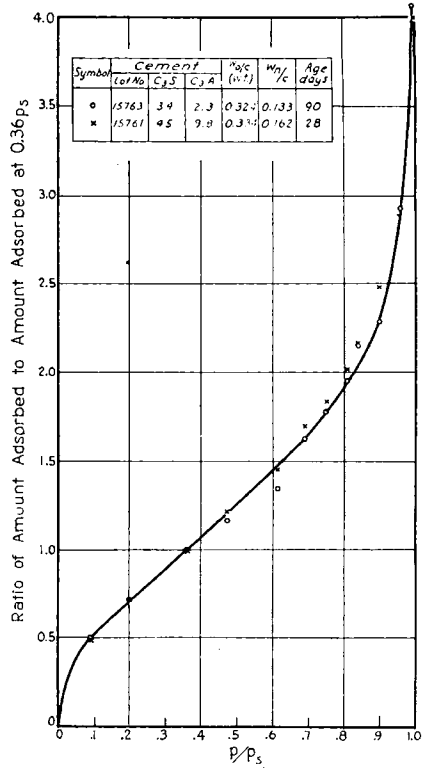

Fig. 2-16 (left)—Adsorption isotherms for which the amount adsorbed is expressed as a ratio to the amount adsorbed at $p/p_s = 0.36$
Different degrees of hydration

Fig. 2-17 (right)—Adsorption isotherms for which the amount adsorbed is expressed as a ratio to the amount adsorbed at $p/p_s = 0.36$
Different cements and different degrees of hydration

amount taken up at a pressure of 0.36 p_s. The coincidence in the lower range of pressures proves that the lower part of the curves can be represented by the same form of mathematical expression.

Empirical relationship between the amount of adsorption at low pressures and the non-evaporable water content

Fig. 2-18 shows typical relationships between the amount of water held at low vapor pressure and the non-evaporable water content for samples prepared from two different cements. Symbols of different shape for the same cement designate different original water-cement ratios, and different points of the same shape represent a mix of given water ratio at different stages of hydration.

Although these data were among the first obtained in this investigation and as a consequence show the influence of imperfect laboratory technique, they illustrate adequately the fact that with any given cement

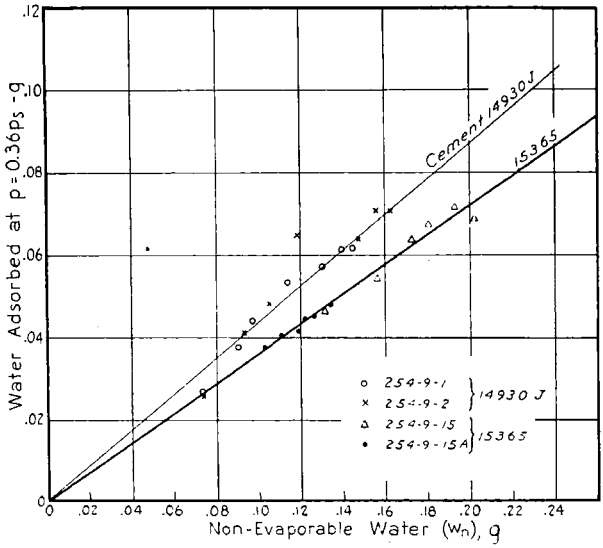

Fig. 2-18—Relationship between amount of water held at low pressure and the non-evaporable water content for two different cements

the adsorption at low vapor pressure (any pressure below about 0.4 p_s) is directly proportional to the extent of hydration as measured by the non-evaporable water content. A study of this relationship will be presented in another part of this paper.

General results from various cements

The results of some of the adsorption tests and measurements of non-evaporable water are shown in graphical form for various cements* in Fig. 2-19 to 2-23. In Fig. 2-19, for example, the total evaporable water is represented by the height of the column above the horizontal reference line and the non-evaporable water by the length of the column extending downward. The proportions of evaporable water held between various relative vapor pressures are shown by the relative lengths of the blocks making up the column. As will be shown later, the length of the first block above the zero line (up to line 0.35) is approximately proportional to the surface area of the cement gel. By assuming that the surface area is proportional to the amount of cement gel, the length of this block may also be taken to indicate the relative amount of cement gel in the sample.

The effect of differences in water-cement ratio for specimens of the same age is shown in Fig. 2-19 and 2-20. The effect of prolonging the period of curing for specimens of the same initial water-cement ratio can best be seen by reference to Fig. 2-21, 2-22, and 2-23. In reading these diagrams it is helpful to remember that at zero age there would be

*For characteristics of the cements, see Appendix to Part 2.

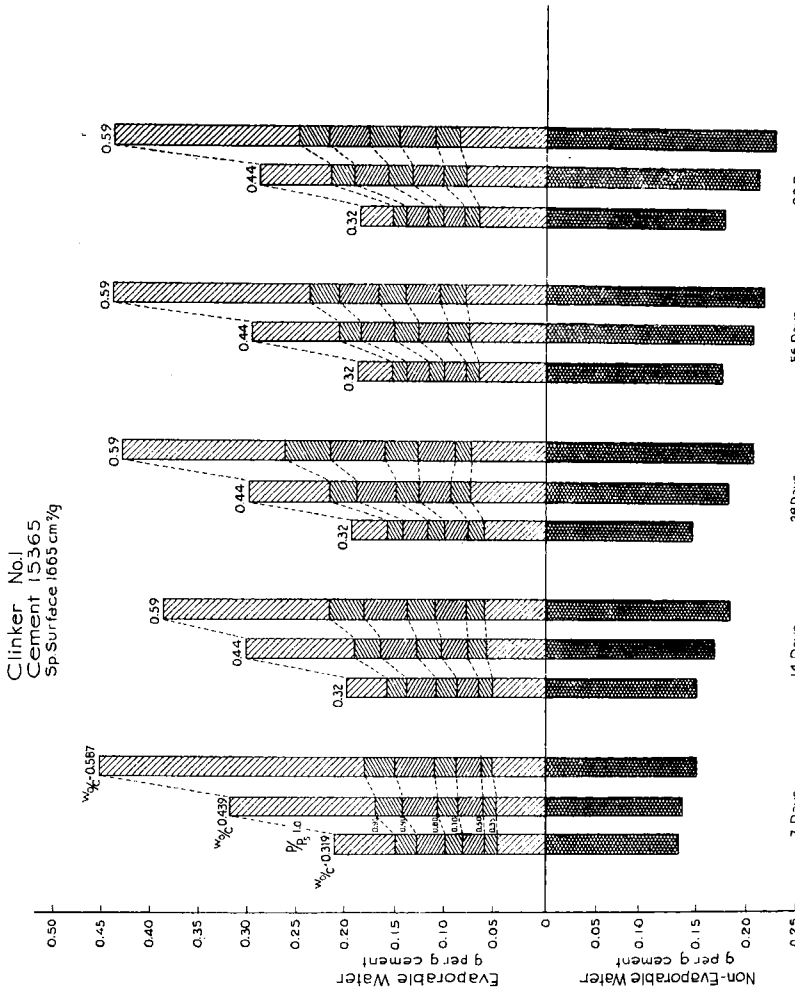

Fig. 2-19—Effect of water-cement ratio on the hardened paste at the ages indicated

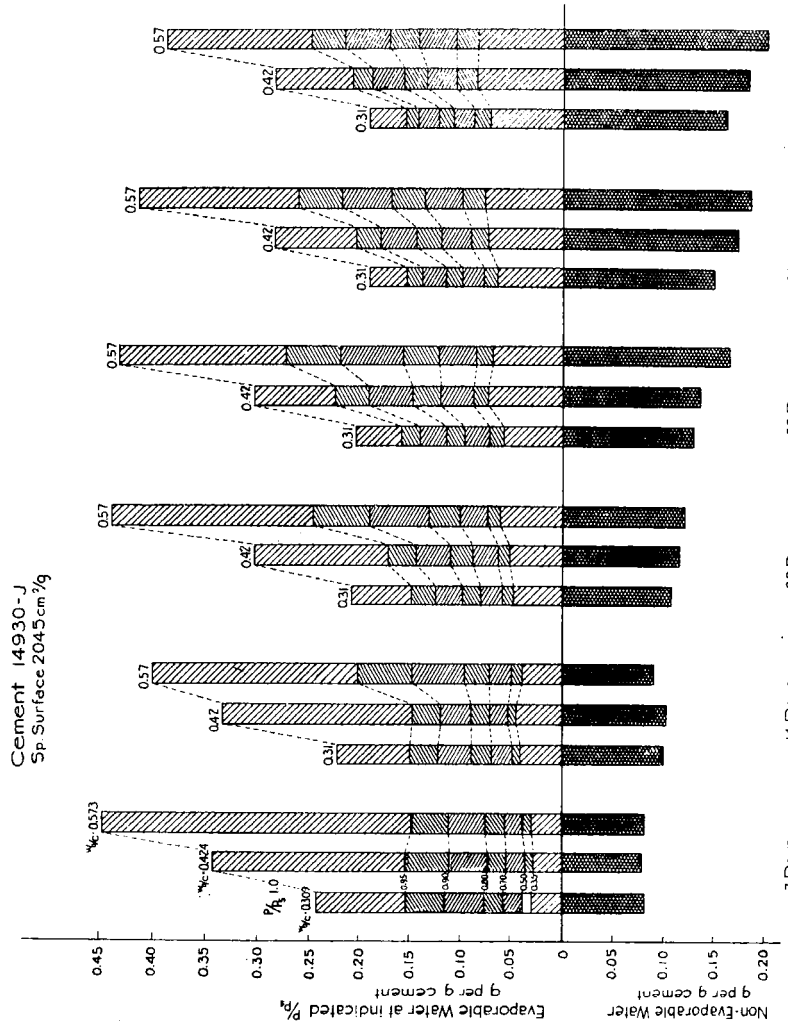

Fig. 2-20—Effect of water-cement ratio on the hardened paste at the ages indicated

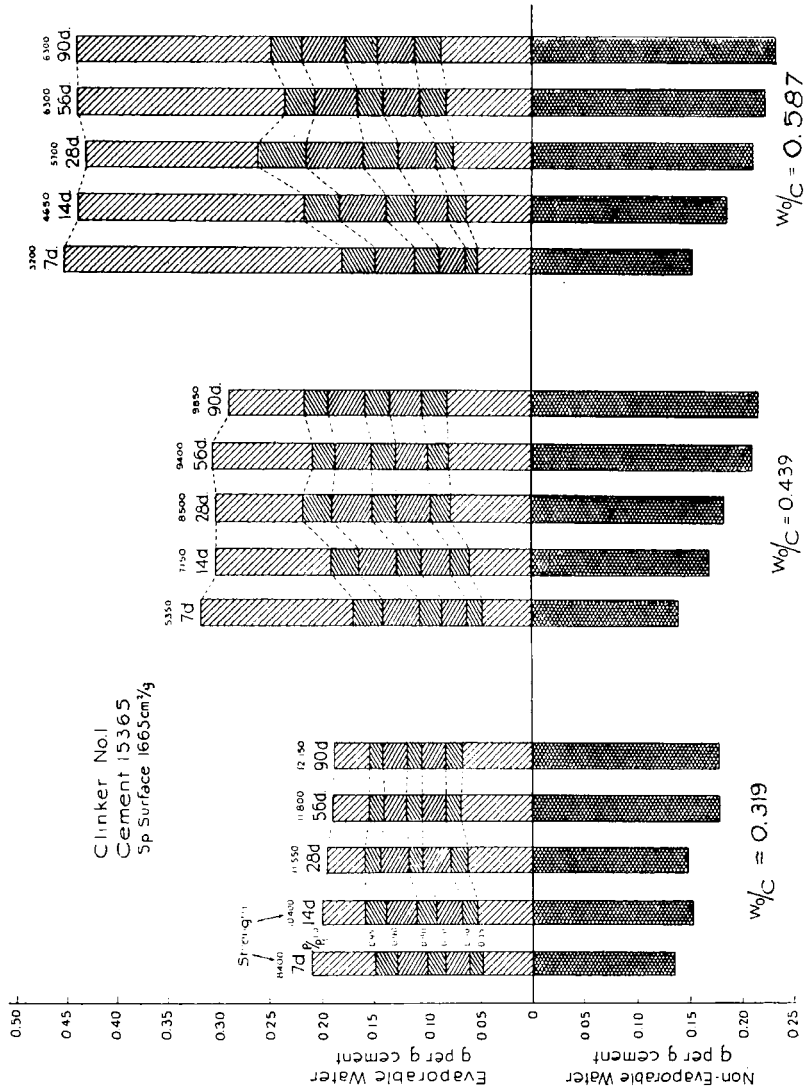

Fig. 2-21—Effect of age on hardened paste at the water-cement ratios indicated

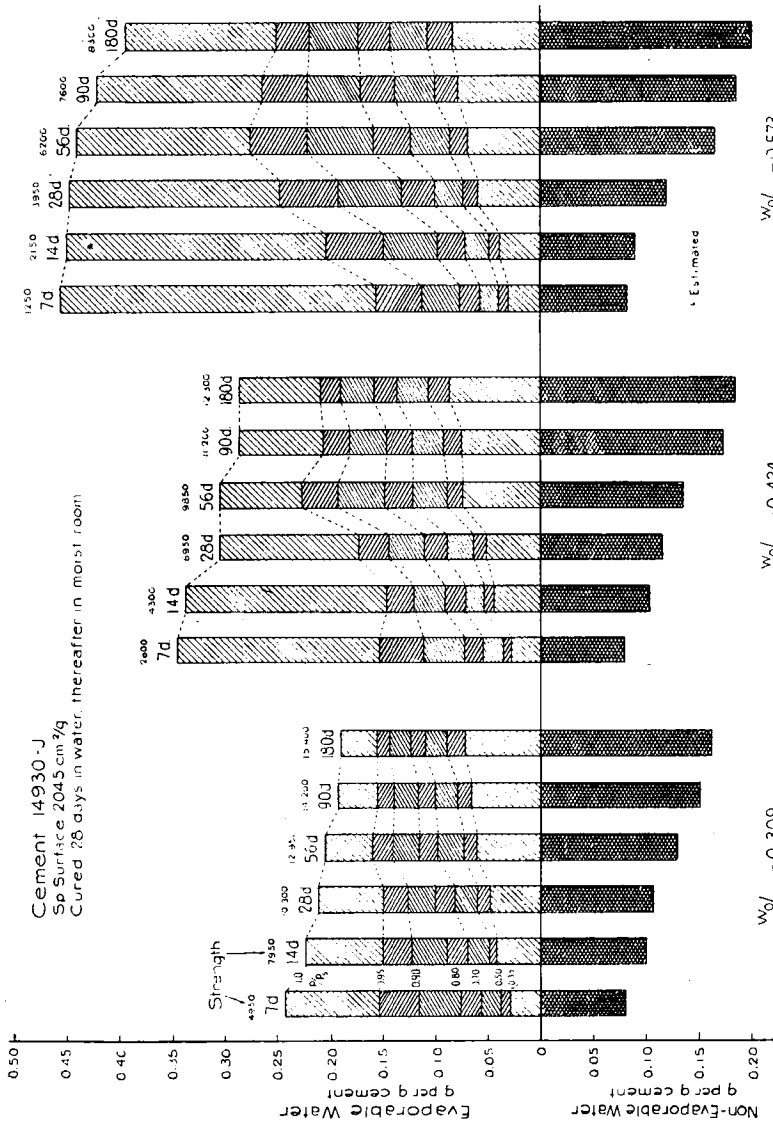

Fig. 2-22—Effect of age on hardened paste at the water-cement ratios indicated

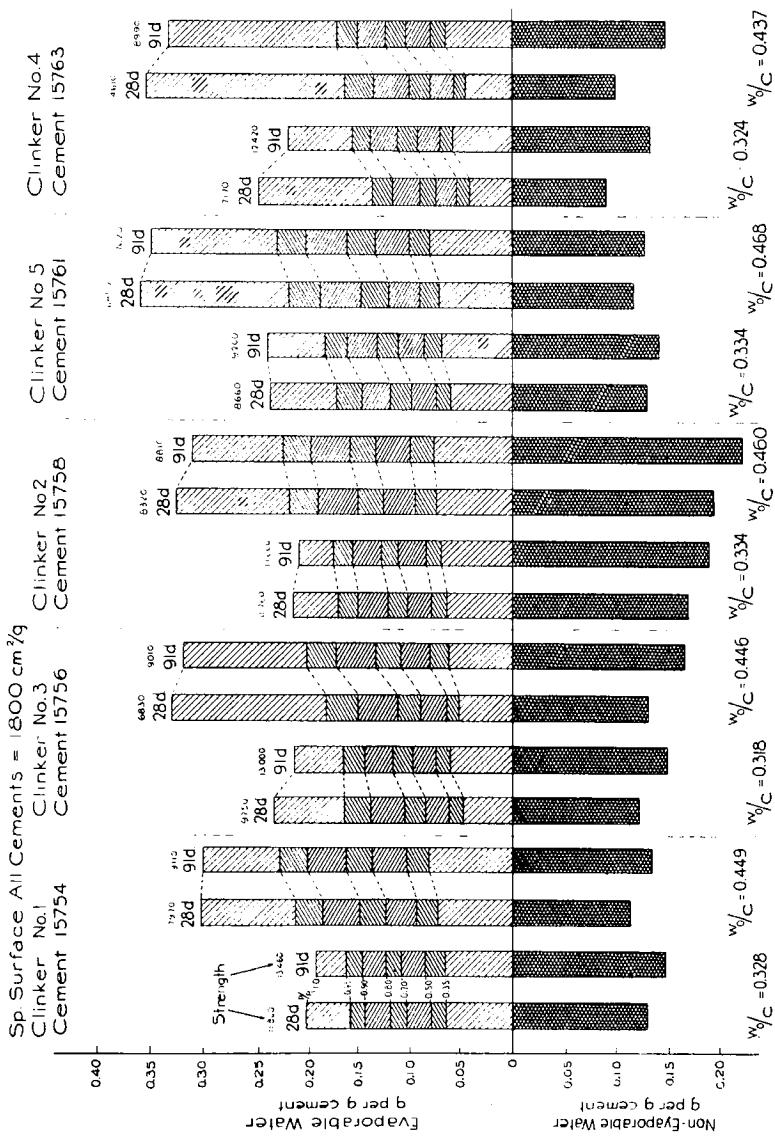

Fig. 2-23—Effect of age on hardened pastes of five different cements

no non-evaporable water and hence no column extending downward and the column for evaporable water would have a height equal to the original water-cement ratio, corrected for bleeding. Therefore, the difference between the height of the evaporable water column and the original water ratio indicates the degree of reduction in porosity brought about by the curing.

Some of the irregularities shown in these diagrams are believed to be due to imperfections in experimental technique. It seems probable that a given group of diagrams representing regular changes in w_o/c or in age should show a regular pattern of change. In most of the interpretations built up in later parts of this paper, these irregularities are ignored.

EFFECT OF STEAM CURING

One test only of steam-cured material was made. The result was so significant, however, that it will be given here. The procedure was as follows: a paste of normal consistency was made, composed of 1 part cement 15756, 0.71 part pulverized silica (Lot 15918), and 0.43 part water, by weight. This was made into two prisms 1x1x11¼ in. The prisms were cured over night in the molds and then were steamed at 420 F in an autoclave for about 6 hours, after which they were immersed in water over night. The bars were then crushed and a 48-80 mesh sample taken for adsorption tests.

Two-inch cubes were made from the same cement-silica mixture, but with slightly higher water-cement ratio—0.50 instead of 0.43. These were cured continuously under water for 28 days. They were then crushed, granular samples were taken, and adsorption characteristics were determined in the usual way.

The results of these tests are given in Table 26 and Fig. 2-24. They show that curing at high temperature radically alters the adsorption characteristics. Note particularly that about 90 percent of all the evaporable water was taken up at pressures above 0.8 p_s. The significance of this will be discussed more fully in the succeeding parts of the paper.

SUMMARY OF PART 2

The water in saturated hardened cement paste is classified as evaporable and non-evaporable. This classification is based on the amount of water retained by a specimen dried in a vacuum desiccator at 23 C over the system $Mg(ClO_4)_2.2H_2O + Mg(ClO_4)_2.4H_2O$. The pores in a hardened paste are defined as those spaces occupied by evaporable water.

This part of the paper deals with measurements of non-evaporable water and the adsorption isotherms of the evaporable water in various samples of hardened cement paste.

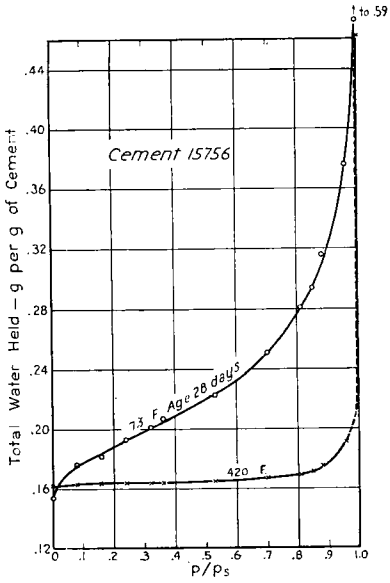

Fig. 2-24—Effect of steam curing on adsorption characteristics

TABLE 26—EFFECT OF STEAM CURING

Cement 15756

Relative vapor pressure	73 F for 28d w_o/c = .478	Autoclaved at 420 F w_o/c = .43
(w_n)*	(.1537)	(.1615)
0.08	.0220	.0015
0.16	.0329	.0017
0.24	.0390	.0028
0.32	.0478	.0025
0.36	.0530	.0026
0.53	.0689	.0038
0.70	.0969	.0052
0.81	.1283	.0081
0.85	.1408	.0090
0.88	.1623	.0131
0.96	.2230	.0300
1.00	.4367	.3009

*w_n = non-evaporable water.

A general description of materials and experimental apparatus and procedures is given, with reference to the Appendix to Part 2 for more complete information. Data are presented on the stability of the hydrates of the constituents of portland cement, in the presence of different desiccating agents. Indications are that of the microcrystalline hydrates that might occur in hardened cement paste, only the calcium sulfoaluminate would be decomposed to an appreciable extent by the desiccant used in these studies.

The experiments were for the most part made on granular samples prepared from the original cylinders or cubes. Data are presented indicating that the granular samples were representative of the original pastes, except for pastes of comparatively high porosity.

The empirical aspects of the experimental results are described and discussed. Adsorption and desorption curves from the same sample present a so-called hysteresis loop similar to those found for other materials. In addition, the curves show some features of irreversibility not commonly found among other materials. Most of the study pertains to adsorption isotherms only.

Adsorption of water vapor from humidified streams of air (air-stream apparatus) was found to be the same as adsorption from water vapor alone (high-vacuum apparatus), except at pressures below about 0.3 p_s, where the adsorption in the absence of air was expected to be greater than that in the presence of air. The curves obtained by the two methods are believed to have the same significance.

Graphs are presented from which the following conclusions are drawn:

(1) The total water held at saturation ($p/p_s = 1.0$) increases as the length of the curing period increases.

(2) The non-evaporable water content also increases.

(3) The amount of water held at any intermediate vapor pressure increases with the length of the curing period.

(4) The evaporable water content, which is the difference between the total and the non-evaporable water, decreases as the length of the curing period increases.

Curves are presented showing that differences in age and original water-cement ratio have no influence on the shape of the lower part of the adsorption curves. On the other hand, the position of the upper part of the curve and the total amount of evaporable water in a saturated specimen depend on both age and original water-cement ratio. These conclusions apply to all cements.

For a given cement the amount of *evaporable* water held at any pressure up to about 0.4 p_s is directly proportional to the *non*-evaporable water content. The proportionality constant is different for cements of different type.

An adsorption curve for cement paste cured for six hours in the autoclave at 420 F is compared with the curve obtained from a similar paste cured at 73 F for 28 days. Results show that curing at high temperature and pressure produces adsorption characteristics radically different from those observed in specimens cured in the ordinary way.

REFERENCES

1. E. Freyssinet, *Science et Industrie* (Jan. 1933).
2. F. M. Lea, *Cement & Cement Mfgr.* v. 5, p. 395 (1932).
3. K. S. Rao, "Hysteresis in Sorption," *J. Phys. Chem.* v. 45 (3) pp. 500-531 (1941).
4. L. H. Cohan, *J. Am. Chem. Soc.* v. 66, p. 98 (1944).
5. N. A. Lange, *Handbook of Chemistry*, 4th Edition, p. 1269.

Appendix to Part 2

CONTENTS

DESCRIPTIONS OF MATERIALS AND TABULATIONS OF ORIGINAL DATA

Information is given in this appendix concerning the materials used in each series and concerning the preparation of test specimens and samples. This information supplements that given in the text.

Also given are tabulations of the original data. The authors regard such a full presentation desirable because of the uniqueness of the data and because of the speculative nature of the interpretation offered in the text. That is, alternative interpretations may occur to other investigators in this field and we consider that they should have access to the original material.

Characteristics of cements

The cements used in any given series can be readily identified in Table A-1. Their chemical and physical properties are tabulated in order of lot numbers in Tables A-2 and A-3.

Description of specimens made in series 254-265

Mortar Specimens: Truncated cones: Base 4 in.; top 1½ in.; altitude 6 in.
Cement: Lot 14502 (see Tables A-2 and A-3 for characteristics).
Aggregate: A mixture of Elgin sand and Ottawa silica graded as follows:

Weight, per cent of size indicated					
Ottawa Silica		Elgin Sand			
200–100	100–48	48–28	28–14	14–8	8–4
2.4	4.9	23.6	29.9	16.3	22.9

TABLE A-1—SERIES INDEX TO CEMENTS

Series	Cement Nos.					
254-265	14502					
254-MRB	14898-39AQ 14904-45AQ 14910-52AQ	14899-40PC 14905-46PC 14911-51PC	14900-41SC 14906-47SC 14912-53SC	14901-42AQ 14907-48AQ 14913-54AQ	14902-43PC 14908-49PC 14914-55PC	14903-44SC 14909-50SC 14915-56SC
254-K4B	13721-1S 13733-5S 13740-7P 13765-15Q 13780-20Q	13722-1P 13734-5P 13741-7Q 13766-16S	13723-1Q 13735-5Q 13752-11P 13767-16P	13730-4S 13736-6S 13753-11Q 13768-16Q	13731-4P 13737-6P 13763-15S 13778-20S	13732-4Q 13738-6Q 13764-15P 13779-20P
254-7	14675					
254-8	14930J 15014J	15007J	15008J	15011J	15012J	15013J
254-9	14930J	15007J	15011J	15013J	15365	
254-11	15495 15761	15497 15763	15669 16198	15754 16213	15756 16214	15758
254-13	15367 15923* 15930*	15498 15924* 15932*	15623 15925* 15933*	15670 15926* 15934*	15699 15927* 15935*	15921* 15929*
254-16	15754 16189	15756	15758	15761	15763	16186
254-18	13495	14675	15365	13723-1Q		

*All cements marked * were ground in the laboratory. The rest were ground in commercial plants.

Mixes: Specimens represented the following mortar mixes, by weight: 1:0 (neat); 1:1½; 1:1, 1:2, 1:3, 1:5, 1:7.

Mixing: Each batch was mixed 30 sec. dry and 2 min. wet in a small power-driven, open-tub mixer.

Molding: Cones were cast in watertight molds of known capacity, the mortar being puddled with a light tamper.

Measurements: The weight of the filled calibrated mold was measured to 1 g immediately after filling, and again after 20-24 hr. in the fog-room. On stripping, the specimens were weighed in air and in water.

Curing: In molds in the fog-room for the first 20-24 hr.; in the fog-room thereafter. Temperature: 70 F.

Drying: The granular samples were dried in air-filled desiccators over concentrated sulfuric acid.

Composition of specimens: See Table A-4.

Analysis of granular samples: See Table A-5.

Adsorption data: See Table A-6.

TABLE A-2—CHEMICAL ANALYSES AND COMPUTED COMPOUND COMPOSITION

All computations are based on the weight of the cement unless otherwise indicated. The computed compositions are based on the oxide analyses corrected for free lime but not for other minor constituents.

Lot No.	Ref. No.	Major Constituents						Loss on Ign.	Insol. Res.	Free CaO	Minor Constituents								Computed Compound Composition				
		SiO_2	Al_2O_3	Fe_2O_3	Total CaO	MgO	SO_3				FeO	TiO_2	P_2O_5	Mn_2O_3	Na_2O	K_2O	$CHCl_3$ Soluble	CO_2	C_3S	C_2S	C_3A	C_4AF	$CaSO_4$
13495		20.79	6.02	3.11	63.57	3.16	1.65	1.00	0.14	1.11					0.22	0.52	.		51	21	11	10	2.8
13721†	1S	21.08	6.10	2.15	64.10	2.91	1.80	0.79	0.24	0.36	0.0				0.10	0.97			50.0	22.7	12.5	6.6	3.06
13722†	1P	20.93	6.18	2.17	63.48	2.94	1.80	0.87	0.23	1.18	0.0	0.31			0.10	1.58			44.8	26.3	12.7	6.6	3.06
13723†	1Q	21.13	5.85	2.17	64.18	2.99	1.80	0.79	0.18	1.49	0.30				0.10	1.11			47.0	25.2	11.8	6.6	3.06
13730†	4S	19.02	4.80	6.85	62.12	4.12	1.80	0.90	0.11	0.29	0.0				0.41	0.10			59.9	9.3	1.2	20.8	3.06
13731†	4P	19.13	4.92	6.70	61.63	4.09	1.80	0.97	0.37	3.80	1.46	0.37			0.53	0.20			42.3	23.0	1.7	20.4	3.06
13732†	4Q	18.79	5.08	7.17	61.72	4.21	1.80	0.78	0.20	1.55	1.27				0.37	0.12			52.6	14.2	1.3	21.8	3.06
13733†	5S	23.16	3.33	4.15	64.47	1.52	1.80	1.20	0.14	0.04	0.0				0.27	0.14			52.8	26.7	1.8	12.6	3.06
13734†	5P	22.61	3.31	4.31	63.23	1.52	1.80	2.40	0.13	0.32	0.0	0.16			0.35	0.46			49.5	27.6	1.5	13.1	3.06
13735†	5Q	22.97	3.27	4.40	63.53	1.50	1.80	1.81	0.10	0.41	0.0				0.37	0.42			49.0	29.0	1.2	13.4	3.06
13736†	6S	21.06	5.85	2.97	65.77	1.38	1.80	0.92	0.20	0.00	0.0				0.07	tr.			59.0	15.8	10.5	9.0	3.06
13737†	6P	20.97	5.99	3.03	65.50	1.39	1.80	0.84	0.17	0.35	0.0	0.26			0.10	0.11			56.0	17.8	10.7	9.2	3.06
13738†	6Q	20.99	5.90	3.03	65.57	1.43	1.80	0.83	0.22	0.45	0.03				0.08	0.08			56.4	17.6	10.5	9.2	3.06
13740†	7P	20.46	6.96	2.31	63.23	3.31	1.80	0.80	0.22	0.40	0.03	0.33			0.42	0.58			45.0	24.7	14.5	7.0	3.06
13741†	7Q	20.48	6.89	2.28	63.55	3.36	1.80	0.82	0.20	0.53	0.36				0.32	0.38			46.0	24.0	14.4	7.0	3.06
13752†	11P	21.18	4.70	4.89	65.10	0.78	1.80	0.94	0.19	0.15	0.0	0.34			0.66	0.16			59.6	15.7	4.2	14.9	3.06
13753†	11Q	21.57	4.26	4.48	65.61	0.79	1.80	0.86	0.16	0.33	0.33				0.51	0.08			61.5	15.4	3.7	13.6	3.06
13763†	15S	21.23	5.58	2.90	62.90	4.07	1.80	0.72*	**	0.11	0.0				0.23	0.41			47.4	25.2	9.9	8.8	3.06
13764†	15P	21.21	5.57	2.89	62.59	4.06	1.80	0.85	0.14	1.28	0.0	0.28			0.28	0.86			41.7	29.4	9.9	8.8	3.06
13765†	15Q	21.23	5.58	2.89	62.92	4.06	1.80	0.76*	**	1.39	0.32				0.20	0.40			42.4	28.9	9.9	8.8	3.06
13766†	16S	21.55	6.10	2.49	64.00	3.16	1.80	0.81*	**	0.00	0.0				0.15	0.15			47.0	26.5	12.0	7.6	3.06
13767†	16P	21.51	6.10	2.49	63.83	3.15	1.80	0.93	0.23	0.39	0.35	0.32			0.20	0.38			45.0	27.8	12.0	7.6	3.06
13768†	16Q	21.53	6.10	2.49	63.95	3.16	1.80	0.81*	**	0.30	0.57				0.15	0.25			45.7	27.3	12.0	7.6	3.06
13778†	20S	19.37	7.35	3.77	65.31	0.98	1.80	0.68*	**	0.32	0.0				0.15	0.42			57.5	12.2	13.1	11.5	3.06
13779†	20P	19.35	7.34	3.77	65.08	0.97	1.80	0.91	0.15	1.24	0.0	0.45			0.18	0.76			53.0	15.5	13.1	11.5	3.06
13780†	20Q	19.34	7.34	3.77	65.28	0.98	1.80	0.73*	**	1.38	0.02				0.15	0.45			53.3	15.3	13.1	11.5	3.06

(Continued on next page)

TABLE A-2—(CONTINUED)

Lot No.	Ref. No.	Major Constituents						Loss on Ign.	Insol. Res.	Free CaO	Minor Constituents								Computed Compound Composition				
		SiO_2	Al_2O_3	Fe_2O_3	Total CaO	MgO	SO_3				FeO	TiO_2	P_2C_5	Mn_2O_3	Na_2O	K_2O	$CHCl_3$ Soluble	CO_2	C_3S	C_2S	C_3A	C_4AF	$CaSO_4$
14502		21.02	6.07	2.75	63.49	2.94	1.76	1.00	0.14	0.96					0.29	0.60			45	26	11	8	3.0
14560		20.78	5.03	3.98	64.99	1.35	2.27	0.99	—	0.39					0.22	0.31			60	17	7	13	4.04
14675		20.76	6.07	2.55	63.83	3.02	1.71	0.95	0.11	1.19					0.26	0.56			48.1	23.2	11.8	7.8	2.90
14898‡	39AQ	20.72	6.45	3.25	63.89	2.6	0.58	0.99	—	0.67									49.4	22.2	11.6	9.9	0.98
14899‡	40PC	20.80	6.52	3.12	63.69	2.5	0.65	0.91	—	1.16									47.5	23.8	12.0	9.5	1.11
14900‡	41SC	20.78	6.64	3.18	64.19	2.5	0.52	0.87	—	0.09									49.2	22.5	12.2	9.7	0.88
14901‡	42AQ	20.68	6.82	3.16	63.78	2.7	0.58	1.04	—	0.67									46.8	24.0	12.7	9.6	0.98
14902‡	43PC	20.72	6.92	3.18	63.63	2.4	0.61	0.92	—	0.97									45.2	25.4	12.9	9.7	1.03
14903‡	44SC	20.78	6.86	3.12	63.78	2.4	0.60	0.99	—	0.13									45.2	25.6	12.9	9.5	1.02
14904‡	45AQ	20.70	6.73	3.35	64.03	2.4	0.52	0.81	—	0.58									48.4	22.9	12.2	10.2	0.88
14905‡	46PC	20.48	6.82	3.12	63.88	2.6	0.57	1.02	—	0.81									48.8	22.0	12.8	9.5	0.96
14906‡	47SC	20.40	6.98	3.14	63.98	2.7	0.36	0.76	—	0.05									49.4	21.3	13.2	9.6	0.60
14907‡	48AQ	20.70	6.95	3.31	63.07	2.7	0.59	0.87	—	0.04									42.7	27.2	12.8	10.0	1.00
14908‡	49PC	20.94	6.79	3.39	63.12	2.7	0.61	1.02	—	0.24									42.0	28.4	12.2	10.3	1.03
14909‡	50SC	21.16	6.72	3.38	63.14	2.7	0.52	0.75	—	0.07									41.3	29.6	12.1	10.3	0.88
14910‡	52AQ	20.92	6.87	3.47	63.30	2.7	0.52	0.18	—	0.10									42.5	28.0	12.3	10.6	0.88
14911‡	51PC	20.88	7.23	3.51	63.09	2.7	0.48	0.23	—	0.04									39.6	30.1	13.2	10.7	0.82
14912‡	53SC	21.04	7.09	3.41	63.40	2.6	0.48	0.30	—	0.06									40.8	29.6	13.0	10.4	0.82
14913‡	54AQ	21.18	7.13	3.39	62.89	2.6	0.75	0.28	—	0.96									36.6	33.2	13.1	10.3	1.28
14914‡	55PC	21.08	7.09	3.49	62.84	—	0.76	0.37	—	0.63									37.3	32.4	12.9	10.6	1.29
14915‡	56SC	21.06	6.59	3.37	62.43	2.5	0.78	0.35	—	0.46									39.3	30.8	11.7	10.2	1.32
14930J		25.42	4.36	3.21	62.46	1.65	1.55	0.81	0.09	tr.					0.22	0.41		0.24	22.7	55.8	6.1	9.8	2.64
15007J		22.78	4.77	3.46	64.92	1.32	1.30	0.84	0.07	0.62					a	a		0.49	48.0	29.1	6.8	10.5	2.22
15008J		22.69	4.87	4.10	64.51	1.27	1.26	0.78	0.09	0.08					0.23	0.51	0.029d		47.7	29.1	6.0	12.5	2.14
15011J		23.09	4.73	3.45	64.62	1.19	1.43	0.67	0.12	0.40					b	b	0.014	0.66	45.1	29.1	6.7	10.5	2.43
15012J		23.65	4.39	3.25	64.53	1.09	1.34	0.77	0.15	0.37					0.22	0.49	0.054		43.0	35.4	6.1	9.9	2.28
15013J		20.98	6.85	2.43	62.75	3.52	1.71	0.74	0.07	0.64					c	c	***		39.0	29.0	14.0	7.0	3.00
15014J		21.18	6.42	2.40	62.96	3.61	1.61	0.70	0.08	0.59					0.32	0.49	0.041		41.7	29.3	13.0	7.3	2.73
15365		20.78	6.42	2.20	63.86	2.48	2.48	0.96	0.19	0.93	0.60	0.28	0.03	0.51	0.17	0.16	0.039	0.32	45.0	28.0	13.3	6.7	4.22
15367K		21.87	6.83	2.23	65.30	2.63	0.41	0.15	0.33	0.98	"	"	"	"	"	"	"	"	45.5	28.4	14.3	6.7	0.70
15495		20.04	5.52	2.50	66.42	1.28	1.82	1.71	0.26	3.14	0.03	0.26	0.08	0.06	0.30	0.40	0.005	0.16	59.4	13.0	10.4	7.6	3.10
15497		19.98	5.55	2.59	66.55	1.33	1.82	1.52	0.15	3.14	"	"	"	"	"	"	"	"	60.1	11.9	10.3	7.9	3.10
15498K		20.92	5.82	2.53	67.71	1.36	0.19	0.85	0.25	2.71	"	"	"	"	"	"	"	"	62.5	13.0	11.2	7.7	0.32

(Concluded on next page)

15623K		23.30	4.58	4.35	65.01	1.44	0.03	1.05	0.25	0.73	nil	0.30	0.14	0.09	0.05	0.17	0.002	0.22	47.6	30.9	4.8	13.2	0.06
15669		27.57	2.09	1.92	63.88	1.72	1.82	0.73	0.06	0.15	nil	0.11	0.03	0.09	0.05	0.22	0.009	0.26	33.0	54.2	2.3	5.8	3.10
15670K		27.95	2.07	1.87	65.61	1.83	0.17	0.26	0.13	0.23	"	"	"	"	"	"	"	"	37.4	51.9	2.4	5.7	0.27
15699K		22.72	5.38	2.48	64.06	3.43	0.20	0.37	0.16	nil	nil	0.25	0.13	0.09	1.13	0.44	0.006	0.16	47.9	29.0	10.1	7.6	0.34
15754		20.85	6.44	2.20	63.96	2.50	2.36	0.92	0.19	0.93	0.60	0.28	0.03	0.51	0.17	0.16	0.039	0.32	45.0	27.7	13.4	6.7	4.0
15756		22.50	4.39	4.14	64.31	1.46	1.73	1.28	0.13	0.49	nil	0.30	0.14	0.09	0.05	0.17	0.002	0.22	48.6	27.9	4.7	12.6	2.9
15758		19.98	5.50	2.55	66.57	1.25	1.84	1.55	0.17	3.14	0.03	0.26	0.08	0.06	0.30	0.40	0.005	0.16	60.6	11.6	10.2	7.7	3.2
15761		22.00	5.25	2.47	62.98	3.42	1.82	0.53	0.07	nil	nil	0.25	0.13	0.09	1.13	0.44	0.006	0.16	44.9	29.2	9.8	7.5	3.1
15763		27.52	2.09	1.96	63.93	1.70	1.88	0.75	0.07	0.15	nil	0.11	0.03	0.09	0.05	0.22	0.009	0.26	33.5	53.6	2.3	6.0	3.2
15921§		21.87	6.83	2.23	65.30	2.63	0.41	0.15	0.33	0.98	0.60	0.28	0.03	0.51	0.17	0.16	0.039	0.32	45.5	28.4	14.3	6.7	0.7
15922§		21.43	6.69	2.19	63.99	2.58	2.36	0.15	0.32	0.96	"	"	"	"	"	"	"	"	44.6	27.8	14.0	6.6	4.0
15923§		20.81	6.50	2.12	62.15	2.50	5.00	0.14	0.31	0.93	"	"	"	"	"	"	"	"	43.3	27.0	13.6	6.4	8.5
15924§		20.92	5.82	2.53	67.71	1.36	0.19	0.85	0.25	2.71	0.03	0.26	0.08	0.06	0.30	0.40	0.005	0.16	62.5	13.0	11.2	7.7	0.3
15925§		20.57	5.72	2.49	66.57	1.34	1.85	0.84	0.25	2.66	"	"	"	"	"	"	"	"	61.4	12.8	11.0	7.6	3.1
15926§		19.86	5.53	2.40	64.28	1.29	5.00	0.81	0.24	2.57	"	"	"	"	"	"	"	"	59.3	12.3	10.6	7.3	8.5
15927§		23.30	4.58	4.35	65.01	1.44	0.03	1.05	0.25	0.73	nil	0.30	0.14	0.09	0.05	0.17	0.002	0.22	49.2	28.5	4.4	12.8	2.7
15929§		22.08	4.34	4.12	61.61	1.36	5.00	1.00	0.24	0.69	"	"	"	"	"	"	"	"	46.6	27.0	4.2	12.1	8.5
15930§		27.95	2.07	1.87	65.61	1.83	0.17	0.26	0.13	0.23	nil	0.11	0.03	0.09	0.05	0.22	0.009	0.26	37.4	51.9	2.4	5.7	0.3
15932§		26.53	1.96	1.78	62.28	1.74	5.00	0.25	0.12	0.22	"	"	"	"	"	"	"	"	35.5	49.3	2.3	5.4	8.5
15933§		22.72	5.38	2.48	64.06	3.43	0.20	0.37	0.16	nil	nil	0.25	0.13	0.09	1.13	0.44	0.006	0.16	47.9	29.0	10.1	7.6	0.3
15934§		22.35	5.29	2.44	63.01	3.37	1.81	0.36	0.16	nil	"	"	"	"	"	"	"	"	47.1	28.5	9.9	7.5	3.1
15935§		21.57	5.11	2.35	60.82	3.26	5.00	0.35	0.15	nil	"	"	"	"	"	"	"	"	45.5	27.5	9.6	7.2	8.5
16186		21.13	6.42	2.20	63.89	2.49	2.45	0.95	0.19	0.93	0.60	0.28	0.03	0.51	0.17	0.16	0.039	0.32	45.0	27.9	13.3	6.7	4.1
16189		22.50	4.38	4.16	64.31	1.46	1.72	1.28	0.13	0.49	nil	0.30	0.14	0.09	0.05	0.17	0.002	0.22	48.7	27.9	4.7	12.6	2.9
16198		27.54	2.09	1.95	63.91	1.71	1.86	0.74	0.07	0.15	nil	0.11	0.03	0.09	0.05	0.22	0.009	0.26	33.4	53.9	2.3	5.9	3.2
16213		20.88	6.48	2.21	63.99	2.52	2.27	0.91	0.25	0.93	0.60	0.28	0.03	0.51	0.17	0.16	0.039	0.32	44.8	27.1	13.4	6.8	3.9
16214		20.81	6.43	2.20	63.90	2.49	2.42	0.94	0.21	0.93	"	"	"	"	"	"	"	"	44.9	27.7	13.3	6.7	4.1

† Minor constituents on clinker basis.
‡ These analyses were made in the plants furnishing the clinker, except for SO_3 and free CaO which were determined in this laboratory. The values are based on clinker weights instead of cement weights.
§ Ground in laboratory.
K Clinker
* The loss on ignition for the clinker was not determined. The values shown here represent the loss on ignition from the gypsum and that from the clinker.
** Not determined.
*** 0.008% tallow; 0.005% Vinsol resin.
a Alkali analyses made on 15008J.
b " " " " 15012J.
c " " " " 15014J.
d Tallow.

TABLE A-3—DENSITY, SPECIFIC VOLUME,

Lot No.	Density and Specific Volume, as Computed from Displacement in				Specific Surface cm^2/g A.S.T.M.
	Kerosene		Water		
	Density g/cm^3	Sp. Vol. cm^3/g	Density g/cm^3	Sp. Vol. cm^3/g	
13495	3.161	0.316			1868
13721	3.130	0.320			1645
13722	3.110	0.322			1745
13723	3.109	0.322			1535
13730					1735
13731					1800
13732					1705
13733					1790
13734					1715
13735					1665
13736	3.163	0.316			1685
13737	3.152	0.317			1815
13738	3.139	0.319			1715
13740					1655
13741					1655
13752					1740
13753					1610
13763	3.165	0.316			1780
13764	3.143	0.318			1630
13765	3.104	0.322			1800
13766					1845
13767					1735
13768					1745
13778	3.145	0.318			1705
13779	3.135	0.319			1730
13780	3.128	0.320			1695
14502	3.145	0.318			1820*
14560	3.154	0.317	3.184	0.314	1085
14560	3.150	0.318	3.170	0.316	1540
14560	3.155	0.317	3.192	0.314	2045
14560	3.156	0.317	3.206	0.312	2550
14675	3.143	0.318			1865
14898	3.140	0.318			1620
14899					1610
14900					1620
14901	3.150	0.318	3.197	0.313	1640
14902					1590
14903	3.167	0.316	3.225	0.310	1630
14904					1580
14905					1610
14906					1620
14907					1660
14908					1630

a. All those cements marked a were ground in the laboratory. The rest were ground in commercial plants.
b. This includes +325 material.
c. Densities of these cements were not determined. The values given are for cements of similar fineness made from the same clinker, but no allowance was made for differences in gypsum content.
* 1560 cm^2/g by the permeability method.

AND SPECIFIC SURFACE OF CEMENTS

Lot No.	Density and Specific Volume, as Computed from Displacement in				Specific Surface, cm^2/g	
	Kerosene		Water			
	Density g/cm^3	Sp. Vol. cm^3/g	Density g/cm^3	Sp. Vol. cm^3/g	A.S.T.M.	Permeability Method
14909					1630	
14910	3.165	0.316	3.207	0.312	1610	
14911					1620	
14912	3.181	0.314	3.228	0.310	1640	
14913					1640	
14914	3.144	0.318			1610	
14915					1650	
14930J	3.218	0.311	3.290	0.304	2045	
15007J	3.189	0.314	3.260	0.307	2015	
15008J	3.201	0.312	3.239	0.309	1825	
15011J	3.204	0.312	3.263	0.306	1835	
15012J	3.191	0.314			1740	
15013J	3.162	0.316	3.247	0.308	1810	
15014J	3.174	0.315			2010	
15365	3.135	0.319	3.187	0.314	1640	3120
15495	3.101	0.322	3.136	0.319	1440	2780
15497	3.109	0.322	3.178	0.315	2500	5150
15669	3.215	0.311	3.257	0.307	2290	3810
15754	3.135	0.319	3.174	0.315	1800	3420
15756	3.174	0.315	3.209	0.312	1800	3060
15758	3.107	0.322	3.158	0.317	1800	3570
15761	3.155	0.317	3.210	0.312	1800	2950
15763	3.215	0.311	3.252	0.308	1800	2760
15921 a	3.135 c	0.319	3.190 c	0.314	1820	2870
15922 a	"	"	"	"	1890	3350
15923 a	"	"	"	"	2070	4850
15924 a	3.107 c	0.322	3.16 c	0.316	1815	2930
15925 a	"	"	"	"	1870	3360
15926 a	"	"	"	"	2020	4580
15927 a	3.176 c	0.315	3.22 c	0.310	1800	2860
15929 a	"	"	"	"	2080	4770
15930 a	3.215 c	0.311	3.25 c	0.308	1795	2630
15932 a	"	"	"	"	2050	4280
15933 a	3.155 c	0.317	3.21 c	0.312	1820	2960
15934 a	"	"	"	"	1855	3480
15935 a	"	"	"	"	2080	4480
16186	3.135	0.319	3.188	0.314	1702 b	3200
16189	3.174	0.315	3.214	0.312	1849 b	3200
16198	3.215	0.311	3.254	0.308	2014 b	3200
16213	3.135	0.319	3.179	0.315	1263	2430
16214	3.135	0.319	3.184	0.314	1528	2920

TABLE A-4—UNIT ABSOLUTE VOLUME COMPOSITION OF THE MORTARS USED IN SERIES 254-265

Ref. No.	Unit Absolute Volume Composition				Water-Cement Ratio		
	Cement	Sand	Water	Air	Volume Basis	Wt. Basis	Gal/Sk.
323	0.5601	—	0.4169	0.0192	0.744	0.236	2.66
506	0.4046	0.2438	0.3331	0.0189	0.823	0.262	2.95
509	0.3195	0.3850	0.2826	0.0129	0.884	0.268	3.17
512	0.2221	0.5353	0.2264	0.0162	1.019	0.323	3.65
515	0.1666	0.6022	0.2075	0.0237	1.245	0.395	4.46
518	0.1062	0.6399	0.2250	0.0289	2.118	0.670	7.59
521	0.0787	0.6638	0.2216	0.0359	2.816	0.893	10.09

TABLE A-5—ANALYSES OF GRANULAR SAMPLES USED FOR ADSORPTION AND NON-EVAPORABLE WATER MEASUREMENTS IN SERIES 254-265

Ref. No.	Cement Cont. Sol. SiO_2 Meth. % dry weight	Cement Cont. SO_3 Meth. % dry weight	Ignition Loss, % dry weight	CO_2(1) Loss % dry weight	Non-Evap. Water(2) % dry weight	Non-Evap. Water, % cement content		Sand Content (by difference)	
						Sol. SiO_2	SO_3 Meth.	Sol. SiO_2	SO_3 Meth.
323	85.6(3)	—	14.42	0.67	13.7	16	—	0.7	—
506	66	70	17.50	4.99	12.5	19	18	21.0	17.8
509	57	62	19.01	7.58	11.4	20	18	23.1	26.3
512	47	52	20.45	9.91	10.5	22	20	42.4	37.0
515	41	47	22.63	11.86	10.8	26	23	48.0	42.5
518	39	42	21.92	12.40	9.5	24	23	51.8	48.6
521	34	36	21.26	13.22	8.0	23	22	57.7	55.5

(1) CO_2 comes chiefly from calcareous sand (Elgin).
(2) Non-evaporable water obtained by correcting loss on ignition for CO_2-loss.
(3) Ignited weight taken as cement content since this is a neat paste.

TABLE A-6—ADSORPTION DATA FOR SERIES 254-265

Age: 110 days

p/p_s	Total Water Retained at Relative Vapor Pressure Indicated, g/g dry weight						
	Ref. 323	Ref. 506	Ref. 509	Ref. 512	Ref. 515	Ref. 518	Ref. 521
w_n	.137	.125	.114	.105	.108	.095	.080
0.11	.1474	.1384	.1237	.1121	.1141	.1008	.0836
0.20	.1552	.1448	.1310	.1183	.1199	.1060	.0884
0.36	.1649	.1544	.1396	.1254	.1274	.1128	.0945
0.50	.1752	.1626	.1472	.1331	.1353	.1206	.1009
0.61	.1811	.1683	.1526	.1382	.1400	.1264	.1052
0.75	.1947	.1800	.1634	.1491	.1532	.1443	.1224
0.80	.1962	.1826	.1649	.1510	.1558	.1453	.1252
0.826	.2013	.1862	.1703	.1569	.1636	.1560	.1327
0.888	.2085	.1941	.1776	.1629	.1731	.1651	.1431
0.93	.2201	.2022	.1868	.1730	.1850	.1865	.1592
0.98	.2225	.2053	.1887	.1767	.1888	.1991	.1718
SSD	.250	.220	.210	.197	.227	.267	.259

w_n = non-evaporable water, p/p_s = about 24×10^{-6}.
SSD = Water content of granular sample, saturated, surface-dry for sample that had been dried and resaturated.

Description of specimens made in series 254-MRB

Neat Specimens: Cylinders, 1x7 in.

Cements: See Tables A-1 to A-3.

Burning Conditions: Lot Nos. 14910, 14911, 14912: hard burned; Lot Nos. 14913, 14914, 14915; soft-burned; others: normal plant burning. Changes in burning condition were brought about by changing length of burning zone.

Cooling Condition: The symbol PC signifies cooling by regular plant method; SC signifies slow cooling by storage in an insulated box where temperatures at or above red-heat were maintained for about 24 hours; AQ signifies cooling to temperatures below dull-red within 10 seconds by use of an air-blast.

Grinding: In the laboratory mill with enough added gypsum for 1.8 percent total SO_3.

Mixing: The cement was placed with water in a kitchen-type mixer and mixed for 2 minutes, allowed to rest for 1 minute, and then mixed for 1 minute. w/c = 0.5 by weight at mixing.

Casting: The pastes were poured into 1x7-in. waxed-paper cylinders.

Curing: In the molds under water. Molds stored horizontally.

Drying: The granular samples were dried in a vacuum desiccator over $Mg(ClO_4)_2 \cdot 2H_2O$.

Adsorption Data: See Table A-7.

TABLE A-7—ADSORPTION DATA FOR SERIES 254-MRB

Water-cement ratio corrected for bleeding

p/p_s	Total Water Retained at Relative Vapor Pressure Indicated, g/g cement								
	14898-1AQ w_o/c = .382 Age 120d	14899-1PC w_o/c = .388 Age 120d	14900-1SC w_o/c = .446 Age 126d	14901-2AQ w_o/c = .391 Age 126d	14902-2PC w_o/c = .393 Age 133d	14903-2SC w_o/c = .424 Age 133d	14904-3AQ w_o/c = .425 Age 162d	14905-3PC w_o/c = .411 Age 162d	14906-3SC w_o/c = .476 Age 173d
w_n	.2171	.2225	.2274	.2228	.2273	.2271	.2284	.2299	.2355
.088	.2615	.2614	.2684	.2629	.2665	.2664	.2723	.2757	.2794
.20	.2737	.2781	.2848	.2755	.2825	.2823	.2891	.2924	.2966
.355	.2977	.3034	.3111	.2992	.3092	.3091	.3143	.3184	.3271
.51	.3179	.3209	.3245	.3116	.3285	.3277	.3333	.3393	.2510
.61	.3298	.3355	.3534	.3332	.3422	.3448	.3485	.3529	.3702
.69	.3461	.3511	.3656	.3437	.3578	.3602	.3578	.3631	.3831
.75	.3610	.3666	.3852	.3649	.3743	.3797	.3749	.3811	.4048
.80	.3675	.3724	.3918	.3700	.3807	.3842	.3824	.3879	.4107
.84	.3782	.3813	.4000	.3803	.3883	.3926	.3941	.3982	.4217
.89	.3971	.3983	.4100	.3908	.3981	.3996	.4168	.4176	.4438
.96	.4318	.4225	.4459	.4491	.4475	.4401	.4553	.4469	.4737
SSD	.4604	.4581	.5082	.4911	.5013	.5106	.4897	.4898	.5496
SSDO	—	—	.5267	.5031	.5108	.5261	.4993	.5021	.5673

p/p_s	Total Water Retained at Relative Vapor Pressure Indicated, g/g cement								
	14907-4AQ w_o/c = .406 Age 173d	14908-4PC w_o/c = .394 Age 200d	14909-4SC w_o/c = .483 Age 200d	14910-5AQ w_o/c = .460 Age 204d	14911-5PC w_o/c = .464 Age 204d	14912-5SC w_o/c = .489 Age 212d	14913-6AQ w_o/c = .410 Age 212d	14914-6PC w_o/c = .423 Age 222d	14915-6SC w_o/c = .437 Age 222d
w_n	.2191	.2250	.2255	.2282	.2294	.2252	.2206	.2253	.2240
.088	.2605	.2673	.2669	.2704	.2723	.2703	.2665	.2675	.2667
.20	.2789	.2853	.2846	.2865	.2940	.2883	.2839	.2847	.2830
.355	.3037	.3108	.3119	.3142	.3166	.3167	.3075	.3101	.3097
.51	.3231	.3327	.3346	.3365	.3383	.3416	.3275	.3293	.3299
.61	.3354	.3463	.3496	.3470	.3496	.3558	.3389	.3443	.3441
.69	.3459	.3573	.3639	.3533	.3571	.3698	.3514	.3537	.3562
.75	.3629	.3764	.3871	.3793	.3832	.3907	.3678	.3736	.3759
.80	.3683	.3835	.3948	.3844	.3905	.3956	.3704	.3771	.3787
.84	.3766	.3920	.4061	.3952	.4017	.4048	.3771	.3847	.3869
.89	.4027	.4136	.4333	.4280	.4365	.4300	.4061	.4137	.4149
.96	.4279	.4394	.4659	.4706	.4801	.4547	.4314	.4347	.4327
SSD	.4606	.4771	.5477	.5131	.5259	.5473	.4767	.4870	.5203
SSDO	.4741	.4922	.5725	.5348	.5458	.5675	.4932	—	.5296

Key: *SSD* = Water content of granular sample, saturated, surface-dry for sample that had been dried and resaturated.
SSDO = Water content of granular sample that was brought to saturated condition without preliminary drying.
AQ = Air quenched.
PC = Plant cooled.
SC = Slow cooled.
w_n = Non-evaporable water; p/p_s = about 24×10^{-6}.

Description of specimens made in series 254-K4B

Neat Specimens: Cylinders, 1x7½ in.

Cements: See Tables A-1 to A-3.

Cooling: Symbol P signifies regular plant cooling; S signifies slow cooling after reheating clinker; Q signifies quick cooling after reheating clinker.

Grinding: In the laboratory mill with enough added gypsum for 1.8 percent total SO_3.

Mixing: The cement was placed with water in a kitchen-type mixer and mixed for 2 minutes, allowed to rest for 2 minutes, and then mixed for 2 minutes. w/c = 0.5 by weight at mixing.

Casting: The pastes were poured into 1x7½-in. cylindrical molds.

Curing: In the molds stored horizontally under water for 20-24 hrs.; under water thereafter. Temperature: 70 F.

Drying: The granular samples (48-100 mesh) were dried in a vacuum desiccator over $Mg(ClO_4)_2.2H_2O$.

Adsorption Data: See Table A-8.

Description of specimens made in series 254-7

Mortar Specimens: Truncated cones: base, 4 in.; top, 2 in.; altitude, 6 in.

Cement: Lot 14675. See Tables A-2 and A-3 for characteristics.

Batches: The batches were made up as follows:

Ref. No.	Mix by Wt.	Weights, gms. per batch						Cement g	Water, ml
		Ottawa Silica			Cow Bay Sand				
		200–100	100–48	48–28	28–14	14–8	8–4		
7–1	1–0	—	—	—	—	—	—	4000	1010
7–2	1–½	36	73	125	579	301	386	3000	830
7–3	1–1	54	110	187	868	453	578	2250	675
7–4	1–2	77	157	266	1234	644	822	1600	570
7–5	1–3	86	177	299	1389	724	925	1200	545
7–6	1–4	90	184	311	1447	654	1064	938	590
7–7	1–5	90	184	311	1447	654	1064	750	570

Mixing: Each batch was mixed 30 sec. dry and 2 min. wet, in a small power-driven, open-tub mixer.

Molding: From each batch 3 watertight molds of known capacity were filled. The mortar was puddled with a light tamper.

Measurements: The weight of the filled calibrated mold was measured to 1 g immediately after filling, and again after 20-24 hr. in the fog-room. On stripping, the weights of the specimen in air and in water were obtained.

Curing: In molds in the fog-room for the first 20-24 hr.; under water thereafter. Temperature: 70 F. Some of the molds were not stripped until the specimens were 48 hr. old, but the specimens were nevertheless immersed after the first 24 hr.

Drying: The granular samples were dried in a vacuum desiccator over $Mg(ClO_4)_2.2H_2O$.

Cement-Silica Specimens: Cylinders cast in test tubes (⅞ x 6 in.)

Cement: Lot 14675. See Tables A-2 and A-3 for characteristics.

Silica: Lot 13239. 95 percent passing No. 200-mesh sieve.

Proportions:

Ref. No.	Proportions by Wt.			c/SiO_2	Nominal w/c	
	Cement c	Silica SiO_2	Water w		wt.	gal/sk
1	0.736	0	0.264	100/0	0.36	4.06
2	0.590	0.148	0.262	80/20	0.444	5.00
3	0.483	0.260	0.257	65/35	0.530	5.97
4	0.411	0.336	0.253	55/45	0.618	6.96
5	0.376	0.376	0.248	50/50	0.660	7.43

Mixing: Cement and silica were premixed by tumbling them together in a large glass bottle. The dry material was placed with water in a kitchen-type mixer, and mixed for 2 minutes, allowed to rest for 3 minutes, and then mixed for 2 minutes.

Casting: The pastes were poured into ⅞ x 6 in. test tubes which had previously been calibrated by filling them with water from a burette.

Curing: The level-full test tubes were stored under water until the third day after casting, at which time the glass molds were broken off and the specimens were reimmersed in water where they remained until tested.

Drying: The granular samples were dried in a vacuum desiccator over $Mg(ClO_4)_2 \cdot 2H_2O$.

Test Results: All test results are given in Part 5.

Description of specimens made in series 254-8

Mortar Specimens: Cubes, 2 in.

Cements: See Tables A-1 to A-3.

Pulverized Silica: About same fineness, volume basis, as cement.

Proportions:

Mix	Relative Proportions			w/c by weight (approx.)
	Cement	Pulverized Silica	Std. Ottawa Sand	
A	1	0	1.64	0.33
B	1	0.330	2.30	0.46
C	1	0.707	3.07	0.61

Mixing: Each batch was mixed 30 sec. dry and 2 min. wet, in a small power-driven, open-tub mixer before making slump test. Slump-sample returned to tub and batch mixed additional 30 sec. before casting.

Slump Test: Made in duplicate on 6-in. cone. Water adjusted to give 1½-2-in. slump.

Molding: From each batch 3 cubes were cast in previously weighed, 3-gang, steel molds.

Measurements: The weight of the filled molds was measured to 1 g immediately after filling, and again 2-2¼ hr. later after carefully removing any accumulated water with a suitable absorbent. The molds were dried and weighed again just prior to stripping. After stripping, the cubes were weighed in air and in water.

Curing: In molds in the fog-room for the first 20-24 hr.; then under water for 27 days; thereafter in the fog-room.

Drying: The granular samples were dried in a vacuum desiccator over $Mg(ClO_4)_2 \cdot 2H_2O$.

Composition of Specimens: The composition of the hardened cubes, derived from the measurements mentioned above, are given in Table A-9.

TABLE A-8—ADSORPTION DATA FOR SERIES 254-K4B

Water-cement ratios corrected for bleeding

p/p_s	Total Water Retained at Relative Vapor Pressure Indicated, g/g cement											
	13721–1S $w_o/c = .470$ Age 174d	13722–1P $w_o/c = .473$ Age 180d	13723–1Q $w_o/c = .425$ Age 180d	13730–4S $w_o/c = .463$ Age 144d	13731–4P $w_o/c = .460$ Age 138d	13732–4Q $w_o/c = .450$ Age 138d	13733–5S $w_o/c = .427$ Age 150d	13734–5P $w_o/c = .453$ Age 146d	13735–5Q $w_o/c = .456$ Age 150d	13736–6S $w_o/c = .471$ Age 196d	13737–6P $w_o/c =$ Age 191d	13738–6Q $w_o/c = .447$ Age 191d
w_n	.2231	.2332	.2290	.1786	.1772	.1773	.1650	.1589	.1650	.2148	.2297	.2220
.09	.2666	.2769	.2709	.2128	.2072	.2087	.1994	.1936	.1983	.2568	.2729	.2612
.20	.2830	.2934	.2863	.2268	.2173	.2211	.2136	.2071	.2140	.2723	.2904	.2764
.355	.3123	.3208	.3143	.2464	.2363	.2396	.2337	.2253	.2311	.2978	.3181	.3011
.50	.3910	.3478	.3405	.2646	.2516	.2554	.2502	.2404	.2491	.3266	.3487	.3277
.61	.3561	.3595	.3508	.2772	.2647	.2689	.2608	.2517	.2610	.3397	.3634	.3368
.69	.3746	.3783	.3673	.2917	.2783	.2777	.2770	.2667	.2756	.3574	.3818	.3535
.75a	.3899	.3894	.3799	.2159	.3056	.2999	.2975	.2889	.2968	.3675	.3940	.3667
.80b	.3962	.3999	.3878	.3180	.3121	.3037	.2999	.2922	.2996	.3761	.4020	.3734
.84	.4029	.4079	.3943	.3259	.3215	.3112	.3091	.3010	.3088	.3824	.4095	.3801
.89	.4294	.4457	.4269	.3718	.3698	.3528	.3482	.3446	.3513	.4099	.4337	.4145
.96	.4477	.4727	.4497	.4116	.4056	.3916	.3839	.3842	.3890	.4318	.4554	.4478
SSD	.5433	.5590	.5022	.5098	.5122	.4949	.4976	.5093	.5139	.5085	.5189	.5125
SSDO	.5572	.5755	.5149	.5249	.5349	.5148	.5102	.5193	.5268	.5295	.5462	.5361

(Concluded on next page)

p/p_s	Total Water Retained at Relative Vapor Pressure Indicated, g/g cement												
	13740–7P w_o/c = .473 Age 164d	13741–7Q w_o/c = .480 Age 171d	13752–11P w_o/c = .445 Age 164d	13753–11Q w_o/c = .440 Age 172d	13763–15S w_o/c = .485 Age 202d	13764–15P w_o/c = Age 196d	13765–15Q w_o/c = .445 Age 202d	13766–16S w_o/c = Age 322d	13767–16P w_o/c = .464 Age 223d	13768–16Q w_o/c = .456 Age 223d	13778–20S w_o/c = .472 Age 170d	13779–20P w_o/c = .462 Age 167d	13780–20Q w_o/c = .436 Age 176d
w_n	.2395	.2390	.1864	.1896	.2173	.2109	.2201	.2096	.2256	.2250	.2308	.2329	.2262
.09	—	.2810	—	.2267	.2589	.2494	.2591	.2501	.2709	.2689	.2736	.2730	.2664
.20	.3051	.2988	.2386	.2403	.2735	.2653	.2735	.2695	.2869	.2854	.2914	.2894	.2816
.355	.3372	.3256	.2611	.2651	.3017	.2874	.2972	.2933	.3163	.3131	.3183	.3130	.3073
.50 c	.3653	.3536	.2782	.2826	.3224	.3133	.3050	.3094	.3379	.3324	.3443	.3383	.3326
.61	.3812	.3660	.2904	.2944	.3343	.3238	.3234	.3323	.3522	.3427	.3597	.3531	.3447
.69	.4003	.3840	.3074	.3125	.3665	.3387	.3583	.3441	.3749	.3673	.3766	.3636	.3624
.747 d	.4098	.3960	.3188	.3240	.3794	.3514	.3596	.3595	.3869	.3778	.3888	.3821	.3740
.802 e	.4215	.4048	.3316	.3346	.3758	.3588	.3604	.3693	.3987	.3927	.3974	.3908	.3811
.84	.4284	.4110	.3378	.3401	.3906	.3634	.3749	.3844	.4048	.3925	.4035	.3977	.3870
.89	.4518	.4450	.3767	.3770	.4202	.3979	.4174	.4114	.4331	.4255	.4301	.4245	.4157
.96	.4671	.4671	.4098	.4148	.4391	.4244	.4542	.4376	.4500	.4426	.4499	.4440	.4366
SSD	.5564	.5489	.5162	.5087	.5362	.5008	.5290	.5459	.5253	.5021	.5426	.5424	.5080
SSDO	.5751	.5639	.5323	.5158	.5613	.5167	.5445	.5641	.5413	.5196	.5544	.5548	.5194

a–p/p_s = 0.747 for Refs. 6-S, 6-P and 6-Q.
b– " = 0.802 for Refs. " " " ".
c– " = 0.476 for Refs. 15-S, 15-P, and 15-Q; p/p_s = 0.47 for Refs. 16-S, 16-P, and 16-Q.
d- " = 0.75 for 16-S, 16-P, and 16-Q.
e- " = 0.805 for " " " ".

Key: *SSD* = Water content of granular sample, saturated, surface-dry for sample that had been dried and resaturated.
SSDO = Water content of granular sample that was brought to saturated condition without preliminary drying.
S = Slow cooled after reheating clinker.
P = "Plant cooled."
Q = Quick-cooled after reheating clinker.
w_n = Non-evaporable water; p/p_s = about 24×10^{-6}.

TABLE A-9—UNIT ABSOLUTE VOLUME COMPOSITION OF THE MORTARS USED IN SERIES 254-8

Cement No.	Ref. No.	Unit Absolute Volume Composition at End of the 2nd Hour				w/c at 2 hours	Cement Content of Paste
		Cement	Water	Air	Silica		
14930J	8–1	.2375	.2431	.035	.4843	.311	.494
	8–2	.1692	.2466	.032	.5521	.443	.407
	8–3	.1271	.2492	.029	.5953	.595	.338
15007J	8–28	.2363	.2649	.021	.4776	.344	.471
	8–29	.1698	.2567	.025	.5491	.464	.398
	8–30	.1288	.2500	.024	.5978	.595	.340
15008J	8–32	.1647	.2477	.055	.5322	.462	.399
	8–33	.1251	.2405	.055	.5796	.590	.342
15011J	8–40	.2407	.2508	.022	.4870	.319	.490
	8–41	.1730	.2494	.018	.5598	.442	.410
	8–42	.1298	.2522	.015	.6029	.595	.340
15012J	8–44	.1606	.2419	.077	.5207	.461	.399
	8–45	.1202	.2472	.068	.5636	.624	.329
15013J	8–46	.2345	.2532	.040	.4721	.332	.481
	8–47	.1713	.2520	.025	.5516	.453	.405
	8–48	.1260	.2455	.046	.5825	.599	.339
15014J	8–50	.1566	.2595	.079	.5045	.510	.376
	8–51	.1201	.2511	.074	.5548	.644	.324

Adsorption Data: See Table A-10.

TABLE A-10—ADSORPTION DATA FOR SERIES 254-8

Water-cement ratio corrected for bleeding

p/p_s	Total Water Retained at Relative Vapor Pressure Indicated, g/g cement								
	14930J-8-1 w_o/c = .311 Age 447d	14930J-8-2 w_o/c = .443 Age 362d	14930J-8-3 w_o/c = .595 Age 362d	15007J-8-28 w_o/c = .344 Age 479d	15007J-8-29 w_o/c = .464 Age 440d	15007J-8-30 w_o/c = .595 Age 479d	15008J-8-32 w_o/c = .462 Age 463d	15008J-8-33 w_o/c = .590 Age 463d	15011J-8-40 w_o/c = .319 Age 478d
w_n	.1808	.2006	.2101	.1980	.2169	.2323	.2105	.2208	.1843
.09	.2199	—	.2616	.2370	.2578	.2760	.2472	.2604	.2210
.20	.2360	.2641	.2765	.2538	.2759	.2939	.2641	.2798	.2375
.36	.2566	.2889	.3048	.2765	.2997	.3183	.2863	.3022	.2565
.47	.2681	.3042	.3224	.2918	.3191	.3367	.3024	.3237	.2699
.61	.2798	.3205	.3444	.3100	.3411	.3574	.3221	.3480	.2836
.69	.2888	.3346	.3624	.3179	.3591	.3752	.3361	.3690	.2912
.75	.2994	.3495	.3842	.3249	.3739	.3972	.3471	.3828	.2979
.81	.3057	.3626	.3975	.3350	.3832	.4126	.3673	.4084	.3080
.84	.3132	.3732	.4082	.3401	.3919	.4298	.3789	.4278	.3107
.89	.3290	.4024	.4674	.3489	.4221	.4831	.3933	.4461	.3218
.96	.3479	.4234	.4909	.3762	.4477	.5266	.4442	.5206	.3460
SSD	.3934	.5314	.6852	.4248	.5267	.6711	.5383	.6763	.2892
SSDO	.4132	.5431	.7060	.6228	.5600	.7178	—	—	—

p/p_s	Total Water Retained at Relative Vapor Pressure Indicated, g/g cement								
	15011J-8-41 w_o/c = .442 Age 368d	15011J-8-42 w_o/c = .595 Age 368d	15012J-8-44 w_o/c = .461 Age 464d	15012J-8-45 w_o/c = .624 Age 464d	15013J-8-46 w_o/c = .332 Age 339d	15013J-8-47 w_o/c = .453 Age 333d	15013J-8-48 w_o/c = .599 Age 333d	15014J-8-50 w_o/c = .510 Age 487d	15014J-8-51 w_o/c = .644 Age 487d
w_n	.2102	.2218	.2109	.2227	.2185	.2407	.2527	.2472	.2527
.09	.2503	.2640	.2519	.2657	.2567	.2829	.2932	.2885	.2961
.20	.2667	.2817	.2694	.2835	.2737	.2991	.3103	.3079	.3152
.36	.2921	.3073	.2922	.3080	.2934	.3252	.3348	.3373	.3439
.47	.3149	.3329	.3137	.3315	.3076	.3446	.3546	.3587	.3685
.61	.3345	.3548	.3336	.3586	.3163	.3643	.3793	.3834	.3951
.69	.3463	.3745	.3504	.3761	.3333	.3746	.3942	.4050	.4205
.75	.3581	.3931	.3613	.3892	.3424	.3931	.4148	.4199	.4422
.81	.3657	.4003	.3794	.4145	.3468	.4002	.4281	.4359	.4627
.84	.3828	.4232	.3906	.4320	.3514	.4089	.4387	.4436	.4732
.89	.4131	.4659	.4066	.4546	.3673	.4375	.4820	.4656	.5065
.96	.4338	.4975	.4608	.5295	.3826	.4619	.5203	.5116	.5701
SSD	.5246	.6426	.5738	.6978	.4245	.5587	.6886	.6355	.7769
SSDO	.5306	.6756	—	—	.4461	—	—	—	—

Key: *SSD* = Water content of granular sample, saturated, surface-dry for sample that had been dried and resaturated.
SSDO = Water content of granular sample that was brought to saturated condition without preliminary drying.
w_n = Non-evaporable water; p/p_s = about 24×10^{-6}.

Description of specimens made in series 254-9

Mortar Specimens: Cubes, 2-in.; Prism, 2x2x9½ in.

Cements: See Tables A-1 to A-3.

Pulverized Silica: Lot 15282. Specific surface, volume basis, about the same as that of cement.

Batches: The batches were made up as follows:

Mix	Weights, gms. per batch			Water (approx.)	Nominal w/c by Weight
	Cement	Pulverized Silica	Std. Ottawa Sand		
A	1900	—	3100	620	0.326
B	1350	450	3100	610	0.452
C	1000	730	3100	600	0.600

Mixing: As in Series 254-8.

Slump Test: As in Series 254-8.

Molding: From each batch 12 cubes and 1 prism were cast in previously weighed steel molds.

Measurements: Cubes: as in Series 254-8. Prism: the prism was weighed in air and in water at 28 days.

Curing: As in Series 254-8.

Drying: As in Series 254-8.

Test results for series 254-9

Composition of Hardened Specimens: The composition of the mortars in the hardened cubes, derived as in Series 254-8, is given in Table A-11.

TABLE A-11—UNIT ABSOLUTE VOLUME COMPOSITION OF THE MORTARS USED IN SERIES 254-9

Cement No.	Ref. No.	Mix	Unit Absolute Volume Composition at the End of the 2nd Hour				w/c at 2 hrs. (wt. basis)
			Cement	Water	Air	Silica	
14930J	9–1	A	.2401	.2437	.0308	.4863	.309
	9–2	B	.1718	.2397	.0284	.5610	.424
	9–3	C	.1268	.2380	.0292	.6072	.573
15007J	9–4	A	.2402	.2474	.0312	.4821	.316
	9–5	B	.1721	.2422	.0289	.5568	.433
	9–6	C	.1292	.2434	.0211	.6062	.570
15011J	9–7	A	.2415	.2493	.0245	.4852	.316
	9–8	B	.1727	.2445	.0240	.5593	.432
	9–9	C	.1288	.2394	.0251	.6073	.582
15013J	9–10	A	.2407	.2538	.0248	.4813	.324
	9–11	B	.1709	.2457	.0341	.5504	.443
	9–12	C	.1260	.2500	.0337	.5912	.611
15365	9–13	A	.2366	.2462	.0439	.4752	.319
	9–14	B	.1711	.2453	.0313	.5536	.439
	9–15	C	.1295	.2388	.0224	.6101	.587
	9–15A	Neat	.5316	.4220	.0487	—	.244

Adsorption Data: See Tables A-12 to A-27.

Chemical Analyses of Dried Granular Samples: See Table A-28.

Compressive Strength: Cubes were tested in compression, two at each age. See Tables 6-2 to 6-6, Part 6 for results. Samples for adsorption measurements were prepared from the broken cubes.

Modulus of Elasticity: The modulus of elasticity was determined from sonic measurements on the prism. See Table A-29 for results.

TABLE A-12—ADSORPTION DATA FOR REF. 254-9-1, CEMENT 14930J

w/c (by wt.): Original 0.316; after bleeding 0.309
w_n = non-evaporable water; p/p_s = about 24×10^{-6}
w_t = total water
(w_e = evaporable water can be obtained from the relationship $w_e = w_t - w_n$)

p/p_s	Total Water, w_t, Retained at Relative Vapor Pressure and Age Indicated, g/g cement						
	7 days	14 days	28 days	56 days	90 days	180 days	365 days
w_n	.0804	.0994	.1071	.1292	.1497	.1620	.1704
.088	.0957	.1183	—	—	—	—	—
.089	—	—	.1327	.1598	.1812	.2000	—
.090	—	—	—	—	—	—	.2080
.20	.1018	.1273	.1421	.1725	.1963	.2160	.2232
.355	.1097	.1407	—	—	—	—	—
.36	—	—	.1557	.1893	.2155	.2335	.2422
.47	—	—	.1680	.2024	.2271	.2482	.2547
.51	.1185	.1473	—	—	—	—	—
.61	.1247	.1533	.1738	.2109	.2338	.2598	.2654
.69	.1341	.1661	.1898	.2240	.2477	.2678	.2743
.75	.1477	.1763	.2007	.2323	.2558	.2754	.2800
.80	.1547	.1879	.1905	.2347	.2608	.2811	—
.81	—	—	—	—	—	—	.2904
.84	.1599	.1925	.2136	.2521	.2715	.2915	.2963
.89	.1863	.2201	.2408	.2697	.2851	.3054	.3012
.96	.2152	.2421	.2623	.2974	.3105	.3184	.3282
SSD	.3258	.3324	.3493	.3473	.3522	.3576	.3627
SSDO	.3457	.3520	.3516	.3605	.3667	.3703	—

Key: *SSD* = Water content of granular sample in saturated, surface-dry condition for sample that had been dried and resaturated.
SSDO = Water content of granular sample that was brought to saturated condition without preliminary drying.

TABLE A-13—ADSORPTION DATA FOR REF. 254-9-2, CEMENT 14930J

w/c (by wt.): Original 0.441; after bleeding 0.424
w_n = non-evaporable water; p/p_s = about 24×10^{-6}
w_t = total water
(w_e = evaporable water can be obtained from the relationship $w_e = w_t - w_n$)

p/p_s	Total Water, w_t, Retained at Relative Vapor Pressure and Age Indicated, g/g cement						
	7 days	14 days	28 days	56 days	90 days	180 days	365 days
w_n	.0798	.1029	.1165	.1352	.1735	.1853	.1953
.088	.0957	.1227	—	—	—	—	—
.089	—	—	.1444	.1697	.2093	.2268	—
.090	—	—	—	—	—	—	.2396
.20	.1020	.1315	.1542	.1889	.2254	.2473	.2569
.355	.1075	.1487	—	—	—	—	—
.36	—	—	.1700	.2089	.2485	.2693	.2791
.47	—	—	.1819	.2194	.2643	.2873	.2987
.51	.1160	.1511	—	—	—	—	—
.61	.1214	.1551	.1892	.2388	.2751	.3075	.3154
.69	.1335	.1722	.2076	.2516	.2939	.3184	.3286
.75	.1446	.1797	.2142	.2666	.3065	.3295	.3358
.80	.1517	.1928	.2051	.2671	.3133	.3347	—
.81	—	—	—	—	—	—	.3507
.84	.1573	.1976	.2359	.2955	.3240	.3520	.3614
.89	.1879	.2426	.2784	.3238	.3496	.3720	.3735
.96	.2189	.2693	.3103	.3684	.3797	.3894	.4114
SSD	.3981	.4426	.4769	.4738	.4879	.4852	.5109
SSDO	.3995	.4626	.4936	.4864	.5017	.5024	—

Key: *SSD* = Water content of granular sample in saturated, surface-dry condition for sample that had been dried and resaturated.
SSDO = Water content of granular sample that was brought to saturated condition without preliminary drying.

TABLE A-14—ADSORPTION DATA FOR REF. 254-9-3, CEMENT 14930J

w/c (by wt.): Original 0.600; after bleeding 0.573
w_n = non-evaporable water; p/p_s = about 24×10^{-6}
w_t = total water
(w_e = evaporable water can be obtained from the relationship $w_e = w_t - w_n$)

p/p_s	Total Water, w_t, Retained at Relative Vapor Pressure and Age Indicated, g/g cement						
	7 days	14 days	28 days	56 days	90 days	180 days	365 days
w_n	.0822	.0896	.1214	.1638	.1850	.2008	.2142
.089	.1022	.1118	.1521	.1979	.2238	.2422	.2625
.20	.1054	.1180	.1635	.2130	.2409	.2601	.2842
.36	.1125	.1289	.1814	.2343	.2637	.2841	.3125
.47	.1192	.1337	.1848	.2484	.2814	.3032	.3327
.61	.1271	.1464	.2086	.2634	.3068	.3251	.3508
.69	.1385	.1626	.2173	.2882	.3207	.3308	.3700
.75	.1411	.1712	.2371	.3043	.3372	.3573	.3838
.80	.1553	.1721	.2354	.3182	.3470	.3700	—
.81	—	—	—	—	—	—	.4012
.84	.1673	.2026	.2713	.3380	.3647	.3835	.4176
.89	.1955	.2318	.3099	.3761	.4114	.4261	.4450
.96	.2297	.2807	.3642	.4385	.4485	.4515	.5062
SSD	.4822	.4599	.5944	.6344	.6393	.5640	.6971
SSDO	.4732	.4851	.6021	.6579	.6562	.6028	—

Key: *SSD* = Water content of granular sample in saturated, surface-dry condition for sample that had been dried and resaturated.
SSDO = Water content of granular sample that was brought to saturated condition without preliminary drying.

TABLE A-15—ADSORPTION DATA FOR REF. 254-9-4, CEMENT 15007J

w/c (by wt.): Original 0.338; after bleeding 0.316
w_n = non-evaporable water; p/p_s = about 24×10^{-6}
w_t = total water
(w_e = evaporable water can be obtained from the relationship $w_e = w_t - w_n$)

p/p_s	Total Water, w_t, Retained at Relative Vapor Pressure and Age Indicated, g/g cement					
	7 days	14 days	28 days	56 days	90 days	180 days
w_n	.1259	.1404	.1538	.1681	.1729	.1835
.089	.1503	.1687	.1824	.2147	.2105	—
.09	—	—	—	—	—	.2170
.20	.1612	.1816	.1950	.2167	.2234	.2311
.36	.1759	.1982	.2126	.2353	.2419	.2513
.47	.1848	.2111	.2270	.2496	.2574	.2672
.61	.1949	.2243	.2449	.2651	.2752	.2814
.69	.2082	.2378	.2587	.2752	.2821	.2907
.75	.2185	.2440	.2657	.2810	.2891	.2962
.80	.2215	—	.2715	.2856	.2941	—
.81	—	—	—	—	—	.3026
.84	.2319	.2584	.2781	.3004	.3030	.3092
.89	.2520	.2810	.2979	.3077	.3146	.3235
.96	.2856	.2921	.3131	.3269	.3276	.3378
SSD	.3541	.3643	.3654	.3794	.3712	.3773
SSDO	.3716	—	.3747	.3853	—	.3921

Key: *SSD* = Water content of granular sample in saturated, surface-dry condition for sample that had been dried and resaturated.
SSDO = Water content of granular sample that was brought to saturated condition without preliminary drying.

TABLE A-16—ADSORPTION DATA FOR REF. 254-9-5, CEMENT 15007J

w/c (by wt.): Original 0.467; after bleeding 0.433
w_n = non-evaporable water; p/p_s = about 24×10^{-6}
w_t = total water
(w_e = evaporable water can be obtained from the relationship $w_e = w_t - w_n$)

p/p_s	Total Water, w_t, Retained at Relative Vapor Pressure and Age Indicated, g/g cement					
	7 days	14 days	28 days	56 days	90 days	180 days
w_n	.1334	.1498	.1714	.1847	.1924	.2018
.089	.1585	.1801	.2026	.2336	.2341	—
.09	—	—	—	—	—	.2396
.20	.1698	.1942	.2169	.2399	.2500	.2555
.36	.1843	.2128	.2357	.2593	.2714	.2778
.47	.1972	.2243	.2522	.2751	.2917	.2979
.61	.2085	.2415	.2763	.2975	.3158	.3152
.69	.2232	.2570	.2906	.3128	.3284	.3315
.75	.2312	.2657	.3020	.3249	.3394	.3411
.80	.2364	—	.3132	.3302	.3460	—
.81	—	—	—	—	—	.3520
.84	.2517	.2867	.3191	.3527	.3607	.3614
.89	.2774	.3158	.3432	.3713	.3802	.3994
.96	.3157	.3254	.3695	.3899	.3980	.4111
SSD	.4667	.4764	.4913	.5002	.5092	.5502
SSDO	.5000	.4971	.5106	.5156	—	.5605

Key: *SSD* = Water content of granular sample in saturated, surface-dry condition for sample that had been dried and resaturated.
SSDO = Water content of granular sample that was brought to saturated condition without preliminary drying.

TABLE A-17—ADSORPTION DATA FOR REF. 254-9-6, CEMENT 15007J

w/c (by wt.): Original 0.610; after bleeding 0.570
w_n = non-evaporable water; p/p_s = about 24×10^{-6}
w_t = total water
(w_e = evaporable water can be obtained from the relationship $w_e = w_t - w_n$)

p/p_s	Total Water, w_t, Retained at Relative Vapor Pressure and Age Indicated, g/g cement					
	7 days	14 days	28 days	56 days	90 days	180 days
w_n	.1560	.1634	.1839	.2035	.2049	.2132
.089	.1824	.1921	.2191	—	—	—
.09	—	—	—	.2398	.2428	—
.20	.1918	.2066	.2341	.2561	.2603	.2758
.36	.2078	.2210	.2536	.2781	.2811	.3006
.47	.2209	.2342	.2668	.2975	.3038	.3218
.61	.2423	.2523	.2943	.3240	.3266	.3460
.69	.2545	.2694	.3136	.3405	.3407	.3589
.75	.2705	.2864	.3297	.3524	.3578	.3810
.80	.2816	.2870	.3347	.3585	—	—
.81	—	—	—	—	.3656	.3918
.84	.2998	.3140	.3634	.3836	.3818	.4151
.89	.3240	.3409	.3921	.4132	.4155	.4430
.96	.3597	.3774	.4244	.4456	.4413	.4780
SSD	.5084	.5300	.5845	.5900	.6019	.6676
SSDO	.5630	.5846	.6219	.6347	.6186	—

Key: *SSD* = Water content of granular sample in saturated, surface-dry condition for sample that had been dried and resaturated.
SSDO = Water content of granular sample that was brought to saturated condition without preliminary drying.

TABLE A-18—ADSORPTION DATA FOR REF. 254-9-7, CEMENT 15011J

w/c (by wt.): Original 0.353; after bleeding 0.316
w_n = non-evaporable water, p/p_s = about 24×10^{-6}
w_t = total water
(w_e = evaporable water can be obtained from the relationship $w_e = w_t - w_n$)

p/p_s	Total Water, w_t, Retained at Relative Vapor Pressure and Age Indicated, g/g cement						
	7 days	14 days	28 days	56 days	90 days	180 days	365 days
w_n	.1137	.1333	.1430	.1557	.1643	.1705	.1760
.089	.1415	.1584	.1785	.1892	.1961	.2039	—
.09	—	—	—	—	—	—	.2111
.20	.1484	.1686	.1953	.2035	.2098	.2191	.2276
.36	.1617	.1838	.2069	.2211	.2268	.2359	.2468
.47	.1703	.1960	.2193	.2295	.2410	.2509	.2573
.61	.1808	.2038	.2312	.2401	.2531	.2632	.2685
.69	.1935	.2197	.2448	.2535	.2622	.2716	.2764
.75	.1942	.2289	.2534	.2627	.2704	.2817	.2861
.80	.2112	.2319	.2548	.2684	.2746	.2873	—
.81	—	—	—	—	—	—	.2931
.84	.2209	.2535	.2738	.2767	.2812	.2951	.3002
.89	.2480	.2787	.2955	.2905	.3015	.3125	.3109
.96	.2697	.3059	.3186	.3140	.3138	.3216	.3341
SSD	.3487	.3575	.3619	.3591	.3617	.3646	.3721
SSDO	.3587	.3710	.3696	.3713	.3685	.3794	—

Key: *SSD* = Water content of granular sample in saturated, surface-dry condition for sample that had been dried and resaturated.
SSDO = Water content of granular sample that was brought to saturated condition without preliminary drying.

TABLE A-19—ADSORPTION DATA FOR REF. 254-9-8, CEMENT 15011J

w/c (by wt.): Original 0.459; after bleeding 0.432
w_n = non-evaporable water; p/p_s = about 24×10^{-6}
w_t = total water
(w_e = evaporable water can be obtained from the relationship $w_e = w_t - w_n$)

p/p_s	Total Water, w_t, Retained at Relative Vapor Pressure and Age Indicated, g/g cement					
	7 days	14 days	28 days	56 days	90 days	180 days
w_n	.1228	.1527	.1654	.1781	.1913	.1986
.089	.1514	.1824	.2054	.2154	.2278	—
.09	—	—	—	—	—	.2359
.20	.1618	.1940	.2116	.2269	.2444	.2521
.36	.1762	.2064	.2300	.2464	.2647	.2751
.47	.1828	.2205	.2444	.2656	.2798	.2956
.61	.2005	.2357	.2562	.2858	.3023	.3126
.69	.2140	.2470	.2764	.3000	.3165	.3250
.75	.2254	.2634	.2890	.3119	.3289	.3364
.80	—	.2718	.2993	.3226	.3380	—
.81	—	—	—	—	—	.3437
.84	.2517	.2875	.3108	.3313	.3591	.3587
.89	.2829	.3249	.3251	.3618	.3816	.3827
.96	.3310	.3579	.3778	.3864	.4055	.4108
SSD	.4661	.4932	.4843	.4922	.4952	.4975
SSDO	—	.5155	.5045	.5075	.5165	.5119

Key: *SSD* = Water content of granular sample in saturated, surface-dry condition for sample that had been dried and resaturated.
SSDO = Water content of granular sample that was brought to saturated condition without preliminary drying.

TABLE A-20—ADSORPTION DATA FOR REF. 9-9, CEMENT 15011J

w/c (by wt.): Original 0.610; after bleeding 0.582
w_n = non-evaporable water; p/p_s = about 24×10^{-6}
w_t = total water
(w_e = evaporable water can be obtained from the relationship $w_e = w_t - w_n$)

p/p_s	Total Water, w_t, Retained at Relative Vapor Pressure and Age Indicated, g/g cement					
	7 days	14 days	28 days	56 days	90 days	180 days
w_n	.1314	.1567	.1756	.1953	.2046	.2136
.089	.1573	.1871	.2176	.2332	.2427	—
.09	—	—	—	—	—	.2523
.20	.1693	.1994	.2231	.2484	.2600	.2693
.36	.1804	.2132	.2418	.2688	.2831	.2914
.47	.1901	.2244	.2562	.2897	.2977	.3139
.61	.2037	.2385	.2695	.3121	.3212	.3364
.69	.2160	.2529	.2948	.3294	.3408	.3526
.75	.2290	.2679	.3065	.3413	.3566	.3684
.80	—	.2804	.3179	.3590	.3692	—
.81	—	—	—	—	—	.3756
.84	.2574	.2999	.3344	.3684	.3939	.3990
.89	.2946	.3381	.3527	.4134	.4291	.4344
.96	.3453	.3931	.4233	.4469	.4588	.4670
SSD	.5576	.5258	.5793	.6471	.6212	.5800
SSDO	—	.5657	.6146	.6726	.6306	.6156

Key: *SSD* = Water content of granular sample in saturated, surface-dry condition for sample that had been dried and resaturated.
SSDO = Water content of granular sample that was brought to saturated condition without preliminary drying.

TABLE A-21—ADSORPTION DATA FOR REF. 9-10, CEMENT 15013J

w/c (by wt.): Original 0.326; after bleeding 0.324
w_n = non-evaporable water; p/p_s = about 24×10^{-6}
w_t = total water
(w_e = evaporable water can be obtained from the relationship $w_e = w_t - w_n$)

p/p_s	Total Water, w_t, Retained at Relative Vapor Pressure and Age Indicated, g/g cement					
	7 days	14 days	28 days	56 days	90 days	180 days
w_n	.1488	.1639	.1711	.1802	.1913	.1877
.089	.1748	.1909	.2028	.2147	—	—
.09	—	—	—	—	.2260	.2299
.20	.1859	.2042	.2161	.2277	.2409	.2426
.36	.2001	.2186	.2324	.2452	.2586	.2615
.47	.2110	.2304	.2472	.2602	.2760	.2763
.61	.2287	.2465	.2634	.2790	.2912	.2907
.69	.2386	.2604	.2761	.2899	.3015	.2917
.75	.2509	.2705	.2843	.2952	.3100	.3058
.80	.2541	.2680	.2857	.2979	—	—
.81	—	—	—	—	.3135	.3103
.84	.2653	.2863	.3004	.3104	.3212	.3151
.89	.2729	.2997	.3114	.3218	.3342	.3307
.96	.3019	.3110	.3228	.3335	.3417	.3418
SSD	.3745	.3831	.3781	.3852	.3873	.3784
SSDO	.3745	.3831	.3914	.3995	.4018	—

Key: *SSD* = Water content of granular sample in saturated, surface-dry condition for sample that had been dried and resaturated.
SSDO = Water content of granular sample that was brought to saturated condition without preliminary drying.

TABLE A-22—ADSORPTION DATA FOR REF. 9-11, CEMENT 15013J

w/c (by wt.): Original 0.459; after bleeding 0.443
w_n = non-evaporable water; p/p_s = about 24×10^{-6}
w_t = total water
(w_e = evaporable water can be obtained from the relationship $w_e = w_t - w_n$)

p/p_s	Total Water, w_t, Retained at Relative Vapor Pressure and Age Indicated, g/g cement					
	7 days	14 days	28 days	56 days	90 days	180 days
w_n	.1556	.1828	.1770	.2085	.2152	.2356
.089	.1830	.2143	.2131	—	—	—
.09	—	—	—	.2460	.2530	.2761
.20	.1932	.2269	.2272	.2604	.2695	.2933
.36	.2079	.2434	.2455	.2843	.2940	.3179
.47	.2190	.2572	.2626	.3017	.3124	.3372
.61	.2369	.2814	.2822	.3212	.3306	.3572
.69	.2447	.2911	.2985	.3363	.3426	.3660
.75	.2578	.3026	.3129	.3518	.3555	.3797
.80	.2614	.3051	—	—	—	—
.81	—	—	—	.3557	.3649	.3908
.84	.2788	.3228	.3316	.3690	.3763	.3958
.89	.2991	.3481	.3690	.3927	.4034	.4127
.96	.3247	.3698	.3933	.4115	.4265	.4547
SSD	.4435	.4831	.5248	.5298	.5643	.5705
SSDO	.4793	.5137	.5419	—	—	—

Key: *SSD* = Water content of granular sample in saturated, surface-dry condition for sample that hap been dried and resaturated.
SSDO = Water content of granular sample that was brought to saturated condition without preliminary drying.

TABLE A-23—ADSORPTION DATA FOR REF. 9-12, CEMENT 15013J

w/c (by wt.): Original 0.635; after bleeding 0.611
w_n = non-evaporable water; p/p_s = about 24×10^{-6}
w_t = total water
(w_e = evaporable water can be obtained from the relationship $w_e = w_t - w_n$)

p/p_s	Total Water, w_t, Retained at Relative Vapor Pressure and Age Indicated, g/g cement					
	7 days	14 days	28 days	56 days	90 days	180 days
w_n	.1583	.1828	.2028	.2208	.2357	.2447
.089	.1841	.2129	.2368	—	—	—
.09	—	—	—	.2582	.2778	.2856
.20	.1941	.2238	.2502	.2737	.2937	.3029
.36	.2063	.2395	.2663	.2971	.3173	.3272
.47	.2176	.2532	.2850	.3151	.3372	.3460
.61	.2345	.2747	.3075	.3396	.3579	.3690
.69	.2432	.2848	.3232	.3578	.3747	.3841
.75	.2584	.3003	.3395	.3731	.3946	.3983
.80	—	.3034	—	—	—	—
.81	—	—	—	.3796	.4029	.4166
.84	.2792	.3229	.3576	.3974	.4191	.4221
.89	.3018	.3507	.3995	.4296	.4557	.4468
.96	.3244	.3763	.4244	.4563	.4930	.5102
SSD	.5148	.5497	.5798	.6136	.7162	.6707
SSDO	.5743	.6200	.6438	—	—	—

Key: *SSD* = Water content of granular sample in saturated, surface-dry condition for sample that had been dried and resaturated.
SSDO = Water content of granular sample that was brought to saturated condition without preliminary drying.

TABLE A-24—ADSORPTION DATA FOR REF. 9-13, CEMENT 15365

w/c (by wt.): Original 0.326; after bleeding 0.319
w_n = non-evaporable water; p/p_s = about 24×10^{-6}
w_t = total water
(w_e = evaporable water can be obtained from the relationship $w_e = w_t - w_n$)

p/p_s	Total Water, w_t, Retained at Relative Vapor Pressure and Age Indicated, g/g cement					
	7 days	14 days	28 days	56 days	90 days	180 days
w_n	.1326	.1515	.1488	.1786	.1789	.1815
.09	.1596	.1803	.1803	.2133	.2133	.2168
.20	.1681	.1903	.1933	.2275	.2269	.2311
.36	.1809	.2043	.2106	.2461	.2460	.2495
.47	.1925	.2181	.2242	.2574	.2591	.2608
.61	.2052	.2313	.2414	.2725	.2734	.2740
.69	.2134	.2434	.2489	.2796	.2824	.2870
.75	.2244	.2541	.2571	.2898	.2926	.2922
.81	.2319	.2625	.2649	.2962	.2973	.2992
.84	.2391	.2688	.2783	.3017	.3026	.3078
.89	.2662	.2907	.2938	.3190	.3184	.3173
.96	.2906	.3123	.3036	.3367	.3341	.3344
SSD	.3570	.3669	.3639	.3847	.3702	.3791
SSDO	—	.3842	—	—	—	—

Key: *SSD* = Water content of granular sample in saturated, surface-dry condition for sample that had been dried and resaturated.
SSDO = Water content of granular sample that was brought to saturated condition without preliminary drying.

TABLE A-25—ADSORPTION DATA FOR REF. 254-9-14, CEMENT 15365

w/c (by wt.): Original 0.459; after bleeding 0.439
w_n = non-evaporable water; p/p_s = about 24×10^{-6}
w_t = total water
(w_e = evaporable water can be obtained from the relationship $w_e = w_t - w_n$)

p/p_s	Total Water, w_t, Retained at Relative Vapor Pressure and Age Indicated, g/g cement					
	7 days	14 days	28 days	56 days	90 days	180 days
w_n	.1394	.1711	.1841	.2105	.2150	.2224
.09	.1665	.2031	.2230	.2502	.2571	.2651
.20	.1758	.2142	.2377	.2655	.2730	.2819
.36	.1893	.2315	.2599	.2889	.2962	.3088
.47	.2009	.2470	.2757	.3062	.3165	.3250
.61	.2138	.2619	.2961	.3257	.3346	.3460
.69	.2237	.2767	.3102	.3366	.3512	.3626
.75	.2343	.2894	.3256	.3518	.3638	.3699
.81	.2419	.3008	.3322	.3621	.3717	.3830
.84	.2512	.3104	.3476	.3681	.3791	.3925
.89	.2828	.3399	.3761	.3968	.4044	.4094
.96	.3098	.3646	.3966	.4188	.4288	.4429
SSD	.4182	.4724	.5034	.5133	.5113	.5344
SSDO	—	.4877	—	—	—	—

Key: *SSD* = Water content of granular sample in saturated, surface-dry condition for sample that had been dried and resaturated.
SSDO = Water content of granular sample that was brought to saturated condition without preliminary drying.

TABLE A-26—ADSORPTION DATA FOR REF. 254-9-15, CEMENT 15365

w/c (by wt.): Original 0.610; after bleeding 0.587
w_n = non-evaporable water; p/p_s = about 24x10^{-6}
w_t = total water
(w_e = evaporable water can be obtained from the relationship $w_e = w_t - w_n$)

p/p_s	Total Water, w_t, Retained at Relative Vapor Pressure and Age Indicated, g/g cement					
	7 days	14 days	28 days	56 days	90 days	180 days
w_n	.1530	.1855	.2102	.2213	.2296	.2546
.09	.1820	.2194	.2495	.2653	.2741	.2967
.20	.1922	.2321	.2646	.2820	.2918	.3139
.36	.2063	.2496	.2872	.3032	.3176	.3406
.47	.2162	.2636	.3030	.3249	.3357	.3609
.61	.2298	.2819	.3262	.3484	.3611	.3821
.69	.2395	.2937	.3382	.3641	.3783	.4056
.75	.2531	.3108	.3541	.3767	.3910	.4175
.81	.2578	.3139	.3637	.3898	.4074	.4347
.84	.2716	.3306	.3773	—	.4177	.4456
.89	.3060	.3706	.4197	.4228	.4461	.4681
.96	.3489	.4139	.4587	.4809	.5104	.5318
SSD	.5157	.5804	.6272	.6400	.6614	.6637
SSDO	.5707	.6031	—	—	—	—

Key: *SSD* = Water content of granular sample in saturated, surface-dry condition for sample that had been dried and resaturated.
SSDO = Water content of granular sample that was brought to saturated condition without preliminary drying.

TABLE A-27—ADSORPTION DATA FOR REF. 254-9-15A, CEMENT 15365

w/c (by wt.): Original 0.246; after bleeding 0.244
w_n = non-evaporable water; p/p_s = about 24x10^{-6}
w_t = total waer
(w_e = evaporable water can be obtained from the relationship $w_e = w_t - w_n$)

p/p_s	Total Water, w_t, Retained at Relative Vapor Pressure and Age Indicated, g/g cement							
	7 days	14 days	28 days	56 days	90 days	180 days	270 days	
							A	B
w_n	.1152	.1259	.1358	.1396	.1452	.1554	.1691	.1722
.081	—	—	—	—	—	—	.1910	.1918
.09	.1380	.1501	.1611	.1684	.1741	.1856	—	—
.161	—	—	—	—	—	—	.2000	.1999
.20	.1465	.1591	.1709	.1785	.1837	.1956	—	—
.238	—	—	—	—	—	—	.2053	.2063
.322	—	—	—	—	—	—	.2111	.2116
.36	.1572	.1713	.1830	.1901	.1967	.2090	.2159	.2152
.47	.1658	.1811	.1933	.2002	.2061	.2177	—	—
.53	—	—	—	—	—	—	.2275	.2277
.61	.1763	.1918	.2034	.2123	.2182	.2266	—	—
.69	.1846	.1993	.2116	.2211	.2240	.2355	—	—
.70	—	—	—	—	—	—	.2397	.2402
.75	.1988	.2133	.2217	.2256	.2306	.2399	—	—
.81	.2021	.2146	.2259	.2324	.2389	.2459	.2509	.2504
.84	.2116	.2254	.2305	—	.2412	.2489	—	—
.85	—	—	—	—	—	—	.2582	.2588
.88	—	—	—	—	—	—	.2634	.2619
.89	.2317	.2414	.2487	.2426	.2509	.2536	—	—
.96	.2508	.2599	.2613	.2594	.2698	.2724	.2775	.2771
SSD	.3064	.2948	.3028	.2960	.2969	.2836	.2906	.3024
SSDO	.3128	.3076	—	—	—	—	—	—

Key: *SSD* = Water content of granular sample in saturated, surface-dry condition for sample that had been dried and resaturated.
SSDO = Water content of granular sample that was brought to saturated condition without preliminary drying.
A and B refer to separate rounds.

TABLE A-28—ANALYSES OF GRANULAR SAMPLES USED FOR ADSORPTION AND NON-EVAPORABLE WATER MEASUREMENTS IN SERIES 254-9

w/c at 2 hr. (wt. basis)	Composition of Dry Samples at Age Indicated, percent dry weight																				
	7 days			14 days			28 days			56 days			90 days			180 days			365 days		
	Cmt.	SiO_2	H_2O	Cmt.	SiO_2	H_2O	Cmt.	SiO_2	H_2O	Cmt.	SiO_2	H_2O	Cmt.	SiO_2	H_2O	Cmt.	SiO_2	H_2O	Cmt.	SiO_2	H_2O
Cement 14930J																					
0.309	84.7	7.9	7.5	80.4	11.7	8.0	70.6	22.0	7.6	73.9	16.6	9.6	69.9	19.6	10.5	76.9	10.6	12.5	70.1	18.0	11.9
0.424	66.1	27.9	5.3	62.5	30.2	6.4	52.0	42.0	6.1	48.5	45.0	6.6	55.1	35.4	9.6	60.4	28.4	11.2	54.4	35.0	10.6
0.573	46.5	49.8	3.8	33.8	63.6	3.0	40.4	54.7	4.9	46.0	46.5	7.5	46.8	44.5	8.7	49.7	40.3	10.0	46.4	43.6	9.9
Cement 15007J																					
0.316	76.3	14.1	9.6	74.3	15.3	10.4	74.2	14.4	11.4	77.5	9.5	13.0	77.6	9.0	13.4	75.8	10.3	13.9			
0.433	60.5	31.5	8.1	58.2	33.1	8.7	57.4	32.8	9.8	60.8	27.9	11.2	60.6	27.7	11.7	47.9	42.5	9.7			
0.570	48.1	44.4	7.5	48.1	44.0	7.9	48.4	42.8	8.9	47.9	42.4	9.7	47.5	42.3	10.2	32.6	60.5	7.0			
Cement 15011J																					
0.316	79.0	12.1	9.0	71.7	18.9	9.6	75.5	13.7	10.8	72.8	15.7	11.3	73.7	14.2	12.1	78.6	8.0	13.4	78.8	7.3	13.9
0.432	51.0	42.8	6.3	58.9	32.1	9.0	58.5	31.8	9.7	58.1	31.5	10.4	61.0	27.3	11.7	57.9	30.6	11.5			
0.582	47.5	46.2	6.2	47.3	45.3	7.4	45.9	46.0	8.1	44.6	46.7	8.7	48.0	42.3	9.8	45.7	44.5	9.8			
Cement 15013J																					
0.324	80.3	7.7	12.0	80.2	6.7	13.1	79.1	7.3	13.5	79.1	6.7	14.2	78.0	7.1	14.9	62.5	25.8	11.7			
0.443	62.7	27.5	9.8	59.4	29.8	10.8	25.1	70.5	4.4	58.1	29.7	12.1	51.0	37.0	11.0	53.4	34.1	12.6			
0.611	46.1	46.6	7.3	47.7	43.6	8.7	45.4	45.4	9.2	45.0	45.1	9.9	35.2	56.5	8.3	40.4	49.8	9.9			
Cement 15365																					
0.319	82.2	7.0	10.9	78.3	9.8	11.9	50.1	42.4	7.5	76.8	9.4	13.7	76.6	9.7	13.7	72.5	14.3	13.2			
0.439	62.2	29.2	8.7	60.6	29.0	10.4	51.9	38.6	9.6	60.0	27.4	12.6	58.6	28.6	12.8	56.1	31.3	12.5			
0.587	45.4	47.6	7.0	48.5	42.5	9.0	44.8	45.8	9.4	46.6	43.0	10.3	46.5	42.9	10.7	47.7	40.2	12.1			

Cement content estimated from CaO determination. Water content estimated from ignition loss corrected for ignition loss of cement. Silica content found by difference.

TABLE A-29—YOUNG'S MODULUS OF MORTARS USED IN SERIES 254-9

Cement No.	w/c at 2 hrs. (wt. basis)	Young's Modulus at Age Indicated* millions of lb/in²					
		7 days	14 days	28 days	56 days	90 days	180 days
14930J	.309	4.47	4.98	5.45	5.50	5.75	6.00
	.424	3.67	4.30	4.85	5.14	5.36	5.66
	.573	2.57	3.34	4.13	4.71	4.87	5.20
15007J	.316	5.18	5.35	5.58	5.54	5.48	5.73
	.433	4.65	4.85	5.08	5.14	5.35	5.32
	.570	4.23	4.50	4.92	5.03	5.08	(a)
15011J	.316	5.10	5.45	5.62	5.76	5.88	6.00
	.432	4.55	4.85	5.20	5.30	5.42	5.48
	.582	4.13	4.48	4.83	4.89	5.00	5.00
15013J	.324	5.05	5.17	5.30	5.40	5.47	5.65
	.443	4.37	4.68	4.85	(a)	(a)	(a)
	.611	3.78	3.97	4.36	4.45	4.50	4.65
15365	.319	5.30	5.42	5.58	5.78	5.78	—
	.439	4.64	5.27	5.03	5.18	5.40	—
	.587	4.40	4.81	4.96	5.03	5.03	—

*Values are for a single prism.
(a) Prism broken.

TABLE A-30—UNIT ABSOLUTE VOLUME COMPOSITION OF THE MORTARS USED IN SERIES 254-11

Cement No.	Ref. No.	(See page 317)	Unit Absolute Volume Composition at 2 hours				w/c at 2 hours, (wt. basis)
			Cement	Silica	Air	Water	
15758	11–1	A	.2395	.4660	.0437	.2526	.334
	11–2	B	.1721	.5398	.0382	.2506	.460
15756	11–3	A	.2443	.4828	.0233	.2551	.318
	11–4	B	.1781	.5604	.0087	.2525	.446
15763	11–5	A	.2434	.4827	.0237	.2508	.324
	11–6	B	.1741	.5562	.0245	.2458	.437
15761	11–7	A	Note 1	—	—	—	.334
	11–8	B	—	—	—	—	.468
15754	11–9	A	.2409	.4746	.0315	.2540	.328
	11–10	B	.1727	.5484	.0271	.2526	.449
16213	11–11	B	.1775	.5592	.0135	.2497	.443
16214	11–12	B	.1766	.5580	.0131	.2522	.448
16198	11–13	B	.1745	.5621	.0121	.2512	.443
15669	11–14	B	.1725	.5579	.0157	.2538	.451
15495	11–15	B	.1764	.5488	.0302	.2445	.442
15497	11–16	B	.1731	.5453	.0266	.2549	.464

Note 1: The specimens with Cement 15761, expanded in the molds and hence it was impossible to obtain satisfactory data for calculating the composition.
See p. 333 for description of specimens.

TABLE A-31—ANALYSES OF GRANULAR SAMPLES USED FOR ADSORPTION AND NON-EVAPORABLE WATER MEASUREMENTS IN SERIES 254-11

Cement No.	*w/c* at 2 hrs. (wt. basis)	Cement-, Silica-, and Non-Evaporable Water-Content of 35-100-Mesh Samples at Age Indicated, g/g dry weight					
		28 days			90 days		
		Cement	Silica	Non-Evap. Water	Cement	Silica	Non-Evap. Water
15758	.334	.783	.084	.134	.773	.079	.148
	.460	.598	.284	.117	.607	.258	.135
15756	.318	.788	.115	.097	.776	.108	.116
	.446	.616	.302	.082	.617	.279	.104
15763	.324	.834	.089	.077	.788	.107	.105
	.437	.647	.288	.065	.169	.289	.092
15761	.334	.802	.068	.130	.798	.059	.144
	.468	.630	.253	.117	.611	.260	.130
15754	.328	.767	.102	.131	.760	.091	.148
	.449	.591	.293	.116	.588	.277	.135
16213	.443	.5834	.3082	.1084			
16214	.448	.5864	.3130	.1006			
16198	.443	.6160	.3165	.0675			
15669	.451	.6287	.2976	.0736			
15495 (1)	.442	.5422	.3873	.0705			
15497 (1)	.464	.5560	.3424	.1016			

(1) Age 6 days.
See p. 333 for description of specimens.

TABLE A-32—FLEXURAL STRENGTH AND YOUNG'S MODULUS OF ELASTICITY OF MORTARS MADE WITH SPECIAL CEMENTS FOR THE BASIC-RESEARCH PROGRAM—SERIES 254-11

Cement No.	*w/c* at 2 hrs. (wt. basis)	Flexural Strength at Age Indicated lb/in²		Young's Modulus at Age Indicated millions of lb/in²	
		28 days	90 days	28 days	90 days
15758	.334	1395	1275	6.0	6.1
	.460	1090	970	5.5	5.4
15756	.318	1170	1295	5.8	6.4
	.446	915	1010	5.1	5.6
15763	.324	1035	1345	5.4	6.0
	.437	765	1115	4.7	5.5
15761	.334	1145	980	5.6	5.7
	.468	1015	790	5.2	5.3
15754	.328	1275	1210	6.0	6.5
	.449	1035	945	5.4	5.7

Flexural strength is the average of results for two prisms.
Young's modulus was calculated from the resonance frequency of vibration found by the electrodynamic method. The values for 28 days are the average of results for 12 prisms; those at 90 days, the average for 2 prisms.
See p. 333 for description of specimens.

TABLE A-33—ADSORPTION DATA FOR SERIES 254-11

Water-cement ratios corrected for bleeding

p/p_s	Total Water Retained at Relative Vapor Pressure Indicated, g/g cement													
	Cement 15758 Ref. No. 11-1 w_o/c = 0.334		Cement 15758 Ref. No. 11-2 w_o/c = 0.460		Cement 15756 Ref. No. 11-3 w_o/c = 0.318		Cement 15756 Ref. No. 11-4 w_o/c = 0.446		Cement 15763 Ref. No. 11-5 w_o/c = 0.324		Cement 15763 Ref. No. 11-6 w_o/c = 0.437		Cement 15761 Ref. No. 11-7 w_o/c = 0.334	
	28 days	90 days	28 days	90 days	28 days	90 days	28 days	90 days	28 days	90 days	28 days	90 days	28 days	90 days
w_n	.1707	.1912	.1962	.2227	.1229	.1492	.1325	.1684	.0922	.1335	.1013	.1487	.1621	.1798
.09	.2019	.2255	.2326	.2601	.1472	.1802	.1578	.1997	.1128	.1624	.1231	.1802	.1908	.2141
.20	.2153	.2401	.2472	.2767	.1581	.1931	.1690	.2141	.1216	.1750	.1330	.1952	.2037	.2287
.36	.2331	.2596	.2680	.2993	.1725	.2105	.1839	.2313	.1328	.1909	.1447	.2118	.2211	.2476
.47	.2448	.2730	.2844	.3179	.1813	.2217	.1940	.2457	.1414	.2005	.1535	.2246	.2339	.2615
.61	.2606	.2879	.3045	.3375	.1931	.2445	.2055	.2598	.1530	.2112	.1651	.2343	.2483	.2755
.69	.2741	.3008	.3212	.3571	.2071	.2507	.2204	.2791	.1653	.2273	.1803	.2548	.2621	.2911
.75	.2817	.3060	.3300	.3637	.2170	.2566	.2323	.2867	.1737	.2355	.1903	.2630	.2706	.3003
.81	.2931	.3176	.3452	.3798	.2295	.2706	.2469	.3065	.1833	.2458	.2012	.2782	.2808	.3137
.84	.3004	.3266	.3548	.3918	.2373	.2754	.2556	.3128	.1910	.2544	.2097	.2910	.2899	.3206
.89	.3186	.3420	.3772	.4144	.2520	.2908	.2746	.3298	.2042	.2653	.2267	.3055	.3079	.3355
.96	.3504	.3752	.4273	.4605	.2973	.3215	.3310	.3924	.2416	.3015	.2777	.3651	.3490	.3733
SSD	.3975	.4162	.5247	.5682	.3751	.3764	.4721	.5127	.3554	.3674	.4287	.5030	.3978	.4144

p/p_s	Total Water Retained at Relative Vapor Pressure Indicated, g/g cement										
	Cement 15761 Ref. No. 11-8 w_o/c = 0.468		Cement 15754 Ref. No. 11-9 w_o/c = 0.328		Cement 15754 Ref. No. 11-10 w_o/c = 0.449		p/p_s	Cement 16213 Ref. No. 11-11 w_o/c = 0.443	Cement 16214 Ref. No. 11-12 w_o/c = 0.448	Cement 16198 Ref. No. 11-13 w_o/c = 0.443	Cement 15669 Ref. No. 11-14 w_o/c = 0.451
	28 days	90 days	28 days	90 days	28 days	90 days		28 days	28 days	28 days	28 days
w_n	.1852	.2120	.1703	.1951	.1967	.2301	w_n	.1720	.1854	.1098	.1084
.09	.2192	.2501	.2020	.2284	.2336	.2704	.081	.2043	.2188	.1322	.1283
.20	.2346	.2673	.2150	.2418	.2480	.2866	.161	.2152	.2302	.1400	.1385
.36	.2555	.2899	.2337	.2615	.2695	.3114	.238	.2229	.2380	.1454	.1472
.47	.2722	.3071	.2475	.2766	.2869	.3308	.322	.2338	.2491	.1537	.1545
.61	.2882	.3256	.2617	.2904	.2959	.3488	.36	.2394	.2552	.1569	.1582
.69	.3056	.3454	.2737	.3059	.3223	.3699	.53	.2579	.2778	.1692	.1726
.75	.3166	.3545	.2806	.3125	.3338	.3788	.70	.2826	.3080	.1944	.1951
.81	.3304	.3734	.2926	.3227	.3482	.3942	.81	.2864	.3288	.2174	.2226
.84	.3415	.3827	.2986	.3297	.3562	.4063	.85	.3144	.3401	.2262	.2334
.89	.3666	.4001	.3118	.3387	.3758	.4187	.88	.3356	.3550	.2484	.2528
.96	.4221	.4562	.3381	.3578	.4161	.4616	.96	.3691	.3906	.2903	.3090
SSD	.5350	.5626	.3887	.3991	.5289	.5560	*SSD*	.4880	.5084	.4748	.4784

p/p_s	Total Water Retained at Relative Vapor Pressure Indicated, g/g cement	
	Cement 15495 Ref. No. 11-15 w_o/c = 0.442 Age 6 days	Cement 15497 Ref. No. 11-16 w_o/c = 0.464 Age 6 days
w_n	.1300	.1825
.081	.1525	.2125
.161	.1604	.2237
.238	.1659	.2309
.322	.1728	.2402
.36	.1810	.2456
.53	.1873	.2765
.70	.2100	.2990
.81	.2306	.3228
.85	.2435	.3386
.88	.2625	.3539
.96	.3151	.4028
SSD	.4515	.5100

SSD = Water content of granular sample, saturated, surface-dry for sample that had been dried and resaturated.
w_n = Non-evaporable water;
p/p_s = about 24×10^{-6}

TABLE A-34—UNIT ABSOLUTE VOLUME COMPOSITION OF THE MORTARS USED IN SERIES 254-13

Clinker No.	Ref. No.	Unit Absolute Volume Composition at 2 hours				*w/c* at 2 hours (wt. basis)
		Cement	Silica	Air	Water	
15367*	13–1	.2853	.2444	.0201	.4506	.494
	13–2	.2870	.2458	.0147	.4528	.493
	13–3	.2909	.2492	.0045	.4553	.489
	13–4	.2879	.2466	.0133	.4523	.491
15367**	13–1B	.2828	.2422	.0362	.4400	.486
	13–2B	.2828	.2422	.0297	.4458	.488
	13–3B	.2822	.2417	.0358	.4414	.488
	13–4B	.2849	.2441	.0240	.4476	.492
15623	13–5	.2931	.2529	.0053	.4489	.470
	13–6	.2919	.2519	.0058	.4504	.474
	13–7	.2920	.2520	.0063	.4497	.473
	13–8	.2898	.2501	.0073	.4528	.480
15699	13–9	.2827	.2436	.0204	.4537	.498
	13–10	.2824	.2433	.0219	.4530	.499
	13–11	.2816	.2427	.0232	.4529	.499
	13–12	.2796	.2410	.0297	.4503	.498
15498	13–13	.2888	.2444	.0200	.4472	.488
	13–14	.2909	.2462	.0154	.4480	.487
	13–15	.2905	.2458	.0114	.4524	.493
	13–16	.2909	.2462	.0124	.4509	.491

*First round of measurements.
**Second round of measurements.

TABLE A-35—ANALYSES OF THE GRANULAR SAMPLES USED FOR ADSORPTION AND NON-EVAPORABLE WATER MEASUREMENTS IN SERIES 254-13

Clinker No.	Ref. No.	Wt. % SO_3	*w/c* at 2 hrs. (wt. basis)	Composition of 35-100-Mesh Samples, g/g dry weight		
				Cement	Silica	Water
15367*	13–1	1.5	0.493	.518	.370	.111
	13–2	1.9	0.493	.519	.371	.110
	13–3	2.4	0.489	.520	.372	.108
	13–4	3.5	0.491	.524	.374	.102
15367**	13–1B	1.5	0.486	.519	.371	.110
	13–2B	1.9	0.488	.518	.370	.112
	13–3B	2.4	0.488	.518	.370	.112
	13–4B	3.5	0.492	.521	.372	.106
15623	13–5	1.5	0.470	.536	.383	.081
	13–6	2.0	0.474	.536	.383	.081
	13–7	2.5	0.473	.536	.383	.081
	13–8	3.5	0.480	.538	.384	.078
15699	13–9	1.5	0.498	.523	.373	.104
	13–10	2.0	0.499	.524	.374	.102
	13–11	2.5	0.499	.525	.374	.101
	13–12	3.5	0.498	.527	.376	.097
15498	13–13	1.5	0.488	.521	.371	.108
	13–14	2.0	0.487	.523	.373	.104
	13–15	2.5	0.493	.523	.372	.105
	13–16	3.5	0.491	.525	.375	.100

*First round of measurements.
**Second round of measurements.

Description of specimens made in series 254-11

Mortar Specimens: Cubes, 2 in.

Cements: See Tables A-1 to A-3.

Pulverized Silica: Lot 15918. Specific surface (Wagner), 6000 cm^2/cm^3.

Batches: Same as Mixes A and B of Series 254-9.

Mixing: Each batch was mixed 30 sec. dry, 1½ min. wet, allowed to rest 3 min., and then mixed 2 min. more in a small, power-driven, open-tub mixer. Batches remixed 30 sec. after slump test.

Slump Test: As in Series 254-8.

Molding: As for cubes in Series 254-9, except 15 per batch.

Measurements: As in Series 254-8.

Drying: As in Series 254-8.

Composition of Hardened Specimens: Computed as in Series 254-8. See Table A-30.

Chemical Analyses of Dried Granular Samples: See Table A-31. Determinations by same procedure as in Series 254-9.

Compressive Strength: See Table 6-1, Part 6.

Flexural Strength and Modulus of Elasticity: From prisms made from same materials in same proportions as in Series 290. See Table A-32.

Adsorption Data: See Table A-33.

Description of specimens made in series 254-13

Specimens: 2-in. cubes made of cement-silica pastes.

Cements: See Tables A-1 to A-3. Cements were prepared in the laboratory mill from plant-made clinkers. Three grinds of each clinker were made, one with no added gypsum, one with enough added gypsum to give a total SO_3 content of about 2.4 percent, and one with enough to give about 5 percent SO_3. Blends were made to give cements having 1.5, 2.0, 2.5, and 3.5 percent SO_3 and specific surface area (Wagner) of 1800 cm^2/g.

Pulverized Silica: Lot 15918. Specific surface area (Wagner), 6000 cm^2/cm^3.

Weight Proportions: Cement: pulverized silica: water = 1.0 : 0.714 : 0.5.

Mixing: Each batch was mixed with a kitchen-type mixer 2 min., allowed to rest 3 min., and then mixed 2 min. more. Mixing water was cooled before use to give batch temperature of 73 ± 2 F after mixing.

Molding: Three cubes were molded from each batch.

Measurements: As in Series 254-8.

Curing: In water at 73 F. Curing water replaced with fresh water after first 24 hr., twice weekly thereafter.

Drying: As in Series 254-8.

Composition of Hardened Specimens: See Table A-34.

Analyses of Granular Samples: See Table A-35.

Compressive Strengths: See Table 6-7, Part 6.

Adsorption Data: See Table A-36.

Series 254-16

The specimens of this series were prepared for the heat of adsorption studies described in Part 4.

Cements: The cements used were 16186 and 16189, which were prepared from two of the groups of cements described in Series 254-11. No. 16186 was a blend of two cements prepared from clinker 15367, the blend having a specific surface area of 3200 cm^2/g by the permeability method. No. 16189 had the same specific surface area, being a blend of cements prepared from clinker 15623. The clinkers were of Type I and Type II compositions, respectively.

TABLE A-36—ADSORPTION DATA FOR SERIES 254-13

Water-cement ratios corrected for bleeding

Age 28 days

p/p_s	Total Water Retained at Relative Vapor Pressure Indicated, g/g cement				p/p_s	Total Water Retained at Relative Vapor Pressure Indicated, g/g cement		
	Clinker 15367 Ref. No. 13-1 w_o/c = 0.493	Clinker 15367 Ref. No. 13-2 w_o/c = 0.493	Clinker 15367 Ref. No. 13-3 w_o/c = 0.489	Clinker 15367 Ref. No. 13-4 w_o/c = 0.491		Clinker 15367 Ref. No. 13-1B w_o/c = 0.486	Clinker 15367 Ref. No. 13-2B w_o/c = 0.488	Clinker 15367 Ref. No. 13-3B w_o/c = 0.488
w_n	.2147	.2108	.2083	.1938	w_n	.2115	.2158	.2151
.09	.2542	.2504	.2462	.2295	.081	.2500	.2550	.2527
.20	.2732	.2660	.2619	.2438	.161	.2631	.2681	.2653
.36	.2989	.2903	.2864	.2631	.238	.2737	.2779	.2749
.47	.3181	.3101	.3027	.2774	.322	.2893	.2920	.2861
.61	.3403	.3317	.3258	.2961	.36	.2957	.2990	.2957
.69	.3605	.3540	.3439	.3159	.53	.3251	.3274	.3245
.75	.3683	.3610	.3510	.3224	.70	.3563	.3611	.3563
.81	.3854	.3765	.3681	.3396	.81	.3821	.3862	.3847
.84	.3931	.3833	.3779	.3495	.85	.3987	.4034	.3995
.89	.4091	.4046	.3987	.3730	.88	.4131	.4157	.4174
.96	.4502	.4466	.4435	.4313	.96	.4515	.4543	.4591
SSD	.6229	.5781*	.6223	.6176	*SSD*	.6279	.6199	.6206

p/p_s	Total Water Retained at Relative Vapor Pressure Indicated, g/g cement						
	Clinker 15367 Ref. No. 13-4B w_o/c = 0.492	Clinker 15623 Ref. No. 13-5 w_o/c = 0.470	Clinker 15623 Ref. No. 13-6 w_o/c = 0.474	Clinker 15623 Ref. No. 13-7 w_o/c = 0.473	Clinker 15623 Ref. No. 13-8 w_o/c = 0.480	Clinker 15699 Ref. No. 13-9 w_o/c = 0.498	Clinker 15699 Ref. No. 13-10 w_o/c = 0.499
w_n	.2035	.1518	.1509	.1515	.1444	.1992	.1937
.081	.2407	.1779	.1744	.1737	.1671	.2346	.2290
.161	.2518	.1833	.1843	.1838	.1773	.2478	.2423
.238	.2607	.1923	.1910	.1919	.1846	.2568	.2504
.322	.2706	.2018	.2009	.2004	.1931	.2704	.2618
.36	.2783	.2072	.2054	.2056	.1989	.2771	.2693
.53	.3002	.2261	.2238	.2230	.2162	.3000	.2891
.70	.3310	.2520	.2596	.2580	.2565	.3322	.3215
.81	.3569	.2783	.2816	.2931	.2920	.3680	.3519
.85	.3752	.2988	.3003	.3112	.3115	.3739	.3603
.88	.3941	.3224	.3169	.3312	.3292	.4113	.3900
.96	.4498	.3858	.3699	.3861	.3834	.4614	.4490
SSD	.6308	.5772	.5959	.5965	.6054	.6210	.6110

(Concluded on next page)

p/p_s	Total Water Retained at Relative Vapor Pressure Indicated, g/g cement					
	Clinker 15699 Ref. No. 13-11 w_o/c = 0.499	Clinker 15699 Ref. No. 13-12 w_o/c = 0.498	Clinker 15498 Ref. No. 13-13 w_o/c = 0.488	Clinker 15498 Ref. No. 13-14 w_o/c = 0.487	Clinker 15498 Ref. No. 13-15 w_o/c = 0.493	Clinker 15498 Ref. No. 13-16 w_o/c = 0.491
w_n	.1917	.1839	.2082	.1992	.2004	.1895
.081	.2247	.2156	.2468	.2355	.2352	.2232
.161	.2373	.2183	.2600	.2474	.2472	.2352
.238	.2462	.2346	.2688	.2554	.2558	.2430
.322	.2561	.2439	.2796	.2659	.2677	.2548
.36	.2643	.2507	.2902	.2747	.2717	.2581
.53	.2828	.2667	.3151	.2957	.2945	.2781
.70	.3144	.3082	.3487	.3273	.3243	.3162
.81	.3501	.3411	.3758	.3523	.3507	.3478
.85	.3587	.3511	.3901	.3661	.3675	.3662
.88	.3920	.3762	.4130	.3848	.3927	.3857
.96	.4526	.4390	.4485	.4374	.4444	.4407
SSD	.6308	.6087	.5485	.5478	.5600	.5742

SSD = Water content of granular sample, saturated, surface-dry for sample that had been dried and resaturated.
* This figure is probably incorrect. By comparison with others, it should be about 0.617.
w_n = Non-evaporable water; p/p_s = about 24×10^{-6}.

Specimens: The specimens were 1½x3-in. neat cement cylinders, nominal w/c = 0.50 by weight. The pastes were mixed with a kitchen-type mixer, following the 2-3-2 schedule described for earlier series. The specimens were cured continuously in water until they were used.

Results of Experiments: Experimental procedures and the results are given in Part 4 of the text.

Series 254-18

This series comprises several experiments using the high-vacuum adsorption apparatus.

Cements: The cements used were 13495, 13723-1Q, 14675, and 15365. These are cements of about average Type I composition.

Specimens: The original specimens were neat-cement pastes. As explained in the text, the samples made with cements 15365 and 13723-1Q were granules prepared previously for Series 254-9 (Ref. 15A, age 180 days) and 254-K4B (Ref. 1Q), respectively. The original specimens from which granular samples were taken were 2-in. cubes.

The specimen made with cement 13495 was a slab, cast on edge, about 0.25 cm thick and 10 cm square. The paste was mixed with a kitchen-type mixer, 2 min. mixing, 3 min. rest, followed by 2 more min. of mixing, w/c = 0.5 by weight. The mold was stored under water immediately after casting. When the paste was 1 day old, the square was cut into 1x10x0.25 cm slabs and these were stored in sealed bottles containing water-saturated cotton. After 7 years and 116 days of such storage, one of the 1x10x0.25 slabs was ground on a plate-glass surface with water and powdered emery until the thickness was reduced to an average of about 0.3 mm. This thin slab was used for adsorption measurements.

The specimen made with cement 14675 was a cylinder about 3 cm in diameter by 4 cm high. The original water-cement ratio was 0.12 by weight. The cement was mixed with the water by kneading with a stiff spatula on a steel plate. The moist mix was then loosely packed into a steel mold. By means of a close-fitting plunger and hydraulic press, the sample was compacted. The applied pressure was 24,000 lb/in^2, which was just enough to bring water to the surface of the specimen. A cross-section of the specimen at time of test was free of visible voids.

The cylinder was removed from the mold immediately after casting and then cured continuously under water in a covered can. It was 4 years 29 days old when used for these experiments.

The sample for adsorption measurements was obtained by sawing out a thin slab parallel to the vertical axis of the cylinder and grinding it to a thickness of about 0.3 mm as described above. The sample used actually comprised two such slabs, each about 1.2 x 3.8 x 0.03 cm.

Test Results. All the experimental data are given in the text.

Title 43-5c —a part of PROCEEDINGS, AMERICAN CONCRETE INSTITUTE Vol. 43

JOURNAL
of the
AMERICAN CONCRETE INSTITUTE
(copyrighted)

Vol. 18 No. 4 7400 SECOND BOULEVARD, DETROIT 2, MICHIGAN December 1946

Studies of the Physical Properties of Hardened Portland Cement Paste*

By T. C. POWERS†
Member American Concrete Institute
and T. L. BROWNYARD‡

Part 3. Theoretical Interpretation of Adsorption Data§

CONTENTS

*Received by the Institute July 8, 1946—scheduled for publication in seven installments; October 1946 to April, 1947. In nine parts:

Part 1. "A Review of Methods That Have Been Used for Studying the Physical Properties of Hardened Portland Cement Paste". ACI Journal, October, 1946.
Part 2. "Studies of Water Fixation"—Appendix to Part 2. ACI Journal, November, 1946.
Part 3. "Theoretical Interpretation of Adsorption Data."
Part 4. "The Thermodynamics of Adsorption"—Appendix to Parts 3 and 4.
Part 5. "Studies of the Hardened Paste by Means of Specific-Volume Measurements."
Part 6. "Relation of Physical Characteristics of the Paste to Compressive Strength."
Part 7. "Permeability and Absorptivity."
Part 8. "The Freezing of Water in Hardened Portland Cement Paste."
Part 9. "General Summary of Findings on the Properties of Hardened Portland Cement Paste."

†Manager of Basic Research, Portland Cement Assn. Research Laboratory, Chicago 10, Ill.
‡Navy Dept., Washington, D. C., formerly Research Chemist, Portland Cement Assn. Research Laboratory, Chicago 10, Ill.

§The characteristics of the cements mentioned in this section may be found in the Appendix to Part 2.

The adsorption isotherms obtained from hardened cement paste are identical in several respects with those obtained from other materials that are very different in chemical and physical properties. For example when glass spheres[1]* or oxide-coated cathodes of radio tubes[2] are exposed to nitrogen vapor (at the temperature of liquid air), or when a plane mercury surface is exposed to CCl_4 vapor (11 C),[3] the adsorption curves obtained are of the same type as those for water vapor on cement paste. Also, the same type of curve is obtained when crystalline solids such as titanic oxide, stannic oxide, zinc oxide or pulverized quartz are exposed to water vapor at room temperature[4]. Moreover, curves of the same type may be obtained with different vapors on the same solid[5].

The similarities just mentioned exist not only among materials that are not porous, that is, materials on which adsorption is confined to the visible surfaces, but also among many porous solids having negligible superficial surface areas. With suitable vapors the following materials, some porous, some not, all give the same type of isotherm: building stone[6]; cotton[7, 8]; asbestos fibre[9]; wood[10]; wood pulp[11]; carbon black[12]; titania gel, ferric oxide gel, rice grains[13]; cellophane[14]; bone-char[15]; cellulose[16]; silica gel[17]; proteins[18]; soils[19]; wool[20].

It appears therefore that the curves found for portland cement paste are not characteristic of the particular substances composing the paste but represent some factor common to many dissimilar substances. We will see in what follows that this common factor is probably nothing other than a solid surface that has an attraction for the adsorbed substance.

B.E.T. THEORY

Various theories have been advanced to explain the taking up of gases and vapors by solid materials[5]. Among the most recent, and at present the most useful, is the theory of Brunauer, Emmett and Teller, [21, 22] known as the multimolecular-adsorption theory, or the B.E.T. theory for brevity. It is beyond the scope of this paper to discuss the B.E.T. theory in full; reference should be made to Brunauer's book[5] or to the original papers for an adequate treatment. However, it is necessary to review here the main features of the theory.

The theory rests on a concept advanced earlier by Langmuir. The taking up of a gas by a solid is considered to be the result of a physical attraction between the molecules of the gas and the surface molecules of the solid.† This field of force is believed to arise from three different

*See references end of Part 3.
†Chemical reaction with the solid is not excluded by the theory but it will not be considered here.

causes, or to be made up of three different forces that are known collectively as *van der Waal's forces.* Hence, the process under discussion is called *van der Waal's adsorption.* These forces are of a lesser order of intensity than those involved in most chemical reactions, but they may be effective over greater distances.

A solid surface exposed to a continuous bombardment of gas molecules catches and holds some of the gas molecules, at least momentarily. Moreover, when the gas is also a vapor such as water, the molecules caught on the surface are in a condensed state and may be considered as a separate phase. Hence, when they are adsorbed, the molecules must give up their latent heat of vaporization. Besides this, adsorption usually is accompanied by a further evolution of heat which may be said to represent the energy of interaction between the solid and the condensed substance; this is called the *net heat of adsorption.*

Some of the adsorbed molecules acquire enough kinetic energy to escape from the force field of the solid surface. The over-all result is a continuous interchange between the surface region and the interior of the vapor phase, but the average molecular concentration at the solid surface remains higher than that of the interior of the vapor phase by virtue of the surface attraction.

The derivation of the mathematical statement of the theory starts with the assumption that the rate of condensation is directly proportional to the frequency of impact between the solid and the vapor molecules, which frequency is proportional to the vapor pressure when temperature is constant. The rate of evaporation is expressed as a function of the amount of energy a condensed molecule must acquire to escape from a particular situation in the condensed phase. In the derivation of the mathematical expressions that have found use, only two situations of a molecule in the condensed phase are recognized: (1) a molecule may be condensed on bare surface; (2) a molecule may be condensed on a layer of previously condensed molecules. It is assumed that a molecule in the second situation can escape when it acquires energy exactly equal to its heat of vaporization; a molecule in the first situation must acquire a different (usually greater) amount of energy to escape. In other words, the net heat of adsorption is assumed to be zero for all molecules not in the first layer.*

The theory requires that at any given vapor pressure the amount adsorbed is directly proportional to the surface area of the solid.

A logical extension of the assumptions made in the derivation is that at the saturation pressure there is no limit to the number of layers that might be condensed on an open surface.

*Brunauer, Emmett, and Teller have published an equation representing the assumption that the net heat of adsorption from the second layer also differs from zero. This equation includes also the assumption that the packing of molecules is different in the first from that in the succeeding layers. This equation does not appear to have found use (See Ref. 21, p. 313).

The most widely used mathematical statement of the theory is the following expression:

$$\frac{w}{V_m} = \frac{C(p/p_s)}{(1 - p/p_s)\,(1 - p/p_s + C(p/p_s))} \qquad \text{(A)}$$

in which

w = quantity of vapor adsorbed at vapor pressure p
V_m = quantity of adsorbate required for a complete condensed layer on the solid, the layer being 1 molecule deep
p = existing vapor pressure
p_s = pressure of saturated vapor

C is a constant related to the heat of adsorption as follows:

$$C = k\,e^{\frac{Q_1 - Q_L}{RT}}$$

where

k is a constant assumed to be 1.0 in computations.
Q_L = normal heat of condensation of the vapor per mole of vapor
Q_1 = total heat of adsorption per mole of vapor
$(Q_1 - Q_L)$ = net heat of adsorption per mole of vapor
R = the gas constant
T = absolute temperature
e = base of natural logarithms

Owing to the assumptions made in the derivation, eq. (A) would be expected to hold only for adsorption on exterior surfaces. It could hardly be expected to hold for surfaces on the interior of a porous solid where unlimited adsorption would obviously be impossible. Brunauer, Emmett, and Teller recognized this and introduced another constant n which was intended to be the maximum number of layers adsorbed. The resulting four-constant equation does not fit any known data from a porous adsorbent over the whole pressure range. However, Pickett[23] discovered a way to improve the derivation of the B.E.T. four-constant equation and supplied a better expression. This equation has the same four constants as the original. It fits many adsorption curves over about 90 percent of pressure range. In some cases it conforms to the extremes, but in the middle range the theoretical curve is above the experimental. There are also many curves that this equation does not fit in the high-pressure range. One reason for this will be explained in connection with the theory of capillary condensation, discussed below.

In general, the four-constant equations did not prove to be very useful in this study; hence, they are not given here. However, the three-constant eq. (A) can be used to represent the low-pressure part of the curve precisely. Of the three constants, p_s is the same for all curves and C is the same for most of them. Consequently, in most cases adsorption characteristics can be represented by V_m alone.

THE THEORY OF CAPILLARY CONDENSATION

Condensation of vapor in a porous cement paste seems to be most adequately explained by a combination of a theory based on the energy available at the solid surface, such as the B.E.T. theory discussed above, and a theory based on energy available at the surface of a liquid, the capillary-condensation theory.

The capillary-condensation theory rests on the fact that the surface of a liquid is the seat of available energy. The molecules at the surface of a liquid not being completely surrounded by other molecules of like kind are under an inwardly directed intermolecular force. When a given body of water is changed in shape so as to increase its surface area, work must be done against the forces tending to draw the molecules out of the surface. Consequently, when left to itself, a small body of liquid tends to become spherical, since that is the form giving a minimum of surface.

This phenomenon has an effect on the vapor pressure of the liquid. How this comes about can be seen by considering the behavior of water in a small glass cylinder, as shown in Fig. 3-1. The solid curve at the top

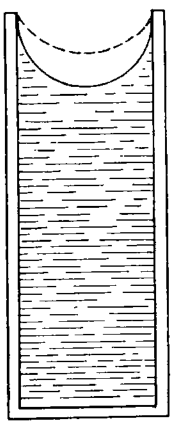

Fig. 3-1

represents the meniscus of the water surface. Owing to the surface tension, which strives to straighten the meniscus, that is, to reduce its curvature and thus reduce the surface area, the water in the vessel is under tension. Consequently, the vapor pressure of the water in the tube will be less than normal for the existing temperature. The greater the curvature of the meniscus, the greater the tension in the water and hence the lower the vapor pressure. The relationship between surface-curvature and vapor pressure was worked out by Lord Kelvin. It may be written

$$ln\ p/p_s = -\frac{2\sigma M}{d_f RTr} \qquad (1)$$

where

p_s = vapor pressure over plane surface at temperature T, the saturated vapor pressure
p = the existing vapor pressure over a concave surface
σ = surface tension of liquid
d_f = density of liquid
M = molecular weight of liquid
R = the gas constant
T = absolute temperature
r = radius of curvature of the circular meniscus

Under the conditions pictured in Fig. 3-1 the greatest curvature that the liquid can have is limited by the radius of the container. When the liquid surface has this curvature, the liquid can be in equilibrium with only one vapor pressure, p, corresponding to the radius of curvature r, as given in eq. (1). If the pressure of the vapor is kept below p, all the liquid in the vessel will evaporate. If the pressure is maintained above p, some vapor will condense, increasing the amount of water in the vessel. But under the conditions pictured, condensation would lessen the curvature of the liquid as indicated by the dotted line and there would be a corresponding rise in the equilibrium vapor pressure. If the vapor pressure is kept equal to the saturation pressure, that is, the maximum possible over a plane surface at the existing temperature, condensation will proceed until the tube fills and the surface curvature disappears ($r = \infty$).

The minimum relative vapor pressure at which the liquid in the vessel can retain its meniscus depends on the maximum possible curvature of the meniscus. This in turn depends on the bore of the cylinder. Table 3-1 gives an idea of the curvature required to produce a given effect on vapor pressure.

The main point to note in Table 3-1 is that the surface must have a high degree of curvature to produce an appreciable effect on the vapor pressure of the liquid. For example, if the radius of curvature is 0.1 micron, the vapor pressure is 99 percent of the normal value, p_s. A radius of curvature of 0.0015 micron would reduce the pressure to 50 percent of p_s. The figures given should not be taken too literally; they are undoubtedly in error through the low-pressure range, for the equation takes no account of the fact that the physical properties of the liquid are affected by capillary and adsorption forces. The table serves only to indicate what the order of magnitude of the curvatures must be when capillary condensation occurs.

An "adsorption curve" of almost any shape could easily be accounted for by the capillary condensation theory. The simplest approach is to imagine first that the voids in a porous solid are cylindrical pores of

TABLE 3-1—RELATIONSHIP BETWEEN AQUEOUS RELATIVE VAPOR PRESSURE AND RADIUS OF CURVATURE

Calculated from Kelvin's Equation—Temperature = 25 C

Relative vapor pressure, p/p_s	Radius of curvature of meniscus	
	cm	microns
0.10	4.6×10^{-8}	.0005
0.20	6.6×10^{-8}	.0007
0.30	8.8×10^{-8}	.0009
0.40	11.5×10^{-8}	.0012
0.50	15.2×10^{-8}	.0015
0.60	20.8×10^{-8}	.0021
0.70	29.5×10^{-8}	.0030
0.80	47.2×10^{-8}	.0047
0.90	100.0×10^{-8}	.0100
0.95	204.0×10^{-8}	.0204
0.98	532.0×10^{-8}	.0532
0.99	1052.0×10^{-8}	.1052
1.00	∞	∞

various sizes and that when a cylinder is partly filled, the radius of curvature of the liquid meniscus equals the radius of the cylinder. At a given pressure p, all cylinders smaller than the corresponding r (see eq. 1) would become or remain full and all larger than r would become or remain empty. The shape of the curve would therefore depend on the range of sizes present and the total capacity of each size.

This simple analogy led Freyssinet [24] and others before him to consider an adsorption curve to be a means of ascertaining pore-size distribution in systems of submicroscopic pores. However, a naturally formed porous solid so constituted is hardly conceivable. It is much more likely that the pore spaces resemble those in an aggregation of particles. The shapes of the particles may be spherical, fibrous, or between these extremes. Capillary condensation could occur in the interstices in the manner illustrated in Fig. 3-2. At the point of contact between two spheres there is a space of wedge-shaped cross section. Condensation in this space would form a circular lens around the point of contact and the liquid would present a curved surface. Similarly, where two prismatic bodies make contact, water condensed in the region of contact would present a curved surface, somewhat as shown.

In the circumstances pictured, the water surface would have two curvatures. Hence, in this case Kelvin's equation would take the general form

$$ln\ p/p_s = -\frac{\sigma M}{d_l RT}\left(\frac{1}{r_1}+\frac{1}{r_2}\right) \quad \ldots\ldots\ldots\ldots\ldots\ldots\ldots\ldots\ldots\ldots (2)$$

where

r_1 and r_2 are the principal radii of curvature.

For the conditions shown in Fig. 3-2 one of the r's would be negative.

Since the structure of paste is probably granular, fibrous, or perhaps plate-like, it is evident that Kelvin's equation provides no simple way of computing the size of the pores; it only gives the *effective* curvature of the water surface. It can, however, explain the condensation of vapor in a porous solid, and we will see evidence in the data indicating that a part of what is here called adsorbed water in cement pastes is taken up by capillary condensation.

COMBINING THE B.E.T. AND CAPILLARY CONDENSATION THEORIES

When adsorption of a vapor occurs in a porous solid of granular or fibrous structure, the liquid surfaces are certain not to be plane. They will be concave, at least in some regions. Therefore, the free surface energy of the solid and the free surface energy of the condensed liquid must both be causes of condensation.*

Brunauer, Emmett, and Teller tried to take this factor into account by adding a fifth constant representing the release of the surface energy of the liquid when two adsorbed layers merge[26]. This five-constant equation is very unwieldy and it embodies the assumption questioned by Pickett[23]. Also, it rests on the oversimplifying assumption that adsorption is occurring only between plane parallel surfaces.

By the B.E.T. theory, vapor would be expected to condense uniformly over all the available surface. But in a porous body, the surface tension

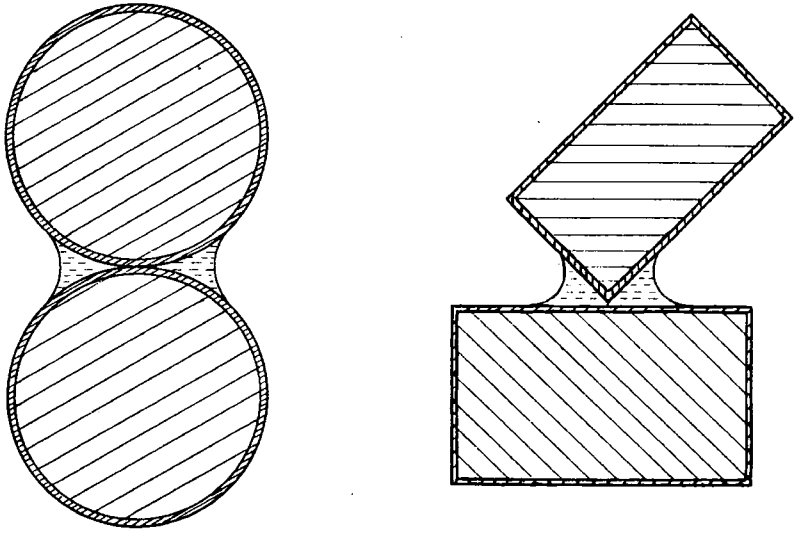

Fig. 3-2

*See Part 4.

of the liquid must influence the distribution of the condensed water, whether it is primarily responsible for the condensation or not. Thus, in Fig. 3-2, B.E.T. adsorption could lead only to a uniform layer of condensate around each sphere, but surface tension would require the liquid to collect as shown, for the condition pictured is the most stable one possible under the circumstances. This follows at once from the fact that if the liquid shown in the lens were spread evenly over the two spheres, the total surface area of the liquid would be increased and the work done would be equal to the product of the increase in area and the surface tension of the liquid.

If, as assumed in the B.E.T. equation, only the molecules in the first layer lose more than their heat of condensation, then all but the first layer should tend to collect in the lens. However, Harkins and Jura[27] have shown that the adsorption forces probably affect more than the first layer. Therefore, the net heat of adsorption probably represents the heat from several layers. This being true we can expect the adsorbed layer to vary in average thickness with the curvature of the liquid meniscus, the greater the curvature the greater the tendency for adsorbed molecules to collect in the lens.

On account of the effect of liquid surface tension the relationship between water content and vapor pressure depends on the characteristics of the pore system. Since the characteristics of the pore system are not predictable from any adsorption theory, it follows that no general equation can be expected to apply to all porous bodies over the whole pressure range. Since, however, no appreciable capillary condensation is to be expected below about $0.4p_s$, general theories may be expected to apply in this low range of vapor pressures.

As will be seen, little quantitative use is made of these theories, except the B. E. T. eq. (A) applied to the range $p = 0.05\ p_s$ to $0.40\ p_s$. However, many features of the interpretations given rest on the theories described above. That is, it was possible to use the theories qualitatively even where the mathematical expressions intended as expressions of the theoretical concepts were found to be inadequate.

Effect of soluble salts on adsorption curves

The foregoing discussion is based on the assumption that the adsorbed liquid is pure water. However, in hardened portland cement paste the water will contain dissolved salts, principally $Ca(OH)_2$, $NaOH$ and KOH.* At any given water content the observed reduction in vapor pressure is due not only to the capillary and surface effects described above, but also to the dissolved salts. The magnitude of the effect of the dissolved salts can be estimated from the vapor-pressure isotherms of the salt

*Because of its low solubility, $Ca(OH)_2$ can be ignored.

solutions and the amount of dissolved alkali in the sample of hardened paste.

Vapor-pressure data [28] for aqueous solutions of *NaOH* and *KOH* are given in Fig. 3-3. The lowering of vapor pressure due to the alkalies can be determined from these curves, for any given concentration of the alkalies.

The amount of dissolved alkali in hardened paste probably varies considerably among the different samples. Sample No. 254-11-2 is considered to be representative of the average. The original mortar was prepared from cement 15758 ($w_o/c = 0.46$) and was cured 28 days in water. The cement originally contained 0.3 percent Na_2O and 0.4 percent K_2O which, in g/g of cement, corresponds to 0.0019 and 0.0024 of *NaOH* and *KOH*, respectively. An unknown portion of these alkalies undoubtedly remained in the unhydrated cement and can be considered insoluble for the present purpose. Some of the soluble alkali was leached from the sample during the 28-day period of water curing. There is also reason to believe that some of it was adsorbed by the solid phase and thus effectively kept from the solution. Hence, the sample as tested must have contained considerably less than 0.004 g of soluble alkali (total of *NaOH* and *KOH*) per g of cement. The adsorption isotherm from this sample is given in Fig. 3-4, upper curve. This curve presumably represents the combined effect of surface adsorption, capillary condensation, and dissolved alkali. The lower curve in Fig. 3-4 shows the amount of water that could have been held by 0.004 g of sodium hydroxide at any given relative vapor pressure above about 0.07 p_s, the vapor pressure of a saturated solution of sodium hydroxide at 25 C. (See Fig. 3-3.) Since the actual amount of alkali must have been less than 0.004 g, the amount of water that could have been held by the alkali alone would be represented somewhere below the curve as drawn.

It thus becomes apparent that at pressures below about 0.8 p_s only a very small part of the total water taken up by this cement paste could be accounted for by the dissolved alkalies. In the range of higher pressures, the possible effect of the alkali is greater. As p/p_s approaches 1.0, the amount of water that could be held by the alkali approaches infinity. Since, however, the topmost point of the curve is established by saturating the granular sample with liquid water, its position is determined by the capacity of the sample and the assumption that, at saturation, $p/p_s = 1.0$. In this case the capacity of the sample was 0.33 g of water per gram of original cement. With 0.004 g of alkali in 0.33 g of evaporable water the relative vapor pressure would be slightly below 1.0.

Since the effect of the alkali is small, no correction for its effect has been attempted; the topmost point is always plotted at $p/p_s = 1.0$, and

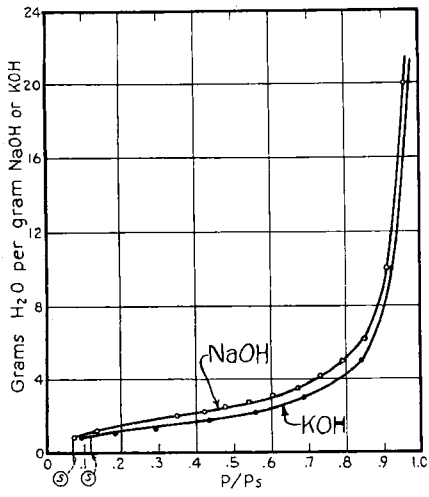

Fig. 3-3 (above)—Vapor pressure isotherms for aqueous solutions of $NaOH$ and KOH

S = Saturated solution

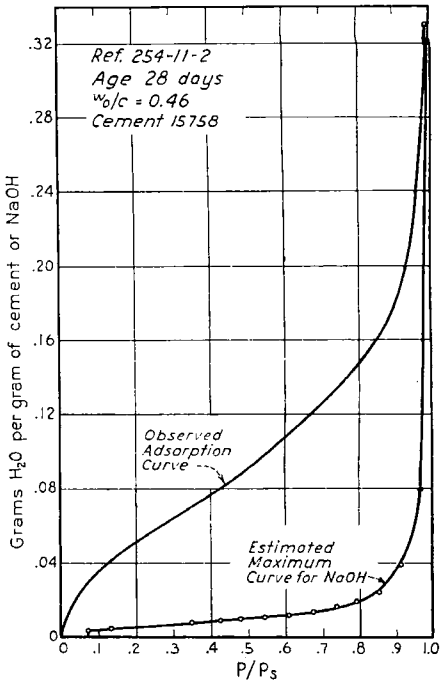

Fig. 3-4 (right)—Estimation of effect of dissolved alkali on adsorption isotherm

all other points are treated as if their positions were determined by surface adsorption and capillary condensation only.

Differences in the amount of soluble alkali among various samples, within the range that might reasonably be expected, probably have little effect on the lower part of the curve, the part that is used in the analyses presented below. However, such differences probably produce considerable effects on the shapes of the upper parts of the curves and hence contribute to the difficulty of interpreting the upper parts.

To minimize the effect of dissolved alkali, most of the specimens were stored in water for the first 28 days of their curing period to leach some of the alkali from the specimens. Longer periods of water storage were avoided because of undesirable leaching of $Ca(OH)_2$.

APPLICATION OF THE B.E.T. EQUATION (A)

Method of evaluating C and V_m

The constants C and V_m were evaluated in the manner recommended by Brunauer, Emmett, and Teller. Eq. (A), written in the form

$$\frac{1}{w}\frac{x}{1-x} = \frac{1}{V_m C} + \frac{C-1}{V_m C}x, \quad (x = p/p_s)$$

shows that a plot of experimental values for $\frac{1}{w}\frac{x}{1-x}$ against x should

give a straight line. The slope of the line will be $\frac{C-1}{V_mC}$ and the intercept on the y-axis will be $1/V_mC$. The application of this method to data from cement pastes is illustrated in Fig. 3-5 and in Tables 3-2 and 3-3. Two of the four diagrams represent data obtained by the air-stream method, and the others represent data obtained by the high-vacuum method.

TABLE 3-2—TYPICAL DATA FOR COMPUTING V_m AND C

Data obtained by air-stream method

p/p_s ($= x$)	w g/g of dry paste	$\frac{x}{1-x}$	$\frac{1}{w}\frac{x}{1-x}$
Ref. 254-11-11—Cement 16213			
0.081	0.0189	0.088	4.65
0.161	0.0253	0.192	7.60
0.238	0.0298	0.312	10.45
0.322	0.0362	0.475	13.1
0.360	0.0395	0.562	14.2
0.530	0.0503	1.128	22.4
Ref. 254-9-15A-180—Cement 15365			
0.09	0.0267	0.099	3.79
0.20	0.0348	0.250	7.18
0.36	0.0464	0.562	12.1
0.47	0.0539	0.887	16.5
Ref. 254-9-15A-270A—Cement 15365			
0.081	0.0187	0.0873	4.68
0.161	0.0264	0.192	7.27
0.238	0.0310	0.312	10.0
0.322	0.0359	0.475	13.2
0.360	0.0400	0.563	14.1
0.530	0.0500	1.127	22.6

C and V_m can be computed conveniently from the intercept on the x-axis and from the ordinate at $x = 0.5$. Thus, when $\frac{1}{w}\frac{x}{1-x} = 0$, $C = 1 - \frac{1}{x}$; and when $x = 0.5$, $V_m = \frac{1+C}{2C}w$. In Fig. 3-5A we see that when $\frac{1}{w}\frac{x}{1-x} = 0$, $x = -0.053$ and when $x = 0.5$, $1/w = 19.3$. Therefore,

$$C = 1 + \frac{1}{0.053} = 19.8, \text{ and } V_m = \frac{1+19.8}{2 \times 19.8} \times \frac{1}{19.3} = 0.027$$

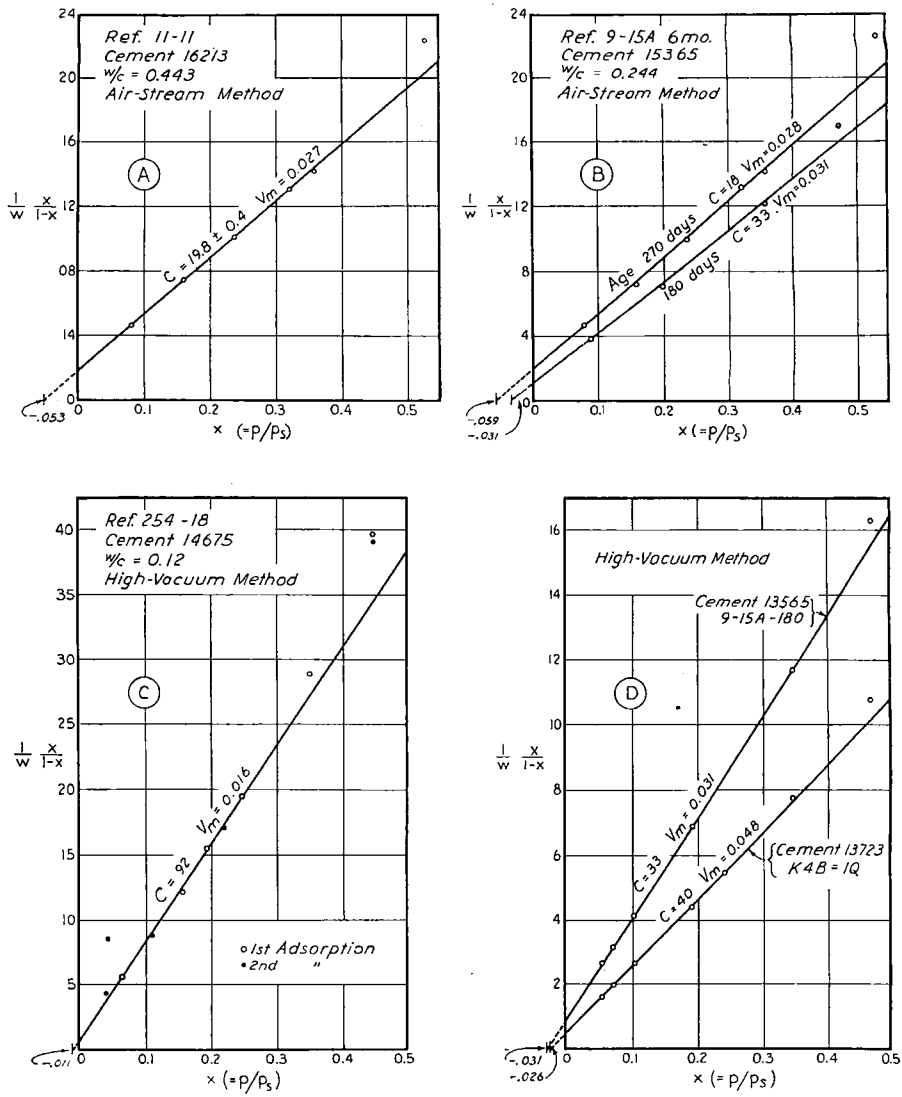

Fig. 3-5—Typical plots of the kind used for evaluating C and V_m
Data from Tables 3-2 & 3-3.

The nomenclature used here is the same as that used by Brunauer et al. except that they used V for the *volume* of gas adsorbed, whereas here w is used for *weight* adsorbed. w is expressed either in grams per gram of dry hardened paste (evaporable water removed) or as grams per gram of original cement. Having become accustomed to thinking of V_m as a factor proportional to surface area, we have somewhat illogically retained this symbol, but express it in grams instead of cc.

TABLE 3-3—TYPICAL DATA FOR COMPUTING V_m AND C

Data obtained by high-vacuum method

p/p_s (= x)	w g/g of dry paste	$\frac{x}{1-x}$	$\frac{1}{w}\ \frac{x}{1-x}$
Ref. 254-18-9-15A-180—Cement 15365			
0.055	0.0227	0.0598	2.63
0.073	0.0249	0.0790	3.17
0.104	0.0284	0.117	4.13
0.193	0.0347	0.240	6.91
0.244	0.0400	0.322	8.06
0.349	0.0455	0.534	11.7
0.472	0.0542	0.885	16.3
Ref. 254-K4B-1Q—Cement 13723			
0.055	0.0369	0.0598	1.62
0.073	0.0397	0.0790	1.99
0.104	0.0435	0.117	2.69
0.193	0.0540	0.240	4.40
0.244	0.0587	0.322	5.49
0.349	0.0686	0.534	7.78
0.472	0.0819	0.885	10.8
Ref. 254-18—Cement 14675			
0.064	0.0552	0.0684	1.24
0.155	0.0646	0.1835	2.84
0.193	0.0675	0.2395	3.55
0.249	0.0720	0.3310	4.60
0.350	0.0817	0.5380	6.58
0.446	0.0910	0.8040	8.84

THE RELATIONSHIP BETWEEN V_m AND NON-EVAPORABLE WATER (w_n) FOR SAMPLES CURED AT 70-75 F

The quantity V_m is considered to be proportional to the internal surface area of the sample. Since the specific surface of microcrystalline material is negligible compared with that of colloidal material, V_m is also considered to be proportional to the amount of colloidal material in the sample. The quantity w_n represents the amount of non-evaporable water in both colloidal and non-colloidal material. Therefore, if a given cement produces the same kind of hydration products at all stages of its hydration, the ratio V_m/w_n should be constant for any given cement under fixed curing conditions. However, the ratio of colloidal to non-colloidal hydration products should be expected to differ among cements of different chemical composition. Hence, the ratio V_m/w_n should be different for different cements.

V_m and w_n are plotted for several different cements and different mixes and ages, in Fig. 3-6 and 3-7. The points in most of the diagrams show a considerable amount of scatter. Some of this is due to random experimental vagaries and some of it is apparently due to variations in drying conditions discussed earlier.

In view of the fact that the variations show no consistent influence of the original water-cement ratio or of the age of the sample, the relationships indicate that for any given cement the ratio V_m/w_n is independent of age or water-cement ratio.

If the points fell on a straight line through the origin, that would indicate that the ratio of colloidal to non-colloidal products is precisely the same at all stages of hydration. The data are not sufficiently concordant to indicate definitely whether this is so or not. There is some reason to believe that the reactions during the first few hours cannot produce exactly the same products as those that occur later. Particularly, the gypsum is usually depleted within the first 24 hours and thus the reactions involving gypsum cannot occur at later periods.

If calcium sulfoaluminate as produced in paste is non-colloidal, the ratio of colloidal to non-colloidal material should be lower during the first 24 hours than it is at any later time. The effect on the graph would be that of causing the proportionality line that holds for the later ages to cut the w_n-axis to the right of the origin. As said before, the plotted data do not indicate definitely where the intercept should be. They do indicate, however, that if the intercept is to the right of the origin, it is nevertheless near the origin, as indeed it should be in view of the relatively small amount of calcium sulfoaluminate that is formed. To simplify the handling of the data, we have assumed that the line passes through the origin and thus have considered the ratio of colloidal to non-colloidal material to be the same at all ages for a given cement.

Fig. 3-6 represents the data from Series 254-8 and 254-9. It represents 5 different commercial cements that had been used in experimental highways. The data on this series are the least concordant of all obtained in the investigation.

Fig. 3-7 represents cements prepared from 5 other commercial clinkers. Different plant grinds of each clinker were blended to give each cement a specific surface of 1800 sq. cm. per g (Wagner).

The ratios determined for the cements in each of these two groups were averaged. The results are shown in Table 3-4.

The figures in the third column give the mean values and those in the fourth give the probable error of the mean. Those in the last column give the probable error of a single test value and thus reflect the degree of scatter of the data.

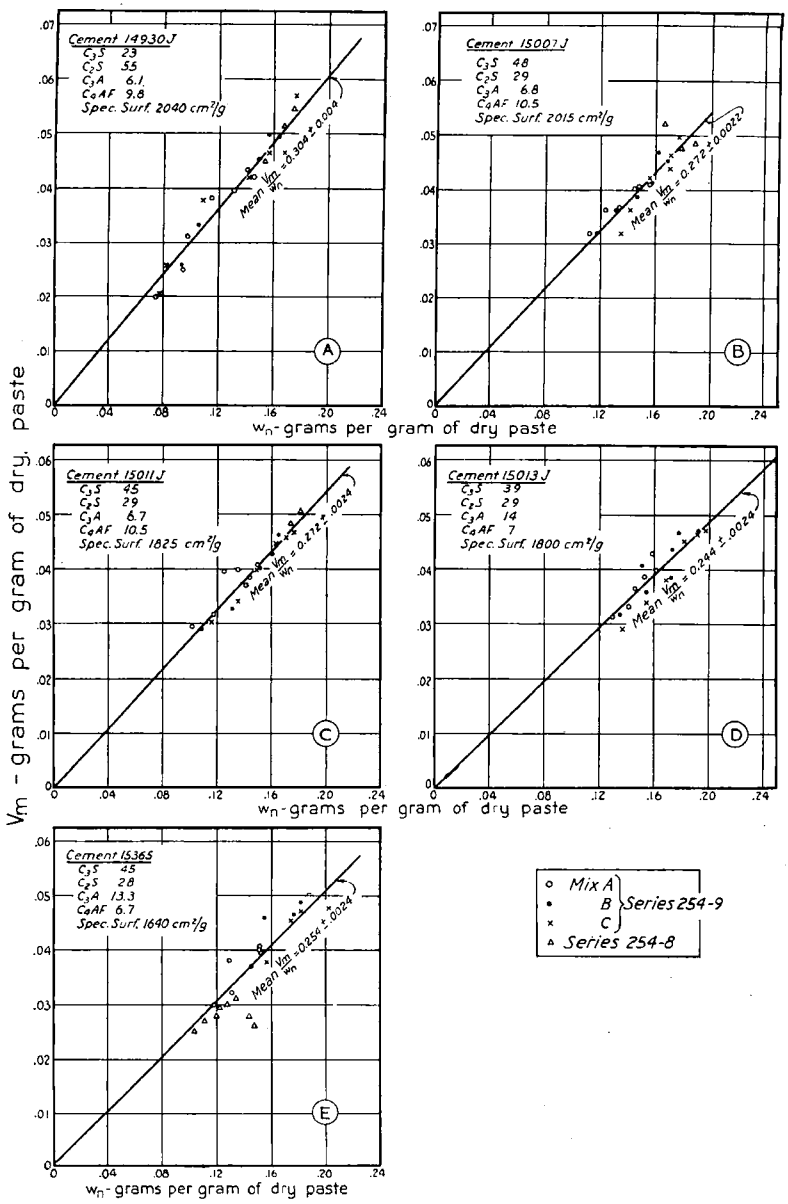

Fig. 3-6—Relationship between V_m and w_n for pastes of Series 254-9

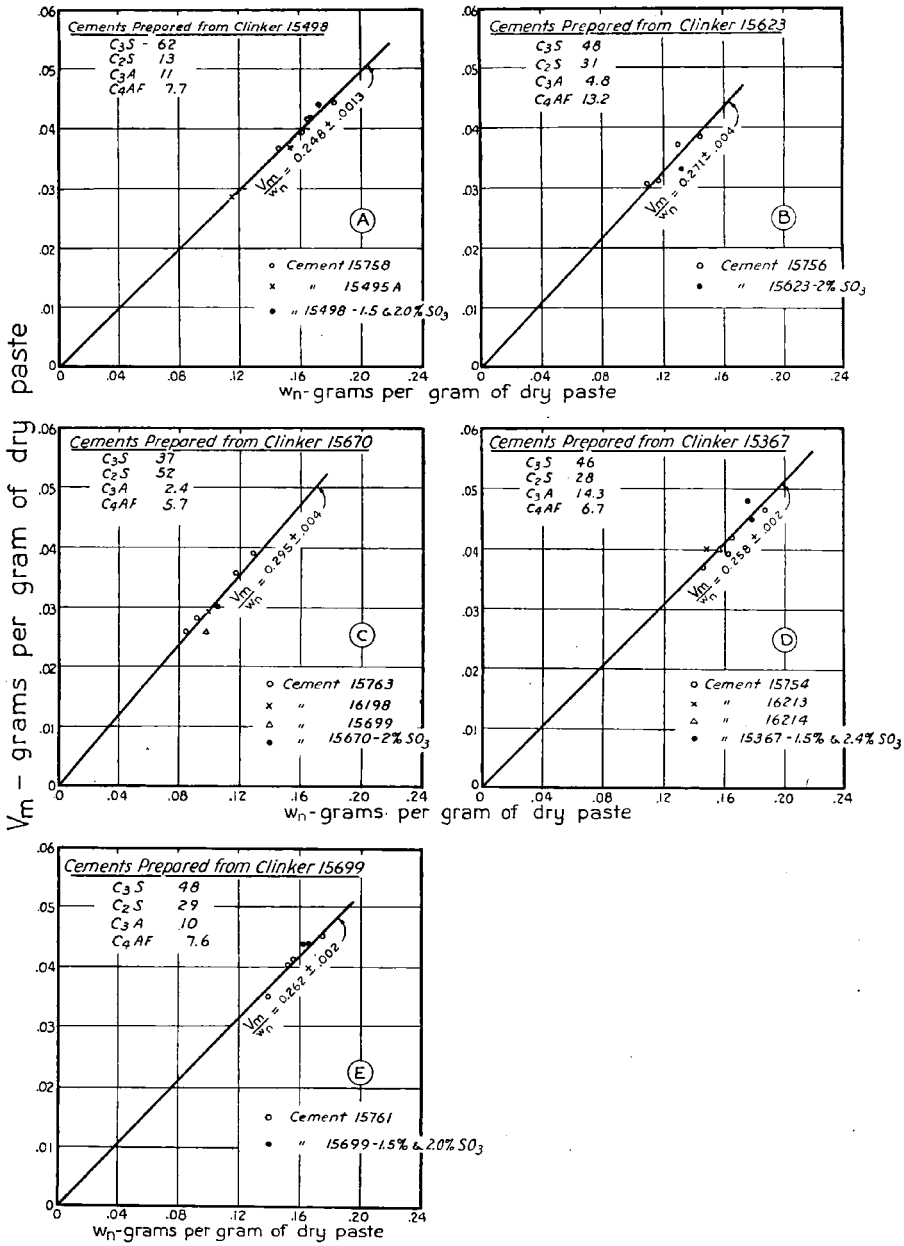

Fig. 3-7—Relationship between V_m and w_n for pastes of Series 254-11 and 254-13

TABLE 3-4—MEAN VALUES OF V_m/w_n FOR TWO GROUPS OF CEMENTS

Cement No.	ASTM classification*	Mean value of V_m/w_n	Probable error of mean	Probable error of single value
		Series 254-9		
14930J	IV	.304	.00392	.0176
15007J	II	.272	.00216	.0089
15011J	II	.272	.00242	.0102
15013J	I	.244	.00259	.0107
15365	I	.254	.00239	.0115
		Series 254-11		
15498	III	.248	.00131	.003
15623	II	.271	.00405	.008
15670	IV	.295	.00411	.010
15367	I	.258	.00244	.006
15699	I	.262	.00203	.004

*ASTM designation C-150-40T. The classification here is based only on the computed quantities of the four major compounds. The surface area requirements are not met in all cases.

To evaluate the effect of composition, the assumption was made that the form of the relationship would be

$$\frac{V_m}{w_n} = A(\%\ C_3S) + B(\%\ C_2S) + C(\%\ C_3A) + D(\%\ C_4AF)$$

The values of the coefficients were determined first from 200 items of data representing about 50 different cements. Then, owing to the fact that 100 of these items represented only 5 cements (Series 254-9), a second analysis was made excluding the data from Series 254-9. The results of the two analyses were as follows:*

For 200 items of data:

$$\text{Eq. (3):}\quad \frac{V_m}{w_n} = \left[\begin{array}{l} .00208(\%C_3S) \\ \pm .00006 \end{array} + \begin{array}{l} .00326(\%C_2S) \\ \pm .00004 \end{array} + \begin{array}{l} .00251(\%C_3A) \\ \pm .00016 \end{array} + \begin{array}{l} .00549(\%C_4AF) \\ \pm .00030 \end{array}\right]$$

For 100 items of data:

$$\text{Eq. (4):}\quad \frac{V_m}{w_n} = \left[\begin{array}{l} .00230(\%C_3S) \\ \pm .00012 \end{array} + \begin{array}{l} .00320(\%C_2S) \\ \pm .00006 \end{array} + \begin{array}{l} .00317(\%C_3A) \\ \pm .00016 \end{array} + \begin{array}{l} .00368(\%C_4AF) \\ \pm .00046 \end{array}\right]$$

The two equations give similar coefficients for C_2S and C_3S but considerably different coefficients for C_3A and C_4AF. However, applied to the same cements, the computed results are not far different, except for

*See footnote, Part 1, page 121.

certain compositions. This is shown by the data given in Table 3-5. Here the observed mean values of V_m/w_n for the cements appearing in Fig. 3-6 and 3-7 are compared with values computed from composition. It appears that the value of V_m/w_n can be computed from composition with fairly satisfactory accuracy by means of either equation. However, eq. (4) probably gives the more correct evaluation of the effect of variations in composition, since individual cements appear in the analysis with approximately equal weights.

The influence of composition as given by eq. (4) is illustrated in Table 3-6.

The results given in the last column of the table show that the influence of composition on this ratio is not very large. The variation occurs mainly among those cements whose compositions differ from the average chiefly in C_3S, C_4AF or both.

TABLE 3-5—COMPARISON OF OBSERVED AND COMPUTED VALUES OF V_m/w_n

Cement No.	ASTM type	Mean V_m/w_n observed	V_m/w_n computed from compound composition	
			Eq. (3)	Eq. (4)
15013J	I	0.244±0.003	0.253	0.256
15365	I	0.254±0.002	0.255	0.260
15367*	I	0.258±0.002	0.253	0.258
15699	I	0.262±0.002	0.254	0.255
Average		0.254	0.254	0.256
15007J	II	0.272±0.002	0.269	0.264
15011J	II	0.272±0.002	0.263	0.257
15623*	II	0.271±0.004	0.284	0.272
Average		0.272	0.272	0.264
14930J	IV	0.304±0.004	0.298	0.286
15670*	IV	0.295±0.004	0.284	0.281
Average		0.300	0.291	0.284
15498*	III	0.248±0.001	0.243	0.249

*This item represents all cements made from this clinker.

The theoretical significance of the coefficients of eq. (3) or (4) found by the method described is not certain, mainly because of the lack of definite knowledge concerning the chemical composition of the hydration products. The data support arguments given elsewhere to the effect that the hydration products of the alumina-bearing compounds are not microcrystalline as they are when these compounds are hydrated alone in an abundance of water; instead, the coefficients for C_3A and C_4AF,

TABLE 3-6—INFLUENCE OF CHEMICAL COMPOSITION ON V_m/w_n

Type of composition	Computed compound composition percent by wt.				Computed $\frac{V_m}{w_n}$ Eq. (4)
	C_3S	C_2S	C_3A	C_4AF	
Type I Normal C_3A	45	29	9.7	7.5	0.255
High C_3A	45	28	14.0	5.0	0.256
Type II High iron	41	29	5.4	14.8	0.259
High silica	40	41	6.4	9.7	0.279
Type III Normal C_3A	59	13	10.4	7.6	0.238
High C_3A	59	13	14.0	5.0	0.240
Type IV High iron	25	48	6.2	13.8	0.282
High silica	33	54	2.3	5.8	0.277

taken literally, indicate that, per gram of compound, these compounds contribute to the total surface area of the hydration products, that is, to V_m, as much as or more than do the two silicates, which are known to produce colloidal hydrates. In any event, the analysis shows that however the Al_2O_3 and Fe_2O_3 enter into combination in the hydration products, they must appear in solids having a high specific surface.

The coefficient of C_3S is less than that of C_2S. This result is compatible with the data of Bogue and Lerch[29] showing that both compounds produce a colloidal hydrous silicate, but only C_3S produces microcrystalline $Ca(OH)_2$. The indications are that $Ca(OH)_2$ does not decompose under the drying conditions of these experiments. Hence, the occurrence of $Ca(OH)_2$ contributes to w_n but contributes very little to V_m.

THE SPECIFIC SURFACE OF HARDENED PASTE

Computation of surface area

From the derivation of the B.E.T. equation it follows that the surface area of the adsorbent should be equal to the product of the number of adsorbed molecules in the first layer and the area covered by a single molecule. Hence, when V_m is expressed in grams per gram of adsorbent (dry paste),

$$S = a_1 \frac{V_m N}{M} \qquad (5)$$

where

S = the surface area of the adsorbent, sq. cm. per g
a_1 = the surface area covered by a single adsorbed molecule

N = 6.06×10^{23}, the number of molecules in a gram-molecular wt. (Avagadro's number)*

M = molecular weight of the adsorbed gas.

The value of a_1 has been estimated in several ways. Livingston[30] found a value for water of 10.6×10^{-16} sq. cm. per molecule. Gans, Brooks, and Boyd[4] used the same figure. Emmett[31] gave a formula for computing a_1 from the molecular weight and density of the condensed vapor which gives nearly the same result if the normal density of water is used. As will be shown, values for molecular area obtained in this way when introduced into eq. (5) actually give surface areas S that are in close agreement with the results obtained by other procedures. Hence, for water we may write,

$$S = \frac{10.6 \times 10^{-16} \times 6.06 \times 10^{23} V_m}{18}$$

$$= (35.7 \times 10^6) V_m \text{ sq. cm. per g} \quad \ldots\ldots\ldots\ldots\ldots\ldots\ldots\ldots (6)$$

Verification of surface areas as computed from V_m

Gaudin and Bowdish[1] used pyrex-glass spheres calibrated by microscope measurements. Low temperature adsorption of nitrogen gave almost exactly the same specific surface as that computed from the mean size of the spheres. Harkins and Jura[32] developed a method of measuring surface area by first covering particles with a complete film of adsorbed water and then measuring the heat evolved when the particles were immersed in water. The results obtained by this method were compared with those from the B.E.T. method for 60 different solids. For 58 of the 60 solids the areas by the Harkins and Jura method differed from those obtained by the B.E.T. method by no more than 9 percent. Emmett[25, 31, 33] presented an extensive array of data showing that wherever particle size can be checked directly, as with the electron microscope, the results of the B.E.T. method look reasonable, to say the least. Because of such evidence as this, the B.E.T. method has been put to use by many investigators during the past few years.

The examples cited above were chosen from experiments made on solids that are non-porous. It is believed that V_m also gives the internal surface area of porous solids, provided that the molecules of the adsorbate are small enough to penetrate the pores and reach all parts of the surface. The fact that V_m is evaluated from data in the low pressure range only, and hence where capillary condensation in the pores is not a factor, supports this belief. With respect to cement paste, the pores are considered to be the spaces vacated by evaporable water when the sample is dried. The drying may be accompanied by irreversible shrinkage so that the

*6.023×10^{23} is now the accepted value for Avagadro's number. This did not come to our attention until all the computations were completed. Since other factors are uncertain, it did not seem worth while to make the slight corrections indicated.

dried sample may not faithfully represent the original paste. The extent of the irreversible alteration is not known but it is considered to be small. Evidence of this is found in the fact that the total pore space, as measured by the total evaporable water, is not greatly altered by the drying; in fact the data indicate that it is increased. (See Table 9, Part 2.) Hence, V_m is considered to give the internal surface area of the solid phase in the dried samples. If drying affects the measured surface area, it would probably be in the direction of making it smaller.

In the remainder of this discussion it is assumed that V_m as determined in this investigation is proportional to the surface area of the solid phase. It will be seen that this assumption leads to highly significant results. Thus the assumption seems justifiable.

Results from hardened paste

The magnitudes of the surface areas and the rates at which surface develops during hydration as computed from eq. (6) are indicated by Table 3-7.

The figures pertain to the whole solid phase; that is, they are based on the combined weights of the hydration products and residue of original clinker. Therefore, the specific surface of the hydration products is higher than the highest figure given except any that might represent completely hydrated cement.

Specific surface in terms of w_n

Since $V_m = kw_n$, the specific surface of a paste can be computed if w_n is known, and if k for the particular cement is known. That is,

$$\frac{S}{c} = 35.7 \times 10^6 \, k \, \frac{w_n}{c} \quad \ldots\ldots (7)$$

$$\frac{S}{w_n} = 35.7 \times 10^6 \, k \quad \ldots\ldots (8)$$

Also

$$\frac{S}{c + w_n} = \frac{35.7 \times 10^6 \, k \, w_n}{c + w_n} = \frac{35.7 \times 10^6 \, k \, w_n/c}{1 + w_n/c} \quad \ldots\ldots (9)$$

Eq. (7) gives the surface area per unit of original cement, and eq. (9) gives it per unit of dry paste.

For the types of cement given in Table 3-6 the surface area per unit weight of non-evaporable water is as given in Table 3-8.

The non-evaporable water content may lie anywhere between zero and about 0.25 g per g of cement. Hence, according to these equations the specific surface may lie between zero and about 2.1 to 2.5 million sq. cm. per g of original cement.

TABLE 3-7—TYPICAL FIGURES FOR SPECIFIC SURFACE OF HARDENED PASTE

Period of hydration, days	Specific surface of paste for cements indicated; w_n/c = 0.45 (approx.)							
	14930J C_3S 23% C_3A 6%		15761 C_3S 45% C_3A 10%		15365 C_3S 45% C_3A 13%		15013J C_3S 40% C_3A 14%	
	Millions of sq. cm. per g of:							
	cement	dry paste	cement	dry paste	cement	dry paste	cement	dry paste
7	0.76	0.71	—	—	1.21	1.06	1.32	1.13
14	1.02	0.92	—	—	1.55	1.32	1.50	1.28
28	1.33	1.19	1.75	1.48	1.94	1.64	1.71	1.46
56	1.75	1.54	—	—	1.96	1.62	1.89	1.57
90	1.89	1.62	1.96	1.62	2.02	1.66	2.04	1.67
180	2.10	1.78	—	—	2.14	1.75	2.07	1.69
365	2.10	1.76	—	—	—	—	—	—

TABLE 3-8—SPECIFIC SURFACE OF HARDENED PASTE IN TERMS OF NON-EVAPORABLE WATER CONTENT

Type of cement		V_m/w_n (= k)	S/w_n
Type I	Normal C_3A	0.261	9.3×10^6
	High C_3A	0.256	9.2×10^6
Type II	High iron	0.259	9.3×10^6
	High silica	0.279	10.0×10^6
Type III	Normal C_3A	0.238	8.6×10^6
Type IV	High iron	0.282	10.1×10^6
	High silica	0.277	9.9×10^6

Of course it cannot be literally true that $S = 0$ when $w_n = 0$, since the initial surface area is that of the original cement. As measured by adsorption, the specific surface of unhydrated cement is much higher than that measured by methods previously used. Using a cement having a specific surface of 1890 sq. cm. per g (Wagner), Emmett and DeWitt[34] found a surface area of 10,800 sq. cm. per g by the nitrogen-adsorption method. By the air-permeability method, this cement would show about 3500 sq. cm. per g, which is probably close to the true *macroscopic* surface area. The difference between the macroscopic surface area and that as measured by adsorption might be due to microscopic, or submicroscopic, cracks in the clinker grains. Surfaces of such cracks would be measured by the adsorption method, but not by the other. Since such

cracks have not been commonly reported, it seems more likely that the difference is due to a slight coating of hydration products on the grain surfaces. As shown above, an average cement shows about 9.3×10^6 sq. cm. per g of non-evaporable water. Hence, to account for the 7400 sq. cm. difference between the two results, it is only necessary to assume that the cement had hydrated to the extent of

$$\frac{7400}{9.3 \times 10^6} = 800 \times 10^{-6} \text{ g of non-evaporable water per g of cement,}$$

or 0.08 percent of the weight of the cement. Such a small amount of hydration could easily occur during the normal handling of a sample during humid weather.

Whether the true surface area of the cement is of the order of 3000 or 10,000, it is clear that the initial surface area is negligible compared with that which finally develops.

THE SPECIFIC SURFACE OF STEAM-CURED PASTE

The effects of high-temperature steam-curing on the adsorption characteristics of cement paste were shown in Part 2, p. 300. In terms of the B.E.T. theory, the effects are as follows:

	Ref. 14-4 Normal curing	Ref. 14-6 Steam curing
C	15.4	20
V_m, g/g of cement	0.037	0.0020
V_m, g/g dry paste	0.032	0.0018
Sp. surface, sq. cm. per g of cement, millions	1.32	0.071
Sp. surface, sq. cm. per g of dry paste, millions	1.15	0.062
V_m/w_n	0.241	0.012
w_n, g/g of cement	0.1537	0.1615

The figures for V_m and specific surface of the steam-cured specimen are probably not very accurate because of the extreme smallness of the amounts of water taken up in the low-pressure range. The order of magnitude relative to the normally cured material is probably correct, however. The result indicates that all but about 5 percent of the colloidal material was converted to the microcrystalline state by high-temperature steam curing.

w/V_m CURVES

The samples of hardened paste used in these studies contained undetermined quantities of unhydrated material. Consequently, the weight of the adsorbent material could not be ascertained directly, a circumstance that increases the difficulty of interpreting the adsorption data. The problem was simplified by expressing the amount of adsorption, w, in terms of the surface area of the solid phase. Since the surface area is proportional to V_m, the ratio w/V_m could be used without computing the surface area.

Typical w/V_m curves are shown in Fig. 3-8. The uppermost curve represents the paste in a mortar specimen having $w/c = 0.587$, cured six months; the middle curve represents the paste from a richer mortar specimen of the same age, $w/c = 0.439$. The lowest curve represents the data given in the first group of Table 3-9. These data include water-cement ratios ranging from 0.12* to 0.32 by weight. The table shows that after long periods of curing and for w/c within this range, w/V_m is virtually the same for all samples at all vapor pressures. (In the lower range of pressures, w/V_m is always the same for all samples except for the effect of differences in C.†) The triangular points plotted in Fig. 3-8 represent the average values from this group.

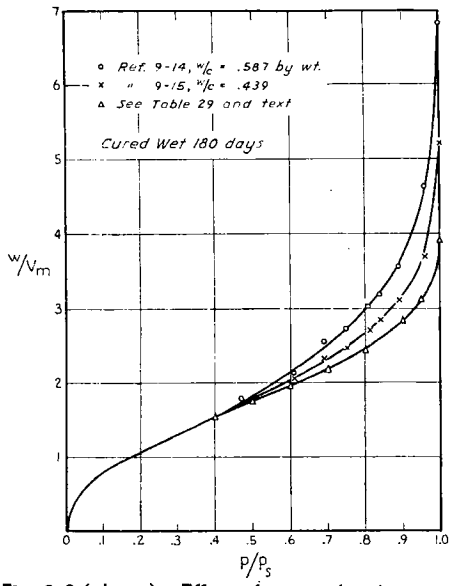

Fig. 3-8 (above)—Effect of original w/c on w/V_m curves

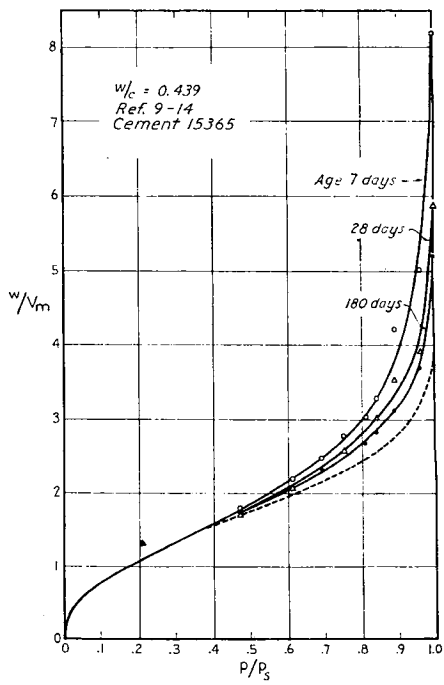

Fig. 3-9 (right)—Effect of wet-curing on w/V_m curves

*This very dry paste was molded by means of a press.
†See discussion in Part 4: "Significance of C of the B.E.T. Equation."

TABLE 3-9—TYPICAL w/V_m DATA

Data obtained by air-stream method, except as noted, and taken from plotted curves.

Ref. No. 254-	Cement No.	Net w/c	Age, days	C	V_m, g/g dry paste	w/V_m at value of p/p_s indicated								v_t‡	w_n/c
						0.4	0.5	0.6	0.7	0.8	0.9	0.95	SSD†		
Samples for which V_{max} = about $4V_m$															
8-1	14930J	—	447	21	.045	1.56	1.66	1.82	2.05	2.32	2.82	3.07	3.99	.88	.1807
9-1	14930J	.309	365	21	.043	1.52	1.72	1.90	2.12	2.40	2.82	3.10	3.89	.86	.1704
9-1	14930J	.309	180	21	.042	1.52	1.72	1.90	2.12	2.40	2.85	3.10	3.88	.86	.1620
9-4	15007J	.316	180	16	.041	1.48	1.72	1.96	2.23	2.42	2.88	3.15	3.99	.87	.1835
9-10	15013J	.324	180	29	.043	1.55	1.80	2.00	2.17	2.40	2.75	2.95	3.73	.86	.1877
9-13	15365	.319	180	25	.039	1.52	1.77	1.98	2.25	2.52	2.92	3.20	4.25	.87	.1815
9-13	15365	.319	90	20	.041	1.55	1.75	1.98	2.20	2.47	2.92	3.20	4.02	.87	.1789
9-15A	15365	.244	180	33	.031	1.57	1.80	2.00	2.25	2.50	2.75	3.18	3.58	—	—
9-15A*	15365	.244	180	33	.031	1.55	1.77	2.02	2.25	2.50	2.90	3.20	—	—	.1554
254-18*	14675	.12	4 yr.	92	.019	1.40	1.60	1.80	2.05	2.30	2.75	3.10	3.9	—	—
Avg.						1.53	1.74	1.94	2.17	2.43	2.84	3.12	3.91	.867	
Samples for which $V_{max} > 4V_m$															
9-14	15365	.439	180	19	.049	1.50	1.75	2.04	2.30	2.65	3.17	3.60	5.22	.89	.2221
9-14	15365	.439	28	19	.046	1.52	1.80	2.08	2.35	2.75	3.40	3.90	5.85	.90	.1841
9-14	15365	.439	7	26	.030	1.55	1.85	2.15	2.55	3.05	4.00	5.25	8.20	.91	.1400
9-15	15365	.587	180	19	.048	1.55	1.80	2.04	2.34	3.16	3.20	3.65	5.23	—	—
254-18	13495	.44§	7 yr.		.055	1.55	1.75	1.95	2.20	2.50	2.90	3.25	4.20	—	—

*Data obtained by high-vacuum method (not included in averages)
†Evaporable water content of saturated, surface-dry samples.
‡See Part 5.
§Estimated.

In Fig. 3-9 the effect of prolonging the period of wet-curing on a given paste is shown together with the lowest curve of Fig. 3-8 for comparison.

Minimum porosity and the cement-gel isotherm

Considering Fig. 3-8 and 3-9 together we may conclude that the densest paste possible contains a pore-volume equal to the volume of the quantity of adsorbed water represented by about $4V_m$.

The shape of the lowest curve in Fig. 3-8 also seems to represent a limit that is approached as the pastes are made denser. Hence, for brevity we will call the lower curve of Fig. 3-8 the *cement-gel isotherm* or just gel-curve, when the meaning is clear. The part of the total evaporable water equal to $4V_m$ will be called *gel-water*.

When a paste is such that at saturation it contains a quantity of evaporable water equal to $4V_m$, we may infer that all the originally water-filled space has become filled with porous hydration products. Thus, in such a paste the space outside the unhydrated clinker residue has only the porosity of the cement-gel itself.

When a paste is such that at saturation it contains a quantity of water exceeding $4V_m$, the excess over $4V_m$ is believed to occupy residual space outside the cement-gel. Water occupying this space is called *capillary water* in this discussion. It should be understood that this distinction between capillary water and gel-water is arbitrary, for some of the gel-water may be taken up by capillary condensation and is thus not different from the rest of the capillary water so far as the mechanism of adsorption is concerned. The distinction is justified by the fact that, in a saturated paste, the quantity of gel-water always bears the same ratio to the amount of gel, whereas the water called capillary water can be present in any amount according to the porosity of the paste as a whole.

Fig. 3-8 and 3-9, which are typical of all other w/V_m curves obtained, show that among various samples any increase in pressure up to about $0.45\ p_s$ is always accompanied by approximately the same increment of adsorption, regardless of differences in porosity.* From this we may infer that the capillaries (the spaces outside the gel) do not begin to fill at pressures below about $0.45\ p_s$. At higher pressures, however, a given increment in pressure will be accompanied by an increment of adsorption that is larger the greater the porosity of the sample. This may be taken as direct evidence of capillary condensation. The amount of water held by capillary condensation at any given pressure is represented by the vertical distance of the point in question above the gel-curve.

These ideas can be represented by a model such as is illustrated in Fig. 3-10. In A the shaded areas represent cross sections of spherical

*Such differences as there may be are due to differences in C of eq. (A), as is explained in Part 4.

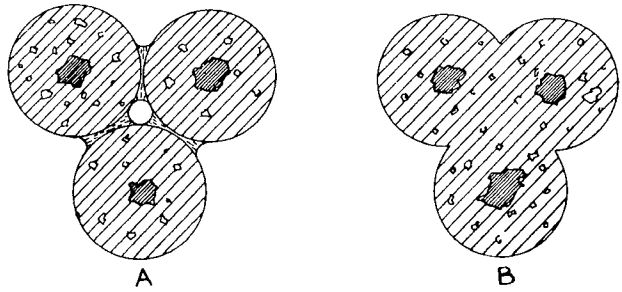

Fig. 3-10

bodies of cement gel with non-colloidal particles (microcrystalline hydrates and unreacted cement) embedded in them. Between the bodies is interstitial space containing capillary-condensed water, here pictured as lenses around the sphere-to-sphere contacts. The water content of the system is assumed to be below saturation, as indicated by the curvature of the lenses. At saturation, the interstitial space would be filled with capillary water, making the total water content equal to $4V_m$ plus the volume of capillary water.

Thus, if we consider the system pictured in Fig. 3-10A to be the sample represented by the upper curve of Fig. 3-8, at equilibrium with the pressure $p = 0.8\ p_s$, the water content of the spheres (the gel-water) would be 2.44 V_m, the capillary water would be 0.56 V_m, making a total of 3.00 V_m. At saturation the gel-water would be $4V_m$ and the capillary water 2.83 V_m, making a total of 6.83 V_m.

Fig. 3-10B represents a paste at the same stage of hydration as that represented in 3-10A but with a lower original w/c. Here the spheres of gel have merged into one body, eliminating all capillary water. The lowest w/V_m curve in Fig. 3-8, the cement-gel isotherm, would correspond to this case.

Estimation of pore- and particle-size

With data obtained from specimens containing no capillary space (as defined above) we can estimate the order of size of the elements of the solid phase and of its characteristic pores. Pore-size can be estimated from the hydraulic radius

$$\text{Hydraulic radius} = m = \frac{\text{volume of pores}}{\text{area of pore-walls}}$$

Pore volume is the space occupied by evaporable water and, in a paste without capillary space, this is equal to the volume of the gel water, i.e., the volume of $4V_m$. The area of the pore-walls is given by eq. (6).

$$S = 35.7 \times 10^6\ V_m$$

Hence,

$$m = \frac{4V_m v_g}{35.7 \text{ x } 10^6 V_m}$$

where

v_g = specific volume of the gel-water.

It will be shown later than the specific volume of the gel-water is about 0.90. Hence,

$$m = \frac{4 \text{ x } 0.90}{35.7 \text{ x } 10^6} = 10.01 \text{ x } 10^{-8} \text{ cm}$$

or approximately 10Å.*

The average size of a pore in the gel having a given hydraulic radius can be estimated by assuming that the cross section of the pore resembles a rectangular slit. Let b, h, and L be the width, thickness, and length, respectively, of the slit. Then

$$m = \frac{hbL}{(2h + 2b)L} = \frac{hb}{2(h + b)}$$

Solutions of this equation for various values of h and b are given below:

$h = b$; $m = 1/4\ b$
$h = 2b$; $m = 1/3\ b$
$h = 4b$; $m = 4/10\ b$
$h = 10b$; $m = 10/22\ b$
$h = 100b$; $m = 100/202\ b$

Thus, as h/b is made larger, m approaches $\frac{1}{2}\ b$ as a limit. This means that the width of the pores is at least twice and at most four times the hydraulic radius. Since m was given as about 10Å, it follows that the average pore is from 20 to 40Å across, probably closer to 40Å than to 20Å if the particles are other than spherical.

The order of size of the colloidal particles cannot be computed directly because there is no way to correct for the volume of non-colloidal material, i.e., microcrystalline hydrates and unhydrated clinker. However, it is of interest to estimate the size without such correction since the volume of non-colloidal hydrates is relatively small and data are available for samples containing very little unhydrated clinker. The estimate is made by finding the size of spheres in an aggregation of spheres that would have the same total volume and surface area as dry hardened paste. The size of sphere is given by the relationship

$$r = \frac{3}{S'}$$

*Å = Ångstrom unit = 10^{-8} cm

where

r = radius of sphere in cm

S' = surface area in sq. cm per cu. cm

$$S' = d_p S$$

where

d_p = density of dry paste, g per cu. cm

and S = surface area of dry paste, sq. cm per g.

For a typical paste cured at least 6 mo.,

$d_p = 2.44$ g per cu. cm.

$S = 1.8 \times 10^6$ sq. cm. per g

$$r = \frac{3}{2.44 \times 1.8 \times 10^6} = 68 \times 10^{-8} \text{ cm},$$

say 70Å.

This indicates that if the solid phase were an assemblage of equal spheres, each sphere would have a diameter of about 140Å. The units of colloid material are probably smaller than this, but not very much smaller since most of the hydration product is colloidal and since there was probably little unhydrated material in the specimen on which this estimate is based.

These figures give a picture of a material made up of solid units averaging about 140Å in diameter, with interstices averaging say 20 to 40Å across. This should, of course, be taken only as an indication of the order of size of the elements of the fine structure. It indicates, for example, the necessary resolving power of a microscope capable of differentiating these features of hardened paste.

* * * * *

It is hardly necessary to add that the authors hold no belief that the gel develops as spheres or that the pores are rectangular slits of uniform cross section. Those assumptions were made only for convenience of illustration and computation. The bodies of hardened gel could be in the form of submicroscopic plates, filaments, prisms, or of no regular form at all. However, as developed above, the evidence points to the conclusion that the gel is a solid having a characteristic porosity.

Data on relative amounts of gel-water and capillary water

The relative amounts of gel-water and capillary water in saturated samples at various stages of hydration are shown in Fig. 3-11 and 3-12, for the materials of Series 254-9. The shaded portion of each column represents gel-water and the open portion capillary water. These charts bring out again the fact that for specimens of sufficiently low water-cement ratio, prolonged curing eliminates all capillary water.

In several instances there is an indication that the ratio of capillary to gel-water *increases* after a minimum is reached. Whether this is real or the result of experimental vagaries cannot be told without further experiment. If it is real, it might be due to the leaching of soluble material from the paste during the curing period. Such leaching would be expected to increase the porosity of the paste. It might also be due to a coarsening of the gel-texture by the formation of microcrystals at the expense of colloids. If so, the change is of considerable significance. Present data warrant no conclusions on this point.

There is a rather definite indication that the gel is able to fill but a limited amount of space, regardless of the length of the curing period. This is brought out in Fig. 3-13, where w_e/V_m (w_e = evaporable water) at saturation is plotted against w/c for all specimens cured 180 days or longer. This shows again that the minimum possible evaporable water content is about $4V_m$ and further that all samples having original water-cement ratios greater than about 0.32 by weight will contain some capillary water. The empirical relationship illustrated can be represented approximately by the equation

$$\left.\frac{w_c}{V_m} = 12.2\ (w/c - 0.32)\right] \quad w/c \geqq 0.32$$

where

w_c is the capillary-water content of specimens cured 6 months or more.

SUMMARY OF PART 3

Adsorption isotherms for water on hardened portland cement pastes show the same characteristics as those for vapors on many different organic and inorganic materials.

The process of adsorption and the conditions for equilibrium are explained in terms of the Brunauer-Emmett-Teller (B.E.T.) theory and the capillary condensation theory.

The B.E.T. eq. (A) is used for representing data over the range $p = 0.05\ p_s$ to $0.45\ p_s$. The equation is

$$\frac{w}{V_m} = \frac{cx}{(1 - x)\ (1 - x - cx)} \qquad \text{(A)}$$

where

w = weight of evaporable water held at equilibrium with pressure p,
V_m = quantity of water required for a complete condensed layer on the solid, the layer being 1 molecule deep on the average,
C = a constant related to the heat of adsorption,
$x = p/p_s$ where p_s = saturation pressure and p the existing pressure.

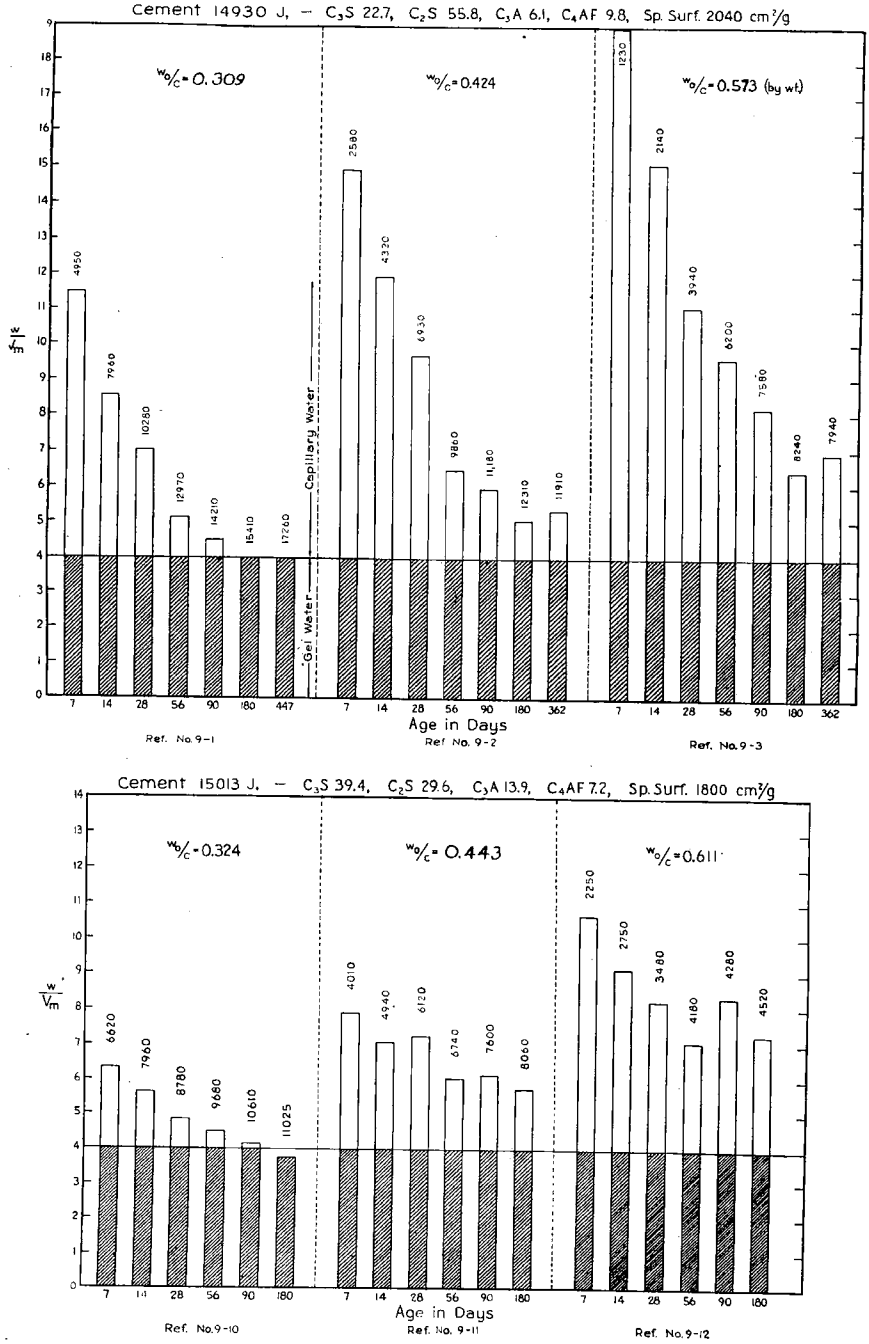

Fig. 3-11—Effect of hydration on w/V_m

Note: Figures over columns are compressive strengths of 2-in. cubes, psi.

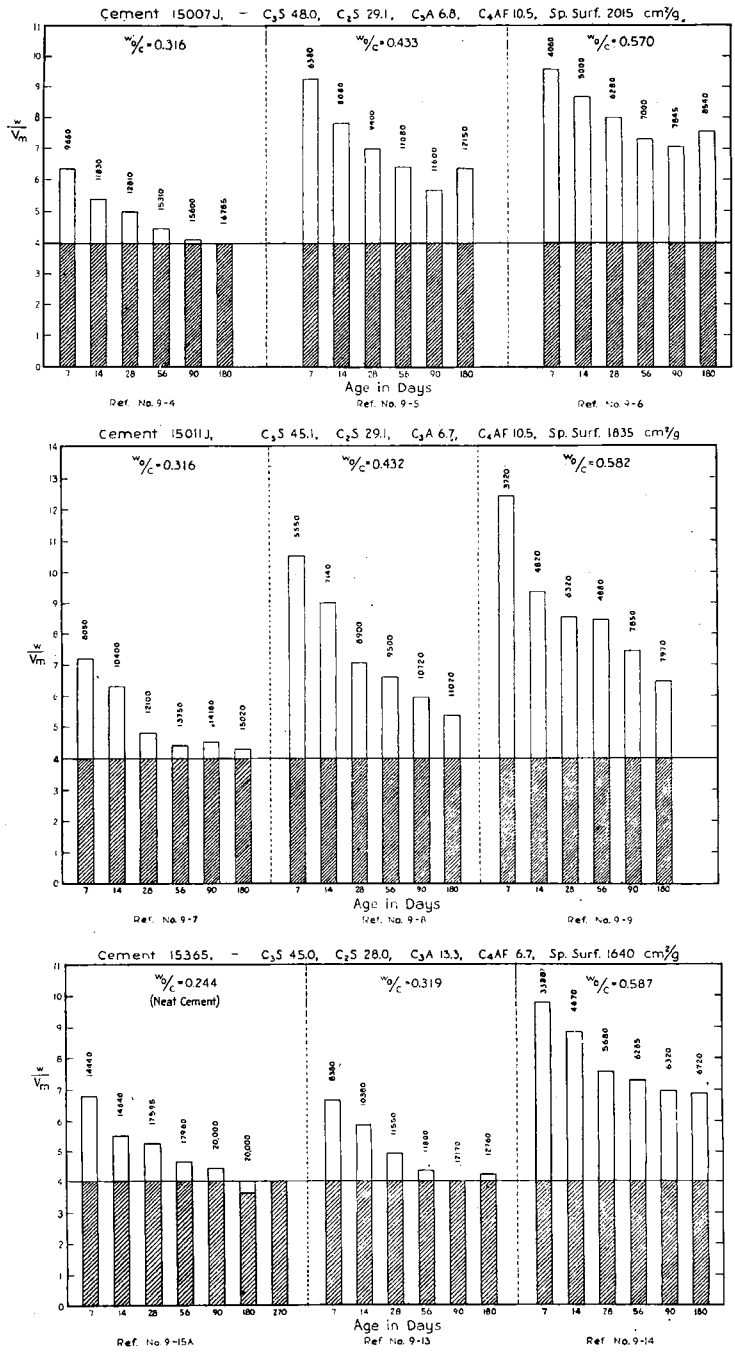

Fig. 3-12—Effect of hydration on w/V_m

Note: Figures over columns are compressive strengths of 2-in. cubes, psi.

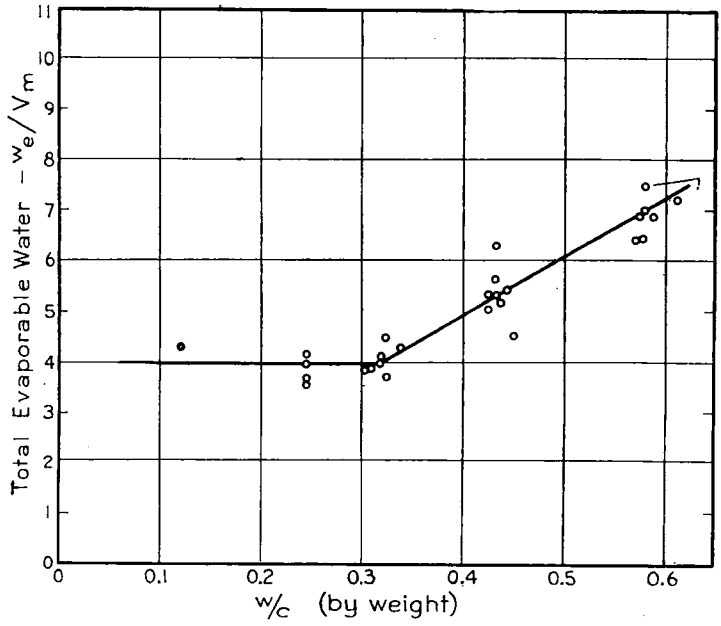

Fig. 3-13—Empirical relationship between total evaporable water per unit V_m and original water-cement ratio for samples cured 180 days or longer

V_m and C can be readily evaluated from experimental data and p_s is a constant depending on temperature. C is about the same for all pastes. Hence differences in adsorption characteristics are indicated by differences in V_m.

The non-evaporable water content, w_n, is regarded as proportional to the total amount of hydration products. Since V_m is porportional to surface area and since practically all the surface is that of the colloids, V_m is considered to be proportional to the colloidal material (gel) only.

The ratio V_m/w_n is considered to be a constant for any given cement. It is influenced by compound composition about as follows:

$$\frac{V_m}{w_n} = 0.00230\ (\%C_3S) + 0.00320\ (\%C_2S) + 0.00317\ (\%C_3A) + 0.00368\ (\%C_4AF)$$

Among the different types of cement V_m/w_n varies from about 0.24 to 0.28.

The above equation implies that the hydrate of each compound is colloidal or at least that all compounds occur as constituents of a complex colloidal hydrate.

The specific surface of hardened paste can be computed from the relationship $S = 35.7 \times 10^6\ V_m$. It increases with the period of curing and reaches about 2 million sq. cm per g of original cement.

The specific surface of the hardened paste is related to w_n as follows:

$$\frac{S}{w_n} = 35.7 \times 10^6 k,$$

where k is a constant for a given cement. Among the different types of cements, S/w_n ranges from about 8.6×10^6 to 10×10^6.

None of the relationships given above apply to paste cured at high temperature. Under steam pressure a sample cured 6 hours at 420 F showed only 0.07×10^6 sq. cm. of surface per g of cement, as compared with 1.3×10^6 for a paste cured 28 days, or about 2.0×10^6 for long curing, at room temperature.

When adsorption data are expressed in terms of w/V_m and p/p_s, the result is an isotherm based on the relative amount of gel. Such curves are virtually identical for all cement pastes over the pressure range $p = 0.05\ p_s$ to $0.45\ p_s$.

For pastes in which the total evaporable water content is about $4V_m$, the curves are identical for the whole pressure range.

For pastes having capacity for evaporable water exceeding $4V_m$, the excess is taken up over the pressure range $p = 0.45\ p_s$ to $p = p_s$.

The evaporable-water capacity is smaller the lower the original water-cement ratio and the longer the period of curing, but it cannot be reduced below about $4V_m$.

Evaporable water in excess of $4V_m$ is believed to occupy interstitial space not filled by gel or other hydration products. The water in this space is called *capillary water.* The rest of the evaporable water is held within the characteristic voids of the gel and is called *gel-water* even though some of it might have been taken up by capillary condensation.

When the total evaporable-water capacity $= 4V_m$, the specimen contains no space for capillary water.

From the surface area of the solid phase, and its characteristic porosity, the average pore in the densest possible hardened paste is estimated to be from 20 to 40Å across.

From the volume of the solid phase and its surface area, the order of particle size, expressed as sphere diameter, is estimated at 140Å.

Data on the relative amounts of gel-water and capillary water in various samples are given graphically.

REFERENCES

(1) A. M. Gaudin and F. W. Bowdish, *Mining Technology,* v. 8 (3) pp. 1-6 (1944).
(2) L. A. Wooten and Callaway Brown, *J. Am. Chem. Soc.* v. 65, p. 113 (1943).
(3) H. Cassel, *Trans. Faraday Soc.* v. 28, p. 177 (1932). Quoted by Brunauer in Ref. 5, p. 289.

(4) D. M. Gans, M. S. Brooks, and G. E. Boyd, *Ind. Eng. Chem.* (Anal. Ed.) v. 14, p. 396 (1942).
(5) Stephen Brunauer, *The Adsorption of Gases and Vapors*, Vol. 1, Princeton University Press (1943).
(6) J. W. McBain and John Ferguson, *J. Phys. Chem.* v. 31, p. 564 (1927).
(7) Urquhart and Williams, *J. Textile Inst.* v. 40, p. T439 (1924).
(8) S. E. Shephard and P. T. Newsome, *Ind. Eng. Chem.* v. 26, p. 285 (1943).
(9) L. M. Pidgeon and A. Van Winsen, *Can. J. Res.* v. 9, p. 153 (1933).
(10) E. Filby and O. Maass, *Can J. Res.* v. 13, Sec. B., p. 5 (1935).
(11) C. O. Seborg, F. A. Simmonds, and P. K. Baird, *Ind. Eng. Chem.* v. 28, p. 1245 (1936).
(12) W. R. Smith, F. S. Thornhill, and R. I. Bray, *Ind. Eng. Chem.* v. 33, p. 1303 (1941).
(13) K. S. Rao, *J. Phys. Chem.*, v. 45, p. 500 (1941).
(14) V. L. Simril and Sherman Smith, *Ind. Eng. Chem.* v. 34, p. 226 (1942).
(15) V. R. Dietz and L. F. Gleysteen, *J. Res.*, Natl. Bur. of Stds. v. 29, p. 191 (1942).
(16) J. D. Babbitt, *Can. J. Res.* v. 20, p. 143 (1942).
(17) L. A. Reyerson and Cyrus Bemmels, *J. Phys. Chem.* v. 46, p. 31 (1942).
(18) Henry B. Hull, *J. Am. Chem. Soc.* v. 66, p. 1499 (1944).
(19) Lyle T. Alexander and M. M. Haring, *J. Phys. Chem.* v. 40, p. 195 (1936).
(20) J. B. Speakman, *Trans. Faraday Soc.* v. 40, p. 6 (1944).
(21) S. Brunauer, P. H. Emmett, and E. Teller, *J. Am. Chem. Soc.* v. 60, p. 309 (1938).
(22) S. Brunauer, L. S. Deming, W. E. Deming, and E. Teller, *J. Am. Chem. Soc.* v. 62, p. 1723 (1940).
(23) Gerald Pickett, *J. Am. Chem. Soc.* v. 67, p. 1958 (1945).
(24) E. Freyssinet, *Science et Industrie* (Jan. 1933).
(25) P. H. Emmett, *Ind. Eng. Chem.* v. 37, p. 639 (1945).
(26) Ref. 5, p. 168.
(27) W. D. Harkins and G. Jura, *J. Chem. Phys.* v. 11, p. 560 (1943) and *J. Am. Chem. Soc.* v. 66, p. 919 (1944).
(28) International Critical Tables, Vol. III. For *NaOH*, pp. 296 and 369. For *KOH*, pp. 298 and 373.
(29) R. H. Bogue and Wm. Lerch, *Ind. Eng. Chem.* v. 26, p. 837 (1934), or Paper No. 27, Portland Cement Association Fellowship, National Bureau of Standards, Washington, D. C.
(30) H. K. Livingston, *J. Am. Chem. Soc.* v. 66, p. 569-73 (1944).
(31) P. H. Emmett, *Advances in Colloid Science*, Interscience Publishers, Inc., New York, 1942, p. 6.
(32) Wm. D. Harkins and Geo. Jura, *J. Chem. Phys.* v. 11, p. 431 (1943).
(33) P. H. Emmett, Symposium on New Methods for Particle-Size Determination in the Subsieve Range, p. 95, A.S.T.M. Publication, 1941.
(34) P. H. Emmett and T. DeWitt, *Ind. Eng. Chem.* (Anal. Ed.) v. 13, p. 28 (1941).

Title 43-5d —a part of PROCEEDINGS, AMERICAN CONCRETE INSTITUTE Vol. 43

JOURNAL
of the
AMERICAN CONCRETE INSTITUTE
(copyrighted)

Vol. 18 No. 5 7400 SECOND BOULEVARD, DETROIT 2, MICHIGAN January 1947

Studies of the Physical Properties of Hardened Portland Cement Paste*

By T. C. POWERS†
Member American Concrete Institute
and T. L. BROWNYARD‡

Part 4. The Thermodynamics of Adsorption of Water on Hardened Paste

CONTENTS

*Received by the Institute July 8, 1946—scheduled for publication in seven installments; October 1946 to April, 1947. In nine parts:

Part 1. "A Review of Methods That Have Been Used for Studying the Physical Properties of Hardened Portland Cement Paste". ACI JOURNAL, October, 1946.
Part 2. "Studies of Water Fixation"—Appendix to Part 2. ACI JOURNAL, November, 1946.
Part 3. "Theoretical Interpretation of Adsorption Data." ACI JOURNAL, December, 1946.
Part 4. "The Thermodynamics of Adsorption"—Appendix to Parts 3 and 4.
Part 5. "Studies of the Hardened Paste by Means of Specific-Volume Measurements."
Part 6. "Relation of Physical Characteristics of the Paste to Compressive Strength."
Part 7. "Permeability and Absorptivity."
Part 8. "The Freezing of Water in Hardened Portland Cement Paste."
Part 9. "General Summary of Findings on the Properties of Hardened Portland Cement Paste."

†Manager of Basic Research, Portland Cement Assn. Research Laboratory, Chicago 10, Ill.
‡Navy Dept., Washington, D. C., formerly Research Chemist, Portland Cement Assn. Research Laboratory, Chicago 10, Ill.

This discussion pertains to the energy changes that take place when water is adsorbed by hardened cement paste. The relationship of these changes to such physical effects as shrinking and swelling, capillary flow, and moisture diffusion will be considered briefly. Comparisons are made of the energy of binding of evaporable and non-evaporable water. Analysis of the energy changes into the two main forms of energy and consideration of the relative amounts of each are of interest in connection with the question of the extent to which water is modified when it is adsorbed on the solid.

THE HEAT OF ADSORPTION

As pointed out in Part 3, the adsorption of a vapor by a solid can be likened to the process of condensation both with respect to the kinetics of the process and the nature of the forces involved. Therefore, it might be expected that the heat liberated when the vapor is adsorbed would be comparable to the heat of liquefaction of the vapor. When the comparison is made, it is usually found that the heat of adsorption exceeds the heat of liquefaction. In the adsorption of water vapor on hardened cement paste, the heat of adsorption for the first increments of water added exceeds the heat of liquefaction by about 65 percent of

the latter. This excess can be attributed, directly or indirectly, to interaction of the adsorbed molecules with the surface of the solid.

THE NET HEAT OF ADSORPTION

Definitions

The excess of the heat of adsorption over the heat of liquefaction is called the *net heat of adsorption.* If Q represents the heat of adsorption and Q_L the heat of liquefaction, then Q_a, the net heat of adsorption, is defined by,

$$Q_a = Q - Q_L \quad \ldots\ldots\ldots\ldots\ldots\ldots\ldots\ldots (1)$$

The definition just given amounts to regarding the adsorption of the vapor as a two-step process, as follows:

(1) Vapor at the saturation pressure, p_s, condenses to liquid, thereby liberating the heat of liquefaction, Q_L.

(2) The liquid water is then adsorbed, liberating the net heat of adsorption, Q_a. In this step, the water comes to equilibrium with vapor at a lower pressure, p.

As pointed out before (Part 3), the free surface energy of the solid and the free surface energy of the condensed liquid must both be causes of adsorption in a porous solid such as hardened paste. Hence, the net heat of adsorption must have its origin in at least two sources. At low vapor pressures, the net heat of adsorption has its origin in the interaction of the adsorbed molecules with the solid surface. When the pressure is increased above 0.45 p_s, where capillary condensation becomes a factor, the surface of the water film formed at lower pressures diminishes and becomes zero, or nearly zero, at saturation. The destruction of the water surface is accompanied by the liberation of the heat of water-surface formation. Thus, the net heat of adsorption is the sum of two terms, *the net heat of surface adsorption* and the *net heat of capillary condensation.* That is,

$$Q_a = Q_s + Q_c, \quad \ldots\ldots\ldots\ldots\ldots\ldots\ldots\ldots (2)$$

where

Q_a = net heat of adsorption,
Q_s = net heat of surface adsorption, and
Q_c = net heat of capillary condensation.

Evaluation of total net heat of capillary condensation

The total amount of heat arising from the destruction of water surface, i.e., the total net heat of capillary condensation, when the paste goes from the dry to the saturated condition can be evaluated by means of the following considerations.

It may be assumed that the maximum extent of water surface is the area of the solid surface. It would seem, however, that this maximum

could not exist at any vapor pressure. At low vapor pressure, the film would be incomplete, even when V_m g. are present, because of the chance distribution of molecules among the layers described in the B.E.T. theory. At higher pressure, the water film would be partly destroyed by capillary condensation. At saturation the water surface would disappear completely except for a negligible area about equal to the superficial area of the granules composing the sample. Nevertheless, each unit of solid surface was covered by a water film at some stage prior to the elimination of the film surface, and the total net heat of capillary condensation should be the same as if the formation of the water surface and its disappearance occurred consecutively.

In accordance with the assumption just stated, the total net heat of capillary condensation, Q_{ct}, is

$$Q_{ct} = Sh_c \quad , \qquad (3)$$

where S = internal surface area of paste, sq. cm., and
h_c = heat of water-surface formation, cal per sq. cm.

According to Harkins and Jura,[1] h_c = 118.5 ergs per sq. cm. at 25 C, or $118.5 \times 2.39 \times 10^{-8} = 2.83 \times 10^{-6}$ cal per sq. cm. Also by eq. (6) of Part 3,

$$S = 35.7 \times 10^6 \, V_m \text{ sq. cm.}$$

Therefore,

$$Q_{ct} = 2.83 \times 10^{-6} \times 35.7 \times 10^6 \times V_m$$
$$= 101 V_m, \text{ say } 100 V_m \text{ cal} \qquad (4)$$

Evaluation of total net heat of surface adsorption

The total amount of heat arising from the interaction of the adsorbed molecules with the solid surface, i.e., the total net heat of surface adsorption is given by

$$Q_{st} = Sh_s \quad , \qquad (5)$$

where Q_{st} = total net heat of surface adsorption, cal per g. of paste,
S = internal surface area of paste, sq. cm. per g, of paste, and
h_s = total net heat of surface adsorption, cal. per cm. of paste.

Hence,

$$Q_{st} = 35.7 \times 10^6 \, V_m h_s \qquad (6)$$

If it can be assumed that h_s is the same for all pastes, and this is a reasonable assumption that will be used, then

$$\frac{Q_{st}}{V_m} = \text{const.} = k. \qquad (7)$$

The total net heat of adsorption

The total net heat of adsorption will be the sum of the total net heat of surface adsorption and the total net heat of capillary condensation.

Thus,

$$Q_{at} = Q_{st} + Q_{ct} \quad (8)$$
$$= kV_m + 100V_m = (k + 100)V_m$$

* * * * * * *

At low vapor pressures, only the net heat of surface adsorption appears. At higher pressures the net heat of capillary condensation also appears. There is at present no basis for evaluating either term at any stage short of saturation.

* * * * * * *

Net heat of adsorption and heat of wetting

When adsorption is considered to be the two-step process mentioned above, step (2) immediately suggests a comparison of the net heat of adsorption with the heat of wetting.

Distinction must be made between the heat evolved when a solid surface is immersed in a body of liquid and the heat evolved when the surface is wetted by causing a film to spread over the surface. The heat of immersion exceeds the heat of spreading-wetting by the heat of formation of water surface.

The total net heat of adsorption, Q_{at}, must be very nearly if not actually, equal to the heat of immersion of the hardened paste. This follows because the water surface at saturation is virtually zero, as pointed out above. This means that if a sample of hardened paste is brought to saturation by adsorption of vapor no measurable amount of heat will be evolved if it is immersed in water.

The net heat of surface adsorption is comparable to the heat of spreading-wetting. If the thickness of the film is not a factor, i.e., if the interaction of the adsorbed molecules with the solid surface affects only the first layer of molecules adsorbed, the net heat of surface adsorption is strictly comparable to the heat of spreading-wetting, except for the possible effect of narrow crevices. (In cement gel, some water may be held in crevices so narrow that a water surface cannot form.) If the thickness of the film is a factor, the net heat of surface adsorption differs from the heat of spreading-wetting but the amount of the difference cannot be evaluated. However, the total net heat of surface adsorption should be equal to the heat of spreading-wetting of what may be called a complete film, i.e., a film so thick that the effect of interaction at the solid surface is no longer evident.

MEASUREMENT OF NET HEAT OF ADSORPTION

Materials and procedure

The net heat of adsorption was measured, using two different hardened pastes. From each paste twelve granular samples were prepared by

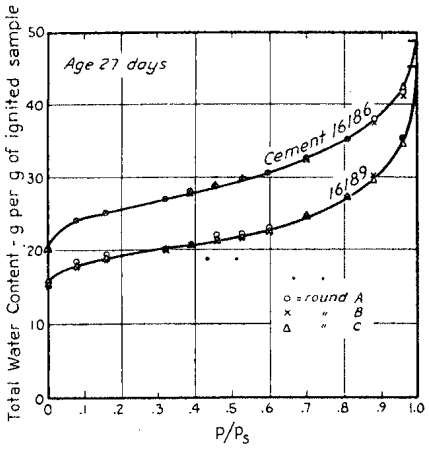

Fig. 4-1 (above)—Adsorption isotherms of samples used for heat of adsorption measurements.

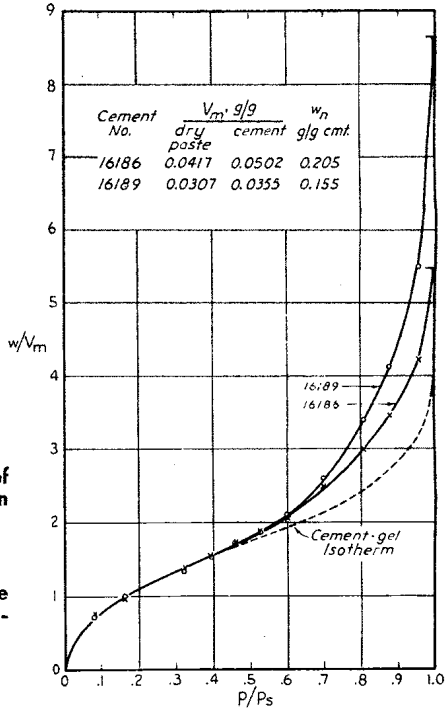

Fig. 4-2 (right)—w/Vm curves for the samples used in heat of adsorption measurements.

Data from Tables 4-1 and 4-2.

first removing the evaporable water and then exposing the samples to different humidified air streams according to the method already described (Part 2).

When the samples had reached equilibrium, each was sealed in a separate glass ampoule, each of the twelve samples from a given paste being at equilibrium with a different vapor pressure. Such samples were prepared in triplicate.

The adsorption isotherms are shown in Fig. 4-1. The total water contents are plotted in order to show also the non-evaporable water contents. The values for $p/p_s = 1.0$, which ordinarily represent the water contents at saturation, were not measured for these samples; the points shown for this pressure represent the water contents before the samples were dried the first time.

w/V_m curves are given in Fig. 4-2. The broken line is the curve for cement-gel, as discussed in Part 3. Both pastes evidently contained space for capillary water.

The heat of adsorption was measured by the same heat-of-solution procedure that is used for measuring the heat of hydration of cement.* The procedure is first to dissolve the dry paste, measuring the heat

*Federal Specification SSC-158a-Sec. 31.

evolved, and then to dissolve a similar sample of paste containing adsorbed water. The indicated reactions are

$$Paste + \text{acid-solution} + nH_2O \rightarrow \text{solution of paste}$$
$$\text{Heat evolved} = Q_o \text{ cal per g of dry paste} \quad (9)$$
$$Paste + nH_2O \rightarrow Paste.nH_2O$$
$$\text{Heat evolved} = Q_a \text{ cal per g of dry paste} \quad (10)$$
$$Paste.nH_2O + \text{acid-solution} \rightarrow \text{solution of paste}$$
$$\text{Heat evolved} = Q_p \text{ cal per g of dry paste} \quad (11)$$

where

$Paste$ = dried paste
Q_o = heat of solution of dry paste
Q_p = heat of solution of paste containing n grams of evaporable water
Q_a = net heat of adsorption.

By Hess's law,

$$Q_a = Q_o - Q_p. \quad (12)$$

This process, in effect, transfers the adsorbed water from the sample to the solution. Hence, the heat of vaporization does not appear and, on the assumption that the heat of solution of the adsorbed water in the acid is zero, the method may be regarded as giving the net heat of adsorption directly.*

The heat-of-solution method was adopted mainly because at the time the project was planned the heat-of-solution calorimeter was already set up. The results obtained are not altogether satisfactory, for in several cases the variation in the observed net heat of adsorption among companion samples was as great as or greater than the difference in heat content due to differences in adsorbed-water content. This results in some uncertainty as to whether certain observed differences are significant or not.

It should be noted that eq. (12) does not take into account the fact that Q_o and Q_p may represent the heats of solution of samples containing different amounts of adsorbed air. This inaccuracy must be accepted, for we have no knowledge of the change in adsorbed air content, or of its heat of desorption. However, the inaccuracy is probably small, owing to the relative smallness of the amount of air adsorbed at room temperature under a pressure of 1 atmosphere.

Experimental results

The experimental results are recorded in Tables 4-1 and 4-2. In Fig. 4-3 the net heats of adsorption are plotted against the equilibrium vapor pressures of the respective samples of each of the two cement pastes. They are plotted in this way to facilitate estimating the total net heats

*The small heat effect of charging n moles of water vapor from pressure p_s to p is considered negligible.

TABLE 4-1—ADSORPTION AND HEAT OF ADSORPTION DATA FOR PASTE MADE WITH CEMENT 16186

Original w/c = 0.50 (not corrected for bleeding). Ref. 16-01A, B, and C. V_m = 0.0502 g/g ignited wt., average of A, B, and C. Heat of solution of orig. cement = 623 cal/g ignited wt. Age at test—27 to 29 days.

Sample No.	p/p_s	Total water, g/g of: dry paste	Total water, g/g of: ign. wt.	Evap. water g/g ign. wt.	Water adsorbed g/g of: dry paste	Water adsorbed g/g of: ign. wt.	w/V_m	Heat of solution cal/g ign. wt	Net heat of adsorption Q_a, cal/g of: dry paste	Net heat of adsorption Q_a, cal/g of: ign. wt.	$\frac{Q_a}{V_m}$
A-12.2a		.1688	.2031		0	0		537.5	0	0	
B-24.2a		.1702	.2051		0	0		539.0	0	0	
C†		.1696	.2042		0	0		538.0	0	0	
Avg.	0	.1695*	.2041*	0	0	0	0	538.2	0	0	—
A-11A		.2010	.2418		.0322	.0387		525.4	9.6	12.2	
B-23a		.2014	.2427		.0312	.0376		527.1	9.5	11.8	
Avg.	.081	.2012	.2422	.0381	.0317	.0381	0.76	526.2	9.6	12.0	239
A-7a		.2092	.2517		.0404	.0486		523.2	11.4	14.3	
B-19a		.2091	.2520		.0389	.0469		525.2	11.0	13.8	
Avg.	.161	.2092	.2518	.0477	.0396	.0478	0.95	524.2	11.2	14.0	279
A-9a		.2258	.2717		.0570	.0686		520.6	13.3	16.9	
B-21a		.2254	.2716		.0552	.0665		521.3	13.8	17.6	
Avg.	.322	.2256	.2716	.0675	.0561	.0676	1.37	521.0	13.5	17.2	342
A-10a		.2336	.2810		.0648	.0779		520.0	13.7	17.5	
B-22a		.2334	.2813		.0632	.0762		518.9	15.7	20.1	
C-10g		.2352	.2832		.0656	.0790		518.9	15.0	19.2	
Avg.	.39	.2340	.2818	.0777	.0645	.0777	1.55	519.3	14.7	18.9	376
A-8a		.2399	.2886		.0711	.0855		519.5	14.0	18.0	
B-20a		.2397	.2889		.0695	.0838		520.8	14.1	18.2	
C-8g		.2428	.2924		.0732	.0882		519.3	14.5	18.8	
Avg.	.46	.2408	.2900	.0859	.0713	.0858	1.71	519.9	14.2	18.3	364
A-1a		.2483	.2987		.0795	.0956		519.1	14.2	18.4	
B-13a		.2473	.2980		.0771	.0929		520.1	14.6	18.9	
C-1g		.2496	.3005		.0800	.0963		516.9	16.3	21.2	
Avg.	.53	.2484	.2991	.0950	.0789	.0949	1.89	518.7	15.0	19.5	388
A-5a		.2550	.3068		.0862	.1037		517.5	15.3	20.0	
B-17a		.2541	.3062		.0839	.1011		519.1	15.2	19.9	
Avg.	.60	.2546	.3065	.1024	.0850	.1024	2.04	518.3	15.3	20.0	398
A-4a		.2726	.3280		.1038	.1249		517.9	14.8	19.6	
B-16a		.2714	.3271		.1012	.1220		516.5	17.0	22.5	
C-4g		.2740	.3300		.1044	.1258		515.7	16.8	22.3	
Avg.	.70	.2727	.3284	.1243	.1031	.1242	2.48	516.7	16.2	21.5	428
A-2a		.2954	.3554		.1266	.1523		515.6	16.2	21.9	
B-14a		.2938	.3541		.1236	.1490		516.6	16.5	22.4	
Avg.	.81	.2946	.3548	.1507	.1251	.1506	3.00	516.1	16.4	22.2	442
A-3a		.3175	.3820		.1487	.1789		513.9	17.1	23.7	
B-15a		.3121	.3761		.1419	.1710		515.0	17.5	24.0	
Avg.	.88	.3148	.3790	.1749	.1453	.1750	3.48	514.4	17.3	23.8	474
A-6a		.3477	.4183		.1789	.2152		510.0	19.4	27.5	
B-18a		.3431	.4135		.1729	.2084		514.3	17.5	24.7	
C-6g		.3522	.4241		.1826	.2199		509.8	19.8	28.2	
Avg.	.96	.3477	.4186	.2145	.1781	.2145	4.28	511.4	18.9	26.8	534
A		.3997									
B†		.4002									
C		.3976									
Avg.	1.0	.3992	.481	.277	—	.277	5.5	509.5‡	—	28.7‡	572‡

*Non-evaporable water. †Estimated graphically from ignition loss; no dry sample available. ‡Estimated

TABLE 4-2—ADSORPTION AND HEAT OF ADSORPTION DATA FOR PASTE MADE WITH CEMENT 16189

Original w/c = 0.5 (not corrected for bleeding). Ref. 16-02A, B, and C. V_m = 0.0355 g/g ignited wt., average of A, B, and C. Heat of solution of orig. cement = 606 cal/g ignited wt. Age at test—42 to 44 days.

Sample No.	p/p_s	Total water, g/g of: dry paste	Total water, g/g of: ign. wt.	Evap. water, g/g ign. wt.	Water adsorbed, g/g of: dry paste	Water adsorbed, g/g of: ign. wt.	w/V_m	Heat of solution cal/g ign. wt.	Net heat of adsorption Q_a, cal/g of: dry paste	Net heat of adsorption Q_a, cal/g of: ign. wt.	$\frac{Q_a}{V_m}$
A-24.2g		.1375	.1594		0	0		542.2	0	0	
B-12.2c		.1340	.1547		0	0		546.2	0	0	
C†		.1336	.1542		0	0		546.6	0	0	
Avg.	0	.1350*	.1561*	0	0	0	0	545.0	0	0	—
A-23g		.1602	.1847		.0227	.0253		536.1	5.1	6.1	
B-11c		.1557	.1798		.0217	.0251		539.1	5.9	7.0	
C-23c		.1562	.1803		.0226	.0261		540.6	5.1	6.0	
Avg.	.081	.1574	.1816	.0255	.0223	.0255	0.72	538.6	5.4	6.4	180
A-19g		.1682	.1950		.0294	.0356		534.8	6.3	7.5	
B-7c		.1634	.1887		.0305	.0340		534.6	9.7	11.5	
C-19c		.1641	.1894		.0307	.0348		537.0	8.1	9.6	
Avg.	.161	.1652	.1910	.0349	.0302	.0348	0.98	535.5	8.0	9.5	268
B-9c		.1741	.2010		.0401	.0463		534.0	10.2	12.2	
C-21c		.1757	.2028		.0421	.0486		535.4	9.0	11.1	
Avg.	.322	.1749	.2019	.0458	.0411	.0474	1.34	534.7	9.6	11.6	327
B-10c		.1803	.2082		.0463	.0535		532.9	10.9	13.1	
C-22c		.1818	.2098		.0482	.0556		534.1	10.3	12.5	
Avg.	.39	.1810	.2090	.0539	.0472	.0546	1.54	533.5	10.6	12.8	360
A-20g		.1905	.2209		.0530	.0615		529.2	10.6	13.0	
B-8c		.1857	.2144		.0517	.0597		533.2	10.7	13.0	
C-20c		.1876	.2165		.0540	.0623		532.6	11.4	13.9	
Avg.	.46	.1879	.2173	.0612	.0529	.0612	1.72	531.7	10.9	13.3	375
A-13g		.1943	.2253		.0568	.0659		528.7	11.0	13.5	
B-1c		.1907	.2202		.0567	.0655		532.2	11.4	14.0	
C-13c		.1914	.2209		.0578	.0667		533.6	10.6	13.0	
Avg.	.53	.1921	.2221	.0660	.0571	.0660	1.86	531.5	11.0	13.5	380
A-17g		.2011	.2331		.0636	.0737		527.7	11.8	14.5	
B-5c		.1976	.2282		.0636	.0735		—	—	—	
C-17c		.1984	.2290		.0648	.0748		532.4	11.6	14.2	
Avg.	.60	.1990	.2301	.0740	.0640	.0740	2.08	530.0	11.7	14.4	406
A-16g		.2153	.2496		.0778	.0902		526.6	12.5	15.6	
B-4c		.2149	.2482		.0809	.0935		529.0	13.7	17.1	
C-16c		.2145	.2476		.0810	.0934		530.7	12.7	15.8	
Avg.	.70	.2149	.2485	.0924	.0799	.0924	2.60	528.8	13.0	16.2	456
B-2c		.2383	.2752		.1043	.1205		528.2	14.0	17.9	
C-14c		.2385	.2753		.1049	.1211		528.8	14.0	17.8	
Avg.	.81	.2384	.2752	.1191	.1046	.1208	3.40	528.5	14.0	17.8	501
B-3c		.2635	.3043		.1295	.1496		526.7	14.9	19.4	
C-15c		.2572	.2969		.1246	.1447		(537.8)	14.4	18.7	
Avg.	.88	.2604	.3006	.1445	.1270	.1472	4.15	526.7	14.6	19.0	535
A-18g		.3062	.3550		.1697	.1966		(518.9)	(17.2)	(23.3)	
B-6c		.3058	.3531		.1718	.1984		526.8	14.3	19.4	
C-18c		.3003	.3466		.1669	.1924		523.3	14.7	19.8	
Avg.	.96	.3041	.3516	.1965	.1695	.1958	5.50	525.0	14.5	19.6	552
A		.3991	.4627								
B†		.3872	.4489								
C		.3894	.4515								
Avg.	1.0	.3919	.4544	.2983	—	.298	8.65	—	—	20.3‡	572‡

*Non-evaporable water. †Estimated graphically from ignition loss; no dry sample available. ‡Estimated

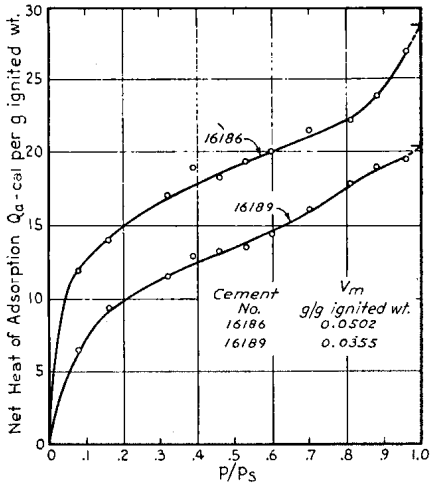

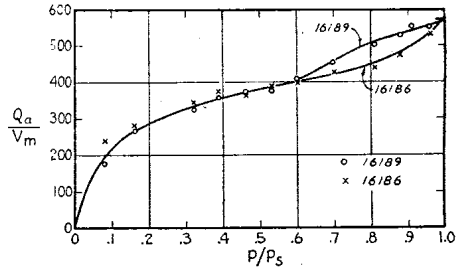

Fig. 4-3 (left)—Heat of adsorption vs. relative vapor pressure.
Data from Tables 4-1 and 4-2.

Fig. 4-4 (above)—$\frac{Q_a}{V_m}$ vs. p/p_s

of adsorption for the saturated samples, which were not measured. The terminus of the lower curve was estimated to be at 20.3 cal per g of ignited weight. Then, in accordance with eq. (8) the total net heat of adsorption was assumed to be proportional to V_m and the terminus of the upper curve estimated on this basis. That is,

$$\frac{(Q_{at})_1}{(V_m)_1} = \frac{(Q_{at})_2}{(V_m)_2}$$

From the data given in Fig. 4-3 and from the estimated value of $(Q_{at})_1$ we have the following:

$$(Q_{at})_1 = 20.3 \text{ cal per g ign. wt.}$$
$$(V_m)_1 = 0.0355 \text{ g per g ign. wt.}$$
$$(V_m)_2 = 0.0502 \text{ g per g ign. wt.}$$

Hence,

$$(Q_{at})_1/(V_m)_1 = 20.3/0.0355 = 572 \text{ cal per g}$$

and

$$(Q_{at})_2 = 572 \times 0.0502 = 28.7 \text{ cal per g}$$

Reference to the upper curve of Fig. 4-3 will show that this estimate results in a reasonable terminus for that curve.

According to the discussion leading up to eq. (8) the amount of heat evolved by adsorption at a given pressure should be proportional, or nearly so, to the amount of surface covered at that pressure. According to the B.E.T. theory, the fraction of the total surface that is covered at a given relative vapor pressure is the same for all adsorbents having the same value for the constant C. This could be strictly true only in the absence of capillary condensation, unless the various adsorbents had pores of exactly the same size and shape. Thus, at least for the low pressure range, we could predict from theory that the relationship be-

tween Q_a/V_m and p/p_s should be the same for both samples, at least up to $p = 0.45\ p_s$.

The relationship found between Q_a/V_m and p/p_s for the two cement pastes is shown in Fig. 4-4. If plotted separately the two series of points would be judged to describe different curves. However, in view of the possibility of considerable experimental error, it is doubtful whether the differences are significant, at least in the lower range of pressures. At any rate, differences in the lower range cannot be accounted for on the basis of current theory. In the upper range the separation of the curves might be due to a difference in size and shape of the pores and hence to a difference in the rate of change of water surface with change in pressure. The curves as drawn indicate that only those pores, or those parts of the pores, that fill at pressures above 0.6 p_s differ in size and shape.

Comparison of net heat of adsorption of water by cement paste with that of water on other solids

The total net heat of adsorption, Q_{at}, was estimated above to be 572 V_m. Since $V_m = \dfrac{S}{35.7 \times 10^6}$, the heat per unit of surface $= \dfrac{572}{35.7 \times 10^6}$ $= 16 \times 10^{-6}$ cal per sq. cm. of solid surface or $16 \times 10^{-6} \times 4.18 \times 10^7 =$ 670 ergs per sq. cm. of solid surface. Harkins and Boyd[2] measured the heats of immersion in liquid water of several different solids. The results were as follows:

$BaSO_4$	490 ergs per sq. cm. of solid surface
TiO_2	520
Si	580
SiO_2	600
ZrO_2	600
SnO_2	680
$ZrSiO_4$	850
Graphite	265

It is evident that the total net heat of adsorption for water in hardened cement paste is about the same as the heat of immersion of various non-porous minerals. As brought out before, the heat of immersion per sq. cm. of surface of these minerals should be about equal to their total net heats of adsorption per unit of surface if they were porous adsorbents.

Comparison of heat of hydration with net heat of adsorption

In another project, W. C. Hansen* measured the non-evaporable water contents and the heats of hydration on a group of 27 commercial cements comprising all types. The samples were neat pastes, $w/c = 0.40$ by

*Formerly of PCA laboratory. At present, Manager, Research Laboratories, Universal Atlas Cement Co.

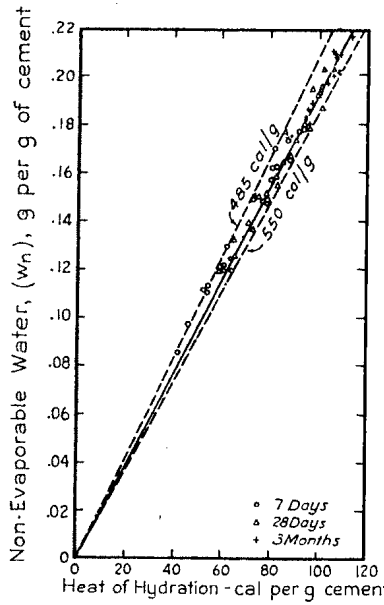

Fig. 4-5—Relationship between heat of hydration and non-evaporable water.

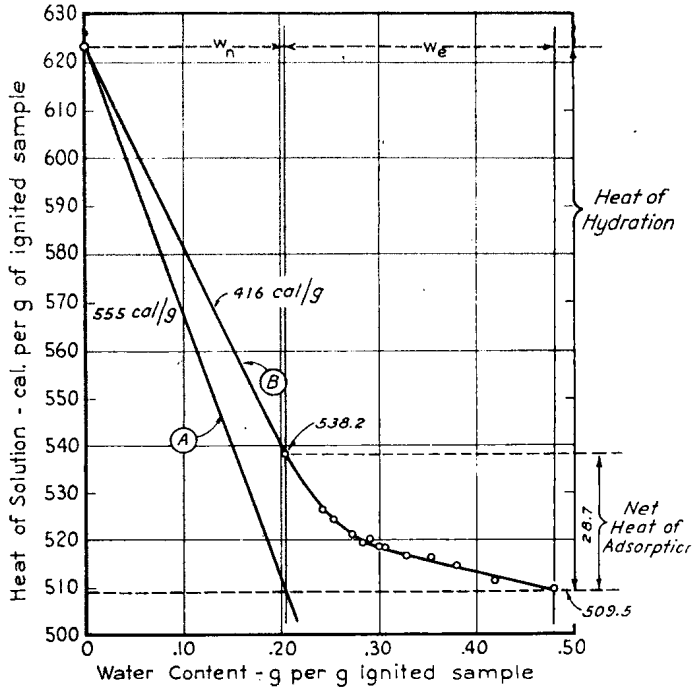

Fig. 4-6—Heat of solution data for pastes made with cement 16186.

Data from Table 4-1.

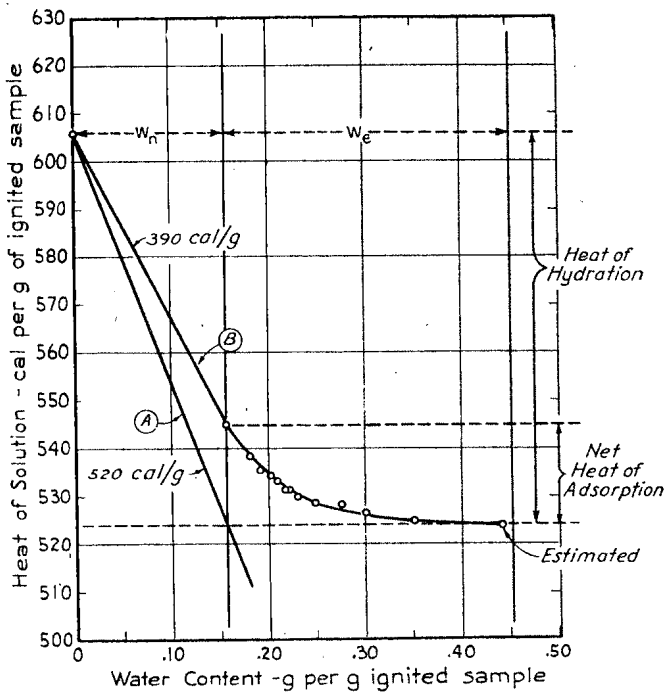

Fig. 4-7—Heat of solution data for pastes made with cement 16189.
Data from Table 4-2.

weight (not corrected for bleeding). They were cured in sealed vials at 70 F for periods ranging from 7 days to 1 year. The heat of hydration at each age was determined by the same heat-of-solution method described above. The non-evaporable water content was determined by the method already described. (Part 2)

The results are shown in Fig. 4-5. This graph indicates that the heat of hydration is directly proportional to the non-evaporable water content, and that the proportionality constants for the different cements differ, but do not differ widely.

Fig. 4-6 and 4-7 bring out the relationship between heat of hydration and heat of adsorption for the two samples used for the present study. In each diagram the point plotted for zero water content represents the heat of solution of the original cement. All the other points represent the hardened paste after 27 days of wet curing. In Fig. 4-6, for example, we see that the heat of solution of the original cement was 623 cal per g and that after hydration the heat of solution was 509.5 cal per g.† The difference, 113.5 cal, is the heat of hydration. When the evaporable water was removed before determining the heat of solution of the hy-

†This particular point was not obtained directly but was estimated from Fig. 4-1 in the manner already described. The same is true of the lowest point in Fig. 4-7.

drated cement, the heat of solution was 538.2 cal per g. The difference between 538.2 and 509.5, or 28.7 cal per g ignited weight, is the total net heat of adsorption, Q_{at}. The other points on the curve represent samples containing intermediate amounts of evaporable water.

The heat of hydration per g of non-evaporable water is about 555 cal for 16186 and 520 cal for 16189, which values agree fairly well with the data given in Fig. 4-5. These values are computed from the slopes of the lines marked A in Fig. 4-6 and 4-7.

The heat of reaction of the non-evaporable water alone is 416 cal per g of non-evaporable water for 16186 and 390 cal per g for 16189. These figures (based on lines B) indicate that the heat of reaction of the non-evaporable water is different for cements of different chemical composition.

From these results we may picture the heat of hydration as developing in the following way:

(1) Chemical reactions between the cement and water in the fresh paste produce new solid phases in which the non-evaporable water is an integral part. These reactions release a definite amount of heat for each unit of water combined, but the amount is different for cements of different chemical composition. (For cement 16186 the amount is 416 cal per g of non-evaporable water, or $416 \times 0.204 = 84.8$ cal per g of cement.)

(2) As the new solid phases (the reaction products) form, they adsorb water and the net heat of adsorption is released. This, according to the above estimates, is $572V_m$ cal per g for all cements, and is equal to the heat of immersion of the dried paste. (For the paste made from cement 16186 this amounts to $572 \times 0.0502 = 28.7$ cal per g of cement.)

(3) The total heat of hydration is the sum of the heat of combination of the non-evaporable water and the net heat of adsorption ($84.8 + 28.7 = 113.5$ cal per g for 16186).

The amount of heat that adsorption generally contributes to the total heat of hydration can be estimated from the data given above. Let

Q_r = heat of reaction of the non-evaporable water, cal per g.

Then

$$Q_r = k_1 w_n ,$$

where

k_1 = a constant for a given cement. Also, as assumed before,

$$Q_{at} = 572\ V_m \text{ cal per g} .$$

Since

$$w_n = k_2\ V_m ,$$

where

k_2 = a constant for a given cement (see Part 3),

$$\frac{Q_{at}}{Q_r} = \frac{572\ V_m}{k_1 w_n} = \frac{572}{k_1 k_2};$$

or

$$\frac{Q_{at}}{Q_r + Q_{at}} = \frac{572}{k_1 k_2 + 572}$$

The data for the two cements discussed above are:

Cement No.	k_1	k_2	$\frac{Q_{at}}{Q_r + Q_{at}}$
16186	416	4.07	0.25
16189	392	4.39	0.24

This shows that for the cements cited the total net heat of adsorption of the evaporable water is about ¼ of the total heat of hydration.

The results from these two cements suggest that the ratio of the heat of adsorption to the heat of combination of the non-evaporable water is a constant, or nearly so. However, the close similarity in this case is evidently fortuitous. Q_r is the heat of combination of the water that is a part of the solid phase and Q_{at} depends on the surface area of the solid phase. Hence, only Q_r is appreciably influenced by chemical composition and the two quantities therefore should not always bear the same ratio to each other. However, for most portland cements cured under the same conditions, the ratios probably do not differ widely from those found for these two cements.

THE FREE-ENERGY AND ENTROPY CHANGES OF ADSORPTION

Underlying concepts

It will be shown that the net heat of adsorption represents a change in the internal energy of the system in which the reaction takes place. As expressed by Glasstone,[3] the internal energy content of a substance "is made up of the translational kinetic energy of the moving molecules . . . . . of the energies of rotation and vibration within the molecule, of the internal potential energy determined by the arrangements of the atoms and electrons and other forms of energy involved in the structure of matter. From the standpoint of thermodynamics, however, it is not necessary to know anything about the structure of the atom or molecule, and so it is sufficient to divide the internal energy into two parts only: these are (a) the kinetic energy of translation or, in brief, the kinetic energy, and (b) all other forms of energy." For the present purpose this statement can be amplified by adding that it is not necessary to distinguish energy resident at the surface of a phase from energy within the phase. It can all be regarded as internal energy.

Although the principles of thermodynamics can be applied without knowledge of the mechanism of the change from the initial to final conditions, it seems helpful to picture what is believed to occur.

In the introduction to this section, adsorption was likened to the wetting of a solid by immersion in a liquid or by the spreading of a liquid film. Although in the following discussion this analogy is not explicitly used, the treatment is not in conflict with the concept set forth earlier. In the earlier discussion, emphasis was placed on the change from the completely dry to the completely water-covered or saturated state. In the following discussion attention is centered on changes from one intermediate state to another.

As indicated in Part 3, a field of force exists over the surface of the solid matter of the hardened paste. When molecules, in this case water molecules, enter this force field, they are attracted to the surface. In the direction normal to the surface the force field of the surface supplements the normal cohesive forces between water molecules. The result is that the proportion of molecules having enough energy to escape from the adsorbed liquid during a given time interval is less than normal for the existing temperature. The vapor pressure is correspondingly below that of free water at the same temperature.

The mean specific volume of adsorbed water is *less* than that of free water (see Part 5). The adsorbed water thus appears to be in compression. This observation has led to the belief that adsorbed water is in the same state as would be produced by an external compressive force of sufficient magnitude to reduce the specific volume of free water to that of adsorbed water. This conclusion was reached by Lamb and Coolidge[4] from their experiments showing that for the adsorption of the vapors of eleven different liquids, the net heats of adsorption were roughly proportional to the compressibilities of the respective liquids. However, for several reasons this is regarded as an oversimplified interpretation of the data. We may note in the first place that increasing the external pressure on a liquid densifies it and *raises* its vapor pressure. Although adsorption densifies the liquid, it *decreases* the vapor pressure. In the second place we may note (as will appear later) that the change in entropy caused by applying an external force is very much smaller than that caused by adsorption, unless the applied force causes a change of state. An external pressure produces a uniform compression throughout the liquid. The force of adsorption acts, like gravitation, on the water molecules individually and the effect therefore must vary with the distance from the surface, or from the centers of greatest attraction, according to the gradients in intensity of the force-field.

It seems reasonable to regard the net heat of adsorption as representing the result of changes in the internal structure of the water

(changes in the association and orientation of the molecules) and in the potential energy of the water molecules caused by the mutual attraction between the water molecules and the surface. The surface of the solid probably remains structurally unchanged.

Internal energy

A system in a given state is regarded as possessing a definite quantity of internal energy. The system may undergo a gain or a loss of internal energy by a gain or a loss of energy in the form of heat, by doing mechanical work, or by having mechanical work done on it. In thermodynamics, heat gained by the system and work done by the system are conventionally regarded as positive quantities.

According to the first law of thermodynamics the increase in internal energy is equal to the difference between the energy gained as heat and the energy lost by the system if it does mechanical work on its surroundings during the process. That is,

$$\Delta U = Q - w , \quad (13)$$

where

ΔU = increase in internal energy,
Q = heat gained, and
w = work done by the system.

When the external pressure is constant, the work term is proportional to the increase in volume. That is,

$$w = P\Delta v , \quad (14)$$

in which

P = the constant external pressure, and
Δv = the increase in volume of the system.

It is conventional to subtract the initial value from the final to obtain the increment. For example, $\Delta U = U_2 - U_1$ and $\Delta v = v_2 - v_1$. The increment is called an increase whether in any given case it is positive or not. In the case of adsorption the final energy content and the final volume are less than the corresponding initial values. Hence, it is advantageous to write in terms of decreases, that is, in terms of $-\Delta U$, $-\Delta v$, etc. This is done in the rest of this discussion.

Enthalpy, free energy, and unavailable energy

For reactions at constant pressure it is customary to let

$$-\Delta H = -\Delta U - P\Delta v \quad (15)$$

$-\Delta H$ is usually called the decrease in heat content, but, as will be seen, it is generally not that and is preferably called the decrease in enthalpy.[6]

The decrease in enthalpy accompanying an isothermal adsorption represents a decrease in two general classes of energy, namely, *free energy* and *unavailable energy*. That is,

$$-\Delta H = -\Delta G - T\Delta S, \quad \ldots\ldots\ldots\ldots\ldots\ldots (16)$$

where

$-\Delta G$ = decrease in free energy,
$-\Delta S$ = decrease in entropy, and
T = absolute temperature.

The term $-T\Delta S$ represents the decrease in unavailable energy for an isothermal reaction. It is that part of the total energy decrease which, at constant temperature, cannot be converted into external work. If released, it can appear only as heat. Therefore, the unavailable energy can be regarded as stored heat.* In the freezing of water, it is the latent heat of freezing. Without reference to underlying concepts, entropy, S, can be regarded simply as a capacity factor giving the quantity of stored heat in calories per degree of temperature above absolute zero. Hence, TS is the quantity of stored heat, and $T\Delta S$ a change in stored heat, in calories or in whatever energy unit is adopted.

The decrease in free energy, $-\Delta G$, that accompanies an isothermal reaction at constant pressure is that part of the enthalpy-decrease that might be converted into external work. It is that which promotes all spontaneous processes at constant temperature and pressure. In this case it is the energy that promotes hydration, adsorption, swelling, capillary flow, and moisture diffusion. Such processes always take place in such a way as to tend to equalize initial differences in free energy. Thus adsorption occurs when the free energy of the free water or free vapor is greater than the free energy of the adsorbed or capillary condensed water. Moisture diffusion occurs when adsorbed or capillary-condensed water in adjacent regions is at different free-energy levels. The free energy per mole of a given substance is known also as its chemical potential, or thermodynamic potential.

For the conditions of most of these experiments (adsorption in small granules of paste at constant temperature and atmospheric pressure) the decrease in free energy may be assumed to appear entirely as heat. But if work is done by the process, as for example against forces tending to restrain swelling, the free energy expended for such work will not appear as heat.†

*This concept is developed at length in an office memorandum by H. H. Steinour. (Special Report No. 1, Series 330, 1945).

†Very recent developments in this subject indicate that adsorption in a comparatively rigid solid such as hardened paste should not be considered to be occurring under a constant external pressure of 1 atmosphere. Since, in a rigid body, swelling or shrinkage may give rise to elastic forces that act on the adsorbed layer, the pressure on the layer is a function of the degree of swelling of the paste, and hence of p/p_s as shown in the section below on Swelling Pressure. Such a variation in external pressure was dealt with by A.B.D. Cassie. See "Adsorption of Water by Wool," *Trans. Faraday Soc.* v. 41, p. 458 (1945) and earlier papers by Barkas in the same journal.

Cassie assumed that the swelling of dry wool fiber produced tension in the filaments of the fiber and compression in the adsorbed water. This assumption may not apply to cement paste. The gel is formed in the fully swollen-state and the elastic bonds that hold the mass together should therefore be considered free of stress in that state, rather than in the dry state as assumed by Cassie. However, since the same reasoning may be applied to the growth of wool fiber, Cassie's results seem to indicate that the reasoning is incorrect. In view of these uncertainties and the recent date of Cassie's paper, the authors have adopted the usual procedures and assumptions for the present paper. A more exact analysis will not be attempted until more experimental data are available.

We may note in passing that Δv of eq. (15) is in the present case the small contraction accompanying adsorption from the liquid state. It amounts, on the average, to about 0.13 cc per cc of water adsorbed. Hence, for an external pressure of 1 atmosphere, 10^6 dynes per sq. cm.,

$$w = 0.13 \times 10^6 \text{ ergs.}$$

or $0.13 \times 10^6 \times 2.39 \times 10^{-8} = .003$ cal. per g. of water adsorbed. Thus it is seen that the work term of eq. (15) is negligible and hence the net heat of adsorption represents the change in internal energy of the system.

Relationship between net heat of adsorption and decreases in internal energy, enthalpy, free energy, and entropy

Since by eq. (13), (14), and (15) $-\Delta H = -Q$, it follows from eq. (16) that:

$$-Q = -(\Delta G + T\Delta S), \quad \ldots\ldots\ldots\ldots (17)$$

$$-\Delta G = -(Q - T\Delta S), \quad \ldots\ldots\ldots\ldots (18)$$

$$-\Delta S = \frac{-(Q - \Delta G)}{T}, \quad \ldots\ldots\ldots\ldots (19)$$

$-\Delta G$ can be computed from the vapor pressure, as will be shown below, and ΔS can be estimated from the measured value of $-Q$ and the corresponding value of $-\Delta G$.

Relationship between change in vapor pressure and change in free energy

As said before, adsorption can occur only when water in the free state has a higher vapor pressure than it has after it is adsorbed. When water in the free state is adsorbed, the change in its free energy is equal to the corresponding change in the free energy of its vapor. Hence, the change in free energy when water changes from one equilibrium condition to another can be calculated from the corresponding change in the free energy of the water vapor.

The relationship between change in free energy and change in vapor pressure may be written

$$dG = v\,dp\,, \quad \ldots\ldots\ldots\ldots (20)$$

where v and p are the volume and pressure, respectively, of 1 mole of vapor at temperature T. Hence, if p_1 is the initial equilibrium vapor pressure of the free water and p_2 the pressure after adsorption, the change in free energy is, for such a finite change,

$$\Delta G = \int_{p_1}^{p_2} v\,dp\,; \quad \ldots\ldots\ldots\ldots (21)$$

Assuming that the vapor behaves as an ideal gas, we have

$$v = \frac{RT}{p}. \quad \ldots\ldots\ldots\ldots (22)$$

Thus,

$$\Delta G = RT \int_{p_1}^{p_2} \frac{dp}{p}; \quad \ldots\ldots\ldots\ldots\ldots\ldots\ldots\ldots (23)$$

or,

$$\Delta G = RT' \ln p_2/p_1 \text{ (cal per mole of water)} \ldots\ldots\ldots\ldots (24)$$

This is the change in free energy when 1 mole of free water, or water vapor, at vapor pressure p_1 is adsorbed by a paste under conditions such that the pressure after adsorption is p_2. The decrease in free energy when the initial vapor pressure is the saturation pressure, p_s, and the final pressure is a smaller pressure, p, is given—in calories per g of water taken up—by the following equation:

$$\Delta G = -\frac{RT}{M} \ln p/p_s, \quad \ldots\ldots\ldots\ldots\ldots\ldots\ldots (25)$$

where M = the molecular weight of the adsorbate.

For our experiments,

M = 18.02 (molecular weight of water)
R = 1.986 cal per deg. per mole
T = 298 K.

Using these values and letting $\ln p/p_s = 2.303 \log_{10} p/p_s$, we obtain

$$-\Delta G = -75.6 \log_{10} p/p_s \text{ cal per g of water} \ldots\ldots\ldots\ldots\ldots (26)$$

It is to be noted that the solid phase is not directly represented in this equation for reduction in free energy (eq. 26). It is indirectly represented by the difference between p and p_s. Since temperature is constant and since condensed water is present, p can be smaller than p_s only through the action of a solute or some agency external to the water. The nature of this agency is immaterial so far as the thermodynamic relationships are concerned.

Estimation of decrease in entropy from experimental results

From eq. (19) it is seen that the decrease in entropy can be obtained from the difference between $-\Delta G$ and $-Q$. In the present case, $-Q = Q_a$, the net heat of adsorption in cal per g of adsorbent, an integral quantity.* But the decrease in free energy, $-\Delta G$, is given by eq. (26) as the calories lost per gram of water adsorbed when 1 gram of water having vapor pressure p_s is added to a large quantity of paste having vapor pressure p, the quantity of paste being so large that the added gram of water does not change the vapor pressure. In other words, $-\Delta G$ is a differential. It is therefore necessary to obtain the differential net heat of adsorption in cal per g of adsorbed water. This can be done by differentiating the empirical Q_a vs. w relationship.

*Note that the tabulated values of Q_a, the heat lost, are given as positive quantities. This is customary in recording adsorption data. Hence, the recorded values must be multiplied by — 1 before being used in the thermodynamic equations in place of Q.

The Q_a vs. w relationship found in these experiments is similar to those found by Katz[6] and others for various materials. Katz found that these curves could be represented by empirical equations of the form

$$Q_a = \frac{Aw}{B + w}, \quad \ldots\ldots\ldots\ldots\ldots\ldots\ldots\ldots\ldots\ldots (27)$$

where Q_a = net heat of adsorption, cal per g of solid,
w = vapor adsorbed, g per g of solid, and
A and B = constants for a given system.

Differentiation gives

$$\frac{dQ_a}{dw} = \frac{AB}{(B + w)^2} \quad \ldots\ldots\ldots\ldots\ldots\ldots\ldots\ldots\ldots\ldots (28)$$

The constants A and B of eq. (27) and (28) can be obtained by using the following form of eq. (27):

$$\frac{w}{Q_a} = \frac{B}{A} + \frac{w}{A}$$

This shows that if experimental values of w/Q_a are plotted against w, a straight line should result, from which the constants can be evaluated. The data for the two pastes used in this study are given in Table 4-3.

The corresponding values of w/V_m and w/Q_a up to $p = 0.81\ p_s$ are plotted in Fig. 4-8. The points for 16186 lie close to a straight line. Those for 16189 appear more erratic, but between $w/V_m = 1$ and $w/V_m = 2$ they seem to follow the same line as the other points. At any rate,

TABLE 4-3—DATA FOR EVALUATING CONSTANTS OF NET HEAT OF ADSORPTION EQUATION

p/p_s	Cement 16186			Cement 16189		
	$\frac{Q_a}{V_m}$ cal/g	$\frac{w}{V_m}$	$\frac{w}{Q_a}$ g/cal $\times 10^3$	$\frac{Q_a}{V_m}$ cal/g	$\frac{w}{V_m}$	$\frac{w}{Q_a}$ g/cal $\times 10^3$
0.0	0	0		0	0	
0.081	239	0.76	3.18	180	0.72	4.0
0.161	279	0.95	3.40	268	0.98	3.66
0.322	342	1.37	4.00	327	1.34	4.10
0.39	376	1.55	4.12	360	1.54	4.28
0.46	364	1.71	4.70	375	1.72	4.59
0.53	388	1.89	4.88	380	1.86	4.90
0.60	398	2.04	5.13	406	2.08	5.12
0.70	428	2.48	5.80	456	2.60	5.70
0.81	442	3.00	6.79	501	3.40	6.80
0.88	474	3.48	7.34	535	4.15	7.76
0.96	534	4.28	8.02	552	5.50	9.95
1.00	572	5.50	9.6	572	8.65	15.10

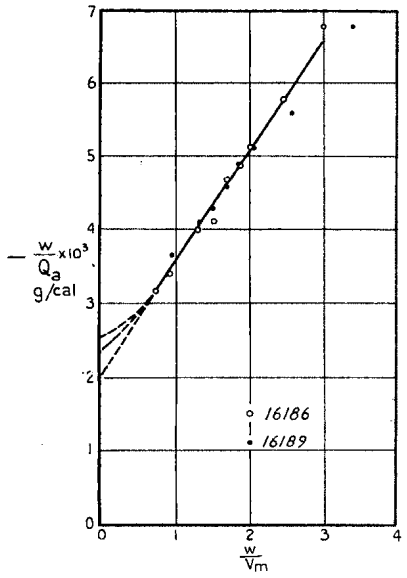

Fig. 4-8—Plot for evaluating constants of net heat of adsorption equation.

no distinction between the two pastes seems justifiable on the basis of these data alone.

The constants for the line as drawn are

$$\frac{B}{A} = 0.0020 \quad ; \quad \frac{A}{B} = 500;$$

$$\frac{V_m}{A} = 0.00152 \quad ; \quad A = 655\ V_m\ ;$$

$$B = 1.31 V_m \quad ; \quad AB = 858 V_m^2.$$

Hence, for these experimental data,

$$\frac{Q_a}{V_m} = \frac{655\ w/V_m}{1.31 + w/V_m}, \qquad (29)$$

and

$$\frac{dQ_a}{dw} = \frac{858}{(1.31 + w/V_m)^2} \qquad (30)$$

Solutions of eq. (26) and (30) are given in Table 4-4 and in Fig. 4-9. These data show, for example, that if 1 g of water were added to a very large quantity of paste having a water content corresponding to $p = 0.2\ p_s$, the quantity of paste being so large that the addition of 1 g would not change the vapor pressure, the total heat evolved would be 154 cal per g of water. Of this total, 53 cal per g would be due to the change in free energy. The curves and tabulated data based on the equations represent

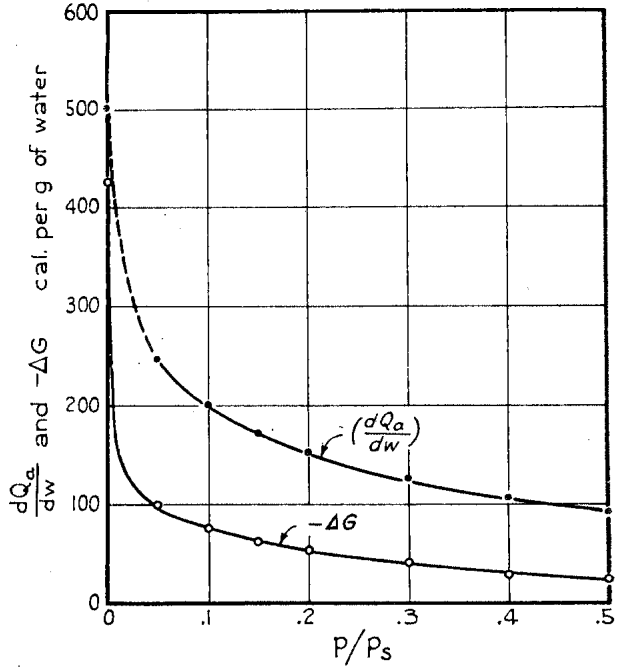

Fig. 4-9—Comparison of differential net heat of adsorption with change in free energy.

—ΔG from eq. (25).
$\frac{dQa}{dw}$ from eq. (29)

the original data rather closely between $p = 0.05\ p_s$ and $p = 0.5\ p_s$ at least for 16186. For lower pressures, the trend of the dQ_a/dw curve is uncertain. This will be discussed more fully below.

Table 4-5 gives solutions of eq. (19) and thus gives the change in unavailable energy and entropy for the same data as Table 4-4. These data show that for the pressure range $p = 0.05\ p_s$ to $p = 0.5\ p_s$, from 60 to 70 percent of the heat-loss represents unavailable energy. For adsorption of water on cellulose over the same pressure range, Babbitt[7] found the change in unavailable energy to be 44 to 60 percent of the total. This may be taken to indicate that when water is adsorbed by cement paste, it undergoes a similar but somewhat greater change than it does when it is adsorbed by cellulose.

Significance of change of entropy

The decrease in entropy is shown in the last column of Table 4-5. That these are relatively large changes in entropy may be judged by comparing them with the change in entropy of water in the various physical and chemical processes given below:

(1) For water at 25 C an increase in pressure from 50 atm. to 400 atm. causes a decrease in entropy of 0.0023 cal per g per deg.[8]

(2) The transition of water to ice at 0 C is accompanied by an entropy decrease of 0.29 cal per g per deg.[9]

TABLE 4-4—COMPUTATION OF DIFFERENTIAL NET HEAT OF ADSORPTION dQ_a/dw AND FREE ENERGY ΔG

$$\frac{dQ_a}{dw} = \frac{858}{(1.31 + w/V_m)^2}\ ;\ -\Delta G = -75.6\ log_{10} p/p_s$$

p/p_s	w/V_m*	$1.31 + w/V_m$	$(1.31+ w/V_m)^2$	$\frac{dQ_a}{dw}$	$-\Delta G$
>0	—	—	—	500	—
.05	0.57	1.86	3.46	248	98
.10	0.76	2.07	4.28	200	76
.15	0.92	2.23	4.97	172	62
.20	1.05	2.36	5.57	154	53
.30	1.30	2.61	6.81	126	40
.40	1.52	2.83	8.01	107	30
.50	1.75	3.06	9.36	92	23

*Values taken from curve in Fig. 4-2.

TABLE 4-5—COMPUTATION OF DECREASE IN UNAVAILABLE ENERGY, $-T\Delta S$ AND DECREASE IN ENTROPY, $-\Delta S$

$$-T\Delta S = \frac{dQ_a}{dw} + \Delta G$$

$$T = 298\ K$$

p/p_s	w/V_m*	$\frac{dQ_a}{dw}$ cal/g	$-\Delta G$ cal/g	$-T\Delta S$ cal/g	$\frac{-\Delta S \text{ cal/g}}{\text{deg}}$
>0	—	500	—	—	—
.05	0.57	248	98	150	0.50
.10	0.76	200	76	124	0.42
.15	0.92	172	62	110	0.37
.20	1.05	154	53	101	0.34
.30	1.30	126	40	86	0.29
.40	1.52	107	30	77	0.26
.50	1.75	92	23	69	0.23

*Values taken from curve in Fig. 4-2. $T\Delta S$ from eq. (19).

(3) At 25 C, a pressure of about 9000 atm. will change liquid water to a solid of density 1.35 (specific volume 0.74) known as ice VI. This change in phase is accompanied by a decrease in entropy of 0.26 cal per g per deg.[9]

(4) The entropy change of a system comprising $CaSO_4$ and H_2O when the $CaSO_4$ acquires two molecules of water of hydration can be computed as follows:[10]

Compound	Entropy, S, at 25 C
$CaSO_4$	25.5
$2H_2O$	33.5
Total	59.0 cal/deg
$CaSO_4.2H_2O$	46.4
$-\Delta S$	= 12.6 cal/deg

If this decrease in entropy of the system is ascribed wholly to the water, as is done in the calculations for adsorption, $-\Delta S$ in cal per g of water is

$$\frac{12.6}{2\times 18} = 0.35 \text{ cal per g per deg}$$

(5) For the system Na_2SO_4 and H_2O reacting to form $Na_2SO_4.10H_2O$, the change in entropy of the system expressed in terms of the water is, when computed as above, also $-$ 0.35 cal per g per deg.[10]

(6) For the system CaO and H_2O, reacting to form $Ca(OH)_2$, the change in entropy, computed and expressed as above, is $-$ 0.49 cal per g per. deg. [10a]*

A comparison of these figures with those in the last column of Table 4-5 shows that the data have the following indications with respect to the change of state of the water adsorbed in the low-pressure range indicated by the decrease in entropy:

(1) The change in entropy is far greater than could be produced by pressures lower than the pressure required for solidification of water at 25 C.

(2) The change in entropy is fully as great as that corresponding to the transition from normal liquid to ice VI, or to water of crystallization.

(3) The change in entropy for the water taken up at very low pressure, $p = 0.05\ p_s$, may be as great as the change accompanying the change from normal water to hydroxyl groups chemically combined in $Ca(OH)_2$.

The third conclusion is less valid than the other two. As will be brought out below, there is reason to question whether eq. (27) and (28), on which Table 4-5 is based, are of the correct form for the low pressure range, about $p = 0.05\ p_s$ and below. If it is not, the estimated $-\Delta S$ may be considerably in error in the direction of being too large. Evidence can be found to show that $-\Delta S$ reaches a maximum in absolute value below $p = 0.05 p_s$. At very low relative vapor pressures, the absolute value of ΔS may be about the same as that estimated for $p/p_s = 0.50$. This would indicate that the estimated decrease in entropy is the resultant of several factors and that the full significance of the entropy decrease cannot be seen until these factors are known in detail.

*In Part 2, in connection with Table 5, it was pointed out that the equilibrium relative vapor pressure of water over CaO may be much less than that given in the table. The evidence for this statement is found in the values for change in entropy and enthalpy for the system CaO-H_2O. (The enthalpy change is 847 cal/g of water. The equilibrium relative vapor pressure may be calculated by reversing the steps in the procedure for calculating the entropy change of adsorption. The result is $p/p_s = 5.6 \times 10^{-10}$. This is to be compared with 1.3×10^{-4} given in Table 5, Part 2. Although the calculated value may be somewhat in error, the error is not likely to be great enough to account for a million-fold difference. The experimental value is open to more question. It is derived from measurements of the relative efficiency of desiccants. The conditions were such as to warrant the conclusion that the value of p/p_s cannot exceed that given; the true value can be much less.

No evidence has been obtained in this laboratory that any of the desiccants listed in Table 5, Part 2, actually removed water from $Ca(OH)_2$. If the calculated value is accepted as being of the right order of magnitude, then the dehydration of $Ca(OH)_2$ by these desiccants would not be expected.

In general, the data indicate that some of the adsorbed water undergoes a pronounced modification, but the nature of the modification cannot be deduced from the data alone. In Part 3, reasons were given for considering the adsorption process to be a physical one—van der Waal's adsorption. These data are generally compatible with that view, although the estimated $-\Delta S$ values in the low pressure range appear to be rather larger than might be expected. Thus, the possibility of some of the water being taken up by a chemical process is not precluded by these data.

THE ENERGY OF BINDING OF WATER IN HARDENED PASTE

The heat of adsorption is a measure of the energy that must be supplied to enable adsorbed water molecules to break away from the force field of the adsorbent and become vapor. Similarly, the net heat of adsorption (dQ_a/dw) is a measure of the energy required to restore adsorbed water to the normal liquid state. That is, the net heat of adsorption is a measure of the energy of binding between the evaporable water and the solid phase. In the same way, the heat of reaction of the non-evaporable water is a measure of the energy of its binding.

In this connection the value of dQ_a/dw when evaporable water = zero is of special interest. According to eq. (27), this value is equal to A/B. For the data of Fig. 4-9, A/B = 500 cal per g. Steinberger[11] remarked that when the vapor pressure is near zero, the surface is so sparsely populated with adsorbed molecules that the molecules can be regarded as having no effect on each other, and therefore the net heat of adsorption at the limit where, in this case, w/V_m approaches zero is a measure of the binding energy of the evaporable water molecules in the gel. In this case it has the further significance that it should also be a measure of the energy of binding of the *least firmly bound part of the non-evaporable water*. This will become evident when it is remembered that in Part 2, Tables 3 and 4, it was shown that the water content of the sample dried over $Mg(ClO_4)_2$. $2H_2O$ is a point on a smooth curve relating water content to vapor pressure. If the chosen drying agent had been P_2O_5, the non-evaporable water contents would have been 80 percent of the present values, and the evaporable water contents would have been correspondingly higher. For example, in Fig. 4-6, the non-evaporable water content would have been 0.163 instead of 0.204. If the heat of reaction of the increment of water (0.204 − 0.163) is the same as the average for all the non-evaporable water, the heat of solution of the dry sample would have been 555 cal per g, represented by the point of intersection of line B and the ordinate at w = 0.163. If the heat of reaction

of this increment is less than the average, the heat of solution would fall below line B.*

Similarly, had a desiccant of higher vapor pressure been used, the non-evaporable water content would have been higher and the heat of solution of the dried sample lower, the point falling somewhere on the curve now representing evaporable water. The average heat of reaction of the non-evaporable water would have appeared lower.

It is thus clear that the *maximum* net heat of adsorption cannot be greater than the *minimum* heat of reaction of the non-evaporable water. Since the minimum heat of reaction of the non-evaporable water cannot be greater than the average for all the non-evaporable water, the maximum net heat of adsorption cannot exceed the average heat of reaction of the non-evaporable water and is probably less.

This is rather positive evidence that eq. (28) cannot represent the data all the way to $w = 0$. Hence, the value 500 cal per g for $w = 0$ obtained from eq. (30) cannot be accepted; it is too high.† This conclusion is represented by the curved dotted lines in Fig. 4-8. The line terminating at $w/Q_a = 2.40 \times 10^{-3}$ g per cal corresponds to the average heat of reaction of the non-evaporable water in sample 16186, 416 cal per g. It is therefore the *lowest* possible terminus for the line representing that sample. The other point, at 2.55×10^{-3} g per cal, is the lowest possible terminus for sample 16189. It corresponds to the average heat of reaction, 392 cal per g of non-evaporable water.

As discussed in Part 2, one microcrystalline hydrate known to occur in hardened paste is $Ca(OH)_2$. The heat of formation of this compound from CaO and H_2O is about 15,260 cal per mole.[12] Expressed on the basis of the water, as for the net heat of adsorption or the heat of reaction of non-evaporable water, this amounts to about 847 cal per g of water. This figure is to be compared with the 392 and 416 cal per g of water found as the heat of reaction of the non-evaporable water for the two paste samples. It is thus apparent that a considerable portion of the non-evaporable water in hardened paste has much less energy of binding than the part that is in $Ca(OH)_2$. From the relationship pointed out above it follows also that the most firmly bound adsorbed water is loosely bound as compared with that in $Ca(OH)_2$.

The total net heat of adsorption has already been shown to be about $572V_m$ cal per g of sample. The *average* for the gel water alone is therefore about $572V_m \div 4V_m = 143$ cal per g of gel water. We can now observe that the *maximum* net heat of adsorption is of the order of 400 cal per g (392 cal per g of water for one paste and 416 cal per g for the

*It could not fall very far below line B, however, since the curve would still have to pass through the point at $w = 0.204$ in line with the smooth curve. It is estimated that the lowest point in Fig. 4-6 that would meet this requirement would be at about 550 cal per g and $w = 0.163$.

†This conclusion may be true also with respect to the use made of eq. (28) by Katz, Steinberger, Babbitt, and others.

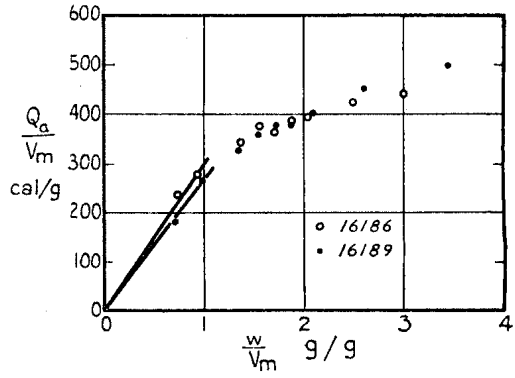

Fig. 4-10—Estimate of the net heat of adsorption for the water in the first layer.

other). How much of the adsorbed water has this relatively higher energy of binding cannot be told from these data. However, an estimate can be made of the *average* binding energy of the first layer with the aid of Fig. 4-10. This is a plot of Q_a/V_m vs. w/V_m for both sets of data up to about $w/V_m = 3$. This shows that the average net heat of adsorption of the first layer is about 300 cal per g of water for 16186 and about 270 cal per g for 16189. This estimate embodies the assumption that all the water taken on in the low pressure range is held in the first layer, that is, that the layers form consecutively as the pressure is raised. This is probably not true. According to the B.E.T. theory, when $w/V_m = 1.0$, p = about 0.2 p_s and about 85 percent of the water would be in the first layer at this pressure. The rest would be in higher layers. Such a correction, very doubtful as to accuracy, would indicate an average net heat of adsorption of about 320 to 350 cal per g of water in the first layer.

Data published by Harkins and Jura[13] are instructive in this respect. These authors found, by direct calorimetric measurement, the net heat of adsorption of water on anatase (titanium dioxide) to be as follows:

Average for:	
1st layer	364 cal per g of water
2nd layer	76
3rd layer	25
4th layer	4.4
5th layer	2.2 (?)
All above 5	1.7 (?)
Total	473 cal per g of water

Since these quantities were computed from experimental data on the assumption that the layers formed consecutively, the average per layer is directly comparable with the figures obtained from Fig. 4-10 without

correction for the overlapping of layer-formation. Thus, 364 cal per g for the first layer adsorbed on anatase is comparable with 270 to 300 for the first layer on dried paste. At least a part of the difference is due to the presence of air in our experiments, for the adsorption on anatase occurred in a high-vacuum system. The general indication is that the first layer of water on cement paste is bound with about the same energy as the first layer on anatase.

A comparison of the average heats for successive layers is not feasible because the shapes of our curves are undoubtedly influenced by capillary condensation and the presence of air.

NET HEAT OF ADSORPTION AND C OF THE B.E.T. EQ. (A)

As previously indicated, the constant C of the B.E.T. eq. A is related to the heat of adsorption as follows,

$$C = ke^{\frac{Q_1 - Q_L}{RT}}$$

where

Q_1 = heat of adsorption for the first layer, cal per mole,
Q_L = heat of liquefaction, cal per mole
R = gas constant = 1.986 cal per mole per deg
T = absolute temperature
k = constant

Brunauer et al. assumed that constant k does not differ significantly from unity, and, hence, that

$$Q_1 - Q_L = 2.303\ RT\ log_{10}\ C$$

This assumption no longer appears valid in the light of the derivation of the equation by statistical-mechanical methods recently reported by Cassie.[23] On the contrary, it appears that k is of the order 0.02 or less. It follows that $(Q_1 - Q_L)$ calculated on the assumption that k is unity must be too low. However, in some cases, k might approach unity so that $(Q_1 - Q_L)$ calculated on this assumption would approach the experimental values.

The experimental data obtained by the air-stream method show that, for cement pastes, about 90 percent of the values of C lie between 17 and 23. For the particular samples used in the calorimeter tests, $C = 22$. On the assumption that k is unity, $C = 22$ corresponds to 102 cal per g. This is to be compared with 472 cal per g found experimentally. That is, the value of k appears to be far less than unity.

Similar results were obtained in the adsorption of water on nonporous adsorbents by Harkins and Boyd, as shown by the following data:[14]

Kind of solid	Q_a (B.E.T.) cal/g	Q_a (Observed) cal/g
TiO_2 (anatase)	133	445
SiO_2 (quartz)	139	511
$BaSO_4$	178	416

Here also k must be much less than unity to account for the results.

The analysis made by Cassie clarifies somewhat the significance of C, making it appear as a factor which expresses the distribution of molecules between the first and higher layers and placing less emphasis upon its relationship to the heat of adsorption. At the same time, it clarifies the significance of constant V_m. So long as k was assumed to be unity, the discrepancies between calculated and experimental net heat of adsorption raised doubts about the acceptance of V_m on theoretical grounds. Now it appears that this doubt can be dissolved to a considerable extent, though not completely. In any case, it may be noted that the acceptance of V_m as a measure of surface area, discussed in Part 3, rests mainly on the outcome of empirical tests, rather than on literal acceptance of the assumptions used in the derivation of the B.E.T. equation.

SWELLING PRESSURE

Limited-swelling gels

When some kinds of gel are placed in contact with a suitable liquid, they imbibe liquid and swell until they have become molecular or colloidal solutions. This is called *unlimited swelling*. The same gels with another type of liquid may imbibe only a limited amount and show correspondingly *limited swelling*. Such observations suggest that the tendency to swell on contact with a liquid is a manifestation of a tendency of the material to dissolve or at least to peptize to the colloidal-solution state. When swelling is of the limited type, the tendency of the liquid to penetrate and disperse the solid is evidently opposed by cohesive forces that bind the mass together.

Portland cement gel in water belongs to the limited-swelling class. Like other gels of its class, it is not able to swell beyond the dimensions established at the time of its formation. However, it will shrink on loss of evaporable water and swell when evaporable water is regained. As mentioned elsewhere (see Part 2) it undergoes a permanent shrinkage on first drying; that is, only a part of the initial shrinkage is reversible.

When the tendency of a swelling body to expand is resisted, the body may be able to exert great force. For example, dry wooden wedges driven into rock seams will split the rock when the wedges are allowed

to take up water, a method of quarrying used by the ancient Egyptians.[15]

It is thus understood that swelling is a movement of the solid units of the gel that can be prevented only by suitable application of force. The magnitude of the force required to prevent swelling, the so-called swelling pressure, can be ascertained from a consideration of the free-energy changes that occur when a swelling body takes up a liquid at a given constant temperature.

Idealized cement gel

In the following derivation it will be assumed, contrary to fact, that the solid particles of the cement gel are not interconnected. Also, the possible effects of any non-gel constituents will be ignored. It will be assumed that these disconnected gel-elements are colloidal particles and that they are packed together in such a way that all interstitial space is filled with adsorbed water. Thus we assume that we are dealing with a highly concentrated colloidal solution. These assumptions make it possible to ascertain the conditions governing the movements of adsorbed water in an actual paste, without the modifying effects of elastic forces in the solid phase. Also, it eliminates the complication introduced by the presence of capillary space. This will be dealt with later.

The thermodynamics of the swelling of such an idealized gel can be treated as if the gel were a true solution. The swelling pressure is related to vapor pressure in the same way that osmotic pressure is related to vapor pressure. The following treatment follows Glasstone's treatment of osmotic pressure.[16] (See also references (7) and (11)).

Derivation of equation for swelling force

Imagine a vessel containing the idealized gel, its water content such as to give a vapor pressure less than that of pure water at the same temperature. If pure water were placed in contact with this gel, the gel would imbibe water and swell until the vapor pressure of the water within the gel became equal to the vapor pressure of pure water. If the external pressure on the gel (which acts alike on both the solid and the liquid phases) were increased sufficiently, the vapor pressure of the water in the gel could thereby be made equal to that of free water at the same temperature. Under this higher external pressure, the gel would be unable to imbibe water and swell. The increase in pressure required to prevent swelling when a dry or partially dry gel has access to free water is, as said above, defined as the swelling pressure.

Let P_s = existing external pressure,

P = external pressure on the gel when it is in equilibrium with free water under external pressure P_s,

$P - P_s = \Delta P$ = swelling pressure,

G_s = free energy of pure water at external pressure P_s, and
G = free energy of adsorbed water at external pressure P_s.

The increase in external pressure required to equalize the free energies of the adsorbed and free water is given by the following expression

$$G_s = G + \int_{P_s}^{P} \left(\frac{\partial G}{\partial P}\right)_T dP \quad \ldots\ldots\ldots\ldots\ldots\ldots (31)$$

For a system such as this the change in free energy with pressure at constant temperature can be shown to be equal to the rate of change in volume of the system with change in water content—on the molar basis, the "partial molal volume" of the adsorbed water, $\overline{V}$. That is,

$$\left(\frac{\Delta G}{\Delta P}\right)_T = \overline{V} \quad \ldots\ldots\ldots\ldots\ldots\ldots\ldots\ldots (32)$$

Hence,

$$G_s = G + \int_{P_s}^{P} \overline{V}\, dP \quad \ldots\ldots\ldots\ldots\ldots\ldots\ldots\ldots (33)$$

The increase in free energy of the adsorbed water that takes place when the external pressure is increased can be expressed in terms of the corresponding changes in vapor pressure. If

G = free energy of adsorbed water under initial external pressure, P_s and G_s = free energy of adsorbed water under external pressure P, then $G_s - G = \Delta G$ = increase in free energy when external pressure is raised from P_s to P. The respective free-energies are related to vapor pressures as follows:

$$G = G_r + RT \ln p/p_r \quad \ldots\ldots\ldots\ldots\ldots\ldots\ldots\ldots (34)$$

and

$$G_s = G_r + RT \ln p_s/p_r\,, \quad \ldots\ldots\ldots\ldots\ldots\ldots (35)$$

where

G_r = free energy of free water in a chosen reference state, and
p_r = vapor pressure of free water in the chosen reference state.

Hence,

$$G_s - G = \Delta G = RT \ln p_s/p \quad \ldots\ldots\ldots\ldots\ldots\ldots (36)$$

and, by eq. (33)

$$\int_{P_s}^{P} \overline{V}\, dP = -RT \ln p/p_s \quad \ldots\ldots\ldots\ldots\ldots\ldots (37)$$

An exact solution of eq. (37) for swelling pressure would require knowledge of the relationship between the specific volume of the adsorbed water and change in external pressure. This relationship is unknown; in a real paste containing capillary water as well as gel water it must be rather complicated. Although the water is densified by adsorption forces in a

partially dried sample containing capillary water, it is also subjected to capillary forces that tend to extend it. Without knowledge of the relationship, it is necessary to assume $\overline{V}$ to be independent of pressure and hence a constant. On this assumption, integrating eq. 37 gives

$$P - P_s = \Delta P = -\frac{RT}{\overline{V}} ln\ p/p_s \quad \ldots\ldots\ldots\ldots (38)$$

In terms of ordinary logarithms and specific volume, $\overline{V}$ becomes Mv_f and the swelling pressure becomes

$$\Delta P = -\frac{RT}{Mv_f} 2.303\ log_{10} p/p_s \quad \ldots\ldots\ldots\ldots\ldots\ldots\ldots\ldots (39)$$

Solutions of eq. 39 are given in Table 4-6. The value of specific volume of adsorbed water used in these computations is 0.87, the mean specific volume of the gel water. (See Part 5). This value is no doubt too low for swelling at high vapor pressures and too high at low pressures, but it should be preferable to the specific volume of free water, ordinarily used for this computation.

TABLE 4-6—COMPUTED POTENTIAL SWELLING PRESSURE

$\Delta P = -\frac{RT}{Mv_f} 2.303\ log_{10} p/p_s$; $T = 298K$; $M = 18.02$; $v_f = 0.87$; $R = 82.07$ cc, atm per deg per mole; $\Delta P = -3593\ log_{10} p/p_s$ atmospheres or $\Delta P = -52{,}810\ log_{10} p/p_s$ psi

p/p_s	Swelling pressure, ΔP	
	atmospheres	psi
1.00	0	0
0.95	80	1178
0.90	165	2419
0.80	348	5118
0.70	557	8181
0.60	797	11710
0.50	1081	15900
0.40	1430	21010
0.30	1879	27620

Computed values such as those given in Table 4-6 have never been satisfactorily tested experimentally, owing to experimental difficulties. For an idealized gel, there is little reason to question the results, except for the error introduced by assuming the specific volume of the adsorbed water to remain constant. At least, they are in line with general observations as to the enormous forces that swelling bodies are able to develop when the tendency to swell is restrained.

It should be understood that the pressures indicated cannot exist unless the movement of swelling is *prevented*; the so-called swelling pressure is really the *potential* pressure. Also, the potential pressures

given correspond only to a condition wherein a specimen at initial vapor pressure p is exposed to liquid water or to vapor of pressure p_s. If the specimen is exposed to vapor having a pressure p' such that p' is greater than p but smaller than p_s, the potential swelling pressure may be computed from the pressure ratio p/p'.

Relation of idealized behavior to that of cement paste or concrete

A hardened cement paste or concrete differs from the idealized gel discussed above. The gel in the paste is not composed of discrete particles but is apparently a coherent, porous mass held together by solid-to-solid bonds. Moreover, it contains microcrystals and aggregate particles that resist the shrinkage of the gel. Consequently, swelling (or shrinkage) in concrete is partially opposed by the elastic forces developed throughout the mass according to the relationship

$$\Delta P_e = \alpha \, \Delta V \ , \quad \ldots\ldots\ldots\ldots\ldots\ldots\ldots\ldots (40)$$

where

α = the coefficient of compressibility,
ΔP_e = change in elastic force, and
ΔV = change in over-all volume of concrete.

Thus, a change in volume induced by the swelling or shrinking of the gel may be partially opposed by a force that is, presumably, proportional to the change in volume.

However, swelling pressure, as defined above, should be very nearly the same for concrete as for the idealized gel, for if the swelling is *prevented*, ΔV of eq. (40) is zero and the increase in external pressure required to prevent swelling is only that required by eq. (39). However, the required increase in external pressure per unit *gross* area of concrete may be less than ΔP of eq. (39) if the adsorbed water is effective over less than 100 percent of the cross-sectional area of the concrete. In other words, the maximum externally manifested swelling pressure could be less than the theoretical, but not greater.

MECHANISM OF SHRINKING AND SWELLING

Volume change as a liquid-adsorption phenomenon

When volume change is regarded as a swelling phenomenon, as was done in deriving eq. (39), the force is considered to arise from attraction between the liquid and the solid surface. In regions where the solid surfaces are separated slightly, the solid-to-solid attraction tends to draw the solid surfaces together, and at the same time the solid-to-liquid attraction tends to draw the water in between the surfaces. If the water is exposed, its tendency to evaporate or its surface tension, or both, give rise to an opposing force that tends to draw the water out of the adsorbed layer. Thus, the adsorbed water in the gel is the

subject of competing forces, and when these opposing forces are in equilibrium the rate of volume change is zero.

From this conception of the mechanism of shrinking and swelling it would appear that the over-all volume change of the paste should be proportional to the change in spacing of the solid bodies that are held apart by adsorbed water. This spacing should decrease as adsorbed water is withdrawn and increase as adsorbed water is added. Since the first layer is much more strongly held than the higher layers, the volume change should be of the order of magnitude that could be accounted for by changing the spacing of the particles by only 2 molecular diameters, about 5 or 6 Ångstrom units, per particle.

To see whether this is within the bounds of possibility, we may consider the data on the particle-size of the solid phase. Imagine the solid matter to be made up of equal spheres having a specific surface equal to that of the hardened paste. The spheres are in some characteristic array that encloses voids equal to the observed pore-volume in the paste. The addition of an adsorbed layer of water will be regarded as equivalent to increasing the sphere radii and hence their center-to-center spacing. The corresponding change in over-all volume is related to the change in radius by the well known relationship for small changes,

$$\frac{\Delta V}{V} = \frac{3\Delta r}{r} \quad , \qquad (41)$$

where

V = over-all volume,
ΔV = change in over-all volume,
r = sphere-radius, and
Δr = change in sphere radius.

When hardened paste is dried to equilibrium with a very low vapor pressure, virtually all the adsorbed water is removed. Hence, the possible change in volume may be computed from the thickness of the adsorbed layer and the particle-size of the solid phase. The thickness of the adsorbed layer may be conservatively estimated at one water-molecule diameter, or about 2.7Å. The equivalent sphere radius of the paste particles is estimated at 70Å (see Part 3). Hence,

$$\frac{\Delta V}{V} = \frac{3 \times 2.7}{70} = 0.16 \quad .$$

That is, a change in particle spacing corresponding to the addition or loss of one molecular layer per particle would, under the assumptions given, result in an over-all volume change of 16 percent.

Shrinkage measurements on thin, neat-cement slabs, $w_o/c = 0.5$ by weight, showed a linear shortening of 0.7 percent when all the evaporable water was removed. This corresponds to a volume-shrinkage of

about 2 percent, or about one-eighth the amount theoretically possible.

Thus, it appears that the loss or gain of the first adsorbed layer could more than account for the observed amount of volume change. The smallness of the observed volume change, relative to the calculated, could be explained as being due to the restraining effect of non-shrinking bodies embedded in the gel, and elastic forces developed at points where the gel particles are joined by solid-to-solid bonds.

However, the figures should not be taken too literally. If the particles composing the mass are not of equal size and shape, the above computation does not apply exactly. However, unless the simplifying assumption leads to as much as an eight-fold error, which seems unlikely, the conclusion that swelling could be due to changes in adsorbed water content is well within the limit of possibility.

* * * *

It should be observed particularly that by the theory outlined above the change in volume is not considered to be the result of forces acting on the solid phase. Instead, the change is assumed to be the result of an unbalance of the forces acting on the adsorbed water, and the consequent changes toward establishing an equilibrium between those forces.

Volume change as a capillary phenomenon

The shrinkage and swelling of rigid porous bodies that undergo volume changes much smaller than the corresponding changes in water content are regarded by some as capillary phenomena. Plummer and Dore,[17] for example, describe shrinkage of some soils as the result of tension in the capillary water. The reaction of this tension produces compressive stress in the solid phase and thus causes a reduction in volume or length. The force of capillary tension is given by the following equation[18].

$$F = \sigma\left(\frac{1}{r_1} + \frac{1}{r_2}\right), \quad \ldots\ldots\ldots\ldots\ldots\ldots \quad (42)$$

where F = force of capillary tension,
σ = surface tension of water, and
r_1 and r_2 = principal radii of curvature of the menisci.

The curvature of the water surface is determined by the size and shape of the pores in the solid. Apparently the pores are such that as the water content of the body diminishes, the curvature (concavity) of the water surface increases (the radius decreases) and thus the shrinkage force increases.

Swelling on increase in water content can be accounted for by this theory only by assuming that shrinkage produces elastic strains and thus, when the shrinkage force is released, elastic recovery causes expansion.

When concrete undergoes shrinkage for the first time, it is unable to regain its original dimensions when it becomes resaturated. This can be accounted for in terms of the capillary theory by assuming that the stresses of shrinkage cause plastic flow in the solid phase. Hence, the permanent shrinkage, that is, the irreversible part of the initial shrinkage, can be regarded as permanent set.

According to the capillary-tension theory, any porous body containing small liquid-filled capillaries should contract as the water is removed until the evaporable water content and vapor pressure pass the limit below which a meniscus cannot exist. When this limit is passed, the body should expand. In concrete, this limit might be found at the water content corresponding to $p = 0.45\ p_s$; it certainly would be found at some pressure greater than $p = 0.00$. However, concrete and, as Plummer and Dore[17] point out, fine-grained soils shrink and swell with changes in moisture content even when the moisture content is too low for the existence of a meniscus. In concrete at least, shrinkage is at a maximum when the evaporable water content is zero.* It is thus apparent that the capillary theory alone will not suffice.

The relationship between tension in the capillary water and volume change of cement paste can be clarified with the aid of Fig. 4-11. Here, as in Part 3, the paste is represented by a model composed of spheres. Each sphere represents gel substance together with its associated voids (gel water) and non-gel solids. The interstices between the spheres represent capillary spaces outside the gel.†

Each sphere of Fig. 4-11 is supposed to contain gel water and be in a state of swelling determined by its water content. The water content

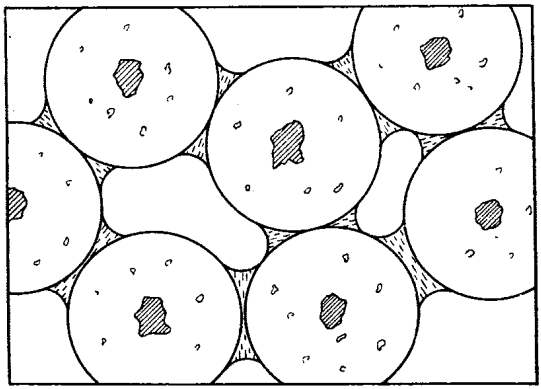

Fig. 4-11.

*Shrinkage probably increases further with loss of some of the non-evaporable water on heating in dry air. No data are available, however.

†It must be emphasized that the authors do not know the shapes of the solid bodies composing hardened paste (except for small amounts of microscopic material) or how they are linked together. The model is offered only because the conditions pictured thereby are such as to give the same adsorption characteristics as hardened cement paste.

in turn is determined by the existing vapor pressure. The capillary water is represented as lenses around points of contact or near-contact between the spheres. The volume of water in each lens is determined by the curvature and position of the spheres and the curvature of the water-surfaces. The latter is determined by the existing vapor pressure according to the relationship

$$\frac{1}{r_1} + \frac{1}{r_2} = - \frac{RT}{Mv_f\sigma} \ln p/p_s \,, \quad \ldots\ldots\ldots\ldots\ldots\ldots\ldots\ldots (43)$$

where

r_1 and r_2 = principal radii of water-surface curvature,

σ = surface tension of the water,

and the other symbols have the same significance as before. Eq. (43) is the Kelvin equation discussed in Part 3.

For finite values of $\frac{1}{r_1} + \frac{1}{r_2}$ the capillary water is in tension, the tensile force F being

$$F = \sigma \left(\frac{1}{r_1} + \frac{1}{r_2} \right) = - \frac{RT}{Mv_f} \ln p/p_s \,. \quad \ldots\ldots\ldots\ldots\ldots\ldots (44)$$

Comparison of this with the swelling-pressure equation (eq. 39) shows, as must needs be, that for equilibrium with a given vapor pressure p, capillary tension equals potential swelling pressure. That is, potential swelling force is the result of the tendency of water to enter the gel and capillary tension opposes that tendency; at equilibrium the two forces balance.*

Fig. 4-11 is drawn so as to depict a condition in which the gel is only partly covered with capillary-condensed water. In those areas not covered, the tendency of the water molecules to enter the gel is opposed by their tendency to evaporate. This has the same effect as tension arising from a meniscus.

It has been remarked before that the classification of gel water and capillary water adopted in this discussion is somewhat arbitrary. Some of the gel water may occupy space beyond the force-field of the solid material and may therefore be properly classed as capillary water. Nevertheless, even if a less arbitrary definition of capillary water were adopted, the concepts developed above would seem to apply: The spheres in Fig. 4-11 would represent the gel-substance together with whatever part of the total water-fillable space is predominantly in-

*Strictly speaking, the *free energies* of the adsorbed water and capillary water are equal at equilibrium, rather than the intensity of forces. That is, at equilibrium.

$\Delta P v_f = F v_f$. (Eq. (39) and (44))

Since v_f for the adsorbed water is not the same as that for capillary water, ΔP and F cannot be exactly equal. The discussion in the text, though perhaps not rigorously correct, leads to easily visualized concepts that should not be misleading.

fluenced by van der Waal forces. The interstices would represent the rest of the water-fillable space in the paste.

Relationship between change in volume and change in water content

According to the concepts set forth above, swelling and shrinking should depend on the amount of adsorbed water in the gel. That is, presumably,

$$\Delta V = k \frac{\Delta w_a}{V_m} , \quad \ldots\ldots\ldots\ldots\ldots\ldots\ldots\ldots (45)$$

where k is a proportionality constant connecting change in over-all volume, ΔV, with change in the amount of adsorbed water, Δw_a, per unit surface of the gel, as represented by V_m. In the range of vapor pressures where capillary condensation takes place ($p > 0.45\ p_s$), any change in adsorbed-water content would be accompanied by a change in capillary water content, Δw_c, so that Δw_t, the change in *total* water content = $\Delta w_a + \Delta w_c$. Hence,

$$\Delta V = \frac{k}{V_m} (\Delta w_t - \Delta w_c) \quad \ldots\ldots\ldots\ldots\ldots\ldots\ldots\ldots (46)$$

It follows from this that the change in over-all volume will be related to the total change in water content differently in different samples according to the ratios of adsorbed water to capillary water in the respective samples. We should expect, therefore, that the greater the ratio $\Delta w_c/\Delta w_a$, the smaller the average $\Delta V/\Delta w_t$ for a specimen containing a given amount of gel.

A wholly satisfactory experimental check of this deduction cannot be offered at this time because available volume-change data pertain to shrinkage accompanying *desorption* whereas data leading to the evaluation of V_m and w_a are derived from adsorption measurements. However, shrinkage data bear out eq. (46) in a general way. The best available example of this is given in Fig. 4-12, representing a part of a study of shrinkage by Pickett.[19] It was found that the course of shrinkage during the drying of a concrete prism could be represented by an equation analogous to the heat-flow equation. If shrinkage were directly proportional to the concomitant water-loss, the same equation should apply also to water-loss. Pickett found, however, that the water-loss-vs.-time curve could not be represented by a single equation of the heat-flow type. But, by assuming that two classes of water are lost simultaneously during drying, the loss of water in each class following its own law, he could represent the experimental results with two equations of the heat-flow type. This is shown in Fig. 4-12. Pickett called the water that seemed to be unrelated to shrinkage W_a and the rest W_b. The relative proportions W_a and W_b assumed for the computations were arrived at by trial. In the figure the "a" water is represented

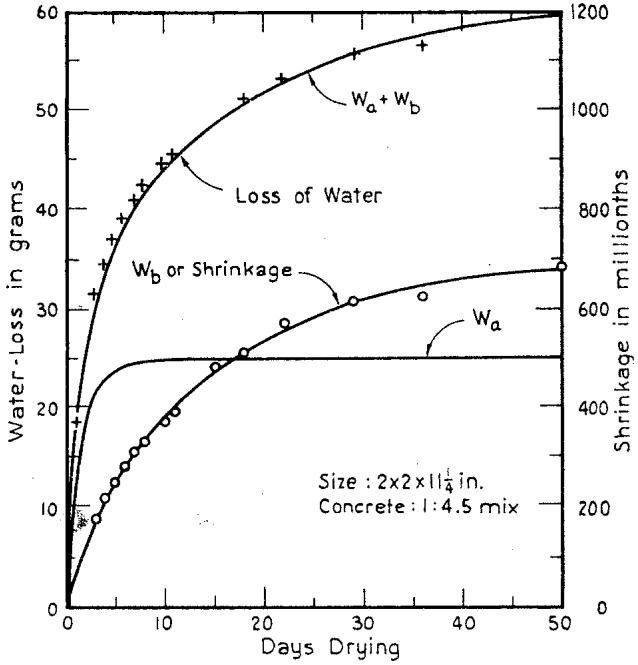

Fig. 4-12—Time relationships for shrinkage and water-loss for a concrete specimen stored in air at 50 per cent relative humidity.

by the computed curve marked W_a. The "b" water is represented by the computed curve marked W_b, which also represents shrinkage when appropriate ordinate scales are used. The sum of the ordinates of these two curves gives the curve marked $W_a + W_b$. The crosses represent the observed total water-losses and the circles the observed shrinkage.

Thus Pickett's experimental data support the deduction expressed in eq. (45) and (46) that volume change is directly proportional to a *part* of the total water-loss. It remains for future experiments to prove or disprove the deduction that the part responsible for volume change is the adsorbed water. It is of interest in this connection that in Fig. 4-12 the "b" water constitutes 60 percent of the total lost at 50 percent relative humidity. The highness of this proportion suggests that shrinkage is proportional to the loss of gel water rather than to the loss from the first adsorbed layer only. This indicates that w_a of eq. (45) includes about the first four layers of adsorbed water.

CAPILLARY FLOW AND MOISTURE DIFFUSION

In connection with this discussion of the thermodynamics of adsorption, about all that need be said about capillary flow and moisture diffusion is that these phenomena take place as a result of inequalities in free energy. Under isothermal conditions, capillary water will move

if the effective radius of curvature (see eq. (42)) is not the same on all exposed surfaces of a continuous body of capillary water. In Fig. 4-11 it is apparent that the addition of water, by condensation or otherwise, to the outer concave water-surfaces, would decrease the curvature of those surfaces. Water would therefore flow inward until the inner water-surfaces would have acquired the same curvature as the outer.

Where capillary water is absent, adsorbed water will move along any continuous surface if a gradient in the free energy of the adsorbed water exists. If an inequality in free energy exists between water on disconnected areas, the transfer of water will occur by distillation through the vapor phase. If surface migration and distillation are both physically possible, both will occur simultaneously. However, in an extremely fine-pored substance such as the gel in hardened paste, most of the transfer is believed to be effected through surface migration.

Inequalities in free energy

Inequalities in free energy under isothermal conditions arise from inequalities in moisture content, as shown indirectly by the water-content-vs.-vapor-pressure isotherms shown in Part 2. Hardened cement paste is of such nature that a change in moisture content of a given region in the paste, however slight the change may be, changes the free energy of the water in that region.*

Inequalities in free energy under isothermal conditions may also arise from deformations of the solid phase. In Fig. 4-11 we can see that if the spacing of any pair of spheres were changed, the surface curvature of the water lens would likewise change. This would require a redistribution of moisture to restore equality in free energy of the capillary water throughout the system. Also, a change in external pressure acting on the adsorbed water would change the free energy of the adsorbed water, as indicated by eq. (32) and (33).

Thus inequalities in stress and strain produce inequalities in the free energies of both the adsorbed water and capillary water and thereby induce redistributions of moisture within the mass. This, as has been pointed out by Lynam,[20] Carlson,[22] and others, is an important factor in the gradual yielding of concrete under sustained stress known as creep or plastic flow. The changes in moisture distribution cause localized shrinkings and swellings with consequent changes in the deformation of the body as a whole.

EFFECT OF TEMPERATURE CHANGES

The experimental part of these studies has not included measurements of the effect of temperature changes. However, some of these

*If, however, the external pressure on the adsorbed water changes at the same time, the relationship between water content and vapor pressure will not be the same as when external pressure remains constant. See later discussion.

effects can be deduced qualitatively with the aid of the theories and principles introduced above.

Effect on swelling

It was shown in eq. (44) that at equilibrium the capillary tension equals the potential swelling pressure. That is,

$$\Delta P = F = \sigma \left[\frac{1}{r_1} + \frac{1}{r_2} \right] = - \frac{RT}{Mv_f} \ln p/p_s \quad \ldots\ldots\ldots\ldots\ldots\ldots (47)$$

Since an increase in temperature causes an expansion of the adsorbed water, the surface curvature of the water in the lenses must decrease. Moreover, the surface tension of water decreases with increase in temperature. Hence, the capillary tension must decrease with increase in temperature, provided the water content remains constant. This in turn would mean that an increase in temperature would cause expansion owing to swelling, in addition to the thermal expansion. However, if the specimen is initially saturated, no change in swelling pressure can occur because for this condition capillary tension is zero, or insignificantly small. Obviously, if the specimen contains no evaporable water, no swelling due to moisture can occur when the temperature is increased.

Evidence of this may be found in data published by Meyers.[21] The coefficients of thermal expansion of neat cement and concrete prisms were measured at various degrees of saturation, with results as shown in Table 4-7.

TABLE 4-7—MEYERS' DATA ON THERMAL EXPANSION FOR SATURATED AND PARTLY SATURATED SPECIMENS

(Temperature range 70 to 120 F)

Type of material	Thermal coefficient in millionths for condition indicated	
	Sealed storage for 9 mo.	After soaking for 1 week
Normal portland cement	10.3	5.7
Concrete (flint aggregate)	8.1	4.9
Cement-sand mortar 1:1	9.2	6.3
High-C_3S cement	11.4	5.6

Note that the sealed specimens* show much greater expansion than the same specimens after soaking. According to the foregoing discussion, the figures in the last column represent the true thermal coefficient of the solid phase, whereas those in the first column represent the combined effect of thermal expansion and swelling caused by the decrease in swelling pressure.

*The specimens were stored in copper-foil jackets with soldered seams. Even though sealed they could not remain fully saturated.

It was stated above that if all the evaporable water is removed, a rise in temperature would not cause swelling. This too is confirmed by Meyers' data, as shown in Table 4-8. These data show that driving out all the evaporable water (or most of it) reduced the thermal coefficient of a specimen below that of the same specimen in the partially saturated state. Comparison of Tables 4-7 and 4-8 indicates that the thermal coefficient for the "bone-dry" and saturated states are about equal.

TABLE 4-8—MEYERS' DATA ON THERMAL EXPANSION—EFFECT OF EXTREME DESICCATION

(Temperature range 70 to 120 F)

Type of material	Thermal coefficient in millionths for condition indicated	
	Before drying	Dried 1 week at 100 C
High early strength cement	9.1	6.0
White cement	10.4	6.5
Normal portland cement	8.0	6.0
Concrete (limestone aggregate)	4.1	2.1

Meyers found that the introduction of a liquid that does not cause swelling, kerosene, did not change the thermal coefficient appreciably.*

Effect on diffusion

If temperature gradients are established in a concrete mass, water must move in the direction of descending temperatures. This follows from rather simple considerations. An increase in temperature in any region of the mass must be accompanied by an increase in the water vapor pressure in that region in accordance with the Clausius-Clapeyron equation. Water then moves toward the regions of lower temperature where the vapor pressure is lower.

The movement of water thus induced is accompanied by shrinkage in the regions where the temperature is increased which tends to offset the expansion due to swelling and thermal expansion. Conversely, in the regions where the temperature is lowered, swelling tends to offset the shrinkage and thermal contraction. However, these effects cannot be evaluated quantitatively at present.

Combined effect of stress, strain, and temperature gradients

It can readily be seen that deformations of the solid phase and temperature changes together or separately cause moisture movements in

*It should be observed that a single thermal coefficient cannot correctly be assigned to a given specimen of concrete. The "coefficient" is a variable that changes with evaporable water content. The function must be such that the coefficient is a minimum for the bone-dry and saturated states and a maximum for some intermediate evaporable water content. Meyers' data indicate that the variation with change in evaporable water content is far from insignificant.

concrete. The separate effects may combine in different ways so that they may offset or augment each other at a given point in the mass. During a period of heating, cooling, or changing external force, the separate effects may combine in different ways at different times at the same point. The over-all result is that in concrete subjected to changing external forces or temperature or both, the evaporable water must be in a continual state of flux. If the ambient humidity also fluctuates, the internal moisture movements are still further complicated. Possibly these effects have an influence on the ability of concrete to withstand weathering.

SUMMARY OF PART 4

(1) This part deals with energy changes of adsorption and with their relationship to shrinking and swelling, capillary flow, and moisture diffusion.

(2) The net heat of adsorption is the heat in excess of the normal heat of condensation that is released when water vapor is adsorbed. The total net heat of adsorption of hardened paste is approximately equal to the heat of immersion of the adsorbent.

(3) The net heat of *surface* adsorption is that part of net heat of adsorption that has its origin in interaction of the adsorbed molecules and the solid surface. It is related to the heat of spreading-wetting and in cement paste is equal to about $472V_m$.*

(4) The net heat of capillary condensation is the total heat of water-surface formation. It is about equal to the difference between the heat of immersion and the heat of spreading-wetting. In cement paste it is equal to about $100V_m$ cal per g.

(5) The net heats of adsorption at 11 different initial water contents were measured, using two different samples of hardened paste.

(6) The total net heat of adsorption was found to be about $572V_m$ cal per g or about 670 ergs per sq cm of solid surface. This is about the same as the heat of immersion of various mineral oxides in water.

(7) Among portland cements of all types the total heat of hydration ranges from about 485 to 550 cal per g of non-evaporable water. Data from two cements indicate that of this amount about three-fourths is due to the heat of reaction of the non-evaporable water and the rest is due to the net heat of adsorption of the evaporable water.

(8) The total internal energy change of adsorption is equal to the change in enthalpy minus a small "$P\Delta v$" work term representing the contraction in volume under constant external pressure that accompanies adsorption. The enthalpy change is thus essentially equal to the net heat

*V_m = weight of adsorbed water required to cover the surface of the solid phase with a monomolecular layer.

of adsorption and is the sum of the free energy and unavailable energy changes, i.e.,

$$Q_a = \Delta H = \Delta G + T\Delta S,$$

where

$-Q_a$ = net heat of adsorption,
ΔH = change in enthalpy,
ΔG = change in free energy,
ΔS = change in entropy,
T = absolute temperature,
$T\Delta S$ = change in unavailable energy.

(9) The free energy change of water that occurs when the water becomes adsorbed can be expressed in terms of vapor pressure change alone. When the initial and final vapor pressures are p_s and p, respectively,

$$-\Delta G = -75.6\ log_{10} p/p_s.$$

where

p = existing vapor pressure
p_s = saturation vapor pressure

(10) Unavailable energy is equal to the difference between the net heat of adsorption and the corresponding free-energy term, i.e.,

$$T\Delta S = Q_a - \Delta G.$$

(11) Entropy change, ΔS, is an indication of the extent to which adsorption modifies the adsorbed water. The data show that for water isothermally adsorbed at low vapor pressure the entropy change of adsorption is of the same magnitude as that accompanying solidification, or the combining of water in a salt as water of crystallization.

(12) The differential net heat of adsorption is the differential of the Q_a-vs.-w relationship. It is at a maximum for the first increment adsorbed, and becomes zero with the last increment at $p = p_s$.

(13) The maximum differential net heat of adsorption is about 400 cal per g of water. This is also the *minimum* heat of reaction of the non-evaporable water. Expressed on the same basis, the heat of combination of water in $Ca(OH)_2$ is 847 cal per g of water. This shows that the maximum energy of binding for evaporable water and the minimum for non-evaporable water is much less than that of the bond of water (i.e., hydroxyl groups) to calcium.

(14) The *average* net heat of adsorption of the *gel water* appears to be about 143 cal per g of gel water. The average for the first layer of adsorbed water appears to be about 270 to 300 cal per g. These figures are probably too low owing to the effect of adsorbed air.

(15) The logarithm of the constant C of the B.E.T. equation is theoretically proportional to the net heat of adsorption. Recent work has shown that assumptions concerning the proportionality constant made by

B.E.T. are invalid and that values of net heat of adsorption based on this assumption are too low.

(16) Cement gel belongs to the *limited swelling* class of gels.

(17) Swelling pressure is the increase in external pressure required to prevent swelling. It can be estimated from the following relationship:

$$\Delta P = -\frac{RT}{Mv_f} 2.303 \log_{10} p/p_s ,$$

where

ΔP = swelling pressure, excess over normal external pressure,
R = the universal gas constant,
M = molecular weight of adsorbate,
v_f = specific volume of adsorbate.

This gives the pressure required to prevent the isothermal swelling of a gel dried to vapor pressure p when it has access to free water.

(18) The externally manifested swelling pressure of concrete would probably be less than that calculated from the above equation.

(19) The order of magnitude of the total volume change of hardened cement paste can be accounted for on the assumption that the change is due to the removal or addition of the first layer of adsorbed water molecules.

(20) Total volume change cannot be regarded solely as a capillary phenomenon, since expansion does not occur when the evaporable water, and hence meniscuses, disappear. When capillary water is present, capillary tension is equal to swelling pressure when the system is at equilibrium.

(21) Experimental data show that volume change is directly proportional to a *part* of the total change in water content. This agrees with 19, which implies that volume change is independent of the change in capillary-water content. The data suggest that volume change may be proportional to the change in gel-water content, rather than to the change in the first layer only.

(22) Capillary flow or moisture diffusion or both occur under isothermal conditions when there are inequalities in the free energy of the evaporable water in different regions in the specimen. Inequalities in free energy under isothermal conditions arise from inequalities in moisture content, from deformations of the solid phase, and from inequalities in external pressure on the adsorbed water. Resulting moisture movement is an important factor in plastic flow.

(23) An increase in temperature causes a decrease in swelling pressure of partially saturated pastes and thus causes an effect on volume change in addition to the usual thermal expansion. Evidence of this is found in data obtained by Meyers.

(24) Changes in external forces and changes in ambient temperature and humidity keep the evaporable water of a partially saturated specimen in a continual state of flux. This possibly influences durability.

REFERENCES

(1) Wm. D. Harkins and Geo. Jura, *J. Am. Chem. Soc.* v. 66, p. 1362 (1944).
(2) Wm. D. Harkins and Geo. E. Boyd, *J. Am. Chem. Soc.* v. 64, p. 1197 (1942), Table I.
(3) Samuel Glasstone, *Physical Chemistry* (D. Van Nostrand, 1940), p. 175.
(4) A. B. Lamb and A. S. Coolidge, *J. Am. Chem. Soc.* v. 42, p. 1146 (1920).
(5) Luke E. Steiner, *Introduction to Chemical Thermodynamics* (McGraw-Hill, 1941), p. 46.
(6) J. R. Katz, Ergibnisse der Exacten Naturwiss v. 3, p. 316 (1924); v. 4, p. 154 (1925); *Trans. Faraday Soc.* v. 29, p. 279 (1933).
(7) J. D. Babbitt, *Can. J. Res.* v. 20, Sec. A, p. 143 (1942).
(8) E. E. Dorsey, *Properties of Ordinary Water Substance* (Reinhold, 1940), Table 123, p. 267.
(9) Ref. 8, Table 201, p. 467.
(10) R. R. Wenner, *Thermochemical Calculations* (McGraw-Hill, 1941), pp. 177 and 216.
(10a) Ref. 10, p. 178.
(11) R. L. Steinberger, *Textile Research* v. 4, p. 451 (1934).
(12) Ref. 10, p. 44.
(13) Wm. D. Harkins and Geo. Jura, *J. Am. Chem. Soc.* v. 66, p. 919 (1944).
(14) Ref. 2, Table VI.
(15) H. Freundlich, *Colloid and Capillary Chemistry* (E. P. Dutton, 1922), p. 673.
(16) Ref. 3, p. 659.
(17) F. L. Plummer and S. M. Dore, *Soil Mechanics and Foundations* (Pitman, 1940), p. 60.
(18) N. K. Adam, *The Physics and Chemistry of Surfaces* (Oxford University Press, 1930), pp. 8, 9.
(19) Research Reports of the Portland Cement Association Research Laboratory, Appendix 3, July 1942, unpublished.
(20) C. G. Lynam, *Growth and Movement in Portland Cement Concrete* (Oxford University Press, 1934).
(21) S. L. Meyers, *Ind. Eng. Chem.* v. 32, p. 1107 (1940).
(22) R. W. Carlson, *Proc A. S. T. M.*, v. 35, Part II, p. 370 (1935).
(23) A. B. D. Cassie, *Trans. Faraday Soc.* v. 41, p. 450 (1945).

Appendix to Parts 3 and 4

This appendix gives tables of non-evaporable water, w_n, water required for the first monomolecular layer of adsorbed water, V_m, the ratio V_m/w_n, the B.E.T. constant C, and the computed surface of the dry paste for all the series used in this discussion.

In estimating V_m for some of the groups of data from plots of $\frac{1}{w}\frac{x}{1-x}$ versus w,* the same value of C could be used for all items in the group. In other groups the data could be represented best by using different values of C for different items. In some instances the points were too few and too scattered to establish the slope of the line. When this was true, a value of C was estimated and the line was drawn in such a way as to conform to the experimental points and the assumed value of C as closely as possible.

The samples of Series 254-265 were dried over concentrated H_2SO_4 instead of $Mg(ClO_4)_2.2H_2O$. This accounts for the relatively low ratio of V_m/w_n and low values of C for this group.

*See Part 3.

TABLE 1—V_m, C, COMPUTED SPECIFIC SURFACE AND OTHER DATA FOR SERIES 254-265*

Cement 14502

Ref. No.	Age at test, days†	w_n, g per g of:		V_m, g per g of:		$\frac{V_m}{w_n}$	C	Sp. surface of dry paste, cm²/g millions
		Original cement	Dry paste	Original cement	Dry paste			
323	110	.160	.137	.024	.0210	.152	8.6	0.75
506	110	.179	.158	.030	.0266	.168	11.7	0.95
509	110	.183	.167	.031	.0287	.172	8.5	1.19
512	110	.200	.182	.030	.0272	.150	7.8	0.97
515	110	.232	.208	.037	.0336	.160	5.2	1.20
518	110	.226	.197	.036	.0311	.158	5.7	1.11
521	110	.219	.189	.037	.0324	.170	3.7	1.16

*Samples of this group were dried over concentrated H_2SO_4 instead of over $Mg(ClO_4)_2.2H_2O$ as in the other tests. †Approximate.

TABLE 2—V_m, C, COMPUTED SPECIFIC SURFACE AND OTHER DATA FOR SERIES 254-MRB

Cement No.	Net w/c	Age at test, days	w_n, g/g of:		V_m, g/g of:		$\frac{V_m}{w_n}$	C	Sp. surf. of dry paste, cm²/g millions
			Original cement	Dry paste	Original cement	Dry paste			
14898-1AQ	.382	120	.2171	.1784	.057	.047	.269	18	1.68
14899-1PC	.388	120	.2225	.1820	.056	.046	.253	18	1.64
14900-1SC	.446	126	.2274	.1853	.058	.047	.254	18	1.68
14901-2AQ	.391	126	.2228	.1822	.054	.044	.242	18	1.57
14902-2PC	.393	133	.2273	.1852	.056	.046	.238	18	1.57
14903-2SC	.424	133	.2271	.1851	.056	.046	.248	18	1.64
14904-3AQ	.425	162	.2284	.1859	.061	.050	.268	18	1.79
14905-3PC	.411	162	.2261	.1869	.063	.052	.278	18	1.86
14906-3SC	.476	173	.2344	.1906	.063	.051	.268	18	1.82
14907-4AQ	.406	173	.2185	.1797	.060	.049	.273	18	1.75
14908-4PC	.394	200	.2249	.1836	.060	.049	.267	18	1.75
14909-4SC	.483	200	.2255	.1840	.059	.048	.261	18	1.71
14910-5AQ	.460	204	.2282	.1858	.059	.048	.258	18	1.75
14911-5PC	.464	204	.2294	.1866	.060	.049	.262	18	1.71
14912-5SC	.489	212	.2252	.1838	.062	.051	.276	18	1.82
14913-6AQ	.410	212	.2206	.1807	.062	.051	.282	18	1.82
14914-6PC	.423	222	.2253	.1839	.060	.049	.266	18	1.75
14915-6SC	.437	222	.2240	.1830	.060	.049	.268	18	1.75

TABLE 3—V_m, C, COMPUTED SPECIFIC SURFACE AND OTHER DATA FOR SERIES 254-K4B

Cement No.	Net w/c	Age at test, days	w_n, g/g of:		V_m, g/g of:		$\frac{V_m}{w_n}$	C	Sp. surf. of dry paste, cm²/g millions
			Original cement	Dry paste	Original cement	Dry paste			
13721-1S	.470	174	.2231	.1824	.0634	.0518	.284	18	1.85
13722-1P	.473	180	.2332	.1891	.0618	.0501	.265	18	1.79
13723-1Q	.425	180	.2290	.1863	.0597	.0486	.261	18	1.74
13730-4S	.463	144	.1786	.1515	.0486	.0412	.272	18	1.47
13731-4P	.460	138	.1772	.1505	.0426	.0362	.240	18	1.29
13732-4Q	.450	138	.1773	.1506	.0447	.0380	.252	18	1.36
13733-5S	.427	150	.1650	.1416					
13734-5P	.453	146	.1589	.1371					
13735-5Q	.456	150	.1650	.1416					
13736-6S	.471	196	.2148	.1768	.0591	.0486	.275	18	1.74
13737-6P	—	191	.2297	.1868	.0637	.0518	.277	18	1.85
13738-6Q	.447	191	.2220	.1817	.0559	.0457	.252	18	1.63
13740-7P	.473	164	.2395	.1932	.0682	.0550	.285	18	1.96
13741-7Q	.480	171	.2390	.1929	.0617	.0498	.258	18	1.78
13752-11P	.445	164	.1864	.1571	.0537	.0453	.288	18	1.62
13753-11Q	.440	172	.1896	.1594	.0530	.0446	.280	18	1.59
13763-15S	.485	202	.2173	.1785	.0597	.0490	.275	18	1.75
13764-15P	—	196	.2109	.1742	.0545	.0450	.258	18	1.61
13765-15Q	.445	202	.2201	.1804	.0553	.0453	.251	18	1.62
13766-16S	—	322	.2096	.1733	.0594	.0491	.283	18	1.75
13767-16P	.464	223	.2256	.1841	.0640	.0522	.284	18	1.86
13768-16Q	.456	223	.2250	.1837	.0623	.0509	.277	18	1.82
13778-20S	.472	170	.2308	.1875	.0611	.0496	.265	18	1.77
13779-20P	.462	167	.2329	.1889	.0565	.0458	.242	18	1.64
13780-20Q	.436	176	.2262	.1845	.0569	.0464	.252	18	1.66

TABLE 4—V_m, C, COMPUTED SPECIFIC SURFACE AND OTHER DATA FOR SERIES 254-8

Ref. No.	Age at test, days	Net w/c	w_n, g/g of:		V_m, g/g of:		$\frac{V_m}{w_n}$	C	Sp. surf. of dry paste, cm²/g millions
			Original cement	Dry paste	Original cement	Dry paste			
Cement 14930J									
254-8-1	447	.312	.1808	.1530	.053	.045	.294	21.0	1.61
254-8-2	362	.443	.2006	.1671	.062	.052	.310	21.0	1.83
254-8-3	362	.592	.2101	.1736	.066	.054	.313	21.0	1.94
Cement 15007J									
254-8-28	479	.351	.1980	.1652	.063	.052	.316	18.0*	1.86*
254-8-29	440	.464	.2169	.1782	.058	.048	.268	17.0	1.70
254-8-30	479	.595	.2323	.1885	.060	.049	.256	20.6	1.73
Cement 15011J									
254-8-40	478	.319	.1843	.1556	.051	.043	.276	18.0	1.54
254-8-41	368	.442	.2102	.1737	.058	.048	.276	16.4	1.73
254-8-42	368	.596	.2218	.1815	.062	.051	.280	15.0	1.81
Cement 15013J									
254-8-46	339	.333	.2185	.1793	.052	.043	.239	19.2	1.53
254-8-47	333	.454	.2407	.1940	.058	.047	.242	17.6	1.67
254-8-48	333	.599	.2527	.2017	.057	.045	.224	17.6	1.63

*Estimated; $\frac{1}{w}\frac{x}{1-x}$ vs. x does not give straight line.

TABLE 5—V_n, C, COMPUTED SPECIFIC SURFACE AND OTHER DATA FOR SERIES 254-9

Ref. No.	Age at test, days	w_n, g/g of: Original cement	w_n, g/g of: Dry paste	V_m, g/g of: Original cement	V_m, g/g of: Dry paste	$\frac{V_m}{w_n}$*	C	Sp. surf. of dry paste, cm²/g millions
Cement 14930J; w/c at 2 hr. 0.309								
254-9-1 Mix A	7	.0804	.0744	.021	.019	.258	18	0.70
	14	.0994	.0904	.027	.024	.274	18	0.88
	28	.1071	.0967	.034	.031	.321	18	1.11
	56	.1292	.1144	.043	.038	.330	18	1.35
	90	.1497	.1302	.046	.040	.304	18	1.41
	180	.1620	.1400	.050	.043	.310	21	1.55
	365	.1704	.1456	.049	.042	.290	21	1.51
w/c at 2 hr. 0.424								
254-9-2 Mix B	7	.0798	.0739	.021	.020	.268	18	0.71
	14	.1029	.0933	.028	.025	.276	18	0.92
	28	.1165	.1044	.037	.033	.319	18	1.19
	56	.1352	.1191	.049	.043	.363	22	1.54
	95	.1735	.1479	.053	.045	.306	18	1.62
	183	.1853	.1564	.059	.050	.319	21	1.78
	365	.1953	.1634	.059	.049	.302	21	1.76
w/c at 2 hr. 0.573								
254-9-3 Mix C	7	.0822	.0760	.022	.020	.270	18	0.73
	14	.0896	.0822	.028	.026	.313	18	0.92
	28	.1214	.1083	.043	.038	.351	18	1.36
	56	.1638	.1407	.049	.042	.298	18	1.50
	90	.1850	.1561	.055	.046	.298	18	1.66
	180	.2008	.1672	.056	.047	.279	18	1.66
	365	.2142	.1764	.069	.057	.324	18	2.04
Cement 15007J; w/c at 2 hr. 0.318								
254-9-4 Mix A	7	.1259	.1118	.036	.032	.284	18	1.17
	14	.1404	.1231	.041	.036	.295	18	1.30
	28	.1538	.1332	.042	.036	.276	16	1.31
	56	.1681	.1439	.047	.040	.281	22	1.44
	90	.1729	.1474	.048	.041	.276	25	1.45
	180	.1835	.1550	.048	.041	.265	16	1.46
w/c at 2 hr. 0.432								
254-9-5 Mix B	7	.1334	.1177	.036	.032	.270	18	1.14
	14	.1498	.1303	.042	.037	.278	23	1.29
	28	.1714	.1463	.045	.038	.265	18	1.39
	56	.1847	.1559	.049	.041	.266	68	1.48
	90	.1924	.1614	.056	.047	.290	20	1.67
	180	.2018	.1679	.055	.046	.271	16	1.63
w/c at 2 hr. 0.582								
254-9-6 Mix C	7	.1560	.1350	.037	.032	.235	18	1.13
	14	.1634	.1405	.042	.036	.258	20	1.29
	28	.1839	.1553	.050	.042	.272	18	1.51
	56	.2035	.1690	.053	.044	.259	18	1.57
	90	.2049	.1700	.056	.046	.272	16	1.66
	180	.2132	.1757	.060	.050	.283	20	1.78
Cement 15011J; w/c at 2 hr. 0.338								
254-9-7 Mix A	7	.1137	.1020	.033	.029	.288	25	1.05
	14	.1333	.1176	.036	.032	.268	16	1.13
	28	.1430	.1251	.045	.040	.317	22	1.42
	56	.1557	.1347	.046	.040	.296	22	1.43
	90	.1643	.1411	.043	.037	.263	22	1.33
	180	.1705	.1457	.045	.038	.264	25	1.37
	365	.1760	.1497	.048	.041	.273	25	1.46
w/c at 2 hr. 0.433								
254-9-8 Mix B	7	.1228	.1094	.037	.033	.304	22	1.19
	14	.1527	.1325	.038	.033	.247	27	1.17
	28	.1654	.1419	.045	.039	.272	23	1.38
	56	.1781	.1512	.047	.040	.266	23	1.44
	90	.1913	.1606	.051	.043	.267	23	1.53
	180	.1986	.1657	.056	.046	.280	16	1.66

*Calculated before rounding V_m values to 2 significant figures.

(Concluded on p. 599)

TABLE 5—CONCLUDED

Ref. No.	Age at test, days	w_n, g/g of: Original cement	w_n, g/g of: Dry paste	V_m, g/g of: Original cement	V_m, g/g of: Dry paste	$\frac{V_m^*}{w_n}$	C	Sp. surf. of dry paste, cm^2/g millions
Cement 15011J; w/c at 2 hr. 0.570								
254-9-9 Mix C	7	.1314	.1161	.034	.030	.261	27	1.08
	14	.1567	.1355	.039	.034	.252	22	1.22
	28	.1756	.1494	.047	.040	.268	18	1.43
	56	.1953	.1634	.054	.045	.274	17	1.60
	90	.2046	.1698	.056	.046	.272	16	1.65
	180	.2136	.1760	.057	.047	.266	16	1.67
Cement 15013J; w/c at 2 hr. 0.324								
254-9-10 Mix A	7	.1488	.1295	.036	.031	.240	21	1.11
	14	.1639	.1408	.039	.033	.236	20	1.19
	28	.1711	.1461	.043	.036	.250	23	1.30
	56	.1802	.1527	.046	.039	.254	22	1.38
	90	.1913	.1606	.047	.040	.248	22	1.42
	180	.1877	.1580	.051	.043	.272	29	1.54
w/c at 2 hr. 0.443								
254-9-11 Mix B	7	.1556	.1346	.037	.032	.235	21	1.13
	14	.1828	.1545	.042	.036	.232	21	1.28
	28	.1770	.1504	.048	.041	.271	21	1.46
	56	.2085	.1725	.053	.044	.254	18	1.57
	90	.2152	.1771	.057	.047	.263	15	1.67
	180	.2356	.1907	.058	.047	.248	16	1.69
w/c at 2 hr. 0.611								
254-9-12 Mix C	7	.1583	.1367	.033	.029	.211	27	1.03
	14	.1828	.1545	.040	.034	.219	21	1.21
	28	.2028	.1686	.046	.038	.226	21	1.36
	56	.2208	.1809	.055	.045	.250	16	1.62
	90	.2357	.1907	.058	.047	.245	19	1.67
	180	.2447	.1966	.059	.047	.239	17	1.68
Cement 15365; w/c at 2 hr. 0.322								
254-9-13 Mix A	7	.1326	.1171	.034	.030	.254	24	1.06
	14	.1515	.1316	.037	.032	.243	24	1.14
	28	.1488	.1295	.044	.038	.294	20	1.36
	56	.1786	.1515	.047	.040	.264	22	1.43
	90	.1789	.1518	.048	.040	.267	20	1.45
	180	.1815	.1536	.046	.039	.256	25	1.40
w/c at 2 hr. 0.439								
254-9-14 Mix B	7	.1394	.1223	.034	.030	.244	26	1.06
	14	.1711	.1461	.043	.037	.253	20	1.32
	28	.1841	.1555	.054	.046	.295	19	1.64
	56	.2105	.1739	.055	.045	.261	19	1.62
	90	.2150	.1770	.056	.046	.263	20	1.66
	180	.2224	.1819	.060	.049	.269	19	1.75
w/c at 2 hr. 0.587								
254-9-15 Mix C	7	.1530	.1327	.037	.032	.242	25	1.15
	14	.1855	.1565	.045	.038	.241	22	1.35
	28	.2102	.1737	.055	.045	.261	19	1.62
	56	.2213	.1812	.057	.047	.259	22	1.68
	90	.2296	.1867	.062	.051	.271	19	1.81
	180	.2546	.2029	.060	.048	.235	19	1.70
w/c at 2 hr. 0.244								
254-9-15A Neat Cement	7	.1152	.1033	.028	.025	.244	33	0.90
	14	.1259	.1118	.030	.027	.242	33	0.96
	28	.1358	.1196	.032	.028	.232	33	0.99
	56	.1396	.1225	.034	.029	.240	33	1.05
	90	.1452	.1268	.034	.030	.236	33	1.07
	180	.1554	.1345	.035	.031	.230	33	1.09
Isotherm A	270	.1691	.1446	.032	.028	.193	19	0.99
Isotherm B	270	.1722	.1469	.031	.026	.178	16	0.94

*Calculated before rounding V_m values to 2 significant figures.

TABLE 6—V_m, C, COMPUTED SPECIFIC SURFACE AND OTHER DATA FOR SERIES 254-11

Cement No.	Ref. No. 254-	w/c at 2 hr.	w_n, g/g of:		V_m, g/g of:		$\frac{V_m}{w_n}$*	C	Sp. surf. of dry paste, cm^2/g millions
			Original cement	Dry paste	Original cement	Dry paste			
Age at test 28 days									
15758	11–1	.334	.1707	.1458	.043	.037	.252	18	1.31
"	11–2	.460	.1962	.1640	.050	.042	.254	18	1.49
15756	11–3	.318	.1229	.1094	.034	.031	.281	18	1.10
"	11–4	.446	.1325	.1170	.035	.031	.267	18	1.11
15763	11–5	.324	.0922	.0844	.028	.026	.307	18	0.92
"	11–6	.437	.1013	.0920	.031	.028	.305	18	1.00
15761	11–7	.334	.1621	.1395	.041	.035	.251	18	1.25
"	11–8	.468	.1852	.1563	.049	.042	.266	18	1.48
15754	11–9	.328	.1703	.1455	.044	.037	.256	18	1.33
"	11–10	.449	.1967	.1644	.050	.042	.256	18	1.50
16213	11–11	.443	.1720	.1468	.047	.040	.273	18	1.43
16214	11–12	.448	.1854	.1564	.048	.040	.258	18	1.44
16198	11–13	.444	.1098	.0989	.032	.029	.296	18	1.05
15669	11–14	.452	.1084	.0978	.028	.025	.262	21	0.92
Age at test 90 days									
15758	11–1	.334	.1912	.1605	.047	.039	.245	21	1.41
"	11–2	.460	.2227	.1821	.054	.044	.244	18	1.59
15756	11–3	.318	.1492	.1298	.043	.037	.287	21	1.33
"	11–4	.446	.1684	.1441	.045	.038	.267	18	1.37
15763	11–5	.324	.1335	.1178	.041	.036	.304	18	1.28
"	11–6	.437	.1487	.1295	.045	.039	.303	18	1.40
15761	11–7	.334	.1798	.1524	.048	.040	.264	18	1.44
"	11–8	.468	.2120	.1749	.055	.045	.259	18	1.62
15754	11–9	.328	.1951	.1632	.047	.039	.241	18	1.41
"	11–10	.449	.2301	.1871	.058	.047	.250	18	1.67
Age at test 6 days									
15495A	11–15	.442	.1300	.1150	.032	.029	.249	19	1.02
15497	11–16	.464	.1825	.1543	.044	.037	.240	18	1.32

*Calculated before rounding V_m values to 2 significant figures.

TABLE 7—V_m, C, COMPUTED SPECIFIC SURFACE AND OTHER DATA FOR SERIES 254-13

Ref. No. 254–	w/c at 2 hr.	SO_3 content of cement, percent	w_n, g/g of:		V_m, g/g of:		$\frac{V_m}{w_n}$*	C	Sp. surf. of dry paste, cm^2/g millions
			Original cement	Dry paste	Original cement	Dry paste			
Cements made from clinker 15367									
13–1	.493	1.5	.2147	.1768	.059	.049	.275	15.4	1.74
13–2	.493	1.9	.2108	.1741	.056	.046	.265	17.7	1.65
13–3	.489	2.4	.2083	.1724	.054	.044	.257	17.7	1.59
13–4	.491	3.5	.1938	.1623	.048	.041	.250	21.0	1.45
13-1B	.486	1.5	.2115	.1746	.058	.048	.276	16.5	1.72
13–2B	.488	1.9	.2158	.1775	.058	.048	.268	18.0	1.70
13–3B	.488	2.4	.2151	.1770	.055	.045	.254	21.0	1.60
13–4B	.492	3.5	.2035	.1691	.050	.041	.245	23.3	1.48
Cements made from clinker 15623									
13–5	.470	1.5	.1518	.1317	.038	.033	.248	17.7	1.17
13–6	.474	2.0	.1509	.1311	.038	.033	.253	15.4	1.19
13–7	.473	2.5	.1515	.1316	.038	.033	.252	13.5	1.19
13–8	.480	3.5	.1444	.1262	.038	.034	.265	13.5	1.20
Cements made from clinker 15699									
13– 9	.498	1.5	.1992	.1661	.053	.044	.268	16.5	1.59
13–10	.499	2.0	.1937	.1623	.052	.044	.268	17.7	1.55
13–11	.499	2.5	.1917	.1609	.049	.041	.258	17.7	1.48
13–12	.498	3.5	.1839	.1553	.046	.039	.251	17.7	1.39
Cements made from clinker 15498									
13–13	.488	1.5	.2082	.1723	.053	.044	.256	21.0	1.57
13–14	.487	2.0	.1992	.1661	.050	.042	.252	21.0	1.49
13–15	.493	2.5	.2004	.1669	.049	.041	.244	21.0	1.46
13–16	.491	3.5	.1895	.1593	.047	.040	.250	21.0	1.42
Cements made from clinker 15670									
13–17	.476	1.5	.1108	.0997	.031	.028	.282	18.0	1.01
13–18	.479	2.0	.1182	.1057	.034	.030	.287	18.0	1.08
13–19	.483	2.5	.1842	.1555	.042	.036	.231	18.0	1.28
13–20	.486	3.5	.2087	.1727	.050	.042	.241	18.0	1.49

*Calculated before rounding V_m values to 2 significant figures.

TABLE 8—V_m, C, COMPUTED SPECIFIC SURFACE AND OTHER DATA FOR SERIES 254-16

Ref. No.	Age at test, days	w_n, g/g of:		V_m, g/g of:		$\frac{V_m}{w_n}$*	C	Sp. surf. of dry paste, cm^2/g millions
		Original cement	Dry paste	Original cement	Dry paste			
Based on maximum weights attained during adsorption test								
16-01A	27	.2031	.1688	.053	.044	.259	22	1.56
16-01B	27	.2051	.1702	.053	.044	.258	22	1.57
16-01C	29	.2042	.1696	.052	.043	.256	22	1.55
Avg.		.2041	.1695	.053	.044	.258	22	1.56
16-02A	42	.1594	.1375	.037	.032	.230	22	1.13
16-02B	44	.1547	.1340	.035	.030	.226	22	1.08
16-02C	44	.1542	.1336	.036	.031	.233	22	1.11
Avg.		.1561	.1350	.036	.031	.230	22	1.11
16-03A	56	.1412	.1237	.036	.032	.255	22	1.12
16-03B	56	.1416	.1240	.037	.032	.258	22	1.15
16-03C	63	.1502	.1306	.039	.034	.260	22	1.21
16-03D	63	.1510	.1312	.039	.034	.258	22	1.21
Avg.		.1460	.1274	.038	.033	.258	22	1.17
Based on weights at time heat-of-solution measurements were made								
16-01A	27	.2031	.1688	.051	.042	.250	22	1.51
16-01B	27	.2051	.1702	.050	.041	.242	22	1.47
16-01C	29	.2042	.1696	—	—	—	—	—
Avg.		.2041	.1695	.050	.042	.246	22	1.49
16-02A	42	.1594	.1375	.036	.031	.223	22	1.09
16-02B	44	.1547	.1340	.035	.030	.224	22	1.08
16-02C	44	.1542	.1336	.036	.032	.235	22	1.12
Avg.		.1561	.1350	.036	.031	.227	22	1.10

*Calculated before rounding V_m values to 2 significant figures.

Title 43-5e . —a part of PROCEEDINGS, AMERICAN CONCRETE INSTITUTE Vol. 43

JOURNAL
of the
AMERICAN CONCRETE INSTITUTE
(copyrighted)

Vol. 18 No. 6 7400 SECOND BOULEVARD, DETROIT 2, MICHIGAN February 1947

Studies of the Physical Properties of Hardened Portland Cement Paste*

By T. C. POWERS†
Member American Concrete Institute
and T. L. BROWNYARD‡

Part 5. Studies of the Hardened Paste by Means of Specific-Volume Measurements§

CONTENTS

*Received by the Institute July 8, 1946—scheduled for publication in seven installments; October 1946 to April, 1947. In nine parts:

Part 1. "A Review of Methods That Have Been Used for Studying the Physical Properties of Hardened Portland Cement Paste". ACI JOURNAL, October, 1946.
Part 2. "Studies of Water Fixation"—Appendix to Part 2. ACI JOURNAL, November, 1946.
Part 3. "Theoretical Interpretation of Adsorption Data." ACI JOURNAL, December, 1946.
Part 4. "The Thermodynamics of Adsorption"—Appendix to Parts 3 and 4. ACI JOURNAL, January 1947.
Part 5. "Studies of the Hardened Paste by Means of Specific-Volume Measurements."
Part 6. "Relation of Physical Characteristics of the Paste to Compressive Strength."
Part 7. "Permeability and Absorptivity."
Part 8. "The Freezing of Water in Hardened Portland Cement Paste."
Part 9. "General Summary of Findings on the Properties of Hardened Portland Cement Paste."

†Manager of Basic Research, Portland Cement Assn. Research Laboratory, Chicago 10, Ill.
‡Navy Dept., Washington, D. C., formerly Research Chemist, Portland Cement Assn. Research Laboratory, Chicago 10, Ill.

§The characteristics of the cements mentioned in this section may be found in the Appendix to Part 2.

CLASSIFICATION OF WATER IN SATURATED PASTE ACCORDING TO MEAN SPECIFIC VOLUME

The total water content of a saturated sample of hardened paste has already been classified according to its evaporability, i.e., into evaporable and non-evaporable water. We have seen also that the evaporable water can be subdivided into gel water and capillary water on the basis of vapor pressure data. The following discussion will show that the same conclusion can be reached on the basis of the mean specific volume of the total water.

The non-evaporable water is regarded as an integral part of the solid phase in hardened cement paste. In becoming a part of the solid material some or all of it may have lost its identity as water. Nevertheless, the absolute volume of the solid phase can be considered as being equal to the original volume of the cement plus the volume of the non-evaporable water. If the absolute volume of the original cement, the absolute volume of the whole solid phase, and the weight of the non-evaporable water are known, a hypothetical specific volume can be assigned to the non-evaporable water such as will account for the known volume of the solid phase. This hypothetical specific volume is known to be less than 1.0; that is, the non-evaporable water occupies less space than an equal volume of free water. Moreover, the physically adsorbed part of the evaporable water also has a specific volume less than 1.0. Thus, in any given specimen the mean specific volume of the non-evaporable and adsorbed water is less than 1.0.

On the other hand, any capillary water present will either be in a state of tension or under no stress at all. If the specimen is not saturated, so that the vapor pressure of the contained water is less than p_s but more than about 0.45 p_s, capillary water will be present and under tension. (The magnitude of the tension is theoretically equal to the potential swelling pressure. See eq. (39), Part 4.) If the paste is saturated, so that $p = p_s$, the capillary water will be under no tension. Hence, when capillary water is present, but the paste is not saturated, the specific volume of the capillary water will be greater than 1.0, and if the specimen is saturated, the specific volume will be 1.0, except for a slight effect of the dissolved salts.

Thus, we can divide the total water content of a *saturated* specimen into two categories:

(1) Water that has a specific volume less than 1.0;

(2) Water that has a specific volume equal to 1.0.

The part of the total water in a saturated paste that has a mean specific volume less than 1.0 will be called *compressed water* for want of a better descriptive term. As applied to adsorbed water, the term is appropriate, if used with the reservations discussed in Part 4. Applied to non-evaporable water the term can hardly be taken literally. It does, however, fit the fact that non-evaporable water occupies less space as a part of the solid than it does when free.

The weight-composition of the total water in a sample of saturated paste can be expressed as follows:

$$w_t = w_d + w_c \,, \qquad (1)$$

where

w_d is the weight of the compressed water, g and

w_c is the weight of the capillary water, g.

The *volume* of the total water can be expressed as

$$w_t v_t = w_d v_d + w_c \,, \qquad (2)$$

where v_d is the mean specific volume of the compressed water, and

v_t is the mean specific volume of the total water.

The specific volume of the capillary water is assumed to be 1.0.

Since $w_c = w_t - w_d$, eq. (2) can be rewritten

$$w_d (1 - v_d) = w_t (1 - v_t) \qquad (3)$$

Experimental values of the mean specific volume of the total water content, v_t, were obtained by direct measurement. If the weight of the compressed water also could be measured, its mean density could be obtained by means of eq. (3). However, this cannot be done directly. It can be estimated by making certain assumptions, as will be shown below.

Of the water, w_d, that has a specific volume less than 1.0, a part is the non-evaporable water and the rest is adsorbed water, specifically, water within the range of the force-field of the solid phase. That is,

$$w_d = w_n + w_a \,, \qquad (4)$$

where w_n is the weight of non-evaporable water, g and

w_a is the weight of adsorbed water, g.

For samples made with a given cement we may safely assume that

$$w_a = B' w_n \,, \qquad (5)$$

where B' is a constant for the particular cement. That is, it is assumed that the amount of adsorbed water is proportional to the total amount

of hydration products* which in turn is in proportion to the amount of non-evaporable water. Hence,

$$w_d = w_n + B' w_n = (1 + B')w_n = B w_n \quad \ldots\ldots\ldots\ldots\ldots\ldots (6)$$

Substitution from eq. (6) into eq. (3) gives

$$v_t = 1 - B(1 - v_d)\frac{w_n}{w_t} \quad \ldots\ldots\ldots\ldots\ldots\ldots\ldots\ldots (7)$$

Eq. (7) shows that a plot of experimentally determined values of v_t versus the corresponding values for w_n/w_t should give a straight line beginning at $v_t = 1$ when $w_n/w_t = 0$ and having a slope which would equal the product of the decrease in mean specific volume of the *compressed water* and the factor B, which is the ratio of the total amount of compressed water to the non-evaporable water, eq. (6). Experimental data are given in Tables 5-1 to 5-8.

The mean specific volumes of the total water, v_t, were determined as follows: Granular samples were dried to remove all the evaporable water. A portion of each dried sample was analyzed for non-evaporable water, portland cement, and pulverized silica, when present. Another part of the dried sample was brought to the saturated, surface-dry condition by the method described under "Experimental Procedures" (Part 1), and the amount required for saturation was noted. This amount, added to the non-evaporable water, gave the total water content of the sample. The specific volume of the saturated sample was then determined by a conventional pycnometer method, using water as the displacement medium.

Examination of these tables will show how the mean specific volume of the total water was computed. In Table 5-2, for example, columns 5, 6, and 7 give the weight-compositions of the saturated granular samples. Column 8 gives the measured density of the same granules.

Columns 9, 10, 11, and 12 give the weight-composition of 1 cc of each saturated sample. The values were obtained by multiplying the corresponding values in columns 5, 6, and 7 by the density of the saturated sample.

The volumes of cement in 1 cc of each saturated sample appear in column 13. These were obtained by multiplying the values in column 9 by the respective specific volumes of the original cements as measured by displacement of kerosene.

The figures in column 14 are the differences between the total volumes and the volumes of the cements as given in column 13. The difference was taken to be the volume of water. This involved the assumption that the air content was zero. For these particular neat cement specimens the air contents of the original specimens were very low. In the mortar specimens from which the samples represented in other tables were ob-

*Because $w_a \sim V_m \sim w_n$ for a given cement.

TABLE 5-1—COMPOSITIONS OF GRANULAR SAMPLES USED IN ADSORPTION AND OTHER TESTS AND COMPUTATION OF MEAN SPECIFIC VOLUME OF TOTAL WATER CONTENT AND OTHER FACTORS

Series 254-MRB

(1)	(2)	(3)	(4)	(5)	(6)	(7)	(8)	(9)	(10)	(11)	(12)	(13)	(14)	(15)	(16)	(17)
Cement No.	Ref. No.	Age, days	v_c*	Grams per g of sat'd sample			Density, saturated, g/cc	Grams per cc of saturated sample				Vols. per unit vol. sat'd sample		Avg. sp. vol. of water v_t	$\frac{w_n}{w_t}$	$\frac{1 - v_t}{w_n/w_t}$
				Cement	Non-evap. water	Evap. water		Cement	Non-evap. water	Evap. water	Total water	Cement	1 − cement			
Clinker No. 1																
14898	1AQ	120	0.3155	0.685	0.149	0.167	2.040	1.397	0.304	0.341	0.645	0.441	0.559	0.867	0.471	0.282
14899	1PC	120	0.3155	0.686	0.153	0.162	2.040	1.399	0.312	0.330	0.642	0.441	0.559	0.871	0.486	0.265
14900	1SC	126	0.3155	0.664	0.151	0.186	1.976	1.312	0.298	0.368	0.666	0.414	0.586	0.880	0.447	0.268
Clinker No. 2																
14901	2AQ	126	0.3175	0.671	0.149	0.180	2.004	1.345	0.299	0.361	0.660	0.427	0.573	0.868	0.453	0.291
Clinker No. 3																
14904	3AQ	162	0.3155	0.671	0.153	0.175	2.020	1.355	0.309	0.354	0.663	0.428	0.572	0.863	0.466	0.294
14905	3PC	162	0.3155	0.671	0.154	0.174	2.013	1.351	0.310	0.350	0.660	0.426	0.574	0.870	0.470	0.277
14906	3SC	173	0.3155	0.645	0.152	0.203	1.939	1.251	0.295	0.394	0.689	0.395	0.605	0.878	0.428	0.285
Clinker No. 4																
14907	4AQ	173	0.3155	0.685	0.150	0.165	2.045	1.401	0.307	0.337	0.644	0.442	0.558	0.866	0.477	0.281
14908	4PC	200	0.3155	0.677	0.152	0.171	2.028	1.373	0.308	0.347	0.655	0.433	0.567	0.866	0.470	0.285
14909	4SC	200	0.3155	0.646	0.146	0.208	1.936	1.251	0.283	0.403	0.686	0.395	0.605	0.882	0.413	0.286
Clinker No. 5																
14910	5AQ	204	0.3155	0.655	0.150	0.194	1.964	1.286	0.295	0.381	0.676	0.406	0.594	0.879	0.436	0.278
14911	5PC	204	0.3160	0.661	0.151	0.188	1.978	1.307	0.299	0.372	0.671	0.413	0.587	0.875	0.446	0.280
14912	5SC	212	0.3144	0.646	0.146	0.208	1.930	1.247	0.282	0.401	0.683	0.392	0.608	0.890	0.413	0.266
Clinker No. 6																
14913	6AQ	212	0.3155	0.677	0.149	0.173	2.026	1.372	0.302	0.350	0.652	0.433	0.567	0.870	0.463	0.281
14914	6PC	222	0.3155	0.672	0.152	0.176	2.008	1.349	0.305	0.353	0.658	0.426	0.574	0.872	0.464	0.276
14915	6SC	222	0.3155	0.658	0.147	0.194	1.964	1.292	0.289	0.381	0.670	0.408	0.592	0.884	0.431	0.269

*For most of these cements v_c was not measured. The figure 0.3155 is the average for those that were measured. Avg. 0.279

TABLE 5-2—COMPOSITION OF GRANULAR SAMPLES USED IN ADSORPTION AND OTHER TESTS AND COMPUTATION OF MEAN SPECIFIC VOLUME OF TOTAL WATER CONTENT AND OTHER FACTORS

Series 254-K4B

(1)	(2)	(3)	(4)	(5)	(6)	(7)	(8)	(9)	(10)	(11)	(12)	(13)	(14)	(15)	(16)	(17)
Cement No.	Ref. No.	Age, days	v_c	Grams per g of sat'd sample			Density, saturated, g/cc	Grams per cc of saturated sample				Vols. per unit vol. sat'd sample		Avg. sp. vol. of water, v_l	$\frac{w_n}{w_l}$	$\frac{1 - v_l}{w_n/w_l}$
				Cement	Non-evap. water	Evap. water		Cement	Non-evap. water	Evap. water	Total water	Cement	1 − cement			
Cements Made from Clinker No. 1																
13721	1-S	174	0.3195	0.648	0.145	0.208	1.925	1.247	0.279	0.400	0.679	0.398	0.602	0.886	0.411	0.277
13722	1-P	180	0.3215	0.641	0.150	0.209	1.910	1.224	0.287	0.399	0.686	0.394	0.606	0.883	0.418	0.280
13723	1-Q	180	0.3216	0.666	0.152	0.182	1.980	1.319	0.301	0.360	0.661	0.424	0.576	0.871	0.455	0.284
Cements Made from Clinker No. 4																
13730	4-S	144	0.3100*	0.662	0.118	0.222	1.953	1.293	0.230	0.434	0.664	0.401	0.599	0.902	0.346	0.283
13731	4-P	138	0.3100*	0.661	0.117	0.222	1.960	1.296	0.229	0.435	0.664	0.402	0.598	0.901	0.345	0.287
13732	4-Q	138	0.3100*	0.669	0.119	0.212	1.981	1.325	0.236	0.420	0.656	0.411	0.589	0.898	0.360	0.283
Cements Made from Clinker No. 5																
13733	5-S	150	0.3100*	0.668	0.110	0.222	1.960	1.309	0.216	0.435	0.651	0.406	0.594	0.912	0.332	0.265
13734	5-P	146	0.3100*	0.663	0.105	0.232	1.936	1.284	0.203	0.449	0.652	0.398	0.602	0.923	0.311	0.248
13735	5-Q	150	0.3100*	0.661	0.109	0.230	1.937	1.280	0.211	0.446	0.657	0.397	0.603	0.918	0.321	0.255
Cements Made from Clinker No. 6																
13736	6-S	196	0.3162	0.663	0.142	0.195	1.966	1.303	0.279	0.383	0.662	0.412	0.588	0.888	0.421	0.266
13737	6-P	191	0.3172	0.658	0.151	0.190	1.956	1.287	0.295	0.372	0.667	0.408	0.592	0.888	0.442	0.253
13738	6-Q	191	0.3186	0.661	0.147	0.192	1.974	1.305	0.290	0.379	0.669	0.416	0.584	0.873	0.433	0.293
Cements Made from Clinker No. 7																
13740	7-P	164	0.3190†	0.643	0.154	0.204	1.926	1.238	0.297	0.393	0.690	0.395	0.605	0.877	0.430	0.286
13741	7-Q	171	0.3190†	0.646	0.154	0.200	1.934	1.249	0.298	0.387	0.685	0.398	0.602	0.879	0.435	0.278
Cements Made from Clinker No. 11																
13752	11-P	164	0.3100*	0.660	0.123	0.218	1.951	1.288	0.240	0.425	0.665	0.399	0.601	0.904	0.361	0.266
13753	11-Q	172	0.3100*	0.663	0.126	0.212	1.956	1.297	0.246	0.415	0.661	0.402	0.598	0.905	0.372	0.255
Cements Made from Clinker No. 15																
13763	15-S	202	0.3160	0.651	0.141	0.208	1.932	1.258	0.272	0.402	0.674	0.398	0.602	0.893	0.404	0.265
13764	15-P	196	0.3182	0.666	0.141	0.193	1.976	1.316	0.279	0.381	0.660	0.419	0.581	0.880	0.423	0.284
13765	15-Q	202	0.3222	0.654	0.144	0.202	1.953	1.277	0.281	0.395	0.676	0.411	0.589	0.871	0.416	0.310

(Concluded opposite page.)

(Table 5-2 concluded)

Cements Made from Clinker No. 16																
13766	16-S	322	0.3190*	0.647	0.136	0.218	1.918	1.241	0.261	0.418	0.679	0.396	0.604	0.890	0.384	0.286
13767	16-P	223	0.3190*	0.656	0.148	0.196	1.952	1.281	0.289	0.383	0.672	0.409	0.591	0.879	0.430	0.281
13768	16-Q	223	0.3190*	0.666	0.150	0.184	1.976	1.316	0.296	0.364	0.660	0.420	0.580	0.879	0.448	0.270
Cements Made from Clinker No. 20																
13778	20-S	170	0.3180	0.648	0.150	0.202	1.942	1.258	0.291	0.392	0.683	0.400	0.600	0.878	0.426	0.286
13779	20-P	167	0.3190	0.648	0.151	0.201	1.954	1.266	0.295	0.393	0.688	0.404	0.596	0.866	0.429	0.312
13780	20-Q	176	0.3197	0.663	0.150	0.187	1.984	1.315	0.298	0.371	0.669	0.420	0.580	0.867	0.445	0.299

*Assumed value for Type IV cements—Density of cement = 3.22; v_c = 0.310. Avg. 0.278
†Average value for Type I cements.

TABLE 5-3—COMPOSITIONS OF GRANULAR SAMPLES USED IN ADSORPTION AND OTHER TESTS AND COMPUTATION OF MEAN SPECIFIC VOLUME OF TOTAL WATER CONTENT AND OTHER FACTORS

Series 254-7

(1)	(2)	(3)	(4)	(5)	(6)	(7)	(8)	(9)	(10)	(11)	(12)	(13)	(14)	(15)	(16)	(17)	(18)
		Grams per g of saturated sample					Grams per cc of saturated sample					Vols/unit vol. sat'd sample					
Ref. No.	Age, mo.	Cement	Sand	Non-evap. water	Evap. water	Density, saturated, g/cc	Cement	Sand	Non-evap. water	Evap. water	Total water	Cement	Sand	1 − (Cement + sand)	Avg. sp. vol. of water, v_t	$\frac{w_n}{w_t}$	$\frac{1 - v_t}{w_n/w_t}$
Cement 14675; Density of cement = 3.143 g/cc; v_c = 0.3182																	
7-1	6	0.772	—	0.126	0.103	2.268	1.751	—	0.286	0.234	0.520	0.558	—	0.442	0.850	0.550	0.273
7-2	6	0.598	0.199	0.105	0.098	2.270	1.358	0.452	0.238	0.222	0.460	0.432	0.170	0.398	0.865	0.517	0.261
7-3	6	0.554	0.249	0.101	0.096	2.278	1.262	0.567	0.230	0.219	0.449	0.402	0.213	0.385	0.858	0.512	0.277
7-4	6	0.467	0.331	0.096	0.106	2.237	1.045	0.740	0.215	0.237	0.452	0.332	0.278	0.390	0.863	0.476	0.288
7-5	6	0.420	0.349	0.099	0.133	2.144	0.900	0.748	0.212	0.285	0.497	0.286	0.281	0.433	0.871	0.427	0.302
7-6	6	0.322	0.452	0.075	0.151	2.098	0.676	0.948	0.157	0.317	0.474	0.215	0.356	0.429	0.905	0.331	0.287
7-7	6	0.284	0.493	0.065	0.158	2.084	0.592	1.027	0.135	0.329	0.464	0.188	0.386	0.426	0.918	0.291	0.281
7-S-1	6	0.709	—	0.154	0.137	2.104	1.492	—	0.324	0.288	0.612	0.475	—	0.525	0.858	0.530	0.268
7-S-2	6	0.574	0.131	0.133	0.162	2.024	1.162	0.265	0.269	0.328	0.597	0.370	0.100	0.530	0.888	0.451	0.248
7-S-3	6	0.471	0.235	0.115	0.179	2.000	0.942	0.470	0.230	0.358	0.588	0.300	0.177	0.523	0.890	0.391	0.281
7-S-4	6	0.397	0.316	0.099	0.188	2.000	0.794	0.632	0.198	0.376	0.574	0.253	0.238	0.509	0.887	0.345	0.328
7-S-5	6	0.377	0.351	0.093	0.179	2.019	0.761	0.709	0.188	0.361	0.549	0.242	0.267	0.491	0.894	0.342	0.310

Avg. 0.284

TABLE 5-4—COMPOSITION OF GRANULAR SAMPLES USED IN ADSORPTION AND OTHER TESTS AND COMPUTATION OF MEAN SPECIFIC VOLUME OF TOTAL WATER CONTENT AND OTHER FACTORS

Series 254-8

(1)	(2)	(3)	(4)	(5)	(6)	(7)	(8)	(9)	(10)	(11)	(12)	(13)	(14)	(15)	(16)	(17)	(18)
		Grams per g of saturated sample					Grams per cc of saturated sample					Vols/unit vol. sat'd sample					
Ref. No.	Age, days	Cement	Silica	Non-evap. water	Evap. water	Density, saturated, g/cc	Cement	Silica	Non-evap. water	Evap. water	Total water	Cement	Silica	1 − (Cement + silica)	Avg. sp. vol. of water, v_t	$\frac{w_n}{w_t}$	$\frac{1 - v_t}{w_n/w_t}$
Cement 14930; Density of cement = 3.218 g/cc; v_c = 0.3108																	
8–1	448	0.645	0.102	0.116	0.137	2.157	1.391	0.220	0.250	0.296	0.546	0.432	0.083	0.485	0.888	0.458	0.244
8–2	363	0.498	0.238	0.100	0.165	2.070	1.031	0.493	0.207	0.342	0.549	0.320	0.185	0.495	0.901	0.377	0.262
8–3	363	0.401	0.325	0.084	0.190	2.004	0.804	0.651	0.168	0.381	0.549	0.250	0.245	0.505	0.920	0.306	0.261
Cement 15007J; Density of cement = 3.189 g/cc; v_c = 0.3136																	
8–28	481	0.623	0.112	0.123	0.141	2.115	1.318	0.237	0.260	0.298	0.558	0.413	0.089	0.498	0.892	0.467	0.231
8–29	441	0.474	0.276	0.103	0.147	2.093	0.992	0.578	0.216	0.308	0.524	0.311	0.217	0.472	0.901	0.412	0.240
8–30	441	0.359	0.401	0.083	0.157	2.078	0.746	0.833	0.172	0.326	0.498	0.234	0.313	0.453	0.910	0.345	0.261
Cement 15008; Density of cement = 3.181 g/cc; v_c = 0.3144																	
8–32	464	0.520	0.197	0.110	0.173	2.026	1.054	0.399	0.223	0.350	0.573	0.331	0.150	0.519	0.906	0.390	0.241
8–33	464	0.400	0.329	0.088	0.182	1.994	0.798	0.656	0.175	0.363	0.538	0.251	0.247	0.502	0.933	0.326	0.205
Cement 15011J; Density of cement = 3.204 g/cc; v_c = 0.3121																	
8–40	479	0.647	0.101	0.119	0.133	2.162	1.399	0.218	0.257	0.288	0.545	0.437	0.082	0.481	0.883	0.472	0.248
8–41	368	0.518	0.211	0.109	0.163	2.067	1.071	0.436	0.225	0.337	0.562	0.334	0.164	0.502	0.893	0.400	0.268
8–42	368	0.400	0.343	0.089	0.168	2.056	0.822	0.705	0.183	0.345	0.528	0.256	0.265	0.479	0.907	0.347	0.268
Cement 15012J; Density of cement = 3.191 g/cc; v_c = 0.3134																	
8–44	465	0.493	0.225	0.104	0.179	2.000	0.986	0.450	0.208	0.358	0.566	0.309	0.169	0.522	0.922	0.368	0.212
8–45	465	0.395	0.329	0.088	0.188	1.992	0.787	0.655	0.175	0.374	0.549	0.247	0.246	0.507	0.923	0.320	0.240
Cement 15013J; Density of cement = 3.163 g/cc; v_c = 0.3162																	
8–46	440	0.663	0.049	0.145	0.143	2.089	1.385	0.102	0.303	0.299	0.602	0.438	0.038	0.524	0.870	0.502	0.259
8–47	434	0.510	0.204	0.123	0.162	2.040	1.040	0.416	0.251	0.330	0.581	0.329	0.156	0.515	0.886	0.432	0.265
8–48	434	0.413	0.303	0.104	0.180	2.000	0.826	0.606	0.208	0.360	0.568	0.261	0.228	0.511	0.900	0.367	0.273
Cement 15014J; Density of cement = 3.175 g/cc; v_c = 0.3150																	
8–50	488	0.479	0.217	0.118	0.186	1.957	0.937	0.425	0.231	0.364	0.595	0.295	0.160	0.545	0.916	0.388	0.216
8–51	488	0.380	0.324	0.096	0.199	1.936	0.736	0.627	0.186	0.385	0.571	0.232	0.236	0.532	0.932	0.327	0.214
																	Avg. 0.245

TABLE 5-5—COMPOSITIONS OF GRANULAR SAMPLES USED IN ADSORPTION AND OTHER TESTS AND COMPUTATION OF MEAN SPECIFIC VOLUME OF TOTAL WATER CONTENT AND OTHER FACTORS

Series 254-9

(1)	(2)	(3)	(4)	(5)	(6)	(7)	(8)	(9)	(10)	(11)	(12)	(13)	(14)	(15)	(16)	(17)	(18)	(19)
			Grams per g of saturated sample					Grams per cc of saturated sample					Vols/unit vol. sat'd sample					
Ref. No.	w/c	Age, days	Cement	Silica	Non-evap. water	Evap. water	Density, saturated, g/cc	Cement	Silica	Non-evap. water	Evap. water	Total water	Cement	Silica	1 − (cement + silica)	Avg. sp. vol. of water, v_t	$\frac{w_n}{w_t}$	$\frac{1 - v_t}{w_n/w_t}$
Cement 14930J; Density of cement = 3.218 g/cc; v_c = 0.3108																		
9–1	.310	7	0.701	0.065	0.062	0.172	2.210	1.549	0.144	0.137	0.380	0.517	0.481	0.054	0.465	0.899	0.265	0.381
		14	0.677	0.099	0.067	0.157	2.222	1.504	0.220	0.149	0.349	0.498	0.467	0.083	0.450	0.904	0.299	0.321
		28	0.603	0.188	0.065	0.146	2.236	1.348	0.420	0.145	0.326	0.471	0.419	0.158	0.423	0.898	0.308	0.331
		56	0.636	0.142	0.082	0.139	2.226	1.416	0.316	0.182	0.309	0.491	0.440	0.119	0.441	0.898	0.371	0.275
		90	0.612	0.172	0.092	0.124	2.236	1.368	0.385	0.206	0.277	0.483	0.425	0.145	0.430	0.890	0.427	0.258
		180	0.668	0.092	0.108	0.131	2.202	1.471	0.203	0.238	0.288	0.526	0.457	0.076	0.467	0.888	0.452	0.248
		365	0.618	0.158	0.105	0.119	2.202	1.361	0.348	0.231	0.262	0.493	0.423	0.131	0.446	0.905	0.469	0.203
9–2	.424	7	0.546	0.230	0.043	0.175	2.166	1.183	0.498	0.093	0.379	0.472	0.368	0.187	0.445	0.943	0.197	0.289
		14	0.516	0.249	0.053	0.175	2.139	1.104	0.533	0.113	0.374	0.487	0.343	0.200	0.457	0.938	0.232	0.267
		28	0.438	0.354	0.051	0.158	2.160	0.946	0.765	0.110	0.341	0.451	0.294	0.288	0.418	0.927	0.244	0.299
		56	0.416	0.386	0.056	0.141	2.190	0.911	0.845	0.123	0.309	0.432	0.283	0.318	0.399	0.924	0.285	0.266
		95	0.470	0.301	0.082	0.148	2.153	1.012	0.648	0.177	0.319	0.496	0.314	0.244	0.442	0.891	0.357	0.306
		183	0.512	0.240	0.095	0.153	2.114	1.082	0.507	0.201	0.323	0.524	0.336	0.191	0.473	0.903	0.384	0.252
		365	0.464	0.299	0.091	0.146	2.117	0.982	0.633	0.193	0.309	0.502	0.305	0.238	0.457	0.910	0.384	0.234
9–3	.573	7	0.392	0.419	0.032	0.157	2.197	0.861	0.921	0.070	0.345	0.415	0.268	0.346	0.386	0.930	0.169	0.414
		14	0.300	0.565	0.027	0.111	2.301	0.690	1.300	0.062	0.255	0.317	0.214	0.489	0.297	0.937	0.196	0.322
		28	0.339	0.460	0.041	0.160	2.144	0.727	0.986	0.088	0.343	0.431	0.226	0.371	0.403	0.935	0.204	0.318
		56	0.378	0.382	0.062	0.178	2.080	0.786	0.795	0.129	0.370	0.499	0.244	0.299	0.457	0.916	0.259	0.325
		90	0.386	0.367	0.072	0.176	2.062	0.796	0.757	0.148	0.363	0.511	0.247	0.285	0.468	0.916	0.290	0.290
		180	0.421	0.341	0.084	0.153	2.100	0.884	0.716	0.176	0.321	0.497	0.275	0.269	0.456	0.918	0.354	0.231
		365	0.379	0.357	0.081	0.183	2.022	0.766	0.722	0.164	0.370	0.534	0.238	0.271	0.491	0.919	0.307	0.264
Neat Paste; Cement 14930J; Density of cement = 3.218 g/cc; v_c = 0.3108																		Avg. 0.290
14930J		330	0.6431	—	0.1404	0.2157	1.918	1.233	—	0.269	0.414	0.683	0.383	—	0.617	0.903	0.394	0.246
Cement 15007J (15372); Density of cement = 3.189 g/cc; v_c = 0.313																		
9–4	.318	7	0.650	0.120	0.082	0.148	2.198	1.429	0.264	0.180	0.325	0.505	0.448	0.099	0.453	0.897	0.356	0.290
		14	0.637	0.131	0.089	0.142	2.194	1.398	0.287	0.195	0.312	0.507	0.438	0.108	0.454	0.895	0.385	0.273
		28	0.641	0.125	0.099	0.136	2.194	1.406	0.274	0.217	0.298	0.515	0.441	0.103	0.456	0.885	0.421	0.273
		56	0.666	0.081	0.112	0.141	2.168	1.444	0.176	0.243	0.306	0.549	0.453	0.066	0.481	0.876	0.443	0.280
		90	0.673	0.078	0.116	0.133	2.175	1.464	0.170	0.252	0.289	0.541	0.459	0.064	0.477	0.882	0.466	0.240
		180	0.661	0.090	0.121	0.128	2.182	1.442	0.196	0.264	0.279	0.543	0.452	0.074	0.474	0.873	0.486	0.261

(Continued p. 678.)

TABLE 5-5—CONTINUED

Series 254-9

(1)	(2)	(3)	(4)	(5)	(6)	(7)	(8)	(9)	(10)	(11)	(12)	(13)	(14)	(15)	(16)	(17)	(18)	(19)
			Grams per g of saturated sample					Grams per cc of saturated sample					Vols/unit vol. sat'd sample					
Ref. No.	w/c	Age, days	Cement	Silica	Non-evap. water	Evap. water	Density, saturated, g/cc	Cement	Silica	Non-evap. water	Evap. water	Total water	Cement	Silica	1 − (cement + silica)	Avg. sp. vol. of water, v_t	$\frac{w_n}{w_t}$	$\frac{1-v_t}{w_n/w_t}$
Cement 15007 J (15372); Density of cement = 3.189 g/cc; v_c = 0.313 (Continued)																		
9–5	.432	7	0.503	0.262	0.067	0.168	2.120	1.066	0.555	0.142	0.356	0.498	0.334	0.209	0.457	0.918	0.285	0.288
		14	0.489	0.278	0.073	0.160	2.120	1.037	0.589	0.155	0.339	0.494	0.325	0.221	0.454	0.919	0.314	0.258
		28	0.485	0.277	0.083	0.155	2.114	1.025	0.586	0.175	0.328	0.503	0.321	0.220	0.459	0.912	0.348	0.253
		56	0.510	0.234	0.094	0.161	2.097	1.069	0.491	0.197	0.338	0.535	0.335	0.185	0.480	0.897	0.368	0.280
		90	0.508	0.233	0.098	0.161	2.085	1.059	0.486	0.204	0.336	0.540	0.332	0.183	0.485	0.898	0.378	0.270
		180	0.410	0.364	0.083	0.143	2.132	0.874	0.776	0.177	0.305	0.482	0.274	0.292	0.434	0.900	0.367	0.273
9–6	.582	7	0.411	0.380	0.064	0.144	2.170	0.892	0.825	0.139	0.312	0.451	0.280	0.310	0.410	0.909	0.308	0.295
		14	0.409	0.374	0.067	0.150	2.136	0.874	0.799	0.143	0.320	0.463	0.274	0.300	0.426	0.920	0.309	0.259
		28	0.405	0.358	0.074	0.162	2.094	0.848	0.750	0.155	0.339	0.494	0.266	0.282	0.452	0.915	0.314	0.270
		56	0.404	0.358	0.082	0.156	2.092	0.845	0.749	0.172	0.326	0.498	0.265	0.282	0.453	0.910	0.345	0.261
		56	0.404	0.358	0.082	0.156	2.004	0.810	0.717	0.164	0.313	0.477	0.254	0.270	0.476	(0.998)	0.344	——
		90	0.401	0.358	0.086	0.166	2.070	0.830	0.741	0.178	0.344	0.522	0.260	0.279	0.461	0.883	0.341	0.343
		180	0.284	0.527	0.060	0.129	2.171	0.617	1.144	0.130	0.280	0.410	0.193	0.430	0.377	0.920	0.317	0.253
Cement 15011J; Density of cement = 3.204 g/cc; v_c = 0.3121																		Avg. 0.273
9–7	.338	7	0.666	0.102	0.076	0.156	2.208	1.471	0.225	0.168	0.344	0.512	0.459	0.085	0.456	0.891	0.328	0.332
		14	0.618	0.163	0.082	0.138	2.214	1.368	0.361	0.182	0.306	0.488	0.427	0.136	0.437	0.895	0.373	0.282
		28	0.655	0.119	0.094	0.143	2.058	1.348	0.245	0.193	0.294	0.487	0.421	0.092	0.487	1.000	0.396	——
		28	0.655	0.119	0.094	0.143	2.206	1.445	0.263	0.207	0.315	0.522	0.451	0.099	0.450	0.862	0.397	0.348
		56	0.634	0.137	0.099	0.129	2.222	1.409	0.304	0.220	0.287	0.507	0.440	0.114	0.446	0.880	0.434	0.277
		90	0.643	0.124	0.106	0.127	2.206	1.418	0.274	0.234	0.280	0.514	0.443	0.103	0.454	0.883	0.455	0.257
		180	0.683	0.069	0.116	0.132	2.176	1.486	0.150	0.252	0.287	0.539	0.464	0.056	0.480	0.891	0.468	0.233
		365	0.683	0.063	0.120	0.134	2.160	1.475	0.136	0.259	0.289	0.548	0.460	0.051	0.489	0.892	0.473	0.228
9–8	.433	7	0.434	0.364	0.053	0.149	2.182	0.947	0.794	0.116	0.325	0.441	0.296	0.299	0.405	0.918	0.263	0.350
		14	0.490	0.268	0.075	0.167	2.115	1.036	0.567	0.159	0.353	0.512	0.323	0.213	0.464	0.906	0.311	0.302
		28	0.493	0.269	0.082	0.157	2.131	1.051	0.573	0.175	0.335	0.510	0.328	0.215	0.457	0.896	0.343	0.304
		28	0.493	0.269	0.082	0.157	2.123	1.047	0.571	0.174	0.333	0.507	0.327	0.215	0.458	0.903	0.343	0.283
		56	0.492	0.266	0.088	0.154	2.120	1.043	0.564	0.187	0.326	0.513	0.326	0.212	0.462	0.901	0.365	0.271
		90	0.515	0.231	0.098	0.156	2.105	1.084	0.486	0.206	0.328	0.534	0.338	0.183	0.479	0.897	0.386	0.267
		180	0.494	0.261	0.098	0.148	2.118	1.046	0.553	0.208	0.313	0.521	0.326	0.208	0.466	0.894	0.399	0.266
9–9	.570	7	0.395	0.384	0.052	0.168	2.116	0.836	0.813	0.110	0.355	0.465	0.261	0.306	0.433	0.931	0.237	0.291
		14	0.403	0.386	0.063	0.149	2.152	0.867	0.831	0.136	0.321	0.457	0.271	0.312	0.417	0.912	0.298	0.295
		28	0.387	0.388	0.068	0.156	2.130	0.824	0.826	0.145	0.332	0.477	0.257	0.311	0.432	0.906	0.304	0.309
		56	0.371	0.389	0.072	0.168	2.080	0.772	0.809	0.150	0.349	0.499	0.241	0.304	0.455	0.912	0.301	0.292
		90	0.400	0.352	0.082	0.167	2.088	0.836	0.735	0.171	0.349	0.520	0.261	0.276	0.463	0.890	0.329	0.335
		180	0.392	0.381	0.084	0.144	2.127	0.834	0.810	0.179	0.306	0.485	0.260	0.305	0.435	0.897	0.369	0.280
(Concluded opposite page.)																		Avg. 0.290

(Table 5-5 concluded)

Cement 15013J; Density of cement = 3.162 g/cc; v_e = 0.3162

9–10	.324	7	0.686	0.066	0.102	0.146	2.176	1.493	0.144	0.222	0.318	0.540	0.472	0.054	0.474	0.878	0.411	0.297
		14	0.689	0.057	0.113	0.140	2.174	1.498	0.124	0.246	0.304	0.550	0.474	0.047	0.479	0.871	0.447	0.289
		28	0.680	0.063	0.116	0.141	2.168	1.474	0.136	0.251	0.306	0.557	0.466	0.051	0.483	0.867	0.451	0.295
		56	0.680	0.057	0.123	0.140	2.155	1.465	0.123	0.265	0.302	0.567	0.463	0.046	0.491	0.866	0.467	0.287
		90	0.676	0.062	0.129	0.133	2.158	1.459	0.134	0.278	0.287	0.565	0.461	0.050	0.489	0.865	0.492	0.274
		180	0.558	0.230	0.105	0.106	2.235	1.247	0.514	0.235	0.237	0.472	0.394	0.193	0.413	0.875	0.498	0.251
9–11	.443	7	0.531	0.233	0.083	0.153	2.112	1.121	0.492	0.175	0.323	0.498	0.354	0.185	0.461	0.926	0.351	0.211
		14	0.504	0.253	0.902	0.151	2.126	1.072	0.538	0.196	0.321	0.517	0.339	0.202	0.459	0.888	0.379	0.296
		28	0.231	0.648	0.041	0.080	2.346	0.542	1.520	0.096	0.188	0.284	0.171	0.572	0.257	0.905	0.338	0.281
		56	0.490	0.251	0.102	0.157	2.088	1.023	0.524	0.213	0.328	0.541	0.323	0.197	0.480	0.887	0.394	0.287
		90	0.433	0.314	0.093	0.151	2.101	0.910	0.660	0.195	0.317	0.512	0.288	0.248	0.464	0.906	0.381	0.246
		180	0.453	0.289	0.107	0.152	2.086	0.945	0.603	0.223	0.317	0.540	0.299	0.227	0.474	0.878	0.413	0.295
9–12	.611	7	0.396	0.401	0.063	0.141	2.170	0.859	0.870	0.137	0.306	0.443	0.272	0.327	0.401	0.905	0.309	0.307
		14	0.406	0.371	0.074	0.149	2.134	0.866	0.792	0.158	0.318	0.476	0.274	0.298	0.428	0.899	0.332	0.305
		28	0.387	0.388	0.079	0.146	2.126	0.823	0.825	0.168	0.310	0.478	0.260	0.310	0.430	0.900	0.351	0.285
		56	0.382	0.383	0.084	0.150	2.106	0.804	0.807	0.177	0.316	0.493	0.254	0.303	0.443	0.899	0.359	0.282
		90	0.301	0.484	0.071	0.145	2.122	0.639	1.027	0.151	0.308	0.459	0.202	0.386	0.412	0.898	0.329	0.310
		180	0.344	0.424	0.084	0.147	2.102	0.723	0.891	0.177	0.309	0.486	0.229	0.335	0.436	0.897	0.364	0.283

Cement 15365; Density of cement = 3.135 g/cc; v_e = 0.319 — Avg. 0.282

9–13	.322	7	0.694	0.059	0.092	0.156	2.147	1.490	0.127	0.198	0.335	0.533	0.475	0.048	0.477	0.895	0.371	0.283
		14	0.671	0.084	0.102	0.144	2.158	1.448	0.181	0.220	0.311	0.531	0.462	0.068	0.470	0.885	0.414	0.278
		28	0.452	0.383	0.067	0.097	2.291	1.036	0.877	0.153	0.222	0.375	0.330	0.330	0.340	0.907	0.408	0.227
		56	0.663	0.081	0.118	0.137	2.157	1.430	0.175	0.255	0.296	0.551	0.456	0.066	0.478	0.868	0.463	0.285
		90	0.668	0.084	0.120	0.128	2.172	1.451	0.182	0.261	0.278	0.539	0.463	0.068	0.469	0.870	0.484	0.269
		180	0.634	0.125	0.115	0.125	2.169	1.375	0.271	0.249	0.271	0.520	0.439	0.102	0.459	0.883	0.479	0.245
9–14	.439	7	0.530	0.248	0.074	0.148	2.156	1.143	0.535	0.160	0.319	0.479	0.365	0.201	0.434	0.906	0.334	0.281
		14	0.513	0.245	0.088	0.154	2.104	1.079	0.515	0.185	0.324	0.509	0.344	0.194	0.462	0.908	0.363	0.253
		28	0.445	0.331	0.082	0.142	2.134	0.950	0.706	0.175	0.303	0.478	0.303	0.265	0.432	0.904	0.366	0.262
		56	0.508	0.232	0.107	0.154	2.084	1.059	0.483	0.223	0.321	0.544	0.338	0.182	0.480	0.882	0.410	0.273
		90	0.498	0.243	0.109	0.150	2.084	1.038	0.506	0.227	0.313	0.540	0.331	0.190	0.479	0.887	0.420	0.269
		180	0.478	0.267	0.106	0.149	2.082	0.995	0.556	0.221	0.310	0.531	0.317	0.209	0.474	0.893	0.416	0.257
9–15	.587	7	0.390	0.409	0.060	0.142	2.154	0.840	0.881	0.129	0.306	0.435	0.268	0.331	0.401	0.922	0.297	0.262
		14	0.407	0.356	0.076	0.161	2.074	0.844	0.738	0.158	0.334	0.492	0.269	0.277	0.454	0.923	0.321	0.271
		28	0.376	0.384	0.079	0.157	2.085	0.784	0.801	0.165	0.327	0.492	0.250	0.301	0.449	0.913	0.335	0.260
		56	0.390	0.360	0.086	0.163	2.053	0.801	0.739	0.177	0.335	0.512	0.255	0.278	0.467	0.912	0.346	0.254
		90	0.387	0.357	0.089	0.167	2.046	0.792	0.730	0.182	0.342	0.524	0.253	0.274	0.473	9.903	0.347	0.280
		180	0.399	0.336	0.102	0.163	—	—	—	—	—	—	—	—	—	—	—	—
9–15A	.244	7	0.7654	—	0.0882	0.1464	2.214	1.695	—	0.195	0.324	0.519	0.541	—	0.459	0.884	0.376	0.309
		14	0.7723	—	0.0972	0.1304	2.240	1.730	—	0.218	0.292	0.510	0.552	—	0.448	0.878	0.427	0.286
		28	0.7676	—	0.1043	0.1282	2.238	1.718	—	0.233	0.287	0.520	0.548	—	0.452	0.869	0.448	0.292
		56	0.7716	—	0.1077	0.1206	2.250	1.727	—	0.241	0.270	0.511	0.551	—	0.449	0.879	0.472	0.257
		90	0.7710	—	0.1120	0.1170	2.248	1.733	—	0.252	0.263	0.515	0.553	—	0.447	0.868	0.489	0.270
		180	0.7790	—	0.1211	0.0999	—	—	—	—	—	—	—	—	—	—	—	—
		270(a)	0.7747	—	0.1310	0.0944	2.264	1.754	—	0.297	0.214	0.511	0.559	—	0.441	0.863	0.581	0.236

Avg. 0.268

TABLE 5-6—COMPOSITIONS OF GRANULAR SAMPLES USED IN ADSORPTION AND OTHER TESTS AND COMPUTATIONS OF MEAN SPECIFIC VOLUME OF TOTAL WATER CONTENT AND OTHER FACTORS—Series 254-11

(1)	(2)	(3)	(4)	(5)	(6)	(7)	(8)	(9)	(10)	(11)	(12)	(13)	(14)	(15)	(16)	(17)	(18)
		Grams per g of saturated sample				Density, saturated, g/cc	Grams per cc of saturated sample					Vols/unit vol. sat'd sample			Avg. sp. vol. of water, v_t	$\frac{w_n}{w_t}$	$\frac{1 - v_t}{w_n/w_t}$
Ref. No.	Age, days	Cement	Silica	Non-evap. water	Evap. water		Cement	Silica	Non-evap. water	Evap. water	Total water	Cement	Silica	1 − (Cement + silica)			
Clinker No. 2; Cement 15758; Density of cement 3.107; v_c = 0.3219; Sp. surf. 1800 (turb.); 3567 (perm.)																	
11–1	28	0.665	0.071	0.114	0.151	2.110	1.403	0.150	0.240	0.319	0.559	0.452	0.056	0.492	0.880	0.429	0.280
11–2	28	0.500	0.237	0.098	0.164	2.038	1.019	0.483	0.200	0.334	0.534	0.328	0.182	0.490	0.918	0.375	0.219
11–1	90	0.659	0.072	0.126	0.148	2.094	1.380	0.151	0.264	0.310	0.574	0.444	0.057	0.499	0.869	0.460	0.285
11–2	90	0.502	0.213	0.112	0.173	2.014	1.011	0.429	0.226	0.348	0.574	0.325	0.161	0.514	0.895	0.394	0.266
Clinker No. 3; Cement 15756; Density of cement 3.174; v_c = 0.3151; Sp. surf. 1800 (turb.); 3060 (perm.)																	
11–3	28	0.658	0.096	0.081	0.166	2.139	1.407	0.205	0.173	0.355	0.528	0.443	0.077	0.480	0.909	0.328	0.277
11–4	28	0.510	0.250	0.068	0.173	2.094	1.068	0.524	0.142	0.362	0.504	0.337	0.197	0.466	0.925	0.282	0.266
11–3	90	0.660	0.092	0.098	0.150	2.162	1.427	0.199	0.212	0.324	0.536	0.450	0.075	0.475	0.886	0.396	0.288
11–4	90	0.509	0.230	0.086	0.175	2.030	1.033	0.467	0.175	0.355	0.530	0.325	0.176	0.499	0.942	0.330	0.176
Clinker No. 4; Cement 15763; Density of cement 3.215; v_c = 0.3110; Sp. surf. 1800 (turb.); 2760 (perm.)																	
11–5	28	0.684	0.073	0.063	0.180	2.148	1.469	0.157	0.135	0.387	0.522	0.457	0.059	0.484	0.927	0.259	0.282
11–6	28	0.534	0.238	0.054	0.175	2.137	1.141	0.509	0.115	0.374	0.489	0.355	0.191	0.454	0.928	0.235	0.306
11–5	90	0.665	0.091	0.089	0.156	2.169	1.442	0.197	0.193	0.338	0.531	0.448	0.074	0.478	0.900	0.364	0.275
11–6	90	0.508	0.237	0.076	0.180	2.078	1.056	0.492	0.158	0.374	0.532	0.328	0.185	0.487	0.915	0.297	0.286
Clinker No. 5; Cement 15761; Density of cement 3.155; v_c = 0.3170; Sp. surf. 1800 (turb.); 2951 (perm.)																	
11–7	28	0.674	0.057	0.109	0.159	2.114	1.425	0.120	0.230	0.336	0.566	0.452	0.045	0.503	0.889	0.406	0.273
11–8	28	0.516	0.208	0.096	0.181	2.038	1.052	0.424	0.196	0.369	0.565	0.333	0.159	0.508	0.899	0.347	0.291
11–7	90	0.672	0.049	0.121	0.158	2.097	1.409	0.103	0.254	0.331	0.585	0.447	0.039	0.514	0.879	0.434	0.279
11–8	90	0.503	0.214	0.107	0.176	2.038	1.025	0.436	0.218	0.359	0.577	0.325	0.164	0.511	0.886	0.378	0.302
Clinker No. 1; Cement 15754; Density of cement 3.135; v_c = 0.3190; Sp. surf. 1800 (turb.); 3417 (perm.)																	
11–9	28	0.657	0.089	0.112	0.143	2.144	1.409	0.191	0.240	0.307	0.547	0.449	0.072	0.479	0.876	0.439	0.282
11–10	28	0.494	0.245	0.097	0.164	2.069	1.022	0.507	0.201	0.339	0.540	0.326	0.191	0.483	0.894	0.372	0.285
11–9	90	0.658	0.079	0.128	0.134	2.136	1.405	0.169	0.273	0.286	0.559	0.448	0.064	0.488	0.873	0.488	0.260
11–10	90	0.493	0.232	0.114	0.161	2.050	1.011	0.476	0.234	0.330	0.564	0.323	0.179	0.498	0.883	0.415	0.282
Clinker No. 1; Cement 16213; Density of cement 3.135; v_c = 0.3190; Sp. surf. 2426 (perm.)																	
11–11	28	0.494	0.265	0.085	0.156	2.110	1.042	0.559	0.179	0.329	0.508	0.332	0.210	0.458	0.902	0.352	0.278
Clinker No. 1; Cement 16214; Density of cement 3.135; v_c = 0.3190; Sp. surf. 2923 (perm.)																	
11–12	28	0.491	0.259	0.091	0.159	2.086	1.024	0.540	0.190	0.332	0.522	0.327	0.203	0.470	0.900	0.364	0.275

(Concluded opposite page)

(Table 5-6 concluded)

Clinker No. 4; Cement 16198; Density of cement 3.215; v_c = 0.3110; Sp. surf. 3200 (perm.)																	
11–13	28	0.503	0.258	0.055	0.184	2.104	1.058	0.543	0.116	0.387	0.503	0.329	0.204	0.467	0.928	0.231	0.312
Clinker No. 4; Cement 15669; Density of cement 3.215; v_c = 0.3110; Sp. surf. 3810 (perm.)																	
11–14	28	0.551	0.201	0.060	0.188	2.082	1.147	0.418	0.125	0.391	0.516	0.357	0.157	0.486	0.942	0.242	0.240

Avg. 0.274

TABLE 5-7—COMPOSITONS OF GRANULAR SAMPLES USED IN ADSORPTION AND OTHER TESTS AND COMPUTATIONS OF MEAN SPECIFIC VOLUME OF TOTAL WATER CONTENT AND OTHER FACTORS—Series 254-13

(1)	(2)	(3)	(4)	(5)	(6)	(7)	(8)	(9)	(10)	(11)	(12)	(13)	(14)	(15)	(16)	(17)	(18)
		Grams per g of saturated sample					Grams per cc of saturated sample					Vols/unit vol. sat'd sample					
Ref. No.	SO_3 Content of cement, %	Cement	Silica	Non-evap. water	Evap. water	Density, saturated, g/cc	Cement	Silica	Non-evap. water	Evap. water	Total water	Cement	Silica	1 − (Cement + silica)	Avg. sp. vol. of water, v_t	$\frac{w_n}{w_t}$	$\frac{1 - v_t}{w_n/w_t}$
Clinker No. 1 (15367); Density of cement* = 3.135; v_c = 0.319																	
13–1	1.5	0.428	0.306	0.092	0.175	2.034	0.871	0.622	0.187	0.356	0.543	0.278	0.234	0.488	0.899	0.344	0.294
13–2	1.9	0.436	0.312	0.092	0.160	2.067	0.901	0.645	0.190	0.331	0.521	0.287	0.243	0.470	0.902	0.365	0.269
13–3	2.4	0.428	0.306	0.089	0.177	2.027	0.868	0.620	0.180	0.359	0.539	0.277	0.233	0.490	0.909	0.334	0.272
13–4	3.5	0.429	0.306	0.083	0.182	3.067	0.887	0.633	0.172	0.376	0.548	0.283	0.238	0.479	0.874	0.314	0.401
Clinker No. 1 (15367); Density of cement* = 3.135; v_c = 0.319																	
13-1B	1.5	0.427	0.305	0.090	0.178	2.026	0.865	0.618	0.182	0.361	0.543	0.276	0.232	0.492	0.906	0.335	0.280
13-2B	1.9	0.428	0.306	0.092	0.173	2.028	0.868	0.621	0.187	0.351	0.538	0.277	0.233	0.490	0.911	0.348	0.256
13-3B	2.4	0.428	0.306	0.092	0.174	2.087	0.893	0.639	0.192	0.363	0.555	0.285	0.240	0.475	0.856	0.346	0.415
14-4B	3.5	0.426	0.305	0.087	0.182	1.969	0.839	0.601	0.171	0.358	0.529	0.268	0.226	0.506	0.957	0.323	0.133
Clinker No. 3 (15623); Density of cement* = 3.175; v_c = 0.315																	
13–5	1.5	0.436	0.312	0.066	0.186	2.040	0.889	0.636	0.135	0.379	0.514	0.280	0.239	0.481	0.936	0.263	0.243
13–6	2.0	0.433	0.309	0.065	0.193	2.028	0.878	0.627	0.132	0.391	0.523	0.277	0.236	0.487	0.931	0.252	0.274
13–7	2.5	0.433	0.309	0.066	0.193	2.016	0.873	0.623	0.133	0.389	0.522	0.275	0.234	0.491	0.941	0.255	0.231
13–8	3.5	0.431	0.308	0.062	0.199	2.022	0.871	0.623	0.125	0.402	0.527	0.274	0.234	0.492	0.934	0.237	0.278
Clinker No. 5 (15670); Density of cement* = 3.155; v_c = 0.317																	
13–9	1.5	0.428	0.306	0.085	0.181	2.031	0.869	0.621	0.173	0.368	0.541	0.275	0.233	0.492	0.909	0.320	0.285
13–10	2.0	0.430	0.307	0.083	0.179	2.033	0.874	0.624	0.169	0.364	0.533	0.277	0.235	0.488	0.916	0.317	0.265
13–11	2.5	0.426	0.304	0.082	0.187	2.018	0.860	0.613	0.165	0.377	0.542	0.273	0.230	0.497	0.917	0.304	0.273
13–12	3.5	0.430	0.307	0.079	0.183	2.027	0.872	0.622	0.160	0.371	0.531	0.276	0.234	0.490	0.923	0.301	0.255
Clinker No. 2 (15498); Density of cement* = 3.108; v_c = 0.322																	
13–13	1.5	0.443	0.315	0.092	0.150	2.010	0.890	0.633	0.185	0.302	0.487	0.286	0.238	0.476	0.977	0.380	0.606
13–14	2.0	0.442	0.316	0.088	0.154	2.052	0.907	0.648	0.181	0.316	0.497	0.292	0.244	0.464	0.934	0.364	0.181

*Effect of varying gypsum neglected.

TABLE 5-8—COMPOSITIONS OF GRANULAR SAMPLES USED IN ADSORPTION AND OTHER TESTS AND COMPUTATIONS OF MEAN SPECIFIC VOLUME OF TOTAL WATER CONTENT AND OTHER FACTORS

Series 254-14. Age, 28 days

(1)	(2)	(3)	(4)	(5)	(6)	(7)	(8)	(9)	(10)	(11)	(12)	(13)	(14)	(15)	(16)	(17)	(18)	(19)
			Grams per g of saturated sample					Grams per cc of saturated sample					Vols/unit vol. sat'd sample					
Cement No.	Ref. No.	v_c	Cement	Silica	Non-evap. water	Evap. water	Density, saturated, g/cc	Cement	Silica	Non-evap. water	Evap. water	Total water	Cement	Silica	$1 -$ (cement + silica)	Avg. sp. vol. of water, v_t	$\frac{w_n}{w_t}$	$1 - \frac{v_t}{w_n/w_t}$
Cured 24 hr. at 43 C, 27 days at 23 C																		
15954	14–1	0.3176	0.437	0.312	0.085	0.166	2.064	0.902	0.644	0.175	0.343	0.518	0.286	0.242	0.472	0.911	0.338	0.263
15756	14–5	0.3111	0.436	0.311	0.066	0.187	2.040	0.889	0.634	0.135	0.381	0.516	0.277	0.238	0.485	0.940	0.262	0.229
16215	14–11	0.3190	0.430	0.307	0.087	0.176	2.037	0.876	0.625	0.177	0.359	0.536	0.279	0.235	0.486	0.907	0.330	0.282
16195	14–12	0.3216	0.438	0.313	0.080	0.170	2.078	0.910	0.650	0.166	0.353	0.519	0.293	0.244	0.463	0.892	0.320	0.338
Cured 28 days at 23 C																		
15954	14–2	0.3176	0.433	0.309	0.087	0.171	2.051	0.888	0.634	0.178	0.351	0.529	0.282	0.238	0.480	0.907	0.336	0.277
15756	14–4	0.3111	0.434	0.310	0.067	0.189	2.038	0.884	0.632	0.137	0.385	0.522	0.275	0.238	0.487	0.933	0.262	0.256
16186	14–7	0.3190	0.427	0.305	0.091	0.177	2.030	0.867	0.619	0.185	0.359	0.544	0.277	0.233	0.490	0.901	0.340	0.291
16195	14–8	0.3216	0.426	0.305	0.086	0.183	2.024	0.862	0.617	0.174	0.370	0.544	0.277	0.232	0.491	0.903	0.320	0.303
Cured 24 hr. at 5 C, 27 days at 23 C																		
15756	14–3	0.3111	0.436	0.312	0.068	0.184	2.055	0.896	0.641	0.140	0.378	0.518	0.279	0.241	0.480	0.927	0.270	0.270
Cured 24 hr. at 4 C, 27 days at 23 C																		
16186	14–9	0.3190	0.425	0.304	0.090	0.180	2.022	0.859	0.615	0.182	0.364	0.546	0.274	0.231	0.495	0.907	0.333	0.279
16195	14–10	0.3216	0.433	0.310	0.085	0.172	2.059	0.892	0.638	0.175	0.354	0.529	0.287	0.240	0.473	0.894	0.331	0.320
Autoclaved at 350 F for 6 hr.																		
15756	14–6	0.3111	0.459	0.328	0.074	0.138	2.240	1.028	0.735	0.166	0.309	0.475	0.320	0.276	0.404	0.851	0.349	0.427

tained, the air contents were considerable. However, it is believed that the small granules taken for these measurements were smaller than most of the air voids and therefore would contain little air, if any.

Column 15 was obtained by dividing the figures given in column 14 by corresponding figures in column 12.

Plots of v_t vs. w_n/w_t for most of these data are given in Fig. 5-1 to 5-4.

Since v_t depends on the measured volume of the saturated, granular samples, and the computed volume of the original cement and (when present) pulverized silica, small inaccuracies in measurement have rather large effects on v_t. Moreover, any inaccuracies in the corresponding figures for non-evaporable water, due either to errors or to inadvertent departures from the standard drying condition discussed earlier, contribute to random scattering of the plotted points. Nevertheless, when all the plots are considered together, they support the conclusion that the total water content is made up of two components, one being free water and the other being water having a mean specific volume less than 1.0.

This conclusion may not seem wholly convincing in view of the rather wide scatter of points in some cases and the fewness of the points in others. If so, one should consider that the main factor determining the magnitude of w_n is the length of the period of hydration. In the graphs for Series 254-9, Fig. 5-3, the points represent ages ranging from 7 days to 6 months or a year. In every case, the sample at *zero age* would have to be represented by a point at $w_n = 0$, $v_t = 1.0$, for at that time all the water would obviously be free. Consequently, the only uncertainty is whether the real relationship is a straight line beginning at $v_t = 1.0$, or a curve, beginning at that point. If the real relationship were a curve bending upward from the line as now drawn, it would indicate that the specific volume of the compressed water that is combined when w_n is large is greater than when w_n is small. If the curve turned downward, the indication would be the opposite. In either case the indication would be that the products formed at one time would be different from those formed in the same paste at another time.

There is some basis for believing that the products formed at first are different from those formed later. During the first few hours the reactions with gypsum are completed, as mentioned before. Also, the products formed from the finest flour in the cement would differ from those formed later because of the difference between the composition of the flour and that of the coarser particles. However, the effects are apparently not large. This was shown earlier when discussing the relationship between V_m and w_n (Part 3). All things considered, it seems justifiable to assume that one straight line represents the data for any given cement and accordingly that both B eq. (6) and v_d eq. (7) are constant for a given cement.

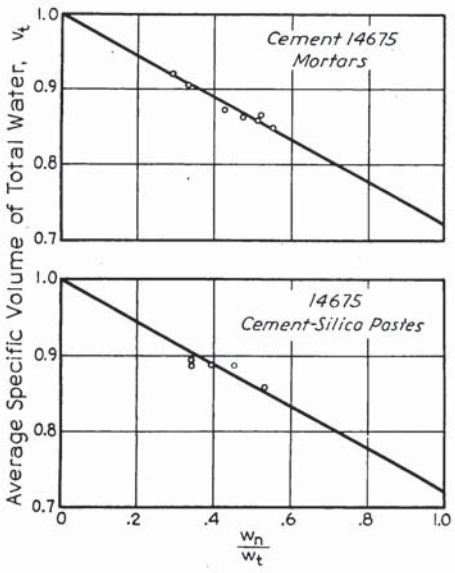

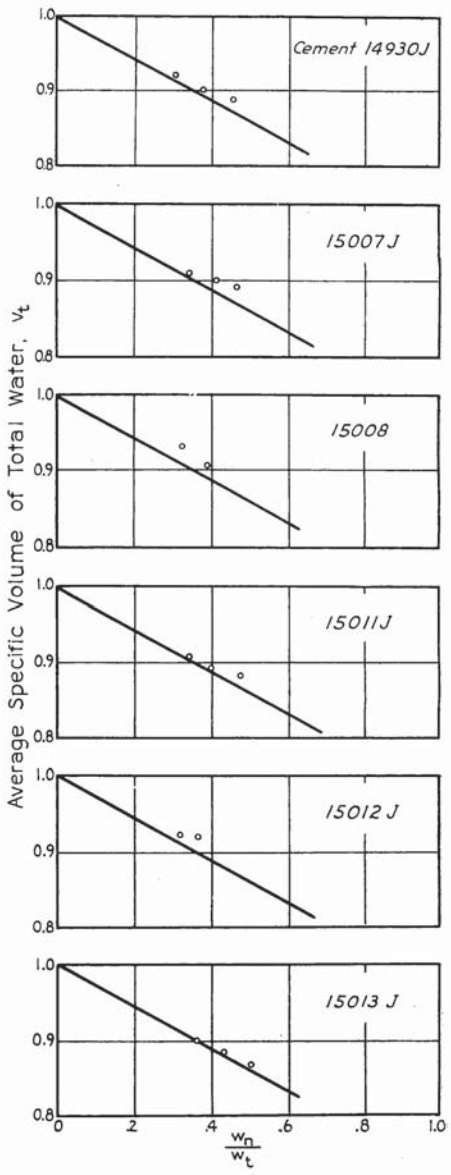

Fig. 5-1 (above)—v_t versus $\frac{w_n}{w_t}$
Series 254-7

Fig. 5-2 (right)—v_t versus $\frac{w_n}{w_t}$
Series 254-8

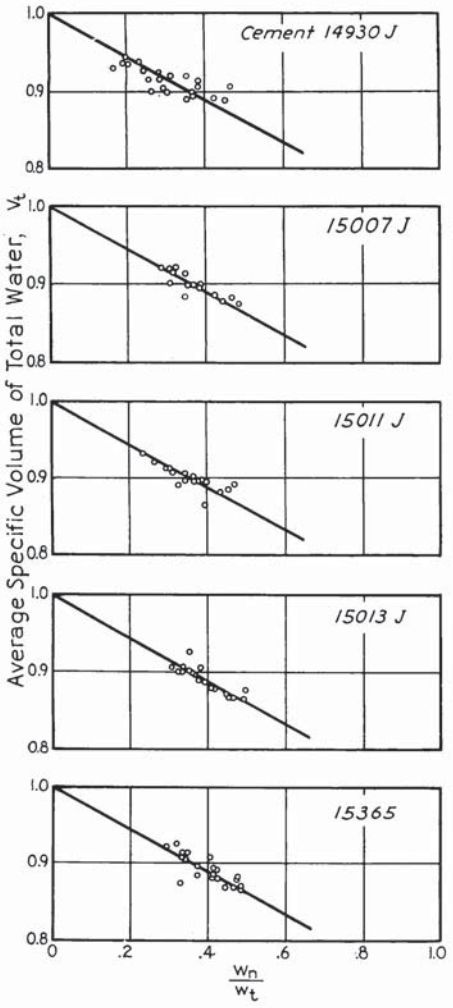

Fig. 5-3—v_t versus $\frac{w_n}{w_t}$

Series 254-9

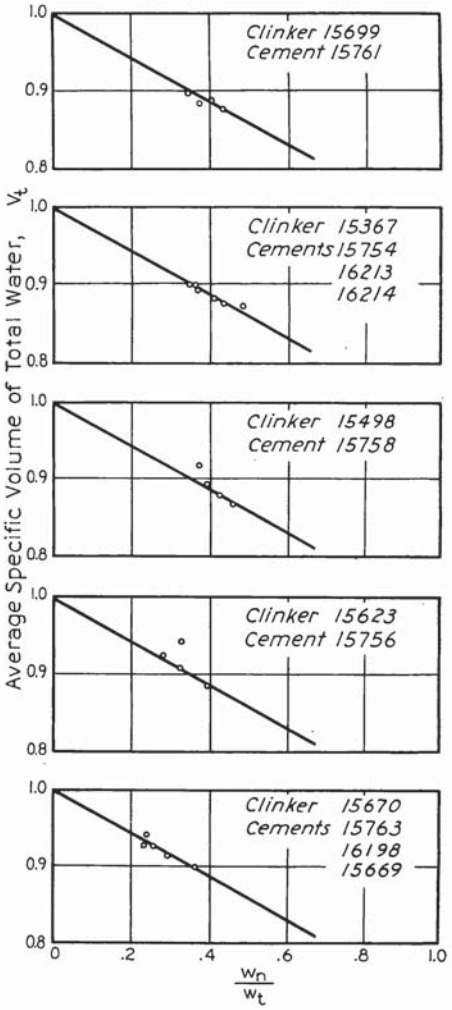

Fig. 5-4—v_t versus $\frac{w_n}{w_t}$

Series 254-11, 254-13

Mean ratio of $(1 - v_t)$ to w_n/w_t

As stated before, the compressed part of the total water is considered to be the sum of the non-evaporable water and the adsorbed water. The degree of compression of the adsorbed water is probably the same for all cements. This is indicated from data on the heat of adsorption already considered. The degree of "compression" of the non-evaporable water might be different for different cements, however, since there are differences in the proportions of the various reaction products. For example, the proportion of $Ca(OH)_2$ should depend on the C_3S content of the clinker, and the amount of aluminate-hydrates should vary with the C_3A content. With this in mind, the data were classified according to C_3A content, and for each class the values of $\frac{(1 - v_t)}{w_n/w_t}$ were averaged separately. The results are shown in Table 5-9.

Application of methods of statistical analysis indicate that the largest difference between the mean ratios of the group are not larger than could be accounted for by chance variation alone. Nevertheless, some of the variation must be due to differences in the chemical compositions of the cements, as mentioned above.

On the whole, the data seem to support the presumption that $(1 - v_t)/(w_n/w_t)$ varies with the composition of the cement but at the same time they show the influence of cement composition to be small. Certainly the random variations are too great to warrant trying to evaluate the effect of cement composition from these data. Accordingly, eq. (8) below, representing the grand average, will be applied to all cements alike in further treatments of the data:

$$v_t = 1 - 0.279\, w_n/w_t \quad \ldots\ldots\ldots\ldots\ldots\ldots\ldots\ldots\ldots\ldots\ldots\ldots (8)$$

According to Table 5-9, this equation will give v_t for an individual item with a probable error of about 7 percent. The degree of agreement between the data and the equation is shown in Fig. 5-1 to 5-4. In each diagram the line represents eq. (8).

TABLE 5-9—RATIO OF MEAN SPECIFIC VOLUME OF TOTAL WATER TO w_n/w_t

Type of cement	Mean $\frac{1 - v_t}{w_n/w_t}$	Probable error of mean	Probable error of single value	Number of samples
Low C_3A	0.279	± .0028	± .0259	88
Med. C_3A	0.283	± .0024	± .0137	31
High C_3A	0.278	± .0015	± .0129	70
Grand avg.	0.279	± .0015	± .0200	189

Lower limit of mean specific volume of total water

From eq. (8) it is apparent that the greater the weight-fraction of non-evaporable water, w_n/w_t, the smaller will be the mean specific volume, v_t. However, there is an upper limit to w_n/w_t and hence a lower limit to v_t. This conclusion follows from the fact that the evaporable water content of a saturated paste cannot be less than about $4V_m$ (see Part 3). That is, the minimum amount of evaporable water is

$$w_e = w_t - w_n = 4V_m \text{ (min.)} ,$$

or

$$\frac{w_t}{w_n} - 1 = \frac{4V_m}{w_n} \text{ (min.)} .$$

Since $V_m/w_n = k$, for a given cement,

$$\frac{w_t}{w_n} = 1 + 4k \text{ (min.)} ,$$

or

$$\frac{w_n}{w_t} = \frac{1}{1 + 4k} \text{ (max.)} .$$

From the values for k, i.e., V_m/w_n, for different types of cement given in Table 3-6, Part 3, the limits of w_t/w_n and w_n/w_t were computed with the results given in Table 5-10.

TABLE 5-10—LIMITS OF w_n/w_t AND w_t/w_n FOR DIFFERENT TYPES OF CEMENT

	Type of Cement	$\frac{V_m}{w_n}$ $(=k)$	$\frac{w_t}{w_n}$	$\frac{w_n}{w_t}$
Type I	Normal C_3A	0.255	2.02	0.50
	High C_3A	0.256	2.02	0.50
Type II	High iron	0.259	2.04	0.49
	High silica	0.279	2.12	0.47
Type III	Normal C_3A	0.238	1.99	0.50
	High C_3A	0.240	1.96	0.51
Type IV	High iron	0.282	2.13	0.47
	High silica	0.277	2.11	0.47

From these results we may conclude that *the non-evaporable water cannot become more than about one-half the total water content of a saturated paste.*

From the data given in Table 5-10 and the empirical relationship given in eq. (8), the mean of the specific volumes of the non-evaporable water and gel water can be estimated. That is, when w_n/w_t is a maximum,

w_n/w_t is between 0.47 and 0.51. For most cements w_n/w_t would be about 0.50. Hence, the lower limit of v_t is about

$$(v_t) \text{ min.} = 1 - (0.279 \times 0.50) = 0.860.$$

Since these considerations pertain to pastes in which the total evaporable water $= 4V_m$, hence, to pastes containing no space outside the gel, it follows that *0.860 is the mean specific volume of the total water in a saturated sample that contains no capillary water outside the gel.*

Estimation of the bulk volume of the solid phase and volume of capillary water

With the mean of the specific volumes of the gel water and non-evaporable water established, as given above, it is possible to compute the *bulk volume* of the solid phase and the volume of capillary water at any stage of hydration.

The bulk volume of the solid phase is here defined as the sum of the absolute volumes of the solid material in the hardened paste and the volume of the pores that are characteristic of the gel. In other words, it is the sum of the volumes of the gel-substance, the pores characteristic of the gel, other hydrates, and residues of unhydrated clinker. Or, for a saturated paste, the bulk volume of the solid phase is the sum of the volumes of the solids plus the volume of the gel water. It differs from the over-all volume of the paste by the volume of the capillary water.

The volume-composition of a unit volume of paste can be expressed in terms of its weight-composition as follows:

$$c\,v_c + (w_n + w_g)v_d + w_c = 1 \quad ,$$

where

c = weight of cement, g per cc of saturated paste,
w_n = weight of non-evaporable water, g per cc of saturated paste,
w_g = weight of gel water,* g per cc of saturated paste,
w_c = weight or volume of capillary water, g per cc of saturated paste,
v_c = specific volume of original cement, and
v_d = mean specific volume of $(w_n + w_g)$.

Let

$$V_B = 1 - w_c = c\,v_c + (w_n + w_g)v_d$$

where

V_B = bulk volume of solid phase.

Since $w_g = 4V_m$, and $V_m = kw_n$ (see Part 3), $w_g = 4kw_n$.
Hence,

$$V_B = c\,v_c + w_n(1 + 4k)v_d \quad \ldots\ldots\ldots\ldots\ldots\ldots\ldots\ldots (9)$$

This equation holds for $V_B = 0$ to $V_B = 1.0$.

*In this equation w_g, the weight of the gel water, may be identical with w_a, the weight of the adsorbed water appearing in eq. (4). However, until this is proved it is necessary to assume that a saturated gel may contain some water held by capillary condensation, that is, that gel water may comprise both adsorbed water and capillary water. However, the term "capillary water" as used in this discussion includes only the water that is in excess of the gel water.

For an average Type I cement, for which $k = 0.255$ (see Table 5-10) and $v_c = 0.315$, and for $v_d = 0.860$ as given above, this reduces to

$$\frac{V_B}{c\,v_c} = 1 + 5.5\,\frac{w_n}{c} \qquad \text{.....(10)}$$

The significance of this equation is illustrated in Fig. 5-5. This diagram gives the bulk volume of the solid phase, or of capillary water, per unit volume of paste at any stage of hydration for any paste. For example, if a paste was originally 0.3 cement and 0.7 water by absolute volume, by the time it had hydrated to an extent such that the non-evaporable water is 0.2 g per g of original cement, the bulk volume of the solid phase will be 0.63 and the volume of the capillary water will be 0.37 cc per cc of paste. The other lines give the compositions at lesser degrees of hydration. At $w_n/c = 0$, a point on the line gives, of course, the original water or cement content of the fresh paste, by absolute volume. The increase in volume due to hydration is also clearly seen in this diagram.

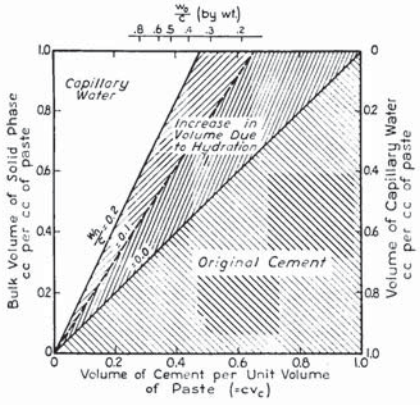

Fig. 5-5—Graphical illustration of eq. (10)

$$V_B = \left[1 + 5.5\frac{w_n}{c}\right] cv_c$$

It should be noted that for any given stage of hydration (given w_n/c) there is a certain cement content above which the paste can contain no capillary water. For example, as shown in Fig. 5-5, when $w_n/c = 0.1$, capillary-water content is zero when the absolute volume of the original cement is 0.65 cc per cc of paste; or, when $w_n/c = 0.2$, $w_c = 0$ when the cement content of the paste is 0.48.

Conversely, for a given cement content there is a degree of hydration at which capillary water disappears. This conclusion is restricted, however, by the fact that for any given cement, w_n/c cannot exceed a certain limit, which is usually about 0.25. This topic will be considered further after the following discussion of the *absolute* volume of the solid phase in hardened paste.

ESTIMATION OF THE ABSOLUTE VOLUME OF THE SOLID PHASE

The absolute volume of the solid phase in hardened paste is defined here as the sum of the volumes of all the hydrated solids and the volume of the unreacted cement. For a saturated paste it differs from the overall volume by the volume of the evaporable water and from the bulk volume of the solid phase by the volume of the gel water. It cannot be determined from the weight of the evaporable water because the mean specific volume of the evaporable water varies with the porosity of the paste and the extent of hydration of the cement. For that reason, attempts to measure the specific volume of the solid phase were made.

Method of measuring volume of solid phase

In preliminary work, the volume of the solid phase was computed from the displacement of the dried granules in water and in other liquids. Owing to the effects of adsorption and to other factors which will be discussed presently, it was necessary to adopt an inert gas as the displacement medium and to develop special apparatus—a volumenometer—for the purpose. This apparatus and its operation are described below.

The apparatus developed for measuring the volume of the solid phase in a hardened paste is illustrated in Fig. 5-6. The volumenometer proper is that part, shown with surrounding water bath, which is located between stopcocks, 1, 2, and 5. This comprises:

(1) A sample bulb, S, which is joined to the rest of the apparatus through a standard-taper, ground-glass joint, and which can be cut off from communication with the rest of the system by means of stopcock 3.

(2) A mercury barometer, B, for measuring the pressure within the volumenometer.

(3) A burette bulb, V, the free volume of which can be altered at will by introducing or withdrawing mercury through stopcock 5, thus altering the gas pressure within the volumenometer.

(4) A stopcock, 4, which enables the sample bulb to be evacuated without evacuating the rest of the volumenometer.

Stopcock 2 connects with a line to the vacuum pump. Beyond stopcock 5 is a mercury reservoir R. The pressure in the volumenometer is maintained at somewhat less than atmospheric so that mercury will siphon into bulb V when R is open to the air and stopcock 5 is open. To withdraw mercury from V, the side-tube on R is connected to the vacuum pump by means of rubber tube T and is evacuated before stopcock 5 is opened.

Stopcock 1 connects the volumenometer to a helium reservoir H in direct communication with a mercury manometer M, which gives the

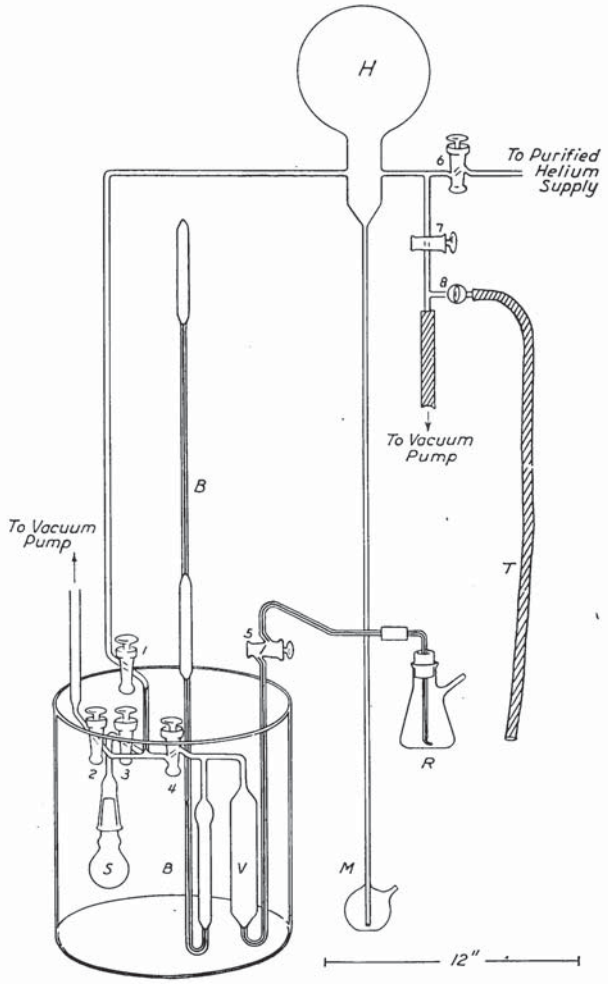

Fig. 5-6

difference between atmospheric and helium pressures. Stopcock 6 connects with the helium supply through two cold traps (not shown) filled with activated charcoal for removing impurities.

Tests are made with the volumenometer to obtain the free volume of the sample bulb S (up to cock 3) with and without a sample in place. The absolute volume of the sample is then found by difference. Volumes are measured by determining the volume of mercury that must be admitted to bulb V in order to restore the helium pressure in the volumenometer after the cock to the evacuated sample bulb is opened.

At the start of a volume measurement the mercury is withdrawn from bulb V until only the capillary remains filled. The flask R with

its content of mercury is then removed, weighed, and replaced. Next, the volumenometer inclusive of the sample bulb S is evacuated through cock 2 using a mercury diffusion pump backed by a Cenco-Hyvac pump. If the volumenometer is already filled with pure helium beyond stopcock 4, this cock can be left closed. After evacuation, stopcocks 2 and 3 are closed and 4 is opened. Helium is then admitted through cock 1 until the desired pressure, somewhat less than atmospheric, is obtained. Readings are taken on the lower level of mercury in barometer B until a steady, reliable value is obtained. A micrometer microscope reading to 0.001 mm is used. After the reading has been obtained, a little mercury is withdrawn to flask R to eliminate any air that may have become trapped at the mouth of the siphon-tube when the flask was replaced after the previous weighing. This clears the line for subsequent manipulations.

Next, stopcock 3 is opened, admitting helium to the sample bulb, and the pressure drops. The pressure is then restored by opening stopcock 5, thus allowing mercury to flow into bulb V. The mercury content of V is adjusted until the reading taken on barometer B is the same as before the helium was admitted to the sample bulb. The apparatus is allowed to stand in this condition with further additions of mercury when necessary, until it is obvious that the desired reading is being maintained. Then the weight of flask R and its content of mercury is found and subtracted from the previous weight. When the weight of mercury given by this difference is multiplied by the specific volume of mercury, the volume of the free space in the sample bulb is obtained.

When bulb S contains a paste sample, the times required for evacuation and for helium contact are necessarily much longer than when the volume of the empty bulb is measured. Experience with cement pastes has indicated that overnight pumping out and one or more days of contact with the helium are advisable.

Choice of displacement medium

The displacement medium was chosen on the basis of results of preliminary tests given in Table 5-11. The object in making these measurements was to find a medium that would measure the space occupied by the evaporable water, or its complement, the space occupied by solids. The medium should be able to penetrate any region that can be reached by water, without undergoing the volume change that water does.

The upper half of the table represents data obtained by pycnometer measurements; the lower half represents results obtained with gases as displacement media using an earlier form of the volumenometer described above. These data were obtained when the methods were being

TABLE 5-11

Displacement-fluid	Volume of 1 g of dry sample for samples indicated: (cc)							
	20Q	1S	39	40	41	42	62	N.B.
Liquid displacement fluids								
Water	.395	—	.392	—	.389	.391	—	.450
Acetone	.408	.404	—	—	—	—	.424	—
Carbon tetrachloride	—	—	—	—	—	—	.465	—
Toluene	.429	.444	—	—	—	—	—	—
Gaseous displacement fluids								
Air	—	—	.327	.362	.336	.338	.312	—
Hydrogen	—	—	.392	.422	.392	.396	—	.206
Helium	.424	.433	—	—	—	—	—	.420

N. B.—Silica-gel Lot 15106.

developed and may not be very accurate; however, they serve well enough for the present purpose.

The wide differences among the results shown in Table 5-11 are due, we presume, to such factors as differences in size of molecule and differences in the interaction between the solid and the fluid. The size of the molecules of the various gases is about the same as that of water, or slightly smaller; but the organic liquids have molecules considerably larger than the water molecule, as shown by the following data:

Kind of liquid	Molar volume	Relative volume
Water	18	1.0
Acetone	73	4.0
Carbon tetrachloride	96	5.3
Toluene	106	5.9

Since the sizes of the molecules of the organic liquids ranged from four to six times that of the water molecule, the gases were preferable so far as this factor is concerned.

Among the gases, air and hydrogen proved to be unsatisfactory because they were adsorbed by the solid material. In air, the apparent specific volume of the hydrated cement appeared to be little or no higher than that of the original cement. This obvious absurdity was probably due mainly to the adsorption of oxygen. Hydrogen is adsorbed also; it happened to give apparent displacements virtually the same as those in water. These results with air and hydrogen left only the inert gases as being able to meet the requirements with respect to molecule-size and absence of interaction, for these gases have small molecules and besides

are not adsorbed to a measurable degree at ordinary temperature and pressure. Helium was chosen because it was readily available and had been used by others for the purpose.[1]

It cannot be said that the displacement of a sample in helium is an accurate basis for computing the space that had been occupied by evaporable water. An inaccuracy would arise from the salts that appear as solids in the dry paste but which are in solution in the saturated paste. The error from this source is probably small. Another inaccuracy, perhaps more serious, arises from the ability of water to swell the solid and thus possibly to open up and enter regions that are inaccessible to an inert gas. Whether or not helium is excluded from any regions accessible to water is not known. The existence of such regions does not necessarily imply an inaccuracy in the helium determination. That is, if the loss of water from such a region causes a shrinkage equal to the volume of water lost, the helium measurement would correctly indicate the density of the solid phase and the space available to the water even though the helium were not able to penetrate it. However, if the volume change in such a region is not equal to the volume of water lost from that region, the helium displacement will not accurately indicate the space available to water. This is a question which must be left open for the present. However, it might be noted that the possibility of a gel-shrinkage equal to the amount of water removed from the gel is not as remote as might at first be supposed. Although it is true that the over-all volume-change is only about 1/40 of the volume of water removed, there is evidence that the gel itself undergoes much greater shrinkage than the specimen as a whole, the difference being due to mechanical restraints.

Other sources of error are inherent in the apparatus itself. Although the apparatus was constructed and manipulated with care, leakage through the stopcocks seemed to occur occasionally. Also, the readings of the mercury level in the barometer with the micrometer microscope were sometimes affected by changes in the shape of the meniscus in the course of the manipulation of the apparatus.

EXPERIMENTAL RESULTS

Many measurements were made on samples of various descriptions, but the original determinations were later found to be in error because not enough time had been allowed for the helium to penetrate the fine structure of the granules. As was found for carbon black by Rossman and Smith,[2] the first period of rapid penetration is followed by a very long period of slow penetration. Different pastes differed in the time required for the attainment of practical equilibrium. In one case 5 or 6 days of contact seemed to be necessary. The procedure finally adopted

was to evacuate the sample for 1 or 2 days and then to maintain contact with the helium for 1, 2, or as many days as were necessary to establish apparent equilibrium. Even under these circumstances it was difficult to attain as good duplicability in repeat tests as was desired, partly because the long time periods increased the effects of any slight leaks. These sometimes developed at the stopcocks.

Test measurements had to be repeated several times to obtain values for the specific volume of the non-evaporable water with an apparent accuracy of about + 0.01 cc per g. Only four different samples were tested by the final technique, but the cements represented a considerable range of compositions. The specific volumes of the dried pastes (about 6 months old) were all found to be close to 0.41 cc per g (density: 2.44 g per cc). From the individual values the specific volume of the non-evaporable water was computed as explained below.

Specific volume of non-evaporable water

The volume of the solid phase can be considered as being equal to the sum of the volumes of original cement and the volume of the non-evaporable water. That is,

$$V_s = c\, v_c + w_n v_n \,, \qquad (11)$$

where

V_s = volume of solid matter,

v_n = hypothetical specific volume of non-evaporable water, and the other symbols have the same significance as before.

The specific volume of the non-evaporable water may have no literal significance, since at least a part of the non-evaporable water probably loses its identity when it enters into chemical combination with the cement constituents. Nonetheless, a figure can be obtained which represents the increase in volume of solid phase per gram of water combined with the cement and which is thus virtually the specific volume of the water. Since this specific volume does not vary widely among cements of various compositions, general use can be made of it for estimating the absolute volume of the solid phase from the non-evaporable water content. This makes available for this study a considerable number of data from samples on which helium-displacement measurements were not made.

The hypothetical specific volume of the non-evaporable water can conveniently be computed from the following form of eq. (11):

$$v_n = \frac{V_s - c\, v_c}{w_n} \qquad (12)$$

The values of v_n found from the final, most reliable experiments were as follows:

Cement No.	Computed composition				v_n
	C_3S	C_2S	C_3A	C_4AF	
13721-1P	44.8	26.3	12.7	6.6	0.82
13738-6Q	56.4	17.6	10.5	9.2	0.83
13765-15Q	42.4	28.9	9.9	8.8	0.81
13779-20P	53.0	15.5	13.1	11.5	0.82

In the computations that follow v_n is taken as 0.82 for all cements, on the basis of the results tabulated above.

Specific volume of gel water

With the data now at hand, the approximate specific volume of the gel water can be estimated.

Let v_g = mean specific volume of gel water;
w_g = weight of gel water;
$v_n w_n + v_g w_g = v_t w_t$.

In a saturated sample, made of normal Type I cement, containing no capillary space,

$$w_n = 0.50\ w_t\ ;$$
$$w_g = 0.50\ w_t\ ;$$
$$v_t = 0.860\ ;\text{ and}$$
$$v_n = 0.82\ .$$

Hence,

$$v_g = \frac{0.860 - 0.50 \times 0.82}{0.50} = 0.90, \text{ approximately.}$$

Computation of volume of solid phase from non-evaporable water

Eq. (11) can be written

$$\frac{V_s}{c\ v_c} = 1 + \frac{v_n}{v_c}\frac{w_n}{c} \quad \ldots\ldots\ldots\ldots\ldots\ldots\ldots\ldots\ldots\ldots\ldots\ldots\ldots\ldots (13)$$

This gives the ratio of the volume of the solid phase to the volume of the original cement in terms of the non-evaporable water (g per g of cement) and the ratio of the specific volume of the non-evaporable water to that of original cement, v_n/v_c. For any given cement v_n/v_c is constant and indeed the same value may be used for various cements without introducing much error. In the following computations v_n is taken as 0.82 for all cements, v_c is the measured value when known and 0.317 when no measured value is available. That is, the value is either $\frac{0.82}{v_c}$ or $\frac{0.82}{0.317}$ = 2.59.

Computations of solid-phase volumes are recorded in Tables 5-12 to 5-16. These data include results from five different cements and three

TABLE 5-12—COMPUTATION OF VOLUME OF SOLID PHASE

Cement 14930J

$\frac{v_n}{v_c} = \frac{0.82}{0.31} = 2.64$; C_3S 23 percent; C_2S 56 percent; C_3A 6 percent; C_4AF 10 percent; Specific surface = 2040 sq cm per g; Computations based on eq. (12)

(1)	(2)	(3)	(4)	(5)	(6)	(7)
Ref. No. Series 254-8 & 9	w_o/c	Age, days	$\frac{w_n}{c}$ (g/g)	$\frac{V_s}{c\,v_c}$	$c\,v_c$ cc. per cc. of paste	V_s
			Mix A			
9–1	.309	7	.080	1.21	.498	.60
"	"	14	.099	1.26	"	.63
"	"	28	.107	1.28	"	.64
"	"	56	.129	1.34	"	.67
"	"	90	.150	1.40	"	.70
"	"	180	.162	1.43	"	.71
"	"	365	.170	1.45	"	.72
8–1	.311	447	.181	1.48	.494	.73
			Mix B			
9–2	.424	7	.080	1.21	.418	.51
"	"	14	.103	1.27	"	.53
"	"	28	.116	1.31	"	.55
"	"	56	.135	1.36	"	.57
"	"	90	.174	1.46	"	.61
"	"	180	.185	1.49	"	.62
"	"	365	.195	1.52	"	.63
8–2	.443	362	.201	1.53	.407	.62
			Mix C			
9–3	.573	7	.082	1.22	.347	.42
"	"	14	.090	1.24	"	.43
"	"	28	.121	1.32	"	.46
"	"	56	.164	1.43	"	.50
"	"	90	.185	1.49	"	.52
"	"	180	.201	1.53	"	.53
"	"	365	.214	1.56	"	.54
8–3	.595	362	.210	1.55	.338	.52

different mixes and from six to eight different curing periods for each cement. The increases in solid volume during the course of hydration are shown for each of the cements in Fig. 5-7.*

These curves show that during the first month or so the average rate of hydration of a given cement is greater the greater the original water-cement ratio. After the first 3 months the rate is very low. Because of this the data do not indicate very definitely the trends of the curves at the later ages. Nevertheless, it is clear that even with the slow hardening cements, hydration virtually ceases within a year.

*For description of mixes see S-254-8 & 9, Appendix to Part 2.

TABLE 5-13—COMPUTATION OF VOLUME OF SOLID PHASE

Cement 15007J

$\frac{v_n}{v_c} = \frac{0.82}{0.314} = 2.61$; C_3S 48 percent; C_2S 29 percent; C_3A 7 percent; C_4AF 10 percent; Specific surface = 2015 sq cm per g; Computations based on eq. (12).

(1) Ref. No. Series 254-8 & 9	(2) w_o/c	(3) Age, days	(4) $\frac{w_n}{c}$ (g/g)	(5) $\frac{V_s}{c\,v_c}$	(6) $c\,v_c$ cc per cc of paste	(7) V_s
			Mix A			
9–4	.316	7	.126	1.33	.493	.66
"	"	14	.140	1.36	"	.67
"	"	28	.154	1.40	"	.69
"	"	56	.168	1.44	"	.71
"	"	90	.173	1.45	"	.72
"	"	180	.184	1.48	"	.73
8–28	.344	480	.198	1.52	.471	.71
			Mix B			
9–5	.433	7	.133	1.35	.416	.56
"	"	14	.150	1.39	"	.58
"	"	28	.171	1.45	"	.60
"	"	56	.185	1.48	"	.62
"	"	90	.192	1.50	"	.62
"	"	180	.202	1.53	"	.64
8–29	.464	440	.217	1.57	.398	.62
			Mix C			
9–6	.570	7	.156	1.41	.347	.49
"	"	14	.163	1.42	"	.49
"	"	28	.184	1.48	"	.51
"	"	56	.204	1.53	"	.53
"	"	90	.205	1.54	"	.53
"	"	180	.213	1.56	"	.54
8–30	.595	440	.232	1.61	.340	.55

Table 5-17 gives the volumes of the solid phase in pastes that had apparently closely approached the maximum possible extent of hydration. The average results from each mix are plotted in Fig. 5-8. This diagram is like Fig. 5-5 except that the solid volume rather than bulk volume is shown. Fig. 5-9 represents a Type I cement cured 6 months. The original specimens were truncated cones of 4-in. base diameter, 1½-in. top diameter, and 6-in. altitude. Some were made of sand-cement mortar; others from cement and pulverized silica.* (See Table 5-18.)

These two diagrams show that as the cement approaches ultimate hydration the volume of the solid phase per unit over-all volume of paste is directly proportional to the original cement content of the paste for

*For complete description see Appendix to Part 2, Series 254-7.

TABLE 5-14—COMPUTATION OF VOLUME OF SOLID PHASE

Cement 15011J

$\frac{v_n}{v_c} = \frac{0.82}{0.312} = 2.63$; C_3S 45 percent; C_2S 29 percent; C_3A 7 percent; C_4AF 10 percent; Specific surface = 1835 sq cm per g; Computations based on eq. (12).

(1)	(2)	(3)	(4)	(5)	(6)	(7)
Ref. No. Series 254-8 & 9	w_o/c	Age, days	$\frac{w_n}{c}$ (g/g)	$\frac{V_s}{c\,v_c}$	$c\,v_c$ cc per cc of paste	V_s
			Mix A			
9–7	.316	7	.114	1.30	.492	.64
"	"	14	.133	1.35	"	.66
"	"	28	.143	1.38	"	.68
"	"	56	.156	1.41	"	.69
"	"	90	.164	1.43	"	.70
"	"	180	.170	1.45	"	.71
"	"	365	.176	1.46	"	.72
8–40	.319	478	.184	1.48	.490	.72
			Mix B			
9–8	.432	7	.123	1.32	.413	.54
"	"	14	.153	1.40	"	.58
"	"	28	.165	1.43	"	.59
"	"	56	.187	1.47	"	.61
"	"	90	.191	1.50	"	.62
"	"	180	.199	1.52	"	.63
8–41	.442	368	.210	1.55	.410	.64
			Mix C			
9–9	.582	7	.131	1.34	.350	.47
"	"	14	.157	1.41	"	.49
"	"	28	.176	1.46	"	.51
"	"	56	.195	1.51	"	.53
"	"	90	.205	1.54	"	.54
"	"	180	.214	1.56	"	.55
8–42	.595	368	.222	1.58	.340	.54

those pastes in which the original cement content does not exceed about 45 percent of the over-all paste volume. For this lower range of cement contents the position of the line OB corresponds to $w_n/c = 0.224$; hence, eq. (13) becomes

$$V_s = 1.58\ c\ v_c \Big]_{c\ v_c \leqq 0.45} \quad \text{(14)}$$

For pastes having cement contents greater than 45 percent of the over-all volume, the ultimate volume of the solid phase in the hardened paste is not directly proportional to $c\ v_c$. Instead, the relationship, as shown in Fig. 5-8, is

$$V_s = 0.5 + 0.5\ c\ v_c \Big]_{0.45 \leqq cv_c \leqq 1.0} \quad \text{(15)}$$

Eq. (14) is represented in Fig. 5-8 by line OB; eq. (15), by BC.

TABLE 5-15—COMPUTATION OF VOLUME OF SOLID PHASE

Cement 15013J

$\frac{v_n}{v_c} = \frac{0.82}{0.316} = 2.60$; C_3S 39 percent; C_2S 29 percent; C_3A 14 percent; C_4AF 7 percent; Specific surface = 1810 sq cm per g; Computations based on eq. (12).

(1) Ref. No. Series 254-8 & 9	(2) w_o/c	(3) Age, days	(4) $\frac{w_n}{c}$ (g/g)	(5) $\frac{V_s}{c\,v_c}$	(6) $c\,v_c$ cc per cc of paste	(7) V_s
			Mix A			
9–10	.324	7	.149	1.39	.488	.68
"	"	14	.164	1.43	"	.70
"	"	28	.171	1.44	"	.70
"	"	56	.180	1.47	"	.72
"	"	90	.191	1.50	"	.73
"	"	180	.188	1.49	"	.73
8–46	.332	339	.218	1.57	.481	.75
			Mix B			
9–11	.443	7	.156	1.41	.410	.58
"	"	14	.183	1.48	"	.60
"	"	28	.177	1.46	"	.60
"	"	56	.208	1.54	"	.63
"	"	90	.215	1.56	"	.64
"	"	180	.236	1.61	"	.66
8–47	.453	333	.241	1.63	.405	.66
			Mix C			
9–12	.611	7	.158	1.41	.335	.47
"	"	14	.183	1.48	"	.49
"	"	28	.203	1.53	"	.51
"	"	56	.221	1.58	"	.53
"	"	90	.236	1.61	"	.54
"	"	180	.245	1.64	"	.55
8–48	.599	333	.253	1.66	.339	.56

Lines OD and DC in Fig. 5-8 represent the bulk volumes of the solid phase (see Fig. 5-5) corresponding to the solid volumes represented by OB and BC. Line OD corresponds to eq. (10) with $w_n/c = 0.224$. For a saturated paste vertical distances in the area above OD represent capillary water; those in the area between ODC and OBC represent gel water; those in the area $OBCO$ represent non-evaporable water.

In Part 3, data were presented showing that the evaporable water cannot be less than $4V_m$. (V_m = weight of water in first adsorbed layer.) It was shown that as a consequence of this the maximum weight ratio of the non-evaporable to the total water would be between about 0.47 and 0.51, depending on the type of cement. For a Type I cement it would be about 0.50. It is of interest to compare these weight ratios with the volume ratio indicated by BC in Fig. 5-8. (The points along

TABLE 5-16—COMPUTATION OF VOLUME OF SOLID PHASE

Cement 15365

$\frac{v_n}{v_c} = \frac{0.82}{0.319} = 2.57$; C_3S 45 percent; C_2S 28 percent; C_3A 13 percent; C_4AF 7 percent; Specific surface = 1640 sq cm per g; Computations based on eq. (12).

(1) Ref. No. Series 254-8 & 9	(2) w_o/c	(3) Age, days	(4) $\frac{w_n}{c}$ (g/g)	(5) $\frac{V_s}{c\,v_c}$	(6) $c\,v_c$ cc per cc of paste	(7) V_s
			Neat cement			
9–15A	.244	7	.115	1.30	.558	.72
"	"	14	.126	1.32	"	.74
"	"	28	.136	1.35	"	.75
"	"	56	.140	1.36	"	.76
"	"	90	.145	1.37	"	.77
"	"	180	.155	1.40	"	.78
			Mix A			
9–13	.319	7	.133	1.34	.490	.66
"	"	14	.152	1.39	"	.68
"	"	28	.149	1.38	"	.68
"	"	56	.179	1.46	"	.72
"	"	90	.179	1.46	"	.72
"	"	180	.182	1.47	"	.72
			Mix B			
9–14	.439	7	.139	1.36	.412	.56
"	"	14	.171	1.44	"	.59
"	"	28	.184	1.47	"	.61
"	"	56	.210	1.54	"	.63
"	"	90	.215	1.55	"	.64
"	"	180	.222	1.57	"	.65
			Mix C			
9–15	.587	7	.153	1.39	.351	.49
"	"	14	.186	1.48	"	.52
"	"	28	.210	1.54	"	.54
"	"	56	.221	1.57	"	.55
"	"	90	.230	1.59	"	.56
"	"	180	.255	1.66	"	.58

this line represent cements of average Type I composition.) To make this comparison it is necessary to convert the volume ratio represented by BC to the corresponding weight ratio:

$$w_n v_n = 0.5\, w_t v_t \quad \text{(Fig. 5-8)} \qquad (16)$$

$$v_t = 1 - 0.279\,\frac{w_n}{w_t} \quad \text{(eq. (8))}.$$

$$v_n = 0.82 \quad \text{(assumed)} \qquad (17)$$

Substitution of eq. (8) and (17) into eq. (16) gives

$$\frac{w_n}{w_t} = 0.52\,.$$

Thus, the maximum weight ratio of w_n to w_t as estimated from the specific-volume measurements is higher than that estimated from the adsorption measurements by 6 percent of the smaller value. This discrepancy is probably the result of applying eq. (8) for v_t instead of experimental values for the particular cements represented in Fig. 5-8, using the approximate value 0.82 for v_n, and using the estimated weight

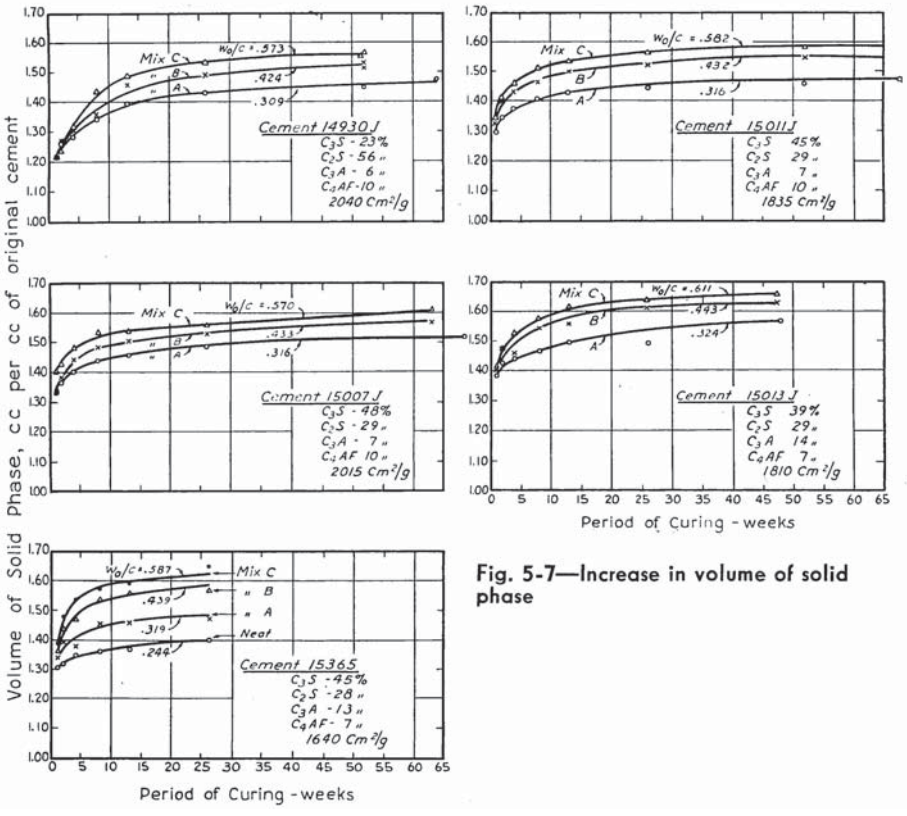

Fig. 5-7—Increase in volume of solid phase

TABLE 5-17—COMPUTATION OF VOLUME OF SOLID PHASE FROM w_n/c FOR PASTES 6 MONTHS OLD OR OLDER

All pastes were from mortar cubes unless otherwise indicated.

(1)	(2)	(3)	(4)	(5)	(6)	(7)	(8)	(9)	(10)	(11)
Cement No.	Specific surface, cm^2/g	Ref. No. Series 254-8 & 9	w_o/c	Age, days	w_n/c	v_c	$\frac{0.82}{v_c}$ $(= k)$	$\frac{V_s}{c\,v_c}$	Cement content of paste $(= c\,v_c)$	V_s
					Neat cement					
14675	—	254–18	.120	4 yr.	.079*	.318	2.58	1.20	.72	.86
15365	1640	9–15A	.244	.180	.155	.319	2.57	1.40	.558	.78
					Mix A					
14930J	2040	8–1	.311	447	.181	.311	2.64	1.48	.494	.73
15007J	2015	8–28	.344	480	.198	.314	2.61	1.52	.471	.72
15011J	1835	8–40	.319	478	.184	.312	2.63	1.48	.490	.73
15013J	1810	8–46	.332	339	.218	.316	2.60	1.57	.481	.75
15365	1640	9–13	.319	180	.182	.319	2.57	1.47	.490	.72
Average								1.50	.485	.73
					Mix B					
14930J	2040	8–2	.443	362	.201	.311	2.64	1.53	.407	.62
15007J	2015	8–29	.464	440	.217	.314	2.61	1.57	.398	.62
15011J	1835	8–41	.442	368	.210	.312	2.63	1.55	.410	.64
15013J	1810	8–47	.453	333	.241	.316	2.60	1.63	.405	.66
15365	1640	9–14	.439	180	.222	.319	2.57	1.57	.412	.65
Average								1.57	.406	.64
					Mix C					
14930J	2040	9–3	.573	365	.214	.311	2.64	1.56	.347	.54
15007J	2015	8–30	.595	440	.232	.314	2.61	1.61	.340	.55
15011J	1835	8–42	.595	368	.222	.312	2.63	1.58	.340	.54
15013J	1810	8–48	.599	333	.253	.316	2.60	1.66	.339	.56
15365	1640	9–15	.587	180	.255	.319	2.57	1.66	.351	.58
Average								1.61	.343	.55

*w_n computed from V_m.

ratio based on an average ratio between V_m and w_n that may be in error by as much as 10 percent for a particular cement.

It may be concluded that Table 5-10 and line BC of Fig. 5-8 are substantially in agreement in showing that the maximum possible weight ratio of non-evaporable water to total water is about ½.

Limit of hydration for pastes of high cement content

As already noted, line BC appears to be an upper limit to the amount of hydration (in terms of w_n) that can occur in pastes of high cement content. The data at hand are not sufficient to prove whether this is an absolute limit or whether, given sufficient time, the points will gradually move higher. However, the fact that one of the points represents a water-cured paste 4 years old gives strong support to the supposition that the line as shown marks the upper limit. The significance of the position of line BC and whether or not its slope remains the same may not at first be apparent. Consider the following alternative possibilities.

(1) The process of filling the available space with hydration products could be likened to filling a vessel with like-size spheres; at any given stage in the filling the total void space in the vessel would represent the unfilled space plus the pore space between the spheres; the void space

TABLE 5-18—COMPUTATION OF THE VOLUMES OF THE SOLID PHASE IN SPECIMENS FROM SERIES 254-7

Cement 14675

$$\frac{V_s}{c\,v_c} = 1 + \frac{v_n}{v_c}\frac{w_n}{c} \quad ; \quad \frac{v_n}{v_c} = \frac{0.82}{0.318} = 2.58$$

Ref. No. 254-7	w_n/c			$1 + 2.58(w_n/c)$			cv_c cc per cc of paste	$(1 + 2.58\ w_n/c)cv_c = V_s$ cc/cc of paste		
	28d	56d	6 mo.	28d	56d	6 mo.		28d	56d	6 mo.
Mortar specimens										
7–1	.1445	.1485	.1626	1.37	1.38	1.42	.554	.76	.77	.79
7–2	.1585	.1605	.1763	1.41	1.41	1.46	.534	.75	.76	.78
7–3	.1665	.1705	.1817	1.43	1.44	1.47	.515	.74	.74	.76
7–4	.1895	.1870	.2046	1.49	1.48	1.53	.477	.71	.71	.73
7–5	.2045	.2115	.2351	1.53	1.55	1.61	.421	.64	.65	.68
7–6	.2115	.2275	.2337	1.55	1.59	1.60	.354	.55	.56	.57
7–7	.2155	.2275	.2303	1.56	1.59	1.59	.306	.48	.49	.49
Cement-silica specimens										
	35d	63d	6 mo.	35d	63d	6 mo.		35d	63d	6 mo.
7–1S	.1995	.2007	.2160	1.52	1.52	1.56	.472	.72	.72	.74
7–2S	.2133	.2164	.2324	1.55	1.56	1.60	.421	.65	.66	.67
7–3S	.2246	.2270	.2433	1.58	1.59	1.63	.373	.59	.59	.61
7–4S	.2323	.2303	.2497	1.60	1.59	1.64	.340	.54	.54	.56
7–5S	.2351	.2304	.2456	1.61	1.59	1.63	.326	.52	.52	.53

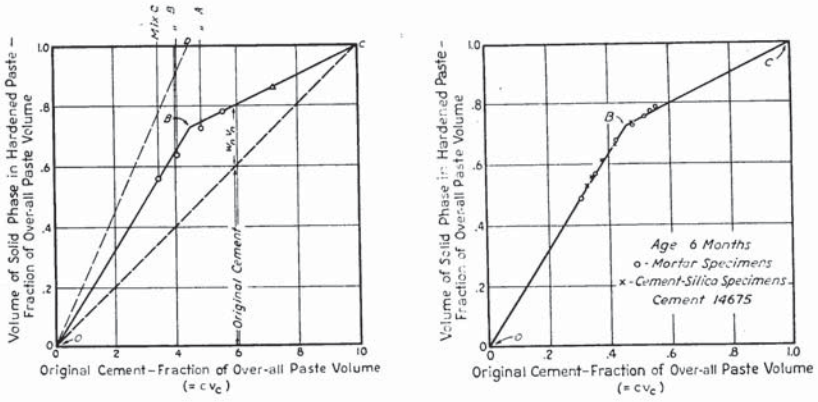

Fig. 5-8 (left) —Relationship between volume of solid phase and original cement content at virtually ultimate hydration
Data from Table 5-17

Fig. 5-9 (right)—Relationship between volume of solid phase and volume of original cement
Data from Table 5-18
See Appendix to Part 2 for description of original specimens

within the vessel could not be reduced below the total volume of the spaces between the spheres when the vessel is full of spheres.

(2) The process could be likened to that of filling a vessel with relatively large spheres and then sifting in smaller spheres that could occupy the spaces between the larger spheres.

If the amount of non-evaporable water reached a point on the line *BC* and then remained there regardless of the length of the period of curing, thus indicating an unchanging ratio between evaporable and non-evaporable water, the indication would be that the hydration products have a characteristic minimum porosity that cannot be reduced. This would indicate that the space becomes filled by a process analogous to that described in (1). If with continued hydration the slope of *BC* should become smaller, this would show that the ratio of non-evaporable to evaporable water gradually increases and that the colloidal hydration products become less porous as hydration proceeds. This would indicate that the space becomes filled in the manner pictured in (2); that is, the pores of the gel first formed would become partly filled by hydration products formed at a later time. As pointed out above, the fact that the specimen cured 4 years is represented by a point on *BC* of Fig. 5-8 is strong evidence that the porosity of the hydration products does not decrease as hydration proceeds. Hence, hydration seems to be a process of forming new products without changing the characteristics of products already formed.

This evidence that the hydration products have a characteristic porosity is compatible with the theory of formation of the gels. When the solid material precipitates from solution, the colloidal particles initially formed by the aggregating molecules are drawn together by interparticle forces having an intensity characteristic of the system. The gel is pictured as a mass of colloidal particles drawn together in random arrangement and held by the forces of flocculation and probably to some extent by rudimentary, submicroscopic crystal growths. If the particles composing the gel (the "micelles") are larger than the normal spaces in the gel, later deposition of new gel in such spaces would seem unlikely. (See Part 3.)

Limit of hydration with capillary water continuously available

For mixes falling to the left of point B, the time required for the solid phase in a given paste to attain a volume represented by a point on the line OB is greater the greater the original cement content of the paste. (It should be noted that time is not represented in Fig. 5-8 or 5-9.) But apparently this line is reached eventually and it marks a limit to the amount of hydration even though capillary water is present in the paste. Such a result would be expected if the position of line OB corresponded to complete hydration of all the cement. However, complete hydration probably does not occur except in cements of unusually high specific surface. Observations by Brownmiller[3] on pastes of $w/c = 0.4$ by weight ($c\ v_c = 0.44$ cc per cc of paste) indicate that all but the coarsest particles of cement, probably those having diameters less than about 40 microns, become completely hydrated if water-cured long enough. According to Brownmiller, a Type III cement of about 2600 specific surface appeared to be about 99 percent hydrated at the seventh day. A Type I cement, specific surface 1800, appeared about 85 percent hydrated at the 28th day. In a section from concrete pavement 6 years old, the cement (specific surface unknown but probably not over 1800) in the part photographed appeared to be completely hydrated except for one 75-micron particle.

Fig. 5-10 gives data obtained in this laboratory on the influence of fineness on the extent of hydration as indicated by the non-evaporable water content. These results indicate that the ultimate increase in solid volume per cc. of original cement is smaller the coarser the cement. These indications that coarse particles of cement remain unhydrated for an indefinite period even when free water is present show that the apparent cessation of hydration is, for cements of ordinary fineness, not due to the attainment of chemical equilibrium. Apparently, the gel around the coarser cement grains becomes so dense that water cannot penetrate it. Absolute stoppage of flow through the gel is hardly conceivable, however.

It is more likely that water continues to penetrate to the cement but does it so slowly that we are unable to detect the effect.

Estimation of volume of unreacted cement

The amount of unreacted cement in hardened paste can be expressed as follows:

$$\frac{V_{uc}}{cv_c} = 1 - n\,\frac{w_n v_n}{c\,v_c} \quad , \ldots\ldots\ldots\ldots\ldots\ldots\ldots\ldots\ldots\ldots (18)$$

where

$\frac{V_{uc}}{cv_c}$ = volume of unreacted cement per unit volume of original cement, and

n = cc. of hydration products per cc. of non-evaporable water.

As said before, we have no data on the amount of unreacted cement in the specimens used in these studies. However, from Brownmiller's observations, mentioned above, it seems reasonable to assume that at ultimate hydration, about 90 percent of a Type I cement becomes hydrated. Making this assumption, assuming that $w_n/c = 0.24$ at ultimate hydration, and letting $v_n/v_c = 2.59$, we obtain

$$0.1 = 1 - n(2.59 \times 0.24).$$

Hence, $$n = 1.45.$$

With n thus estimated we may write

$$\frac{V_{uc}}{cv_c} = 1 - 3.75\,w_n/c \ldots\ldots\ldots\ldots\ldots\ldots\ldots\ldots (19)$$

It should be understood that this relationship is only a rough estimate. The value of n will depend on the fineness of the cement, the coarser the cement, the smaller n. For example, if when $w_n/c = 0.24$ the cement is actually completely hydrated, n would equal about 1.6; if 80

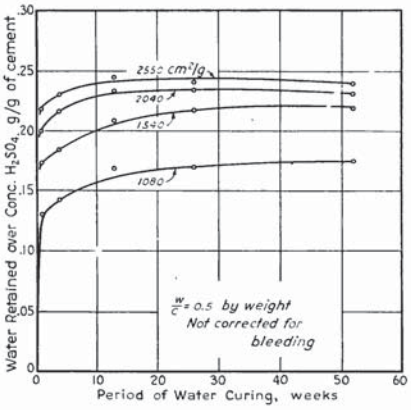

Fig. 5-10—Effect of fineness of grinding on rate and amount of hydration
Cement 14560
C_3S-60%, C_2S-17%, C_3A-7%, C_4AF-13%

percent hydrated, about 1.3. The purpose of the computation is to show the order of magnitude of n and to provide a basis for showing, in the following section, how the correct data would be represented graphically if we had them.

Graphical summary of data on volumes of various phases in hardened cement paste

Fig. 5-11 gives a summary of the relationships brought out in the preceding discussions.

It should be understood that the diagrams represent average values. The slope of BC (eq. (15)) would vary slightly among pastes made with different cements, according to differences in the ratios w_n/w_t for the various cements. Likewise, the relationship between the slope of OB (eq. (13)) and that of OD (eq. (9)) depends on V_m/w_n. The slope of OB at ultimate hydration would be smaller the coarser the cement. Moreover, the slope of OE (eq. (18)) would depend on the fineness and other characteristics of the cement.

With respect to eq. (18), it should be clear that this equation can hold only up to the ordinate of point B. Beyond that point the locus of the point representing unreacted cement must be the straight line EC.

At 0 percent hydration, only the diagonal line would appear, representing unreacted cement and capillary water. At this stage, the capillaries are the spaces between the original cement grains. The manner in which the new phases develop as hydration proceeds may be seen by comparing the four diagrams in consecutive order.

SOME PRACTICAL ASPECTS OF THE RESULTS

No attempt was made in this paper to discuss the implications of the data and the relationships that have been presented. However, the following fairly obvious matters may be pointed out:

(1) Pastes in which the original cement constitutes more than 45 percent of the over-all volume cannot become hydrated to the same extent as pastes containing less cement. In terms of weight ratio, this means that if w_o/c is less than 0.40, ultimate hydration will be restricted. Therefore, conclusions about the extent of hydration of cement in ordinary concrete should not be drawn from data obtained from standard test-pieces—w/c = about 0.25. (The numerical limits mentioned above probably are different for cements of different specific surfaces; the coarser the cement the lower the limiting w_o/c. For specific surfaces between 1600 and 2000, the figures given are satisfactory.)

(2) The average rate of hydration is lower the lower w_o/c. Therefore, the age-strength relationship for ordinary concrete cannot be the same as that for standard test pieces of low w_o/c.

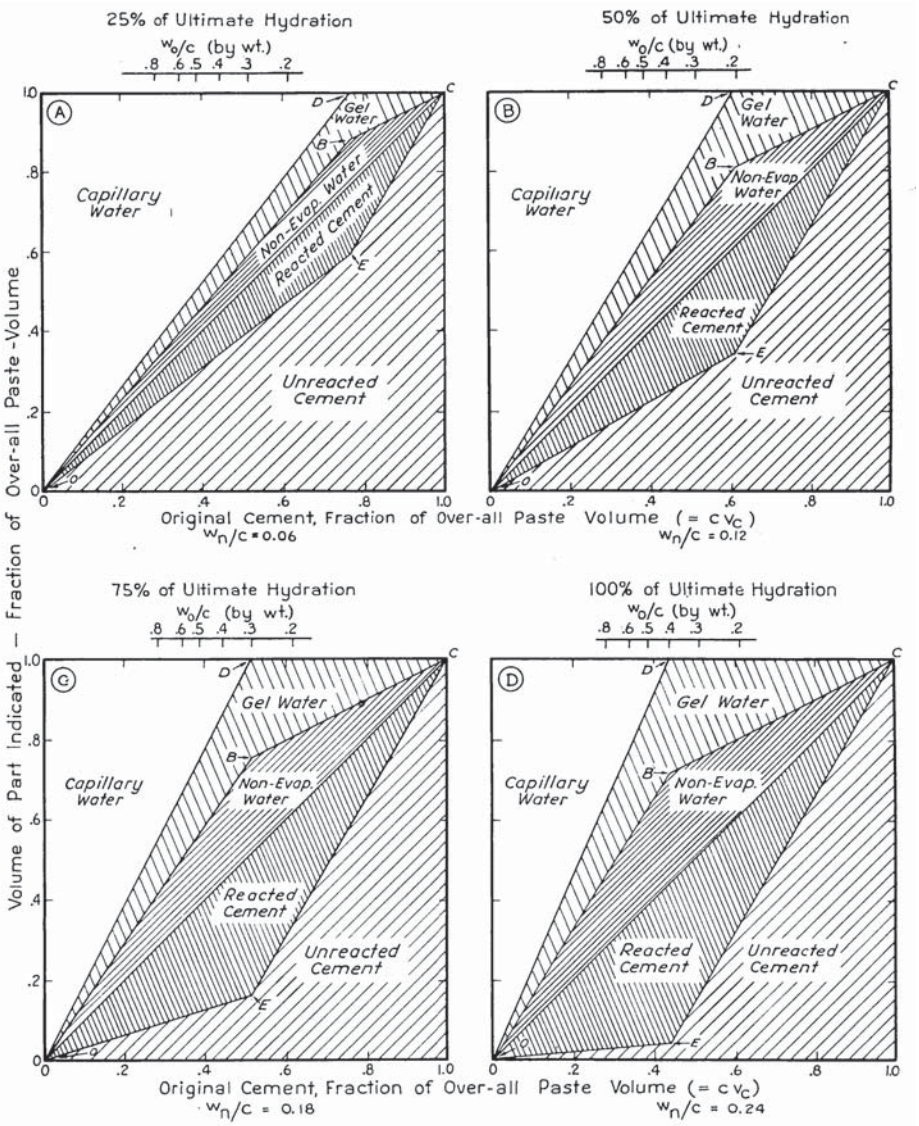

Fig. 5-11—Relationship between volumes of various phases in saturated hardened paste and original cement content at ultimate hydration

(3) The substance that gives concrete its strength and hardness is the solid material formed by the hydration of portland cement. In Fig. 5-11 this cementing substance is represented by the vertical distance from *OEC* to *ODC* at the point on the scale of abscissas representing the original cement content of the paste. The capillary spaces, when present, are distributed through this

substance and weaken it. Therefore, the cementing substance (not the paste as a whole) has its maximum possible strength if the hardened paste can be represented by the ordinate passing through points *E*, *B*, and *D*, or by any ordinate to the right of that one.

(4) It might seem from the foregoing paragraph that a paste represented by the ordinate through *EBD* has the maximum possible strength and therefore that still richer pastes (necessarily molded under pressure) would be no stronger. However, a limited amount of data obtained from specimens molded under high pressure indicates that the strength of the paste as a whole increases as the composition is made to fall farther to the right of the ordinate passing through *EBD*. In view of the evidence that the density of the cementing substance is the same in all such pastes, it is concluded that the increase in strength is due to the decrease in the thickness of the layer of cement between the particles of mineral aggregate. In this connection, the unreacted cement may be considered to be a part of the aggregate. The increase may also be due in part to an increase in the degree of "self-desiccation" of the gel, which would be expected to increase with the proportion of unreacted cement.

(5) The hydraulic radius of the pores in the paste and the porosity are smaller the smaller the proportion of capillary space in the hardened paste. The hydraulic radius is at its lowest possible value when the composition of the hardened paste can be represented on the ordinate passing through points *E*, *B*, and *D* of Fig. 5-11. Porosity of the paste as a whole continues to decrease as the composition is made to fall farther to the right, but the hydraulic radius is not further reduced.

(6) The permeability of hardened pastes to fluids under external pressure probably depends almost entirely on the proportion of capillary water, owing to the extreme smallness of the gel-pores. Hence, permeability is practically zero when the paste can be represented by the ordinate passing through points *E*, *B*, and *D*. This is discussed further in Part 7.

GENERAL SUMMARY OF PART 5

Nomenclature:

c = cement, g per g of saturated paste
w_t = total water, g per g of saturated paste
w_n = non-evaporable water, g per g of saturated paste
w_d = compressed water, g per g of saturated paste
w_c = capillary water, g per g of saturated paste
w_a = adsorbed water, g per g of saturated paste

w_g = gel water, g per g of saturated paste
v_c = specific volume of cement
v_t = " " " total water
v_n = " " " non-evaporable water
v_d = " " " compressed water
v_g = " " " gel water
B' = ratio of adsorbed water to non-evaporable water
B = $(1 + B')$
k = ratio of V_m to w_n
V_m = constant of B.E.T. equation, proportional to surface area of the gel
V_B = bulk volume of solid phase. It differs from the over-all volume of the paste by the volume of the capillary space outside the gel.
V_s = volume of solid matter in the paste
V_{uc} = volume of unreacted cement in the paste
n = cc of hydration product per cc of non-evaporable water

(1) The total water in a saturated specimen can be divided into two categories: (a) that which has a specific volume less than 1.0; (b) that which has a specific volume equal to 1.0. All the water having a specific volume less than unity is called compressed water. It comprises the non-evaporable water and a part of the evaporable water.

(2) The mean specific volumes of the total water contents were computed from the measured volumes of the saturated granular samples and the volumes and weights of the ingredients, assuming that the cement retained its original volume.

(3) The mean specific volume of the total water in a saturated paste is given by the expression

$$v_t = 1 - 0.279 \frac{w_n}{w_t}.$$

w_n/w_t can vary from zero to about 0.50. Hence, the mean specific volume of the total water varies from 1.0 as a maximum ($w_n = 0$) to about 0.860 as a minimum ($w_n/w_t = 0.50$). Among different types of cement, w_n/w_t (maximum) ranges from 0.47 to 0.51.

(4) When w_n/w_t = about 0.50, the sample contains no capillary water. Hence, 0.860 is the mean of the specific volumes of the non-evaporable water and the gel water.

(5) The mean specific volume of the gel water is estimated to be about 0.90; that of the capillary water is 1.0.

(6) The bulk volume of the solid phase as a fraction of the over-all volume of the paste is given by the expression

$$\frac{V_B}{c\,v_c} = 1 + \frac{w_n}{c}(1 + 4k)\frac{0.860}{v_c} \quad (\text{for } 0 \lesssim V_B \lesssim 1)$$

For an average Type I cement, $k = 0.255$ and V_B becomes

$$V_B = \left[1 + 5.5\frac{w_n}{c}\right] c\,v_c$$

(7) The absolute volume of the solid phase as a fraction of the total paste volume is given as

$$V_s = \left[1 + \frac{v_n}{v_c}\cdot\frac{w_n}{c}\right] c\,v_c$$

(8) The ratio of the solid volume after hydration to the solid volume of the original cement, $V_s/(c\,v_c)$, varies from 1.0 when $w_n/c = 0$ to about 1.63 when w_n/c is maximum. The upper limit is probably lower than 1.63 for cements coarser than those used in this study (1600 to 2000 sq cm per g and may be slightly higher for finer cements.

(9) For pastes having original cement contents greater than about 0.45 of absolute volume, the ultimate solid volume is about

$$V_s = 0.5 + 0.5\,cv_c \Big]_{0.45 \leqq cv_c \leqq 1.0}$$

(10) The extent of hydration in water-cured pastes having original cement contents below 0.45 by absolute volume is apparently limited by the relative amount of +40 micron particles in the original cement. In the richer pastes it is limited by the space available for the hydration products.

* * * * *

For comments on some practical implications of the results, see the section immediately preceding this General Summary.

REFERENCES

(1) A. J. Stamm and L. A. Hansen, *J. Phys. Chem.* v. 41, p. 1007 (1937); G. F. Davidson, *J. Textile Inst.* v. 18, T175 (1927); Stephen Brunauer, *The Adsorption of Gases and Vapors*, v. 1 (Princeton University Press, 1943), Chapter XII.

(2) R. P. Rossman and W. R. Smith, *Ind. Eng. Chem.* v. 35, p. 972 (1943).

(3) L. T. Brownmiller, *Proc.* ACI, v. 39, p. 193 (1943).

Title 43-5f —a part of PROCEEDINGS, AMERICAN CONCRETE INSTITUTE Vol. 43

JOURNAL
of the
AMERICAN CONCRETE INSTITUTE
(copyrighted)

Vol. 18 No. 7 7400 SECOND BOULEVARD, DETROIT 2, MICHIGAN March 1947

Studies of the Physical Properties of Hardened Portland Cement Paste*

By T. C. POWERS†
Member American Concrete Institute
and T. L. BROWNYARD‡

Part 6. Relation of Physical Characteristics of the Paste to Compressive Strength

Part 7. Permeability and Absorptivity§

CONTENTS PART 6

RELATION OF PASTE STRUCTURE TO COMPRESSIVE STRENGTH

The compressive strengths of mortars and concretes depend on many variable factors. The effects of some of the factors, particularly certain properties of the hardened paste, will be discussed in this section.

*Received by the Institute July 8, 1946—scheduled for publication in seven installments; October 1946 to April, 1947. In nine parts:

Part 1. "A Review of Methods That Have Been Used for Studying the Physical Properties of Hardened Portland Cement Paste". ACI JOURNAL, October, 1946.
Part 2. "Studies of Water Fixation"—Appendix to Part 2. ACI JOURNAL, November, 1946.
Part 3. "Theoretical Interpretation of Adsorption Data." ACI JOURNAL, December, 1946.
Part 4. "The Thermodynamics of Adsorption"—Appendix to Parts 3 and 4. ACI JOURNAL, January 1947.
Part 5. "Studies of the Hardened Paste by Means of Specific-Volume Measurements." ACI JOURNAL February, 1947.
Part 6. "Relation of Physical Characteristics of the Paste to Compressive Strength."
Part 7. "Permeability and Absorptivity."
Part 8. "The Freezing of Water in Hardened Portland Cement Paste."
Part 9. "General Summary of Findings on the Properties of Hardened Portland Cement Paste."

†Manager of Basic Research, Portland Cement Assn. Research Laboratory, Chicago 10, Ill.
‡Navy Dept., Washington, D. C., formerly Research Chemist, Portland Cement Assn. Research Laboratory, Chicago 10, Ill.

§The characteristics of the cements mentioned in this section may be found in the Appendix to Part 2.

The ratio of increase in solid phase to available space

At the time when fresh cement paste of normal properties first congeals, its final volume is established except for a relatively minute expansion in volume that occurs during subsequent hydration and the small volume changes that accompany drying and wetting. Therefore, the space available for the increase in volume of the solid phase is initially equal to the volume occupied by water.

We may tentatively assume that the increase in strength that accompanies an increase in extent of hydration is a function of the increase in the volume of the solid phase per unit of volume of initially water-filled space. In this connection it seems logical (though not essential) to consider the volume of the solid phase to be the sum of the volume of the solid matter and the volume of its associated voids, that is, to consider the bulk volume of the solid phase, rather than its absolute volume. (See Part 5.)

As shown in Part 5, the increase in bulk volume of the solid phase is about

$$0.860\ (w_n + 4V_m) \quad .$$

w_n is the weight of the water that has become a part of the solid phase and therefore represents the increase in absolute volume. $4V_m$ is the weight of the water required to fill the voids of the gel. 0.860 is the mean of the specific volumes of these two classes of water. Hence,

$$\frac{\text{increase in solid phase}}{\text{original space available}} = \frac{0.860(w_n + 4V_m)}{w_o} \quad \ldots\ldots\ldots\ldots (1)$$

where w_o is the original water content after bleeding.

For any given cement, V_m/w_n is a constant (see Part 3). Hence, the solid-space ratio is, in general,

$$X' = 0.860\ \frac{w_n}{w_o}\ (1 + 4k) \quad \ldots\ldots\ldots\ldots\ldots\ldots\ldots\ldots\ldots\ldots (2)$$

or

$$X' = 0.860\ \frac{V_m}{w_o}\left(\frac{1 + 4k}{k}\right) \quad \ldots\ldots\ldots\ldots\ldots\ldots\ldots\ldots\ldots\ldots (3)$$

where X' = ratio of increase in solid phase to original water content. It will be shown that compressive strength, f_c, is related to X' by an empirical equation of the form

$$f_c = mX' + B \quad \ldots\ldots\ldots\ldots\ldots\ldots\ldots\ldots\ldots\ldots (4)$$

where m is the slope of the empirical line and B, its intercept on the f_c axis.

Substitution for X' from eq. (2) and (3) gives

$$f_c = M'\ \frac{V_m}{w_o} + B \quad \ldots\ldots\ldots\ldots\ldots\ldots\ldots\ldots\ldots\ldots\ldots\ldots (5)$$

and

$$f_c = kM' \frac{w_n}{w_o} + B \quad , \ldots\ldots\ldots\ldots\ldots\ldots\ldots\ldots\ldots\ldots\ldots\ldots (6)$$

where

$$M' = 0.860 \left(\frac{1 + 4k}{k} \right) m \quad .$$

The constants M' and B can be evaluated by plotting observed values of f_c versus V_m/w_o or w_n/w_o. Such data for four different cements are given in Tables 6-1, 6-2, and 6-4* and are plotted in Fig. 6-1 and 6-2. The points represent mixes A, B, and C of Series 254-9 and the mixes used in Series 254-11, where they were the same as A and B of 254-9. The curing periods ranged from 7 days to about 1 year.

The straight line drawn in Fig. 6-1 represents the relationship

$$f_c = 120{,}000 \frac{V_m}{w_o} - 3600 \quad \ldots\ldots\ldots\ldots\ldots\ldots\ldots\ldots\ldots\ldots\ldots\ldots (7)$$

It will be noted that the deviations of the individual points from this line seem to be random. That is, there is no indication that the points for any particular age or cement or mix can be distinguished by their positions with respect to the line. In view of the fact that V_m/w_n (i.e., k) differs considerably among the four cements, it seems that strength is not much influenced by this ratio. If w_n represents all the hydration products and V_m only the gel (material of high specific surface—see Part 3), this in-

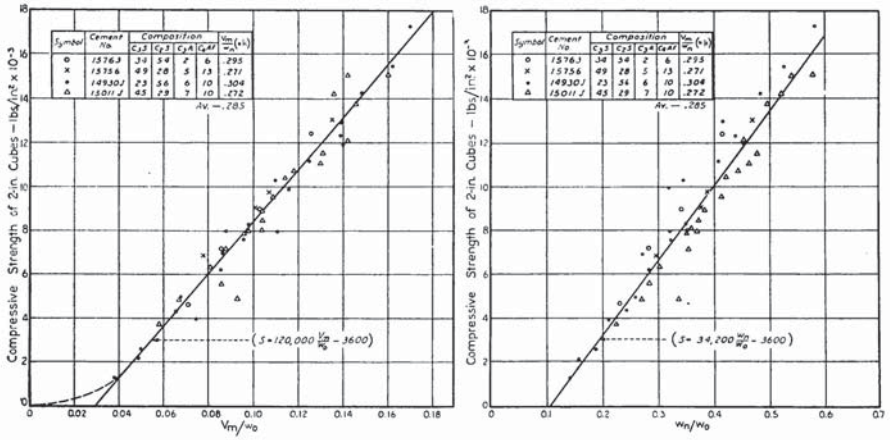

Fig. 6-1 (left)—Relationship between compressive strength and V_m/w_o for cements low in C_3A
Data from Tables 6-1, 6-2, & 6-4; Series 254-8-9 & 11

Fig. 6-2 (right)—Strength versus w_n/w_o for the same materials represented in Fig. 6-1
Series 254-8-9 & 11

*All Part 6 tables follow text pp. 858 to 864.

dicates that strength depends primarily on the gel and is therefore little influenced by differences in w_n when V_m is fixed.

This point is illustrated further by Fig. 6-2, where f_c is plotted against w_n/w_o. The straight line has the slope Mk where $M = 120{,}000$ and $k = 0.285$, the mean value of k for the four cements. That is, the equation for the line is $f_c = 34{,}200 \frac{w_n}{w_o} - 3600$. Although the points scatter to a similar degree, the scattering in Fig. 6-2 differs from that in Fig. 6-1 in that there is clear evidence of segregation of the triangles (representing cement 15011J) whereas in Fig. 6-1 the points are rather well mixed.

The gel-space ratio

It thus appears that the increase in strength is directly proportional to the increase in V_m/w_o regardless of age, original water-cement ratio, or identity of cement. Accordingly, it appears advisable to discard the assumption that strength is a function of the ratio of the total increase in solid phase to available space, in favor of the assumption that it is a function of the ratio of the volume of the gel to the original space available. We may call this the gel-space ratio. Thus, we may assume that

$$X = \beta \frac{V_m}{w_o} \quad , \qquad (8)$$

where X = gel-space ratio

β = proportionality between V_m and the total volume of the gel.

Substitution of eq. (8) into eq. (4) gives

$$f_c = M \frac{V_m}{w_o} + B \quad , \qquad (9)$$

where $M = m\beta$. Comparison of eq. (9), (6), and (4) shows that the above is merely a redefinition of the meaning of the slope of the line represented by eq. (4), the new definition taking into account the observation that k need not be included. Eq. (7) is thus now defined as the relationship between strength and the gel-space ratio.

Limitations of f_c vs. V_m/w_o relationship

Although the four cements represented in Fig. 6-1 differ considerably in C_3S and C_2S content, they are all similarly low in C_3A. When cements of various C_3A contents are included, the f_c vs. V_m/w_o relationship is found to be influenced by the C_3A content of the cement. This is illustrated in Fig. 6-3 and 6-4 (plotted from data of Tables 6-1 through 6-7), in which cements of various C_3A contents, including the cements of Fig. 6-1, are represented. Fig. 6-3 represents cements of low C_3A content;

Fig. 6-4, those of medium or high C_3A content. In each diagram, the diagonal line represents eq. (7).

In Fig. 6-4 it will be seen that the strengths developed by cements of medium or high C_3A content were in general lower than would be computed from eq. (7). (Certain exceptions will be discussed below.) The conclusion follows that cements of different C_3A contents develop different strengths at the same value of V_m/w_o, at least among those cements containing more than about 7 percent C_3A (computed).

Before further discussion of the relation between cement composition and strength, it is necessary to consider some other factors.

Effect of sand particles

In Fig. 6-3 and 6-4 three different series of tests are represented. Series 254-9 comprised three mixes, A, B, and C, as described previously (see Appendix to Part 2). Mix A contained sand and cement only. Mixes B and C contained sand and pulverized silica of cement fineness, the amount of the silica being 33 percent and 73 percent of the weight of the cement, respectively. Series 254-11 comprised mortar mixes of the same proportions as mixes A and B of Series 254-9. The data from these two series are, therefore, directly comparable. On the other hand, the data from Series 254-13 (appearing in Fig. 6-3A, B and Fig. 6-4A, B, and D) represent specimens containing only cement and pulverized silica, the amount of silica being 71 percent of the weight of the cement. The question, therefore, arises as to whether the results from Series 254-13 are comparable with those from the other two series.

In this connection it is of interest to examine Fig. 6-4C, which represents data obtained from mixes A, B, and C, and from neat cement. This is the only case where neat cement and mortar can be compared. Note that the strength of the neat cement at a given V_m/w_o exceeds by a considerable margin that of the specimens containing sand (No. 4 maximum size). The points appearing immediately below those representing neat cement are the ones representing mix A, which contained no pulverized silica, and mix B, which did contain silica. The results indicate, therefore, that the introduction of sand lowered the strength. It is presumed that the decrease in strength resulting from the introduction of sand is due to the decrease in homogeneity with respect to elastic properties, and possibly to a modification of the mode of failure as described by Terzaghi.[1]* On this basis one would not expect the introduction of pulverized silica to affect the strength adversely, owing to the smallness of the silica grains. Therefore, it would seem that neat cement specimens or specimens containing only pulverized silica as aggregate would not be directly comparable with specimens containing relatively coarse sand particles.

*See references at end of text, Part 6.

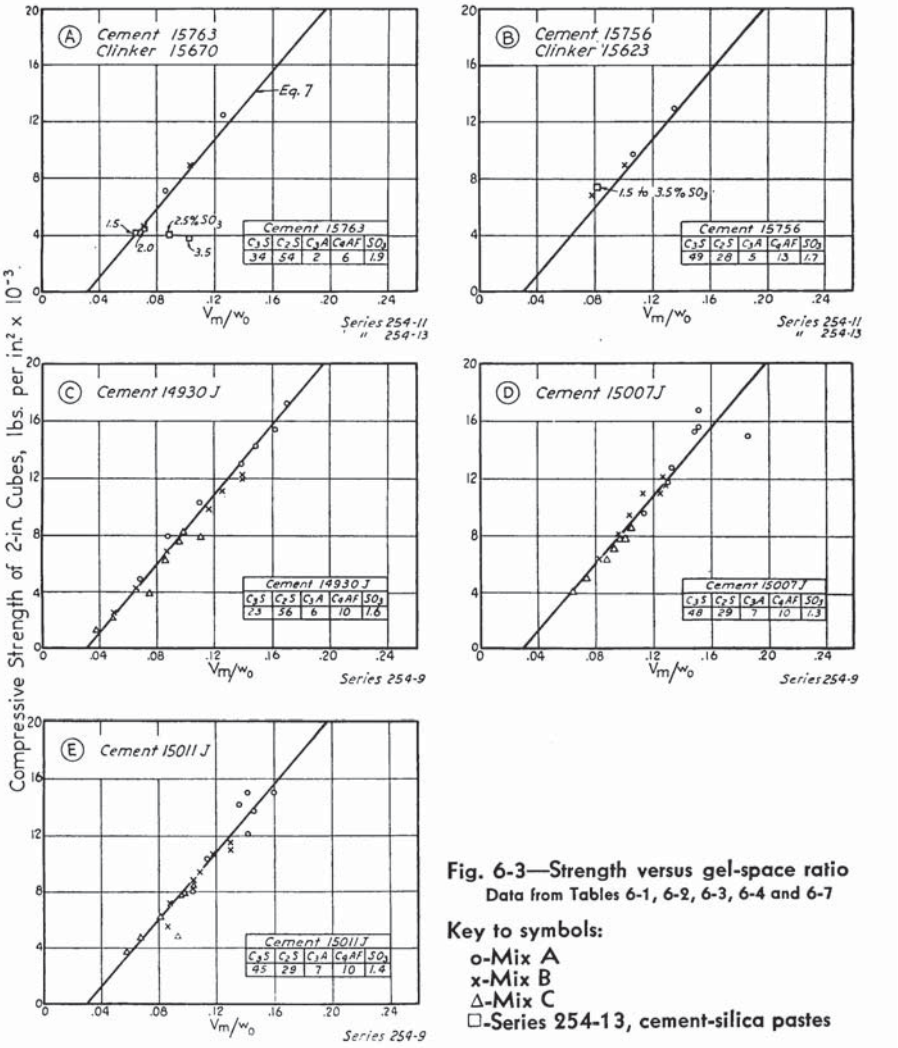

Fig. 6-3—Strength versus gel-space ratio
Data from Tables 6-1, 6-2, 6-3, 6-4 and 6-7

Key to symbols:
o-Mix A
x-Mix B
Δ-Mix C
□-Series 254-13, cement-silica pastes

However, the trend of the neat-cement points is such as to suggest that the strength of the neat cement and mortar would be equal at about $V_m/w_o = 0.10$. It happens that most of the points representing the cement-silica specimens of Series 254-13 fall near this point or lower on the V_m/w_o scale. Also, it may be observed that the strengths of these cement-silica specimens were about the same as or lower than the strengths obtained from the mortar specimens having equal values of V_m/w_o. It thus appears that, at least within the range of gel-space ratios that embraces the results from Series 254-13, the introduction of sand had little or no effect on strength and therefore that the mortars and cement-

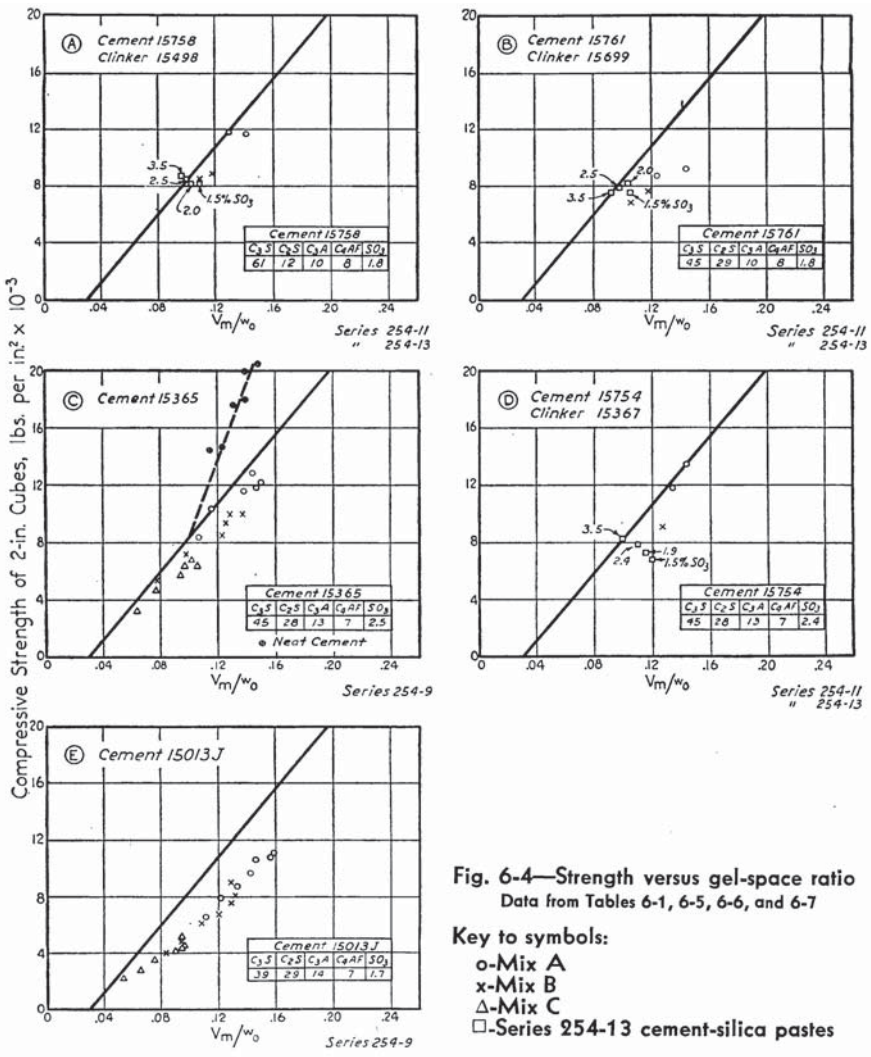

Fig. 6-4—Strength versus gel-space ratio
Data from Tables 6-1, 6-5, 6-6, and 6-7

Key to symbols:
o-Mix A
x-Mix B
Δ-Mix C
□-Series 254-13 cement-silica pastes

silica pastes can be compared directly in this instance. As brought out before, this indication is supported by the trend of the neat cement points appearing in Fig. 6-4C.

Influence of gypsum content of cement

The data from Series 254-13 offer a clue as to the cause of the relatively low strengths at a given V_m/w_o produced by the high C_3A cements. These data are given in Table 6-7 and are plotted in Fig. 6-3 and 6-4, as mentioned above. In this series, four cements were prepared from each of five different clinkers. The SO_3 content in each group of four cements ranged from 1.5 to 3.5 percent. Cement-silica cubes were made and tested after 28 days of water curing.

Note first the diagrams for the cements prepared from clinkers 15498, 15699, and 15367 in Fig. 6-4—medium or medium-high C_3A cements. In each case, increasing the gypsum content *increased* the strength to a value equal to or slightly greater than the mean of the low C_3A cements as represented by eq. (7) (that is, by the diagonal line).

As remarked above, it is somewhat questionable whether the data of Series 254-13 are comparable with eq. (7). Hence, the indications of the data must be taken with some reservation. However, it may tentatively be concluded that the relatively low strengths, at a given V_m/w_o, of cements of the type noted above can be increased and brought into line with the strengths of low C_3A cements by appropriate increases in gypsum content.

This conclusion was reached first by Lerch[2] in an investigation carried on parallel with this one. By means of calorimeter measurements of the rates of reaction and of strength and shrinkage tests, he found that the relatively low strength of high C_3A cements was associated with a premature depletion of gypsum during the early stages of hardening. Maximum strengths were produced when the gypsum content was so adjusted that the dissolved gypsum did not become depleted during the first 24 hours. Marked reductions in drying shrinkage also resulted from such an adjustment in gypsum content. Lerch's results have been confirmed in some respects by Whittaker and Wessels.[3]

It should be noted particularly that increasing the gypsum content of cements prepared from clinkers 15498 and 15367 increased the strength and at the same time *reduced* the ratio V_m/w_o. Since w_o was substantially the same for the different cements of a given group, this indicates that the reduction in the gel-space ratio was due to a reduction in the amount of gel. Thus we have a *reduction* in gel associated with an increase in strength whereas the normal effect would appear to be a reduction in strength. This apparent anomaly cannot yet be explained with assurance. However, it appears that the observed increase accompanying the decrease in gel content could be the result either of a change in the composition of the gel or of a reduction of the proportion of a gel having little intrinsic strength. Lerch[2] has pointed out that gypsum combines with C_3A to form calcium sulfoaluminate, most of the reaction taking place during the first few hours. Therefore, if the hydrate of C_3A is colloidal, as other evidence indicates, and if calcium sulfoaluminate is microcrystalline, the greater the amount of sulfoaluminate produced, the smaller V_m should be. With the type of cement considered here, the C_3A content is in excess of the gypsum on a combining-weight basis, and therefore the amount of calcium sulfoaluminate depends on the proportion of gypsum.

Hence, it appears that with medium- and high-C_3A cements, an increase in gypsum content reduces the ultimate amount of colloidal hydration product of C_3A. If this product is a hydrous calcium aluminate gel, it might have a weakening effect on the paste through an intrinsic weakness of such a gel. Another possibility is that the C_3A that does not react with gypsum becomes a constituent of a complex aluminosilicate gel. Presumably, it has a weakening effect on the gel.

The explanation given above is compatible with the results obtained from one of the low-C_3A cements but is possibly not in accord with the results from the other. As shown in Fig. 6-3, increasing the gypsum content of the low-C_3A cements prepared from clinker 15623 had little effect on either strength or gel-space ratio. This result is in accord with the above explanation. But with the cements prepared from clinker 15670, very low in C_3A, increasing the gypsum content greatly increased the gel content and slightly reduced the strength. This result is definitely not explained above. It might be that in this high-silica, low-R_2O_3 type of cement, the gypsum produces a colloidal hydrate, or causes some normally non-colloidal product to appear in the colloidal state. In either event the new colloidal product would have to be such as to have little effect on strength; that is, it would have no strength of its own and have no effect on the strength of the gel formed from other compounds. This matter will probably not be satisfactorily explained until new information on the constitution of hydration products is available.

Whatever the correct explanation may be, it is apparent that the strength of hardened paste depends on its chemical constitution as well as its gel-space ratio. This is substantially the same conclusion reached earlier by Bogue and Lerch.[4]

Effect of steam curing

The experiment with a steam-cured paste made of cement and pulverized silica was described in Part 2 and Part 3. No strength tests were made on this material, but the effects of the steam treatment can be estimated from the data published by Menzel.[5] These data show that steam-cured mixtures of cement and pulverized silica were as strong as or stronger than companion specimens cured normally. The adsorption data mentioned above indicate that the gel content of steam-cured material is not over 5 percent of that of the specimen normally cured for 28 days. This seems to be a clear demonstration that the gel-space ratio is not the controlling factor when curing temperature and pressure are variable. At least, it proves that the relation of f_c to V_m/w_o found for specimens cured at one temperature and pressure will not hold at another widely different temperature and pressure.

Menzel's data indicate that among specimens cured at different temperatures ranging from 70 to 350 F, the properties of the specimens show no differences that are disproportionate to the difference in curing temperature. This is particularly well illustrated by the data on shrinkage. The plot of total shrinkage at 35 percent relative humidity vs. temperature of curing, results in a smooth curve having a negative slope that diminishes slowly and rather steadily with increase in temperature. (See Menzel's Fig. 8.) Likewise, the initial rate of water-loss increases progressively as the curing temperature increases. From this we conclude that the f_c-vs.-V_m/w_o relationship must change progressively as the temperature of curing is increased above normal. Presumably, it would change also if the temperature were lowered.

DISCUSSION AND SUMMARY

Werner and Giertz-Hedström[6] found that strength could be expressed as a function of the volume of solid phase *per unit volume of hardened paste*. The solid phase was defined as the volume of the original cement plus the water that is not evaporable in the presence of concentrated H_2SO_4. The plotted data of Werner and Giertz-Hedström (see their Fig. 9) showed that the increase in strength was approximately proportional to the increase in the volume of the solid phase over the initial volume in the fresh paste. Thus, the relationship found was virtually the same as that shown in Fig. 6-2 of this paper.

Lea and Jones[7] found a fairly good relationship between fixed water *per unit of original cement* and strength. The fixed water was determined on neat pastes, $w/c = 0.25$, and the strengths on 1:2:4 concrete cubes. Since w_o/c of the concrete was a constant, a measure of the extent of hydration would also be virtually equivalent to our w_n/w_o. However, since the extent of hydration was estimated from companion specimens of much lower w_o/c, the shape of the curve obtained was no doubt influenced by the difference between the rate of hydration of the neat cement and that of the same cement in concrete.

Giertz-Hedström[8] concluded from these experiments and those of several other investigators that "it is thus possible as a first approximation to regard strength as a function of the degree of hydration and independent of the kind of cement." However, he goes on to say, ". . . . this can obviously not be the whole truth, as emerges for instance from the spreading of test values." He points out also that tests by Bogue and Lerch on pastes made of pure C_3S and C_2S "indicate that the silicate gel, which is the sole cause of the hardening of dicalcium silicate, is also chiefly responsible for the hardening of tricalcium silicate, but is to a certain extent helped here by calcium hydroxide." However, the data of Bogue and Lerch are of doubtful significance with respect

to this particular question. The original water-cement ratios of the pastes were not equal and therefore a measure of the extent of hydration alone was not an adequate description of the concentration of the hydration products in the space available to them.

Freyssinet[9] introduced two factors that he regarded as measures of important physical properties of hardened paste. These are:

(1) The "concentration of the cement," defined as:

$$\frac{\text{volume of hydrated cement}}{\text{volume of hydrated cement} + \text{volume of non-combined water}};$$

(2) The total area of the interstitial surfaces per unit volume of paste.

It will be seen that (1) represents the concept on which Giertz-Hedström based his analysis and that (2) is similar to the gel-space ratio as used by the authors.

Any attempt to express the strength of concrete or mortar as a function of only one independent variable is certain to meet with but limited success, at best, for the reason that more than one independent variable is involved. We have seen that in some combinations of paste and sand, the sand lowers the strength below that of the strength of pure paste of the same composition. Another factor influencing the strength of mortars and concretes is the existence of minute fissures under the aggregate particles, especially the larger particles. These fissures are the result of unequal settlement of paste and aggregate during the plastic state.[10,11,12] They occur to different degrees with different materials and proportions.

Another factor influencing strength is the air content, the higher the air content the lower the strength, other factors being equal. Weymouth[13] found that among plastic mixes the air content of fresh concrete depends on the water content and sand-cement ratio. He found also that the air content is approximately constant in different mixes of the same materials if the slump is constant. Therefore, variations in consistency of the fresh concrete will result in variations in strength of the hardened concrete (when other factors are equal) because of the corresponding variations in air content. The effect of air introduced by air-entraining agents is now well known.[14]

Also, although pertinent data are lacking, we may surmise that the strengths of adhesion between the hardened paste and the aggregate differ among concretes made with aggregates of different mineral composition. This will account for differences in strength, especially tensile strength.

All these independent factors influencing strength are secondary to the strength of the paste. Nevertheless, they cannot be ignored either in theoretical studies or construction practice. In the tests described in the foregoing pages most of these factors were absent, or were kept as near constant as possible. Consequently, the results depended mainly on the properties of the hardened paste. However, the problem of evaluating the factors influencing the strength of the paste is not much less complicated than that of the concrete as a whole. The degree of success achieved in this direction is indicated by the following summary of the results described in the foregoing pages.

(1) The strength of 2-in. mortar cubes made with cements of normal gypsum content and low C_3A content (less than about 7 or 8 percent) cured continuously wet at about 73 F conformed (within ± 10 percent) to the following relationship, regardless of differences in age or original water-cement ratio:

$$\text{Compressive strength of 2-in. cubes, psi} = 120{,}000\ \frac{V_m}{w_o} - 3600.$$

(2) Under the same curing conditions, mortar cubes made with cement of medium or high C_3A contents, containing the normal amount of gypsum, produced strengths that are too low to conform with the above equation.

(3) Some cements of medium or high C_3A content could be brought into conformity with the above equation by increasing the gypsum content, the required increase differing among different cements. Increasing the gypsum content of such cements reduced the gel content of the hardened paste.

(4) The tests indicated that with cements low in C_3A both the gel-space ratio and the strength may be unaffected by an increase in gypsum content, or the strength may remain unaffected while the gel-space ratio is increased. In the last-mentioned case, the results were not in conformity with the equation.

(5) The relationship between strength and V_m/w_o given in the above equation did not apply to specimens cured at temperatures other than about 73 F.

(6) In general, strength could be expressed as a function of the volume of the hydration products and the space originally available for them, only when factors such as cement composition and curing conditions were not available.

When cements of ordinary C_3A content are compared, the findings given above show that the strength at a given V_m/w_o is highest for the low-C_3A cements. It should be noted that this observation does not

pertain to the rate of hydration or the rate of strength development. Cements high in C_3A usually hydrate more rapidly and develop higher early strengths than those low in C_3A. The conclusion mentioned means that when two pastes of the same original water-cement ratio reach the same degree of hydration, as indicated by their gel-space ratios, the cement having the lower C_3A content will probably have the higher strength.

REFERENCES

(1) K. Terzaghi, *Proc. A.S.T.M.*, v. 45, p. 777.

(2) Wm. Lerch, A.S.T.M. Preprint A-4, 1946. See *A.S.T.M. Bulletin*, Jan. 1946.

(3) A. G. Whittaker and V. E. Wessels, *Rock Products*, v. 48, p. 95 (Aug. 1945).

(4) R. H. Bogue and Wm. Lerch, *Ind. Eng. Chem.* v. 26, p. 837 (1934) or Paper No. 27, Portland Cement Association Fellowship (Aug. 1934).

(5) Carl A. Menzel, *Proceedings*, ACI v. 31, p. 125 (1934).

(6) D. Werner and S. Giertz-Hedström, *Zement*, v. 20, pp. 984, 1000 (1931).

(7) F. M. Lea and F. E. Jones, *J. Soc. Chem. Ind.* v. 54, p. 63T (1935).

(8) S. Giertz-Hedström, "The Physical Structure of Hydrated Cements," Symposium on the Chemistry of Cements, Stockholm, 1938.

(9) E. Freyssinet, *Science et Industrie* (Jan. 1933).

(10) H. J. Gilkey, *Eng. News-Record*, v. 98, p. 242 (1927).

(11) T. C. Powers, *Proceedings*, ACI v. 25, p. 388 (1929); Bulletin 2, P.C.A. Research Laboratory (1939).

(12) I. L. Collier, *Proc. A.S.T.M.*, v. 30, Part II, p. 731 (1930).

(13) C. A. G. Weymouth, *Proc. A.S.T.M.*, v. 38, Part II, p. 354 (1938).

(14) C. E. Wuerpel, *Proceedings* ACI v. 42, p. 305 (1946); (See particularly bibliography in this paper).

TABLE 6-1—STRENGTHS AND GEL-SPACE RATIOS FOR SERIES 254-11

Ref. No. (S-254)	Mix	w_o/c	Age, days	Strength 2-in. cubes, psi	w_n/c	V_m/c	w_n/w_o	V_m/w_o
Cement 15758; clinker 15498; $V_m/w_n = 0.248$								
11–1	A	.334	28	11760	.171	.043	.512	.129
			90	11660	.191	.047	.572	.141
11–2	B	.460	28	8320	.196	.050	.426	.109
			90	8810	.223	.054	.485	.117
Cement 15756; clinker 15623; $V_m/w_n = 0.271$								
11–3	A	.318	28	9750	.123	.034	.387	.107
			90	13010	.149	.043	.468	.135
11–4	B	.446	28	6830	.132	.035	.296	.078
			90	9010	.168	.045	.377	.101
Cement 15763; clinker 15670; $V_m/w_n = 0.295$								
11–5	A	.324	28	7170	.092	.028	.284	.086
			90	12420	.134	.041	.414	.126
11–6	B	.437	28	4610	.101	.031	.231	.071
			90	8990	.149	.045	.341	.103
Cement 15761; clinker 15699; $V_m/w_n = 0.262$								
11–7	A	.334	28	8660	.162	.041	.485	.123
			90	9200	.180	.048	.539	.144
11–8	B	.468	28	6850	.185	.049	.395	.105
			90	7620	.212	.055	.453	.118
Cement 15754; clinker 15367; $V_m/w_n = 0.258$								
11–9	A	.328	28	11820	.170	.044	.518	.134
			90	13460	.195	.047	.594	.143
11–10	B	.449	28	7970	.197	.050	.439	.111
			90	9110	.230	.057	.512	.127

TABLE 6-2—STRENGTHS AND GEL-SPACE RATIOS FOR CEMENT 14930J—SERIES 254-9

$V_m/w_n = 0.304$

Ref. No. (S-254)	w_o/c	Age, days	Strength 2-in. cubes, psi	w_n/c	V_m/c	w_n/w_o	V_m/w_o
			Mix A				
9–1	.309	7	4950	.080	.021	.259	.068
		14	7960	.099	.027	.320	.088
		28	10280	.107	.034	.346	.110
		56	12970	.129	.043	.417	.139
		90	14210	.150	.046	.485	.149
		180	15410	.162	.050	.524	.162
8–1	.311	447	17260	.181	.053	.582	.170
			Mix B				
9–2	.424	7	2580	.080	.021	.189	.050
		14	4320	.103	.028	.243	.066
		28	6930	.116	.037	.274	.087
		56	9860	.135	.049	.318	.116
		90	11180	.174	.053	.410	.125
		180	12310	.185	.059	.436	.139
8–2	.443	362	11910	.201	.062	.452	.140
			Mix C				
9–3	.573	7	1230	.082	.022	.143	.038
		14	2140	.090	.028	.157	.049
		28	3940	.121	.043	.211	.075
		56	6200	.164	.049	.286	.086
		90	7580	.185	.055	.322	.096
		180	8280	.201	.056	.350	.098
8–3	.595	362	7940	.210	.066	.353	.111

TABLE 6-3—STRENGTHS AND GEL-SPACE RATIOS FOR CEMENT 15007J—SERIES 254-9

$V_m/w_n = 0.272$

Ref. No. (S-254)	w_o/c	Age, days	Strength 2-in. cubes, psi	w_n/c	V_m/c	w_n/w_o	V_m/w_o
			Mix A				
9–4	.316	7	9660	.126	.036	.399	.114
		14	11830	.140	.041	.443	.130
		28	12810	.154	.042	.488	.133
		56	15310	.168	.047	.532	.149
		90	15600	.173	.048	.548	.152
		180	16780	.184	.048	.583	.152
8–28	.344	479	14970	.198	.064	.576	.186
			Mix B				
9–5	.433	7	6380	.133	.036	.307	.083
		14	8080	.150	.042	.346	.097
		28	9400	.171	.045	.395	.104
		56	11080	.185	.049	.427	.113
		90	11600	.192	.056	.443	.129
		180	12150	.202	.055	.467	.127
8–29	.464	440	11120	.217	.058	.468	.125
			Mix C				
9–6	.570	7	4060	.156	.037	.274	.065
		14	5000	.163	.042	.286	.074
		28	6280	.184	.050	.323	.088
		56	7070	.204	.053	.358	.093
		90	7840	.205	.056	.360	.098
		180	8540	.213	.060	.374	.105
8–30	.595	479	7780	.232	.060	.390	.101

TABLE 6-4—STRENGTHS AND GEL-SPACE RATIOS FOR CEMENT 15011J—SERIES 254-9

$V_m/w_n = 0.272$

Ref. No. (S-254)	w_o/c	Age, days	Strength 2-in. cubes, psi	w_n/c	V_m/c	w_n/w_o	V_m/w_o
			Mix A				
9–7	.316	7	8050	.114	.033	.361	.104
		14	10400	.133	.036	.421	.114
		28	12100	.143	.045	.453	.142
		56	13750	.156	.046	.494	.146
		90	14180	.164	.043	.519	.136
		180	15020	.170	.045	.538	.142
8–40	.319	478	15020	.184	.051	.576	.160
			Mix B				
9–8	.432	7	5550	.123	.037	.285	.086
		14	7140	.153	.038	.354	.088
		28	8900	.165	.045	.382	.104
		56	9500	.178	.047	.412	.109
		90	10720	.191	.051	.442	.118
		180	11020	.199	.056	.461	.130
8–41	.442	368	11500	.210	.058	.475	.131
			Mix C				
9–9	.582	7	3720	.131	.034	.225	.058
		14	4820	.157	.039	.270	.067
		28	6320	.176	.047	.302	.081
		56	4880	.195	.054	.335	.093
		90	7850	.205	.056	.352	.096
		180	7970	.214	.057	.368	.098
8–42	.595	368	8440	.222	.062	.373	.104

TABLE 6-5—STRENGTHS AND GEL-SPACE RATIOS FOR CEMENT 15013J—SERIES 254-9

$V_m/w_n = 0.244$

Ref. No. (S-254)	w_o/c	Age, days	Strength 2-in. cubes, psi	w_n/c	V_m/c	w_n/w_o	V_m/w_o
			Mix A				
9–10	.324	7	6620	.149	.036	.460	.111
		14	7960	.164	.039	.506	.121
		28	8780	.171	.043	.528	.133
		56	9680	.180	.046	.555	.142
		90	10610	.191	.047	.590	.145
		180	11020	.188	.051	.580	.158
8–46	.332	339	10820	.218	.052	.656	.157
			Mix B				
9–11	.443	7	4010	.156	.037	.352	.084
		14	4940	.183	.042	.413	.095
		28	6120	.177	.048	.400	.108
		56	6740	.208	.053	.470	.120
		90	7600	.215	.057	.485	.129
		180	8060	.236	.058	.533	.131
8–47	.453	333	9040	.241	.058	.532	.128
			Mix C				
9–12	.611	7	2250	.158	.033	.259	.054
		14	2750	.183	.040	.299	.065
		28	3480	.203	.046	.332	.075
		56	4180	.221	.055	.362	.090
		90	4280	.236	.058	.386	.095
		180	4520	.245	.059	.401	.096
8–48	.599	333	5210	.253	.057	.422	.095

TABLE 6-6—STRENGTHS AND GEL-SPACE RATIOS FOR CEMENT 15365—SERIES 254-9

$V_m/w_n = 0.254$

Ref. No. (S-254)	w_o/c	Age, days	Strength 2-in. cubes, psi	w_n/c	V_m/c	w_n/w_o	V_m/w_o
			Neat cement				
9–15A	.244	7	14440	.115	.028	.471	.115
		14	14640	.126	.030	.515	.123
		28	17600	.136	.032	.556	.131
		56	17960	.140	.034	.573	.139
		90	20000	.145	.034	.594	.139
		180	20500	.155	.036	.635	.148
			Mix A				
9–13	.319	7	8380	.133	.034	.417	.107
		14	10380	.152	.037	.476	.116
		28	11550	.149	.044	.467	.138
		56	11800	.179	.047	.561	.147
		90	12170	.179	.048	.561	.150
		180	12760	.182	.046	.571	.144
			Mix B				
9–14	.439	7	5340	.139	.034	.316	.078
		14	7170	.171	.043	.390	.098
		28	8480	.184	.054	.419	.123
		56	9400	.210	.055	.478	.125
		90	9870	.215	.056	.490	.128
		180	9940	.222	.060	.505	.137
			Mix C				
9–15	.587	7	3220	.153	.037	.260	.063
		14	4670	.186	.045	.317	.077
		28	5680	.210	.055	.358	.094
		56	6280	.221	.057	.376	.097
		90	6320	.230	.062	.392	.106
		180	6720	.255	.060	.435	.102

TABLE 6-7—STRENGTHS AND GEL-SPACE RATIOS WITH THE AMOUNT OF GYPSUM IN THE CEMENT AS A VARIABLE—SERIES 254-13

Cement-silica pastes

Ref. No. (S-254)	w_o/c	SO_3 cont. of cement, percent	28-day strength 2-in. cubes, psi	w_n/c	V_m/c	w_n/w_o	V_m/w_o
Cements made from clinker 15367							
13–1	.493	1.5	6970	.215	.059	.435	.120
13–1B	.486	1.5	6640	.212	.058	.436	.119
13–2	.493	1.9	7630	.211	.056	.428	.113
13–2B	.488	1.9	6870	.216	.058	.442	.119
13–3	.489	2.4	8090	.208	.054	.425	.110
13–3B	.488	2.4	7610	.215	.055	.441	.113
13–4	.491	3.5	8240	.194	.048	.395	.098
13–4B	.492	3.5	8250	.204	.050	.414	.102
Cements made from clinker 15623							
13–5	.470	1.5	7530	.152	.038	.323	.081
13–6	.474	2.0	7440	.151	.038	.319	.080
13–7	.473	2.5	7440	.152	.038	.321	.080
13–8	.480	3.5	7000	.144	.038	.300	.079
Cements made from clinker 15699							
13–9	.498	1.5	7510	.199	.053	.400	.106
13–10	.499	2.0	8160	.194	.052	.389	.104
13–11	.499	2.5	7860	.192	.049	.385	.098
13–12	.498	3.5	7530	.184	.046	.369	.092
Cements made from clinker 15498							
13–13	.488	1.5	8120	.208	.053	.426	.109
13–14	.487	2.0	8120	.199	.050	.409	.102
13–15	.493	2.5	8550	.200	.049	.405	.099
13–16	.491	3.5	8710	.190	.047	.387	.096
Cements made from clinker 15670							
13–17	.476	1.5	4240	.111	.031	.233	.065
13–18	.479	2.0	4440	.118	.034	.246	.071
13–19	.483	2.5	4070	.184	.043	.380	.089
13–20	.486	3.5	3800	.209	.050	.431	.103

Part 7. Permeability and Absorptivity

CONTENTS PART 7

PERMEABILITY OF HARDENED PORTLAND CEMENT PASTE

The following discussion deals with the relationship between the physical properties of hardened paste and the rate at which water may flow through a saturated specimen of paste under a given pressure gradient. In view of the results published by Ruettgers, Vidal, and Wing,[1] we may assume that such flow takes place in accord with Darcy's law.

Darcy's law

Darcy's law for low-velocity flow, first found empirically from experiments with flow through beds of sand, may be written

$$\frac{dq}{dt}\frac{1}{A} = K_1\frac{\Delta h}{L} \quad , \quad \ldots\ldots\ldots\ldots\ldots\ldots\ldots\ldots\ldots\ldots (1)$$

where

$\frac{dq}{dt}$ = rate of volume efflux, cc per sec,
A = area of the porous medium, sq cm,
Δh = drop in hydraulic head across the thickness of the medium, cm,
L = thickness of the medium, cm, and
K_1 = a constant depending on the properties of the porous medium and the kinematic viscosity of the fluid, cm per sec.

K_1 of eq. (1) depends on both the properties of the medium and of the fluid. Thus, K_1 represents the permeability of a porous medium to a specified fluid at a specified temperature. The following, more general expression is preferred:[2]

$$\frac{dq}{dt}\frac{1}{A} = \frac{K_2}{\eta}\frac{\Delta P'}{L} \quad \ldots\ldots (2)$$

in which

η = viscosity of fluid, poises, dyne-sec per sq cm,
$\Delta P'$ = pressure drop across the medium, dynes per sq cm, and
K_2 = coefficient of permeability, sq cm.

In terms of hydraulic gradient rather than pressure differential

$$\frac{dq}{dt}\frac{1}{A} = \frac{K_2 g\, d_f\, \Delta h}{\eta\, L} \quad \ldots\ldots (3)$$

where d_f = density of the fluid, g per cc, and
g = acceleration due to gravity, cm per sec per sec.

As Muskat[2] has pointed out, the coefficient of permeability, K_2, is a constant determined by the characteristics of the medium in question and is entirely independent of the nature of the fluid.

Permeability equation for hardened paste

In the following discussion, the theoretical coefficient of permeability of hardened paste will be evaluated analytically from the original cement content, the non-evaporable water content, and V_m (see Part 3). This is accomplished by means of the following relationship found theoretically by Kozeny[3] and verified experimentally on beds of granules by Carman:[4d]

$$K_2 = k\epsilon\, m^2 \quad \ldots\ldots (4)$$

where k = a dimensionless constant,
ϵ = ratio of pore volume to total volume, and
m = hydraulic radius.

For the derivation of this equation reference should be made to the original articles by Kozeny and especially those by Carman. The equation rests on the assumption that the particles composing the bed have a completely random packing, and on the use of hydraulic radius in Poiseuille's equation for capillary flow. The hydraulic radius is

$$m = \frac{\text{void-volume}}{\text{surface area of void-boundaries}} = \frac{\epsilon}{S} \quad \ldots\ldots (5)$$

Hence

$$K_2 = k\frac{\epsilon^3}{S^2} \quad \ldots\ldots (6)$$

Various experiments of Carman and those of Fowler and Hertel[5] show that $k = 0.2$ can be assumed for a wide variety of media.

Applied to beds of relatively large particles, eq. (6), with $k = 0.2$, was found by Carman to be a satisfactory basis for predicting permea-

bility from the *total* porosity of the bed and the specific surface of the particles. Applied to certain fine-textured media, the equation was found to give permeability coefficients that were much too high if the total porosity was used for ϵ. Carman found such to be the case for beds of clay.[4b] By assuming that a certain amount of the interparticle space was not effective in transmitting water, Carman was able to obtain agreement between the theoretical and experimental results. Powers[6] and Steinour[7] adapted the Kozeny equation (eq. (4)) to the rate of bleeding of portland cement paste and found that a similar modification was necessary. These different experiments show that for certain fine-textured media,

$$\epsilon_e = \epsilon - \alpha(1 - \epsilon) , \quad (7)$$

where ϵ = total porosity,

ϵ_e = effective porosity, and

α = amount of immobile fluid per unit volume of solids in the medium.

Steinour[7] found that for fluid flow through concentrated suspensions of particles, α depended on

(1) the amount of fluid chemically or physically combined with the particle surfaces,

(2) the angularity of the particles, and

(3) the presence or absence of flocculation of the particles.

In a solid porous medium such as hardened paste, item (1) would be the amount of fluid attached to the pore walls, item (2), the irregularity of the wall surfaces, and item (3), the variations in cross-sectional area along the conduits through the medium.

For cement pastes, the total porosity, ϵ, may be taken as being equal to the volume of the total evaporable water. According to eq. (7), the effective porosity, ϵ_e, should be smaller than the total by some quantity proportional to $(1 - \epsilon)$, the volume of the solid phase. However, the effect of the three items mentioned above can be taken care of adequately enough for the present purpose by assuming that the amount of water in a saturated paste that remains immobile is proportional to the total surface area, regardless of the cause of its immobility. Thus, since the total surface area is proportional to V_m,

$$\epsilon_e = w_e - k_1 V_m \quad (8)$$

where w_e = total evaporable water in cc per cc of hardened paste.

Let $w_e/V_m = N$. Then

$$\epsilon_e = V_m(N - k_1) \quad (9)$$

The total surface area in the paste is

$$S = (35.7 \times 10^6) V_m \quad \text{.....(10)}$$

(See Part 3.)

Using ϵ_e for ϵ and substituting from eq. (9) and (10) into eq. (6) gives

$$K_2 = \frac{k}{(35.7 \times 10^6)^2} V_m (N - k_1)^3 \quad \text{.....(11)*}$$

(In the above equations V_m is in g per cc of paste.) Since,

$$k = 0.2 \text{ (Carman)},$$

eq. (11) may be written

$$K_2 = 15.7 \times 10^{-17} V_m (N - k_1)^3 \quad \text{.....(12)}$$

Eq. (12) gives the coefficient of permeability in terms of three factors that are constant for a given sample. V_m and N are measurable. However, k_1 is unknown and cannot be evaluated without further permeability tests.

Comparison with data of Ruettgers, Vidal, and Wing

No experimental data are available for checking eq. (12) quantitatively. However, Ruettgers, Vidal, and Wing[8] published the results of permeability tests on neat cement made with a special cement resembling the present A.S.T.M. Type II, except that it was considerably coarser than present-day cements (15 percent retained on No. 200). From their plotted results, the coefficients of permeability for neat cement cured 60 days were estimated to be as shown in the last column of Table 7-1.

Before comparing the results of the tests and the computations the basis of the computations must be explained. To compute the permeability of the specimens tested by Ruettgers, Vidal, and Wing, V_m and the total evaporable water for the saturated state must be known and a value for k_1 must be assumed. However, only the nominal water-cement ratio, the composition of the cement, and the heat of hydration of the cement were available. The cement content was estimated from the nominal water-cement ratio. w_n/c was computed from the relationship

$$\text{heat of hydration} = 525\, w_n/c \text{ (see Part 4)}$$

and found to be about 0.15. From the composition of the cement and eq. (4) of Part 3, V_m was estimated at $0.256\, w_n$.

Ruettgers, Vidal, and Wing gave their results in terms of K_1 of eq. (1), in ft. per sec, whereas eq. (12) is in terms of K_2 of eq. (3). A comparison of eq. (1) and (3) shows that

$$K_1 = \frac{K_2 d_f g}{\eta}.$$

*It may be noted that, in deriving eq. (11) from eq. (6), the total surface in contact with the flowing water is presumed to be equal to the surface area of the solid phase as measured by water-vapor adsorption. This is exactly correct if the only immobile water is the first adsorbed layer and if the surface area of the first adsorbed layer is equal to the surface area of the solid phase. At present there is no way to check the validity of the final equation, except crudely by the reasonableness of the results obtained.

TABLE 7-1—COMPUTATION OF COEFFICIENT OF PERMEABILITY FROM EQ. (13)

$K_1 = 0.5 \times 10^{-12} V_m(N - k_1)^3$

w/c (nom)	c g per cc of paste	$\frac{w_n}{c}$	$0.256 \times \frac{w_n/c}{} = V_m/c$	$\frac{V_m}{c} \cdot c$	$\frac{w_o - w_n}{c} = w_e/c$	$\frac{w_e/c}{V_m/c} = N$	K_1 computed (ft per sec) $\times 10^{12}$				$K_1 \times 10^{12}$ Ruettgers, Vidal, and Wing
							$k_1 = 1$	$k_1 = 2$	$k_1 = 3$	$k_1 = 4$	
0.5	1.22	0.15	0.038	0.047	0.35	9.2	13	9	6	3	15*
0.6	1.09	0.15	0.038	0.043	0.45	11.8	27	20	15	10	100
0.7	0.98	0.15	0.038	0.037	0.55	14.5	45	36	28	22	550†
0.8	0.90	0.15	0.038	0.034	0.65	17.1	70	59	48	38	1830
1.0	0.76	0.15	0.038	0.029	0.85	22.3	—	—	—	—	3730
1.2	0.66	0.15	0.038	0.025	1.05	27.6	—	—	—	—	8530

*Estimated by extrapolation.
†Estimated by interpolation.

For water, $d_f = 1$, $\eta = 0.01$, and $g = 980$ may be assumed. Hence,

$$K_1, \text{ in cm per sec} = 98000\ K_2,$$

or

$$K_1, \text{ in ft. per sec} = 3220\ K_2.$$

Therefore, from eq. (12)

$$K_1 = 50 \times 10^{-14}\ V_m\ (N - k_1)^3 \text{ ft. per sec} \quad \ldots\ldots\ldots\ldots (13)$$

To be strictly consistent, we would have converted the weights of the total evaporable water to volumes. However, such a refinement seemed unnecessary in view of other uncertainties. Therefore, the estimated weights in grams per unit volume of paste were used.

To k_1, the immobile-water factor, no value could be assigned from known or estimated values of physical composition. Four values were tried, as shown in Table 7-1. The assumption $k_1 = 1.0$ amounts to assuming that only the first adsorbed layer is immobile. The assumption that k_1 is greater than 1 is, of course, that the immobile liquid is more than the amount in the first adsorbed layer.

In Table 7-1 the first indication to be noted is that the computed values are less than the experimental values in all cases. Only for the paste of lowest water-cement ratio do the two values approach equality and then only when k_1 is given its minimum value. Even here, the apparent agreement may be fortuitous because the experimental value given was obtained by an uncertain extrapolation. The second point is that the observed permeabilities increase with increase in w/c much faster than the computed values. Had the computation been based on net rather than nominal w/c, the divergence at high w/c would have been even greater. Possibly the lack of agreement and the divergence just noted are the result of some fault in the theory on which the computations are based, but it cannot be accepted as proof of such faults. There is good reason to believe, as shown in the following paragraph, that the discrepancies between observed and computed values can be accounted for on the basis of decreases in the degree of homogeneity of test specimens accompanying increases in w/c.

Both Powers[6] and Steinour[7c] found from studies of fresh paste made of water and normal portland cement that for w/c's up to about 0.5 by weight, the flocculated cement particles formed a continuous structure having a permeability that could be computed from a modification of the basic Kozeny equation (eq. (4)). At such water ratios, the mass of paste constitutes one continuous floc, and the permeability of the mass as a whole depends on the floc texture. At very high dilution the particles form flocs that are more or less independent of each other. The permeability of such a mass is not determined by the floc texture, but largely by the size of the individual flocs and their concentration.

In an intermediate range of w/c's, the fresh paste exhibits some of the qualities of both extremes. The permeability is determined in part by floc texture and in part by channels that develop in the flocculated mass. This condition is denoted by the appearance of localized channels during the bleeding period. In either the intermediate or the high range of w/c's, the effective size and number of the conduits through the mass of particles cannot be computed from the composition of the mass as a whole, because such masses do not have the homogeneity assumed in the computation.

The homogeneity of a fresh paste, or the lack of it, probably persists in some degree after the paste hardens. Hence, it is probable that for hardened pastes having w/c's greater than 0.6, or thereabouts,* the permeability of a test disk is determined not only by the permeability of the hardened paste, but also by vertical channels that represent discontinuities in the paste—the discontinuities that developed during the bleeding period. In the neat cement disks in question, such channels would extend from the top surface well into the interior and thus greatly increase the permeability of the disk as a whole. The higher the original w/c above the minimum at which channels develop, the greater the number and size of such by-passes around the relatively dense, homogeneous material composing the bulk of the hardened paste.

It is probable that even if channeling did not occur, eq. (13) would not correctly represent the permeability of hardened pastes of all degrees of porosity. This may be inferred from Fig. 5-11 of Part 5. From this figure we may recall the earlier conclusion that saturated, hardened cement pastes may contain only the gel water, or they may contain both gel water and capillary water, depending on the original water-cement ratio and the extent of hydration. Capillary water is absent when the total evaporable water is equal to $4V_m$. It is possible that the permeability of a given paste depends on the permeability of the gel itself and on the size and number of the capillaries outside the gel. The hydraulic radius of these capillaries would be

$$\frac{w_e - 4V_m}{S_c} = \frac{V_m(N - 4)}{S_c} \quad ,$$

where

S_c = superficial area of the gel, and
$N = w_e/V_m$.

S_c is not known. It is probably much smaller than the total surface area of the solid phase as indicated by V_m. If so, the permeability of the capillary space would be of a higher order than that of the gel itself when w_e is greater than $4V_m$.

*The limiting water ratio depends on the characteristics of the cement, particularly its specific surface, and on the character and amount of subsieve aggregate. Air-entraining agents tend to raise the limit.

The discrepancies between computed and observed values of K_1 seen in Table 7-1 are in accord with the considerations expressed above. That is, it appears that the permeability of pastes of relatively high w/c is probably determined in major degree by the by-passes around the hydration products, or in other words, by residues of the original water-filled space not filled by gel or other hydration products; but in pastes of low w/c, well cured, the permeability of the paste as a whole is fixed mainly by the permeability of the gel and the amount of gel per unit volume of paste.

Theoretical minimum permeability

For rich pastes the minimum permeability attainable can be estimated from eq. (13) on the assumption that the equation is valid at least for pastes in which $w_e = 4V_m$. The composition of such pastes may be expressed as follows:

$$cv_c + w_n v_n + w_g v_g = 1 ,$$

where

c = original cement, g per cc of paste,
w_n = non-evaporable water, g per cc of paste,
w_g = gel water, g per cc of paste, and
v_c, v_n, and v_g = the respective specific volumes.

On the basis of data given in Part 5, let

$w_n = 3.9V_m$
$w_g = 4V_m$
$v_n = 0.82$, and
$v_g = 0.90$.

Then

$$V_m = 0.147(1 - cv_c) \quad \ldots\ldots (14)$$

Hence, noting that $N = 4$, we obtain from eq. (13),

$$K_1 = 50 \times 10^{-14} \times 0.147(1 - cv_c)\ (4 - k_1)$$
$$= 7.4 \times 10^{-14}(1 - cv_c)\ (4 - k_1) \quad \ldots\ldots (15)$$

Eq. (15) shows that K_1 can be zero when $cv_c = 1$ or when $k_1 = 4$. The condition that $cv_c = 1$ means that the paste is a voidless mass of unhydrated cement. (As shown in Part 5, cv_c as high as 0.72 can be produced by molding the paste under high pressure. Normally, it is near 0.50.) Hence, the cv_c term cannot make K_1 zero. Constant k_1 has a minimum value of 1. Its maximum value is not known but it is not likely that it can be as great as 4 since this would mean that all the water in such pastes is held immobile by the solid surface. It seems more likely that only the first layer could be wholly immobile and hence that hardened paste cannot be absolutely impermeable. If this is assumed, the minimum permeability would be of the order of 10^{-12} to 10^{-13} ft. per sec.

These estimates indicate that well cured, neat paste of low w/c is practically impermeable. (Ruettgers, Vidal, and Wing[1] give the permeability of granite as ranging from 2 to 10 $\times$ 10^{-12} ft. per sec.).

Relationship between permeability of paste and permeability of concrete

This subject was discussed fully by Ruettgers, Vidal, and Wing and therefore requires only brief mention here. Introduction of aggregate particles into paste tends to reduce the permeability by reducing the number of channels per unit gross cross-section and by lengthening the path of flow per unit linear distance in the general direction of flow. However, during the plastic period, the paste settles more than the aggregate and thus fissures under the aggregate particles develop. In saturated concrete these fissures are paths of low resistance to hydraulic flow and thus increase the permeability of the concrete. In general, with paste of a given composition and with graded aggregate the permeability is greater the larger the maximum size of the aggregate. Obviously, the permeability of concrete as a whole is much higher than the theoretical permeability as developed above for a homogeneous medium.

The above discussions indicate that for well cured concretes having water-cement ratios above about 0.5, the permeability is determined largely by the by-passes around the gel and the by-passes around the paste in the concrete structure as a whole.

THE ABSORPTIVITY OF HARDENED PASTE

The term "absorptivity" pertains to the characteristic rate at which dry or partially dry paste absorbs water without the aid of external hydraulic pressure.

For pastes containing capillary space outside the gel, it is believed that the water is taken in by two different processes. The water enters the capillary system under the influence of capillary force, i.e., surface tension. Probably most of the water entering the gel, if not all, is drawn by adsorption forces. The resistance to the inward flow into the capillary system should be indicated by the coefficient of permeability of the saturated paste. The resistance to the flow into the gel, where the initial flow presumably takes place along surfaces of unfilled channels, would probably not be determined by the permeability, but by a coefficient of diffusivity.

These suppositions are supported by several considerations already discussed. Perhaps the most pertinent consideration is that illustrated by Fig. 4-12, Part 4. This shows that the evaporable water lost when a saturated specimen is exposed to a relative vapor pressure of 0.5 could be divided into two classes—one that was lost rapidly without apparent relation to shrinkage, and one that was lost more gradually and was directly related to shrinkage.

No attempt will be made here to derive a theoretical relationship for absorptivity. However, an empirical relationship between absorptivity and capillary porosity will be shown.

Relationship between absorptivity and the capillary porosity

It can be shown (see later) that for either capillary penetration or diffusion, the adsorption of water during a short initial period, under proper experimental conditions, follows the relationship

$$\frac{q}{A} = (K_a t)^{1/2} \quad \ldots\ldots\ldots\ldots\ldots\ldots\ldots\ldots\ldots\ldots\ldots\ldots\ldots\ldots (16)$$

where q/A = amount of water per unit area absorbed in elapsed time t, and

K_a = a constant characteristic of the absorbent, in its initial state of dryness, called the coefficient of absorptivity. It has the dimensions sq cm per sec.

K_a was evaluated for several mortar prisms, 2 × 2 × 9½ in., that had been water-cured and then dried in air of 50 percent relative humidity for 6 or 7 months. They were broken into halves transversely and then coated with paraffin so that only the broken end was exposed. Each specimen was then suspended under water at 73 F from one end of a beam-balance and its change in weight with time was recorded. Plotting q/A vs. the square root of time for these specimens produced straight lines for about the first 60 minutes.

Two different kinds of cement were used, with the following two mixes for each cement:

Ref. No.	Type of cement (A.S.T.M.)	Parts by weight		
		Cement	Standard sand	Pulverized silica
290–41 & –43	III	1	1.63	—
290–42 & –44	IV	1	2.30	0.33

The pulverized silica was of about the same specific surface (sq cm per cc) as the cement. The mortars were plastic when fresh and relatively homogeneous after hardening, since the paste had relatively low bleeding capacity and the paste content was relatively high. (The above mixes are the same as mixes A and B described in Appendix to Part 2.) The compositions of the specimens were the same as those given in Table A-30, first four lines, Appendix to Part 2. The results of absorptivity tests, together with data derived from Tables A-30 and A-33 are given in Table 7-2.

We may surmise that the coefficient of absorptivity depends on the porosity and on the size of the pores of the specimen. As remarked

TABLE 7-2—ABSORPTIVITY DATA

Ref. No.	W_o g per cc of spec.	C, g per cc of spec.	W_n g per cc of spec.	$0.86 \times (1 + 4k)$	$0.86 \times (1 + 4k) \times W_n$	$W_o - 0.86 \times (1 + 4k) \times W_n$	K_a (observed), sq cm per sec $\times 10^7$	
							Spec. A	Spec. B
Cement 15758 A.S.T.M. Type III, $k = 0.248$*								
290–41	.252	.755	.129	1.71	.220	.032	13.5†	8.3
290–42	.250	.542	.106	1.71	.181	.069	23.5	23.0
Cement 15756 A.S.T.M. Type IV, $k = 0.271$*								
290–43	.255	.769	.095	1.79	.170	.085	27.4	28.0
290–44	.252	.560	.074	1.79	.132	.120	73.5	76.1

*See Part 3, Fig. 3-7A and B.
†Doubtful result based on first 15 minutes only. Others are based on about first hour.

above, it is probable that the initial, comparatively rapid adsorption takes place almost exclusively in the capillary system. That is, although the gel is not saturated, the gel pores are so small that very little water can enter them, as compared with the amount that enters the capillary system during a limited time. On this basis, we may write

$$K_a = f(p_c, r_c) \quad , \ldots\ldots\ldots\ldots\ldots\ldots\ldots\ldots\ldots\ldots\ldots\ldots\ldots\ldots (17)$$

where p_c = volume of capillary pores per cc of mortar—the *capillary porosity*, and r_c = effective radius of the capillaries.

The capillary-porosity can be estimated conveniently in terms of the water content of the fresh mortar (after bleeding) and the increase in the volume of the solid phase due to hydration. That is, the capillary porosity is the difference between the increase in volume of the solid phase (due to hydration) and the original volume of pores:

$$p_c = W_o - V_B - Cv_c \, , \ldots\ldots\ldots\ldots\ldots\ldots\ldots\ldots\ldots\ldots\ldots\ldots\ldots (18)$$

where V_B = bulk volume of the solid phase, including gel pores and unhydrated cement, in cc per cc of specimen,

and C = cement content of specimen, grams per cc of specimen.

From Part 5, eq. (9),

$$V_B = Cv_c - 0.86(1 + 4k)W_n \, , \ldots\ldots\ldots\ldots\ldots\ldots\ldots\ldots\ldots\ldots\ldots\ldots (19)$$

where $0.86 = v_d$ = mean of the specific volumes of gel water and non-evaporable water, and

W_n = non-evaporable water, grams per cc of specimen.

Hence, from eq. (18) and (19),

$$p_c = W_o - 0.86(1 + 4k)W_n \ldots\ldots\ldots\ldots\ldots\ldots\ldots\ldots\ldots\ldots\ldots\ldots\ldots (20)$$

As shown previously, there is no satisfactory way of evaluating the size of the capillaries. However, capillary radius is at a maximum

before hydration begins and becomes zero when all original capillary space ($= W_o$) becomes filled with hydration products. At intermediate stages the relationship may be such that capillary radii are about the same among different pastes when the original capillary space in each paste is filled to the same degree. To the extent that this is true,

$$r_c = f[W_o - 0.86(1 + 4k)W_n] \quad \ldots\ldots\ldots\ldots\ldots\ldots\ldots\ldots (21)$$

A comparison of eq. (17), (20), and (21) indicates that K_a should be some function of $W_o - 0.86(1 + 4k)W_n$ only. The nature of the function is indicated by the plotted experimental data given in Fig. 7-1.

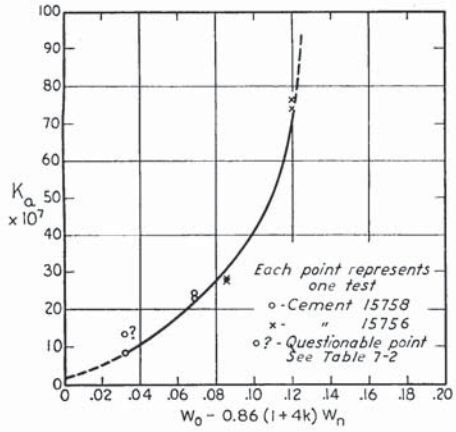

Fig. 7-1—Empirical relationship between coefficient of absorptivity and capillary porosity

Series 254 and 290

It should be noted that according to eq. (21), capillary radius becomes zero when $0.86(1 + 4k)W_n = W_o$, that is, when capillary porosity is zero. Hence, if the assumptions made in arriving at the basis of plotting used in Fig. 7-1 are valid, or approximately so, the curve should appear to go through the origin. Fig. 7-1 shows that a reasonable curve through the points could pass through or very near the origin. This only illustrates, however, the relative smallness of the gel pores, for it is certain that K_a is not zero when capillary porosity is zero. The curve probably should intercept the K_a-axis slightly above zero, possibly about as indicated in Fig. 7-1.

The empirical curve probably does not indicate the relationship between K_a and capillary porosity correctly, for no account is taken of the fact that the capillary pores were not entirely empty at the start of the absorption test. However, at $p = 0.5\ p_s$, reached by desorption, the capillaries are probably not far from empty. The presence of capillary water in the specimen at the start probably reduces K_a below what it would be if the capillaries were entirely empty, but it probably does not influence the indications as to the trend of the curve as capillary porosity approaches zero, the matter of interest here.

On the whole, these absorptivity data support other indications that the capillary pores are much larger than those in the gel, and that relationships given in Part 5 distinguish between water held in capillary spaces and that held in the pores of the gel with satisfactory accuracy.

It should be remembered that when $W_o = 0.86(1 + 4k)W_n$, that is, when capillary porosity is zero, the specimen must be such that, when saturated, the total evaporable water $= 4V_m$. (See Part 3.) These absorptivity data thus constitute a significant independent check of the conclusion reached from other considerations, that the weight of the water required to saturate the gel is equal to $4V_m$.

Dependence of K_a on initial water content of the specimen

It must be remembered that the value of K_a for a given specimen will depend on the initial water content of the specimen, at least for water contents high enough to partly fill the capillaries. If the specimens were first dried completely and then allowed to *ad*sorb vapor before the adsorption test, K_a would probably be about the same for all initial water contents up to that corresponding to about $p = 0.45\ p_s$. This follows from the evidence presented earlier indicating that the capillaries do not begin to fill by capillary condensation below about $p = 0.45\ p_s$ and that the initial rapid *ab*sorption takes place almost exclusively in the capillaries, when capillaries are present. For specimens dried only by *desorption*, data now available do not indicate clearly how low the final vapor pressure must be to empty the capillaries completely. Such data as there are indicate that the required pressure might be as low as $p = 0.1\ p_s$, though theory indicates that it might be about $p = 0.3\ p_s$.[9]

Relationship between absorptivity and permeability

In view of the evidence given above, we may conclude that the initial rapid absorption of water by paste containing capillaries outside the gel is predominantly capillary absorption. Consequently, the rate of absorption should be, according to Darcy's law,

$$\frac{dq}{dt}\frac{1}{A} = \frac{(K_2)_c}{\eta}\, d_f \frac{\Delta h}{L}\, g\ , \qquad (22)$$

in which $(K_2)_c$ is the coefficient of permeability for flow through the capillary system alone, $d_f \Delta h$ is the hydraulic head in g per sq cm causing the flow, and L is the depth of the saturated layer in which the flow is taking place.

For horizontal capillary penetration

$$g\, d_f \Delta h = \sigma\left(\frac{1}{r_1} + \frac{1}{r_2}\right)\ , \qquad (23)^*$$

*Eq. (23) is based on the assumption that the angle of contact between the meniscus and the solid boundary is zero. This assumption seems permissible in this case because of the strong attraction between the solid and the liquid and because of the extreme slowness of the movement of the meniscus. It would not be permissible, however, for specimens that contain stearates or other "water-repellent" substances or for coarsely porous materials in which the capillary penetration is rapid.

where

σ = surface tension of water, dynes per cm,
g = acceleration due to gravity,
r_1 and r_2 = principal radii of curvature of the menisci.

Carman [4d] has shown that $\left(\frac{1}{r_1} + \frac{1}{r_2}\right)$ can be replaced by the reciprocal of the hydraulic radius. That is,

$$\frac{1}{r_1} + \frac{1}{r_2} = \frac{S}{\epsilon_c}, \quad \ldots\ldots (24)$$

where

ϵ_c = volume of the capillaries per unit volume of the specimen,
and S = surface area of capillary boundaries.
For our data,

$$\frac{S}{\epsilon_c} = \frac{S_c}{w_e - 4V_m} = \frac{S_c}{V_m(N-4)}, \quad \ldots\ldots (25)$$

in which

S_c = superficial surface area of the gel, and
w_e = total evaporable water.

We may note also that

$$L = \frac{q}{\epsilon_c A} = \frac{q}{V_m(N-4)A}, \quad \ldots\ldots (26)$$

where A = exposed area of the specimen.
Substitution from eq. (23), (24), (25), and (26) into eq. (22) gives

$$\frac{dq}{dt}\frac{1}{A} = \frac{(K_2)_c}{\eta}\sigma\frac{S_c}{V_m(N-4)}\frac{V_m(N-4)A}{q} = \left[\frac{(K_2)_c A}{\eta}\sigma S_c\right]\frac{1}{q} \quad \ldots\ldots (27)$$

All the quantities within the brackets are constant for a given specimen. Hence, we may write

$$\int q\,dq = \left[\frac{(K_2)_c A^2}{\eta}\sigma S_c\right]\int dt$$

which, when integrated, gives

$$\frac{q}{A} = \left[\frac{2(K_2)_c}{\eta}\sigma S_c\right]^{\frac{1}{2}} t^{\frac{1}{2}} \quad \ldots\ldots (28)$$

From eq. (16) and (28) it follows that

$$K_a = \frac{2(K_2)_c}{\eta}\sigma S_c \quad \ldots\ldots (29)$$

It thus appears that if the superficial surface area of the gel were known, the coefficient of permeability for flow through the capillary system

(which is virtually the total flow) could be computed from the coefficient of absorptivity as determined from the initial rate of absorption. However, S_c cannot be measured by any method now available. We may surmise that in a fresh paste, where the hydration products exist mainly as a thin coating on the cement grains, the superficial area of the hydration products, S_c, must be virtually the same as that of the original cement grains. While hydration proceeds, either an increase or a decrease in S_c is conceivable. If the cement grains were sufficiently separated, and if hydration merely enlarged the grains, S_c would increase until the boundaries of the grains began to merge. After a certain extent of this merging, S_c would begin to decrease and would wither eventually reach zero—if the paste were sufficiently dense—or some finite minimum value. (See Fig. 5-11, Part 5.)

SUMMARY OF PART 7

Permeability

(1) The permeability of well cured neat cement paste of low w/c is, theoretically,

$$K_1 = 50 \times 10^{-14}\, V_m(N - k_1)^3$$

in which K_1 = coefficient of permeability to water in ft. per sec.;
V_m = amount of water required to form the first adsorbed layer, g per cc of paste;
N = ratio of total evaporable water to V_m; and
k_1 is a constant depending on the amount of immobile water per unit of solid surface—k_1 is probably near 1.

(2) For pastes in which N is considerably greater than 4, the permeability is much higher than the theoretical value computed from the above equation. This is believed to indicate that the flow in such pastes is predominantly in the capillary spaces outside the gel and, in tests on neat-cement disks of high w/c, through vertical channels formed during the period of bleeding.

(3) The theoretical permeability of pastes containing no capillary space outside the gel is

$$K_1 = 0.7 \times 10^{-12}(1 - cv_c) \Big]_{0.45 \leqq cv_c \leqq 1.0}$$

where c = cement content, g per cc of paste and v_c = specific volume of the cement. K_1 cannot be zero in practice because cv_c must be less than 1. At $cv_c = 0.45$, approximately the minimum cement content of pastes containing no capillary space outside the gel, $K_1 = 1 \times 10^{-12}$. According to Ruettgers, Vidal, and Wing, this is of the same order as the permeability of granite.

(4) The permeability of concrete is generally much higher than the theoretical permeability owing to fissures under the aggregate that

permit the flow partially to by-pass the paste and owing to the capillaries in the paste that permit the flow in the paste to by-pass the gel.

Absorptivity

(1) The absorption of water by a dry specimen during the first 30 to 60 minutes follows the relationship

$$\frac{q}{A} = (K_a t)^{\frac{1}{2}},$$

in which q/A = the amount absorbed per unit of exposed area and K_a = the coefficient of absorptivity at t = time.

(2) The empirical relationship between K_a and capillary porosity indicates that K_a is near zero when capillary porosity is zero. Hence, the empirical relationship indicates that the initial absorption takes place almost exclusively in the capillaries outside the gel, when such capillaries are present.

(3) The theoretical relationship between absorptivity and permeability is

$$K_a = \frac{(K_2)_c}{\eta} \sigma S_c,$$

in which $(K_2)_c$ = the coefficient of permeability for flow through the capillary system of the paste; σ and η = surface tension and viscosity of water, respectively; g = gravitational constant; S_c = superficial surface area of the gel. This pertains to specimens in which the capillaries are initially empty, or nearly so. S_c has not been measured. It probably diminishes as $(K_2)_c$ diminishes. If so, K_a is a relative measure of $(K_2)_c$.

REFERENCES

(1) A. Ruettgers, E. N. Vidal, and S. P. Wing, *Proceedings* ACI v. 31, p. 382 (1935).

(2) M. Muskat, *The Flow of Homogeneous Fluids through Porous Media* (McGraw-Hill, 1937), p. 71.

(3) J. Kozeny, *S. B. Akad. Wiss. Wien*, v. 136, Part IIa, p. 271 (1927).

(4) P. C. Carman (a) *Symposium on New Methods of Particle Size Distribution in the Subsieve Range*, A.S.T.M. Publication (1941), p. 24.

(b) *J. Agr. Sci.* v. 29, p. 262 (1939).

(c) *J. Soc. Chem. Ind.*, v. 57, p. 225 (1938).

(d) *Soil Science* v. 52, p. 1 (1941).

(5) J. L. Fowler and K. L. Hertel, *J. Applied Phys.* v. 11, p. 496 (1940).

(6) T. C. Powers, "The Bleeding of Portland Cement Paste, Mortar and Concrete," Bulletin 2 of the Research Laboratory, Portland Cement Association, 1939.

(7) H. H. Steinour (a) P.C.A. Research Laboratory Bulletin 3, 1944; or *Ind. Eng. Chem.* (b) v. 36, p. 618 (1944); (c) v. 36, p. 840 (1944); (d) v. 36, p. 901 (1944).

(8) Discussion of paper by A. Ruettgers, E. N. Vidal, and S. P. Wing, *Proceedings* ACI v. 32, p. 378 (1936).

(9) L. H. Cohan, *J. Am. Chem. Soc.* v. 66, p. 98 (1944).

Title 43-5g —a part of PROCEEDINGS, AMERICAN CONCRETE INSTITUTE Vol. 43

JOURNAL
of the
AMERICAN CONCRETE INSTITUTE
(copyrighted)

Vol. 18 No. 8 7400 SECOND BOULEVARD, DETROIT 2, MICHIGAN April 1947

Studies of the Physical Properties of Hardened Portland Cement Paste*

By T. C. POWERS†
Member American Concrete Institute
and T. L. BROWNYARD‡

Part 8. The Freezing of Water in Hardened Portland Cement Paste§

Part 9. General Summary of Findings on the Properties of Hardened Portland Cement Paste

CONTENTS PART 8

*Received by the Institute July 8, 1946—scheduled for publication in seven installments; October 1946 to April, 1947. In nine parts:

Part 1. "A Review of Methods That Have Been Used for Studying the Physical Properties of Hardened Portland Cement Paste". ACI JOURNAL, October, 1946.
Part 2. "Studies of Water Fixation"—Appendix to Part 2. ACI JOURNAL, November, 1946.
Part 3. "Theoretical Interpretation of Adsorption Data." ACI JOURNAL, December, 1946.
Part 4. "The Thermodynamics of Adsorption"—Appendix to Parts 3 and 4. ACI JOURNAL, January 1947.
Part 5. "Studies of the Hardened Paste by Means of Specific-Volume Measurements." ACI JOURNAL February, 1947.
Part 6. "Relation of Physical Characteristics of the Paste to Compressive Strength." ACI JOURNAL, March, 1947.
Part 7. "Permeability and Absorptivity." ACI JOURNAL, March, 1947.
Part 8. "The Freezing of Water in Hardened Portland Cement Paste." ACI JOURNAL, April 1947.
Part 9. "General Summary of Findings on the Properties of Hardened Portland Cement Paste." ACI JOURNAL, April, 1947.

†Manager of Basic Research, Portland Cement Assn. Research Laboratory, Chicago 10, Ill.
‡Navy Dept., Washington, D. C., formerly Research Chemist, Portland Cement Assn. Research Laboratory, Chicago 10, Ill.

§The characteristics of the cements mentioned in this section may be found in the Appendix to Part 2.

This part of the paper contains data on the amount of ice that can exist in hardened portland cement paste under given conditions. Also some theoretical aspects of the data are considered.

THEORETICAL FREEZING POINTS

From the fact that the evaporable water in hardened paste exhibits different vapor pressures when the sample is at different degrees of saturation, we could anticipate the now known fact that not all the evaporable water in a saturated paste can freeze or melt at a fixed temperature. This can readily be deduced from Fig. 8-1, which is a diagram illustrating (on a distorted scale) the relationship between the vapor pressure and temperature for water and ice. The upper curve represents the relationship for pure water under the pressure of its own vapor, p_s. Similarly, the curve marked "ice" represents the relationship for ice under the pressure of its vapor, p_i. The vapor pressures of the two phases are equal only at point A. This is the only point where the free energies of the ice and pure water are equal and hence the only point where ice and pure water can coexist. If a salt is added to the water, the vapor pressure of the solution bears a nearly fixed ratio to the vapor pressure of pure water at all temperatures, as indicated by the line marked "solution." (The position of this line depends on the salt concentration.) Pure ice can coexist with the solution only at point B, which is at a temperature below 0 C.

It is clear, therefore, that the evaporable water in a saturated hardened paste will not begin to freeze at 0 C because of its content of dis-

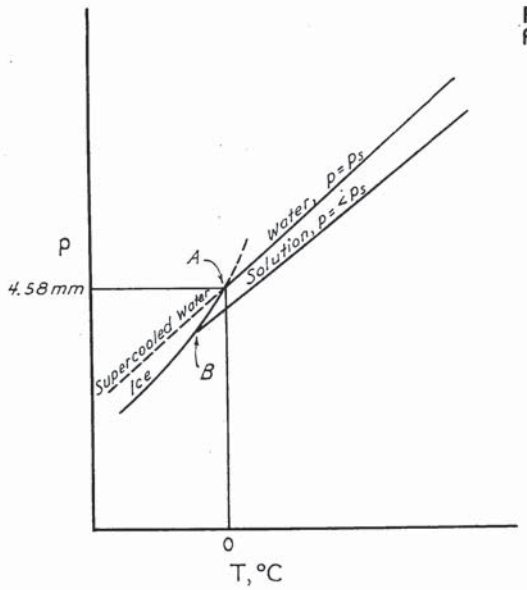

Fig. 8-1—Phase equilibrium diagram for water and ice (distorted)

solved hydroxides. Moreover, when freezing begins, and pure ice separates from the solution, the solution becomes more concentrated and thus the freezing point is lowered further. It follows that the evaporable water will freeze progressively as the temperature is lowered.

At this point we recall the discussion in Part 3 showing that the reduction in the vapor pressure of evaporable water is caused not only by the dissolved salts but also by capillary tension and adsorption. At saturation the effect is due entirely to dissolved material, but as the evaporable water is removed the effect of capillary tension and adsorption increases, and it exceeds that of the dissolved material after only a little of the evaporable water has been removed. A given reduction in vapor pressure signifies the same reduction in freezing point, regardless of the mechanism by which the reduction is effected. Hence, we may conclude that if the ice separates from capillary water or adsorbed water in the same way that it does from a solution, the freezing point will be the same as for a solution of the same vapor pressure.

Application of Washburn's equation

The reduction in freezing point for such a system can be ascertained from the following semi-empirical relationship given by Washburn[1]*

$$\log_{10} \frac{p_i}{p_s} = \frac{1.1489t}{273.1 + t} + 1.33 \times 10^{-5}t^2 - 9.084 \times 10^{-8}t^3, \quad (1)$$

in which

*See references end of Part 8.

p_i = vapor pressure of ice at temperature t,
p_s = vapor pressure of pure water at temperature t, and
t = temperature, deg. C.

Let p = vapor pressure of evaporable water in cement paste.

Then, where the ice and the evaporable water are in equilibrium, that is, at the freezing point, $p = p_i$, and

$$\log_{10} p/p_s = \text{eq. (1)} \quad \ldots\ldots\ldots\ldots\ldots\ldots\ldots\ldots\ldots\ldots (2)$$

Thus, eq. (1) gives the relative vapor pressure of water (or solution) that will be in equilibrium with ice at any given temperature. In other words, it gives the freezing temperature corresponding to any given value of p/p_s for the system. A plot of this equation appears in Fig. 8-2.

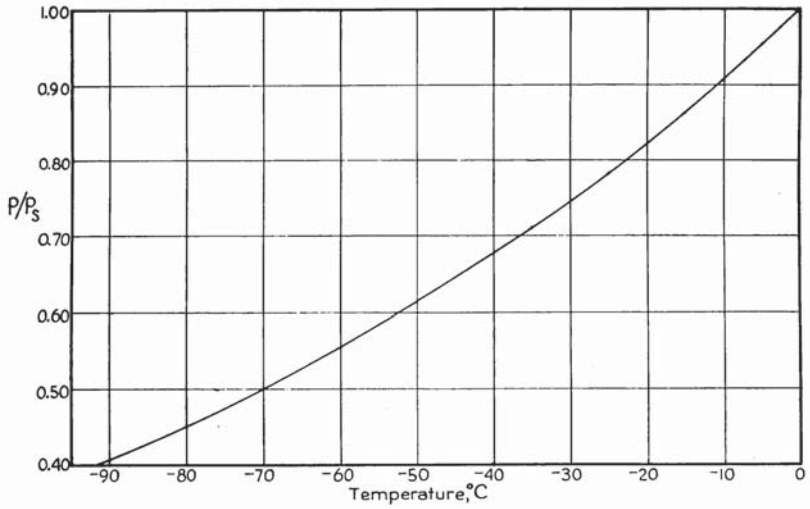

Fig. 8-2—Relationship between p/p_s and freezing point

Eq. (1) gives substantially the same result as the following equation given by Kubelka[2]:

$$\frac{T_o - T}{T_o} = \frac{2v_f\sigma_f}{rq}, \quad \ldots\ldots\ldots\ldots\ldots\ldots\ldots\ldots\ldots\ldots (3)$$

where T_o = normal freezing point, deg. K,
T = freezing point in capillary system, deg. K,
v_f = molar volume of fluid,
σ_f = surface tension of fluid,
r = radius of curvature of fluid surface, and
q = latent heat of fusion of fluid.

This equation was derived from thermodynamic considerations, taking into account the influence of capillary tension. It involves the assump-

tion that the liquid phase is in tension while the ice is under normal pressure.

One of the objects of this investigation was to verify eq. (1) as applied to cement paste, or to find an empirical substitute for it. It is apparent that from the correct relationship the amount of water in a saturated paste that is freezable at any given temperature could be obtained from the adsorption curves, after applying temperature corrections. That is, the amount of freezable water could be obtained from the sorption characteristics measured at 25 C, for example, after correcting the value of p/p_s at 25 C to what it would be at the freezing point.

To apply eq. (1) to the freezing of water in cement paste is tantamount to assuming that the ice forms as a separate microcrystalline phase, the crystals being so large that they exhibit the normal properties of ice, and that the ice is under normal external pressure. As will be seen, the experimental data do not definitely confirm these assumptions, but they indicate that the assumptions are substantially correct, at least for the freezing of saturated pastes. The causes of uncertainty will be discussed later.

APPARATUS AND METHODS

Test samples

The test samples were granules of cement paste or cement-silica paste. They were obtained by the method described in Part 2. The original specimens (cylinders or cubes) were crushed and sieved, the particles caught between the No. 14 and No. 28 sieves being taken for the freezing experiments. Each sample was treated as follows:

The evaporable water was removed from the granulated sample by drying in vacuo over $Mg(ClO_4)_2.2H_2O + Mg(ClO_4)_2.4H_2O$. Then water was added to the dry granules in such quantity as to saturate them. This procedure is described in Part 2.

Most of the sample prepared in this way was then transferred to a dilatometer, without packing the granules in the bulb. All operations involved in the transfer were carried out in a water-saturated atmosphere to minimize losses of moisture from the sample.

Dilatometers

A drawing of a typical dilatometer is shown in Fig. 8-3. This is essentially the same instrument used by Elsner von Gronow[3] in his experiments with hardened paste and by Foote and Saxton,[4] Jones and Gortner,[5] and Bouyoucos,[6] who studied various materials.

Freezing and thawing procedure

The sealed dilatometer was placed in a cryostat (initially at room temperature) with the stem vertical. During the ensuing night, the

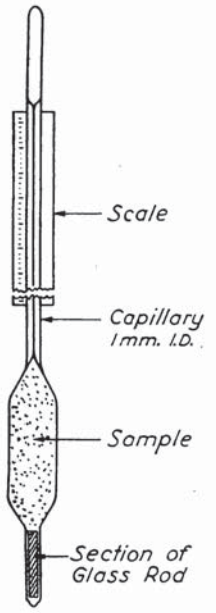

Fig. 8-3 (left)—Sketch of typical dilatometer

Fig. 8-4 (below)—Sketch of apparatus used for filling dilatometers with toluene

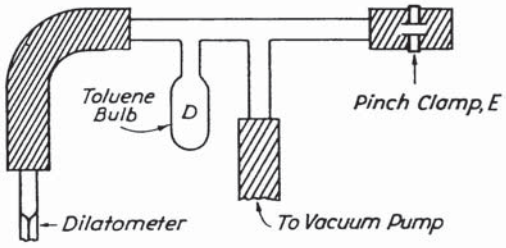

temperature of the cryostat was allowed to drop gradually to about −20 C. The bulb of the dilatometer was then cooled quickly to about −78 C by placing it in a mixture of solid carbon dioxide and alcohol. The stem was connected to a vacuum pump through the apparatus shown in Fig. 8-4. After the air was removed, toluene in bulb D was caused to flow into the dilatometer by manipulating flexible connections and pinch clamp E which admitted atmospheric pressure. By repeating such manipulations, all the space surrounding the frozen grains, as well as the bore of the capillary stem, was filled with toluene.

After the level of the toluene in the stem had been adjusted to a point near the bottom of the scale, the top of the calibrated stem was sealed to prevent loss of toluene by evaporation. Then the loaded dilatometer was transferred back to the cryostat, still at about −20 C, without allowing the sample to thaw during the transfer. The final dilatometer reading at −20 C was taken the following morning.

After the initial −20 C reading was obtained, the temperature was raised stepwise, allowing time for the level of the toluene in the stem to come to rest after each change in temperature. A constant level was usually established in about one-half hour, but each temperature was maintained for at least 1 hour.

The procedure described above was used for most of the data discussed herein. Other data were obtained earlier when the methods were less well developed. In some cases, the saturated sample was sealed in

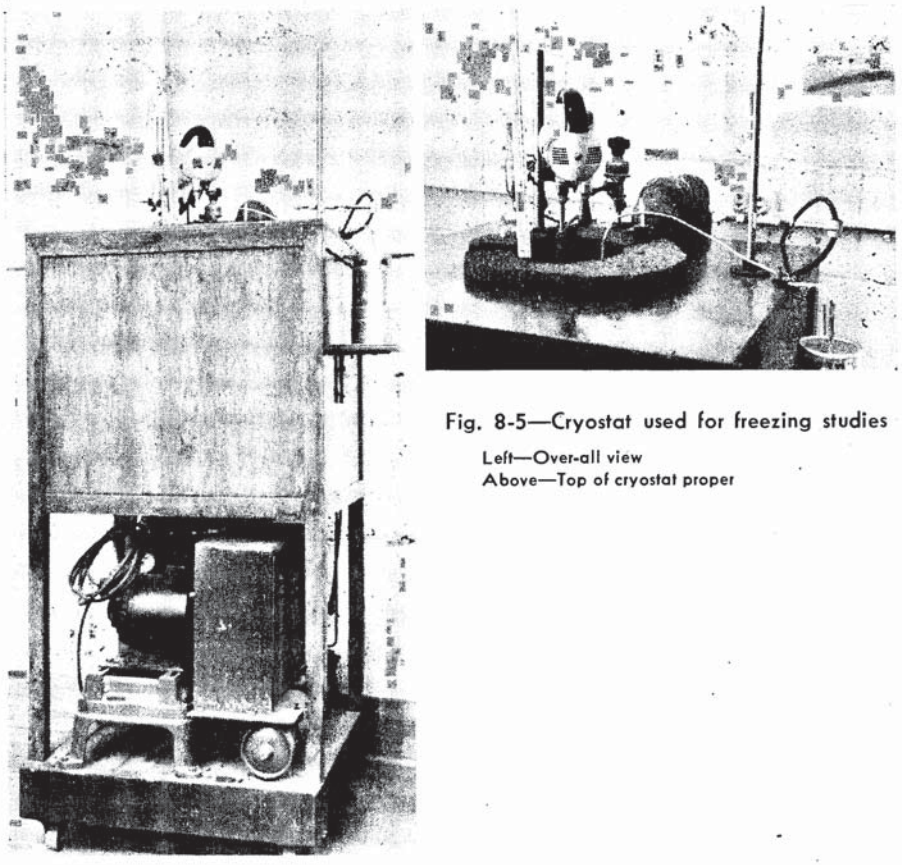

Fig. 8-5—Cryostat used for freezing studies
Left—Over-all view
Above—Top of cryostat proper

the dilatometer and the toluene was introduced with the aid of a vacuum pump without first freezing the sample. Although the granules were wetted with toluene before they were subjected to low pressure, this procedure probably resulted in a small loss of evaporable water. Also, the top of the dilatometer stem was sealed only with a rubber cap. This permitted a small loss of toluene during the course of the experiments. The samples prepared in this manner were usually started above the freezing point and the freezing curves as well as thawing curves were obtained.

Description of cryostat

The cryostat used in these experiments is shown in Fig. 8-5 and diagrammatically in Fig. 8-6. It consists of an alcohol container G, equipped with cooling coils. Within this container is a double-walled glass vessel also containing alcohol. This is the cryostat proper. It contains an electrical heating coil, not shown, a motor-driven stirrer, C, and a mercury-toluene type thermoregulator, B. The temperature of the alcohol

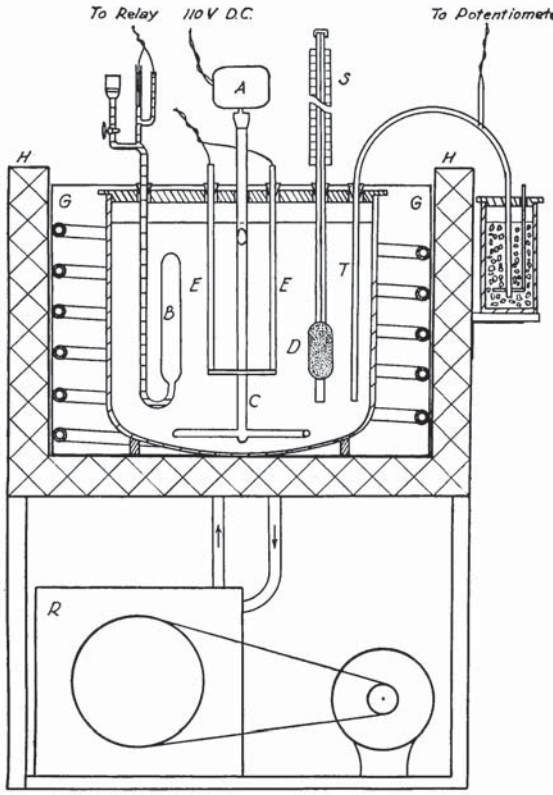

Fig. 8-6—Freezing study apparatus

is indicated by the 8-junction copper-constantan thermopile, T, having its cold junction in melting ice outside the cryostat, as indicated. The e.m.f. of the thermopile is measured by means of a Type K potentiometer and suitable galvanometer. A single dilatometer, D, is shown. Actually, four dilatometers could be accommodated simultaneously.

GENERAL ASPECTS OF EXPERIMENTAL RESULTS

Dilatometer curves

Results of a typical experiment on a saturated sample are given in Fig. 8-7. Beginning at point A, the temperature was lowered stepwise and the corresponding changes in dilatometer readings were observed. These changes were converted into volume change, the volume at −0.2 C being taken as the reference point. As shown, the points describe the straight line AB. This represents the thermal contraction of the whole system, pyrex-glass bulb, toluene, and water-saturated sample. At about −7.5 C, point B, a sudden expansion occurred, giving the rise BC. Further cooling produced the curve CD. Since CD does not fall as steeply as AB, we may conclude that further expansion accompanied the change from −7.5 to −25 C.

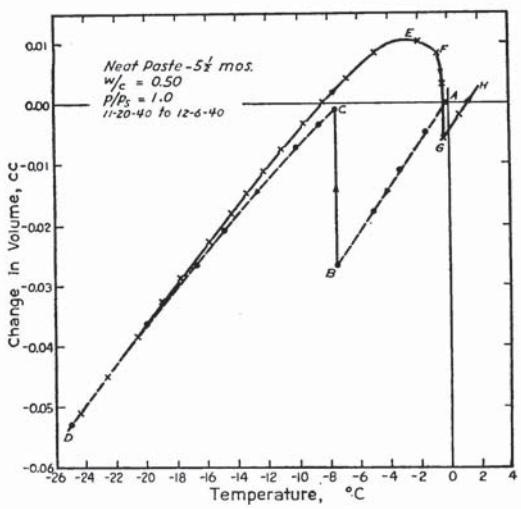

Fig. 8-7—Typical results of dilatometric study of saturated sample

Beginning at −25 C (point D) the temperature was raised stepwise and the curve D to H was obtained. A comparison of the slope of AB with the various slopes of DH shows that each increment of temperature caused expansion up to point E. But the expansion accompanying each increment of temperature was less than the normal thermal expansion. This indicates a progressive melting of ice. Along EF, contraction occurs, showing that the contraction due to melting exceeded the thermal expansion. At temperatures above G, the volume increase is due to thermal expansion only, as shown by the parallelism of GH and AB.

The results described above are typical of all such tests made on saturated granules of paste. During the time when the points fell along AB, below −0.2 C, the water remained in a supercooled state. All the water that might have frozen between −7.5 and −0.2 C changed to ice at −7.5 C. In various experiments the extent of supercooling ranged from about −5 C to −12 C. Sometimes freezing was started by tapping the stem of the dilatometer. It seems likely that at other times chance vibrations determined the extent of supercooling.

The fact that DE and DC do not coincide is probably another manifestation of hysteresis. We have already seen that the progressive drop in freezing point indicates a corresponding progressive drop in relative vapor pressure of the unfrozen evaporable water. The freezing of a part of the evaporable water has an effect on the unfrozen evaporable water similar to the loss of evaporable water by drying. Likewise, the melting of ice has an effect like that of increasing the evaporable water content of a partially dry specimen. Hence, by analogy we can see that the freezing curve is a desorption curve, with temperature representing vapor pressure. The melting curve is conversely an adsorption curve.

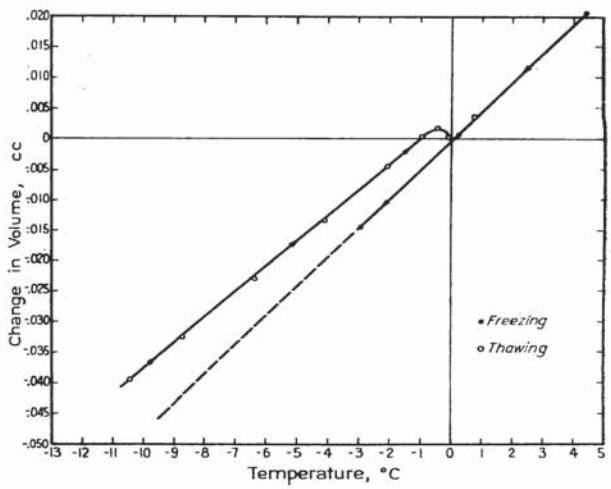

Fig. 8-8—Freezing and thawing of silica gel

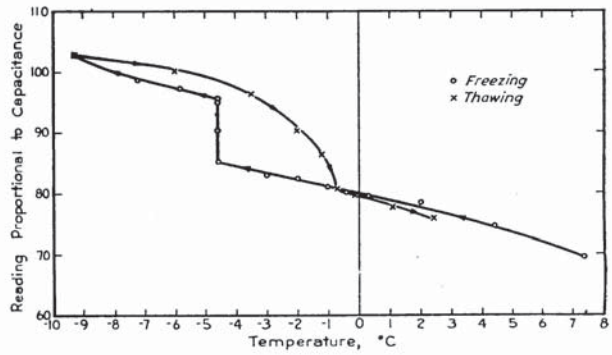

Fig. 8-9—Results of experiment for measuring freezing and thawing of ice in hardened cement paste by the dielectric method

The curves DE and DC in Fig. 8-7 show, by comparison with AB, that the contraction per degree on melting is less than the expansion per degree on freezing. This result is as would be anticipated from the fact that the decrease in evaporable water content per unit decrease in p/p_s is, in the upper range of pressures, less than the increase in evaporable water content per unit increase in p/p_s.

Effect of hydration during the experiment

A significant feature of Fig. 8-7 is the position of point G with respect to A. Point G is that at which all ice disappears—the final melting point. The fact that it is below A shows that the volume of the system decreased permanently during the freezing and thawing cycle.* Repeated cycles on one sample showed that shrinkage increases with each cycle. It was suspected that the shrinkage was due at least in part to hydration of cement in the sample during the test. To check this possi-

*This particular example showed a considerably greater permanent change than did others. It represents a test made before the practice of sealing the dilatometer stem was adopted. Consequently, most of the change may be due to loss of toluene.

bility, some special tests were made on silica gel. Fig. 8-8 gives the result.

The amount of evaporable water that was in this sample of silica gel is not known exactly, owing to losses of moisture during the preparation of the dilatometer. However, it is believed to have been slightly more than the amount required to saturate the granules of silica gel. The feature to be noted especially is that the volume after the cycle was completed was almost exactly the same as the original volume at the same temperature. The same degree of reversibility was found in three other tests on silica gel.

In view of the results obtained from silica gel, it was concluded that the permanent contraction in volume such as is shown in Fig. 8-7 is due, at least in part, to continued hydration of the cement during the course of the experiment. Such an explanation is plausible, even though the original material had been cured under water for several months, because the granulation of the original specimen exposed fresh clinker surfaces and admitted water into fine gel structure that had become partially desiccated in the whole specimen (see Part 2).

Effect of dissolved material

One other feature of Fig. 8-7 should now be noted. Point G, the final melting point, is slightly below 0 C. This is the effect of dissolved materials, chiefly alkalies. It will be seen later that the final melting point of one of the samples was −1.6 C, owing to its unusually high alkali content.

Detection of freezing by means of the change in dielectric constant

Alexander, Shaw, and Muckenhirn studied the freezing of water in soils and other porous media by means of the accompanying change in dielectric constant.[7] The dielectric constant of water is about 80 and that of ice about 4. By using the material to be tested as the dielectric medium between the plates of a fixed condenser, these authors were able to follow the course of ice-formation by measuring the change in capacitance of the condenser.

Through the courtesy of Horace G. Byers, Chief, Soil Chemistry and Physics Research, U. S. Dept. of Agriculture, Washington, D. C., Mr. Alexander very kindly tested a saturated, granular sample of hardened paste for us. The results are shown in Fig. 8-9. Since this represents but a single run, we cannot assume that all the features shown are significant. Nevertheless, they are of considerable interest in connection with the interpretation of the results obtained by the dilatometer method.

In Fig. 8-9 the scale of ordinates gives the dial readings of the apparatus. An increase in reading denotes an equal decrease in the capaci-

tance of the fixed condenser and hence a decrease in the dielectric constant of the sample. The curves show that in the range above 0 C, lowering the temperature decreased the dielectric constant of the sample. As the temperature fell below zero, the water in the sample remained in a supercooled state. At −4.5 C, freezing was started by tapping the condenser, producing the change in dielectric constant indicated. Lowering the temperature further caused a further decrease in dielectric constant, the decrease being greater than could be accounted for by a linear extrapolation of the curve for the supercooled system. After the temperature reached −9.3 C, the temperature was raised stepwise and the melting curve was obtained. The final melting point was at −0.7 C. This depression below 0 C may be due entirely to the alkali content, but it is probably due in part to a slight loss of moisture from the sample that occurred while it was being transferred to the fixed condenser.

The final melting point appears to be exactly on the cooling curve, indicating that the sample returned to its initial state at the end of the cycle. However, the slope of the thawing curve above 0 C is not the same as that of the corresponding part of the freezing curve. This might indicate a permanent change in the dielectric constant of the sample. Such a change would take place if some of the originally evaporable water would become non-evaporable through reaction with unhydrated cement. Since the sample was in the fixed condenser for four days, some additional hydration is not unlikely.

On comparing these results with those given in Fig. 8-7, we find that the major features of the results obtained from the dilatometer method were found also with the electrical method. (A possible exception is the evidence concerning the permanent change in the sample during the cycle.) It seems, therefore, that supercooling and hysteresis are not peculiarities of the dilatometric method but are characteristic of the paste.

METHOD OF ESTIMATING THE AMOUNT OF ICE FROM THE MELTING CURVE

Curves such as that shown in Fig. 8-7 show the algebraic sums of simultaneous expansions and contractions that accompany changes in temperature. To estimate the amount of ice that exists at any given temperature it is necessary to ascertain the net expansion, that is, the difference between the existing volume at the given temperature and the volume that the system would have had, had no freezing occurred. This difference was not determined with exactness for several reasons discussed below.

In those tests where the specimens were cooled stepwise, as in the case represented in Fig. 8-7, the volume change that would have occurred

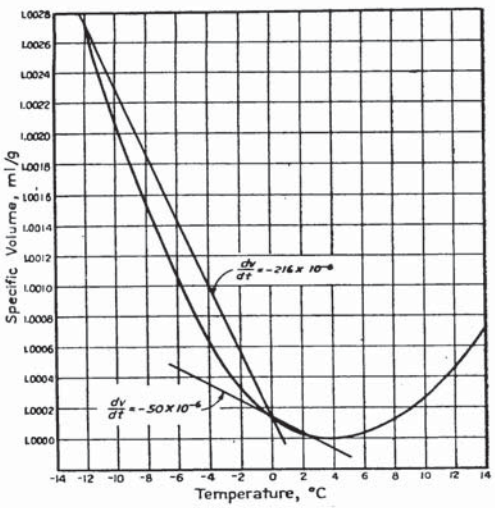

Fig. 8-10—Specific volume of water at a pressure of 1 atmosphere

N. E. Dorsey, *Properties of Ordinary Water Substance* (New York, Reinhold Publishing Corp., 1940) Table 94

had no ice formed could be estimated with satisfactory accuracy from the slope of the line established while the freezable water remained in a supercooled state. However, in the majority of tests only the melting curve was obtained and the volume change in the system when it was free from ice could be observed only in the range from 0 to +2 C. An extrapolation of the line so established into the range below 0 C involves an assumption that the coefficients of expansion of all parts of the system are, in the absence of ice formation, constant throughout the temperature range involved, usually −20 to +2 C. So far as the solid phase of the paste and the pyrex bulb are concerned, this is probably not far from true. With respect to the water and toluene, however, such an assumption is at variance with fact.

As may be seen in Fig. 8-10, water expands as the temperature is changed in either direction from +4 C. Hence, the volume change of the water is in the same direction as that of the rest of the system only when the temperature is above +4 C. Therefore, it follows that at readings taken between 0 and +2 C, the volume change of the water is opposite to that of the rest of the system over all parts of the curve. However, Fig. 8-10 shows that the mean coefficient for the water in the 0 to +2 C range is much different from what it is over a 15-deg. range below 0 C. Hence, a mean slope established by data in the 0 to +2 C range cannot be the same as the mean slope in the lower range. It is necessary, therefore, to find a means of determining the mean slope over the lower range from the empirically established mean slope in the 0 to +2 C range. This may be done as follows:

Let V_o = volume of contents of bulb at 0 C, or volume of pyrex bulb at 0 C,
V_t = volume of contents of bulb at temperature t,
V_{dt} = volume of pyrex bulb at temperature t,
v_{ao} and v_{at} = volume of solids in bulb at 0 and t, respectively,
v_{bo} and v_{bt} = volume of evaporable water in bulb at 0 and t, respectively, and
v_{co} and v_{ct} = volume of toluene in bulb at 0 and t, respectively.

The apparent change in volume for a specified temperature change will be

$$(V_t - V_o) - (V_{dt} - V_o) = V_t - V_{dt} = \Delta V.$$

From the above definitions it follows that

$$\Delta V = (v_{at} - v_{ao}) + (v_{bt} - v_{bo}) + (v_{ct} - v_{co}) - (V_{dt} - V_o)$$

$$v_{at} = v_{ao} + \frac{\Delta v_a}{\Delta t}\Delta t, \text{ etc., for each term of the above equation.}$$

Hence,

$$\frac{\Delta V}{\Delta t} = \frac{\Delta v_a}{\Delta t} + \frac{\Delta v_b}{\Delta t} + \frac{\Delta v_c}{\Delta t} - \frac{\Delta V_d}{\Delta t} \quad \ldots\ldots (4)$$

The mean coefficients for each part are as follows:

For the solid phase of the paste:

$$\frac{\Delta v_a}{\Delta t} = 32 \times 10^{-6}\, v_{ao} \text{ (Ref. 8)}$$

For water:

$$\frac{\Delta v_b}{\Delta t} = -\,50 \times 10^{-6}\, v_{bo}, \text{ for 0 to 2 C (See Ref. 10 and Fig. 8-10)}$$

$$\frac{\Delta v_b}{\Delta t} = -\,216 \times 10^{-6}\, v_{bo}, \text{ for 0 to } -12 \text{ C (See Ref. 10 and Fig. 8-10)}$$

For toluene:

$$\frac{\Delta v_c}{\Delta t} = 1051 \times 10^{-6}\, v_c, \text{ for 0 to 2 C}$$

$$\frac{\Delta v_c}{\Delta t} = 1038 \times 10^{-6}\, v_c, \text{ for 0 to } -12 \text{ C (Ref. 9)}$$

For the bulb (Pyrex-brand glass):

$$\frac{\Delta V_d}{\Delta t} = 10 \times 10^{-6}\, V_o.$$

These figures substituted into eq. (4) give

$$10^6 \frac{\Delta V}{\Delta t} = 32v_{ao} - 50v_{bo} + 1051v_{co} - 10V_o, \text{ for 0 to 2 C} \quad \ldots\ldots (5)$$

and

$$10^6 \frac{\Delta V}{\Delta t} = 32v_{ao} - 216v_{bo} + 1038v_{co} - 10V_o, \text{ for 0 to } -12 \text{ C.} \quad \ldots\ldots (6)$$

Let m = mean slope of dilatometer curve, $\Delta V/\Delta t$, from 0 to 2 C, and
m' = mean slope from 0 to −12 C.

Then, from eq. (5) and (6)

$$10^6(m' - m) = -166v_{bo} + 13v_{co}$$

and

$$\frac{m'}{m} = 1 - \frac{166v_{bo} + 13v_{co}}{10^6\, m} \quad \ldots\ldots (7)$$

Thus the ratio of the mean slope from 0 to −12 C to that from 0 to 2 C is found in terms of the amounts of water, v_{bo}, and toluene, v_{co}, and the experimentally established slope above 0 C. As applied to any specific case the line represented by eq. (4) was extended to −15 C and in some cases to −20 C. This was necessary because data on supercooled water below −12 C were not available.

With the mean slope of the line representing the supercooled system thus established for each test, the amount of ice at any given temperature was estimated from the difference between the observed volume and the corresponding computed volume of the supercooled system, this difference being the observed net expansion. Let

Δv = net expansion,
B_t = expansion resulting from freezing 1 gram of water at the existing temperature, and
w_f = amount of ice (freezable water).

Then

$$w_f = \frac{\Delta v}{B_t} \quad \ldots\ldots (8)$$

B_t is itself a function of temperature, since the coefficients of expansion of water and ice differ both in magnitude and sign. Table 8-1 gives values of B_t at various temperatures calculated from values of the specific volume of ice and water assembled by Dorsey.[10]

The method of obtaining the amount of ice in the dilatometer described above obviously decreases in accuracy as the temperature becomes lower. This is due not only to the inaccuracy of the experimental value for m but also to limitations on the use of Table 8-1. As will be seen later, the water that freezes above a dilatometer temperature of about −6 C is almost entirely capillary water. But below −6 C, some of the gel water is extracted and freezes with the capillary water. Since the mean specific volume of the gel water is about 0.90 (Part 5), Table 8-1 does not correctly represent the volume change of gel water on freezing.

TABLE 8-1—VOLUME CHANGE OF 1 GRAM OF WATER WHEN FREEZING OCCURS AT GIVEN TEMPERATURES

Temp., deg. C	Volume change, ml ($= B_t$)
0	0.0907
− 1.0	0.0904
− 1.5	0.0903
− 2.0	0.0902
− 2.5	0.0900
− 3.0	0.0898
− 3.5	0.0897
− 4.0	0.0896
− 5.0	0.0892
− 6.0	0.0889
− 8.0	0.0881
−10.0	0.0872
−12.0	0.0863
−15.0	0.0849
−20.0	0.0812

Because of these considerations, the method of obtaining w_f described above cannot be considered reliable below about −15 C. A preferable procedure would be to establish the slope by supercooling the sample as far as possible, after the final melting curve has been obtained.

EFFECT OF TOLUENE ON THE MELTING CURVE

Owing to the fact that the paste granules were surrounded with toluene, it is necessary to consider the effect of the toluene on the position of the melting curve. This will be done indirectly by considering its effect on water vapor pressure.

At any given temperature below 0 C, equilibrium between ice and capillary water can be maintained because of the effect of capillary tension on the free energy of the water. The fact that with ice present the capillary tension is maintained indicates that the unfrozen capillary water either becomes separated from the ice so as to maintain its meniscus, or else it retains its continuity and remains in contact not only with the ice but also with the external phase. Such contact might be maintained through channels too small to be frozen at the existing temperature. If the external phase is air, as in the electrical method described earlier, the capillary tension will depend on surface curvature and the interfacial tension at the air-water interface (i.e., the surface tension), according to Kelvin's equation. (See Part 3.) If the external phase is toluene, the capillary tension will depend on surface curvature as before, but now it will depend on the interfacial tension at the toluene-water interface rather than the tension at the air-water interface. There-

fore, the melting curves of the granules submerged in toluene should not be the same as when the granules are exposed to air.

We can estimate the effect of substituting a toluene-water interface for an air-water interface by making use of eq. (3). Let

σ_w = surface tension of water against air,
σ_{wt} = interfacial tension, water against toluene,
T_o = normal freezing point of water, deg. K,
ΔT_1 = depression of freezing point with sample in contact with air,
ΔT_2 = depression of freezing point with sample in contact with toluene, and

let the other symbols have the same meaning as before. Then,

$$\frac{\Delta T_1}{T_o} = \frac{2v_f}{rq}\,\sigma_w$$

and

$$\frac{\Delta T_2}{T_o} = \frac{2v_f}{rq}\,\sigma_{wt}\,.$$

We may assume that v_f and q are the same in both cases. Hence,

$$\frac{\Delta T_1}{\Delta T_2} = \frac{\sigma_w}{\sigma_{wt}}\,.$$

Interfacial tension and surface tension are functions of temperature. For the air-water interface, we may obtain satisfactory figures for given temperatures from published data. For the toluene-air interface no data are available except for 25 C. For the similar liquid, benzene, the temperature coefficient is given as -0.058 for the temperature range 10 to 40 C. We will assume that this holds for toluene and for the lower temperature range.

On the basis just described, the following results were obtained:

t, deg. C	σ_w	σ_{wt}	$\frac{\sigma_w}{\sigma_{wt}}$
0	75.64	37.6	2.01
− 5	76.33	37.8	2.02
−10	77.00	38.1	2.02

Hence, it may be concluded that

$$\Delta T_1 = 2\Delta T_2, \text{ approximately.}$$

That is, the depression of the freezing point with the sample in contact with air would be about twice the amount observed in these experiments. Or, the amount of water freezable in these experiments at −15 C, for

example, is about the same as would be freezable at −30 C if the samples were exposed to air.

QUANTITIES OF ICE FORMED IN VARIOUS SAMPLES

The amounts of ice formed in various samples are given in Tables 8-2 to 8-6 and compositions of the samples in Table 8-7. The relationships between ice-content and temperature are given graphically in Fig. 8-11 and 8-12. The results are analyzed further in succeeding sections.

Influence of soluble alkalies

The curves shown in Fig. 8-11 and 8-12 show that the final melting point differed among the various specimens. These differences are believed to be due to differences in the amount of soluble salts, particularly the alkalies, in the evaporable water. The basis for this conclusion is more clearly indicated by the data as arranged in Table 8-8.

It will be noted that with three of the five cements, the final melting point is higher the higher the original water-cement ratio. This is undoubtedly the result of the leaching out of alkalies during the 28-day period of water storage; the higher w_o/c the higher the rate of leaching.

The dissolved alkali not only lowers the final melting point but also the amounts of ice that can exist at lower temperatures. The effect is probably proportional to the concentration in the part that remains unfrozen. What this concentration is, or how it changes with temperature, cannot be told from information now available, mainly because the effects of adsorption by the solid phase on both the solvent and the solute cannot be evaluated.

THEORETICAL AMOUNT OF FREEZABLE WATER AT A GIVEN TEMPERATURE

Locus of ice in the paste

In the majority of the tests considered here, the samples were first cooled to −78 C. This is the temperature at which ice has about the same vapor pressure as the non-evaporable water. (See Part 2.) Hence, if equilibrium is reached, all the evaporable water should be frozen. However, it should be observed that the *freezing in place* of adsorbed water is very unlikely. As shown in Part 4, when water is adsorbed it undergoes a change, as indicated by its decrease in entropy. The indications are that the entropy change of adsorption is greater than that accompanying the transition from water to ice. It hardly seems possible that water that has already been changed to such an extent could be caused to crystallize only by lowering the temperature. To be considered also are the relative sizes of the gel pores and the capillaries. As shown in Part 3, the hydraulic radius of the gel pores is estimated to be about 10Å. The average width of the pores is probably between 2 and

TABLE 8-2—MELTING-CURVE DATA FOR SAMPLES MADE WITH CEMENT 15754

(For compositions of samples, see Table 8-7.)

Temp., deg. C × (−1)	Ref. 10-4; w_o/c = 0.32				Ref. 10-1; w_o/c = 0.45				Ref. 10-3; w_o/c = 0.62			
	28 days		90 days		28 days		90 days		28 days		90 days	
	w_f/c	w_f/V_m	w_f/c	w_f/V_m	w_f/c	w_f/V_m	w_f/c	w_f/V_m	w_f/c	w_f/V_m	w_f/c	w_f/V_m
0.1	—	—	—	—	—	—	—	—	.0165	0.29	—	—
0.15	—	—	—	—	—	—	—	—	—	—	.0350	0.57
0.25	—	—	—	—	—	—	—	—	.0557	0.99	—	—
0.50	—	—	—	—	.0455	0.86	.0424	0.70	.1160	2.07	.1275	2.09
0.75	.0157	0.35	.0149	0.30	.0744	1.40	.0663	1.09	.1627	2.91	.1562	2.56
1.0	.0293	0.65	.0287	0.59	.0909	1.72	.0762	1.25	.1897	3.39	.1751	2.87
1.5	.0384	0.85	.0376	0.77	.1075	2.03	.0898	1.47	.2243	4.01	.2061	3.38
2.0	.0415	0.92	.0417	0.85	.1207	2.28	.0996	1.63	.2452	4.38	.2259	3.70
2.5	.0449	1.00	.0432	0.88	.1294	2.44	.1045	1.71	.2602	4.65	.2387	3.91
3.0	.0473	1.05	.0452	0.92	.1350	2.55	.1093	1.79	.2724	4.86	.2482	4.07
3.5	.0496	1.10	.0467	0.95	.1404	2.65	.1142	1.87	.2829	5.05	.2547	4.18
4.0	.0520	1.16	.0485	0.99	.1445	2.73	.1177	1.93	.2916	5.21	.2636	4.32
5.0	.0560	1.24	.0507	1.03	.1556	2.94	.1250	2.05	.3055	5.46	.2773	4.55
6.0	.0600	1.33	.0539	1.10	.1655	3.12	.1316	2.16	.3172	5.66	.2885	4.73
8.0	.0663	1.47	.0583	1.19	.1779	3.36	.1449	2.38	.3396	6.06	.3096	5.08
10.0	.0704	1.56	.0622	1.27	.1893	3.57	.1542	2.53	.3616	6.46	.3267	5.36
12.0	.0744	1.65	.0648	1.32	.1993	3.76	.1622	2.66	.3749	6.69	.3397	5.57
15.0	.0823	1.83	.0672	1.37	.2093	3.95	.1738	2.85	.3919	7.00	.3559	5.83
20.0	.0930	2.07	.0734	1.50	.2270	4.28	.1965	3.22	.4240	7.57	—	—
Final Melting Point	− 0.5°		− 0.5°		− 0.25°		− 0.20°		− 0.05°		− 0.05°	

TABLE 8-3—MELTING-CURVE DATA FOR SAMPLES MADE WITH CEMENT 15756

(For compositions of samples, see Table 8-7.)

Temp., deg. C × (−1)	Ref. 10-C; w_o/c = 0.34		Ref. 10-B; w_o/c = 0.48		Ref. 10-A; w_o/c = 0.67		Ref. 10-14; w_o/c = 0.45		Ref. 10-13; w_o/c = 0.63	
	29 days		29 days		29 days		90 days		90 days	
	w_f/c	w_f/V_m	w_f/c	w_f/V_m	w_f/c	w_f/V_m	w_f/c	w_f/V_m	w_f/c	w_f/V_m
0.1	—	—	—	—	.0252	0.60	—	—	—	—
0.25	.0101	0.28	.0470	1.21	.0994	2.37	.0273	0.58	.0448	0.91
0.50	.0242	0.67	.0916	2.35	.1755	4.18	.0558	1.19	.1289	2.63
0.75	.0391	1.09	.1156	2.96	.2260	5.38	.0816	1.74	.2056	4.20
1.0	.0469	1.30	.1345	3.45	.2624	6.25	.0957	2.04	.2168	4.42
1.5	.0600	1.67	.1637	4.20	.3128	7.45	.1161	2.47	.2638	5.38
2.0	.0717	1.99	.1864	4.78	.3489	8.31	.1311	2.79	.2910	5.94
2.5	.0802	2.23	.2068	5.30	.3727	8.87	.1443	3.07	.3138	6.40
3.0	.0889	2.47	.2196	5.63	.3910	9.31	.1549	3.30	.3322	6.78
3.5	.0951	2.64	.2311	5.93	.4071	9.69	.1636	3.48	.3476	7.09
4.0	.1013	2.81	.2410	6.18	.4198	10.00	.1724	3.67	.3608	7.36
5.0	.1139	3.16	.2578	6.61	.4459	10.62	.1863	3.96	.3817	7.79
6.0	.1218	3.38	.2732	7.01	.4624	11.01	.1972	4.20	.3965	8.09
8.0	.1354	3.76	.2934	7.52	.4859	11.57	.2024	4.31	.4175	8.52
10.0	.1413	3.92	.2988	7.66	.4942	11.77	.2251	4.79	.4305	8.79
12.0	.1468	4.08	.3079	7.89	.5030	11.98	.2343	4.99	.4401	8.98
15.0	.1563	4.34	.3184	8.16	.5157	12.28	.2477	5.27	.4557	9.30
20.0	.1721	4.78	.3431	8.80	.5417	12.90	.2691	5.73	.4851	9.90
Final Melting Point	− 0.1°		− 0.1°		− 0.05°		0°		0°	

TABLE 8-4—MELTING-CURVE DATA FOR SAMPLES MADE WITH CEMENT 15758

(For compositions of samples, see Table 8-7.)

Temp., deg. C × (−1)	Ref. 10-12; w_o/c = 0.32				Ref. 10-11; w_o/c = 0.45				Ref. 10-10; w_o/c = 0.62			
	28 days		91 days		28 days		91 days		28 days		91 days	
	w_f/c	w_f/V_m	w_f/c	w_f/V_m	w_f/c	w_f/V_m	w_f/c	w_f/V_m	w_f/c	w_f/V_m	w_f/c	w_f/V_m
0.25	—	—	—	—	—	—	—	—	—	—	.0529	0.96
0.50	—	—	—	—	.0280	0.55	.0177	0.34	.1040	1.93	.1042	1.89
0.75	—	—	—	—	.0510	1.00	.0358	0.69	.1723	3.19	.1474	2.68
1.0	.0019	0.04	.0199	0.45	.0714	1.40	.0538	1.03	.2048	3.79	.1766	3.21
1.5	.0197	0.47	.0335	0.76	.0919	1.80	.0724	1.39	.2386	4.18	.2027	3.68
2.0	.0276	0.66	.0406	0.92	.1045	2.05	.0844	1.62	.2636	4.88	.2272	4.13
2.5	.0324	0.77	.0462	1.05	.1146	2.25	.0933	1.79	.2799	5.18	.2415	4.39
3.0	.0379	0.90	.0493	1.12	.1222	2.40	.1031	1.98	.2925	5.42	.2540	4.62
3.5	.0418	0.99	.0510	1.16	.1272	2.49	.1039	2.00	.3031	5.61	.2586	4.70
4.0	.0449	1.07	.0529	1.20	.1321	2.59	.1082	2.08	.3131	5.80	.2657	4.83
5.0	.0520	1.24	.0583	1.32	.1384	2.71	.1169	2.25	.3229	5.98	.2820	5.13
6.0	.0582	1.38	.0613	1.39	.1445	2.83	.1256	2.42	.3356	6.21	.2909	5.29
8.0	.0694	1.65	.0674	1.53	.1546	3.03	.1397	2.69	.3575	6.62	.3118	5.67
10.0	.0783	1.86	.0727	1.65	.1624	3.18	.1473	2.83	.3741	6.93	.3257	5.92
12.0	.0857	2.04	.0765	1.74	.1678	3.29	.1566	3.01	.3848	7.12	.3376	6.14
15.0	.0924	2.20	.0793	1.80	.1763	3.46	.1673	3.22	.4024	7.45	.3529	6.42
20.0	*	—	*	—	*	—	*	—	.4363	8.08	*	—
Final Melting Point	− 0.9°		− 0.85°		− 0.25°		− 0.25°		− 0.15°		− 0.10°	

*Not available.

TABLE 8-5—MELTING-CURVE DATA FOR SAMPLES MADE WITH CEMENT 15761

(For compositions of samples, see Table 8-7.)

Temp., deg. C × (−1)	Ref. 10-6; w_o/c = 0.32		Ref. 10-2; w_o/c = 0.45				Ref. 10-5; w_o/c = 0.63	
	28 days		28 days		90 days		28 days	
	w_f/c	w_f/V_m	w_f/c	w_f/V_m	w_f/c	w_f/V_m	w_f/c	w_f/V_m
0.75	—	—	—	—	—	—	.1063	1.93
1.0	—	—	—	—	.0191	0.34	.1894	3.44
1.5	—	—	.0854	1.71	.0892	1.59	.2548	4.63
2.0	.0316	0.77	.1199	2.40	.1083	1.93	.2858	5.20
2.5	.0455	1.11	.1357	2.71	.1201	2.14	.3100	5.64
3.0	.0515	1.26	.1459	2.92	.1296	2.31	.3240	5.89
3.5	.0568	1.38	.1547	3.09	.1371	2.45	.3376	6.14
4.0	.0615	1.50	.1630	3.26	.1431	2.56	.3478	6.32
5.0	.0697	1.70	.1779	3.56	.1550	2.77	.3655	6.64
6.0	.0747	1.82	.1918	3.84	.1664	2.97	.3793	6.90
8.0	.0830	2.02	.2130	4.26	.1837	3.28	.4012	7.29
10.0	.0888	2.16	.2289	4.58	.1949	3.48	.4145	7.54
12.0	.0928	2.26	.2410	4.82	.2046	3.65	.4235	7.70
15.0	.0942	2.30	.2542	5.08	.2152	3.84	.4373	7.95
20.0	.0964	2.35	.2780	5.56	.2310	4.12	.4425	8.04
Final Melting Point	− 1.6°		− 0.9°		− 0.85°		− 0.5°	

TABLE 8-6—MELTING-CURVE DATA FOR SAMPLES MADE WITH CEMENT 15763

(For compositions of samples, see Table 8-7.)

Temp., deg. C × (−1)	Ref. 10-9; w_o/c = 0.31				Ref. 10-8; w_o/c = 0.44				Ref. 10-7; w_o/c = 0.62	
					Dil. No. 5		Dil. No. 6			
	28 days		91 days		28 days		28 days		28 days	
	w_f/c	w_f/V_m	w_f/c	w_f/V_m	w_f/c	w_f/V_m	w_f/c	w_f/V_m	w_f/c	w_f/V_m
0.10	—	—	—	—	.0112	0.34	.0092	0.28	.0392	1.12
0.15	.0126	0.42	.0058	0.15	—	—	—	—	—	—
0.25	.0228	0.76	—	—	.0586	1.78	.0478	1.45	.1110	3.17
0.50	.0459	1.53	.0244	0.64	.1003	3.04	.0908	2.75	.1963	5.61
0.75	—	—	.0358	0.94	.1352	4.10	.1269	3.85	.2648	7.57
1.0	.0772	2.57	.0430	1.13	.1600	4.85	.1525	4.62	.3041	8.69
1.5	.0932	3.11	.0538	1.42	.1914	5.80	.1827	5.54	.3580	10.23
2.0	.1046	3.49	.0603	1.59	.2128	6.45	.2036	6.17	.3890	11.11
2.5	.1128	3.76	.0652	1.72	.2276	6.90	.2177	6.60	.4123	11.78
3.0	.1185	3.95	.0698	1.84	.2391	7.24	.2294	6.95	.4306	12.30
3.5	.1231	4.10	.0727	1.91	.2456	7.44	.2386	7.23	.4452	12.72
4.0	.1273	4.24	.0768	2.02	.2523	7.64	.2467	7.48	.4566	13.04
5.0	.1347	4.49	.0822	2.16	.2639	8.00	.2563	7.77	.4705	13.44
6.0	.1378	4.59	.0875	2.30	.2731	8.28	.2658	8.05	.4889	13.97
8.0	.1437	4.79	.0939	2.47	.2828	8.57	.2757	8.35	.4973	14.21
10.0	.1481	4.94	.0983	2.59	.2913	8.83	.2814	8.53	.5061	14.46
12.0	.1509	5.03	.1014	2.67	.2937	8.90	.2846	8.62	.5153	14.72
15.0	.1545	5.15	.1037	2.73	.2962	8.98	.2892	8.76	.5272	15.06
20.0	*	—	.1045	2.75	.3028	9.18	.2963	8.98	.5500	15.71
Final Melting Point	− 0.05°		− 0.05°		− 0.05°		− 0.05°		− 0.05°	

*Not available.

TABLE 8-7—COMPOSITION OF SAMPLES USED IN DILATOMETERS

(For cement characteristics, see Appendix to Part 2.)

Ref. No.	Age, days	$\frac{w_o}{c}$	Composition, g/g of cement					$\frac{w_e}{V_m}$
			$\frac{w_n}{c}$	$\frac{w_e}{c}$	$\frac{w_t}{c}$	$\frac{(w_a)_{.35}}{c}$	$\frac{V_m}{c}$	
Cement 15754; $V_m/w_n = 0.258$								
10–4	28	0.32	0.176	0.213	0.389	0.064	0.045	4.73
10–4	90	0.32	0.189	0.220	0.409	0.065	0.049	4.49
10–1	28	0.45	0.207	0.351	0.558	0.076	0.053	6.63
10–1	90	0.45	0.237	0.335	0.572	0.081	0.061	5.50
10–3	28	0.62	0.217	0.536	0.753	0.081	0.056	9.57
10–3	90	0.62	0.235	0.538	0.773	0.088	0.061	8.82
Cement 15756; $V_m/w_n = 0.271$								
10–C	28	0.34	0.134	0.272	0.406	0.051	0.036	7.56
10–B	28	0.48	0.145	0.443	0.589	0.052	0.039	11.36
10–A	28	0.67	0.154	0.648	0.802	0.057	0.042	15.43
10–14	90	0.45	0.172	0.391	0.563	0.063	0.047	8.32
10–13	90	0.63	0.182	0.611	0.793	0.066	0.049	12.47
Cement 15758; $V_m/w_n = 0.248$								
10–12	28	0.32	0.168	0.224	0.392	0.058	0.042	5.33
10–12	91	0.32	0.179	0.227	0.406	0.061	0.044	5.16
10–11	28	0.45	0.204	0.353	0.557	0.074	0.051	6.92
10–11	91	0.45	0.211	0.365	0.576	0.076	0.052	7.02
10–10	28	0.62	0.218	0.555	0.773	0.078	0.054	10.28
10–10	91	0.62	0.222	0.535	0.757	0.083	0.055	9.73
Cement 15761; $V_m/w_n = 0.262$								
10–6	28	0.32	0.158	0.248	0.406	0.057	0.041	6.05
10–2	28	0.45	0.190	0.390	0.580	0.069	0.050	7.80
10–2	90	0.45	0.215	0.381	0.596	0.078	0.056	6.80
10–5	28	0.63	0.209	0.613	0.822	0.083	0.055	11.15
Cement 15763; $V_m/w_n = 0.295$								
10–9	28	0.31	0.101	0.278	0.379	0.045	0.030	9.27
10–9	91	0.31	0.130	0.237	0.367	0.056	0.038	6.24
10–8	28	0.44	0.113	0.424	0.537	0.048	0.033	12.85
10–7	28	0.62	0.119	0.624	0.743	0.050	0.035	17.83

4 times the hydraulic radius. Thus the average gel pore is estimated to be between 20 and 40Å wide. The width of the average capillary cannot be estimated very accurately, but it is at least 10 or 20 times the width of the gel pore. Owing to the fact that the melting point of a crystal is higher the smaller the crystal—for crystals in the colloidal size-range—any ice that might form in the gel pores would have a higher melting point than that of the ice in the capillaries. It seems, therefore, that if the gel water freezes, it first moves out of the gel and then joins the ice already

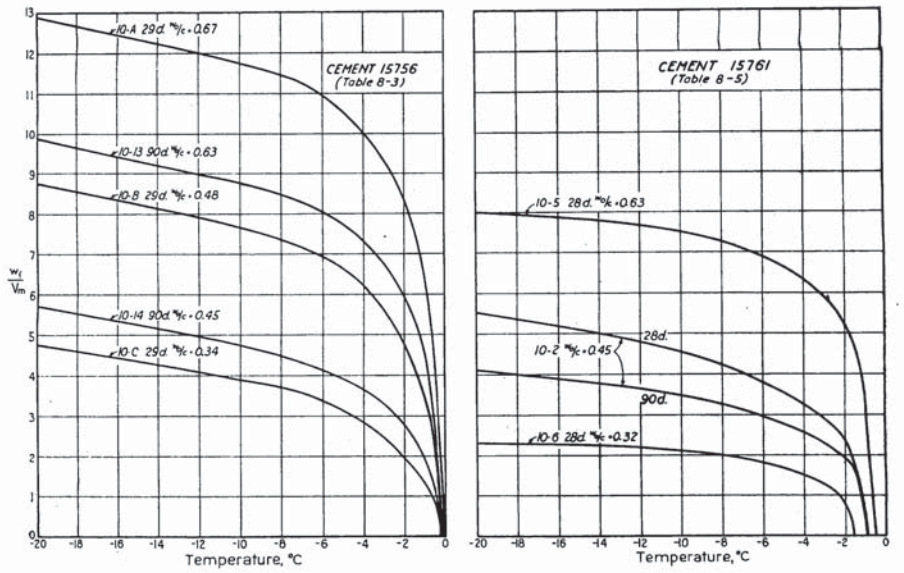

Fig. 8-11—Relationship between ice content and temperature for samples made with cements indicated

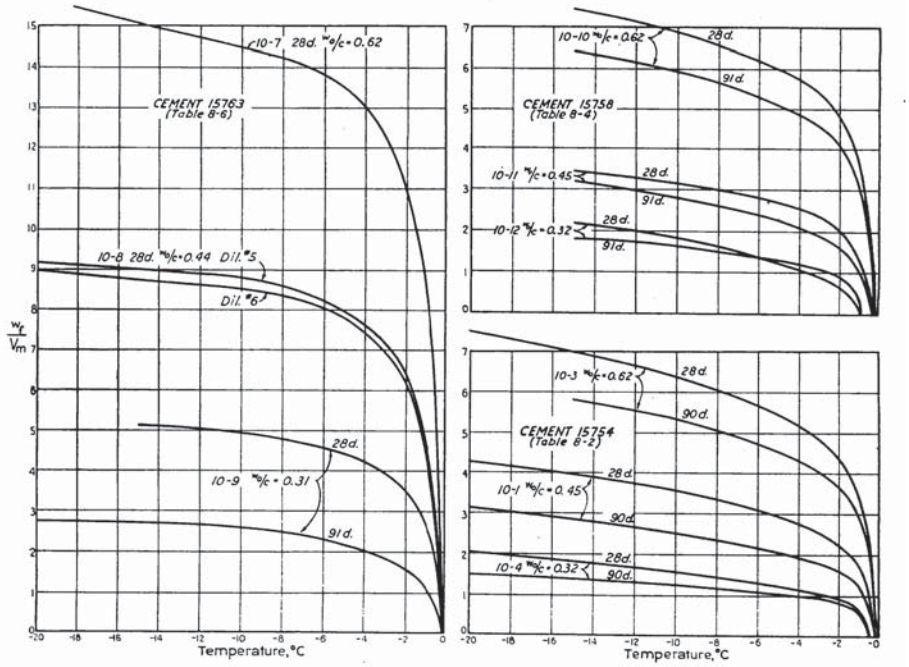

Fig. 8-12—Relationship between ice content and temperature for samples made with cements indicated

formed in the capillaries. The movement of the water could be either by surface migration or by distillation.

Relation of freezing to drying

As mentioned before, the process of freezing out gel water would be fundamentally the same as removing it by evaporation. In either case, the equilibrium vapor pressure of the gel water at any time is determined by the degree of saturation of the gel. Consequently, the amounts of freezable and unfreezable water should be determinable in terms of the vapor pressure isotherm. For the conditions of these experiments, the adsorption isotherm may be used.

TABLE 8-8—INFLUENCE OF ALKALIES ON FINAL MELTING POINT

Cement No.	Alkali content of cement, percent			w_o/c	Final melting point, deg. C	
	Na_2O	K_2O	Total		28 days	90 days
15754	0.17	0.16	0.33	0.32	−0.50	−0.50
				0.45	−0.25	−0.20
				0.62	−0.05	−0.05
15756	0.05	0.17	0.22	0.34	−0.10*	—
				0.45	—	0
				0.48	−0.10*	—
				0.63	—	0
				0.67	−0.05	—
15758	0.30	0.40	0.70	0.32	−0.90	−0.85†
				0.45	−0.25	−0.25†
				0.62	−0.15	−0.10†
15761	1.13	0.44	1.57	0.32	−1.60	—
				0.45	−0.90	−0.85
				0.63	−0.50	—
15763	0.05	0.22	0.27	0.31	−0.05	−0.05†
				0.44	−0.05	—
				0.62	−0.05	—

*29 days.
†91 days.

Relation of freezable water to total evaporable water

We have already seen (Part 3) that the water content that produces a given vapor pressure *in the lower range of pressures* is the same per unit V_m* for all samples. Therefore, for the lower range of vapor pressures, and hence for the lower range of freezing temperatures, the amount of *unfreezable* water at a given temperature per unit V_m should be the same for all samples. Thus if we let

*V_m is the constant in the B.E.T. equation that represents the quantity of water required to cover the surface with a single layer of molecules. It is considered to be proportional to the surface area of the solid phase and a measure of the gel content of well hydrated samples.

w_e = total evaporable water,
w_u = unfreezable water, and
w_f = freezable water,

then $$\frac{w_f}{V_m} = \frac{w_e}{V_m} - u \, , \quad \ldots\ldots (9)$$

where $u = w_u/V_m$ and is a constant for a given temperature.

From eq. (9) it can be seen that plotting w_f/V_m vs. w_e/V_m should produce a straight line having a slope of unity for whatever range of temperatures w_u/V_m is actually constant. Such plots are shown in Fig. 8-13 for six different temperatures. In each diagram the solid straight line has a slope of 1.0 as required by eq. (9). With the exception of those obtained above −6 C, the experimental points conform fairly well to this slope. Hence, we may conclude that for temperatures of about −6 C or lower, the following empirical relationships may be used for estimating the amount of freezable water:

$$\left(\frac{w_f}{V_m}\right)_{-6°} = \frac{w_e}{V_m} - 4.0 \quad \ldots\ldots (10)$$

$$\left(\frac{w_f}{V_m}\right)_{-10°} = \frac{w_e}{V_m} - 3.7 \quad \ldots\ldots (11)$$

$$\left(\frac{w_f}{V_m}\right)_{-15°} = \frac{w_e}{V_m} - 3.2 \quad \ldots\ldots (12)$$

The temperatures indicated are for freezing in toluene. For freezing in air, the temperatures should be multiplied by 2, as shown in a preceding section. That is,

$(w_f)_{-6°}$ in toluene = $(w_f)_{-12°}$ in air, etc.

Reference to Fig. 8-13 shows that at a dilatometer temperature of −6 C or higher, the amount of freezable water is roughly proportional to the amount of capillary water, $w_e - 4V_m$, the proportionality constants being about 1.0 at −6 C, 0.86 at −4 C, 0.7 at −2 C, and 0.6 at −1 C. This indicates that in this upper temperature range, the amount of water extracted from the gel by freezing is negligible. Below − 6 C, the contribution from the gel water is appreciable. As already mentioned it could contribute a maximum of $4V_m$ at about −78 C.

It should be noted that eqs. (10), (11), and (12) can be used only for estimating the *maximum* amount of freezable water. If a specimen were cooled only a few degrees below its final melting point, as is frequently the case for concrete exposed to the weather, the amount of freezable water would probably be smaller than would be indicated by these equations because of the hysteresis in the vapor-pressure-vs.-water-content relationship. Very little specific information on this point can be given until more experimental work is done.

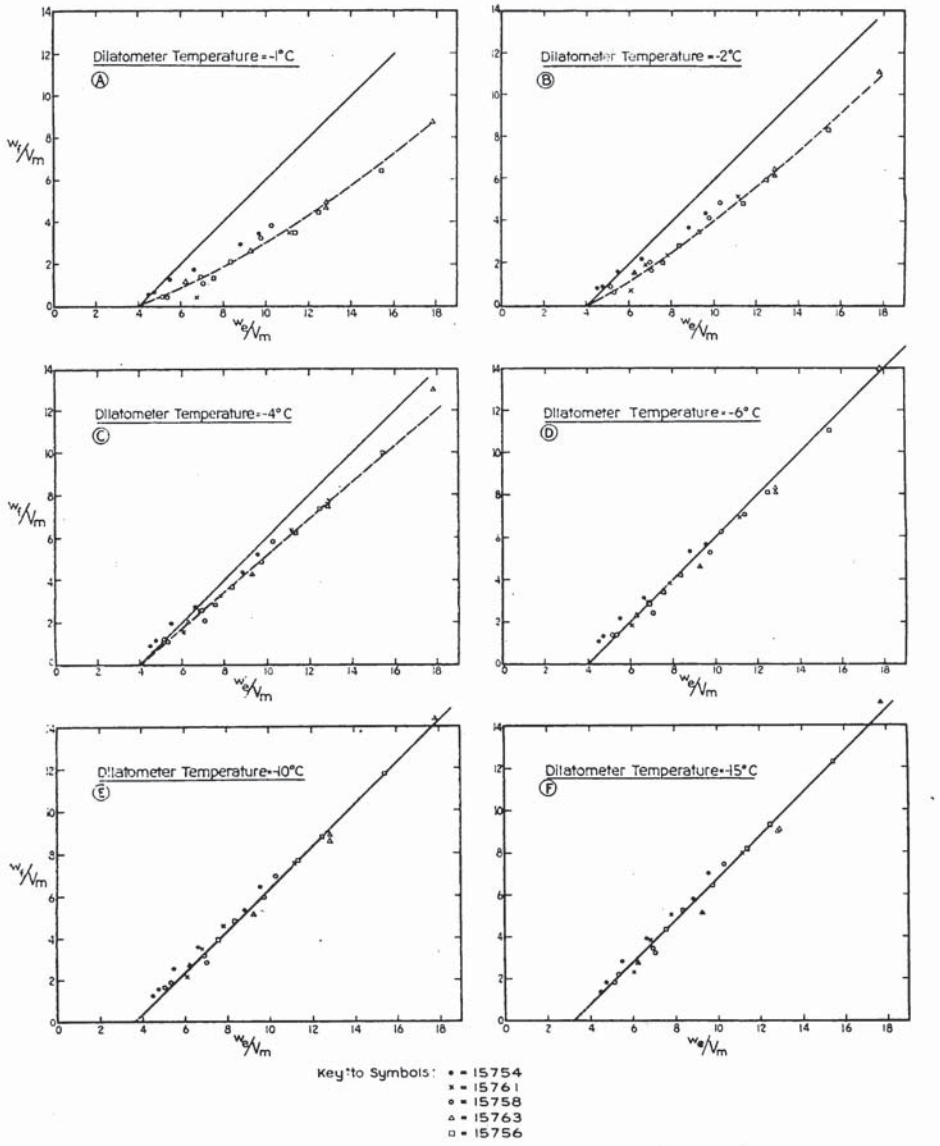

Fig. 8-13—Relationship between maximum freezable water content and total evaporable water in saturated pastes

RELATIONSHIP BETWEEN THE AMOUNT OF WATER UNFREEZABLE AT A GIVEN TEMPERATURE AND THE 25C VAPOR PRESSURE ISOTHERM

Theoretical relationship

As mentioned before, one of the objects of this investigation was to establish the relationship between melting point and vapor pressure so that the amount of water freezable at a given temperature could be estimated from sorption data alone. As pointed out in connection with Fig. 8-1, at any given temperature below 0 C, the vapor pressure of the unfrozen evaporable water must be the same as that of ice at the existing temperature. On the assumption that the ice exists as a pure, microcrystalline phase under atmospheric pressure only, we can ascertain its relative vapor pressure at given temperatures from eq. (1) or (2). The results of such computations are plotted in Fig. 8-2. That curve shows that at −30 C, for example, the vapor pressure of ice is about 0.75 p_s, where p_s is the saturation pressure at −30 C. As shown above, the amount of water freezable at −30 C is about the same as the amount freezable in the toluene-filled dilatometer at −15 C.

To estimate the point on the 25 C adsorption isotherm corresponding to a given relative vapor pressure at a lower temperature, we may use the Kelvin equation (see Part 3):

$$ln\ p/p_s = -\frac{Mv_f\sigma_f}{RT}\left(\frac{1}{r_1}+\frac{1}{r_2}\right), \quad \ldots\ldots\ldots\ldots\ldots\ldots\ (13)$$

where

p/p_s = relative vapor pressure,
M = molecular weight of the fluid,
v_f = molar volume of the fluid,
σ_f = surface tension of the fluid,
r_1 and r_2 = principal radii of surface curvature of the fluid,
R = gas constant, and
T = absolute temperature.

Let

h_{25} = p/p_s at 298 K (25 C),
h_t = p/p_s at temperature T,
σ_{25} = surface tension at 25 C, and
σ_t = surface tension at temperature T.

Then

$$ln\ h_{25} = -\frac{\sigma_{25}\,M(v_f)_{25}}{R298}\left(\frac{1}{r_1}+\frac{1}{r_2}\right)$$

and

$$ln\ h_t = -\frac{\sigma_t\,M(v_f)_t}{RT}\left(\frac{1}{r_1}+\frac{1}{r_2}\right),$$

where

T = the lower temperature, in deg. K, and the other symbols have the same significance as before. Hence,

$$\frac{ln\ h_{25}}{ln\ h_t} = \frac{\sigma_{25}}{\sigma_t}\,\frac{T}{298}\,\frac{(v_f)_{25}}{(v_f)_t} \quad \ldots\ldots\ldots\ldots\ldots\ldots\ldots\ldots (14)$$

The ratio $(v_f)_{25}$ to $(v_f)_t$ varies so little from 1.0000 over the temperature range involved here that it can be taken as unity at all temperatures.

The ratio of σ_{25}/σ_t can be evaluated from the relationship

$$\sigma_t = 75.64 - 0.1391t - 0.00003t^2 \text{ (Ref. 12)} \quad \ldots\ldots\ldots\ldots (15)$$

Solutions of this equation are given below in Table 8-9:

TABLE 8-9—SOLUTIONS OF EQ. (15)

t, deg. C	σ_t	$\frac{\sigma_{25}}{\sigma_t}$
25	71.97	1.0000
0	75.64	0.9515
− 4	76.19	0.9446
− 6	76.46	0.9413
− 8	76.75	0.9377
−10	77.06	0.9339
−12	77.47	0.9290
−15	77.79	0.9251
−20	78.30	0.9192
−30	79.54	0.9048

The above data, substituted into eq. (14), give the results shown in Table 8-10.

TABLE 8-10—SOLUTIONS OF EQ. (14)

t, deg. C	T, deg. K	h_t from Fig. 8-2	h_{25}
0	273.1	1.000	1.000
− 4	269.1	0.958	0.965
− 6	267.1	0.945	0.953
− 8	265.1	0.927	0.939
−10	263.1	0.908	0.924
−12	261.1	0.893	0.911
−15	258.1	0.865	0.890
−20	253.1	0.823	0.859
−30	243.1	0.746	0.806

According to the foregoing discussion, the amount of ice formed in the dilatometer at −15 C, for example, is about the same as that which would form in the same sample exposed to air at −30 C. Table 8-10 shows that the water remaining unfrozen at this temperature would have a relative vapor pressure of 0.806 at 25 C. Thus, if all the assumptions made above are valid, the amount of unfrozen water in a sample at −15 C in the dilatometer should be approximately the same as the evaporable water content of the same sample having a relative vapor pressure of 0.806 at 25 C. The extent to which the data bear out this assumption will be shown after the empirical relationship has been examined.

Comparison of theoretical and empirical relationships

Consider a given sample in a dilatometer at −15 C. It will contain a certain quantity of unfrozen evaporable water in equilibrium with ice. We have already seen that to maintain equilibrium between the same amount of unfrozen water and ice in the absence of toluene, the temperature would have to be −30 C. At this temperature the ice, and hence the unfrozen water, would have a vapor pressure of 0.746 p_s (see Fig. 8-2). According to Table 8-10, the corresponding vapor pressure at 25 C would be 0.806 p_s. Similarly, for dilatometer temperatures of −10 C and −6 C, the corresponding vapor pressures at 25 C would be 0.859 and 0.911, respectively.

Table 8-11 gives the ratio of evaporable water, w, to V_m in samples at equilibrium with these pressures at 25 C. These data were obtained from smooth isotherms, representing samples almost identical with those used in the freezing experiments. They represent the theoretical amounts of unfrozen water at dilatometer temperatures of −6 C, −10 C, and −15 C.

The experimentally observed amounts of unfreezable water are indicated by the intercepts of the straight lines in Fig. 8-13 D, E, and F. These intercepts represent experimental averages, comparable with the grand averages given in Table 8-11.

The two sets of figures may be compared in the following table:

Dilatometer temperature, deg. C	Unfreezable water, w_u/V_m		
	Observed	Theoretical	Ratio
− 6	4.00	3.72	1.08
−10	3.70	3.25	1.13
−15	3.20	2.93	1.09

TABLE 8-11—RATIO OF EVAPORABLE WATER TO V_m IN HARDENED PASTES REPRESENTATIVE OF THOSE USED IN FREEZING STUDIES

w_o/c	Age, days	w/V_m* at p/p_s (25 C) indicated		
		0.911	0.859	0.806
		Cement 15754		
0.33	28	3.35	3.05	2.85
0.33	90	3.10	2.90	2.75
0.45	28	3.60	3.30	3.00
0.45	90	3.45	3.10	2.90
		Avg. 3.38	3.09	2.88
		Cement 15756		
0.32	28	4.10	3.45	3.05
0.32	90	3.45	3.05	2.85
0.45	28	4.40	3.70	3.20
0.45	90	3.90	3.30	2.95
		Avg. 3.96	3.38	3.01
		Cement 15758		
0.33	28	3.70	3.20	2.80
0.33	90	3.35	2.95	2.70
0.46	28	3.80	3.35	3.05
0.46	90	3.70	3.25	2.90
		Avg. 3.64	3.19	2.86
		Cement 15761		
0.33	28	3.80	3.30	2.95
0.33	90	3.50	3.05	2.80
0.47	28	3.80	3.30	2.95
0.47	90	3.55	3.20	2.90
		Avg. 3.66	3.21	2.90
		Cement 15763		
0.32	28	4.25	3.65	3.25
0.32	90	3.45	3.05	2.75
0.44	28	4.35	3.65	3.25
0.44	90	3.85	3.25	2.85
		Avg. 3.98	3.40	3.02
		Grand Avg. 3.72	3.25	2.93

*w = evaporable water, g/g cement; V_m = constant from B.E.T. eq. A, g/g cement.

This indicates that the observed amount of unfreezable water averages about 10 percent greater than the theoretical amount. Such a difference could be due to the smallness of the ice crystals, which would tend to raise their melting point. Or it might be due to an error in the theoretical figure arising from the assumption that the effects of temperature changes on the solutions in the paste are the same as for pure water.

The degree of agreement between the observed and theoretical values is such as to warrant estimating the amount of water freezable at a given temperature from the 25 C isotherm.

EQUATIONS FOR ESTIMATING MAXIMUM FREEZABLE WATER FROM THE NON-EVAPORABLE WATER CONTENT

The maximum amount of water in a saturated paste that may be frozen at a given temperature may be estimated from the non-evaporable and total water contents. The bases for such estimates are developed below:

Eq. (9) may be written

$$w_f = w_e - uV_m .$$

Since, for an average cement,

$$V_m = 0.26\, w_n \text{ (Part 3, eq. (4))},$$

and

$$w_e = w_t - w_n ,$$

then

$$w_f = w_t - w_n(1 + 0.26u) \quad \ldots\ldots (16)$$

Using the values of u given in eqs. (10), (11), and (12), we obtain

$$(w_f)_{-6^\circ} = w_t - 2.04\, w_n \quad \ldots\ldots (17)$$

$$(w_f)_{-10^\circ} = w_t - 1.96\, w_n \quad \ldots\ldots (18)$$

$$(w_f)_{-15^\circ} = w_t - 1.83\, w_n \quad \ldots\ldots (19)$$

The above equations may be used when the *total water content* of the saturated paste is known. When only the *original water-cement ratio* is known (corrected for bleeding), the relationships developed below may be used.

On the assumption that the volume of the hardened paste is the same as that of the fresh paste after bleeding, we may write

$$w_o = w_t v_t \quad \ldots\ldots (20)$$

Since

$$v_t = 1 - 0.279\, \frac{w_n}{w_t} \text{ (Part 5, eq. (8))},$$

$$w_o = w_t - 0.279\, w_n \quad \ldots\ldots (21)$$

Substitution into eq. (16) gives

$$w_f = w_o + 0.279 w_n - w_n(1 + 0.26u)$$

$$= w_o - (0.721 + 0.26u) w_n \quad \ldots\ldots (22)$$

Again using values of u from eqs. (10), (11), and (12) we obtain

$$(w_f)_{-6°} = w_o - 1.76\, w_n ; \quad (23)$$

$$(w_f)_{-10°} = w_o - 1.68\, w_n ; \quad (24)$$

$$(w_f)_{-15°} = w_o - 1.55\, w_n . \quad (25)*$$

It should be noted that all these empirical equations give the amounts of water freezable in the dilatometers, with the saturated paste in contact with toluene. As mentioned before, the temperature drop required to freeze equal amounts of water in the absence of toluene is, theoretically, two times the temperature in degrees C indicated, i.e., −12 C, −20 C, and −30 C, respectively.

SATURATED PASTES CONTAINING NO FREEZABLE WATER

For the range of temperatures over which the equations derived from eq. (9) were found to apply, it seems that the freezable water contents of some saturated hardened pastes should be zero. For example, eq. (25) indicates that $w_f = 0$ when $w_o = 1.55\, w_n$. Thus, when hydration has proceeded to the point where $w_n/c = 0.2$, $w_f/c = 0$ when $w_o/c = 0.2 \times 1.55 = 0.31$. In other words, according to eq. (25), a saturated paste having an original water-cement ratio of 0.31 would contain no water freezable in the dilatometer at −15 C after w_n/c has increased to 0.2. This may not be literally true since all saturated pastes contain a quantity of evaporable water equal to at least $4V_m$, all of which is theoretically freezable at about −78 C, and parts are freezable at higher temperatures, as indicated by the vapor pressure isotherm for gel water. However, in pastes in which the gel fills all available space ($w_e = 4V_m$) freezing may not occur because of the difficulty of starting crystallization in such extremely small spaces. If ice did form in the dilatometer experiment with such a paste, it probably would form as a separate phase on the surface of each granule. This remains a matter for speculation, since no tests were made on pastes containing no capillary space.

Whether or not freezing can occur within such pastes, the quantity that could form at ordinary freezing temperatures is so small that it can be regarded as zero from the practical point of view.

FINAL MELTING POINTS FOR SPECIMENS NOT FULLY SATURATED

As would be expected, the final melting point, that is, the highest temperature at which ice can exist in a specimen of hardened paste, is lower the lower the degree of saturation of the specimen. This is shown

*Note: An equation similar to eq. (25) was given in an earlier publication, *Proc.* ACI v. 41, p. 245, or P.C.A. Research Laboratory Bulletin 5, eq. (3). That equation was based on a preliminary analysis of the data presented in this paper. The difference between the two equations is due mainly to a difference in the assumed relationship between w_o and w_i. In the earlier equation, the relationship for the particular samples used in the freezing studies was used. In this paper, eq. (23) was used instead. For some unknown reason the difference between the w_o and w_i values for the samples used in the freezing study were abnormally high.

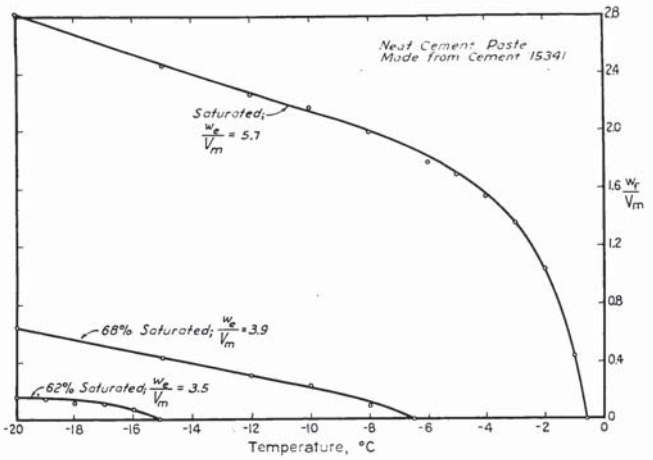

Fig. 8-14—Melting curves for saturated and partially saturated pastes

by the data plotted in Fig. 8-14. The upper curve represents a fully saturated specimen, and the other two lesser degrees of saturation, as indicated. The results agree approximately with eqs. (10), (11), and (12), which were derived empirically from tests on saturated samples.

For the sample represented by the middle curve, the amount of evaporable water was $3.9V_m$. By eq. (10), the amount of water freezable at -6 C should be

$$\left(\frac{w_f}{V_m}\right)_{-6°} = 3.9 - 4.0\,.$$

This indicates that none of the water present was freezable at -6 C, which agrees roughly with the observed fact that the final melting point was -6.5 C.

Similarly for the lowest curve, the amount of water freezable at -15 C is indicated by eq. (14) to be $0.3V_m$. The experimental data show the final melting point to be -15.5 C. This result may be considered as indicating substantial agreement between the equation and the observation.

SUMMARY OF PART 8

(1) Dilatometer studies were made on neat cement and cement-silica pastes to determine the amounts of ice that can exist in hardened paste under given conditions.

(2) Under the conditions of these tests, freezing did not occur on cooling until after the saturated samples had been supercooled 5 to 12 C.

(3) When freezing occurred, further cooling caused more ice to form.

(4) Raising the temperature stepwise from -20 to $+2$ C or higher showed that the melting was progressive. This result is as would be

predicted from the known effects of dissolved salts, adsorption, and capillary tension on the vapor pressure of the evaporable water.

(5) The final melting point in a saturated paste (temperature at which the last increment of ice disappears) ranged from −0.05 to −1.6 C. The temperature seemed to depend on the alkali content of the cement, the higher the alkali content, the lower the final melting point.

(6) The ice is believed to form in the capillary space outside the gel. It is unlikely that the gel water freezes in place, although, at low temperatures, it contributes to the ice.

(7) The maximum amount of water, w_f, that can freeze at a given temperature, can be estimated from the total evaporable water content, w_e, and V_m by use of the following empirical equations:

$$(w_f)_{-6°} = w_e - 4.0V_m$$
$$(w_f)_{-10°} = w_e - 3.7V_m$$
$$(w_f)_{-15°} = w_e - 3.2V_m$$

(8) The maximum freezable water content may be estimated in terms of the total water content, w_t, and the non-evaporable water content, w_n, as follows:

$$(w_f)_{-6°} = w_t - 2.04w_n$$
$$(w_f)_{-10°} = w_t - 1.96w_n$$
$$(w_f)_{-15°} = w_t - 1.83w_n$$

(9) The maximum freezable water content can be estimated from the original water content, w_o, and w_n, as follows:

$$(w_f)_{-6°} = w_o - 1.76w_n$$
$$(w_f)_{-10°} = w_o - 1.68w_n$$
$$(w_f)_{-15°} = w_o - 1.55w_n$$

(10) The temperatures given in the above equations are for freezing in a toluene-filled dilatometer. For freezing in air, the same equations apply (theoretically) if the temperatures (deg. C below zero) are multiplied by 2.

(11) Under freezing conditions differing from those used in these experiments, the amount of freezable water may be less than the amount indicated in the above equations, owing to the hysteresis in the sorption isotherms.

(12) The compositions of pastes that can contain practically no freezable water can be estimated from the above equations.

(13) The maximum amount of water freezable at a given temperature can be estimated from the 25 C isotherm with the aid of Fig. 8-1 and Table 8-10.

(14) When a paste is not fully saturated, the final melting point is lower than that for the same paste when saturated. The maximum

amount of freezable water in a paste at a given degree of saturation can be estimated approximately from the 25 C sorption isotherm and Fig. 8-1.

REFERENCES

(1) E. W. Washburn, *Monthly Weather Review* v. 52, p. 488 (1924); *International Critical Tables* v. 3, 210 (1928).

(2) P. Kubelka, *Z. Electrochem.* v. 38, p. 611 (1932).

(3) E. von Gronow, *Zement*, v. 25, pp. 485-90 (1936).

(4) H. W. Foote, B. Saxton, *J. Am. Chem. Soc.* v. 39, pp. 627-30 (1917).

(5) I. D. Jones, R. A. Gortner, *J. Phys. Chem.* v. 36, pp. 387-436 (1932).

(6) G. J. Bouyoucos, Mich. Agr. College Exp. Station Tech. Bull. No. 36 (1917); also, *J. Agr. Research* v. 8 ,pp. 195, 217 (1917).

(7) L. T. Alexander, T. M. Shaw, and R. J. Muckenhirn, *Proc. Soil Sci. Soc. Am.* v. 1, p. 113 (1937). Also, L. T. Alexander and T. M. Shaw, *J. Phys. Chem.* v. 41, p. 955 (1937).

(8) S. L. Meyers, *Ind. Eng. Chem.* v. 32, p. 1107 (1940).

(9) J. S. Burlew, *J. Am. Chem. Soc.* v. 62, p. 690 (1940).

(10) N. E. Dorsey, *Properties of Ordinary Water Substance* (New York: Reinhold Publishing Corp., 1940), Table 100.

(11) G. Jones and F. C. Jelen, *J. Am. Chem. Soc.* v. 57, p. 2532 (1935).

(12) Ref. 10, p. 514.

Part 9. General Summary of Findings on the Properties of Hardened Portland Cement Paste

CONTENTS PART 9

INTRODUCTION

In this, the final part of the paper, the concepts concerning the characteristics of hardened paste that have emerged from this study are set down in brief. It is not implied that the concepts are new and unique. On the contrary, they agree in general with previously expressed views of those who have believed the colloidal state of the hydration products to be a dominant characteristic of the hardened paste. However, it is now possible to consider these characteristics in more detail and on a quantitative or semi-quantitative basis.

This summary includes only the facts and relationships that can be set down with a minimum of discussion. The reader should not depend on this part alone for an understanding of the subject, since the finer points of interpretation and many significant details and illustrative graphs are omitted.

Some of the relationships given below do not appear in the preceding parts of the paper, but they are derived from relationships already given.

In the preceding parts of this paper the sequence of topics was determined according to the requirements for an orderly development of concepts and interrelationships between variables. In this summary it is assumed that the reader is familiar with the background material and the subject is presented, as far as possible, in the form of an analysis of the properties of hardened paste.

The following should be noted carefully before proceeding with the summary: All the data and relationships discussed below pertain only to specimens cured continuously at about 70 F. Without modification, they do not apply to other curing conditions.

GENERAL

Many of the technically important properties of concrete can be attributed to the peculiar nature of the hydration products of portland cement. The hardened paste is considered to be not a continuous, homogeneous solid, but rather to be composed of a large number of primary units bound together to form a porous structure. The chemical constitution of the units of this structure is not definitely known. However, it appears that many significant characteristics are dependent not primarily on chemical constitution but rather on the physical state of the solid phase of the paste and its inherent attraction for water.

The extreme smallness of the structural units of the paste, the smallness of the interstitial spaces, and the strong attraction of the solid units for water account for the fact that changes in ambient conditions are always accompanied by changes in the moisture content of the hard-

ened paste; moreover, these factors account for the changes in volume, strength, and hardness that accompany changes in moisture content. They also account for the peculiarities of the relationship between ice-content and temperature when saturated or partially saturated paste is cooled below the normal freezing point of water.

Various findings concerning the properties of the solid phase in hardened paste, and the interaction between the solid phase and evaporable water, are summarized in the following sections.

PASTE POROSITY

The pores in hardened portland cement paste are here considered to be the space in the paste that may be occupied by evaporable water. Evaporable water is defined as that which exhibits a vapor pressure greater than about 6×10^{-4} mm Hg at 23 C. It is roughly equivalent to the amount lost when a saturated paste is oven-dried at about 105 C.

The pores in a paste (exclusive of entrained air) are of two kinds: capillary pores and gel pores. The relative proportion of each kind can be determined from suitable data and the relationships given below.

Capillary pores

Before hydration begins, and during the time when the paste remains plastic, a cement paste is a very weak solid held together by forces of interparticle attraction. These forces probably act across thin films of water at points of near-contact between the particles. The water-filled spaces between the particles constitute an interconnected capillary system. After the plastic stage, when the final reactions of hardening begin, the capillary channels of the fresh paste tend to become filled with solids produced by the reaction between water and the constituents of cement. This process rapidly reduces the volume and size of the capillaries, but apparently does not destroy their continuity. The volume of the capillaries at various stages of hydration can be estimated with satisfactory accuracy from the relationships given below.

Before hydration starts,

$$p_c = w \,, \qquad (1)$$

where p_c = volume of capillary pores, and
w = volume of water.*

Eq. (1) is correct only for an instant after the cement and water are mixed. Solution and reaction begin at once, the average rate during the first 5 minutes being higher than during any subsequent 5-min. period. Within the initial 5-min. period, the rate of reaction decreases

*In this and the following equations, cgs units are intended and the same symbol is used for either weight (grams) or volume (cc) of free water. That is, w (general term for free water), w_o (net free water after bleeding), and w_c (capillary water) all are assumed to have a specific volume of 1.0 and thus may represent either grams or cc. The assumption that specific volume is unity introduces no error of practical importance.

abruptly and becomes very low. This low rate persists, under normal, controlled laboratory conditions, for a considerable period, usually about an hour. If the paste has been stirred continuously during the period of rapid initial reaction, or if it is restirred at the end of that period, it will remain plastic during the ensuing, relatively dormant period. If left undisturbed, the paste will "bleed" and its volume will thereby be diminished. After bleeding, its porosity (now equivalent to the remaining water-filled space, entrained air neglected) will be approximately

$$p_c = w_o - (V_B - cv_c) , \quad (2)$$

where w_o = original water content after bleeding, grams (or cc),
V_B = total volume of solid phase including increase due to hydration and pores in the gel,
c = weight of cement,
v_c = specific volume of the cement, i.e., the volume of a unit weight,
$(V_B - cv_c)$ = increase in volume of the solid phase due to hydration.

The volume of the solid phase at any stage of hydration can be evaluated as follows:

$$V_B = cv_c + 0.86(1 + 4k)w_n , \quad (3)$$

where 0.86 = mean specific volume of the non-evaporable water and gel water,
k = a constant characteristic of the cement, and
w_n = weight of non-evaporable water.*

Eliminating V_B and cv_c between eqs. (2) and (3) gives

$$p_c = w_o - 0.86(1 + 4k)w_n . \quad (4)$$

k will range from 0.24 to 0.28 among different cements, but for an average Type I cement, $k = 0.255$ (see Part 5) and eq. (4) becomes

$$p_c = w_o - 1.74w_n . \quad (5)$$

At early stages of hydration, that is, during the first few hours, when w_n is very small, eqs. (4) and (5) probably do not represent the facts very accurately because the numerical constants were evaluated from data obtained over a range of ages during which reactions involving gypsum could not occur. Therefore, the constants are probably not quite correct for periods during which gypsum-reactions are taking place to an appreciable extent.

From eq. (4) it follows that capillary porosity is zero when

$$0.86(1 + 4k)w_n = w_o,$$

or for an average cement, when $1.74w_n = w_o$ (see eq. (5)). For example, when $w_n/c = 0.2$, $p_c = 0$ if w_o/c is equal to or less than $0.2 \times 1.74 = 0.35$.

*Non-evaporable water is that having a vapor pressure equal to or less than about 6×10^{-4} mm *Hg* at 23C. It includes chemically combined water.

The highest possible water-cement ratio at which p_c can be made zero by prolonged curing depends on the magnitude of the highest possible value of w_n and on k. Both $(w_n)_{max}$ and k depend on the characteristics of the cement. $(w_n)_{max}$ depends principally on the degree to which the cement approaches complete hydration, which, in turn, depends principally on the proportion of the cement that is made up of particles finer than about 50 microns. (The coarsest particles fail to hydrate completely even though the wet-curing period is long.) It is related also to the computed chemical composition, as shown by the following relationship for w_n after six months of water-curing at 70 F.*

$$w_n/c = 0.187(C_3S) + 0.158(C_2S) + 0.665(C_3A) + 0.213(C_4AF), \ldots . (6)$$

where the symbols in parentheses represent the computed weight-proportion of the compound indicated. This relationship may be considered to represent the average value of w_n/c when the cement is not far from its ultimate degree of hydration, provided that w_o/c is not less than about 0.44 and that the specific surface of the cement is between 1700 and 2000, by the Wagner turbidimeter. For finer cements $(w_n/c)_{max}$ will be higher, but not much higher. For coarser cements, it will be lower to a degree about proportional to the residue on the 325-mesh sieve. For cements having a specific surface of about 1800 (Wagner), $(w_n/c)_{max}$ ranges from about 0.20 to 0.25, the higher value corresponding to cements relatively high in C_3S and C_3A.

Likewise, k is related to computed compound composition as follows:

$$k = 0.230(C_3S) + 0.320(C_2S) + 0.317(C_3A) + 0.368(C_4AF) \ldots . . . . . (7)$$

This relationship holds for any age with accuracy sufficient for most purposes.

With an average Type I cement, capillary pores will be present, even at ultimate hydration in any paste having an original water-cement ratio greater than about 0.44 by weight.

Gel pores

The quantity $(V_B - cv_c)$ appearing in eq. (2) and implicitly in eq. (4) is the increase in volume of the solid phase including the pores that are characteristic of the hydration products, presumably the pores in the gel. Consequently, the *total* porosity of the paste is greater than that given by the above equations. That is,

$$p_t = p_c + p_g , \ldots . . . . . (8)$$

where p_t = volume of total pores,
p_g = volume of gel pores, and
p_c = volume of capillary pores.

*This empirical relationship was not given in preceding parts of this paper. It was established by the method of least squares using about 100 items of data.

The volume of gel pores is given approximately by the following relationship:

$$p_g = 0.9 \times 4V_m = 3.6V_m \,, \quad (9)$$

where $4V_m$ is the weight of water that would saturate the gel, V_m is a factor proportional to the surface area of the gel (see eq. (12)), and 0.9 is the mean specific volume of the water in saturated gel.

For any given cement,

$$V_m = kw_n \,, \quad (10)$$

where k is the same constant that appears in eqs. (4) and (7). Hence, for an average cement, for which $k = 0.255$,

$$p_g = 0.92w_n \,. \quad (11)$$

SURFACE AREA OF THE SOLID PHASE IN HARDENED PASTE

The surface area of the solid phase in hardened paste is computed by the following relationship

$$S = (35.7 \times 10^6)V_m \,, \quad (12)$$

where S = surface area of solid phase, sq cm, and
V_m = grams of water required to form a complete monomolecular adsorbed layer of water on the solid surface.

Since $V_m = kw_n$, and since $k = 0.255$ for an average cement, the surface area of a hardened paste made from an average cement can be obtained from w_n by using the following relationship:

$$S = (35.7 \times 10^6)0.255w_n$$
$$= (9.1 \times 10^6)w_n \,. \quad (13)$$

In a typical paste, $w_o/c = 0.6$, the surface area per unit volume of paste reaches about 2.4×10^6 sq cm at ultimate hydration.

Since the internal surface area of the paste is predominantly that of the gel, V_m is here usually considered to be proportional to the surface area of the gel, S_g.

MEAN SIZE OF GEL PORES

The mean diameter of the gel pores is probably between 2 and 4 times the hydraulic radius. The hydraulic radius is evaluated as follows:

$$m_g = p_g/S_g \,, \quad (14)$$

where m_g = hydraulic radius of gel pores, cm,
p_g = volume of gel pores, cu cm, and
S_g = surface area in the gel, sq cm.

Thus, from eqs. (9) and (12),

$$m_g = \frac{3.6V_m}{(35.7 \times 10^6)V_m} = 10 \times 10^{-8} \text{ cm} \,. \quad (15)$$

Hence, the mean diameter of the gel pores is from 20 to 40 Ångstrom units.

SIZE OF CAPILLARY PORES

The mean diameter of the capillary pores cannot be determined from data now available. However, results of absorptivity tests indicate that the capillary pores are very much larger than the gel pores, except perhaps in pastes in which the gel nearly fills the available space.

PERMEABILITY

A saturated, hardened paste is permeable to water. Under a given pressure gradient and at a given temperature, the rate of flow is a function of the effective hydraulic radius of the pores and the effective porosity. The general theoretical equation for this function, called the coefficient of permeability, is

$$K_1 = 50 \times 10^{-14}\, V_m (N - k_1)^3 \,, \qquad (16)$$

in which K_1 = coefficient of permeability to water, in ft. per sec,
V_m = weight of water required for the first adsorbed layer, g per cc of paste,
N = ratio of total evaporable water to V_m, and
k_1 = a constant interpreted as the number of layers of immobile water per unit of solid surface, or the difference between total and effective porosity.

Indications of a limited amount of data are that eq. (16) would give results in reasonable agreement with experiment (Ruettgers, Vidal, and Wing) only for pastes in which N is not greater than about 4, that is, for pastes containing no capillary space. For such pastes, the theoretical permeability is given by

$$K_1 = 2.0 \times 10^{-12}(1 - cv_c) \Big| \; 0.45 \leqq cv_c \leqq 1.0$$

where c = cement content, g per cc of paste, and
v_c = specific volume of cement.

This result indicates that cement gel has about the same degree of permeability as granite (Ruettgers, Vidal, and Wing).

For pastes containing much capillary space outside the gel, actual permeability exceeds the theoretical by a wide margin. This is believed to indicate that in such pastes the flow is predominantly in the relatively large capillary pores outside the gel.

The permeability of concrete is generally greater than can be accounted for from the actual permeability of the paste (Ruettgers, Vidal, and Wing). This indicates that the water is able to flow through the fissures

that develop under the aggregate during the bleeding period and thus to partially by-pass the paste.

ABSORPTIVITY

The characteristic rate at which a dry specimen absorbs water is here called the absorptivity of the specimen. The adsorption during the first 30 to 60 minutes follows the relationship

$$q/A = (K_a t)^{1/2} \quad \ldots\ldots\ldots\ldots\ldots\ldots\ldots\ldots\ldots\ldots\ldots\ldots\ldots\ldots (17)$$

in which

q/A = the amount of water absorbed per unit area in time t, and
K_a = coefficient of absorptivity.

An empirical relationship was found between K_a and capillary porosity. That is,

$$K_a = f\left[W_o - 0.86(1 + 4k)W_n\right], \quad \ldots\ldots\ldots\ldots\ldots\ldots\ldots\ldots (18)$$

where the quantity in brackets is the capillary porosity,

W_o = water content of original mix, after bleeding, g (or cc) per cc of specimen,
W_n = non-evaporable water, g per cc of specimen, and
k = a constant characteristic of the cement. (See eq. (3), (7), and (10).)

The quantity $0.86(1 + 4k)W_n$ is the increase in volume of the solid phase due to hydration. When it equals W_o, capillary porosity is zero. The experimental curve showed that K_a was also zero, or nearly so, at this point. Thus the data show that the initial absorption of water by a dried specimen takes place almost exclusively in the capillary spaces outside the gel.

PROPERTIES OF WATER IN HARDENED PASTE

In a saturated, hardened cement paste, three classes of water are here recognized:

(1) non-evaporable water,
(2) gel water, and
(3) capillary water.

Non-evaporable water

Non-evaporable water is defined as that part of the total that has a vapor pressure of not over about 6×10^{-4} mm Hg at 23 C. It is a constituent of the solid material in the paste. Some of it exists as OH groups in $Ca(OH)_2$; some, probably as water of crystallization in calcium sulfoaluminate. The rest is combined in the solid phase in ways not yet

known. Of this part, some may be combined chemically with the hydrous silicates and hydrous alumina-bearing compounds; some may be held by van der Waal forces, that is, physical forces.

For purposes of volume-analysis, the non-evaporable water may be treated as an entity. Its volume added to that of the original cement gives the absolute volume of the solid phase in the paste. Thus,

$$V_S = cv_c + w_n v_n \,, \quad \ldots\ldots\ldots\ldots\ldots\ldots\ldots\ldots\ldots\ldots\ldots\ldots\ldots\ldots (19)$$

where V_S = absolute volume of solid phase in the paste,
c = cement content of the paste,
w_n = non-evaporable water content of the paste,
v_c = specific volume of the cement, and
v_n = mean specific volume of the non-evaporable water.

The specific volume of the non-evaporable water is an empirical factor that will account for the observed increase in the absolute volume of the solid phase per gram increase in amount of non-evaporable water. Its value is about 0.82.

Gel water

The gel water is that contained in the pores of the gel. The pores in the gel are so small that most if not all the gel water is within the range of the van der Waal surface forces of the solid phase. This is indicated by the fact that the mean specific volume of the gel water is about 0.90.

The vapor pressure of the gel water at a fixed temperature is a function of the degree of saturation of the gel. The lowest pressure just exceeds 6×10^{-4} mm at 23 C, which is the highest pressure of the non-evaporable water. The highest pressure is nearly, but not quite, equal to that of pure water in bulk at the same temperature; the difference is due principally to the alkali hydroxides in solution. The vapor pressure at a given intermediate degree of saturation may be any value between limits fixed by the manner in which the existing water content was reached. It will be a maximum if the existing water content was reached by continuous adsorption, beginning with a dry sample. It will be a minimum if the water content was reached by continuous desorption, starting with a saturated sample. Intermediate pressures will be found if the given water content was reached by adsorption after partial desorption, or if it was reached by desorption after partial saturation by adsorption. These peculiar relationships are due to hysteresis in the sorption isotherm. They are found only for water contents that fall within the hysteresis loop. The limits of the loop are not now definitely known.

The weight of gel water in a saturated paste is equal to $4V_m$, where V_m is the weight required to form a complete monomolecular adsorbed layer on the solid phase. For volume analysis of the paste, the weight of

the gel water may be used to determine the total volume (rather than absolute volume) of the solid phase in the paste. Thus,

$$V_B = V_S + 0.9w_g = V_S + 3.6V_m , \quad (20)$$

where V_B = total volume (or bulk volume) of the solid phase,
V_S = absolute volume of solid phase, and
w_g = grams of gel water per cc of saturated paste = $4V_m$.

Capillary water

Like the gel water, the capillary water is really a solution of alkalies and other salts. The capillary water is that which occupies space in the paste other than the space occupied by the solid phase together with characteristic pores of the gel. That is,

$$w_c = V_t - V_B , \quad (21)$$

where w_c = volume of capillary water,
V_t = over-all (total) volume of saturated paste, exclusive of cavities,
V_B = bulk volume of solid phase in the paste.

Practically all the capillary water lies beyond the range of the surface forces of the solid phase. Hence, in a saturated paste, the capillary water is under no stress and its specific volume is the same as the normal specific volume of a solution having the same composition as the capillary water.

In a partially saturated paste, the capillary water is subjected to tensile stress. This stress is due to curvature of the air-water interface and the surface tension of the water. The magnitude of the stress is given by the following equation:

$$F = -\frac{RT}{Mv_f} \ln p/p_s , \quad (22)$$

where F = force of capillary tension,
R = gas constant,
M = molecular weight of water,
v_f = specific volume of water,
p = vapor pressure of capillary water at the existing temperature,
p_s = saturation pressure of water at the existing temperature, and
ln = natural logarithm.

The vapor pressure of the capillary water depends on the degree of saturation of the paste and on the factors arising from hysteresis discussed in the preceding section. However, if the existing vapor pressure is reached by continuous adsorption from the dry state, capillary water does not exist in the paste at pressures below about $0.45\ p_s$.

Since at vapor pressures greater than $0.45\,p_s$ and less than p_s, the capillary water is present and under tension, its specific volume must be greater than 1.0 and a function of F of eq. (22). No attempt has been made to verify this experimentally.

Some of the gel water may be fundamentally the same as capillary water. The distinction used here is made on the basis of relationship to the solid phase. The quantity of gel water always bears a fixed ratio to the quantity of hydration products, whereas the quantity of capillary water is determined by the porosity of the paste.

PHYSICAL STATE OF THE HYDRATION PRODUCTS

Microscopic observation of hardened paste indicates that only $Ca(OH)_2$ crystals and unhydrated residues of the original cement grains can readily be identified. Other microcrystalline constituents, particularly calcium sulfoaluminate, may be present in small amount but are generally obscured by the abundant "amorphous" constituents.

The size and volume of the pores in hardened paste indicate that the solid material is finely subdivided, though the solid units are obviously bonded to each other. If the units were equal spheres, the sphere diameter would be about 140Å. Since the computations leading to this figure included the volume of microcrystalline constituents, the units of "amorphous" material must be somewhat smaller than just indicated. The size indicated is definitely in the colloidal size-range. Since a gel is defined as a coherent mass of colloidal material, it follows that the principal constituent of hardened paste is a gel, here called cement gel.

The cement gel is composed of hydration products that contain all the principal oxides: CaO, SiO_2, Al_2O_3, and Fe_2O_3. This is shown by the fact that the total surface area of the solid phase is related to the computed cement composition in the following way:

$$\frac{V_m}{w_n} = 0.230(C_3S) + 0.320(C_2S) + 0.317(C_3A) + 0.368(C_4AF)\ , \quad \ldots\ (23)$$

where the symbols in parentheses represent the computed weight-fraction of the compounds indicated. The similarity of the numerical coefficients and the magnitude of particle size given above show that all constituents either may be present in a single complex hydrate of high specific surface or they may be constituents of two or more different hydrates having similar specific surfaces. The relative smallness of the coefficient of C_3S is in line with the fact that this compound hydrolyzes to give microcrystalline (low specific surface) $Ca(OH)_2$ as one of its reaction products.

ENERGY CHANGES OF HYDRATION, ADSORPTION, AND CAPILLARY CONDENSATION

Heat of hydration

When cement and water react, the total amount of heat evolved is directly proportional to the total amount of non-evaporable water in the paste. Thus,

$$\text{total heat of hydration} = \text{constant} \times w_n .$$

The proportionality constant varies with cement composition. For all types of portland cement, it ranges from 485 to 550 calories per gram of non-evaporable water.

The total heat of hydration is the sum of the heat of combination of the non-evaporable water, the net heat of adsorption of water on the surface of the solid phase, and the net heat of capillary condensation.

Total net heat of surface adsorption

The net heat of surface adsorption is the amount of heat in excess of the normal heat of liquefaction that is evolved when water vapor interacts with the solid phase. For all cement pastes,

$$Q_{st} = 472V_m \text{ calories (approx.)} , \quad (24)$$

where Q_{st} = total net heat of surface adsorption when the paste is changed from the dry to the saturated state.

Net heat of capillary condensation

Adsorption at low vapor pressures causes the solid phase to become covered with a film of water having a surface area presumably equal to the covered area of the solid phase. At pressures above $0.45p_s$ adsorption is accompanied by capillary condensation which progressively diminishes the exposed water-surface as the pressure is raised. The heat evolved from the destruction of water-surface is the net heat of capillary condensation. When a paste is changed from the dry to the saturated state,

$$Q_{ct} = 100V_m, \text{ calories (approx.)}, \quad (25)$$

where Q_{ct} = total net heat of capillary condensation.

Total net heat of adsorption

The total net heat of adsorption is the sum of the total net heat of surface adsorption and the total net heat of capillary condensation. That is,

$$Q_{at} = 472V_m + 100V_m = 572V_m, \text{ calories (approx.)}, \quad (26)$$

where Q_{at} = total net heat of adsorption. This amounts to about 670 ergs per sq cm of solid surface and is about the same as the heat of immersion of various minerals, particularly the mineral oxides, in water.

Enthalpy change of adsorption

The total net heat of adsorption (eq. (26)) is practically equal to the decrease in enthalpy of the system. The decrease in enthalpy represents

the sum of the decrease in free energy and the decrease in unavailable energy. Thus,

$$-\Delta H = -\Delta G - T\,\Delta S\,, \quad \ldots\ldots\ldots\ldots\ldots\ldots\ldots\ldots\ldots\ldots (27)$$

where $-\Delta H$ = decrease in enthalpy,
$-\Delta G$ = decrease in free energy,
$-\Delta S$ = decrease in entropy,
T = absolute temperature, and
$-T\Delta S$ = decrease in unavailable energy.

Decrease in free energy

Shrinking and swelling, moisture diffusion, capillary flow, and all other effects involving changes in moisture content of the paste at constant temperature are due to the free surface energy of the solid phase, or to the free surface energy of the water, or to both surface energies. All such effects are accompanied by a decrease in free energy and, in this case, a decrease in entropy, but the forces producing these effects are derived solely from the free energy.

The decrease in free energy can be expressed as a function of the ratio of the vapor pressure of the adsorbed water to that of free water at the same temperature without regard to the nature of the underlying solid phase.

$$-\Delta G = -75.6\ log_{10} p/p_s, \text{ cal per g of water} \quad \ldots\ldots\ldots (28)$$

It thus varies from zero when $p = p_s$ to a very large value when p is very much smaller than p_s.

Decrease in entropy

A change in entropy denotes some sort of internal change in the substance or substances involved in a reaction. In this case, the change is assumed to take place solely in the water as it changes from the free to the adsorbed state.

The decrease in entropy was estimated for adsorption over the pressure range $p = 0.05p_s$ to $p = 0.5p_s$. The decrease ranged progressively from $-\Delta S = 0.22$ cal/g/deg at $p = 0.5p_s$ to 0.50 cal/g/deg at $p = 0.05p_s$.

The magnitude of $-\Delta S$ indicates that some of the water is changed by adsorption in this range of pressures more than free water is changed by freezing under ordinary conditions and as much as or more than free water is changed by becoming water of crystallization. Water adsorbed at $p = 0.05p_s$ undergoes a change as great as the change from normal water to hydroxyl groups chemically combined in $Ca(OH)_2$.

Energy of binding of water in hardened paste

The net heat of adsorption (decrease in enthalpy) is a measure of the energy that must be supplied to restore adsorbed water to the normal liquid state.

The maximum energy of binding of the adsorbed water is estimated at about 400 cal/g of water. The average energy of binding of the first complete adsorbed layer is estimated at about 300 cal/g of water. The average energy of binding of the gel water is about 143 cal/g of gel water. These figures are probably somewhat too low inasmuch as the effect of adsorbed air was neglected.

These values indicate that most of the non-evaporable water is less firmly bound than the water in $Ca(OH)_2$ for which the energy of binding is 847 cal/g of water.

The capillary water cannot be considered "bound" in the same sense as the non-evaporable water and gel water. The energy required to remove all the capillary water from a saturated paste, if that could be done separately, would be $100V_m$ calories, regardless of the amount of capillary water in the paste.

VOLUME CHANGE

Mechanism of shrinkage and swelling

Cement paste shrinks and swells as the cement gel loses or gains water. Swelling results when the surface forces of the solid phase are able to draw water into the narrow spaces between the solid surfaces. The magnitude of the swelling can be accounted for by assuming that the total volume change that occurs when a dry specimen is saturated is due to the increase in spacing of the solid surfaces required to accommodate a monomolecular layer on each opposing solid surface.

Shrinking results when water is withdrawn from the gel. It is probably due to the solid-to-solid attraction that tends to draw the solid surfaces together, though capillary tension and elastic behavior may also be involved.

By this theory, volume change is regarded as being the result of an unbalance in the forces acting on the adsorbed water. These forces are the solid-to-liquid attraction and capillary tension. When the solid-to-liquid attraction and capillary tension are equal, the volume of the gel remains constant.

Swelling pressure

Swelling pressure is the force that would be just able to prevent water from entering the gel. For isothermal swelling it is related to the magnitude of the free-energy change that would occur if the water entered the gel. Thus,

$$\Delta P = \Delta G/v_f \,, \qquad (29)$$

where ΔP = increase over existing external pressure required to prevent swelling,

ΔG = increase in free energy of adsorbed water when swelling occurs, and

v_f = specific volume of adsorbed water, assumed to be independent of pressure.

Or, in terms of the change in vapor pressure of the adsorbed water that accompanies swelling,

$$\Delta P = -\frac{RT}{Mv_f} \ln p/p_s \quad \ldots\ldots\ldots\ldots\ldots\ldots\ldots\ldots (30)$$

This equation is probably reasonably accurate (except for low values of p/p_s) for a hypothetical gel composed of discrete colloidal particles. When the gel is composed of interconnected particles and encloses stable microcrystals and aggregate particles, as in concrete, shrinking or swelling is partially opposed by elastic forces. Hence, some difference between the theoretical and actual swelling pressure should be expected.

Capillary tension

In a partially saturated paste the tendency of the water to enter the gel is opposed by tension in the capillary water. The force of capillary tension,

$$F = \sigma\left[\frac{1}{r_1} + \frac{1}{r_2}\right] = -\frac{RT}{Mv_f} \ln p/p_s\,, \quad \ldots\ldots\ldots\ldots\ldots\ldots (31)$$

where σ = surface tension of water,
r_1 and r_2 = principal radii of curvature of the menisci, and
v_f = specific volume of capillary water.

Thus, capillary tension and potential swelling pressure have the same relationship to relative vapor pressure except for a difference in v_f.* When the vapor pressure of the gel water and the capillary water are equal, volume remains constant.

In saturated paste that contains no capillary water ($w_e = 4V_m$) it would appear that there could be no capillary tension. However, some of the gel water may actually be capillary water; that is, menisci may develop as the gel is dried. Whether or not capillary tension can develop in the gel, the tendency of the water to evaporate from the gel would have an effect on adsorbed water equivalent to capillary tension.

Relationship between change in volume and change in water content

When drying occurs, capillary water and gel water are lost simultaneously. Since the resulting change in volume is due only to the change in gel-water content, it follows, theoretically, that

$$\Delta V = (\text{constant})\ \frac{\Delta w_t - \Delta w_c}{V_m}\,, \quad \ldots\ldots\ldots\ldots\ldots\ldots\ldots (32)$$

where ΔV = change in volume of specimen,
Δw_t = change in total water content, grams,
Δw_c = change in capillary-water content, grams,

*See footnote, page 586, Part 4.

$\Delta w_t - \Delta w_c$ = change in gel-water content, grams, and
(constant) = a value characteristic of the concrete in question. (It probably changes slightly as curing proceeds.)

V_m is here considered to be a factor proportional to the amount of gel. Hence,

$$\frac{\Delta V}{\Delta w_t} = (\text{constant}) \frac{1 - \frac{\Delta w_c}{\Delta w_t}}{V_m} . \quad \ldots\ldots\ldots\ldots\ldots\ldots\ldots\ldots (33)$$

Thus, the change in volume per unit change in total water content will depend on the ratio of capillary water to total water.

Contraction in volume of the system cement + water

When cement and water react, there is a diminution in the sum of their absolute volumes. On the assumption that the contraction is confined entirely to the water and that the over-all apparent volume of the hardened paste does not change after bleeding is over,

$$w_t v_t = w_o , \quad \ldots\ldots\ldots\ldots\ldots\ldots\ldots\ldots\ldots\ldots\ldots\ldots\ldots\ldots (34)$$

where w_t = weight of total water in the saturated hardened paste,
v_t = specific volume (mean) of the total water, and
w_o = volume of original water in the paste.

The difference between w_o and w_t is the amount of water that must be absorbed by the specimen during the course of hydration for the specimen to remain saturated.

At any stage of hydration,

$$v_t = 1 - 0.279 \frac{w_n}{w_t} , \quad \ldots\ldots\ldots\ldots\ldots\ldots\ldots\ldots\ldots\ldots\ldots\ldots (35)$$

where

v_t = mean specific volume of the total water (both evaporable and non-evaporable) in saturated paste, and
w_n = non-evaporable water, grams.

Hence,

$$\Delta v_w = w_t - w_o = 0.279 w_n , \quad \ldots\ldots\ldots\ldots\ldots\ldots\ldots\ldots\ldots\ldots (36)$$

where Δv_w = contraction of the water, cc.

Self-desiccation

If a specimen is kept sealed after its bleeding period, so that no extra water is available to it during the course of hydration, the pores in the paste will become partially emptied. This is here called self-desiccation.

The degree to which the pores become emptied can be estimated as follows:

Let w_e = evaporable water content of the saturated paste
$= w_t - w_n$.

Then

$$\frac{\Delta v_w}{w_e} = \text{ratio of empty-pore volume to total-pore volume (ignoring differences in specific volume),}$$

and

$$\frac{\Delta v_w}{w_e} = \frac{0.279 w_n}{w_t - w_n} .$$

Since $w_t = w_o + 0.279 w_n$,

$$\frac{\Delta v_w}{w_e} = \frac{0.279 w_n}{w_o - 0.721 w_n} \quad \ldots\ldots\ldots\ldots\ldots\ldots\ldots\ldots\ldots\ldots (37)$$

This gives the deficiency in evaporable water on a weight-ratio basis, which is close enough to the volume ratio for practical purposes.

For an illustrative example, let $w_o/c = 0.5$ and $w_n/c = 0.2$. Then,

$$\frac{\Delta v_w}{w_e} = \frac{0.279 \times 0.2}{0.5 - (0.721 \times 0.2)} = 0.16 \quad \ldots\ldots\ldots\ldots\ldots\ldots (38)$$

That is, in such a specimen and under conditions that prevent loss or gain of water, the deficiency in evaporable water would be 0.16 g/g of total evaporable water, when hydration had proceeded to the point where $w_n/c = 0.2$.

Such self-desiccation is believed to be an important factor contributing to the frost resistance of concrete. Experimental evidence indicates that when specimens of good quality are stored in moist air, or even under water, they are unable to absorb enough water to compensate completely for self-desiccation. Consequently, cement paste is seldom found in a completely saturated state, and hence is seldom in a condition immediately vulnerable to frost action.

CAPILLARY FLOW AND MOISTURE DIFFUSION

From the standpoint of thermodynamics, capillary flow and moisture diffusion are considered to be the results of inequalities in free energy. Inequalities in free energy under *isothermal* conditions arise from

(1) inequalities in moisture content,
(2) inequalities in deformations of the solid phase, and
(3) inequalities in the external pressure acting on the adsorbed water.

When such inequalities arise, the evaporable water will always tend to redistribute itself in such a way as to equalize its free energy. This has an important influence on plastic flow under sustained stress.

EFFECT OF TEMPERATURE CHANGES AT CONSTANT MOISTURE CONTENT

Effect on swelling

As mentioned above, potential swelling pressure and capillary tension have the following relationships at equilibrium:

$$\Delta P = F = \sigma \left[\frac{1}{r_1} + \frac{1}{r_2} \right] \quad \ldots\ldots\ldots\ldots\ldots\ldots\ldots\ldots\ldots\ldots (39)$$

At constant water content, a rise in temperature would expand the capillary water and thus decrease its surface curvature. Also, it would decrease the surface tension, σ. Consequently, a rise in temperature causes capillary tension to decrease and thus causes water to enter the gel and restore equilibrium between ΔP and F. Thus, a rise in temperature at constant water content causes swelling in addition to the normal thermal expansion. The swelling of the solid phase would be absent in a dry specimen or in a saturated specimen where $p = p_s$.

From the above it follows that the "thermal coefficient" of a given sample of concrete is not a constant, unless the sample is completely dry or saturated.

Effect on diffusion

When counteracting effects are absent, evaporable water moves in the direction of descending temperature.

Combined effect of stress, strain, changes in humidity, and temperature gradients

In concrete subjected to changing external forces, changing temperatures, and fluctuating ambient humidity, the evaporable water must be in a continual state of flux. As a consequence, the concrete swells, shrinks, expands, and contracts under the changing conditions in a highly complicated way. The separate effects may combine in different ways at a given point in the mass so that they offset or augment each other. Possibly these effects have an influence on the ability of concrete to withstand weathering.

FACTORS GOVERNING THE EXTENT AND RATE OF HYDRATION OF PORTLAND CEMENT

Extent of hydration

The principal factors governing the ultimate degree of hydration, regardless of the time required, are the relative proportion of particles having mean diameters greater than about 50 microns, and the original water-cement ratio. Incomplete data indicate that cements containing no particles larger than 50-micron diameter (or thereabouts), become completely hydrated if w_o/c is not too low. The ultimate extent of hydration appears to be about inversely proportional to the 325-mesh residue.

With any given cement the ultimate degree of hydration is proportional to the water content of the paste in all pastes in which w_o/c is less than a definite limiting value. With an average cement the limiting value is about 0.44 by weight. That is, this is the lowest w_o/c that will permit the ultimate degree of hydration with an average cement. Presumably, the greater the 325-mesh residue, the lower this limiting value of w_o/c.

Rate of hydration

With other factors equal, the average rate of hydration is lower the smaller w_o/c, except during a short initial period. Consequently, the time required to reach ultimate hydration becomes longer as w_o/c is made smaller.

During the early stages of hydration, say during the first week or two, the rate of hydration is higher by a large factor, the higher the specific surface. But during the later stages, the rates of hydration for cements of widely different specific surface differ comparatively little.

Self-desiccation influences the rate of hydration. As the pores become partly emptied, the vapor pressure of the remaining evaporable water is correspondingly reduced. Experiments indicate that even though the remaining water is chemically free, its rate of reaction with cement is a function of its relative vapor pressure. If the relative vapor pressure in the paste drops below about 0.85, hydration virtually ceases. Consequently, sealed specimens hydrate more slowly than those having access to water, and they may never reach the ultimate degree of hydration possible when extra water is available. This has a bearing on the efficiency of membrane or seal-coat curing.

The foregoing discussion indicates that conclusions concerning the rate and amount of hydration of portland cement *in concrete* (w/c = 0.45 to 0.70) should not be drawn from data on standard test pieces (w/c = 0.25 ±). Moreover, specimens cured in sealed vials should not be expected to hydrate at the same rate and to the same extent as similar specimens cured in water or fog. Also, it should be noted that for samples in sealed vials, water separated from the paste by bleeding must be considered as extra water.

RELATION OF PASTE POROSITY TO COMPRESSIVE STRENGTH

The compressive strength of 2-in. mortar cubes is, with certain restrictions, given by the relationship

$$f_c = 120{,}000 \frac{V_m}{w_o} - 3600, \quad (40)$$

where f_c is compressive strength, psi, and V_m/w_o is considered to be a

factor proportional to the degree to which the gel fills the originally water-filled space, here called the gel-space ratio. The relationship holds for all ages and apparently for all cements low in C_3A (less than about 7 percent computed).

For cement of average or high C_3A content, and especially for those high in both alkali and C_3A the strengths obtained at a given V_m/w_o are lower than those indicated by the equation. The results obtained with some such cements can be brought into compliance with the equation by increasing the gypsum content of the cement.

The relationship given by eq. (40) is considered to be empirical—neither fundamental nor general. Independent variables that are not adequately taken into account are as follows:

(1) some features of cement composition,
(2) effect of aggregate particles,
(3) entrained air,
(4) fissures under the aggregate particles that form during the bleeding period, and
(5) variations in curing temperature.

FREEZING OF WATER IN HARDENED PASTE

Owing to the nature of the relationship between water content and free energy, as shown by sorption isotherms, the water in a saturated paste freezes or melts progressively as the temperature is varied below the normal melting point. An example of the progressive melting of ice in a particular frozen, saturated paste follows:

Temperature*	Amount of ice, g/g of cement	Amount of ice, as percent of amount at −30 C
0	0	0
− 0.5	0.045	21
− 1.5	0.075	36
− 2.0	0.093	44
− 3.0	0.109	52
− 4.0	0.122	59
− 5.0	0.131	62
− 6.0	0.137	65
− 8.0	0.147	70
−12.0	0.168	80
−16.0	0.181	86
−30.0	0.210	100

*The temperatures indicated are for samples exposed to air or water. For exposure to toluene, as in the experiments, the figures for temperature should be divided by 2.

The capillary water is believed to freeze in place, at least under the conditions of the experiments. However, the gel water probably flows or distills from the gel to the capillaries before it freezes.

The temperature at which the last increment of ice disappears on progressive melting is here called the final melting point. It would be the same as the initial freezing point, were it not for the occurrence of supercooling.

The final melting point in saturated pastes ranges from about −1.6 C to about −0.05 C. The depression of the final melting point is due to dissolved material in the mixing water, principally alkalies.

The final melting point in a paste that is not fully saturated depends not only on the dissolved material but also on the degree of saturation; the lower the degree of saturation the lower the final melting point.

All the evaporable water is freezable, but a minimum temperature of about −78 C is required to freeze all of it.

At any given temperature between −78 and −12 C*, the maximum amount of freezable water in saturated paste is

$$w_f = w_e - uV_m \; ; \quad \ldots\ldots (41)$$

or, approximately,

$$w_f = w_t - w_n\,(1 + 0.26u) \; ; \quad \ldots\ldots (42)$$

or

$$w_f = w_o - (0.721 + 0.26u)w_n \; , \quad \ldots\ldots (43)$$

in which w_f = freezable water,
w_e = total evaporable water,
V_m = factor here considered to be proportional to the gel content of the paste,
w_n = non-evaporable water, and
u = a constant equal to w_u/V_m, where w_u is the amount of water unfreezable at a given temperature.

The following are empirical relationships for the maximum amounts of water freezable in saturated pastes at given temperatures, in terms of w_n and w_o:

$$(w_f)_{-12°} = w_o - 1.76w_n$$
$$(w_f)_{-20°} = w_o - 1.68w_n$$
$$(w_f)_{-30°} = w_o - 1.55w_n$$

At −12 C†, the amount of freezable water is equal to the volume of the capillary water outside the gel. At lower temperatures gel water is frozen, but the gel water probably leaves the gel and becomes a part of the ice already formed in the capillaries.

*See footnote below table on previous page.
†The temperatures indicated are the theoretical values for freezing in air or water. They correspond to −6 C, −10 C, and −15 C, respectively, for freezing in contact with toluene. (See Part 8.)

At temperatures above −12 C, the maximum amount of freezable water is roughly proportional to the amount of capillary water, $w_e - 4V_m$, or (approximately) $W_o - 1.76w_n$. The proportionality constants are about 1.0 at −12 C, 0.86 at −8 C, 0.7 at −4 C, and 0.6 at −2 C.

The maximum amount of ice will not be present unless the temperature has previously dropped to a low value, −50 C or perhaps lower. If the maximum cooling is only a few degrees below the final melting point, the amount of ice formed would probably be less than the amount indicated by the relationship given above. This is a result of the hysteresis in the water content vs. free-energy relationship as indicated by the sorption isotherms.

For practical purposes, the freezable water can be considered to be identical with the capillary water. Hence, pastes that contain no capillary space outside the gel are considered to be without freezable water.